THE UNIVERSITY OF QUEENSLAND

AUSTRALIA

Differential Oxidation of Iron Sulfides to Modify the Au:S Ratio in the Flotation Concentrate Product at Lihir

Joseph John

Bachelor of Pharmacy

Master of Pharmacy

Master of Biotechnology

Master of Chemical Engineering

A thesis submitted for the degree of Doctor of Philosophy at

The University of Queensland in 2017

Sustainable Minerals Institute

Julius Kruttschnitt Mineral Research Centre

Abstract

Sulfide associated refractory gold ores hold a majority of the gold within the pyrite, which has several forms. The high proportion of the gold atomically dispersed in the pyrite has been confirmed by various mineralogy techniques such as laser ablation analysis, optical microscopy, scanning electron microscopy and secondary ion mass spectrometry. Different types of pyrite exist within a refractory ore body and certain types possess a relative abundance of gold compared to other forms.

The low gold pyrite influences the rate at which the concentrate can be processed by any particular route. If the different types of pyrite could be separated by flotation, then the gold grade of the final concentrate can be improved and the invisible gold could be recovered by downstream processing. This separation of low gold pyrite from the gold-rich pyrite would increase the gold:sulfur ratio (*Au:S ratio*) to the autoclave feed, thereby maximising the autoclave throughput and gold production per tonne.

Different methods of extraction such as chemical oxidation, thermal oxidation and biological oxidation liberate gold from refractory ores. However, such oxidation methods have not been reported yet to be successful to allow separation of the low gold pyrite from the gold-rich pyrite and modify the Au:S ratio of a pyrite concentrate. This project is an attempt to develop a hydrometallurgical framework to modify the flotation response of gold-rich pyrite and low gold pyrite so that the Au:S ratio of the final flotation concentrate can be upgraded.

Declaration by the author

This thesis is composed of my original work and contains no material previously published or written by another person except where due reference has been made in the text. I have clearly stated the contribution by others to jointly-authored works that I have included in my thesis.

I have clearly stated the contribution of others to my thesis as a whole, including data analysis, significant technical procedures, professional editorial advice, and any other original research work used or reported in my thesis. The content of my thesis is the result of work I have carried out since the commencement of my research higher degree candidature and does not include a substantial part of work that has been submitted to qualify for the award of any other degree or diploma in any university or other tertiary institution.

I acknowledge that an electronic copy of my thesis must be lodged with the University Library and, subject to the policy and procedures of The University of Queensland, the thesis be made available for research and study in accordance with the Copyright Act 1968 unless a period of embargo has been approved by the Dean of the Graduate School.

I acknowledge that copyright of all material contained in my thesis resides with the copyright holder(s) of that material. Where appropriate I have obtained copyright permission from the copyright holder to reproduce material in this thesis.

Publications during candidature

JOHN, J., JOHNSON, N. W., STEWART, K., TURNER, D., & BRADSHAW, D. (2013). A review of pre-treatment methods to separate the different types of pyrite in gold processing. In *5th World Gold 2013 Conference* (pp. 347-355). AusIMM: Australasian Institute of Mining and Metallurgy.

Publications included in thesis

JOHN, J., JOHNSON, N. W., STEWART, K., TURNER, D., & BRADSHAW, D. (2013). A review of pre-treatment methods to separate the different types of pyrite in gold processing. In *5th World Gold 2013 Conference* (pp. 347-355). AusIMM: Australasian Institute of Mining and Metallurgy. Partially incorporated in Chapter 2 (*Literature Review*).

Contributor	Statement of contribution
Joseph John (Candidate)	Critical Review (100%) Wrote the paper (100%)
Johnson N. W	Feedback (60%) Edited paper (30%)
Kathryn Stewart	Feedback (20%)
Duncan Turner	Feedback (10%)
Dee Bradshaw	Feedback (10%)

Contribution by others to the Thesis

Professor N.W. Johnson (*Bill Johnson*) provided technical support for project design, flotation set-up, experimental design and data analysis. He has regularly reviewed technical outcomes of this thesis and provided valuable advice.

Dr. Cathy Evans provided assistance on mineralogical characterisation of the ore and critically reviewed the thesis.

Dr. Kathryn Stewart provided guidance on the detailed characterization of the ore and to develop a novel technique to establish the oxidation rates of various types of pyrite.

Dr. Duncan Turner provided technical support on designing a novel method based on hydrometallurgical practices to treat the flotation concentrates and cause preferential separation of the various pyrite types.

Newcrest Mining Limited provided funding for this research program.

Critical review and comments on the final draft of the thesis were performed by all five advisors:
Dr. Bill Johnson, Dr. Cathy Evans, Dr. Kathryn Stewart, Dr. Duncan Turner and Dr. Emmy Manlapig.

Statement of parts of the thesis submitted to qualify for the award of another degree

None

Acknowledgements

This thesis would not be possible without the guidance, support and generous contribution of many. Firstly, my deepest gratitude is to principal advisor Prof. Bill Johnson for the continuous support, patience, motivation, and guidance. Special mention to associate advisor Dr. Cathy Evans for her prompt feedback and in helping me to structure the thesis. I also thank my other co- advisors Dr. Kathryn Stewart, Dr. Duncan Turner and Dr. Emmy Manlapig for their overwhelming guidance, timely support and constructive criticisms throughout the candidature. Professor Dee Bradshaw is also thanked in particular for her encouragement and support.

This research was fully sponsored by Newcrest Mining Limited and I take great pride in thanking Newcrest Mining Limited for giving this opportunity to work on a challenging yet exciting project. I thankfully acknowledge all the financial support and personal development courses from Newcrest Mining Limited that have led to the fruitful completion of this project. I would also like to thank other mentors from Newcrest Mining Limited especially David Seaman, Rodolfo Espinosa- Gomez and Paul Griffin for their valuable insights and facilitating site visits.

I would like to acknowledge the financial, academic and technical support of the University of Queensland, Sustainable Minerals Institute and Julius Kruttschnitt Mineral Research Centre and its staff and students because of whom my research experience has been one that I will cherish forever. My sincere thanks also go to Peter Rohner and other Core Resources personnel who provided an opportunity to join their team as an intern, and who gave access to the laboratory and research facilities. Without their precious support, it would not be possible to complete this research. I also would like to acknowledge Newcrest Sumner Park staff personnel for their assistance during the initial experimental stages. Special thanks to Dr. Elaine Wightman and Kelly White for valuable advice regarding MLA and other mineralogical aspects.

Last but not the least by any means, I am deeply grateful to my family for their unequivocal support and inspiration that has led me all the way.

Above all, I thank God, the Almighty for his blessings.

Keywords: Refractory ore, Sulfide minerals, Gold to Sulfur ratio, Pyrite, Hydrometallurgy, Oxidation, Flotation

Australian and New Zealand Standard Research Classifications (ANZSRC)

ANZSRC code: 091403, Hydrometallurgy, 25%
ANZSRC code: 091404, Mineral Processing, 25%
ANZSRC code: 090499, Chemical Engineering not elsewhere classified, 50%

Fields of Research (FoR) Classification

ANZSRC code: 0904, Chemical Engineering, 50%
ANZSRC code: 0914, Resources Engineering and Extractive Metallurgy, 50%

Contribution to Research

- A novel method has been developed to demonstrate the variable rates of oxidation of the different types of pyrite.
- The application of MLA has been extended further by coupling with an etching process and image processing software to understand the effect of oxidation on pyrite.
- Establishing the effectiveness of a preparation step, with its origins from hydrometallurgical practice, to modify the flotation response of gold-rich pyrite and low gold pyrite so that the Au:S ratio of the final flotation concentrate can be upgraded.
- Demonstrating the effectiveness of regrinding conditions prior to oxidation and flotation separation to separate within a mineral family.

Table of Contents

List of Figures

List of Tables

List of Abbreviations

AA - Advanced Argillic

AMD - Acid Mine Drainage

As - Arsenic

Au:As - Gold to Arsenic Ratio

Au:S - Gold to Sulfur Ratio

Au - Gold

BET - Brunauer–Emmett–Teller

BSE - Back Scattered Electron

CAPEX - Capital Expenditure

Ca^{2+}- Calcium Ions

CaO - Calcium Oxide/Lime

CIP - Carbon-in-Pulp

Cum – Cumulative

E.M.U-Electric Multiple Unit

Fe_2O_3 - Hematite

Fe_3O_4 - Magnetite

FGO - Flotation Grade Ore

H_2SO_4 - Sulfuric Acid

HGO - High Grade Ore

HNO_3 - Nitric Acid

$KMNO_4$ - Potassium Permanganate

LA-ICPMS - Laser Ablation Inductively Coupled Plasma Mass Spectrometry

Min - Minutes

MLA - Mineral Liberation Analysis

MOPU - Million Ounce Plant Upgrade

MSDS - Material Safety Data Sheets

NaOH - Sodium Hydroxide

NTS - Newcrest Testing Site

OPEX – Operational Expenditure

PAX - Potassium Amyl Xanthate

QXRD - Quantitative X-ray Diffraction

$S0_3^{2-}$ - Sulfur Trioxide

SEM - Scanning Electron Microscopy

$S_20_3^{2-}$ -Thiosulfate

$S_40_6^{2-}$ −Tetrathionate

S^O - Elemental Sulfur

S^{2-}- Sulfide Sulfur

SO_2-Sulfur Dioxide

SO_4^2-Sulfate

SOx - Sulfide Sulfur Oxidation

SR - Synchrotron Radiation

S – Sulfur

T- Tesla

ToF-SIMS - Time of Flight Secondary Ion Mass Spectroscopy

UFM - Ultra-Fine Milling

XPS - X-Ray Photoelectron Spectroscopy

CHAPTER 1

INTRODUCTION

1. Overview

The past decade has witnessed a considerable deterioration in the availability of the high-grade gold ores. This is because the higher-grade ores are usually processed in the first ten to twenty years of active mining and the lower grade ores are stockpiled or left unmined for future processing. It is necessary and wise to stockpile the low-grade ores because, despite being “below the declining feed cut-off grade, they are still much above the break-even cut-off grade” (Torres et al., 1999, Prasad et al., 1991). Thus, processing them can be economically feasible provided optimum processing methods are adopted thereby sustaining the mining operations for another decade or two.

Hence, in recent years the interest for application of hydrometallurgical processing has increased as the availability of free-milling gold ore deposits has diminished (Sokić et al., 2009, Thomas, 1991). A number of hydrometallurgical developments have resulted in a "high tech gold processing chemical industry” to economically process refractory/double refractory ore types (Fleming, 1992). This is because, in refractory/double refractory ores, the recovery of gold by cyanide treatment is very low (Long and Dixon, 2004, Marsden and House, 2006, John et al., 2013). This necessitates pre-treatment processes for adequate liberation and a high proportion of gold to be recovered (Thomas, 1991). There are a variety of pre-treatment routes such as chlorination, autoclaving and roasting that can be utilised to release the gold from the sulfide mineralisation. Economic evaluations, technical risk factors, metallurgical testing and environmental aspects influence the selection procedure of a suitable process (Thomas, 1991).

A classic example is the Lihir gold mine which is highly refractory in nature yielding much less than 80% gold recovery by direct cyanide usage. The distribution of gold within the sulfides and reaction of the gangue matrix with the sulfide minerals can result in physical or chemical refractoriness of ore (Iglesias and Carranza, 1994, Chen et al., 2013, Marsden and House, 2006). At Lihir, gold is physically locked within pyrite (*physical refractoriness*) and therefore, the process of choice is acid pressure oxidation (*also known as pressure hydrometallurgy as shown in Figure 1.1*) to disintegrate the sulfide matrix. Pressure oxidation refers to the oxidation of sulfides at elevated

temperature and pressure to liberate the valuable mineral (Adams, 2005). This involves oxidising the ore and concentrate slurry in the autoclave using pure oxygen as the reactant at an elevated temperature and absolute pressure of 200^0C and 3100 kPa (Collins et al., 1993).

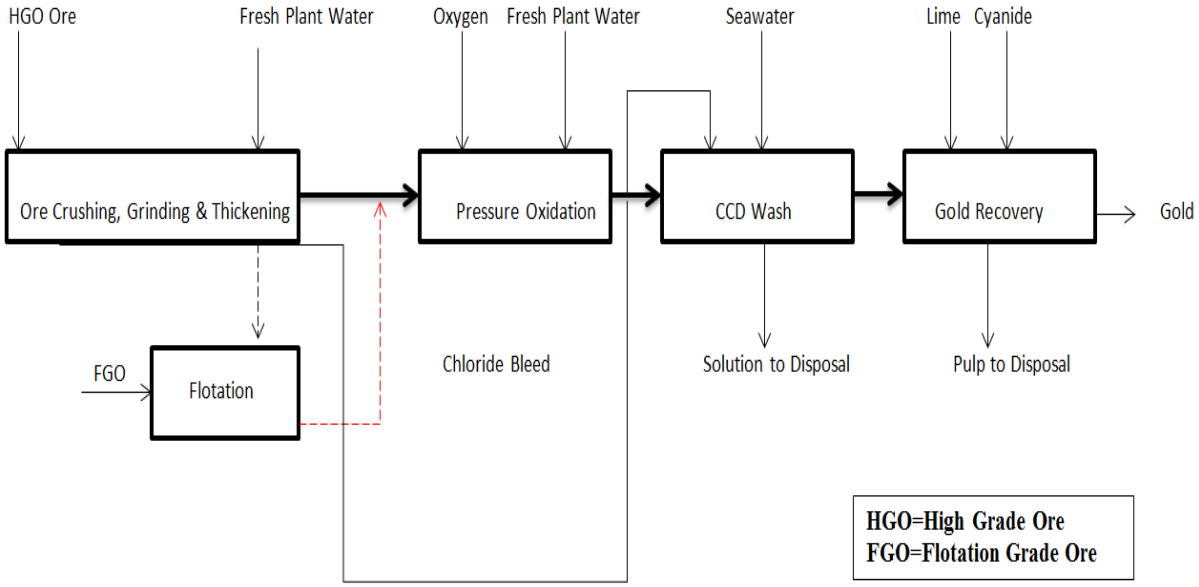

Figure 1.1: Generalised flowsheet for pressure oxidation of Lihir ore

As shown in Figure 1.1, the high-grade ore (*HGO*) is treated in a comminution circuit where the ground ore is ground and washed with fresh plant water to minimise chloride effects. The washed slurry is then fed directly to the oxidising autoclaves. Mitigating the effects of chloride minimises the elemental sulfur which otherwise could have detrimental implications for the sulfide oxidation rate and overall gold recovery (Collins et al., 1993). This is because high chloride levels can impede the oxidation kinetics of sulfides by forming elemental sulfur on the surfaces. In a study by Collins et al. (1993), It was found that increasing the chloride concentrations (*50 to 500 and 2000 g/t*) had an adverse effect on the overall sulfide sulfur oxidation as shown in Table 1.1.

Table 1. 1: Effect of chloride concentration on sulfide sulfur oxidation (Collins et al., 1993)

Test	Temp (^oC)	Pressure (kPa)	Chloride (g/t)	Sulfide sulfur oxidation (%)		
				20 mins	40 mins	60 mins
1	190	1700	50	53	81	96
2	190	1700	500	42	70	87
3	200	2100	50	76	96	98
4	200	2100	500	75	96	98
5	200	2100	2000	49	79	97
6	210	2400	50	86	98	99
7	210	2400	500	82	98	98
8	210	2400	2000	63	97	98

At a temperature of 190 ^{o}C and retention time of 60 minutes, 96% of the sulfide sulfur was oxidised (*Test 1*) compared to 87% oxidation (*Test 2)* when the chloride concentration was increased from 50 g/t to 500 g/t. Increasing the temperature to 200 ^{o}C (*Tests 3 and 4*), 50g/t and 500g/t of chloride concentration yielded the same sulfide sulfur oxidation suggesting that chloride effects could be mitigated with increasing temperature in the autoclave. A similar oxidation rate existed as also observed in the case of Test 5 with 2000g/t of chloride. A further increase in temperature to 210 ^{o}C in Tests 6 to 8 confirmed that sulfide oxidation was similar in all three cases (*50, 500 and 2000 g/t concentrations*) and independent of chloride ions.

The reduction in oxidation kinetics due to elemental sulfur passivation at high chloride levels was confirmed in another study by Ketcham et al. (1993) as shown in Figure 1.2. The deleterious effects of the high chloride concentrations can be counteracted by high temperature and pressure conditions in the autoclave (a*s illustrated in Figure 1.3)* to minimise the formation of elemental sulfur on pyrite. However, corrosion related issues of the non-titanium materials such as nickel alloys still pose a potential impediment. Another complication arising from high chloride concentration is gold chloride complexation resulting in the formation of gold choro complexes $Au(Cl)_4^-$. This involves the adsorption of gold from solution on to iron particles (*and gangue minerals*) via heterocoagulation and re-encapsulation resulting in gold losses as shown in equation 1 (Collins et al.,1993).

$$FeOH + AuCl_4^- \xrightarrow{\text{yields}} FeOHAuCl_3 + Cl^- \quad \ldots\ldots\ldots\

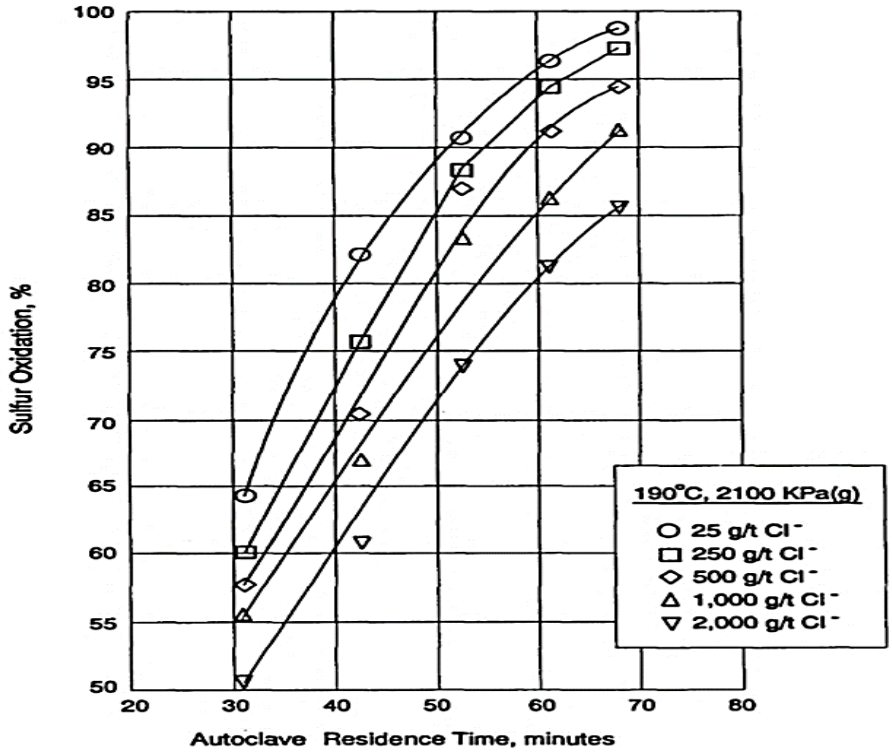

Figure 1.2: Sulfide sulfur oxidation kinetics with increasing chloride levels (Ketcham et al., 1993)

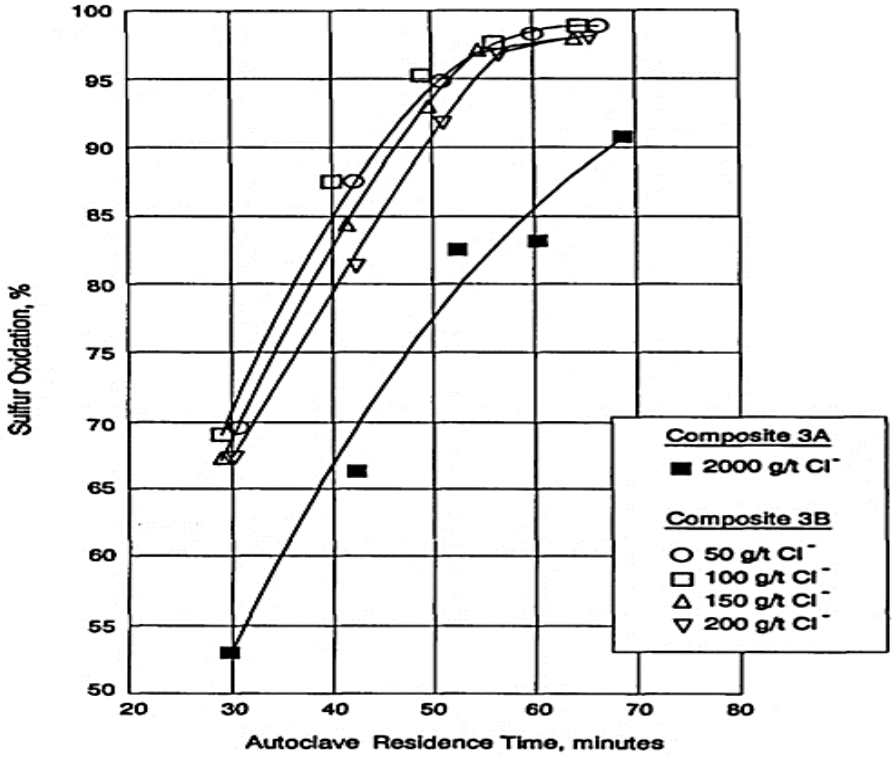

Figure 1.3: Counteracting the effect of chloride concentration on sulfide sulfur oxidation kinetics at a higher temperature of 210 °C (Ketcham et al., 1993).

The second circuit at Lihir processes the flotation-grade ore (*FGO*) with a single roughing stage to generate a sulfide-rich flotation concentrate. The resulting flotation concentrate (*after thickening*) is then blended with HGO stream to attain the required sulfide grade. Blending is done to ensure that autogenous heat is sufficient to achieve the desired reaction temperature and pressure in the autoclave (Rankin, 2013, Thomas et al., 1991). A current process flowsheet of Lihir after the Million Ounce Plant Upgrade (*MOPU*) and design criteria of unit operations is shown in Figure 1.4 and Table 1.2 respectively.

Pyrite oxidation is carried out in an autoclave to destroy the sulfides by severe chemical reactions to render the encapsulated gold amenable to subsequent extraction (Long and Dixon, 2004, Marsden and House, 2006, Rankin, 2013, Ketcham et al., 1993, Collins et al., 1993). This involves oxidising the feed slurry (*HGO and FGO blend*) using pure oxygen as the reactant at an elevated temperature of 200 ^{0}C to totally oxidise the sulfide sulfur to sulfate as shown in equation 2 (Collins et al., 1993). This is followed by leaching gold with sodium cyanide as shown in equation 3 and the gold in the leached solution is adsorbed on to activated carbon in a carbon-in-leach (*CIL*) circuit (Marchbank et al., 1996). Gold is then recovered as bullion by standard metallurgical techniques.

$$2FeS_2 + 7O_2 + 2H_2O \xrightarrow{\text{yields}} 2FeSO_4 + 2H_2SO_4 \quad \ldots\ldots\ldots\

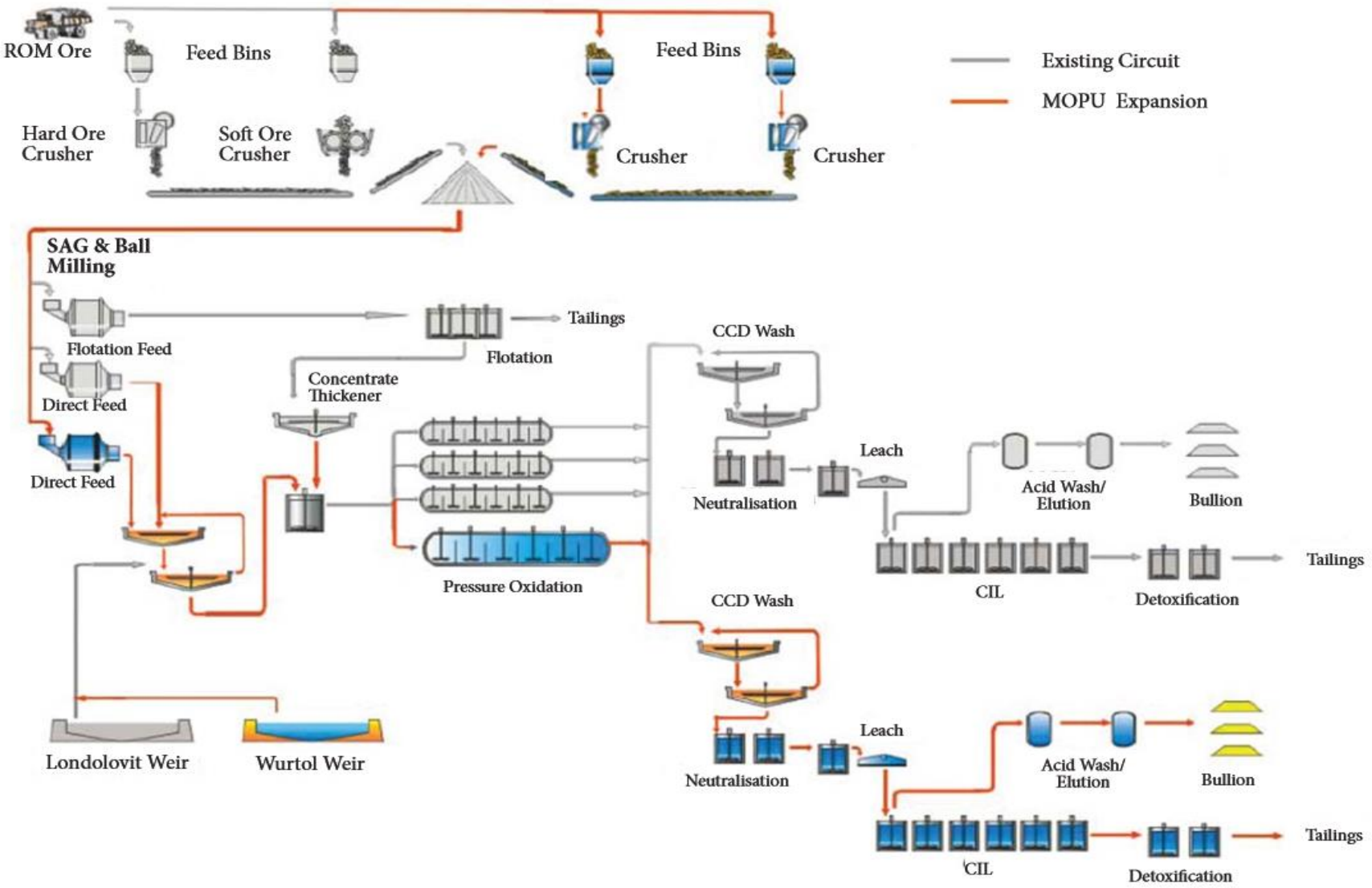

Figure 1.4: Lihir process flowsheet after MOPU Expansion (Rankin, 2013)

Table 1. 2: Design Requirements for the current Lihir process plant

(Ketcham et al., 1993, Rankin, 2013)

Design Criteria		
Annual Throughput	-	9-12 Mt/a
Operation	-	365 days/year
Current Mining	Minifie and Leinetz Ore	
Future Mining	Kapit Ore	
Refractory Ore Grades	Low Medium High	0.95 to 3.5 g/t Au 3.0 to 4.0 g/t Au Above 4.0 g/t Au
Grind	-	80% passing 106 µm
Bond Work Index	-	18.7 kWh/t
Sulfide Sulfur Grade	-	7.2% S^{2-}
Chloride Content	-	50g/t Cl^-
4 parallel pressure Titanium Autoclaves (*exothermic*)	Operating Temperature Operating Pressure Oxygen utilisation Sulfide sulfur oxidation Oxygen Requirement Oxygen to sulfur ratio Residence Time	205-210^oC 2400-2700 kPa 85% 98% 1.90 t per tonne of S 2.0:1.0 65 minutes
Thickeners ***Grinding*** ***CCD and Tailing***	-	 0.11 m^2/tpd 0.08 m^2/tpd
Washed Residue Acid content	-	<0.5 g/L sulfuric acid
Neutralisation, leach and CIL circuit	Residence time Stages for carbon adsorption	14 hours 6
Slurry densities	Grinding and thickening underflow CCD thickener underflow CIL feed Tailings Thickener underflow	55% solids 50% solids 30% solids 45% solids
Gold Circuit	Gold Grade Gold Recovery Carbon Loading Carbon Advance Rate Carbon Regeneration	13 g/t Au 95% 5500g/t Au 20 tpd 15 tpd

1.2 Upgrading the Au:S Ratio

Sulfide oxidation in the Lihir autoclave is in the range of 60 to 70% (*at 55% solids*). Investigations by Rio Tinto in 2004 and 2005 have shown that the limitation in the sulfide oxidation potential (*throughput of sulfides*) in the autoclave at Lihir was due to the fixed Au:S value of the feed. This is because the Lihir ore deposit is a sulfide associated refractory gold ore of epithermal origin containing different types of pyrite with various levels of gold content. It is the presence of porphyroblastic pyrite (*barren in nature or having very low gold assays*) that results in higher consumption of oxygen in the autoclave. This upsets the throughput efficiency and confines the treatment to only the high gold-bearing pyrite types thereby affecting the overall gold production at Lihir (John et al., 2013). The presence of the low gold pyrite types (*of low economic value*) decreases the Au:S value of the Lihir ores as shown in Figure 1.5 clearly specifying that not all pyrite types are contributing equally to the economic performance of the Lihir mine.

Hence, the main driving factor behind this research is to selectively separate (*through hydrometallurgical oxidation and subsequent flotation*) one type of pyrite over the other. Studies by Rio Tinto have suggested that there might be differences in the chemical properties (*i.e. oxidation rates*) of the various pyrite types. The key to a successful separation of the different pyrite types would be the exploitation of the differences in properties (*if any*) that exist between the various types of pyrite thus allowing only the high gold pyrite to be directed to the autoclave at Lihir. However, despite wide speculation regarding the differences in oxidation rates of the various liberated pyrite types, relatively little work has been published which focuses on the effect of oxidation on the different types of pyrite.

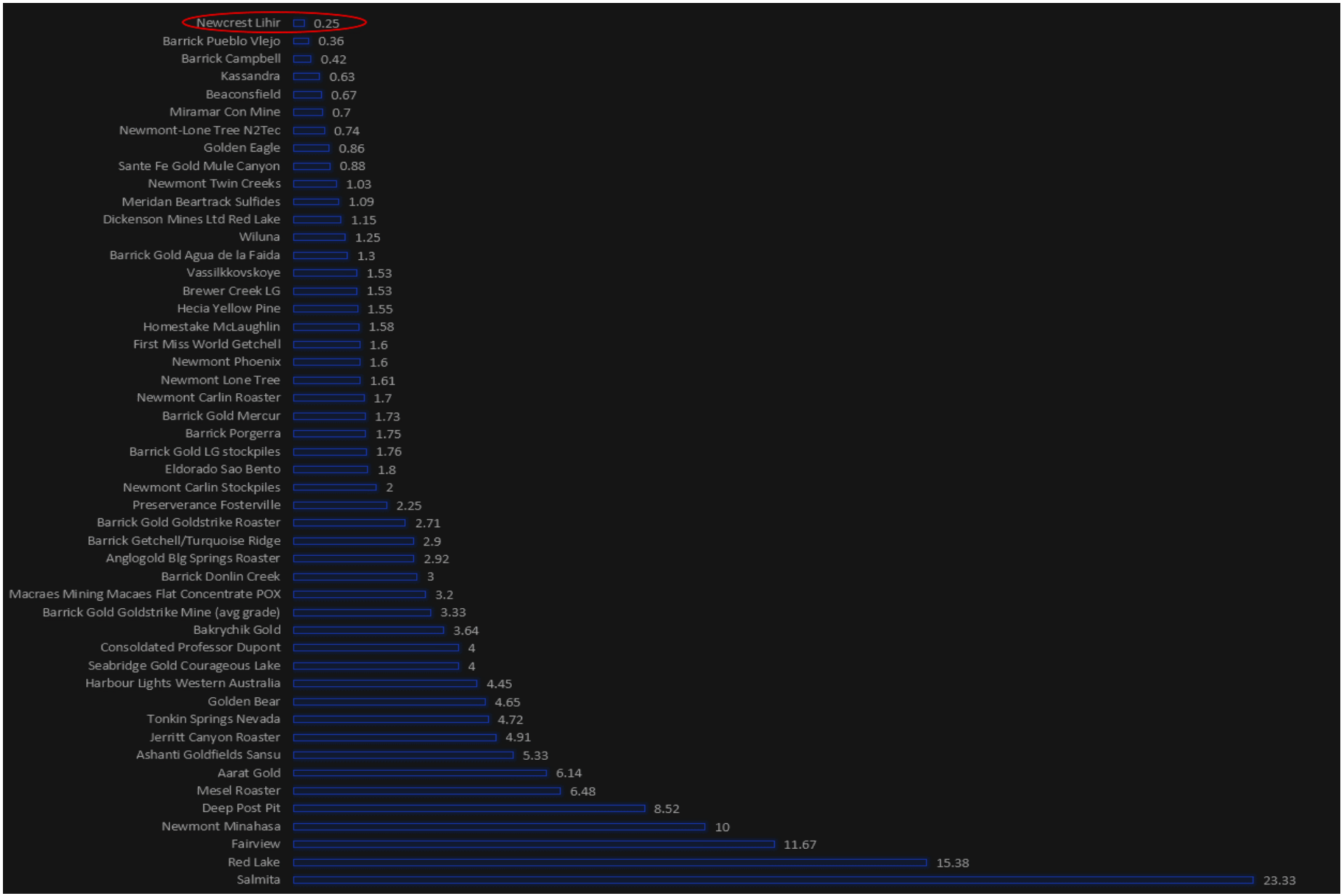

Figure 1.5: Au:S ratio of various ores around the world (Aylmore and Jaffer, 2012, Rankin, 2013)

1.3 Research Questions

A comprehensive review of the published literature (*discussed in Chapter 2*) shows no information that unveils methods to separate within the same mineral family i.e. one type of pyrite from another kind. Therefore, the main questions focussed in this thesis are as follows:

1. Are there differences in the chemical characteristics of the various pyrite types i.e. does each type of pyrite have different oxidation rate?

2. If the oxidation rates are different, can hydrometallurgical oxidation conditions be utilised to oxidise one type of pyrite relative to the other kind and thereby separate them in a subsequent cleaner flotation process?

1.4 Hypothesis:

"Differences exist in the chemical properties of the low gold pyrite relative to the gold-rich pyrite and exploitation of these differences will allow separation of the various types of pyrite in the following separation process".

1.4a Chemical

The differences in the oxidation rates of the various liberated pyrite types in a hydrometallurgical step will be the basis for their separation in a subsequent cleaner flotation process.

1.4b Mechanical and Chemical

The enhanced oxidation rates and other effects from regrinding will cause an improved separation of the various pyrite types resulting in a higher Au:S ratio.

1.5 Aims and Objectives

Oxidation methods as a part of a flotation process have not been reported yet to be successful to show an upgrade of the Au:S ratio of a flotation concentrate. Therefore, this research is an attempt to establish the effectiveness of a preparation step, with its origins from hydrometallurgical practice, to modify the flotation response of gold-rich pyrite versus low gold pyrite so that the Au:S ratio of the final flotation concentrate can be upgraded as shown in Figure 1.6.

As a result, the main objectives (*shown in Figure 1.7*) of this thesis are:

- Measuring and understanding the oxidation rates of the different types of pyrite
- Developing a hydrometallurgical framework to differentially oxidise the various types of pyrite to upgrade the Au:S ratio of a sulfide concentrate (*autoclave feed*) by separating the low gold pyrite from the gold-rich types of pyrite.
- Developing a single step cleaner flotation scheme to minimise the recovery of sulfide sulfur and maximise gold recovery from an oxidised flotation concentrate.

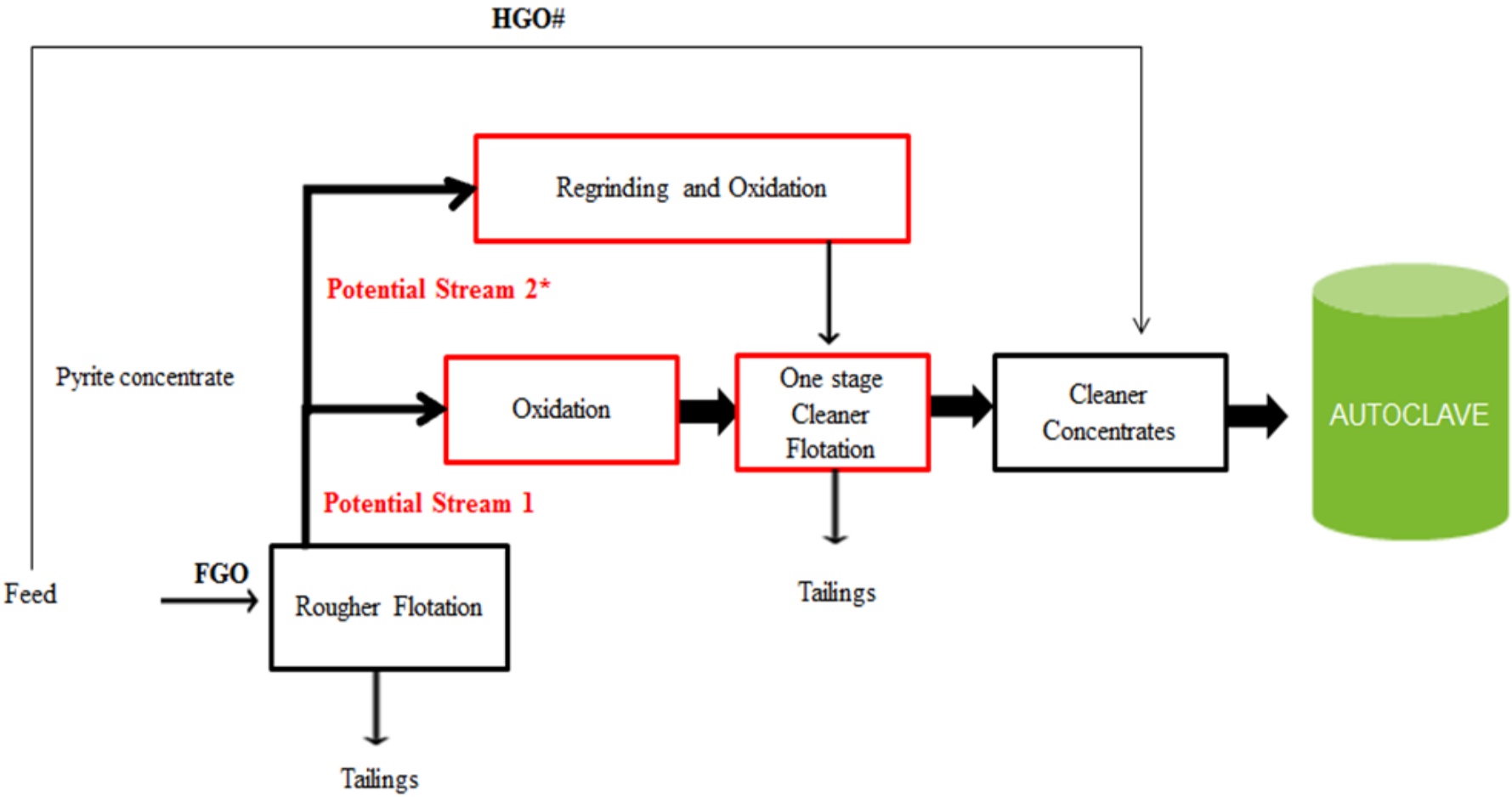

Figure 1.6: Process flowsheet depicting the potential process

1.6 Research Plan

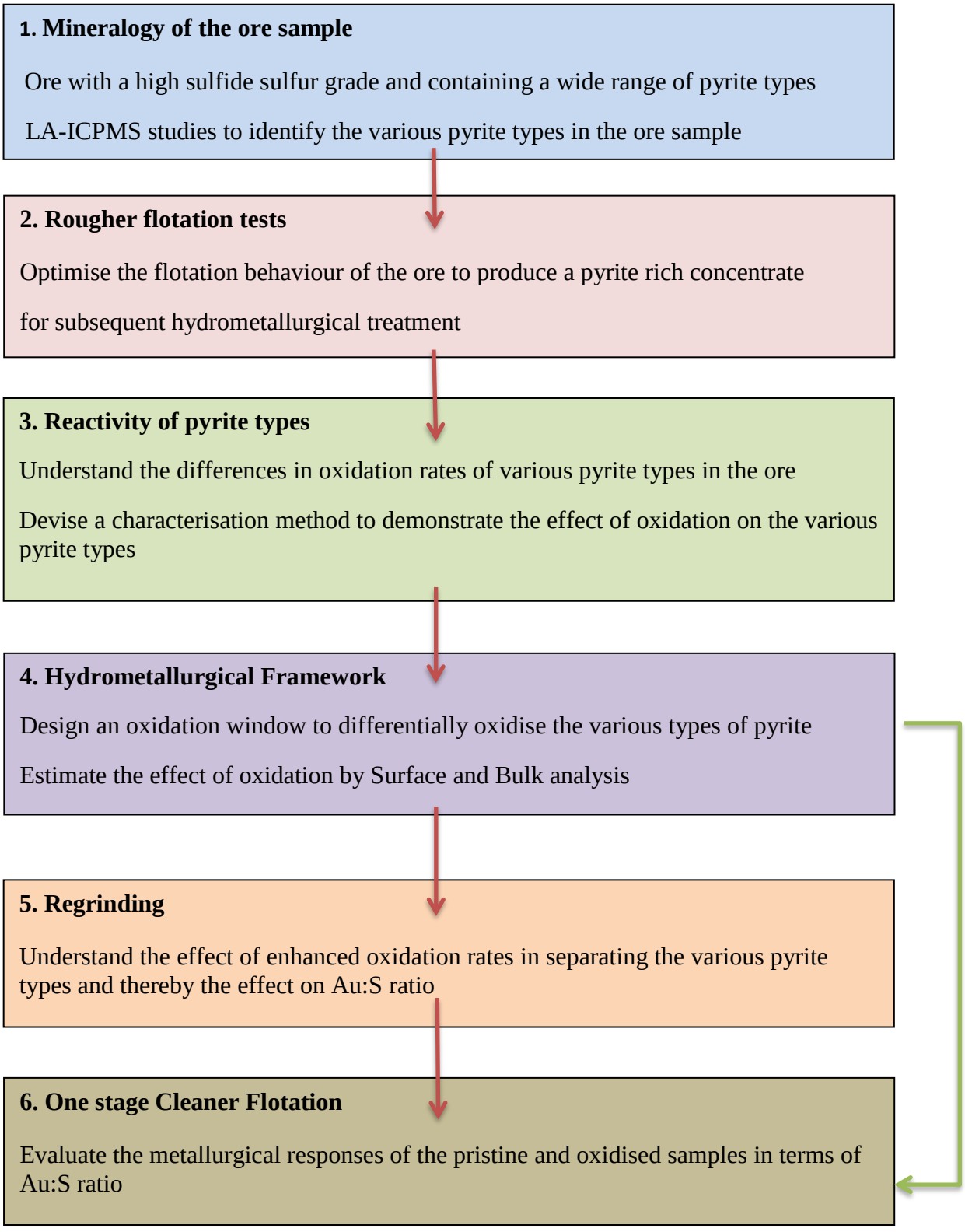

Figure 1.7: Schematic flow diagram of thesis research path

1.7 Thesis Outline

Chapter 2: Literature Review

This review is an evaluation of the separation processes in the industry to separate the various types of pyrite.

Chapter 3: Materials and Methods

This chapter sets out the procedure for sample characterisation, sample preparation, flotation test work and oxidation experiments carried out on the sample of interest.

Chapter 4: Mineralogy and flotation of Advanced Argillic Ores

This chapter discusses the mineralogical and chemical characterisation of the advanced argillic gold ore. This also includes batch scale flotation tests at different pH conditions to understand the gold recovery and grade.

Chapter 5: The Effect of Acid Media on High Arsenic and Low Arsenic Pyrite

This study describes the development of a novel mineral characterisation technique for distinguishing between low arsenic pyrite and high arsenic pyrite species in a refractory gold ore using BSE images from an SEM-based automated mineralogy system, in this case, an MLA system. The technique is based on a chemical etching process which was used to oxidise the surface of the polished blocks of sulfide ore prior to measurement in the MLA system.

Chapter 6: The Influence of Lime and NaOH Conditioning on Sulfide Sulfur in Pyrite Flotation

The focussing question for this study was to determine if there is a promising premise for substituting lime with NaOH as a pH regulator in the flotation of refractory/double refractory ores where there is significant sulfur to be treated for the amount of gold present.

Chapter 7: Nitric Acid Oxidation of Iron Sulfides to Upgrade the Au:S Ratio of a Flotation Concentrate

This chapter is an attempt to establish the effectiveness of a preparation step, with its origins from hydrometallurgical practice, to modify the flotation response of gold-rich pyrite and low gold pyrite so that the Au:S ratio of the final flotation concentrate can be upgraded.

Chapter 8: Sulfuric Acid Treatment of Iron Sulfides to increase the Au:S Ratio of a Flotation Concentrate

Considering that the Lihir mineral deposit is rich in sulfur containing a wide range of pyrite types, it is better from a trade and industry point of view to select an acid that can be generated onsite. In this thesis investigation, sulfuric acid media was used to increase the Au:S ratio of a flotation concentrate.

Chapter 9: Process Implications

Separating one type of pyrite from another is a sensitive process. Unlike most of the hydrometallurgical practices, where aggressive oxidation methods are adopted, separation within a mineral family is driven by a narrow oxidation regime. This chapter discusses the process implications associated with the developed method and its applications in real world practice.

Chapter 10: Conclusions and Recommendations

This chapter summarises the main findings in this thesis and makes corresponding recommendations for future work.

CHAPTER 2

LITERATURE REVIEW

2.1 Overview

The intent of this literature review is to understand and appreciate:

a) Current practices for sulfide (*pyrite*) separation from non-sulfide gangue
b) Flotation separation of minerals
c) Flotation separation within the same mineral family
d) Sulfur Oxidation
e) Pre-treatment methods:
    - Pyrometallurgy
    - Hydrometallurgy
    - Biometallurgy
    - Other emerging pre-treatments
f) Characterization methods for different types of pyrite

Critical analysis in the literature review is crucial to identify and highlight the gaps in the current knowledge regarding the processing of the various pyrite types. This knowledge of relevance can be treatment methods to separate the low gold bearing pyrite from gold-rich pyrite, recorded information on the separation of minerals within the same family and use of surface/bulk analysis techniques to distinguish minerals of the same family.

2.2 Current practices for sulfide separation from non-sulfide gangue

2.2.1 Grinding

Grinding of refractory ores causes distortion and structural fragmentation (*via compression, chipping and abrasion as shown in Figure 2.1*) of the sulfide matrix (Warris and McCormick1997, Wills and Napier-Munn. 2015, Marsden and House, 2006, Corrans and

Angove, 1991). Therefore, it has a significant influence on the subsequent flotation and extraction processes (*oxidative methods of treatments such as hydrometallurgy and biometallurgy*). Gold ore grinding can be divided into wet grinding and dry grinding.

Figure 2.1: Breakage mechanism involved in the grinding process (Wills and Napier-Munn, 2015)

2.2.1.1 Wet Grinding

The application of mechanical forces enhances the reactivity of minerals and this occurs mainly in wet grinding (*the common type of grinding*). Such processes are accompanied by oxidation/reduction reactions resulting in chemical alterations of the reactants. It was shown by Warris and McCormick (1997) that pyrite could be mechano-chemically activated to release the gold encapsulated in the sulfide matrix. To demonstrate this, pyrite samples were mechano-chemically activated with calcium oxide (*CaO*) according to the possible reaction:

$$8FeS_2 + 24CaO \xrightarrow{\text{yields}} 4Ca_2Fe_2O_3 + 13CaS + 3CaSO_4 \ldots\ldots\ldots\ldots\ldots\ldots\ldots\ldots\ldots\ldots\ldots\ldots\ldots\ldots\ldots\ldots 4$$

Sulfur was completely converted to sulfate through the effect of mechano-chemical oxidation and this was confirmed by X-ray diffraction, Mossbauer spectroscopy and thermal analysis techniques (Warris & McCormick, 1997). Though potential might exist for such oxidation processes from an economical and environmental point of view, this is of limited applicability to the present work. This is mainly because the approach in this work is not complete oxidation of sulfur to sulfate but rather the differential oxidation of the different types of pyrite. And for this, it is necessary to adopt a narrow pre-treatment range for preferential oxidation technique(s). Since the work of Warris and McCormick (1997)

provides no indication of the level of oxidation (*or its control*) during the mechano-chemical process, the application of this work may not be the most practical route.

In an another study by Zheng et al. (2010), it was shown that the gold recovery could be improved further with just mechanical activation (Zheng et al., 2010). This is because gold particles occur as inclusions or grains sealed in a sulfide matrix (O'Connor and Dunne, 1994) and therefore further size reduction could liberate such sulfide encapsulated gold. In such circumstances, the application of ultra-fine milling (*UFM*) seems significant (Corrans and Angove, 1991). The sulfide slurries that have undergone UFM treatment have been shown to have better reactivity and this could be a potential alternative to mechano-chemical oxidation, pressure oxidation or bacterial oxidation (Corrans and Angove, 1991).

However, plant economics are hugely dependent on gold grades, energy and media consumption. A major drawback of the UFM process is its energy-intensive nature limiting its application to relatively low tonnages of higher grade concentrates rather than low-grade ores. A concentration method (*preferably flotation*) is usually required for treatment by UFM. Since the approach in this work is the further treatment of a pyrite-rich flotation concentrate (*discussed in Chapter 1*), the effects from regrinding in separating the various pyrite types and Au:S values is a topic of interest and will be discussed further in Chapter 7.

2.2.1.2 Dry Grinding

Dry grinding is an alternative to wet grinding especially considering the savings in energy costs and media wear (Bruckard et al., 2011, Hoberg et al., 1985). Dry grinding technology has been successfully operated at the Barrick Goldstrike operation since August 2000 (Bruckard et al., 2011). The various dry grinding processes involve tertiary grinding and ball milling, semi-autogenous milling, secondary crushing followed by double rotator milling and vertical roller milling followed by ball milling (Bruckard et al., 2011). However, as mentioned, since the focus of this work is based on improving the Au:S value of a pulp containing a pyrite flotation concentrate and not just particle size reduction, the application of dry grinding cannot be considered.

2.2.2 Flotation

Ores consist of mixtures of valuable minerals and it is, therefore, necessary to selectively depress one or more minerals from an economic point of view (O'Connor and Dunne, 1994). This is where flotation plays an important role.

The basis for flotation separation is the difference in hydrophobicities of different minerals (Marsden and House, 2006, Adams, 2005). Though there are chemical treatments to render a mineral's surface hydrophobic or hydrophilic, in-depth investigations to produce flotation concentrates of certain types of pyrite have not been an active topic of research. Different authors have suggested that it would be economical to have a concentration step (*flotation*) to separate one particular type of pyrite from other pyrite types in a concentrate prior to the autoclave process to liberate the gold in the pyrite. Nevertheless, little information exists on its practical application (Zhang et al., 2010, Marsden and House, 2006, Mason, 1992). There is current literature on producing a pyrite concentrate containing all types of pyrite; however, producing a gold-rich pyrite concentrate with an optimised Au:S ratio to be processed in the autoclave is still in its conceptual stage.

Flotation has been, economically and environmentally, successful in separating minerals of different families (*pyrite and arsenopyrite; depression of pyrite by peroxide treatment as shown in Figure 2.2*). Another successful approach is the pre-aeration of the pulp prior to flotation to separate pyrite and arsenopyrite from pyrrhotite (Dunne, 1991). Pre-aeration oxidises pyrrhotite and pyrite differentially and when a collector such as dithiophosphate is used, selective separation of pyrite takes place (O'Connor and Dunne, 1994). Although the probabilities of separating different pyrite types using a secondary collector are low, pre-aeration could be a potential application to vary the oxidation states of different pyrite types and separate them in a subsequent separation process.

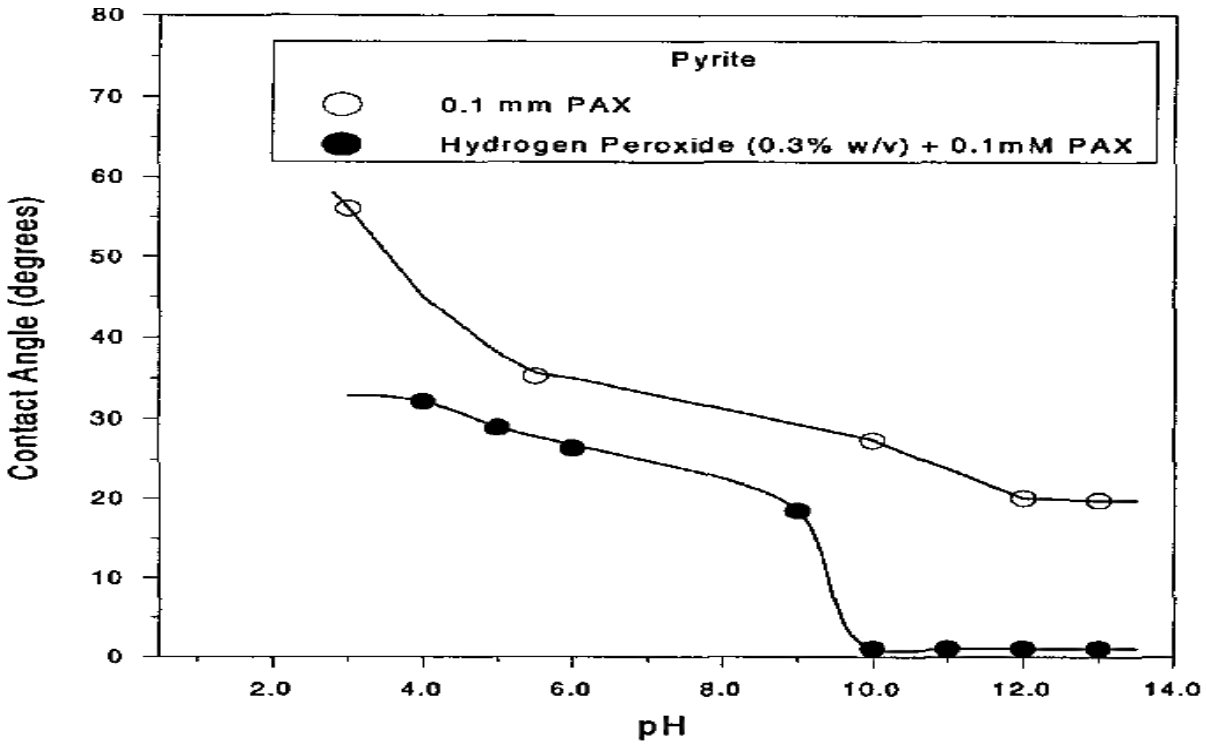

Figure 2.2: Differential flotation of pyrite and free gold by the effect of hydrogen peroxide solution (Monte et al., 1997)

Flotation of free gold from pyrite was possible in this system due to the hydrophilic nature of the gold surface and hydrophobic character of the sulfides (Monte et al., 1997). However, this method is not applicable to refractory/double refractory ores where the submicroscopic gold is locked in sulfide matrices and there is no free gold. Similarly, there has been considerable interest in selectively separating pyrite from arsenopyrite (O'Connor and Dunne, 1994). Arsenopyrite can undergo selective flotation from pyrite by the use of oxidants or reductants to regulate the oxidation state of the pyrite and arsenopyrite as shown in Figures 2.3 and 2.4. Potassium permanganate is a well-known oxidising agent and at a redox potential between 400 and 500mV, it is used as an arsenopyrite depressant (O'Connor and Dunne, 1994). Potassium per-oxo disulfate has also been successfully used to depress the arsenopyrite and activate the pyrite. Recoveries of 60% arsenopyrite and 20% pyrite have also been reported using mixtures of dithiophosphates and dithiocarbamates (O'Connor and Dunne, 1994).

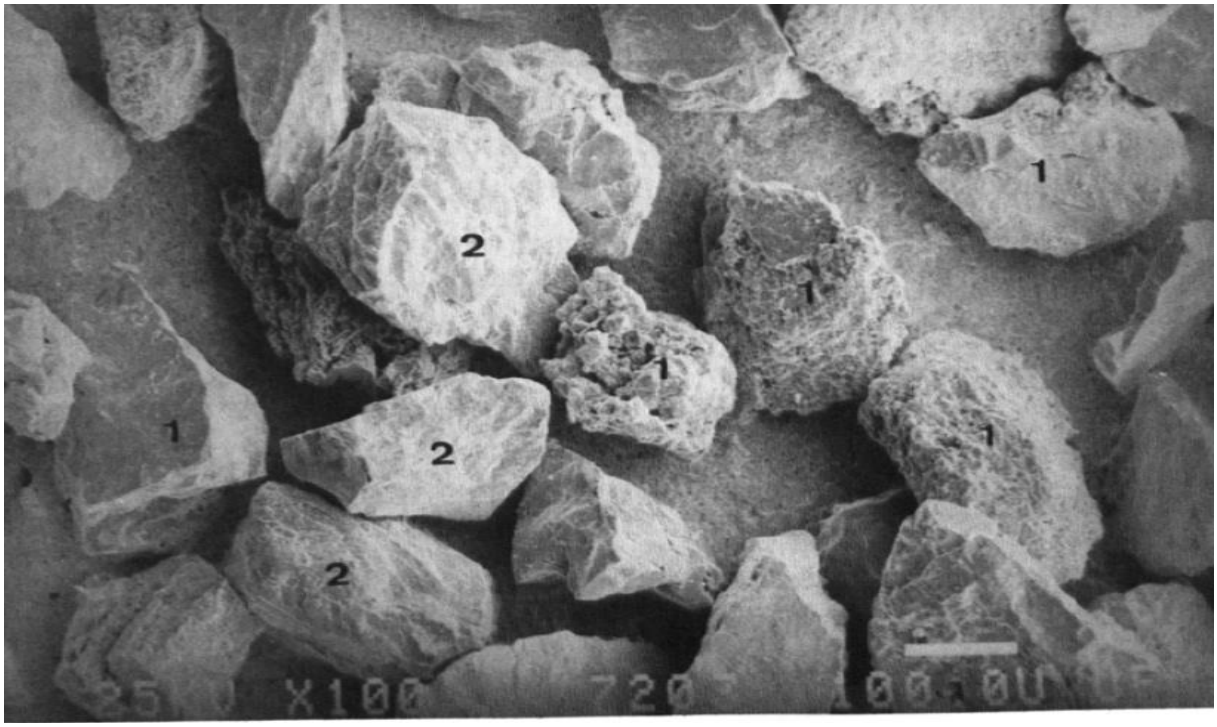

Figure 2.3: SEM micrograph. 1 = unreacted pyrite; 2 = arsenopyrite particles (Koslides and Ciminelli, 1992).

Figure 2.4: SEM micrograph of reacted arsenopyrite and pyrite particles (Koslides and Ciminelli, 1992)

If this property of differential oxidation can be applied to separate different pyrite types by controlling the redox potential of the system, then the chances of separating the minerals of the same family based on their oxidative differences may be increased. Processes, based on such principles, would not only enable separation of the low gold pyrite from gold-rich pyrite based on their chemical reactivity but also provide options to process sulfide refractory/double refractory ores effectively. Sequential flotation (*as shown in Figure 2.5*) is not an effective option and will not be discussed in detail. This is because sequential flotation produces separate concentrates of valuable minerals (*copper and pyrite*) and therefore is not applicable to some mineral systems (*i.e. high gold pyrite from low gold pyrite*).

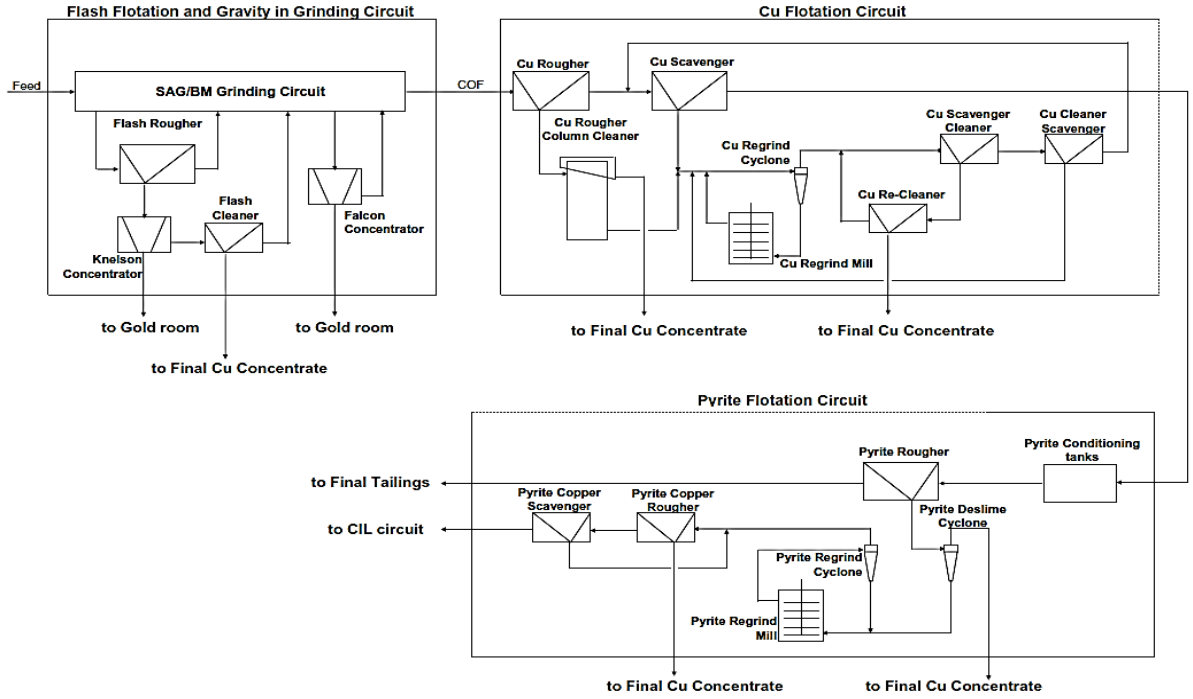

Figure 2.5: Sequential flotation configuration (Zheng et al., 2010)

2.2.2.1 Electrochemical Aspects

Electrochemical aspects have been taken advantage of in differential flotation to separate stibnite from arsenopyrite and pyrite (*also copper-gold bearing minerals from other sulfides*). The presence of antimony complicates the cyanide leaching process and hence it is desirable to separate stibnite from the other sulfide minerals selectively. Flotation usually achieves this at a higher pH (Zhang et al., 2009), use of an activator such as copper sulfate to activate the

arsenopyrite/pyrite and depressing the stibnite (Oberbillig, 1964). Also, bulk flotation of sulfides at neutral pH would activate the stibnite and aid in its removal. Lead nitrate activates the stibnite and the presence of sodium hydroxide facilitates the separation of stibnite from other sulfide minerals (O'Connor and Dunne, 1994). Similarly, separation of copper-gold bearing minerals from other sulfides is achieved by the addition of cyanide and operating at high pH conditions as alkaline pH values depress pyrite.

2.2.2.2 N2TEC Flotation

The N2TEC flotation process has been used to recover the gold-bearing pyrite at Newmont Lone Tree Plant in Nevada (Miller et al., 2006). The processing of a substantial portion of the low-grade sulfide resource at the Newmont Lone Tree Plant was not economically feasible and this problem necessitated the N2TEC flotation process to treat the low sulfur grade ores (Simmons, 1997).

The N2TEC flotation process uses nitrogen as the flotation gas (*as well as the atmosphere*) in grinding and PAX as a collector to create the optimum flotation conditions (Dunne, 2009). Such conditions prevent further oxidation of the mineral surface and minimise the adverse effects of oxidation products such as the inability of the collector to interact with the surface. Nitrogen eliminates oxygen to block the galvanic interaction responsible for forming hydrophilic oxidised pyrites. It was reported that an inert atmosphere (*nitrogen/argon*) not only improves gold recovery for an auriferous sulfide ore but can also enhance selectivity (Dunne et al., 2009). However, the effect of nitrogen to improve the gold recoveries also depends upon the oxidation state of the pyrites. For example, if the microcrystalline pyrite types are not oxidised enough compared to the blocky pyrite, the use of nitrogen may have an adverse effect thereby decreasing gold recoveries. A similar inference was also formulated by Martin et al. (1989) who reported that better recoveries were obtained with nitrogen with PAX.

The effect of the inert gases in the N2TEC process demonstrates that the oxidation rates of some types of pyrites can be quite rapid. This property is a candidate to be considered as a potential basis for separation of types of pyrite. This approach may be utilised to encourage the oxidation of some pyrite types relative to other pyrite types to allow their separation in later stages of processing.

2.3 Pre-Treatment Methods

The refractoriness of gold depends on the ore mineralogy. In general, refractory gold ores are associated with the following physiognomies:

1. Gold encapsulation within the sulfide matrix especially within pyrite and arsenopyrite
2. Gold occurring in solid-solution with other minerals
3. Gold coated with carbonaceous matter

The first two are the most common occurrences found in refractory ores (Afenya, 1991). The current discussion focuses on different processes (*as shown in Figure 2.6*) that break the sulfide framework to liberate the interlocked gold.

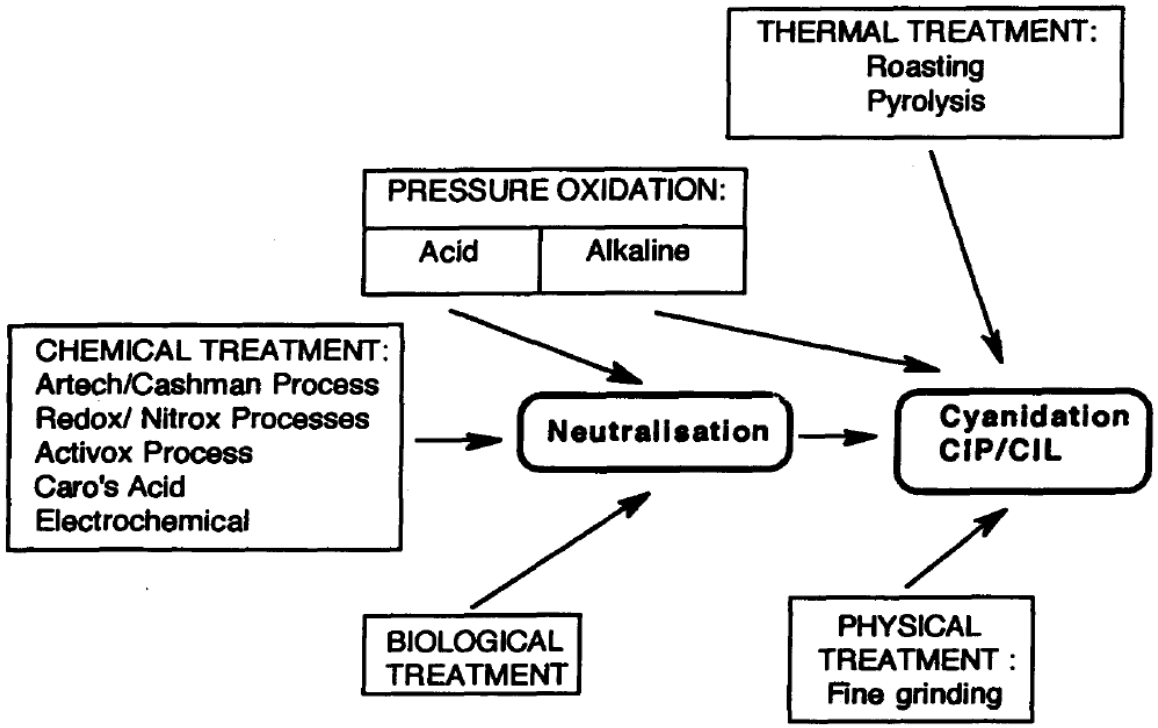

Figure 2.6: Pre-treatment possibilities for refractory ores (La Brooy et al., 1994)

Conventional grinding and cyanidation alone fail to be a feasible treatment for refractory gold ores because they result in low recoveries of gold from 85% down to less than 30% (Corrans and Angove, 1991). Therefore, it is vital to adopt destructive techniques such as thermal (*pyrometallurgy*), chemical (*hydrometallurgy*) or biological oxidation (*biometallurgy*) to liberate the encapsulated gold and thereby increase the gold recoveries (Corrans and Angove, 1991).

A portion of the locked gold can then be recovered from concentrates by cyanide leaching. The low gold recoveries and high cyanide consumptions necessitate the adoption of an efficient and economic pre-treatment strategy prior to cyanide leaching for improving gold extraction by cyanidation such as the following:

a) Pyrometallurgy e.g. roasting

b) Hydrometallurgy e.g. pressure oxidation

c) Biometallurgy e.g. bio-oxidation

d) Other emerging pre-treatments e.g. microwave and magnetic pulses

2.3.1 Pyrometallurgy

The gold-bearing sulfide lattice can be thermally treated to make the gold accessible. The various process options are shown in Figure 2.7.

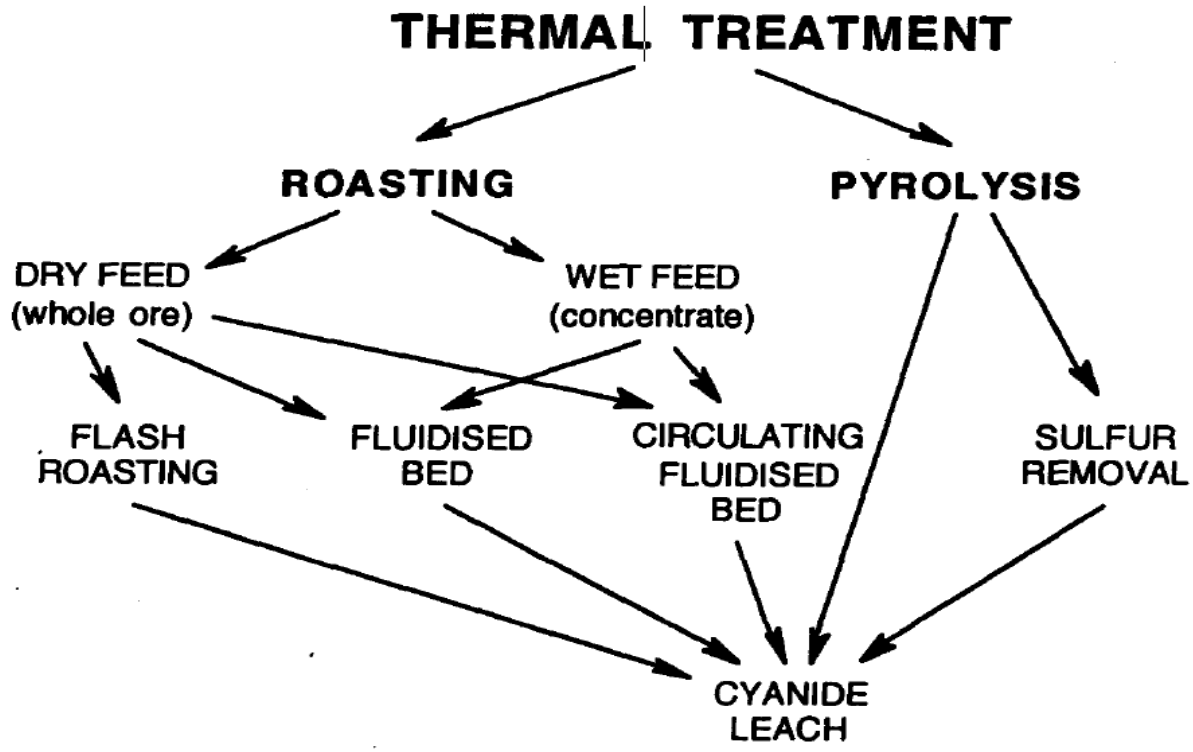

Figure 2.7: Thermal treatment of ores (La Brooy et al., 1994)

Among the various techniques, roasting is commonly utilised to enhance structural destruction of the sulfide phase (*by converting sulfides to oxides as shown in Figure 2.8*) for the subsequent liberation of gold and yield recoveries between 80% and 100%. (Ketcham et al., 1993 Fleming, 1992; Marsden and House, 2006; Ketcham, O'Reilly and Vardill, 1993).

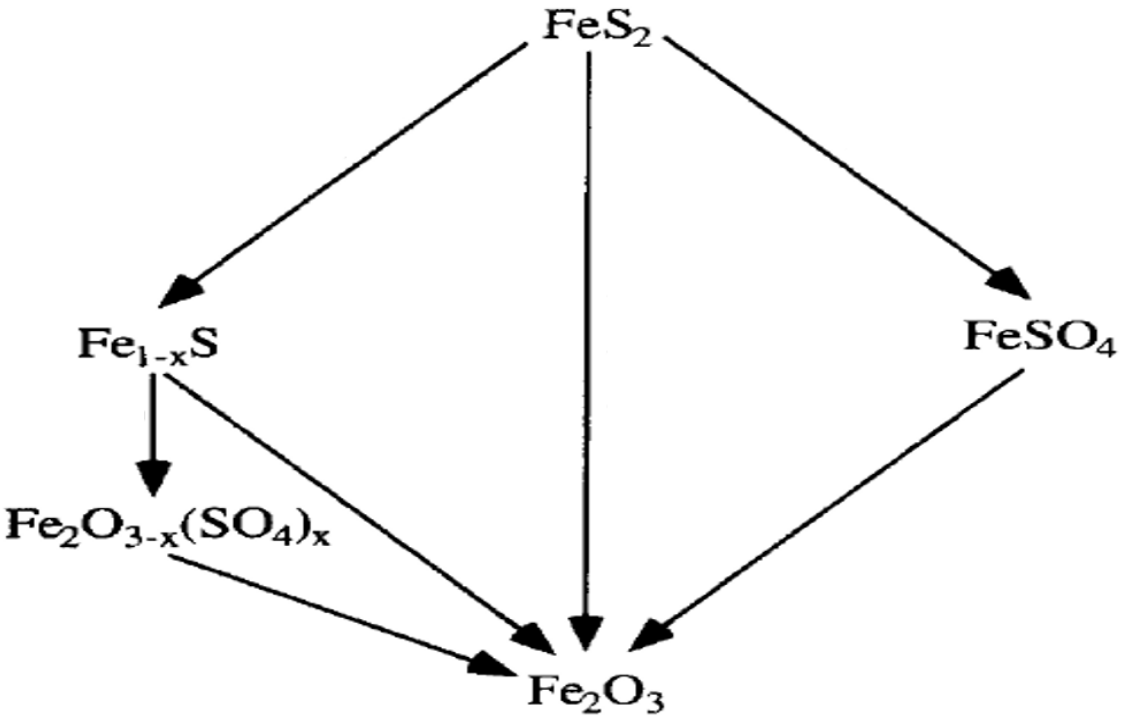

Figure 2.8: Reaction schemes involved in the oxidation of pyrite (Dunn, 1997)

The mechanism and kinetics of pyrite transformations at elevated temperatures have been reported by Hu et al. (2006). It was found that at temperatures below 800^{o}K and high oxygen concentrations, pyrite undergoes direct oxidation. At higher temperatures, it was found that pyrite undergoes a two-step transformation. Firstly, it undergoes thermal decomposition to form porous pyrrhotite and this pyrrhotite is further oxidised in the second step. Hematite (Fe_2O_3) and magnetite (Fe_3O_4) are the main products of pyrite oxidation (*Figure 2.8*) at low and high temperatures respectively (Hu et al., 2006). It was observed that pyrite transformation was controlled by parameters such as temperature, particle size, oxygen concentration and flow and heating conditions. However, differential oxidations of pyrite types were not investigated and the influence of the variables mentioned above on different types of pyrite is not well understood.

Environmental controls requiring reduction of sulfur dioxide (SO_2), mercury and arsenic emissions have necessitated the development of new improvements to roasting or the use of competing technologies (Prasad et al., 1991). The fluid bed roaster has capabilities to treat

both dry ore and flotation concentrates containing moisture. It has been reported that concentrate roasting yields gold recoveries ranging from 85 to 95% compared to dry processing (*75 to 90%*) (Prasad et al., 1991). However, roasting appears to be inefficient in treating ores containing low amounts of arsenic (*0.2% As*). This is mainly due to the concentration of both arsenic and gold in the same impurity-rich regions, thereby limiting the recovery of gold that can be achieved through roasting processes (Ketcham et al., 1993).

2.3.2 Hydrometallurgy

Hydrometallurgical treatment of ores is an economical and technically feasible method for controlled and extensive oxidation of ores (Al-Harahsheh and Kingman, 2004). Pyrite oxidation is a complex process with a variety of oxidation products. Nevertheless, flotation coupled with oxidation may be used to separate valuable minerals. Oxidation can induce hydrophobic or hydrophilic character to a particular mineral surface thereby influencing its interactions with collectors in flotation (Chandra and Gerson, 2010). Since standard Lihir reagents (*PAX as the collector*) will be utilised for the flotation work in this thesis, further discussion regarding reagents will not be undertaken.

2.3.3 Acid oxidation

As mentioned, oxidation can alter the surface properties of sulfide minerals thereby influencing the flotation response. Pyrite oxidation in acidic systems by oxidants like HNO_3, $HClO_4$, and $KMnO_4$ modifies the pyrite surface (*Figures 2.9 and 2.10*) and dictates the species adsorption capacities of flotation collectors (Chirita, 2003). The bulk pyrite concentrates are then selectively floated after using oxidising agents such as permanganate and dichromate. This concept has already been demonstrated by several workers (Glembotskii et al., 1972, Draskic et al., 1982, Antonijević et al., 1993, Beattie and Poling, 1988).

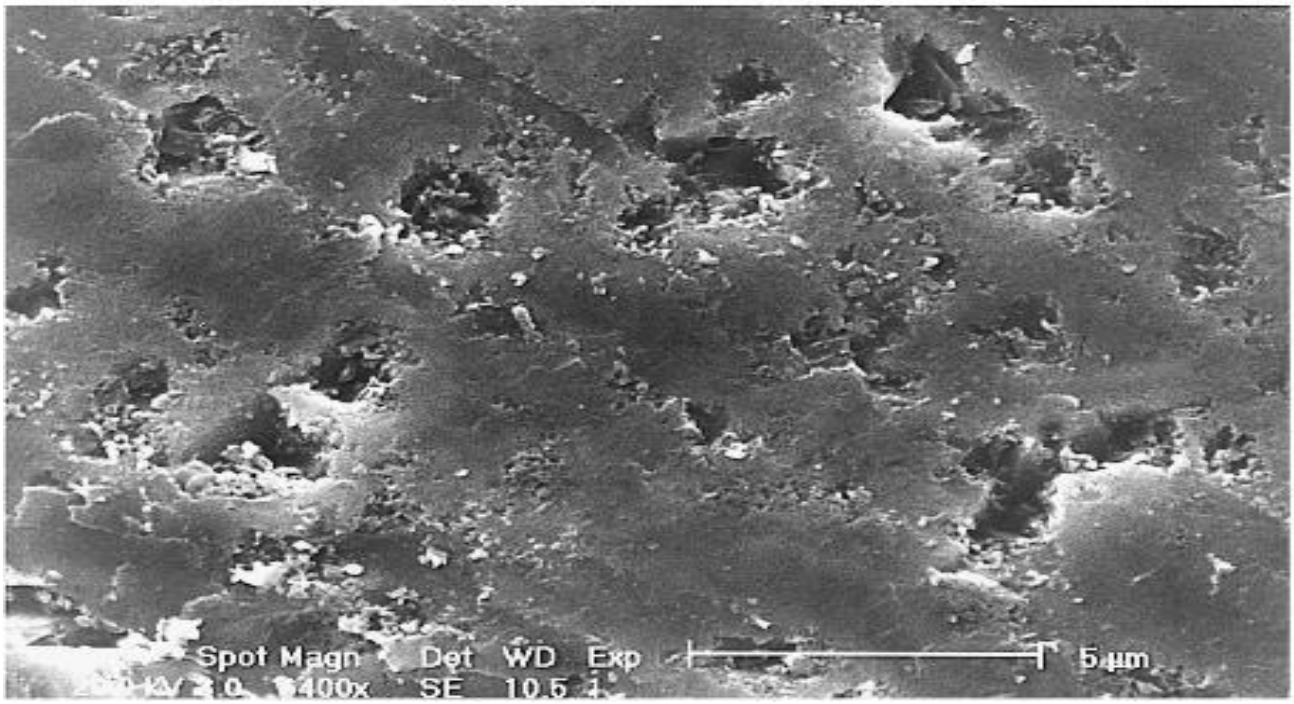

Figure 2.9: SEM image of a fresh pyrite surface (Blight et al., 2000)

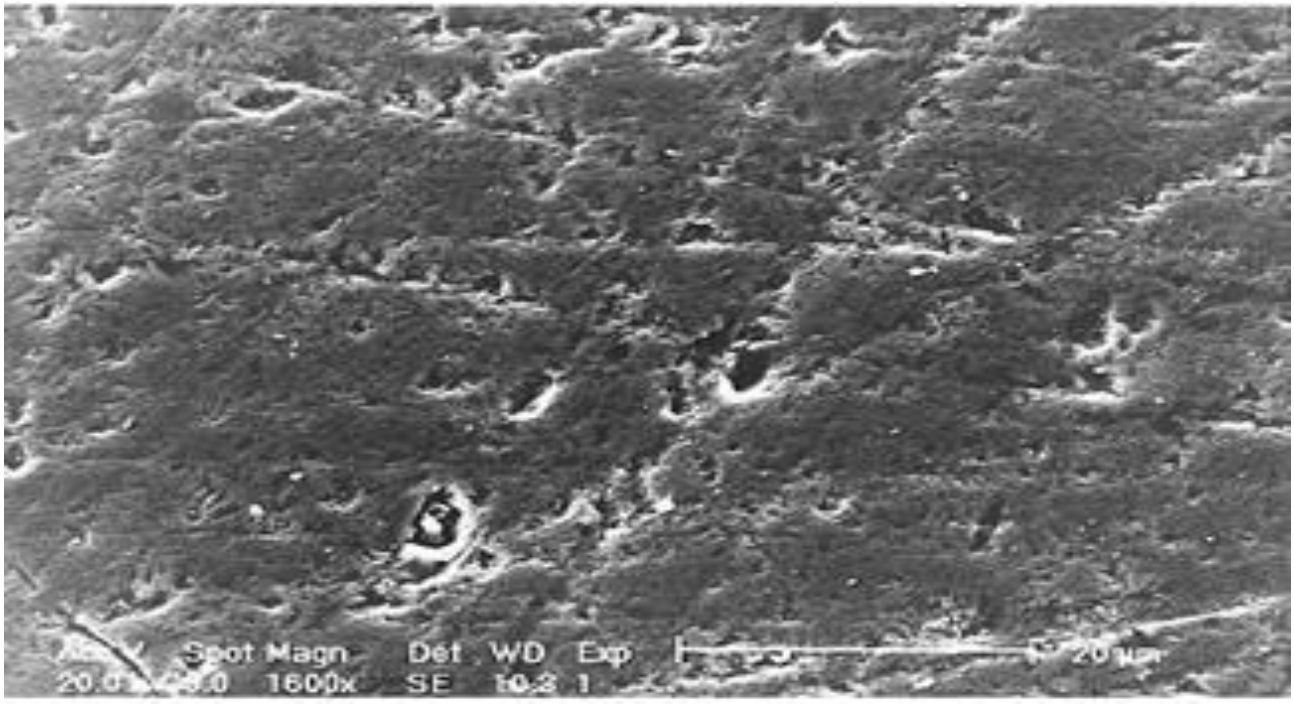

Figure 2.10: SEM image of etched pyrite surface after exposure to sulfuric acid at pH 1.5 showing an uneven surface and more pits from corrosion (Blight et al., 2000)

Although different acid media have been used as suitable oxidants for mineral specific flotation (*shown in Table 2.1*) e.g. permanganates for differential oxidation of pyrrhotite and arsenopyrite, no literature exists on the use of acid media to oxidise a flotation concentrate to separate the different types of pyrite.

Table 2.1: Different pyrite oxidising agents found in literature

Temperature (^0C)	pH	Oxidising Medium
25	2	Ferric chloride
30	1.98	Ferric chloride/Hydrogen peroxide
25	6.7-8.5	Carbonate buffered solution
23	6-7	De-aerated Carbonic Acid
20-50	3	Acidified ferric chloride and ferrous sulfate
20-50	Acidic	Acidified perchloric acid
35	Acidic	Acidified peroxide solution

2.3.4 Alkaline Oxidation

Alkaline pre-oxidation is an efficient pre-treatment technique to treat difficult ores and this has led to the development of the Albion leaching process (*discussed later*). Alkaline oxidation of pyrite (*equation 5*) prior to gold recovery was investigated by Royston et al. (1984). Sodium carbonate, sodium hydroxide and calcium hydroxide were used as the alkaline media and the consequent gold extraction results were studied. Flotation was used to prepare a pyrite concentrate that contained 14g/t gold, 80 g/t silver, 28% sulfur and 36% sulfur. The slurry was agitated in a 1.2-litre glass reaction vessel and the pH was controlled by additions of calcium hydroxide (Royston et al., 1984). Oxidation of pyrite by air was conducted in sodium carbonate, sodium hydroxide and calcium hydroxide solutions. The level of oxidation was measured by the difference between the total sulfur left in the sample compared to the untreated concentrate. It was found that the alkaline oxidation of pyrite had a positive effect on gold recovery by subsequent cyanidation. Comparatively, sodium hydroxide provided the best recoveries, but the downside of the process was the huge consumption of caustic soda (*200 kg/tonne*) (Royston et al., 1984).

$$FeS_2 + 7.5\,H_2O + O_2 \xrightarrow{\text{yields}} Fe^{3+} + (SO_4)^{2-} + H^+ + 7H_2O \quad \ldots\ldots\ldots\ldots\ldots\ldots\ldots\ldots\ldots\ldots\ldots\ldots\ldots 5$$

2.3.5 Pressure oxidation

Pressure oxidation/autoclaving is a destructive treatment used to oxidise metal sulfides to liberate the refractory gold. It involves a post-oxidation step which includes slurry cooling, slurry washing and lime neutralisation as shown in Figure 2.11 (Fraser et al., 1991, Collins et al., 2012). Oxidation of pyrite is vital to collapse the sulfide matrix and facilitate the liberation of gold associated with it. The ore is usually subjected (*without any further treatments*) to high-pressure oxygen and temperature or can be concentrated by flotation prior to pressure oxidation. Concentrates produced by flotation may be preferable because this route helps to minimise the plant cost by adopting low temperature and pressure conditions compared to treating the whole ore (Prasad et al., 1991) and lowers greatly the tonnage of solid to be treated.

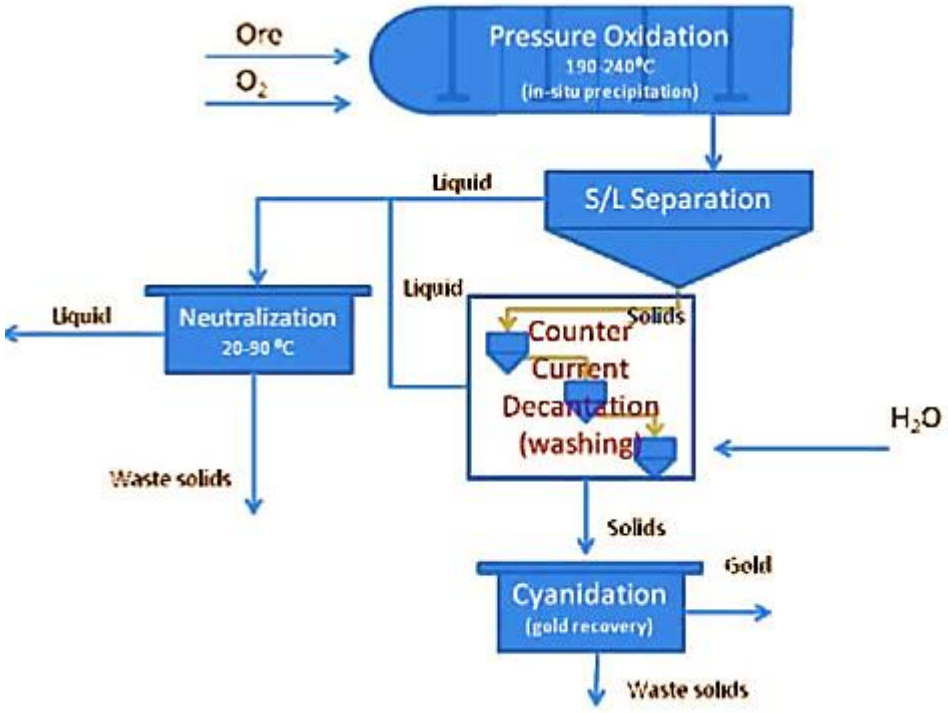

Figure 2.11: General pressure oxidation flowsheet (Collins et al., 2012)

Pressure oxidation is carried out in autoclaves at high temperatures (*180-210 °C*) and pressure (*15 to 20 bars*) to cause the oxidation of sulfides (Prasad et al., 1991). The slurry enters the autoclave at a comparatively lower temperature of 105 °C and at an acidic pH to promote oxidation of sulfides. This is done by the addition of sulfuric acid and the ore is oxidised by purging oxygen into the autoclave. The ore that has undergone pressure oxidation in the autoclave exits at a high temperature (*170-190 °C*) (Prasad et al., 1991) and is cooled

before passing into the thickeners to wash out the acid and lime is added to neutralise the slurry prior to cyanidation extraction. This process has been reported to achieve high gold recoveries of above 90% (Prasad et al., 1991).

Figure 2.12 shows that over a three-hour period, 75% sulfides disintegration was achieved. Just over two-thirds of this maximum breakdown occurred in the first half hour, and then the rate slowed considerably. If this second slower rate were maintained, it would take about a further 3 hours to decompose the sample completely. Figure 2.13 shows that the oxidation produces free acid and this is favourable in terms of increasing the rate of sulfide matrix breakdown. However, an effective residue wash is required to limit the amount of lime needed for neutralisation to the pH value necessary for cyanide leaching (Lehmann et al., 2000).

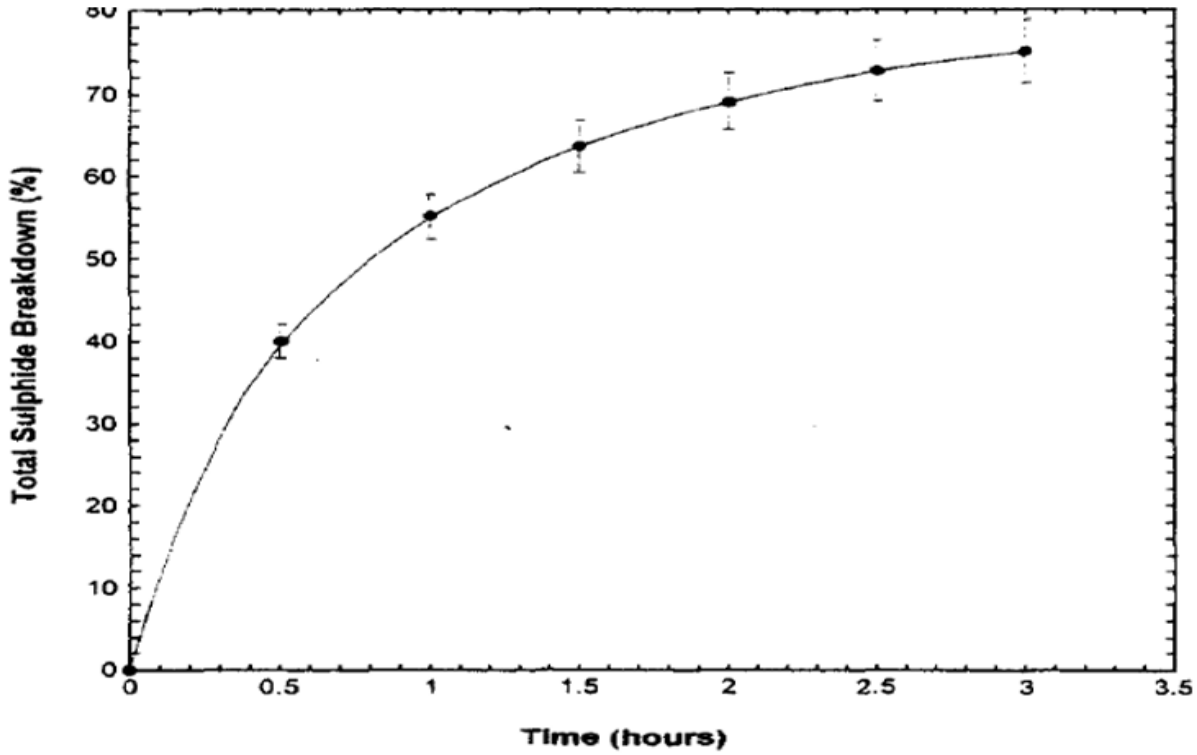

Figure 2.12: Sulfur matrix breakdown from sulfur leached into solution

(Lehmann et al., 2000)

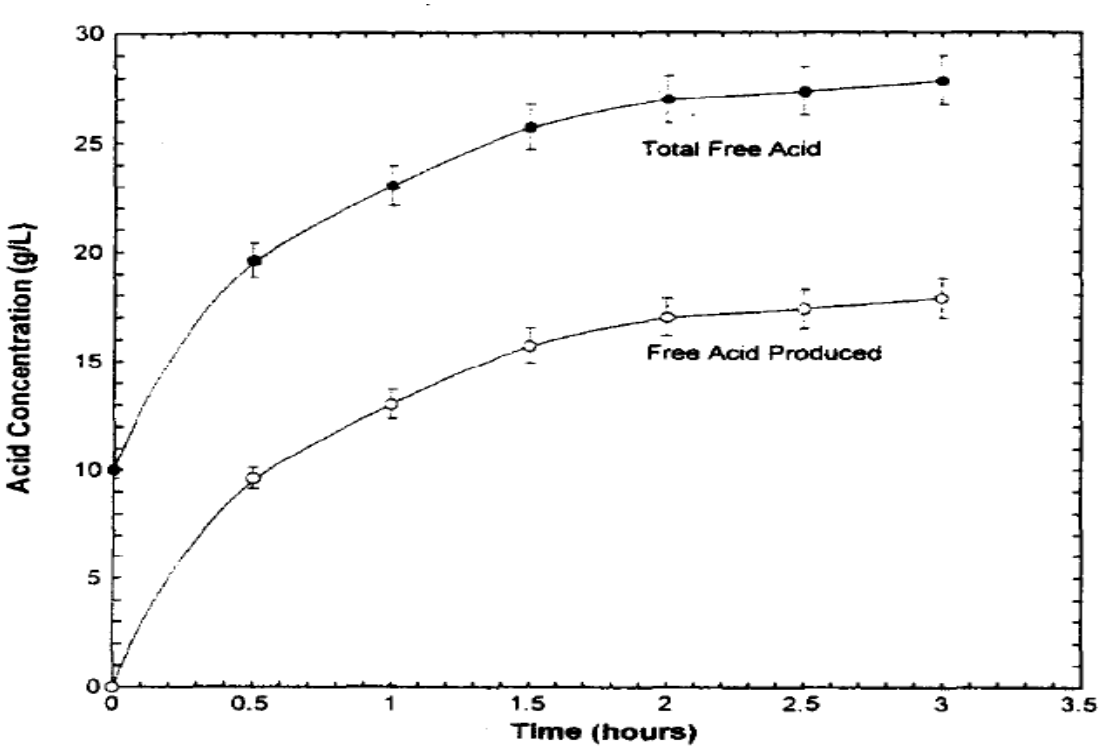

Figure 2.13: Acid concentrations measured during oxidative leach

(Lehmann et al., 2000)

2.3.5.1 Nitrox Process

The Nitrox process, Activox process and electrochemical slurry processes are all based on similar principles. These involve degradation of the sulfide structure in acid media to liberate the gold. However, the technology requires a high oxygen partial pressure and a long oxidation time. Moreover, this technology has high capital and operational costs. Therefore, it is necessary to develop alternative pre-treatment technologies to improve gold recovery.

In the Nitrox process, oxidation is carried out with nitric acid and the coupled Redox process regenerates the consumed nitric acid with oxygen as illustrated in Figure 2.14 and equations 6 and 7. The pressure and temperature conditions for both Nitrox and Redox processes are 100-400 kPa and 90-110 ^{o}C respectively. The Nitrox process involves oxidation of pyrites and arsenopyrites by reacting the ore for a couple of hours in nitric acid in an oxygen environment at atmospheric pressure. This process has demonstrated increased gold recoveries from 30% to 90% (Prasad et al., 1991).

$$3FeS_2 + 18HNO_3 \xrightarrow{\text{yields}} Fe_2(SO_4)_3 + Fe(NO_3)_3 + 3H_2SO_4 + 6H_2O + 15NO \ldots\ldots\ldots\ldots\ldots\ldots 6$$

$$3FeAsS + 14HNO_3 + 2H_2O \xrightarrow{\text{yields}} 3FeAsO_4.2H_20 + 3H_2SO_4 + 14NO \ldots\ldots\ldots\ldots\ldots\ldots\ldots 7$$

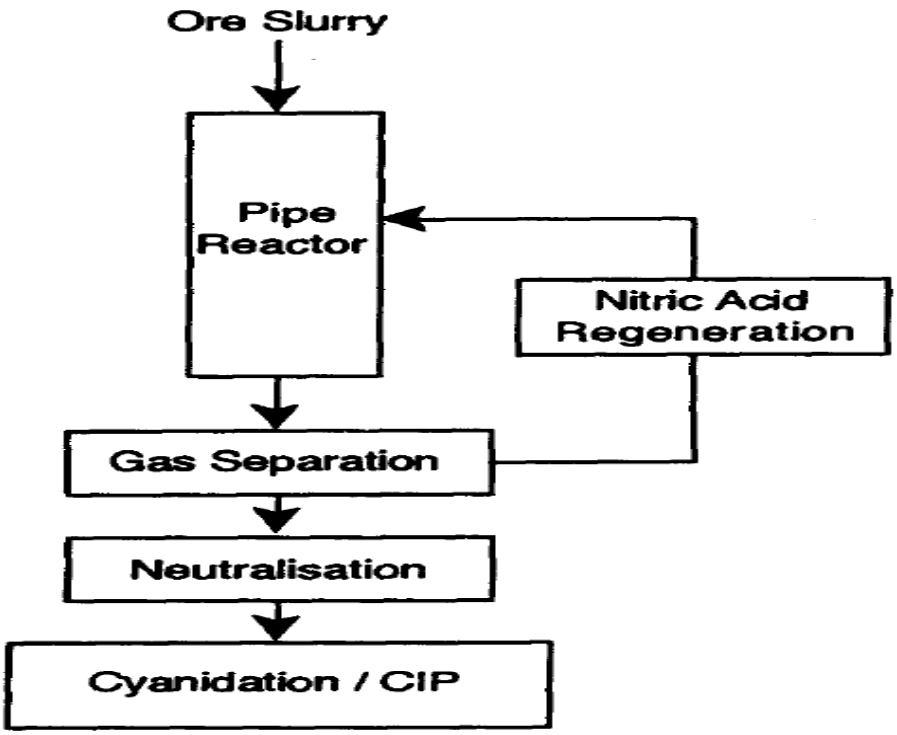

Figure 2.14: Steps in Nitrox process (La Brooy et al., 1994)

Other pressure oxidation methods include high-pressure oxidation, atmospheric-pressure oxidation and catalytic oxidation. (Gao et al., 2009, Huang and Rowson, 2002). These three technologies have particular advantages and disadvantages. Possibly, the catalytically oxidising technology process is the best pre-treatment method, because it has the lowest operating cost, lowest capital investment and easy industrial scale-up (Gao et al., 2009, Kadıoğlu et al., 1995, Papangelakis and Demopoulos, 1991). However, low sensitivity and lack of selectivity compared to bacterial oxidation are shortcomings of the pressure oxidation. Despite these disadvantages, pressure oxidation can still result in good recoveries of gold after ultrafine milling (Corrans and Angove, 1991). The processing conditions involved in various pressure oxidation methods are shown below in Table 2.2.

Table 2.2. Processing conditions involved in various intense pressure oxidation methods

Process	Temperature	Oxidising Time	Acid Concentration	Liquid to Solid Ratio
High-pressure oxidation of refractory gold concentrate	120 to 200 °C	2 to 60 minutes	1 to 3 M nitric acid	6:1
Atmospheric-pressure oxidation with nitric acid	80 to 100 °C	60 to 120 minutes	4 M nitric acid	6:1
Catalytically oxidising technology of NO_x	50 to 60 °C	210 minutes	1.6 M nitric acid	5:1

2.3.5.2 PLATSOL™ Process

The PLATSOL™ process is a high-temperature pressure leaching treatment (*225 ºC and 3200 kPa*) of mixed mineral sulfides, namely 'copper-nickel-cobalt platinum-palladium-gold', using H_2SO_4 (*30-60 g/L*) and halide salts such as sodium chloride for complexation (*10 to 20 g/L NaCl*) (Green et al., 2004, Dreisinger, 2014, Dreisinger et al., 2005, Milbourne et al., 2003, Habashi, 2003). The addition of chloride ions to the autoclave differentiates the PLATSOL™ leaching process (*shown in Figure 2.15*) from the other conventional high-temperature pressure oxidation process (*HTPOX*). Chloride ions modify the autoclave chemistry to facilitate the dissolution and precipitation of metal complexes (Marsden et al., 2003, Ferron and Wang, 2003). The chemistry of the PLATSOL™ process consists of two main steps:

1) Sulfide mineral oxidation of chalcopyrite, pyrite, nickel sulfide and pyrrhotite containing cobalt as shown in equations 8, 9, 10 and 11 (Dreisinger, 2014, Dreisinger et al., 2005) and

2) Extraction of valuable metals like gold, platinum and palladium as a chloro-complexed species according to equations 12, 13 and 14 (Dreisinger, 2014, Dreisinger et al., 2005, Milbourne et al., 2003).

Step 1: Sulfide Oxidation

Chalcopyrite oxidation: $CuFeS_2 + 4.25O_2 + H_2O \xrightarrow{\text{yields}} CuSO_4 + 0.5Fe_2O_3 + H_2SO_4$……..…8

Pyrite oxidation: $FeS_2 + 3.75O_2 + 2H_2O \xrightarrow{\text{yields}} 0.5Fe_2O_3 + 2H_2SO_4$ … … … … . . … … … . … … 9

Nickel Sulfide Oxidation: $NiS + 2O_2 \xrightarrow{\text{yields}} NiSO_4$…….....…10

Pyrrhotite Oxidation: $Fe_7S_8 + 17.25O_2 + 8H_2O \xrightarrow{yields} 3.5Fe_2O_3 + 8H_2SO_4$ … … … . … . … 11

Step 2: Metal Extractions/Complexation

Gold Oxidation/ Chlorocomplexation: $Au + 0.75O_2 + 4HCl \xrightarrow{\text{yields}} HAuCl_4 + 1.5H_2O$……12

Platinum Oxidation/ Chlorocomplexation: $Pt + O_2 + 6HCl \xrightarrow{\text{yields}} H_2PtCl_6 + 2H_2O$…….....13

Palladium Oxidation/ Chlorocomplexation: $Pd + 0.5O_2 + 4HCl \xrightarrow{\text{yields}} H_2PdCl_4 + H_2O$……14

2.3.5.3 Other Current Processes in Extractive Metallurgy

The lntec Copper Process is a hydrometallurgical technique to recover copper from sulfide concentrates (Wood, 2001, Mpinga et al., 2015**)**. The process involves leaching copper sulfides at a temperature of 85 ºC and atmospheric pressure using chloride-bromide lixiviants (280 g/L NaCl and 28 g/L NaBr) as shown in equations 15, 16 and 17 (Wood, 2001, Mpinga et al., 2015, Habashi, 2003**)**. However, it should be noted that chloride bromide is a very strong oxidising agent that causes gold dissolution (Mpinga et al., 2015) and therefore, the application of this mixture for mild oxidation of the various pyrite types may not be possible. The various other pressure leaching process options are described in Table 2.3.

$2CuFeS_2 + 2Cu^{2+} + 3.5O_2 \xrightarrow{\text{yields}} 4Cu^{+} + Fe_2O_3 + 4S^{O}$……..…..15

$4CuFeS_2 + 20HCl + 5O_2 \xrightarrow{\text{yields}} 4CuCl_2 + 4FeCl_3 + 4S^{O} + 10H_2O$……..…..16

$2CuFeS_2 + 5NaBrCl_2 + 5O_2 \xrightarrow{\text{yields}} 2CuCl_2 + 2FeCl_3 + 4S^{O} + 5NaBr$…….…..…...17

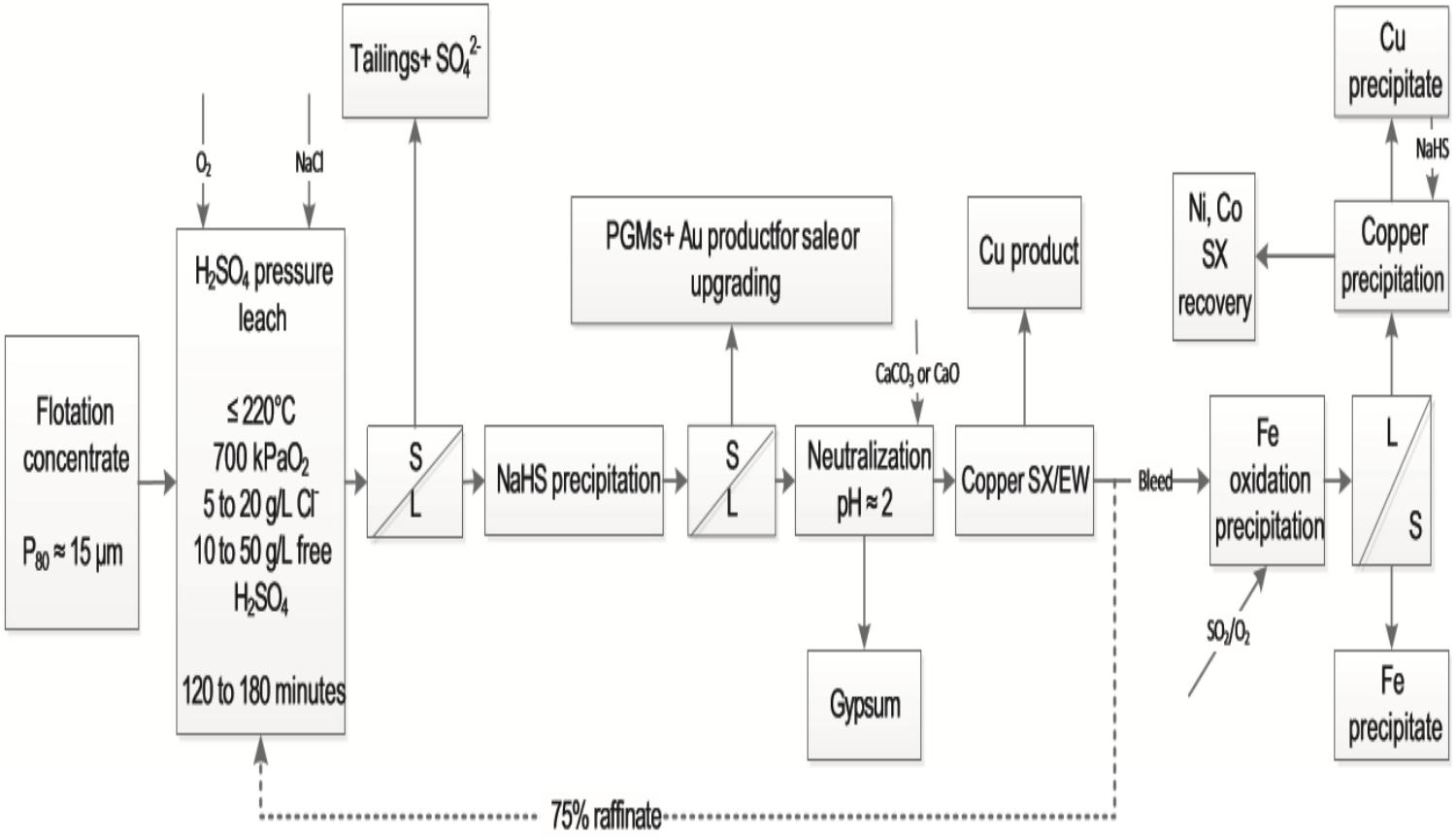

Figure 2.15: Schematic flowsheet of the PLATSOL™ process (Mpinga et al., 2015)

2.3.5.4 Albion Process

The Albion process, developed by Xstrata (*previously MIM Holdings*), involves leaching sulfide concentrates from refractory ores at a temperature of 85 ºC and atmospheric pressure as shown in Figure 2.16. This process (*just like the Activox Process* **(**Palmer and Johnson, 2005)) makes use of ultrafine grinding (*P80 of 10-15 µm*) to accelerate sulfide dissolution (Wood, 2001, Mpinga et al., 2015, Lillkung and Aromaa, 2012**)**. Most of these processes offer excellent gold recovery efficiencies from refractory ore and sulfide feedstocks (Fleming, 1999). Nonetheless, these are high-temperature destructive techniques that destroy the sulfide matrix completely to liberate the encapsulated gold.

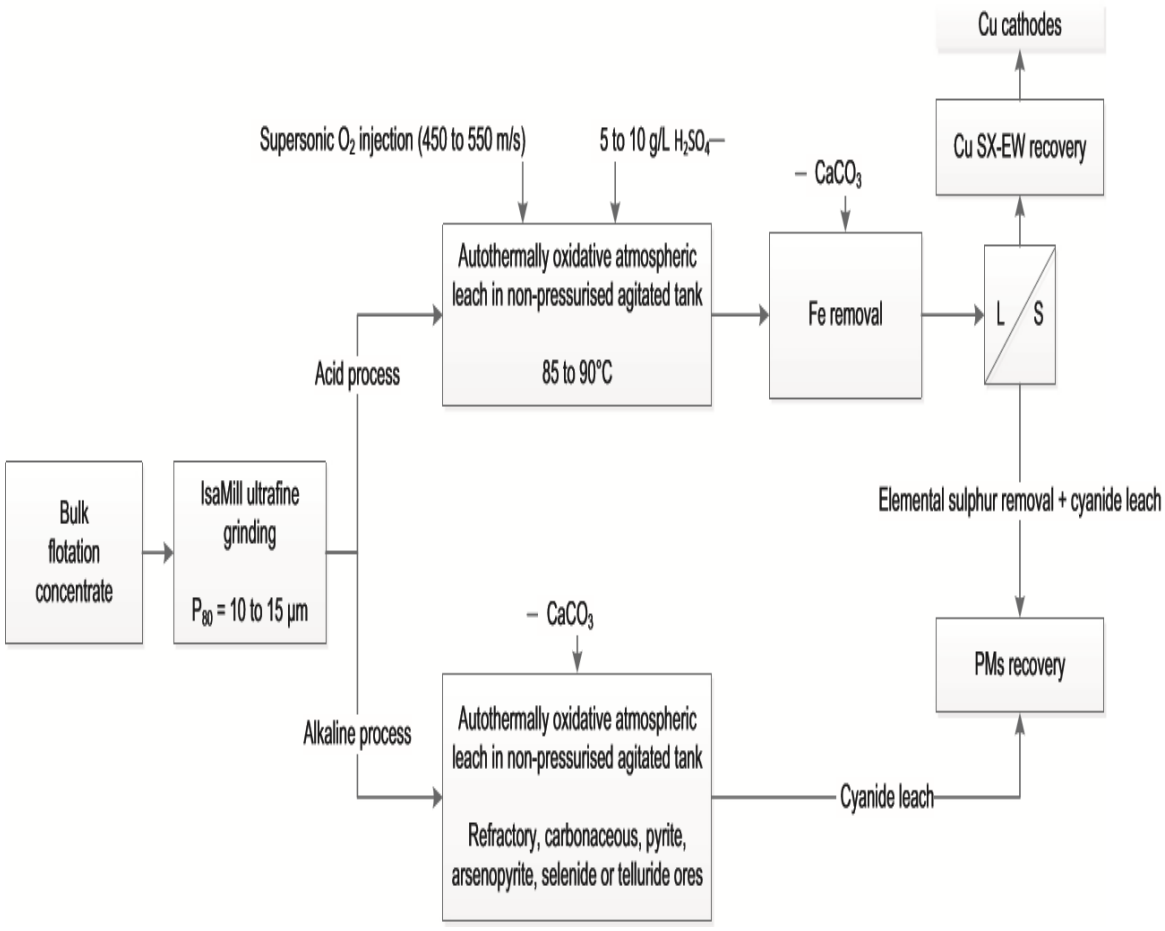

Figure 2.16: Albion process flowsheet for recovery of precious metals (Mpinga et al., 2015)

Table 2.3: Pressure and bio leaching process options (Dreisinger, 2006, Dutrizac, 1992, Fleming, 1999, Cole and Ferron, 2002, La Brooy et al., 1994, Nazari et al., 2011, Palmer and Johnson, 2005, Mpinga et al., 2015, Wood, 2001, Dreisinger, 2014, Milbourne et al., 2003, Dreisinger et al., 2005, Liddell and Adams, 2012, Habashi, 2003, Chmielewski, 2015)

Process	Temperature (^{O}C)	Pressure (kPa)	Reaction Conditions	Main Equations
Sulfate Leach				
Total Pressure Oxidation Process (TPOX)	200-230	3400	H_2O (leach medium)	$CuFeS_2 + 0.5H_2SO_4 + 4O_2 \xrightarrow{\text{yields}} CuSO_4 + 0.5Fe_2(SO_4)_3 + 0.5H_2O$
Galvanox Process	80	Atmospheric	Ag(catalyst)	$CuFeS_2 + O_2 + 2H_2SO_4 \xrightarrow{\text{yields}} CuSO_4 + FeSO_4 + 2H_2O + 2S^O$
Anglo American Corporation/University of British Columbia process (AAC/UBC)	150	700	Acid sulfate system Calcium Lignosulfonate/phenylene diamine	$CuFeS_2 + 4O_2 + H_2SO_4 \xrightarrow{\text{yields}} CuSO_4 + 0.5Fe_2O_3 + H_2O + 2S^O$
Activox Process	100-110	1000		$CuFeS_2 + O_2 + 2H_2SO_4 \xrightarrow{\text{yields}} CuSO_4 + FeSO_4 + 2H_2O + 2S^O$
Albion Process	85-90	Atmospheric	P80 of 10-15 µm	$CuFeS_2 + 3Cu^{2+} + 3Fe^{2+} \xrightarrow{\text{yields}} 2Cu_2S + 4Fe^{3+}$
ConRoast Pocess	1585	Atmospheric	H_2O	**Not Available**

Table 2.3 Continued				
Dynatec Process	150	10-12	Low grade coal	**Not Available**
Mount Gordon Process	90	8	Chalcocite	$FeS_2 + 7Fe_2(SO_4)_3 + 8H_20 \xrightarrow{\text{yields}} 15FeSO_4 + 8H_2SO_4$
Chloride Leach				
Intec Copper	85	Atmospheric	NaCl and NaBr	$2CuFeS_2 + 5NaBrCl_2 + 5O_2 \xrightarrow{\text{yields}} 2CuCl_2 + 2FeCl_3 + 4S^O + 5\ NaBr$
Outokumpu Hydro Copper	80-100	Atmospheric	pH 2	$CuFeS_2 + CuCl_2 + \frac{3}{4}\ O_2 \xrightarrow{\text{yields}} 2CuCl + \frac{1}{2}Fe_2O_3 + 2S^O$

Table 2.3 Continued				
Sulfate + Chloride Leach				
Cominco Engineering Services Limited Process (CESL)	150	700	Chloride Ions	$3CuFeS_2 + 7.5O_2 + \ H_2O + H_2SO_4 \xrightarrow{\text{yields}} CuSO_4.2Cu(OH)_2 + \frac{3}{2}Fe_2O_3 + 6S^O$
PLATSOL™	220	3200	Chloride Ions	$FeS_2 + 3.75O_2 + 2H_2O \xrightarrow{\text{yields}} 0.5Fe_2O_3 + 2H_2$ $Au + 0.75O_2 + 4HCl \xrightarrow{\text{yields}} HAuCl_4 + 1.5H_2$
Kell Process	220	3000	Roasting at 900 ^oC	**Not Available**
Sulfate + Nitrogen				
Nitrogen Species Catalysed Process (NSC)	125	400	H_2SO_4+$NaNO_2$	$2CuFeS_2 + 5NaBrCl_2 + 5O_2 \xrightarrow{\text{yields}} 2CuCl_2 + 2FeCl_3 + 4S^O$+5 NaBr

Table 2.3 Continued				
Cyanide				
Panton Process	60	Atmospheric	5% Chromium	$CuFeS_2 + O_2 + 2H_2SO_4 \xrightarrow{\text{yields}} CuSO_4 + FeSO_4 + 2S^O$
Bio-Oxidation				
BIOCOP	60-80	1	Mesophiles	$4FeS_2 + 6Fe^{3+} + 3H_2O \xrightarrow[\text{Bacteria}]{} S_2O_3^{2-} + 7Fe^{2+} + 6H^+$ $S_2O_3^{2-} + 8Fe^{3+} + 5H_2O \xrightarrow[\text{Bacteria}]{} 2SO_4^{2-} + 8Fe^{2+} + 10H^+$ $4FeS_2 + 15O_2 + 2H_2O \xrightarrow[\text{Bacteria}]{} 2Fe_2(SO_4)_3 + 2H_2SO_4$
BACTECH/MINTEK	35	1	Thermophiles	
BIOX	40	1	Mesophiles	

2.3.5.5 The PARTOX process

The Campo Morado deposits (*Guerrero, Mexico*) are similar to Lihir type refractory deposits where the gold exists as fine-grained mineralised structures in pyrite and hence requires oxidative pre-treatments to increase the amenability to oxidation. However, adding to the complexity of the ore mineralogy is the presence of a wide range of sulfide minerals (*sphalerite, pyrite, chalcopyrite, tetrahedrite and electrum*) encapsulating the valuable metals (*namely zinc, gold, copper and silver*) (Stone et al., 2007). As a part of this, PARTOX (*a selective partial oxidation process*) was developed to extract valuable metals from the sulfide minerals as per the following equations (*18 to 21*).

Pyrite: $FeS_2 + H_2SO_4 + 0.5O_2 \xrightarrow{\text{yields}} FeSO_4 + 2S + H_2O$ ……18

Sphalerite: $ZnS + H_2SO_4 + 0.5O_2 \xrightarrow{\text{yields}} ZnSO_4 + S + H_2O$ ……19

Galena: $PbS + H_2SO_4 + 0.5O_2 \xrightarrow{\text{yields}} PbSO_4 + S + H_2O$ ……20

Chalcopyrite: $CuFeS_2 + 2H_2SO_4 + O_2 \xrightarrow{\text{yields}} CuSO_4 + FeSO_4 + 2S + H_2O$……..…...21

The six steps involved in this partial oxidation process are (Dreisinger et al., 2005):

1. Autoclave leaching of bulk flotation concentrate (*at 20% solids, 100 psi, 150 °C*)
2. 7 stage Counter Current Decantation
3. Copper Solvent Extraction and Electrowinning (SX-EW) for high-grade copper recovery
4. Iron Removal (*by limestone addition*)
5. Zinc Solvent Extraction and Electrowinning (SX-EW) for special grade zinc recovery
6. Gold and Silver Recovery from dore.

A similar approach of 'mild oxidation' is to be developed in this thesis to selectively oxidise the gold bearing pyrite (*by surface modification to alter the surface of one type of pyrite relative to the other types, thus allowing for the selective flotation of the high gold pyrite and rejection of low gold pyrite types*). The PARTOX process targets copper and zinc as main-products and gold as a by-product through autoclave oxidation. Nevertheless, unlike the Campo Morado deposit, pyrite is the main sulfide mineral in Lihir ores (*discussed in Chapter*

4) and for economic reasons, autoclave throughput is critical (John et al., 2013). Therefore, the aim of this work is to maximise the autoclave throughput by directing only the high gold pyrite types into the flotation concentrate and therefore to the autoclave at Lihir.

2.4 Bio-Metallurgy

The terms 'bioleaching' and 'bio-oxidation' have been used interchangeably. However, it should be noted that the bio-oxidation does not solubilise the valuable metal whereas bioleaching does (Mahmoud et al., 2016). Hence, bio-oxidation mainly refers to the microbial treatment of refractory gold ores prior to cyanidation extraction.

Bacterial oxidation is a cost-effective and industrially proven technology that has allowed the industrial processing of low-grade Au ores into mineable resources (Miller and Brown, 2005, Ehrlich, 1997, Rawlings, 2004). Bio-beneficiation is an environmentally benign approach that represents an accelerated natural weathering mechanism to catalyse the breakdown of sulfide minerals (*in this case the FeS_2 lattice*) to liberate the gold occluded in the mineral matrix (Murphy and Strongin, 2009, Mubarok et al., 2016, Komnitsas and Pooley, 1989, Marsden and House, 2006, Whitlock, 1997, Haque, 1987). The exposed gold can be then subsequently recovered by conventional cyanidation or thiosulfate leaching (Komnitsas and Pooley, 1989, Marsden and House, 2006, Whitlock, 1997, Haque, 1987).

A consortium of microorganisms is available for sulfide oxidation and hence, the main design requirements for a bio-oxidation system depends on the mineralogical characteristics of the feedstocks, presence of heavy metals, temperature and pH. Different technologies such as BIOX, BACOX and BacTech-MinTek (*shown previously in Table 2.3*) utilise different genera of microbes for mineral biodegradation with the major difference being the operating temperatures.

A relatively common process philosophy of single stage bacterial oxidation involves crushing and milling of the ores followed by mineral oxidation of the sulfide concentrate by bacteria. The gold liberated from the oxidised sulfide matrix is then recovered by cyanidation/thiosulfate treatment. Nevertheless, the process flowsheet mainly depends on feedstock characteristics (Rawlings, 2004) and Figure 2.17 demonstrates the upstream operations of gravity and flotation processes prior to the downstream microbial oxidation at the Beaconsfield mine in Tasmania, Australia.

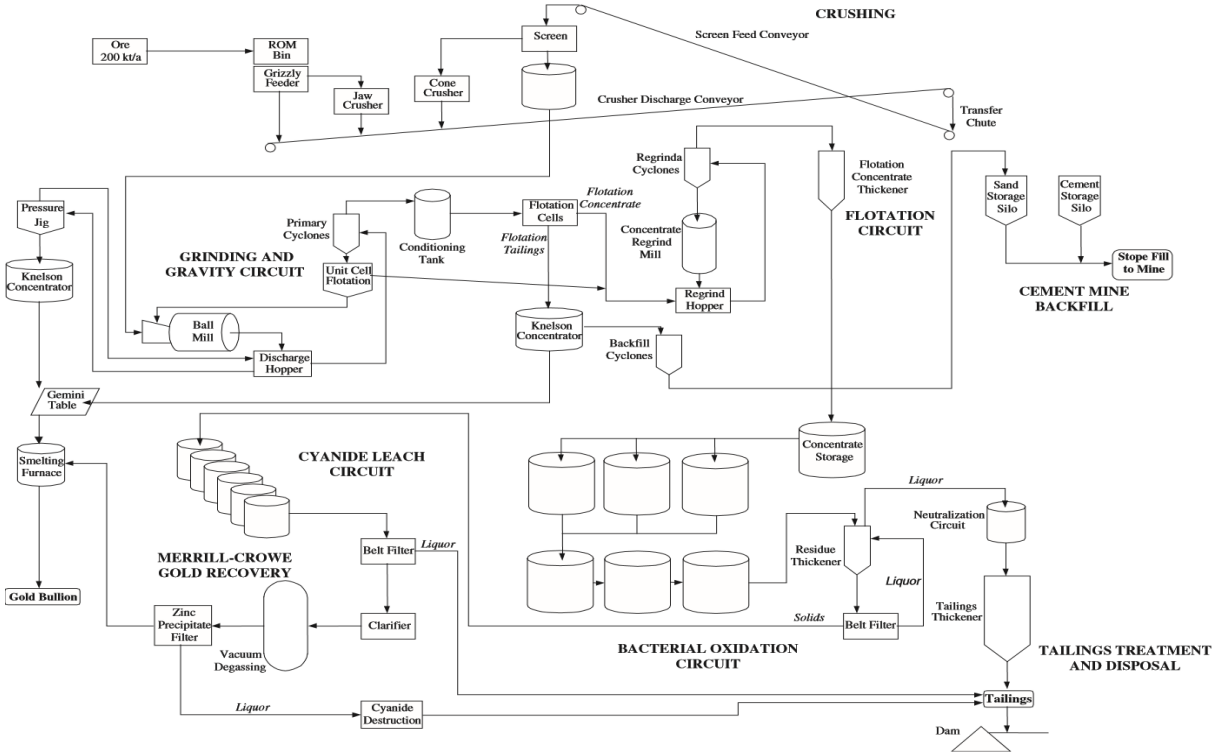

Figure 2.17: Process flowsheet of bacterial oxidation (*Mintek-Bactech*) at Beaconsfield Mining Operation, Australia (Neale et al., 2000)

A dual stage bacterial treatment process, as shown in Figure 2.18, is also carried out in the case of double refractory ores to oxidise the sulfides using *Acidophilus* bacteria in bio-oxidation step I and resolve issues of preg-robbing (*due to the presence of carbonaceous matter*) in bioxidation step II by *Streptomyces Setonii* (Amankwah et al., 2005, Fomchenko et al., 2016).

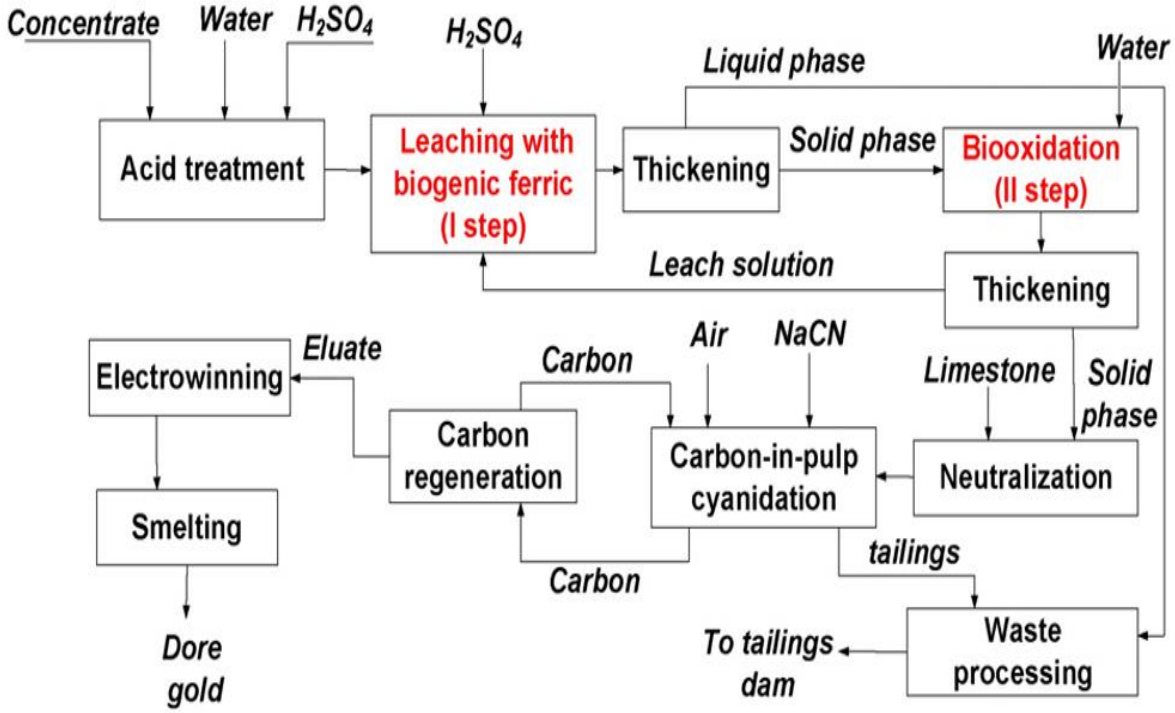

Figure 2.18: Dual stage bacterial treatment process for carbonaceous refractory ores (Fomchenko et al., 2016)

2.4.1 Bacterial Oxidation Mechanisms

The bio-oxidation of refractory Au ores/mineral concentrates is based on the activity of acidophilic iron and sulfur oxidising bacteria such as *Acidithiobacillus ferrooxidans (shown in Figure 2.19),* sulfur oxidising bacteria *Acidithiobacillus Thioxidans* and iron oxidising bacteria *Leptospirillum ferrooxidans* (Hong et al., 2016, Gleisner et al., 2006, Fomchenko et al., 2016, Komnitsas and Pooley, 1989, Marsden and House, 2006, Whitlock, 1997, Haque, 1987, Rawlings, 2004). Metal sulfides that are converted into metal sulfates by 'direct and indirect mechanism' can result in a variety of reaction intermediates. According to Rawlings (2004) and Schippers and Sand (1999), a thiosulfate pathway occurs in the case of pyrite (*as opposed to a polysulfide pathway in sphalerite (ZnS) and chalcopyrite minerals).* The involved reaction pathways are demonstrated in equations 22 to 26 (Rawlings, 2004, Schippers and Sand, 1999).

Thiosulfate Reaction Pathway

$$4FeS_2 + 6Fe^{3+} + 3H_2O \xrightarrow[\text{Bacteria}]{} S_2O_3^{2-} + 7Fe^{2+} + 6H^+ \quad \text{.....22}$$

$$S_2O_3^{2-} + 8Fe^{3+} + 5H_2O \xrightarrow[\text{Bacteria}]{} 2SO_4^{2-} + 8Fe^{2+} + 10H^+ \quad \text{.....23}$$

Polysulfide Reaction Pathway

$$MS + Fe^{3+} + H^+ \xrightarrow[\text{Bacteria}]{} 0.5H_2S_n + M^{2+} + Fe^{2+} \quad \text{.....24}$$

$$0.5H_2S_n + Fe^{3+} + H^+ \xrightarrow[\text{Bacteria}]{} 0.125S_8 + Fe^{2+} + H^{2+} \quad \text{.....25}$$

$$0.125S_8 + 1.5O_2 + H_2O \xrightarrow[\text{Bacteria}]{} SO_4^{2-} + 2H^+ \quad \text{.....26}$$

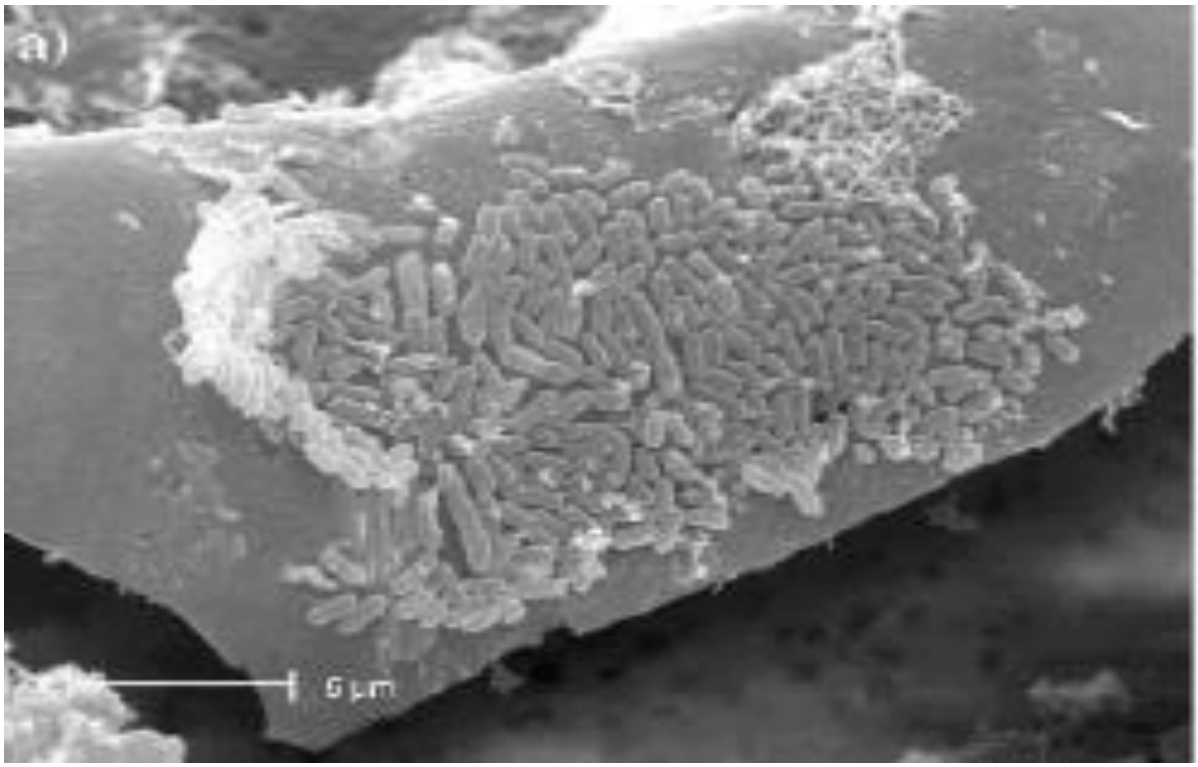

Figure 2.19: SEM pictures of *A. ferrooxidans* attached to pyrite grains (Gleisner et al., 2006)

Nevertheless, it is still not clear if bio-oxidation reactions occur via 'direct or indirect leaching' and this topic is a long-standing subject of debate. However, it is the understanding of the candidate that as long as these processes occur in concert or independently, it is the regeneration of ferric ions that dictates the efficiency of the oxidation reactions.

2.4.1.1 Direct Mechanism

Bacteria are physically adsorbed on the mineral surface (*specific sites as shown in Figure 2.20 and not the whole mineral*) and metal degradation occurs by the oxidation of heavy metal sulfides (FeS_2) to soluble iron sulfates as shown in equations 27, 28 and 29 (Bosecker, 1997, Rawlings, 2004, Sand et al., 2001). This breakdown process of the mineral matrix is catalysed through enzymatic and electrochemical reactions to form a 'ferrous-ferric ion couple' (Holmes et al., 1999, Sand et al., 2001) in the attachment region. While in contact with the mineral, depolarisation of the mineral surface ensues through the oxidation of S and Fe^{2+} culminating in highly oxidising conditions (Komnitsas et al., 1995, Rawlings, 2004, Sand et al., 2001).

$$4FeS_2 + 14O_2 + 4H_2O \xrightarrow[\text{Bacteria}]{} 4FeSO_4 + 4H_2SO_4 \quad \text{.....27}$$

$$4FeSO_4 + O_2 + 4H_2SO_4 \xrightarrow[\text{Bacteria}]{} 2Fe_2(SO_4)_3 + 2H_2O \quad \text{.....28}$$

Summarised as:

$$4FeS_2 + 15O_2 + 2H_2O \xrightarrow[\text{Bacteria}]{} 2Fe_2(SO_4)_3 + 2H_2SO_4 \quad \text{.....29}$$

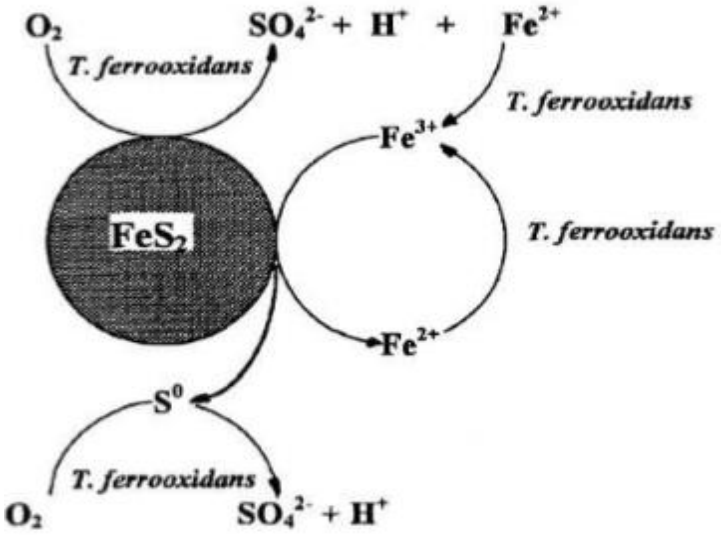

Figure 2.20: Bacteria physically adsorbed on the mineral surface in direct leaching (Nowaczyk and Domka, 1999)

2.4.1.2 Indirect Mechanism

In the indirect mechanism**,** metal oxidation takes place in an acid environment (*pH 2-3*) by chemically oxidising the heavy metal sulfides (FeS_2) to form soluble iron sulfates. This is facilitated by oxidative lixiviants such as ferric ions (Fe^{3+}) and this is shown in Figure 2.21 and equation 30 (Holmes et al., 1999). And therefore, physical adsorption of the bacteria on to the mineral surface is not necessary as they only have a catalytic role to regenerate the ferric ions to oxidise pyrite as shown in equations 30 to 33 (Holmes et al, 1999, Sand et al., 2001) by maintaining a high redox potential and converting sulfur to sulfuric acid as shown in equation 33 (Bosecker, 1997, Sand et al., 2001).

$$MeS + Fe_2(SO_4)_3 \xrightarrow{\text{yields}} MeSO_4 + 2FeSO_4 + S^o \quad \text{.....30}$$

$$4FeS_2 + 14Fe^{3+} + 8H_2O \xrightarrow[\text{Bacteria}]{} 15Fe^{2+} + 2SO_4^{2-} + 16H^+ \quad \text{.....31}$$

$$14Fe^{2+} + 3.5\ O_2 + 14H^+ \xrightarrow[\text{Bacteria}]{} 14Fe^{3+} + 7H_2O \quad \text{.....32}$$

$$2S^o + 3O_2 + 2H_2O \xrightarrow[\text{Bacteria}]{} 2H_2SO_4 \quad \text{.....33}$$

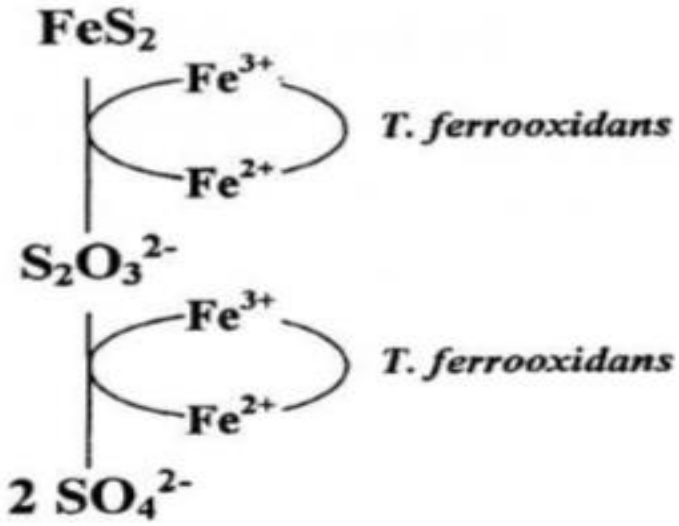

Figure 2.21: Bacteria are not physically adsorbed on the mineral surface but oxidise ferrous to ferric ions for metal bioextraction (Nowaczyk and Domka, 2000)

2.4.2 Industrial Leaching Techniques

Dump leaching (*by sprinklers or flooding*) is the oldest type of leaching (Bosecker, 1997) to treat tonnages of ore in large basins as shown in Figures 2.22 and 2.23.

Figure 2.22: Sprinkler Dump Leaching (Bosecker, 1997)

Figure 2.23: Dump leaching by flooding (Bosecker, 1997)

Heap and submerged leaching are usually used for fine-grained ores whereas *in situ* (*Figure 2.24*) and in-place treatments (*ore is not removed from the ore body*) (Bosecker, 1997, Rawlings, 2004) are also being developed.

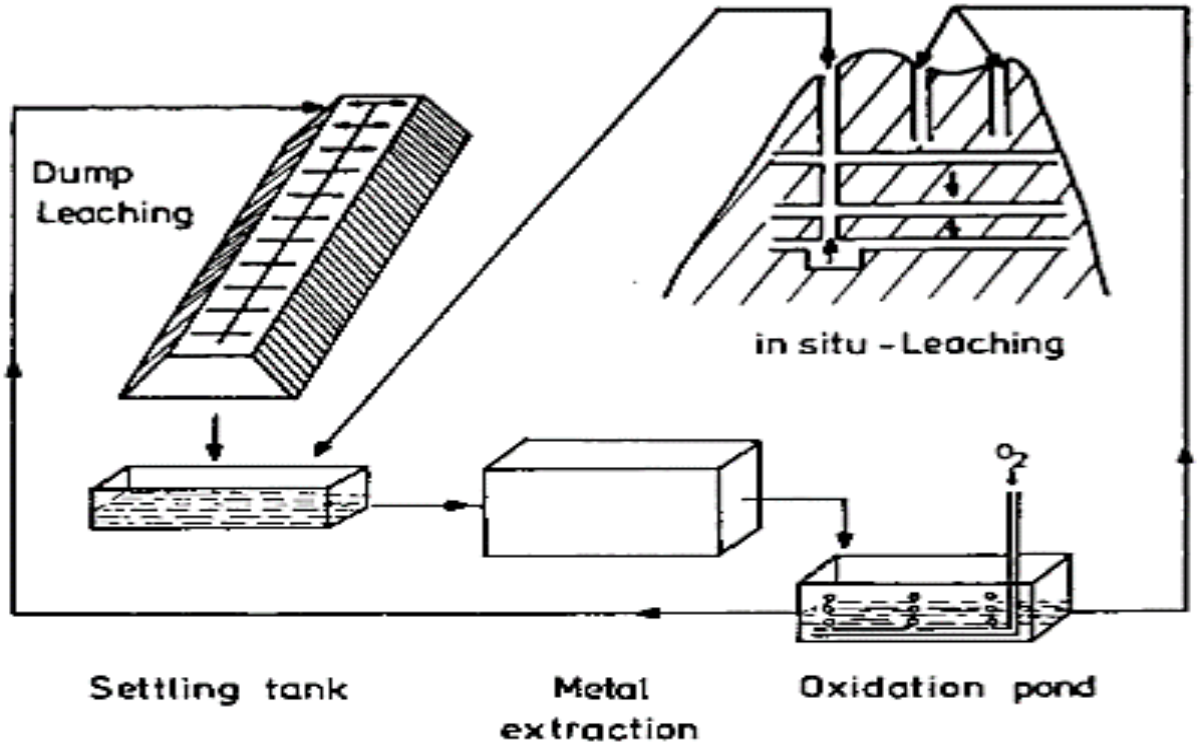

Figure 2.24: Dump and In-situ leaching process (Bosecker, 1997)

Reactor/Tank leaching (*shown in Figure 2.25*) yields the highest rate of metal extraction and is suited for refractory Au ores such as Lihir ores as the ferric ions concentration tends to be usually high to catalyse mineral oxidation (Rawlings, 2004). The sulfide feed (*concentrates from froth flotation*) for bacterial oxidation is diluted with water to maintain a pulp density between 15% and 20% (*w/w*) solids and mixed with essential nutrients such as ammonium and phosphate salts (Bosecker, 1997, Miller and Brown, 2005). A series of agitated aerated reactors as shown in Figure 2.25 are operated to prevent bacterial washout and induce surface air to facilitate the colonisation of the bacterial population. The parallel configuration also ensures adequate residence times (*3 to 5 days for partial oxidation and 7 to 10 days for high-level oxidation*) (Miller, 1997). The reactors are cooled with water due to the exothermic nature of the reaction and to maintain a set temperature depending on the thermal requirements of the bacteria (*28 to 30 ^{0}C for T. ferroxidans*) (Miller and Brown, 2005).

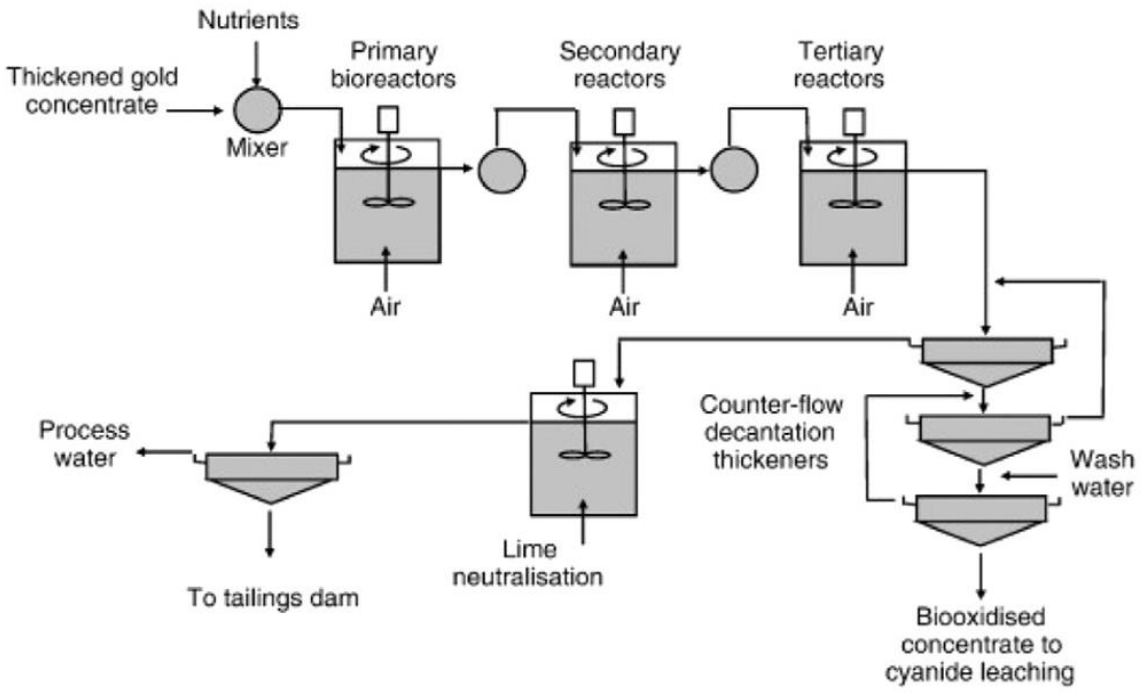

Figure 2.25: Processing of gold-bearing sulfide concentrates in BIOX® reactors (Kaksonen et al., 2014)

The bio-oxidised concentrate leaving the reactors is washed and undergoes a counter-flow decantation (*to remove bacterial cells and flotation reagents*) or filtration process to minimise the iron levels (*below 0.5 g/L*) and the oxidised residue is pH adjusted prior to leaching with cyanide. The liquor filtrate is neutralised using lime and disposed to the tailings dam.

2.4.3 Applications of Bio-Metallurgy for Differential Separation of Pyrite Types

The application of bio-oxidation offers a broad range of benefits over other oxidative methods. Among these the most important one, from an environmental perspective, is the fixing of heavy metals such as arsenic as stable ferric arsenate precipitate which then can be discarded safely into the tailings dam. Other advantages include operational simplicity, competitive CAPEX and OPEX (*two-fold lower capital and operating costs than roasting and pressure oxidation*) (Rawlings, 2004) and the ability to culture consortia of bacteria to suit the location temperature and ore mineralogy.

Nevertheless, the slow rate of reaction involved in the treatment of flotation concentrates (*days compared to hours with conventional hydrometallurgy*), higher cyanide consumption, rigorous temperature and pH requirements, corrosion from acidic slurries, carbon deactivation in the carbon-in-pulp (*CIP*) caused by fouling by dissolved organic residues and

foaming problems limit the application of bio-oxidation. Since the concentrate feed influences the bio-oxidation process, the mineralogy of the ore and concentrates requires the utmost attention to meet operational expectations. For example, the Lihir ore is high in arsenic (John et al., 2013) and this can impair the rate of oxidation and throughput (Miller and Brown, 2005).

The only available literature on the use of microbes to separate the different pyrite types is the study conducted by Boon et al. (1999). The investigation focused on the bacterial oxidation rate of a sulfide concentrate based on the chemical reactivity of the pyrite. It was found that *Thiobacillus Ferroxidans* could be used to oxidise microcrystalline pyrite but not blocky pyrite. This is because the chemical reactivity of microcrystalline pyrite was higher than blocky pyrite (Boon et al., 1999) and also probably due to the lower surface area of blocky pyrite compared to microcrystalline pyrite. This suggests that the various pyrite types have different oxidation rates and exploiting this difference might potentially lead to their relative separation. Nevertheless, the commercial application of a microbial species to separate the minerals of the same family on an industrial scale has not been reported yet.

During the initial stages of this thesis, the capability of the University of Cape Town in Bio-Metallurgy was recognised. However, there are numerous factors that can affect bio-oxidation such as feed concentrate characteristics, choice of bacterial culture, mineral substrate, temperature and pH control and therefore, designing and executing bio-oxidation of Lihir refractory ores is a separate thesis by itself. The potential to preferentially bio-oxidise the various pyrite types exists as demonstrated by Boon et al. (1999). A wide range of bacterial treatment plants for Lihir type gold deposits is shown in Table 2.4 and existing technologies could be modified, for example, the use of mixotrophic bacteria (*instead if chemolithotrophs*) and heterotrophic micro-organisms i.e. fungi such as *Penicillium and Aspergillus* to optimise the oxidation conditions for any given ore type.

Table 2.4: Bacterial Treatment Plants for Refractory Gold Deposits (Miller and Brown, 2005)

Plant Location	Total Reactor Volume (m^3)	S^{2-} in Feed (%)	Technology
Fairview, South Africa	1260	18-24	BIOX
Tonkin Springs, USA	8800	1.3	In House
Sao Bento, Brazil	1300	19	BIOX
Harbor Lights, Western Australia	980	18	BIOX
Wiluna, Western Australia	4230	24	BIOX
Obuasi, Ghana	21600	11	BIOX
Youanmi, Western Australia	3000	28	BacTech
Olympiada, Siberia	NA	NA	BioNord
Proano, Peru	1572	30	BIOX
Beaconsfield, Tasmania	2241	27-34	BIOX
Lazhou, China	4050	21-25	BacTech-Mintek
Suzdal, Kazakhstan	7800	12	BacTech-Mintek
Fosterville, Australia	5400	21	BIOX
Bogosu, Ghana	21000	20	BIOX
Jinfeng, China	16000	9.4	BIOX
Kolpatas, Uzbekistan	43200	20	BIOX
Agnes, South Africa	396	30	BIOX
Runruno, Philippines	10800	17	BIOX

2.5 High Energy Techniques (*Electrical and Magnetic Separations*)

2.5.1 Microwaves

The potential application of microwaves in comminution and extractive metallurgy has been reviewed previously by many researchers to pre-treat sulfide ores (Al-Harahsheh and Kingman, 2004, Orumwense and Negeri, 2004). Microwave energy has been shown to pre-treat refractory sulphidic ores and concentrates leading to enhanced liberation and achievement of high gold extractions (*over 95%*) (Xia and Picklesi, 2000, Haque, 1987). Less environmental constraints, reduced processing duration, localised heating and minimised energy requirements are obvious merits of microwave treatment over conventional thermal methods. However, understanding the interaction of microwaves with minerals is still a poorly explored area and requires further in-depth studies to unlock its full potential for use in extractive metallurgy (Koleini et al., 2012).

Microwave processing is a rapid heating process that occurs at the molecular level in which the polar molecules are rotated rapidly in an externally applied electric field. In the presence of these electromagnetic waves at high frequencies (*up to 500MHz*), the dipoles rotate according to the direction of the applied field. These induced motions, which occur up to 915 million times per second, result in inertial and elastic friction (Vorster, 2001). As a result, volumetric heating is generated in the mass of the material. While conventional thermal treatments rely on heating the material by conduction, electromagnetic waves selectively heat localised phases. The absorption of microwave energy not only improves the reaction kinetics but also causes inter-granular and trans-granular fractures at mineral boundaries as shown in Figure 2.26 ultimately resulting in the differential expansion (Huang and Rawson, 2002, Koleini et al., 2012, Vorster, 2001, Ferrari-John et al., 2016). These inter-granular fractures facilitate the mass transport of lixiviants through the fissures, thereby improving the leaching kinetics to increase gold extraction (Amankwah et al., 2005; Amankwah and Ofori-Sarpong, 2011; Nanthakumar et al., 2007).

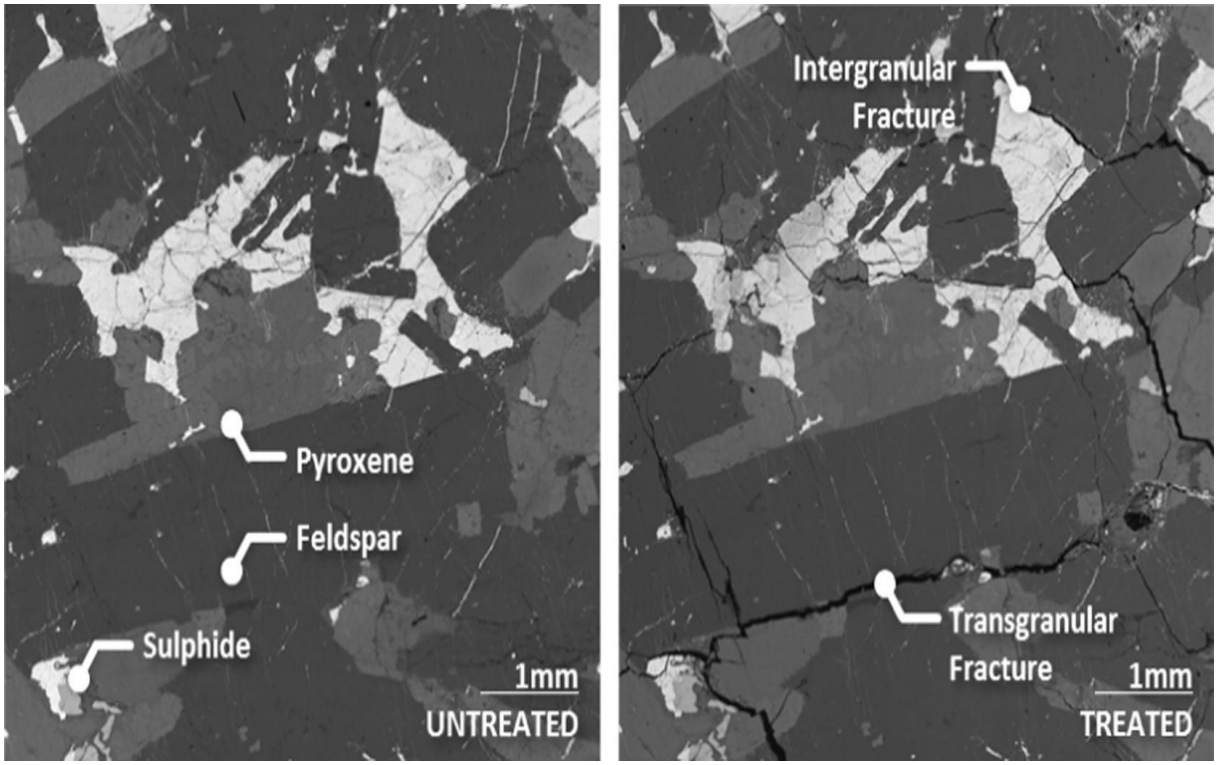

Figure 2.26: Microwave-induced fracture (Batchelor et al., 2015)

Differential expansion by microwaves at the inter-granular fractures is a matter of interest for the separation of various pyrite types. This is because, despite considerable efforts in process development, there is little information recorded on the efficacy of non-ionizing microwave processing to induce fractures in the various pyrite types differentially. If the dielectric properties of both low-gold and high gold pyrite can be understood, then microwave heating could be used to cause differential fragmentation patterns of the individual pyrite types and improve their liberation for the following separation process (*magnetic separation followed by flotation*). Another reason that microwave energy may find successful application in separation of various pyrite types is that gold-bearing minerals tend to be receptive to electromagnetic radiation, whereas many gangue minerals are microwave transparent (Jones et al., 2005). Moreover, since different pyrite types have varying gold tenor (*discussed in Chapter 4*), the responses of the low-gold and gold-rich pyrite types to microwaves might be different.

Sulfide minerals, including pyrite, are materials with high loss factors which are easily heated by microwaves as shown in Figure 2.27 (Vorster, 2001, Koleini et al., 2012, Lovas et al., 2011, Florek et al., 1996, Ferrari-John et al., 2016). Although pyrite is a hyperactive mineral and the heating rate properties of pyrite (*and other minerals*) have been established by

researchers as shown in Table 2.5, the responses of the individual pyrite types to microwaves and the dielectric properties of various pyrite types are an unexplored domain.

Table 2.5: Summary of mineral heating rates (Kingman et al., 2000)

Mineral	Chemical Composition	Max Temp Achieved (°C)	Time (min)	Energy Input (kWh/t)
Chalcopyrite	$CuFeS_2$	920	1	667
Galena	PbS	956	7	4667
Magnetite	Fe_3O_4	1258	2.75	1833
Orthoclase	$KAlSiO_3O_8$	67	6	4000
Pyrite	**FeS_2**	**1019**	**6.75**	**4500**
Quartz	SiO_2	79	7	4667
Sphalerite	ZnS	88	7	4667

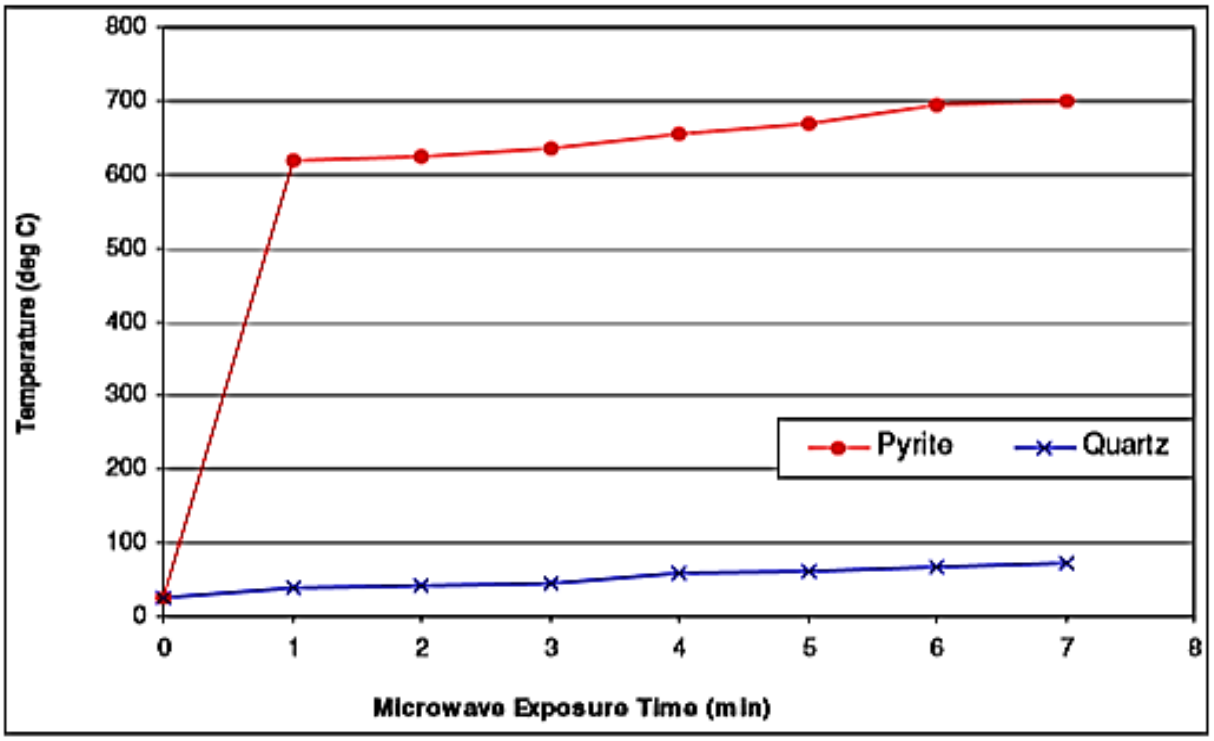

Figure 2.27: Heating rate of microwave receptive pyrite and microwave transparent quartz (Harrison and Rawson, 1996)

Microwave irradiations can also be used to facilitate magnetic separation techniques. Lovas et al. (2005) have shown that chalcopyrite could be magnetically separated from other minerals as a result of the thermal decomposition of Cu-ores by electromagnetic energy to

achieve Cu recovery in the range of 60 to 65%. Uslu et al. (2003) have shown that dielectric heating of pyrite results in the formation of pyrrhotite and γ-hematite which can then be magnetically separated following treatment at various field powers of 0.1T to 0.5T. A similar study by Waters et al., 2007 has also shown that magnetic properties of pyrite can be enhanced after microwave treatment in a multi-modal reactor. If the magnetic properties of the various pyrite types can be modified, say, by increasing the magnetic susceptibility of one pyrite type over another, then different magnetic field strengths can be applied to separate them differentially.

The decomposition of pyrite and marcasite in a nitric acid medium heated by microwave energy has also been investigated by Huang and Rawson (2002). It was found that microwave exposure could effectively improve the leaching kinetics of both minerals. Marcasite had a substantially higher decomposition rate than pyrite. The decomposition rate increased with an increase in leaching temperature and concentration of acid and with a decrease in particle size (Huang and Rawson, 2002). Because microwave energy can give selective and rapid volumetric heating, the combination of sulfide oxidation in a corrosive medium (*oxidising solutions*) with microwave pre-treatment could be another potential alternative for the treatment of refractory pyritic ores (Huang and Rawson, 2002).

Haque (1987) has studied the microwave pre-treatment of refractory sulphidic ores and achieved gold extractions of over 98%. However, there is little information recorded on the influence of microwave processing to oxidise the various types of pyrite differentially. It has been shown by Chen et al. (1984, 2013) that high iron sphalerite had a differential heating rate at low temperatures compared to low iron sphalerite. Also, the successful application of microwaves to separate high and low-titanium content magnetite was demonstrated on Palabora copper ore (Kingman et al., 2000).

Of particular interest to this thesis is the separation of two forms of pyrrhotite ($Fe_{(1-x)}S$) at Sudbury, Canada. Nickel enrichment can be achieved by magnetic separation, flotation or a combination of both (Rao, 2000, Agar, 1991) as shown in Figure 2.28 depending on the mineralogy. The separation of the nickel bearing pyrrhotite (*as shown in Figure 2.29b*) from the relatively barren metal value pyrrhotite (*as shown in Figure 2.29a*) is practised prior to smelting in Sudbury, Canada to minimize the sulfur dioxide emissions from the smelter (*due to stringent limits in Canada*), obtain high grade Ni concentrates and achieve higher circuit throughput (Agar, 1991, Becker et al., 2011).

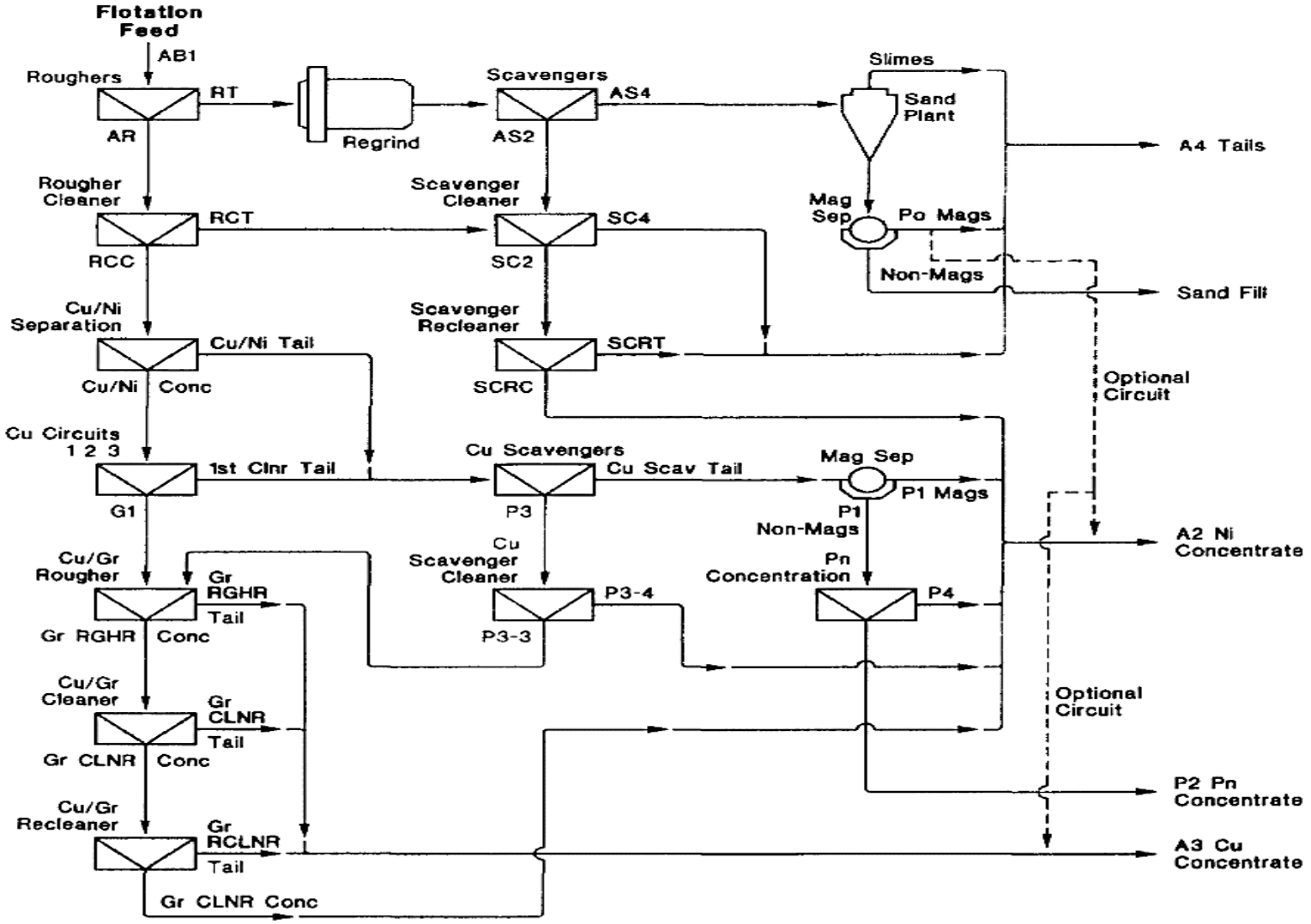

Figure 2.28: Nickel enrichment by magnetic separation and flotation (Agar, 1991)

The differential magnetic separation is achieved by exploiting the magnetic susceptibilities of the two crystallographic forms of pyrrhotite. The non-magnetic less reactive pyrrhotite (*also known as hexagonal 5C pyrrhotite* Fe_7S_8) has a magnetic susceptibility of $1x10^{-5}$ e.m.u/g. and the magnetically reactive pyrrhotite (*known as monoclinic 4C pyrrhotite,* Fe_9S_{10}, $Fe_{11}S_{12}$*)* has a high magnetic signature of 13.1 e.m.u/g. (Miller et al., 2005, Lawson et al., 2005, Becker et al., 2011, Chimbganda et al., 2013, Ekmekci et al., 2010). The application of magnetic separation to separate the various types of pyrite may not be as efficient as pyrrhotite. This because while pyrrhotite is a metallic paramagnetic conductor pyrite is a diamagnetic semiconductor (Wills and Napier-Munn, 2015, Blezile et al., 1997, 2004, Ekmekci et al., 2010). Nevertheless, enhancement of magnetic properties of pyrite through microwave radiation, mild oxidation to hematite (*based on the oxidation rates*) and subsequent differential separation in a magnetic flux might be possible.

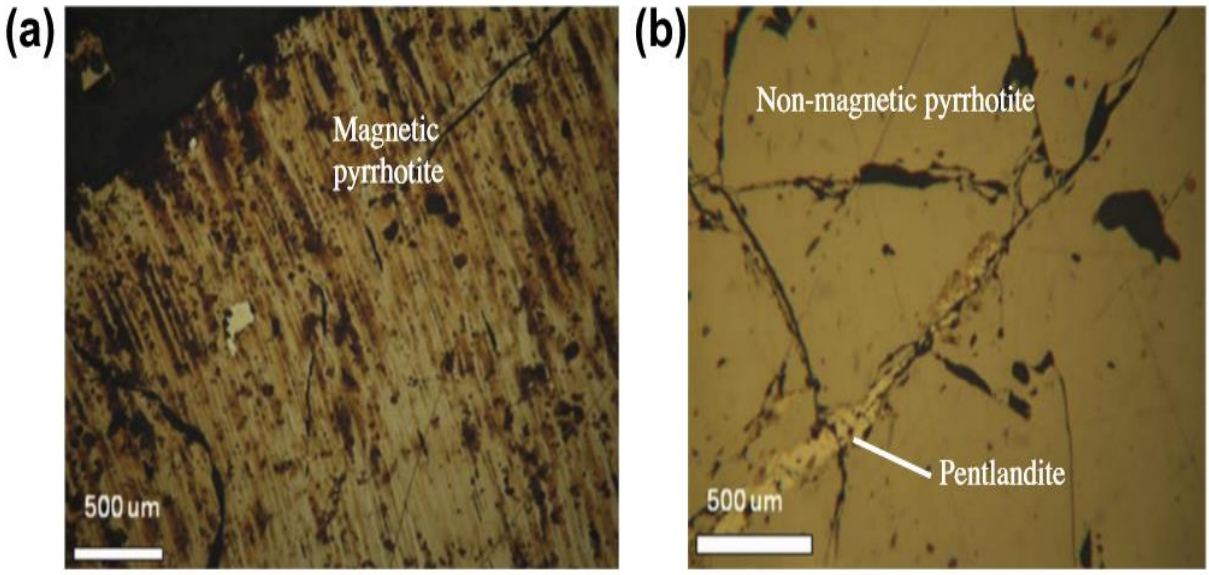

Figure 2.29: Light photomicrographs of a) Magnetic pyrrhotite and b) pentlandite bearing non- magnetic pyrrhotite (Becker et al., 2011, Chimbganda et al., 2013)

Pyrrhotite separation is also achieved by differential flotation in nickel operations (*Phoenix ore, Tati Nickel (Botswana) and Actifloat O2 at Elura Mine in Australia*) to separate the pentlandite locked pyrrhotite from the low-grade pyrrhotite. In such cases, it is the difference in the rates of surface oxidation between pyrrhotite and pentlandite that is manipulated to modify the pyrrhotite flotation performance (Becker et al., 2010 a and b, Miller et al., 2005, Lawson et al., 2005, Becker et al., 2011, Chimbganda et al., 2013). This is because there are 1/8 vacant sites in magnetic pyrrhotite compared to 1/10 vacant sites in non-magnetic pyrrhotite. With a greater frequency of vacancies, a higher oxidation rate is observed (Becker et al., 2010a and b). Hence, in accordance with Becker et al. (2010a), the non-magnetic pentlandite bearing pyrrhotite oxidises at a slower rate than the magnetic pyrrhotite. The differences in the surface reactive sites (*vacancies for preferential*

xanthate attachment and oxygen reduction) (Bozkurt et al., 1998, Becker et al., 2011, Chimbganda et al., 2013) affect the metallurgical performance of the pyrrhotite types in a flotation step.

2.5.2 High Energy Magnetic Pulses (HEMP)

The physical and chemical resistance of refractory ores can be overcome by energy intensive grinding and autoclave treatments. Nevertheless, high energy techniques can also be successfully utilised to break up the sulfide minerals and reduce the textural strength of the ores (Chanturia and Bunin, 2007, Chanturia et al., 2011). This not only improves liberation but also enhances the grindability by reducing the work index and increases the cyanide responsiveness of the ore (Amankwah and Ofori-Sarpong, 2011). The application of HEMP to process refractory ores has been investigated by Chanturia and Bunin (2007). The study involved decomposing the mineral channels by pulse irradiation so that the lixiviant solution permeates into the metal grains through the fissures to enhance the metal recovery (Chanturia and Bunin, 2007, Nanthakumar et al., 2007).

The treatment intensity of HEMP depends on the surface chemical composition of the sulfide minerals. Intensive oxidation of the mineral surface, as a consequence of low treatment energies (*0.1 kilojoules*) results in the formation of sulfur-rich sulfide, iron oxides, iron sulfates and elemental sulfur. Also, irradiation by HEMP results in pyrite activation and depression of arsenopyrite during subsequent flotation. Such findings are crucial for mineral processing projects where pyrite separation is the objective (Chanturiya and Bunin, 2007). It has been reported that pulse treatment of gold ores improved the leaching rate significantly by cracking the sample surface and allowing better percolation of the leaching solutions thereby increasing the gold extraction to over 95% (Amankwah et al., 2005; Amankwah and Ofori-Sarpong, 2011; Nanthakumar et al., 2007). However, there is very limited understanding regarding the physical forces involved in the interaction between HEMP and sulfide minerals and is well beyond the scope of this work (Chanturia et al., 2011).

2.5.3 Applications

There are numerous factors that can affect high energy techniques such as permittivity, loss factors, surface to volume ratio, surface chemical composition, microwave frequencies and the design of microwave applicators and cavities. Specialised knowledge regarding the modelling of microwave heating of materials and high energy pulses is required for mineral processing applications (Whittles et al., 2003). Therefore, the study and application of the high-energy techniques for the thermally assisted liberation of the various pyrite types is a separate study by itself and will not be

covered further in this thesis. The potential to preferentially heat the various pyrite types exists, however, the lack of a suitable characterisation technique to map the fragmentation patterns caused by microwaves still exists.

2.6 Conclusions

Pre-treatment options for refractory ores are greatly dependent on the location of the ore, environmental issues and the associated legislative regulations. The analysis of the treatment methods has pointed to some inadequacies in the current knowledge regarding the separation of low gold pyrite from gold-rich pyrite. The greatest limitation of the pre-treatment methods discussed in the literature is their inability to effectively separate within the same mineral family i.e. various types of pyrite. While not discussed in the literature it is clear that a range of oxidation and other methods may be utilised to separate the low gold pyrite from the gold-rich pyrite. The study by Boon et al., 1999 reinforces the fact that it is possible to separate minerals within the same family. However, there has been no study conducted on an industrial scale to separate pyrites with different gold loadings.

2.7 Characterization Methods

Different characterization methods have been widely used to determine the oxidation states of pyrite and other minerals and also to compare the oxidation rates of the mineral relative to another after a specific surface treatment. However, the disadvantage of these characterization methods is that they are not able to distinguish differences within a mineral family i.e. blocky pyrite from microcrystalline pyrite. This constraint limits the development of specific surface treatment studies that could be used to oxidise one pyrite relative to the other. Hence, this gap in technical expertise necessitates the development of a suitable method. One approach would be adopting electrochemical techniques to construct individual pyrite electrodes (*low gold pyrite electrode and high gold pyrite electrode*). However, it is necessary to have sufficiently larger pyrite grains (*2cm in diameter*) to develop individual electrodes. The other approach is developing a novel staining technique that distinguishes the various types of pyrite (*will be discussed further in Chapter 5*). This would not just be a diagnostic tool to identify the various types of pyrite and the extent of oxidation but would also be helpful to confirm the fact that different pyrite types have different reactivities.

2.7.1 Laser Ablation Analysis

Laser ablation high-resolution ICP-MS (*LA-ICPMS*) is a quantitative technique to identify various elements in sulfide minerals such as pyrite. However, LA-ICPMS is not a surface analysis technique and therefore, only fresh pyrite grains can be used in LA-ICPMS investigations because surface layer coatings (*due to oxidation processes*) can interfere with the readings (Öhlander et al., 2007). This limitation brings into doubt the application of this technique for characterising the different types of pyrite post oxidation.

2.7.2 Cyclic Voltammetry and Raman Spectroscopy

Cyclic voltammetry measurements (*Figure 2.30*) and Raman spectroscopy (*Figure 2.31*) are electrochemical techniques that can be used to identify the nature of the sulfur intermediates (*also known as polysulfides*) formed as a part of an oxidation process. However, these techniques fail to differentiate the various pyrite types and their nature before and after an oxidation process.

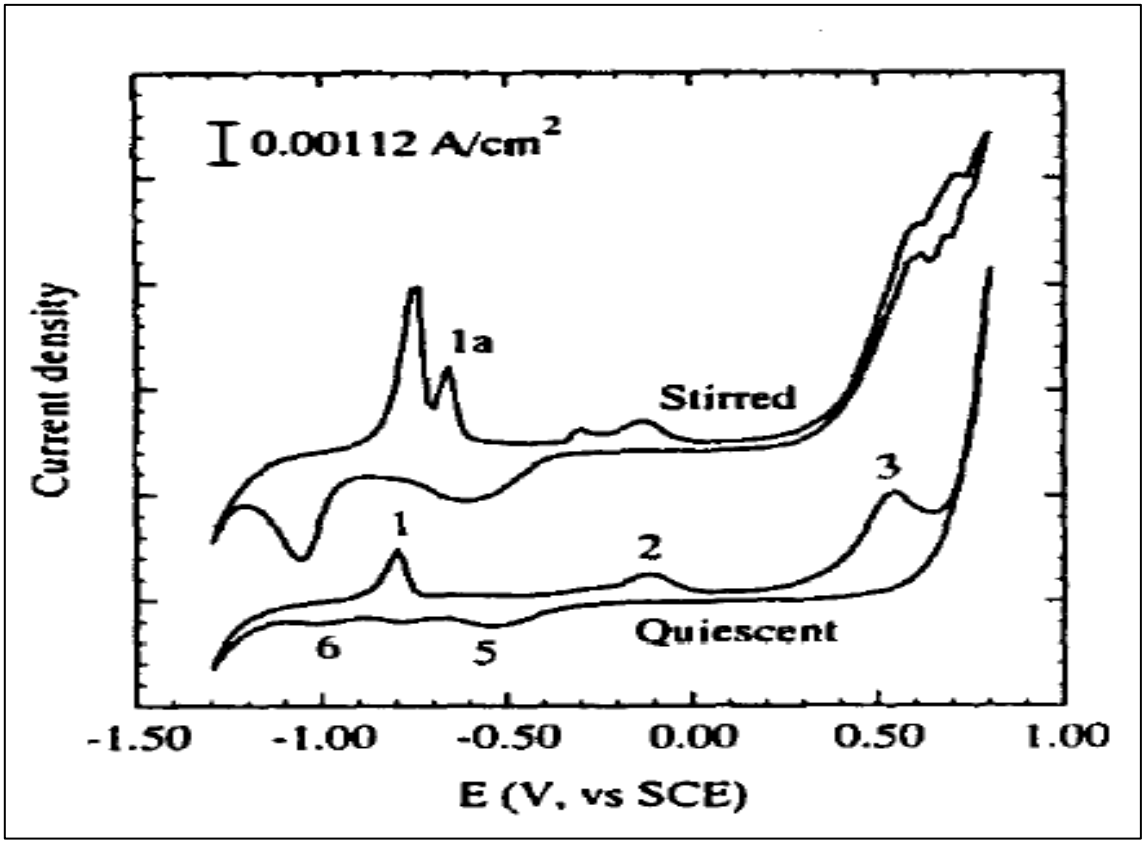

Figure 2.30: Cyclic Voltammograms of pyrite (Zhu et al., 1994) at a sweep rate of 0.5 V/s. Peaks labelled 1 and 2 refers to oxide and hydroxide formation on the pyrite surface as a result of oxidation while peak 3 is an outcome of complete dissolution of pyrite.

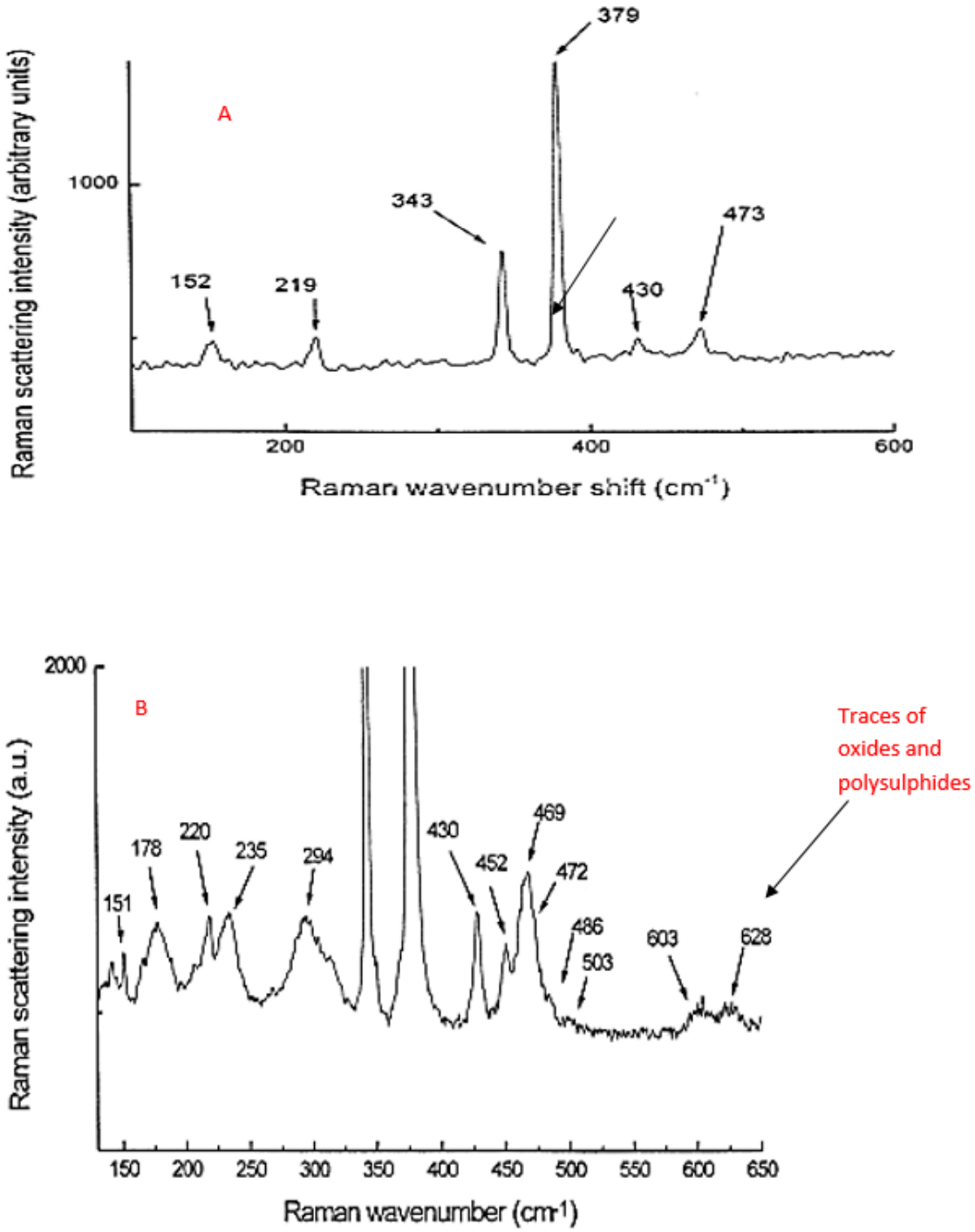

Figure 2.31: A. Raman spectrum pure pyrite surface. B. Raman spectrum of an oxidised pyrite surface showing evidence of polysulfides and oxides (Toniazzo et al., 1999).

2.7.3 Other Characterisation Techniques

A brief summary of the commonly used characterisation methods and the advantages and disadvantages of each technique is shown in Table 2.6.

Table 2.6: Advantages and disadvantages of different characterization techniques (Smart, 2014)

TECHNIQUE	PURPOSE	ADVANTAGE	DISADVANTAGE
X-RAY PHOTOELECTRON SPECTROSCOPY (*XPS*)	Determine the oxidation products at the pyrite surface with a signal covering about 40Å of the mineral	Surface sensitivity Elemental and chemical state analysis Reliable Quantification of the data Valency state of element	*Ex-situ* nature Fails to distinguish different types of pyrite and their oxidation states.
DIFFUSE REFLECTANCE INFRARED FOURIER TRANSFORMED SPECTROSCOPY (*DRIFTS*)	Define Oxidation products present at the pyrite surface with a penetration depth of 25000 Å	Good Sensitivity	Fails to distinguish different types of pyrite and their oxidation states.
SR-XPS TECHNIQUES	Detects oxidation products present at the outmost pyrite surface with a 9-fold increase in the sensitivity compared to XPS alone	Effectively identifies sulphur species Information about early stages of oxidation	Sample damage Destructive technique Fails to provides oxidation states of individual pyrites
TIME OF FLIGHT SECONDARY ION MASS SPECTROMETRY (*ToF-SIMS*)	Of identifying and mapping surface species on individual mineral particles, in the form of secondary ions ejected from the surface after bombardment by an energetic ion beam	Detects H High sensitivity(*ppm*) Element and molecular mapping Mass spectra	Matrix effects and hence not quantitative Sensitive technique and requires cooling for volatile elements. Fails to distinguish different types of pyrite and their oxidation states.

Most of these techniques offer good sensitivity, reliable quantification of the data and straightforward elemental and chemical state analysis. A good example is the XPS spectrum as shown in Figure 2.32. However, the main shortcoming of this technique to analyse the texture of pyrite post oxidation limits its application to identify oxidised surface coatings on pyrite and extract information regarding collector ion attachment. Also, the failure to provide data on different types of pyrite and the valence states (*Fe and S atoms in various pyrite types*) limits their application in this research. Nevertheless, some of these techniques will be used in this project to complement metallurgical and oxidation data.

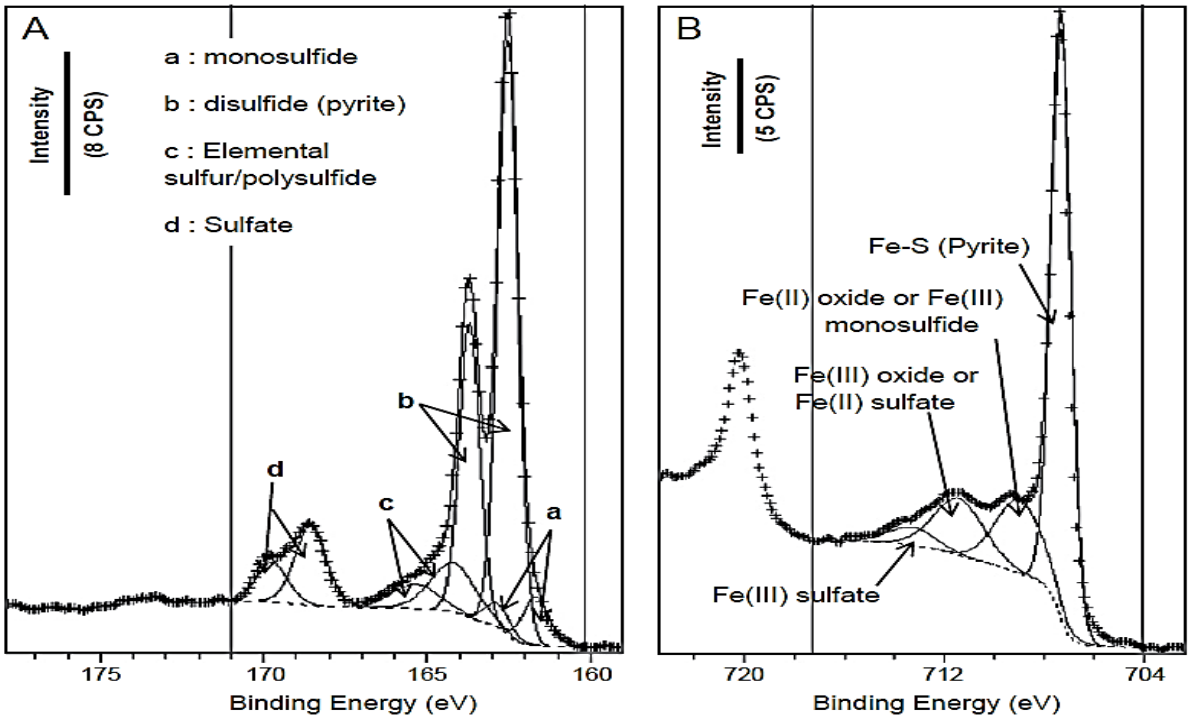

Figure 2.32: Data and band fitting of sulfur and iron spectra in pyrite analysis (Derycke et al., 2013)

2.8 Summary

The critical analysis of the literature review section has pointed to some gaps in the current knowledge regarding the separation of low gold pyrite from gold-rich pyrite.

- A lack of a proper treatment method to separate the low gold bearing pyrite from gold-rich pyrite.
- The knowledge about the variables affecting the separation of low gold pyrite from gold-rich pyrite is vague and incomplete.

- The role of oxidation of different pyrites has not been utilised before for a separation process.
- There is no recorded information in the literature that sheds light on separation of minerals within the same family.
- No attempt has been reported in the literature using differential oxidation as a conditioning step allowing later separation of pyrite types in a flotation process.
- No work has been reported in the literature which uses low-level oxidation technology based on hydrometallurgical practices to condition the various pyrite types and separate them differentially in a flotation process.

As a result of these points, the driving force behind this thesis is to develop a hydrometallurgical treatment to manipulate the preparation conditions prior to flotation separation of the low gold bearing pyrite from the gold-rich pyrite. Hence, hydrometallurgical techniques are to be utilised for the design of the preparation conditions before the separation of pyrite types by flotation. This would provide a clearer understanding regarding the separation within a mineral family but also aid development of expertise to utilise the physical and chemical characteristics of different types of pyrite.

2.9 Bibliography

ADAMS, M. 2005. Advances in gold ore processing, Vol.15. *Elsevier Science*. ISBN: 0-444-51730-8.

AFENYA, P. 1991. Treatment of carbonaceous refractory gold ores. *Minerals Engineering,* 4**,** 1043-1055.

AGAR, G.E., 1991. Flotation of chalcopyrite, pentlandite, pyrrhotite ores. In: K.S,E. Forsberg (Editor), Flotation of Sulfide Minerals 1990. *Int. J. Miner. Process.*, 33: 1-19.

AL-HARAHSHEH, M. & KINGMAN, S. 2004. Microwave-assisted leaching—a review. *Hydrometallurgy,* 73**,** 189-203.

AMANKWAH, R. K., & OFORI-SARPONG, G. 2011. Microwave heating of gold ores for enhanced grindability and cyanide amenability. *Minerals Engineering*, *24*(6), 541-544.

AMANKWAH, R. K., PICKLES, C. A., & YEN, W. T. 2005. Gold recovery by microwave augmented ashing of waste activated carbon. *Minerals Engineering*, *18*(5), 517-526.

AMANKWAH, R. K., YEN, W. T., & RAMSAY, J. A. 2005. A two-stage bacterial pretreatment process for double refractory gold ores. *Minerals Engineering*, *18*(1),103-108.

ANTONIJEVIĆ, M., DIMITRIJEVIĆ, M. & JANKOVIĆ, Z. 1993. Investigation of pyrite oxidation by potassium dichromate. *Hydrometallurgy,* 32**,** 61-72.

AYLMORE, M., & JAFFER, A. 2012. Evaluating process options for treating some refractory ores. *Technical papers are available from the Xstrata ALBION PROCESSTM Available at http://www. Albion process. com/EN/downloads/Pages/TechnicalPapers. aspx*.

BATCHELOR, A. R., JONES, D. A., PLINT, S., & KINGMAN, S. W. 2015. Deriving the ideal ore texture for microwave treatment of metalliferous ores. *Minerals Engineering*, *84*, 116-129.

BEATTIE, M. & POLING, G. 1988. Flotation depression of arsenopyrite through use of oxidising agents. *The Institution of Mining and Metallurgy Transactions. Section C. Mineral Processing and Extractive Metallurgy*, 97.

BECKER, M., BRADSHAW, D., & DE VILLIERS, J. 2011. The mineralogy of pyrrhotite from Sudbury CCN and Phoenix nickel ores and its effect on flotation performance. *Canadian Metallurgical Quarterly*, *50*(1), 10-19.

BECKER, M., DE VILLIERS, J., & BRADSHAW, D. 2010a. The flotation of magnetic and non-magnetic pyrrhotite from selected nickel ore deposits. *Minerals Engineering*, *23*(11), 1045-1052.

BECKER, M., DE VILLIERS, J., & BRADSHAW, D. 2010b. The mineralogy and crystallography of pyrrhotite from selected nickel and PGE ore deposits. *Economic Geology*, *105*(5), 1025-1037.

BELZILE, N., CHEN, Y. W., CAI, M. F., & LI, Y. 2004. A review on pyrrhotite oxidation. *Journal of Geochemical Exploration*, *84*(2), 65-76.

BELZILE, N., MAKI, S., CHEN, Y. W., & GOLDSACK, D. 1997. Inhibition of pyrite oxidation by surface treatment. *The science of the total environment*, *196*(2), 177-186.

BLIGHT, K., RALPH, D. & THURGATE, S. 2000. Pyrite surfaces after bio-leaching: a mechanism for bio-oxidation. *Hydrometallurgy,* 58**,** 227-237.

BOON, M., BRASSER, H., HANSFORD, G. & HEIJNEN, J. 1999. Comparison of the oxidation kinetics of different pyrites in the presence of Thiobacillus Ferrooxidans or Leptospirillum ferrooxidans. *Hydrometallurgy,* 53**,** 57-72.

BOSECKER, K. 1997. Bioleaching: metal solubilization by microorganisms. *FEMS Microbiology Reviews*, *20*(3-4), 591-604.

BOUFFARD, S. C., RIVERA-VASQUEZ, B. F. & DIXON, D. G. 2006. Leaching kinetics and stoichiometry of pyrite oxidation from a pyrite–marcasite concentrate in acid ferric sulfate media. *Hydrometallurgy,* 84**,** 225-238.

BOULTON, A., FORNASIERO, D. & RALSTON, J. 2001. Depression of iron sulfide flotation in zinc roughers. *Minerals Engineering,* 14**,** 1067-1079.

BOZKURT, V., XU, Z., & FINCH, J. A. 1998. Pentlandite/pyrrhotite interaction and xanthate adsorption. *International Journal of Mineral Processing*, *52*(4), 203-214.

BRUCKARD, W., SPARROW, G. & WOODCOCK, J. 2011. A review of the effects of the grinding environment on the flotation of copper sulfides. *International Journal of Mineral Processing,* 100**,** 1-13.

CHANDRA, A. & GERSON, A. 2009. A review of the fundamental studies of the copper activation mechanisms for the selective flotation of the sulfide minerals, sphalerite and pyrite. *Advances in Colloid and Interface Science,* 145**,** 97-110.

CHANDRA, A. & GERSON, A. R. 2010. The mechanisms of pyrite oxidation and leaching: a fundamental perspective. *Surface Science Reports,* 65**,** 293-315.

CHANTURIA, V. & BUNIN, I. Z. 2007. Non-traditional high-energy processes for disintegration and exposure of finely disseminated mineral complexes. *Journal of Mining Science,* 43**,** 311-330.

CHANTURIYA, V. A., BUNIN, I. Z., RYAZANTSEVA, M. V. & FILIPPOV, L. O. 2011. Theory and Applications of High-Power Nanosecond Pulses to Processing of Mineral Complexes. *Mineral Processing & Extractive Metallurgy Review,* 32**,** 105-136.

CHEN, T. T., DUTRIZAC, J. E., HAQUE, K. E., WYSLOUZIL, W., & KASHYAP, S. 2013. The relative transparency of minerals to microwave radiation. *Canadian Metallurgical Quarterly*.

CHEN, T.T., DUTRIZAC, J.E., HAQUE, K.E., WYSLOUZIL, W., KASHYAP, S., 1984, The relative transparency of minerals to microwave radiation. *Can. Metall. Quart*. 23 (1), 349–351.

CHEN, X., PENG, Y. & BRADSHAW, D. 2013. Effect of regrinding conditions on pyrite flotation in the presence of copper ions. *International journal of mineral processing,* 125**,** 129-136.

CHIMBGANDA, T., BECKER, M., BROADHURST, J. L., HARRISON, S. T. L., & FRANZIDIS, J. P. 2013. A comparison of pyrrhotite rejection and passivation in two nickel ores. *Minerals Engineering*, *46*, 38-44.

CHIRITA, P. 2003. Kinetics of aqueous pyrite oxidation by potassium dichromate-An experimental study. *Turkish Journal of Chemistry*, 27**,** 111-118.

CHMIELEWSKI, T. 2015. Development of a hydrometallurgical technology for production of metals from kghm Polska Miedz SA concentrates. *Physicochemical Problems of Mineral Processing*, *51*(1), 335-350.

COLE, S., & FERRON, C. J. 2002. A review of the beneficiation and extractive metallurgy of the platinum-group elements, highlighting recent process innovations. *The Geology, Geochemistry, Mineralogy and Mineral Beneficiation of platinum-group elements. Canadian Institute of Mining, Metallurgy and Petroleum, Special*, *54*, 811-818.

COLLINS, M. J., BEREZOWSKY, R. M. G. S., VARDILL, W. D., KETCHAM, V. J., & STOJSIC, A. 1993. The Lihir Gold project: pressure oxidation process development. In *Proceedings of the Milton E. Wadsworth (IV) International Symposium on Hydrometallurgy, Society for Mining* (pp. 611-628). Metallurgy and Exploration Inc. Littleton.

COLLINS, M., BEREZOWSKY, R., VARDILL, W., KETCHAM, V. & STOJSIC, A. The Lihir Gold project: pressure oxidation process development. IV International Symposium on Hydrometallurgy, Salt Lake City, UT (August 1993), 1993.

COLLINS, M.J., FILIPOU.D., HARLAMOVS J.R., PEEK.E., 2012. Pressure Hydrometallurgy. 51 Annual Conference of Metallurgists of CIM (COM 2012), Niagra Falls.

CORRANS, I. & ANGOVE, J. 1991. Ultra fine milling for the recovery of refractory gold. *Minerals Engineering*, 4**,** 763-776.

DERYCKE, V., KONGOLO, M., BENZAAZOUA, M., MALLET, M., BARRÈS, O., DE DONATO, P., BUSSIÈRE, B. & MERMILLOD-BLONDIN, R. 2013. Surface chemical characterization of different pyrite size fractions for flotation purposes. *International Journal of Mineral Processing*, 118**,** 1-14.

DIMITRIJEVIC, M., ANTONIJEVIC, M. & JANKOVIC, Z. 1996. Kinetics of pyrite dissolution by hydrogen peroxide in perchloric acid. *Hydrometallurgy*, 42**,** 377-386.

DRASKIC, D., MANOJLOVICGIFING, M. & PAVLICE, J. Possibility of arsenic content reduction in pyrite concentrate by a flotation concentration process. CIM BULLETIN, 1982. Canadian Inst Mining Metallurgy Petroleum 101 6th Ave Sw, Ste 320, Calgary Ab Tzp 3p4, Canada, 77-77.

DREISINGER, D. 2006. Copper leaching from primary sulfides: Options for biological and chemical extraction of copper. *Hydrometallurgy*, *83*(1), 10-20.

DREISINGER, D. B. 2014. *U.S. Patent No. 8,741,238*. Washington, DC: U.S. Patent and Trademark Office.

DREISINGER, D., MURRAY, W., HUNTER, D., BAXTER, K., FERRON, J., & FLEMING, C. 2005. The Application of the PLATSOL™ Process To Copper-Nickel-Cobalt-PGE/PGM Concentrates From Polymet Mining's Northmet Deposit. In *Proceedings of the ALTA World Forum on Nickel and Cobalt Hydrometallurgy, Perth Australia* (Vol. 16).

DREISINGER, D., TAGGART, P., BANNER, R., COPELAND, D., JENNINGS, D., WHITTINGTON, D., MEZEI, A.2005. The Hydrometallurgical Treatment of Farallon Resource's Campo Morado Bulk Zn-Pb-Cu-Ag-Au Sulfide Concentrate. Japan.

DUNN, J. 1997. The oxidation of sulfide minerals. *Thermochimica Acta,* 300**,** 127-139.

DUNNE, R. Auriferous sulfide flotation in Australia. Randol Gold Forum Cairns' 91, 1991. Randol Int Golden, Colorado, 239-244.

DUTRIZAC, J. E. 1992. The leaching of sulfide minerals in chloride media. *Hydrometallurgy*, *29*(1), 1-45.

EHRLICH, H. L. 1997. The technical potential for bioleaching and bio beneficiation of ores to recover base metals (other than iron or copper), platinum-group metals and silver. *In Biomining* (pp. 129-150). Springer Berlin Heidelberg.

EKMEKÇI, Z., BECKER, M., TEKES, E. B., & BRADSHAW, D. 2010. The relationship between the electrochemical, mineralogical and flotation characteristics of pyrrhotite samples from different Ni Ores. *Journal of Electroanalytical Chemistry*, *647*(2), 133-143.

FERRARI-JOHN, R. S., BATCHELOR, A. R., KATRIB, J., DODDS, C., & KINGMAN, S. W. 2016. Understanding selectivity in radio frequency and microwave sorting of porphyry copper ores. *International Journal of Mineral Processing*, *155*, 64-73.

FERRON, C. J., & WANG, Q. 2003. Copper arsenide minerals as a sustainable feedstock for the copper industry. *SGS Minerals Services, Technical Bulletin*, *15*, 1-6.

FLEMING, C. 1992. Hydrometallurgy of precious metals recovery. *Hydrometallurgy,* 30**,** 127-162.

FLEMING, C. 1999. PLATSOL™ process provides a viable alternative to smelting. *Africa Mining Journal, pp1-4*.

FLOREK, I., LOVAS, M., MUROVA, I., 1996, The effect of microwave radiation on magnetic properties of grained iron-containing minerals, in: *Proceedings of the 31st International Microwave Power Symposium*, Boston, USA.

FOMCHENKO, N. V., KONDRAT'EVA, T. F., & MURAVYOV, M. I. 2016. A new concept of the biohydrometallurgical technology for Gold recovery from refractory sulfide concentrates. *Hydrometallurgy*, *164*, 78-82.

FRASER, K., WALTON, R. & WELLS, J. 1991. Processing of refractory gold ores. *Minerals Engineering,* 4**,** 1029-1041.

GAO, G., LI, D., ZHOU, Y., SUN, X. & SUN, W. 2009. Kinetics of high-sulfur and high-arsenic refractory gold concentrate oxidation by dilute nitric acid under mild conditions. *Minerals Engineering,* 22**,** 111-115.

GLEISNER, M., HERBERT, R. B. & KOCKUM, P. C. F. 2006. Pyrite oxidation by Acidithiobacillus ferrooxidans at various concentrations of dissolved oxygen. *Chemical Geology,* 225**,** 16-29.

GLEMBOTSKII, V., KLASSEN, V. & PLASKIN, I. 1972. Flotation, Primary Sources, N. York.

GREEN, B. R., SMIT, D. M. C., MAUMELA, H., & COETZER, G. 2004. Leaching and recovery of platinum group metals from UG-2 concentrates. *Journal of the South African Institute of Mining and Metallurgy*, *104*(6), 323-331.

GUDYANGA, F., MAHLANGU, T., ROMAN, R., MUNGOSHI, J. & MBEVE, K. 1999. An acidic pressure oxidation pretreatment of refractory gold concentrates from the KweKwe roasting plant, Zimbabwe. *Minerals Engineering,* 12**,** 863-875.

HABASHI, F. 2003. Chloride Metallurgy 2002, Edgar Peek and Gus Van Weert (Ed.), Canadian Institute of Mining, Metallurgy, and Petroleum, 3400 Maisonneuve W.,# 1210, Montreal, Canada H3Z 3B8, 2 volumes, 800 p.

HAQUE, K. 1987. Gold leaching from refractory ores—literature survey. *Mineral Processing and Extractive Metallurgy Review,* 2**,** 235-253.

HARRISON P.C., & ROWSON, N.A. 1996. The Effect of Heat Treatment on the Grindability of Coal. I. Chem. E. Res. The event, 268-271.

HOBERG, H., LOESCHE, T. & SCHNEIDER, F.-U. 1985. Investigations on the Flotability of Sulfides After Dry Grinding--a Contribution to the Development of an Alternative Energy-Saving Method for the Preparation of Sulfide Ores. *Aufbereit.-Tech.,* 26**,** 171-182.

HOLMES, P. R., FOWLER, T. A., & CRUNDWELL, F. K. 1999. The mechanism of bacterial action in the leaching of pyrite by Thiobacillus ferrooxidans. An electrochemical study. *Journal of the Electrochemical Society*, *146*(8), 2906-2912.

HONG, J., SILVA, R. A., PARK, J., LEE, E., PARK, J., & KIM, H. 2016. Adaptation of a mixed culture of acidophiles for a tank bio-oxidation of refractory gold concentrates containing a high concentration of arsenic. *Journal of bioscience and bioengineering*, *121*(5), 536-542.

HU, G., DAM-JOHANSEN, K., WEDEL, S. & HANSEN, J. P. 2006. Decomposition and Oxidation of pyrite. *Progress in Energy and Combustion Science,* 32**,** 295-314.

HUANG, J. & ROWSON, N. 2002. Hydrometallurgical decomposition of pyrite and marcasite in a microwave field. *Hydrometallurgy,* 64**,** 169-179.

IGLESIAS, N. & CARRANZA, F. 1994. Refractory gold-bearing ores: a review of treatment methods and recent advances in biotechnological techniques. *Hydrometallurgy*, 34**,** 383-395.

JOHN, J., JOHNSON, N. W., STEWART, K., TURNER, D., & BRADSHAW, D. (2013). A review of pre-treatment methods to separate the different types of pyrite in gold processing. In 5th World Gold 2013 Conference (pp. 347-355). AusIMM: Australasian Institute of Mining and Metallurgy.

JONES, D.A, KINGMAN, S.W, WHITTLES, D.N, LOWNDES, I.S. 2005. *Materials Engineering*, 18, 659-669.

KADIOĞLU, Y. Y., KARACA, S. & BAYRAKÇEKEN, S. 1995. Kinetics of pyrite oxidation in aqueous suspension by nitric acid. *Fuel Processing Technology,* 41**,** 273-287.

KAKSONEN, A. H., MUDUNURU, B. M., & HACKL, R. 2014. The role of microorganisms in gold processing and recovery—A review. *Hydrometallurgy*, *142*, 70-83.

KETCHAM, V., O' REILLY, J. & VARDILL, W. 1993. The Lihir gold project; Process plant design. *Minerals Engineering,* 6**,** 1037-1065.

KING, J. & KNIGHT, D. 1992. Autoclave operations at Porgera. *Hydrometallurgy*, 29**,** 493-511.

KINGMAN, S. W., VORSTER, W., & ROWSON, N. A. 2000. The effect of microwave radiation on the processing of Palabora copper ore. *Journal of the South African Institute of Mining and Metallurgy (South Africa)*, *100*(3), 197-204.

KOLEINI, S. J., & BARANI, K. 2012. Microwave heating applications in mineral processing. *INTECH Open Access Publisher*.

KOMNITSAS, C. & POOLEY, F. 1989. Mineralogical characteristics and treatment of refractory gold ores. *Minerals Engineering,* 2**,** 449-457.

KOMNITSAS, K., XENIDIS, A. & ADAM, K. 1995. Oxidation of pyrite and arsenopyrite in sulphidic spoils in Lavrion. *Minerals Engineering,* 8**,** 1443-1454.

KOSLIDES, T. & CIMINELLI, V. 1992. Pressure oxidation of arsenopyrite and pyrite in alkaline solutions. *Hydrometallurgy,* 30**,** 87-106.

LA BROOY, S. R., LINGE, H. G., & WALKER, G. S. 1994. Review of gold extraction from ores. *Minerals Engineering*, *7*(10), 1213-1241.

LAAJALEHTO, K., KARTIO, I. & SUONINEN, E. 1997. XPS and SR-XPS techniques applied to sulfide mineral surfaces. *International Journal of Mineral Processing,* 51**,** 163-170.

LAMB, W. 2004. Optimising the value of the Lihir low-grade resource. Rio Tinto Technical Report No: AR2163. Project Code: GAL 144.

LAWSON, V., KERR, A. N., SHIELDS, Y., WELLS, P. F., XU, M., & DAI, Z. 2005. Improving pentlandite pyrrhotite separation at INCO's Clarabelle Mill. In *Centenary of Flotation Symposium. AusIMM, Brisbane* (pp. 875-885).

LEHMANN, M., O' LEARY, S. & DUNN, J. 2000. An evaluation of pretreatments to increase gold recovery from a refractory ore containing arsenopyrite and pyrrhotite. *Minerals Engineering,* 13**,** 1-18.

LI, J., DABROWSKI, B., MILLER, J., ACAR, S., DIETRICH, M., LEVIER, K. & WAN, R. 2006. The influence of pyrite pre-oxidation on gold recovery by cyanidation. *Minerals Engineering,* 19**,** 883-895.

LIDDELL, K. S., & ADAMS, M. D. 2012. Kell hydrometallurgical process for extraction of platinum group metals and base metals from flotation concentrates. *Journal of the Southern African Institute of Mining and Metallurgy*, *112*(1), 31-36.

LILLKUNG, K., & AROMAA, J. 2012. Hydrometallurgical recovery of platinum group metals. Aalto University publication series SCIENCE + TECHNOLOGY, 17/2012.

LONG, H. & DIXON, D. G. 2004. Pressure oxidation of pyrite in sulfuric acid media: a kinetic study. *Hydrometallurgy,* 73**,** 335-349.

LOVÁS, M., ZNAMENÁČKOVÁ, I., ZUBRIK, A., KOVÁČOVÁ, M., & DOLINSKÁ, S. 2011. The application of microwave energy in mineral processing–a review. *Acta Montanistica Slovaca*, *16*(2), 137.

MAHMOUD, A., CÉZAC, P., HOADLEY, A. F., CONTAMINE, F., & D'HUGUES, P. 2016. A review of sulfide minerals microbially assisted leaching in stirred tank reactors. *International Biodeterioration & Biodegradation*.

MARCHBANK, A. R., THOMAS, K. G., DREISINGER, D. & FLEMING, C. 1996. Gold recovery from refractory carbonaceous ores by pressure oxidation and thiosulfate leaching. U.S. Patent No. 5,536,297. Washington, DC: U.S. Patent and Trademark Office.

MARSDEN, J. & HOUSE, I. 2006. The chemistry of gold extraction, SME. Littleton, Colorado, USA ISBN-13: 978-0-87335-240-6 ISBN-10: 0-87335-240-8.

MARSDEN, J. O., BREWER, R. E., & HAZEN, N. 2003. Copper concentrate leaching developments by Phelps Dodge Corporation. *Electrometallurgy and Environmental Hydrometallurgy, Volume 2*, 1429-1446.

MASON, P. 1992. Examining the economics of some pressure oxidation process options. *Hydrometallurgy,* 29**,** 479-492.

MATIS, K., KYDROS, K. & GALLIOS, G. 1992. Processing a bulk pyrite concentrate by flotation reagents. *Minerals Engineering,* 5**,** 331-342.

MATTILA, S., LEIRO, J. & HEINONEN, M. 2004. XPS study of the oxidised pyrite surface. *Surface Science,* 566**,** 1097-1101.

MILBOURNE, J., TOMLINSON, M., & GORMELY, L. 2003. Use of hydrometallurgy in direct processing of base metal/PGM concentrates. *Hydrometallurgy, 2003,* 625.

MILLER, J. D., LI, J., DAVIDTZ, J. C., & VOS, F. 2005. A review of pyrrhotite flotation chemistry in the processing of PGM ores. *Minerals Engineering, 18*(8), 855-865.

MILLER, J., KAPPES, R., SIMMONS, G. & LEVIER, K. 2006. Pyrite activation in amyl xanthate flotation with nitrogen. *Minerals Engineering,* 19**,** 659-665.

MILLER, P., BROWN, A. 2005.Bacterial oxidation of refractory gold concentrates.

MILLER, P.C., 1997. The design and operating practice of bacterial oxidation plant using moderate thermophiles. In: Rawlings, D.E. (Ed.), *Biomining: Theory, Microbes and Industrial Processes*. Springer-Verlag, Berlin.

MONTE, M., LINS, F. & OLIVEIRA, J. 1997. Selective flotation of gold from pyrite under oxidising conditions. *International Journal of Mineral Processing,* 51**,** 255-267.

MPINGA, C. N., EKSTEEN, J. J., ALDRICH, C., & DYER, L. 2015. Direct leach approaches to Platinum Group Metal (PGM) ores and concentrates: A review. *Minerals Engineering*, *78*, 93-113.

MUBAROK, M. Z., WINARKO, R., CHAERUN, S. K., RIZKI, I. N., & ICHLAS, Z. T. 2016. Improving gold recovery from refractory gold ores through bio-oxidation using iron-sulfur-oxidising/sulfur-oxidising mixotrophic bacteria. *Hydrometallurgy*.

MURPHY, R. & STRONGIN, D. R. 2009. Surface reactivity of pyrite and related sulfides. *Surface Science Reports,* 64**,** 1-45.

NAKAMURA, H., SATO, S. & HARA, Y. 1994. The oxidation of pyrite. *Journal of hazardous materials,* 37**,** 253-263.

NANTHAKUMAR, B., PICKLES, C. A., & KELEBEK, S. 2007. Microwave pre-treatment of a double refractory gold ore. *Minerals Engineering*, *20*(11), 1109-1119.

NAZARI, G., DIXON, D. G., & DREISINGER, D. B. 2011. Enhancing the kinetics of chalcopyrite leaching in the Galvanox™ process. *Hydrometallurgy*, *105*(3), 251-258.

NEALE, J. W., PINCHES, A., & DEEPLAUL, V. 2000. Mintek-BacTech's bacterial-oxidation technology for refractory gold concentrates: Beaconsfield and beyond. *Journal of the South African Institute of Mining and Metallurgy(South Africa)*, *100*(7), 415-421.

NOWACZYK, K., & DOMKA, F. 2000. " Oxidation of Pyrite and Marcasite by Thiobacillus ferrooxidans Bacteria. *Polish Journal of Environmental Studies*, *9*(2), 87-90.

OBERBILLIG, E. 1964. Flotation of antimony ores. *Mining Mag*, 110.

O'CONNOR, C. & DUNNE, R. 1994. The flotation of gold bearing ores—a review. *Minerals Engineering,* 7**,** 839-849.

ÖHLANDER, B., MÜLLER, B., AXELSSON, M. & ALAKANGAS, L. 2007. An attempt to use LA-ICP-SMS to quantify enrichment of trace elements on pyrite surfaces in oxidising mine tailings. *Journal of geochemical exploration,* 92**,** 1-12.

ORUMWENSE, A. & NEGERI, T. 2004. The impact of microwave irradiation on the processing of a sulfide ore. *Minerals and Metallurgical Processing,* 21**,** 44-51.

PALMER, C. M., & JOHNSON, G. D. 2005. The Activox® Process: Growing significance in the nickel industry. *JOM*, *57*(7), 40-47.

PAPANGELAKIS, V. & DEMOPOULOS, G. 1991. Acid pressure oxidation of pyrite: reaction kinetics. *Hydrometallurgy,* 26**,** 309-325.

PRASAD, M., MENSAH-BINEY, R. & PIZARRO, R. 1991. Modern trends in gold processing—overview. *Minerals Engineering,* 4**,** 1257-1277.

RANKIN, W. J. 2013. *New flagship AusIMM Monograph: Australasian mining and metallurgical operating practices*. (The Sir Maurice Mawby Memorial Volume), Third Edition.

RAO, G. V. 2000. Nickel and cobalt ores: flotation. *Encyclopaedia of Separation Science, Academic Press, New York*, 3491-3500.

RAWLINGS, D. E. 2004. Microbially-assisted dissolution of minerals and its use in the mining industry. *Pure and Applied Chemistry*, *76*(4), 847-859.

ROYSTON, D., SPENCER, P. & WINBORNE, D. Alkaline Oxidation of Pyrite in Gold Recovery. Extractive Metallurgy Symposium: 12-14 November 1984, Melbourne, Vic., Australia, 1984. The Institute, 61.

SAND, W., GEHRKE, T., JOZSA, P. G., & SCHIPPERS, A. 2001. (Bio) Chemistry of bacterial leaching—direct vs. indirect bioleaching. *Hydrometallurgy*, *59*(2), 159-175.

SCHIPPERS, A., & SAND, W. 1999. Bacterial leaching of metal sulfides proceeds by two indirect mechanisms via thiosulfate or via polysulfides and sulfur. *Applied and environmental microbiology*, *65*(1), 319-321

SIMMONS, G. 1997. Flotation of Auriferous Pyrite Using Santa Fe Pacific Gold's N~ 2TEC Flotation Process. *PREPRINTS-SOCIETY OF MINING ENGINEERS OF AIME*.

SIRKECI, A. 2000. The flotation separation of pyrite from arsenopyrite using hexyl thioethylamine as a collector. *International Journal of Mineral Processing,* 60**,** 263-276.

SMART, R. S. C. 2014. *Innovations in the measurement of mineral structure and surface chemistry in flotation: Past, present, and future* (Doctoral dissertation, Society for Mining, Metallurgy and Exploration).

SOKIĆ, M. D., MARKOVIĆ, B. & ŽIVKOVIĆ, D. 2009. Kinetics of chalcopyrite leaching by sodium nitrate in sulfuric acid. *Hydrometallurgy,* 95**,** 273-279.

STONE, D. M., ENG, P., GODDEN, S. J., FIMMM, C., GAUNT, J. D.2007. G-9 DEPOSIT, CAMPO MORADO PROJECT.A technical report for Farallon Resources Ltd (*retrieved online*).

THOMAS, K. G. 1991. Alkaline and acidic autoclaving of refractory gold ores. *JOM,* 43**,** 16-19.

THOMAS, K. G., PIETERSE, H. J., BREWER, R. E. & FRASER, K. S. 1991. Process for recovery of gold from refractory ores. U.S. Patent No 5071477 A. Washington, DC: U.S. Patent and Trademark Office.

TONIAZZO, V., MUSTIN, C., PORTAL, J., HUMBERT, B., BENOIT, R. & ERRE, R. 1999. Elemental sulfur at the pyrite surfaces: speciation and quantification. *Applied Surface Science,* 143**,** 229-237.

TORRES, V. M., CHAVES, A. P. & MEECH, J. Intelligold-a fuzzy expert system for gold plant process design. Fuzzy Information Processing Society, 1999. NAFIPS. 18th International Conference of the North American, 1999. IEEE, 899-904.

USLU, T., ATALAY, Ü., & AROL, A. I. 2003. Effect of microwave heating on magnetic separation of pyrite. *Colloids and Surfaces A: Physicochemical and Engineering Aspects*, *225*(1), 161-167.

VORSTER, W. 2001. *The effect of microwave radiation on mineral processing* (Doctoral dissertation, University of Birmingham).

VORSTER, W., ROWSON, N. A., & KINGMAN, S. W. 2001. The effect of microwave radiation upon the processing of Neves Corvo copper ore. *International Journal of Mineral Processing*, *63*(1), 29-44.

WARRIS, C. & MCCORMICK, P. 1997. Mechanochemical processing of refractory pyrite. *Minerals Engineering,* 10**,** 1119-1125.

WATERS, K. E., ROWSON, N. A., GREENWOOD, R. W., & WILLIAMS, A. J. 2007. Characterising the effect of microwave radiation on the magnetic properties of pyrite. *Separation and purification technology*, *56*(1), 9-17.

WHITLOCK, J. L. 1997. Biooxidation of refractory gold ores (the Geobiotics process). *Biomining.* Springer.

WHITTLES, D.N., KINGMAN, S.W., REDDISH, D.J., 2003, Application of Numerical Modelling for Prediction of the Influence of Power Density on Microwave Assisted Grinding, Int. J. Min. Proc., 68, pp. 71-91.

WIGHTMAN, E. 2005. Bench scale testing to determine the potential for removal of low gold pyrite from Lihir ores. Rio Tinto Technical Report No: AR2448. Project Code: GAL 161.

WILLS, B. A., & NAPIER-MUNN, T. 2015. *Wills' Mineral Processing Technology: an introduction to the practical aspects of ore treatment and mineral recovery*. Butterworth-Heinemann.

WOOD, P. 2001. Intec's dendritic copper process poised for commercialization. *Metal Powder Report*, *56*(3), 26-30.

XIA, D. K., & PICKLESI, C. A. 2000. Microwave caustic leaching of electric arc furnace dust. *Minerals Engineering*, *13*(1), 79-94.

ZHANG, J., NGOTHAI, Y., WANG, H., WENG, W., ZHANG, Y., LIANG, W., ZHAO, J., MEI, Y., XIE, M. & JIA, Y. 2009. Flotation of pyritic refractory gold ores at high pH values. Proceedings: 8th World Congress of Chemical Engineering, Montréal, Québec, Canada, August 23–27, 2009: 8 p World Congress of Chemical Engineering (8th : 2009 : Montreal).

ZHANG, J., ZHANG, Y., RICHMOND, W. & WANG, H.-P. 2010. Processing technologies for gold-telluride ores. *International Journal of Minerals, Metallurgy, and Materials,* 17**,** 1-10.

ZHENG, X., MANTON, P., BURNS, F., CRAWFORD, A. & GRIFFIN, P. 2010. Operating strategies to maximise gold recovery at Telfer. *Minerals Engineering,* 23**,** 1159-1166.

CHAPTER 3

METHODOLOGY AND EXPERIMENTAL PROCEDURE

This chapter sets out the experiments (*Figure 3.1*) and experimental procedures adopted to investigate the hypothesis and this includes:

1. Sample preparation and characterisation studies
2. Metallurgical test work (*grinding, flotation and regrinding*)
3. Oxidation experiments
4. Bulk and surface analytical techniques applied to samples from the studies

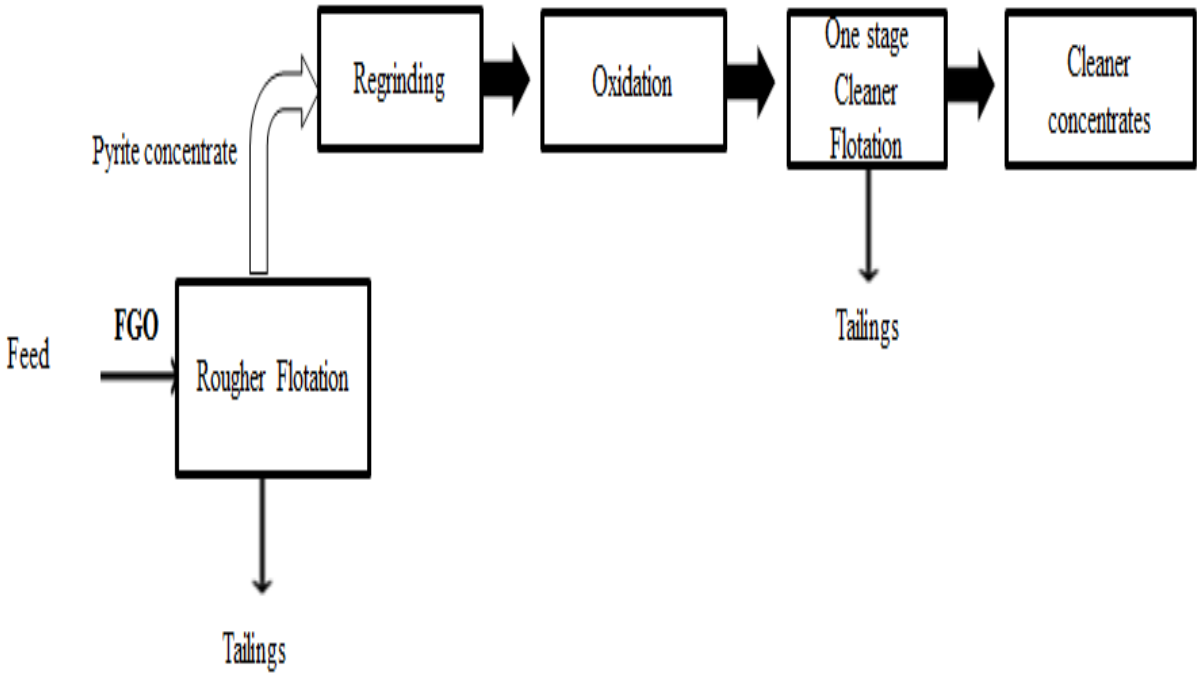

Figure 3.1: Experimental process flowsheet to test the hypothesis

3. Sample Preparation and Characterisation Studies

3.1.1 Ore sample

The sample (*190 kilogrammes*) of Lihir advanced argillic ore (*AA ore*) was used for this study and the sample was labelled as NTS 037 (*Newcrest Testing Site #37*). The ore used in this study was from Lihir gold mine (*Newcrest Mining Ltd*) which is located on Lihir Island in Papua New Guinea (*PNG*) as shown in Figures 3.2 and 3.3. Preliminary examination of the NTS 037 sample was conducted by the Newcrest Principal Mineralogist Dr Kathryn Stewart. The two most important prerequisites involved in the selection of the sample were:

1. Contain a broad range of pyrite types with varying gold content
2. Display a high sulfide sulfur grade (*above 10% S^{2-}*)

Preliminary investigation by Laser Ablation Inductively Coupled Plasma Mass Spectrometry (*LA-ICPMS*) of the advanced argillic ore (*AA ore*) confirmed a wide range of pyrite types in the NTS 037 sample. Head assay of the sample revealed a high sulfide sulfur content as shown in Table 3.1 (*above the Lihir autoclave threshold limit*) and was perfect for this study. The mineralogy of the ore sample will be discussed further in Chapter 4.

Table 3.1: Elemental composition of the AA ore with a very high sulfide sulfur grade

Au (*ppm*)	**As (*ppm*)**	**S_{total} (*%*)**	**$S_{sulfide}$ (*%*)**	**Fe (*%*)**	**Cu (*ppm*)**
3.6	**500**	**14.4**	**13.9**	**9.9**	**167**

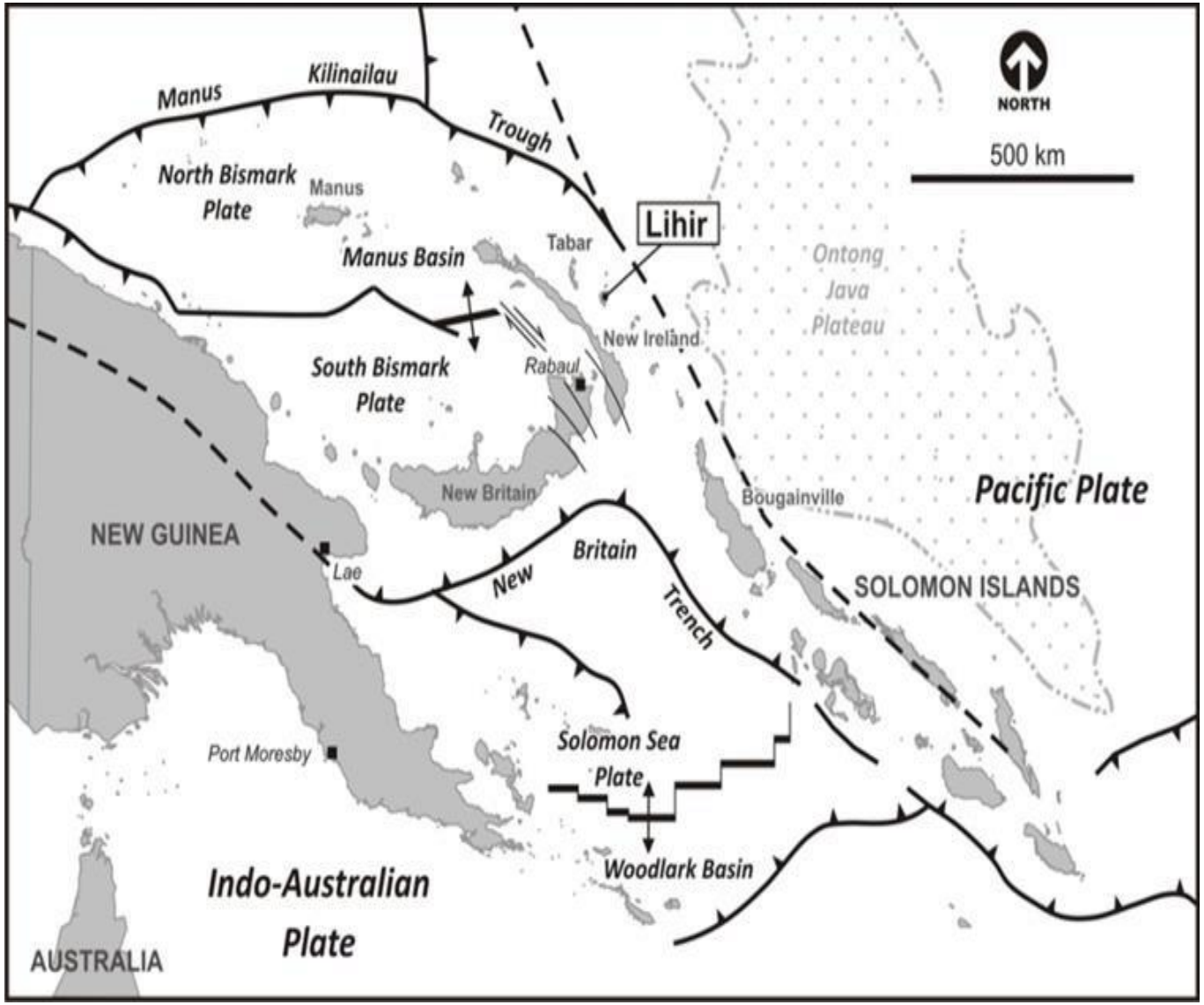

Figure 3.2: Lihir Regional Geology (Colin, 2013)

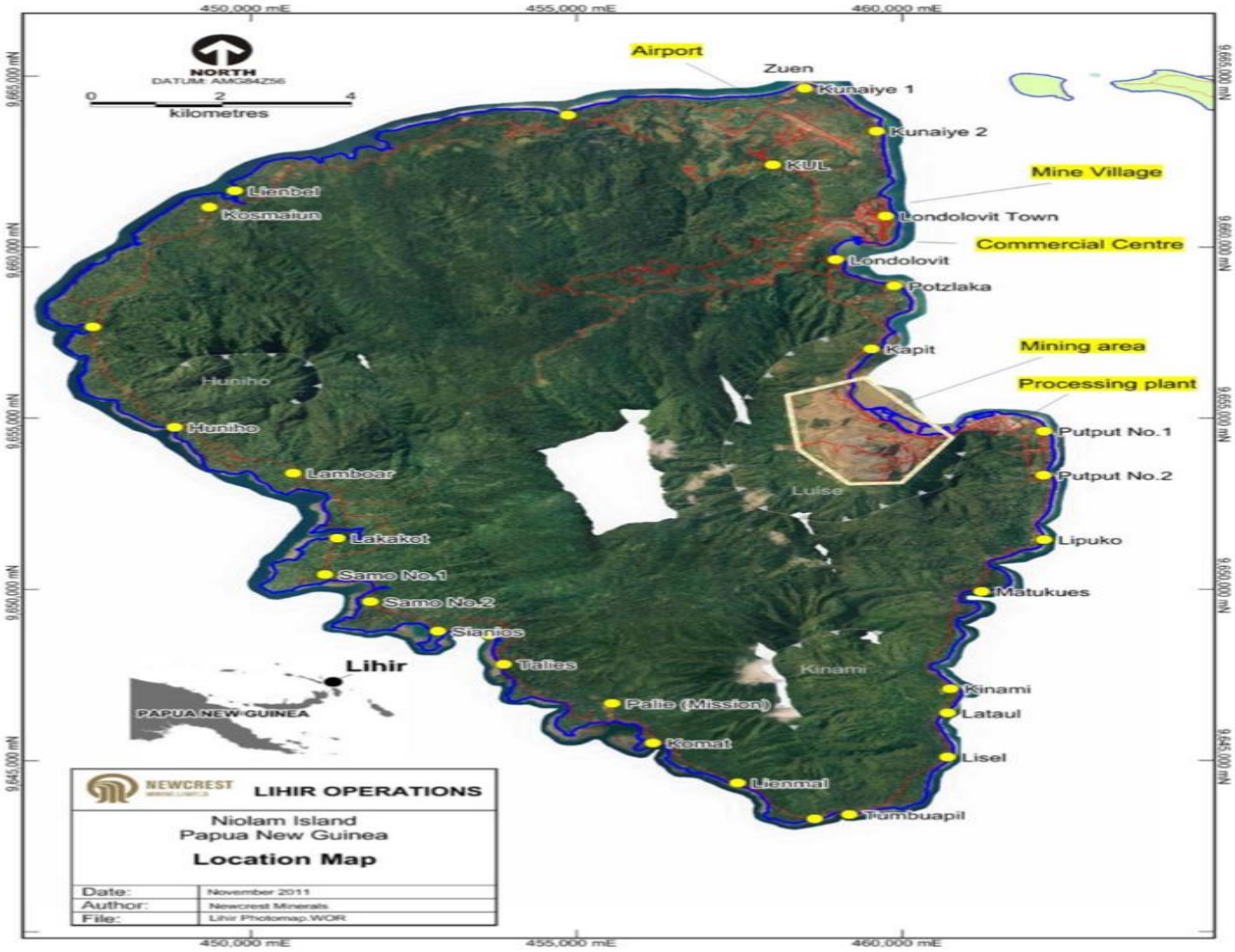

Figure 3.3: Lihir Location Map (Rankin, 2013)

3.1.2 Sample Preparation

The total mass of 190 kilogrammes of the AA ore sample was delivered to the Core Resources Hydrometallurgy Laboratory, Albion, Brisbane (*Queensland, Australia*). The author conducted all sample preparation at the Core Resources Hydrometallurgy Lab, Albion, Brisbane**.** The feed sample was dried prior to stage crushing to 100% minus 3.35 mm in a jaw crusher. After crushing, the sample was homogenised using a rotary divider and placed into sealed plastic sample bags and stored in a freezer. The processing stages involved in sample preparation are illustrated in Figure 3.4.

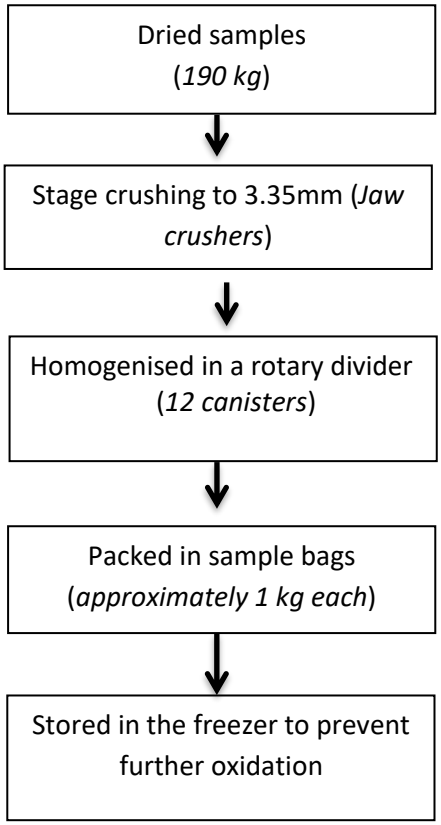

Figure 3.4: Processing Stages Involved in Sample Preparation

3.1.3 Characterisation Tests

Preliminary qualitative mineralogical studies were conducted using a Leica Q-Win Pro 3 optical microscope by the Newcrest mineralogist Dr Kathryn Stewart. Detailed mineralogical characterization of the NTS 037 AA ore sample using quantitative X-ray diffraction (*QXRD*) and the Scanning Electron Microscopy (*SEM*) based Mineral Liberation Analyser (*MLA*) system was also undertaken in the Newcrest laboratory, Brisbane. Gold mineralogy and comprehensive gold and arsenic deportment studies using LA-ICPMS were outsourced to Newcrest funded laboratory at CODES, University of Tasmania.

3.1.4 Mineral Liberation Analysis (MLA)

MLA measurements were also carried out at the JKMRC using an automated FEI Quanta 600 SEM with the MLA software to generate the BSE imagery to segment particles for subsequent analysis by the image processing software. For this purpose, MLA blocks were prepared by mixing the +53µm size fraction in an epoxy resin along with graphite to enhance particle separation. Due to density variations and rapid settling issues of the sulfide particles, the initial mounts were cut vertically into two after hardening and remounted to expose cross sections. After polishing, blocks were coated with a 250Å thickness of carbon to conduct the electron beam on the electrically insulating minerals in the SEM and prevent the build-up of surface charge on the block surfaces. Particular care was taken to prevent agglomeration of the particles. This was because agglomeration would detrimentally affect the particle size distribution and MLA measurements. This was conducted with a procedure that included wet and dry screening at 53 µm. Sizing analysis of samples in the sub-sieve range was performed using a Warman Cyclosizer as shown in Figure 3.5.

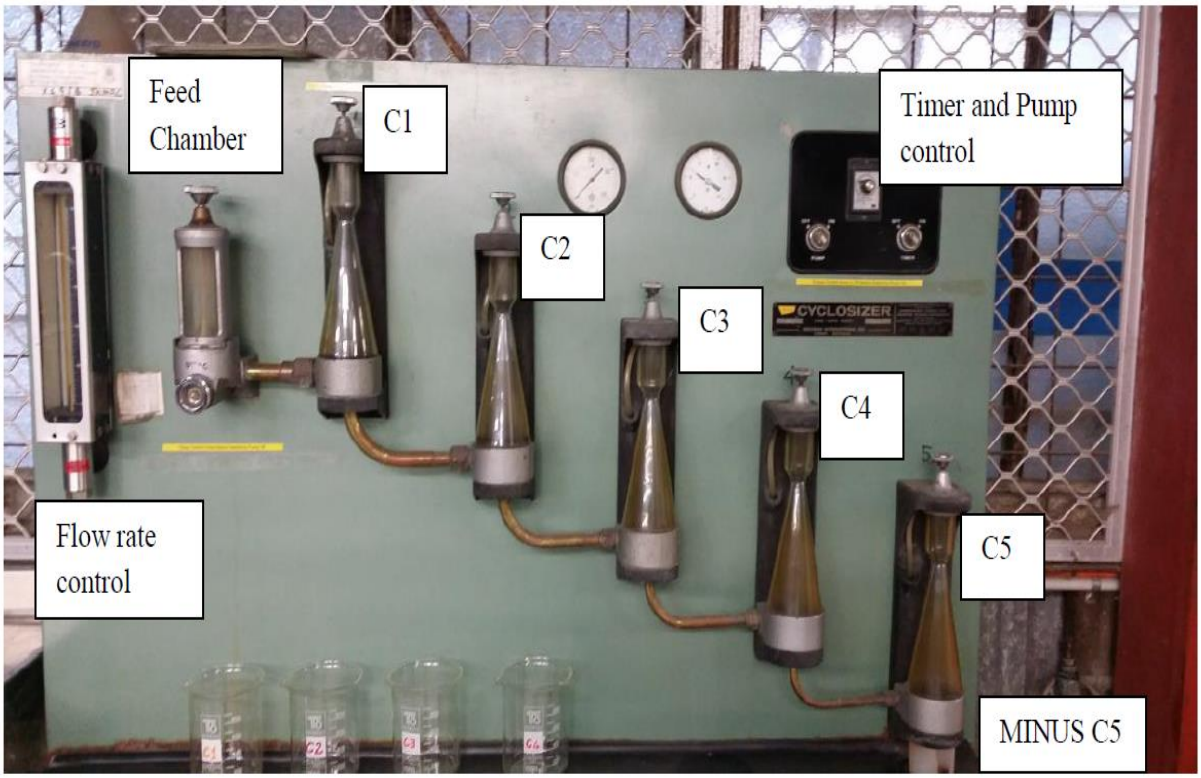

Figure 3.5: Warman cyclosizer at JKMRC, Indooroopilly

3.2 Metallurgical Test Work

3.2.1 Grind Size Establishment

The samples (*mill feed*) stored in the freezer were transferred into the wet laboratory grinding mill. The flotation feed was prepared by grinding the ore prior to each flotation test at a P80 of 106 µm. Grind size establishment was done (*three grind sizes*) to determine the grinding time to achieve a P80 of 106 µm. The required volume of lab water to achieve a 60% grind density was calculated from the flotation worksheet. Sub-samples (*2 kg*) of ore were ground at a solids concentration of 60 Wt. % solids using a rod charge of 29 kg for 2.36 minutes which is derived from the grind establishment curve shown in Figure 3.6. Since the metal ions that are released from the grinding media can affect the surface properties and floatability of the surface particles, stainless steel rods were used to grind the ore in the tests.

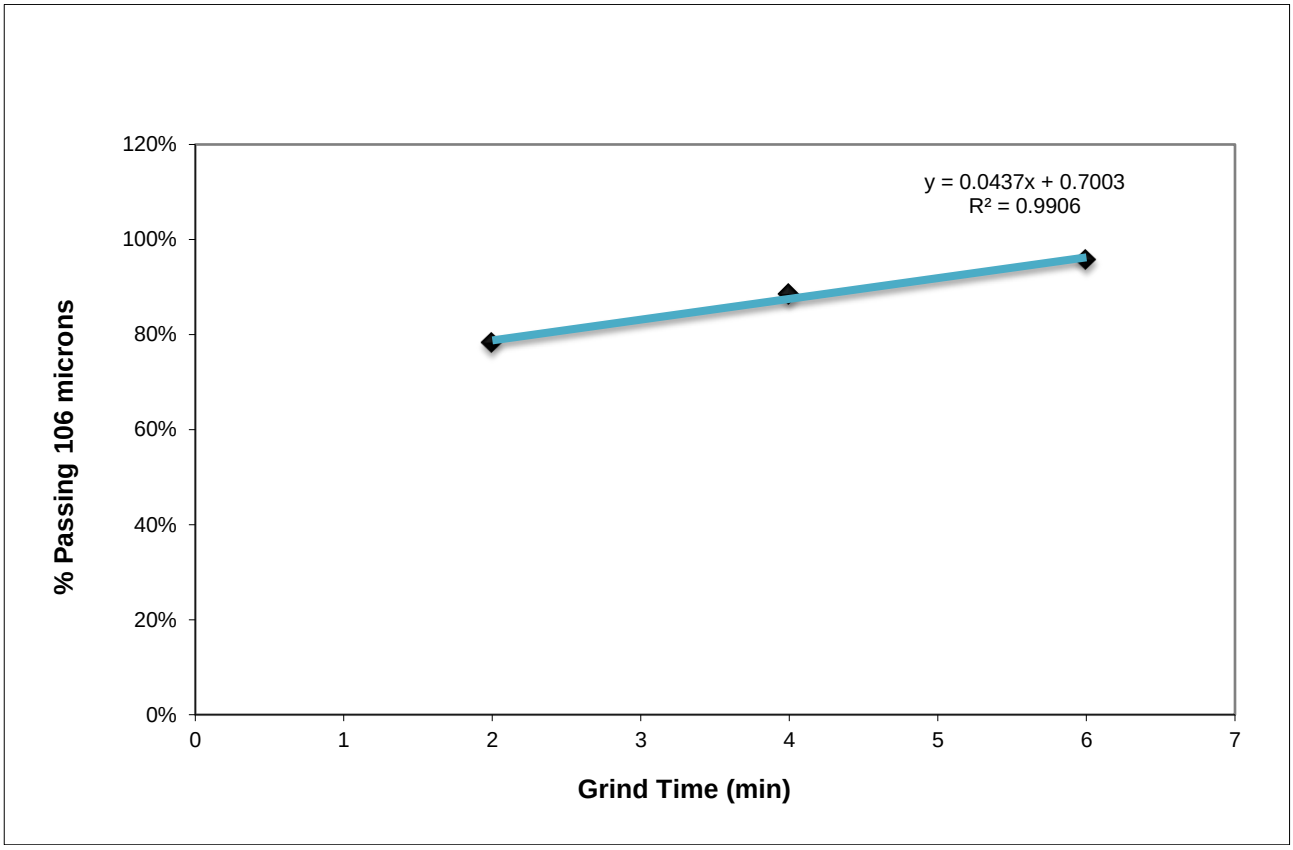

Figure 3.6: Grind size establishment curve for the NTS 037 AA ore sample

3.2.2 Flotation

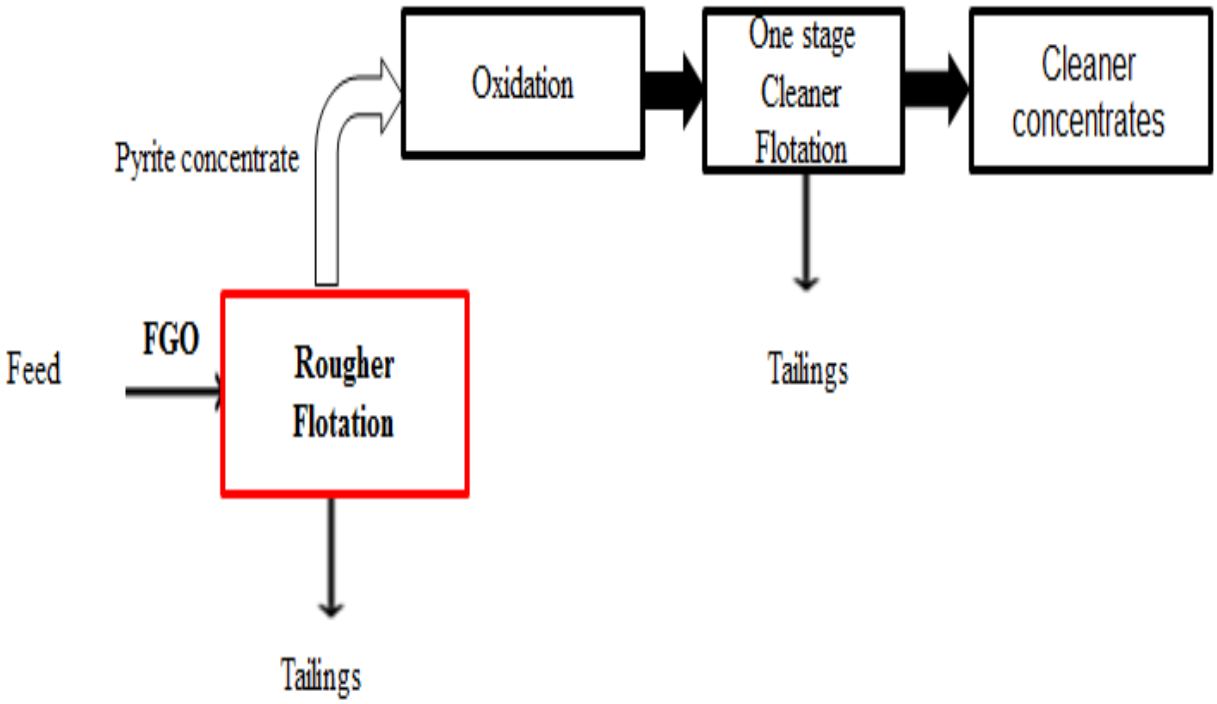

Figure 3.7: Red area highlights the rougher flotation process described in this section

All flotation experiments were conducted by the author at the Core Resources Hydrometallurgy Laboratory Albion, Brisbane. Flotation batch tests were performed using a JKMRC Runge flotation cell**.** The standard flotation conditions are shown in Table 3.2.

Table 3.2: Rougher flotation test conditions

Test Conditions	**Rougher Float Parameters**
Grind Size P80	106 µm
Float Cell Size	5L
Agitation	800 rpm
Air	5 L/min
Reagent	50g/t PAX Nascol 422
Pulp Density	33% solid by weight
Conditioning (*minutes*)	2 minutes
Float pH (*modifier*)	5 (*lime*) (*20kg/tonne)*
Flotation time (*minutes*)	incremental times of 2, 2, 4 and 4 minutes for a total time of 12 minutes

The natural pH of the ore was very acidic (*1.65*); hence to prevent collector degeneration, pH of the slurry was modified using lime (*to pH 5*) and the pulp potential was measured using a digital pH/Eh meter. A Standard reagent scheme, similar to that used at Lihir, was utilised for the experimental work and this consisted of potassium amyl xanthate (*PAX*) as the collector and Nascol 422 as the frother.

Considering the nature of the experiments, in some studies slight variations were made with the flotation time and this will be mentioned in the relevant chapters. The material safety data sheets (*MSDS*) for all the reagents required for the test were consulted prior to handling and usage. The solid PAX (*potassium amyl xanthate*) pellets required to prepare the PAX solution were fresh samples showing no signs of decomposition or ageing. The unused PAX solution was discarded as per laboratory procedures and fresh reagent solutions were prepared each day prior to the testing.

Sample trays (*CON1, CON2, CON3 and CON4 as required*) were placed next to the flotation machine. The weight of the flotation cell, as well as the empty trays, was recorded in the log sheet prior to the test. The mill product ground in the laboratory rod mill was transferred into the flotation cell. The remnants were washed into the cell, making sure that the total volume of contents in the cell did not exceed the static volume. The cell was placed in the housing and the impeller was turned on to agitate the charge to maintain the pulp suspension. Required dosages of the collector (*PAX*) and frother (*Nascol 422*) were added using a syringe and the pulp was conditioned for 2 minutes. The CON 1 tray was placed under the cell lip and the air was introduced to bring the froth level up to the cell lip but not high enough to overflow. Every ten seconds the froth layer was removed from the cell by scraping off the froth into the tray using a single continuous motion for 2 minutes. Laboratory water was used to wash down froth layer remnants from the sides of the cell (*back into the cell*) and the froth on the cell lip and also the scraper (*into the tray*). To replace the water entrained in the froth and maintain the pulp level in the cell, water was added to the cell as required.

Four concentrates (*in some cases 3 concentrates: Chapters 4, 6 and 8*) were collected at intervals of 2, 2, 4 and 4 minutes and the water recoveries were measured. The contents of the cell (*tailing*) were removed and weighed. The concentrates and tailing were filtered using a filter press and dried at 70^{o}C. The dried samples were then weighed and sent to the ALS assay laboratory (*Stafford, Brisbane*) to be analysed for gold (*Fire assay*), sulfide sulfur (*LECO method*), sulfate, carbonates and arsenic. Total sulfur was determined directly using a Leco Carbon/Sulfur Determinator.

Elemental sulfur was determined on a Leco Carbon/Sulfur Analyser combusted at a low temperature (*300°C*). Sulfate sulfur was determined by hydrochloric acid digestion and sulfides were quantified indirectly by difference following the determination of the other sulfur species. Flotation data (*mass recoveries and elemental analyses*) were found reproducible with a standard error of ±1.50%.

3.2.3 Regrinding

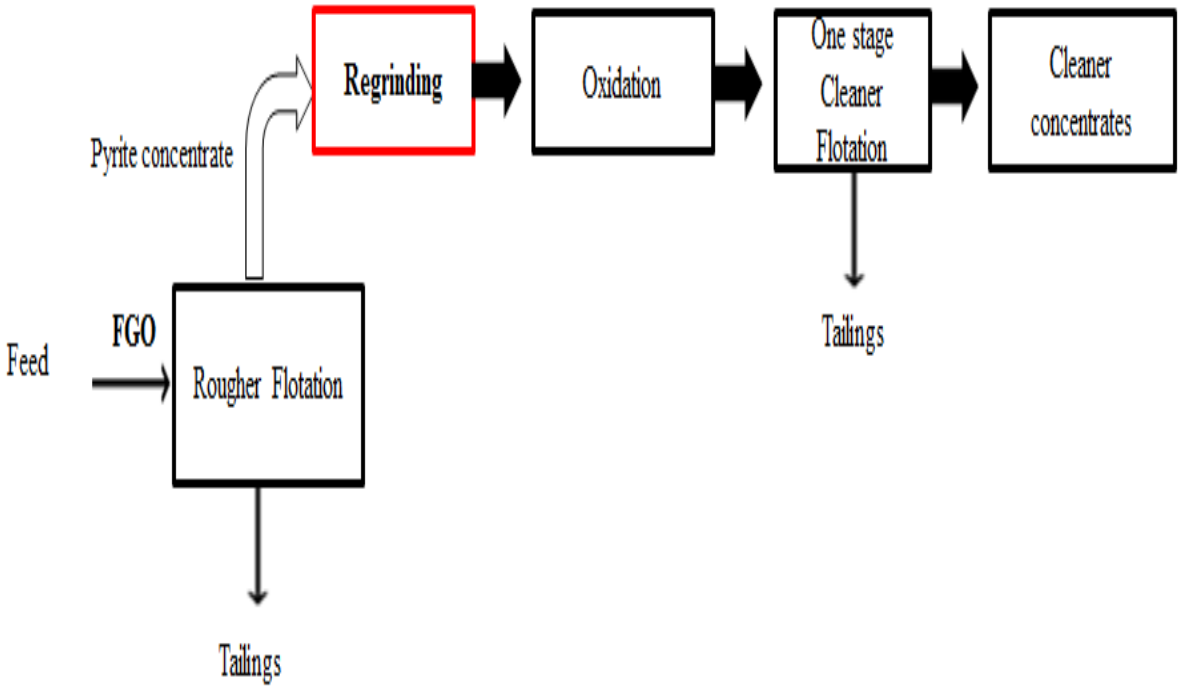

Figure 3.8: Red area highlights the regrinding process described in this section

The four rougher flotation concentrates were combined and then reground in a vertical stirred mill. The regrinding time was 2.5 minutes at a rotational speed of 800 RPM to achieve a P80 of 38 µm (*determined by a Malvern mastersizer*). Ceramic beads with a diameter of 2.5 mm were used as the grinding media. The reground products were then subject to further oxidation tests to verify the hypothesis that enhanced oxidation rates and other effects from regrinding will cause an improved separation of the various pyrite types resulting in a higher Au:S values in comparison with just altered chemical conditions.

3.3 Oxidation

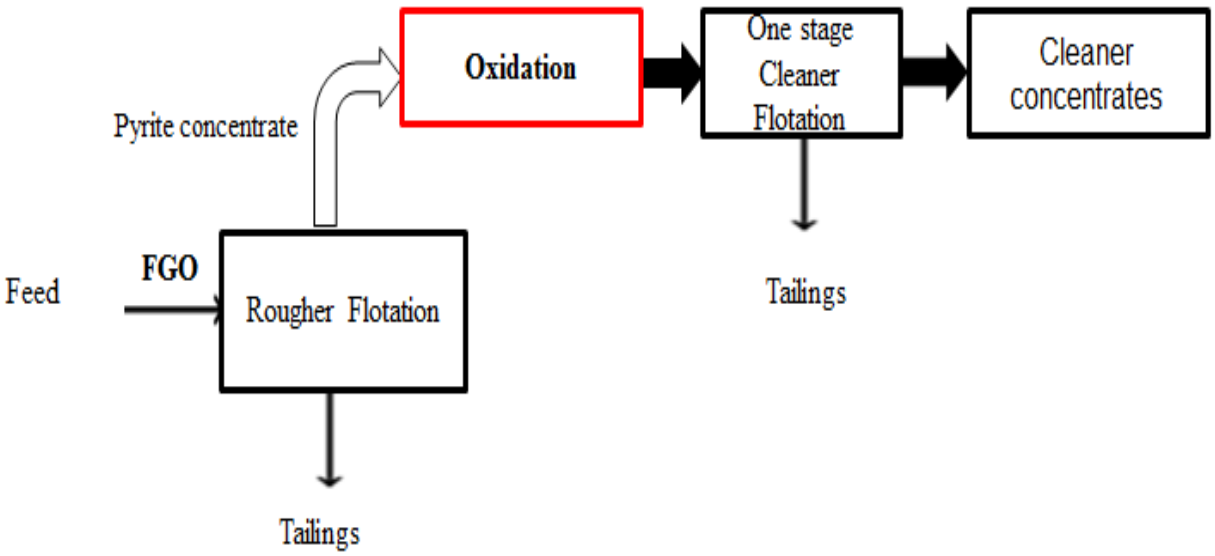

Figure 3.9: Red area highlights the oxidation process described in this section

3.3.1 Percent Solids and Percent Moisture Content

It was important to measure the percent solids in the sample prior to treating the float filter cake in oxidation tests. Hence the following procedure was adopted.

1) The empty sample container weight was recorded.
2) The slurry sample and sample container were weighed on the analytical balance.
3) The sample was filtered by a filter press.
4) The sample was dried in the oven at 70^{o}C
5) After drying, the sample was weighed and the value for the percentage of solids was calculated using the following formula:

$$\% \text{ Solids} = \frac{[(\text{Dry sample weight} + \text{paper weight}) - \text{Paper weight}]}{[(\text{Weight of container} + \text{slurry}) - \text{Container weight}]} * 100 \quad \ldots\ldots 1$$

The percentage moisture was calculated using the formula given below:

$$\% \text{ Moisture} = 100 - \% \text{ Solids} \quad \ldots\ldots 2$$

3.3.2 Oxidation Experiments

Aliquots of the flotation concentrate were reacted in different strengths of oxidising acids to understand the reactivity. The information regarding the reactivity of the acid with the pyrite concentrate and the duration of the reaction helped to design all future oxidation experiments. This included testing various acid strengths from 5 to 50 g/L at ambient temperature and altering the reaction (*oxidation*) time intervals from 10 to 70 minutes.

Visually, 5 g/L was too low concentration to induce any change in the concentrate and the SO_x analysis and flotation data confirmed this (*not shown in this thesis*). These trial experiments (*10% solids*) were conducted in 500 mL conical flasks. The pH was checked periodically but was not adjusted. Among the different oxidising agents, sulfuric acid and nitric acid (*10 g/L*) were found optimum because they did not char the surface of the rougher concentrate but were still effective to oxidise the pyrite concentrate. This was confirmed by SOx and XPS measurements which will be discussed further in Chapters 7 and 8.

3.3.3 Acid Oxidation Set-up

Each oxidation experiment was carried out on a pyrite concentrate generated from the rougher flotation test. The chemical composition of the rougher concentrate is shown in Table 3.3.

Table 3.3: Chemical composition of the pyrite concentrate

Au	Fe	S	As	Cu
7.83 ppm	23.5%	38.2%	1130 ppm	0.10 %

The approach in this work was to preferentially oxidise the high gold pyrite relative to the low gold pyrite in the concentrate and therefore, a mild oxidation process was adopted to prevent the complete destruction of all pyrite types. The pyrite concentrate was oxidised at ambient temperature in a 5000 mL sealed glass vessel (*to prevent air ingress*) as shown in Figure 3.10 under the following conditions: the rate of stirring, 500 rpm; concentration of acid, 10 g/L (*based on concentrated acid*); the volume of aqueous solution, 4500 mL; pulp density *(% solid*s), 10% by weight. Various batch tests for different oxidising times were conducted in duplicate to understand the effect of the extent of oxidation on the metallurgical responses of gold and sulfide sulfur.

Four hundred grams of the concentrate were combined with 4.0 L of the oxidising solution (*nitric acid or sulfuric acid*) in a 5-litre capacity baffled beaker. The oxidation experiments were conducted at an ambient temperature at different durations from to 10 to 70 minutes. The oxidised concentrates were rinsed with water to prevent any further surface changes due to acid reactivity. Aliquots of the samples were frozen in liquid nitrogen and submitted for diagnostic measurements (*surface and bulk analysis*) which will be discussed in detail later. The remaining oxidised sample was filtered and subjected to subsequent cleaner flotation tests.

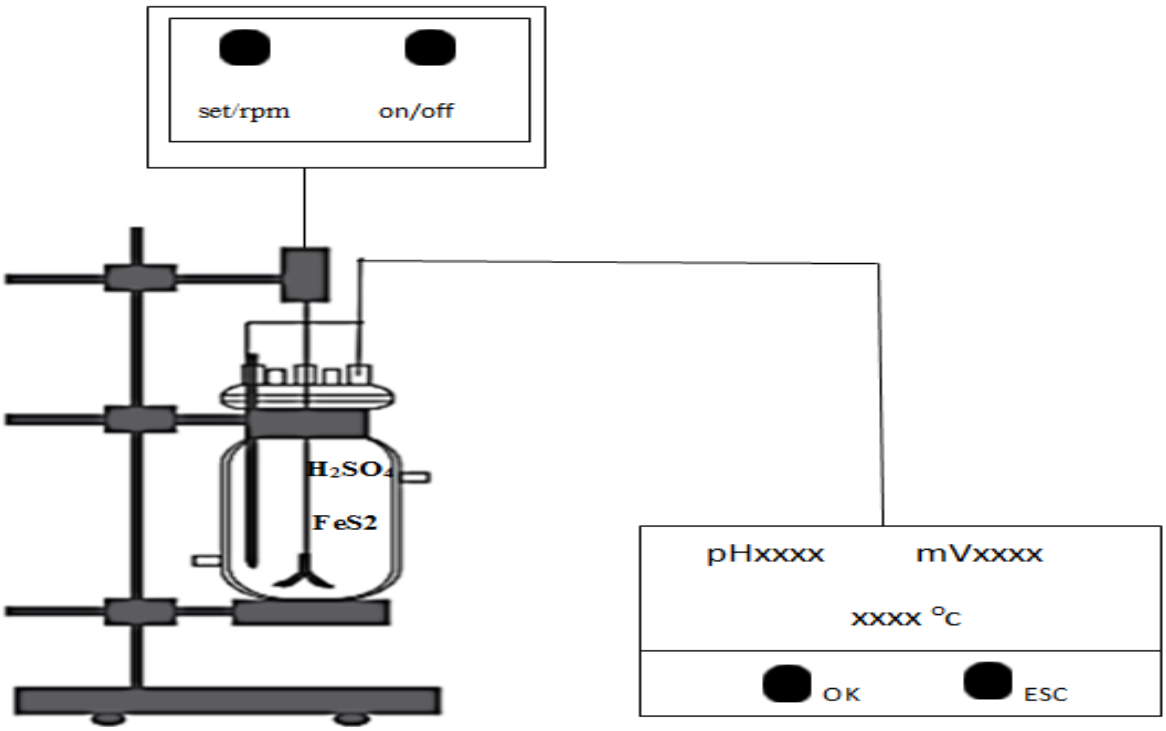

Figure 3.10: Set-up of oxidation of sulfide concentrates. Nitric acid and sulfuric acid (10 g/L) were used as chemical etchants to modify the sulfide concentrate for preferential separation of various pyrite types

3.3.4 Cleaner Flotation

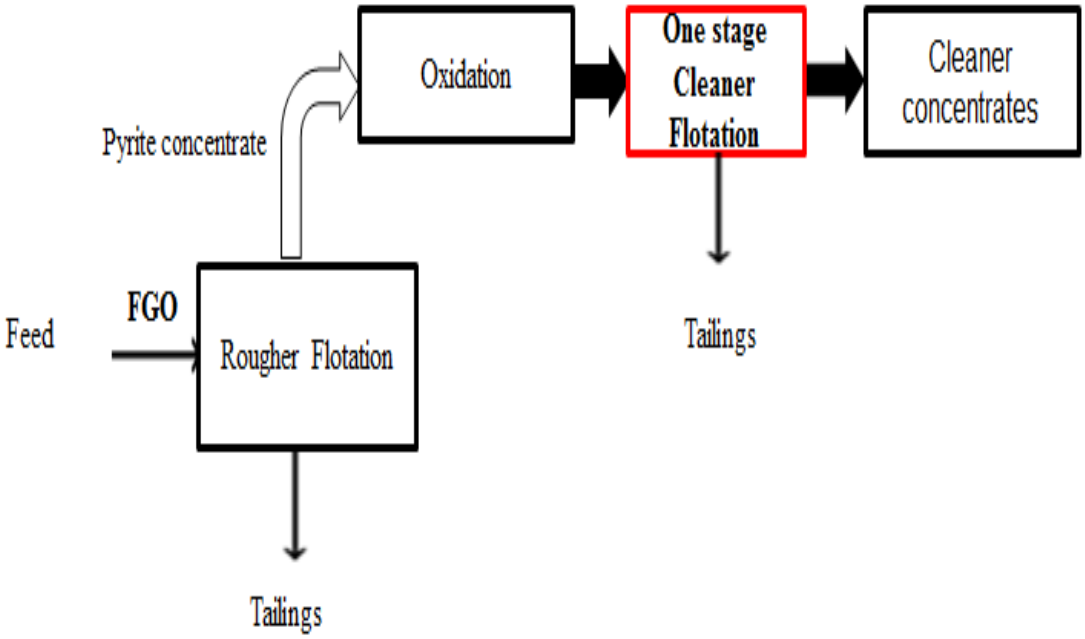

Figure 3.11: Red area highlights the one stage cleaner flotation process described in this section

Metallurgical responses of the oxidised samples were evaluated with one stage cleaner flotation test. The test conditions (*blue column*) are shown in Table 3.4.

Table 3.4: Cleaner flotation test conditions

Test Conditions	Cleaner Float
Float Cell Size	2.5L
Agitation	250 rpm
Air	5 L/min
Reagent	20g/t PAX Nascol 422
Pulp Density	10% solid by weight
Conditioning (*minutes*)	2 minutes
Float pH	11
Flotation Time (*minutes*)	incremental times of 2, 2, 4 and 4 minutes for a total time of 12 minutes

3.4 Diagnostic Measurements

3.4.1 Brunauer–Emmett–Teller (BET)

Surface area determinations were performed at the Department of Chemical Engineering (*University of Queensland*) using a Micrometrics Tri-star unit following the standard BET method (Brunauer et al., 1938). BET results were found reproducible with a standard error of ±1.25%.

3.4.2 Sulfide Sulfur Oxidation

The extent of sulfide sulfur oxidation (*SOx*) is the mass of oxidised sulfides at the end of the oxidation test and was calculated as shown in equations 3, 4, 5 and 6. In this study, the SOx study was modified to suit the purpose as no kinetic samples were withdrawn during the test. The masses of the initial and final residues were recorded and the final SOx calculations were based on these. Detailed calculations have been shown in Appendices 4.1, 4.4 and 5.1.

S^{2-} in head (g) = Mass of Feed x $S^{2\text{-Head}}$ assay……...……3

S^{2-} in Sample (g) = Mass of Test products x $S^{2\text{-sample}}$ assay of Final Kinetic…….4

S^{2-} in Residue (g) = S^{2-} in head - S^{2-} in Sample…….5

Final SOx % by mass of test products= ($S^{2-\ \text{Residue}}$/ $S^{2\text{-Head}}$) *100……..……..……..6

3.4.3 X-Ray Photoelectron Spectroscopy (XPS)

XPS, a surface analysis technique, was used to analyse the changes on pyrite surfaces pre-and post-oxidation, using a KRATOS Axis Ultra (*Kratos Analytical, Manchester, United Kingdom*) at the Centre for Microscopy and Microanalysis (*CMM*), University of Queensland. The analysis spot size was 300 × 700 μm. The frozen samples were placed on a stainless-steel bar and loaded into the XPS spectrometer. Samples were analysed at room temperature using a pass energy of 160 eV. Iron and sulfur spectra (*Fe2p, S2p, and* SO_4^{2-}) were collected at 20 eV pass energy with 2 or 3 sweeps.

3.4.4 Time-of-Flight Secondary Ion Mass Spectrometry (ToF-SIMS)

Time-of-Flight Secondary Ion Mass Spectrometry is a surface analytical technique that was used to identify and map surface species on individual pyrite grains (*pristine and oxidised*). The mass spectra from the highly surface sensitive technique were used for elemental and molecular mapping to generate information regarding collector attachment and copper ion activation. ToF-SIMS

experiments were conducted on a Physical Electronics Inc. PHI TRIFT V nano TOF instrument under a vacuum of $5x10^{-6}$ Pa. The spatial resolution of +SIMS and –SIMS images were optimised using unbunched Au_1 ToF-SIMS settings and calibrated using the standard WincadenceN software. Data were collected from ~25 pyrite particles to ensure representative data from each sample.

3.4.5 Image Analysis

The lack of suitable surface and bulk analytical techniques to distinguish one type of pyrite from another motivated the development of a novel mineral characterisation technique for distinguishing between low arsenic pyrite and high arsenic pyrite species in a refractory gold ore using BSE images from an SEM-based automated mineralogy system, in this case, an MLA system. The scientific image analysis program ImageJ was used to perform a full set of imaging manipulations of the unoxidised (*pristine*) and oxidised samples and this will be discussed in detail in Chapter 5. Although the MLA system is equipped with advanced image analysing capabilities for particle de-agglomeration and phase segmentation (Fandrich et al., 2007), the use of ImageJ program to analyse the BSE images helped to develop a new approach to identify the oxidation characteristics of various pyrite types. The BSE images generated by the MLA system were analysed using the ImageJ program as shown by the flowsheet in Figure 3.12. Ease of use, license-free application, compatibility with all operating systems and support for all common file formats used in mineral imaging uniquely positions ImageJ among other image processing programs. The application of image analysing software enabled comparison of the effect of oxidation between different pyrite types.

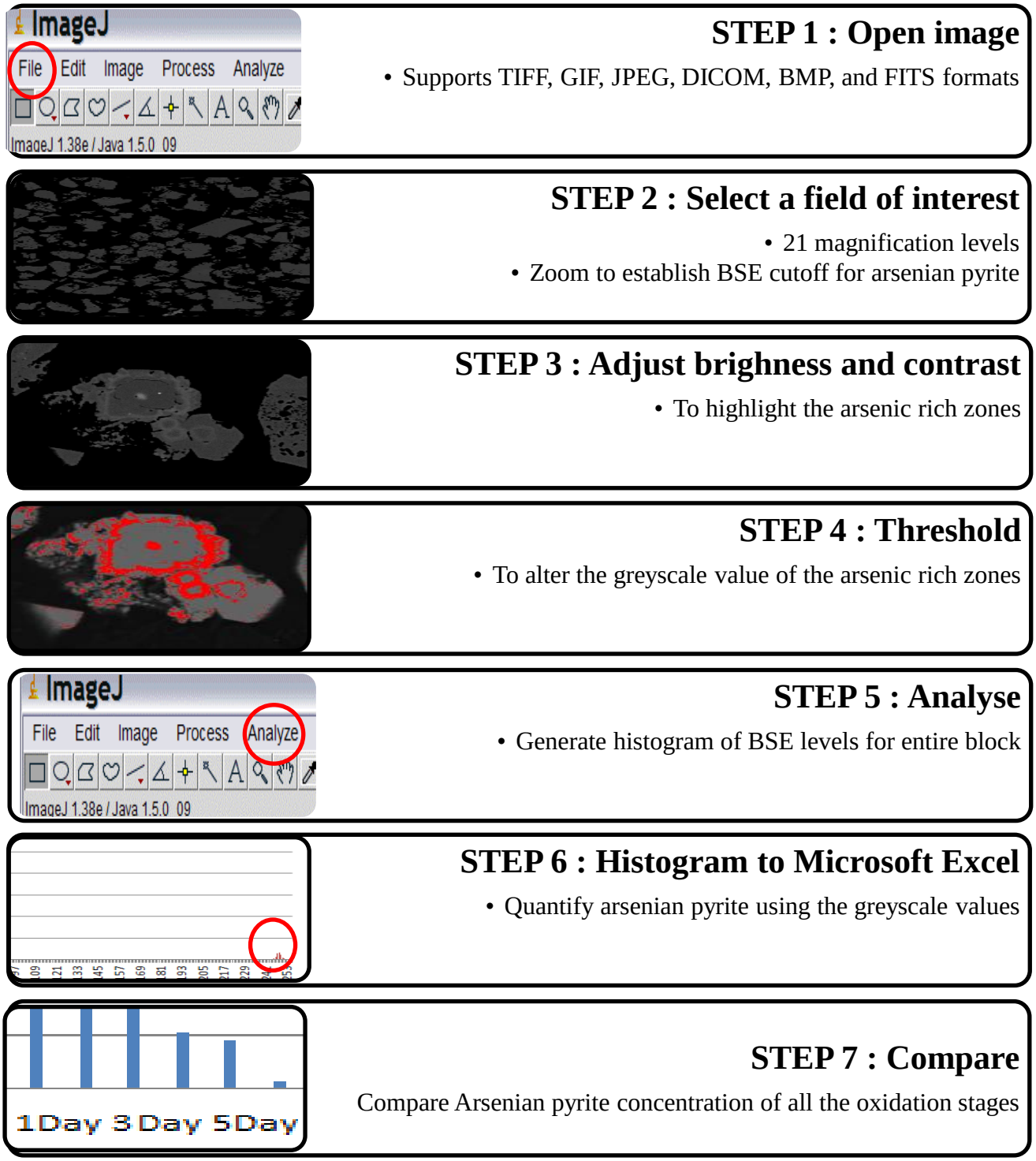

Figure 3.12: Screenshots of the steps involved in ImageJ processing of BSE images

3.5 Bibliography

BRUNAUER, S., EMMETT, P. H. & TELLER, E. 1938. Adsorption of gases in multimolecular layers. *Journal of the American Chemical Society,* 60**,** 309-319.

COLIN, M .2013.Technical report on the Lihir property in Papua New Guinea (*Prepared by Newcrest Mining Limited in accordance with the requirements of National Instrument 43-101, Standards for Disclosure of Mineral Projects, of the Canadian Securities Administrators).*

FANDRICH, R., GU, Y., BURROWS, D. & MOELLER, K. 2007. Modern SEM-based mineral liberation analysis. *International journal of mineral processing,* 84**,** 310-320.

WHITE, S. P., CREIGHTON, A. L., BIXLEY, P. F. & KISSLING, W. M. 2004. Modelling the dewatering and depressurization of the Lihir open-pit gold mine, Papua New Guinea. *Geothermics,* 33**,** 443-456.

CHAPTER 4

Process Mineralogy and Flotation Response of an Advanced Argillic Ore

This chapter discusses the mineralogical and chemical characterisation of an advanced argillic gold ore. Mineralogical analysis revealed gold was associated with sulfides in the ore and occurred in a sub-microscopic form in solid solution. The ore was categorised as advanced argillic due to the high amounts of alunite, manganese-bearing carbonates, leucoxene and K-Feldspar associated with a suite of pyrophyllite type clays, kaolinite, barite, illite, chlorite and muscovite. Since the aim of this work includes producing a pyrite-rich concentrate for subsequent oxidation process, batch scale flotation tests at different pH conditions were conducted to optimise the sulfide sulfur and gold recoveries.

Keywords: Mineralogy, Flotation, Advanced Argillic, Gold, Pyrite, Arsenic

4. Introduction

Lihir is an open pit mining operation comprising three separate mining deposits: Minifie, Lienetz and Kapit (Ketcham et al., 1993, Rankin, 2013). Newcrest Mining Ltd owns 100 percent of the property and gold dore is the main metal of economic significance from the operation. The deposit contains an estimated mineable resource of about 43 million ounces of gold (Müller et al., 2001).

4.2 Hydrothermal alterations

The deposit is a mixture of brecciated volcanics of epithermal origin (White et al., 2010) with a vast majority of the deposit undergone argillic alteration. The refractory nature of the deposit is attributed to the occurrence of sub-microscopic gold in the pyrite grains. Exploration has identified potassic and proplytic phases of alteration leading to five main assemblages of the Lihir mineral deposit as shown in Figure 4.1 and they are:

1. Argillic
2. Advanced Argillic (*AA*)
3. Boiling Zone (*BZ*)
4. Leach-soaked (*LS*)
5. Anhydrite Seal (*AS*)

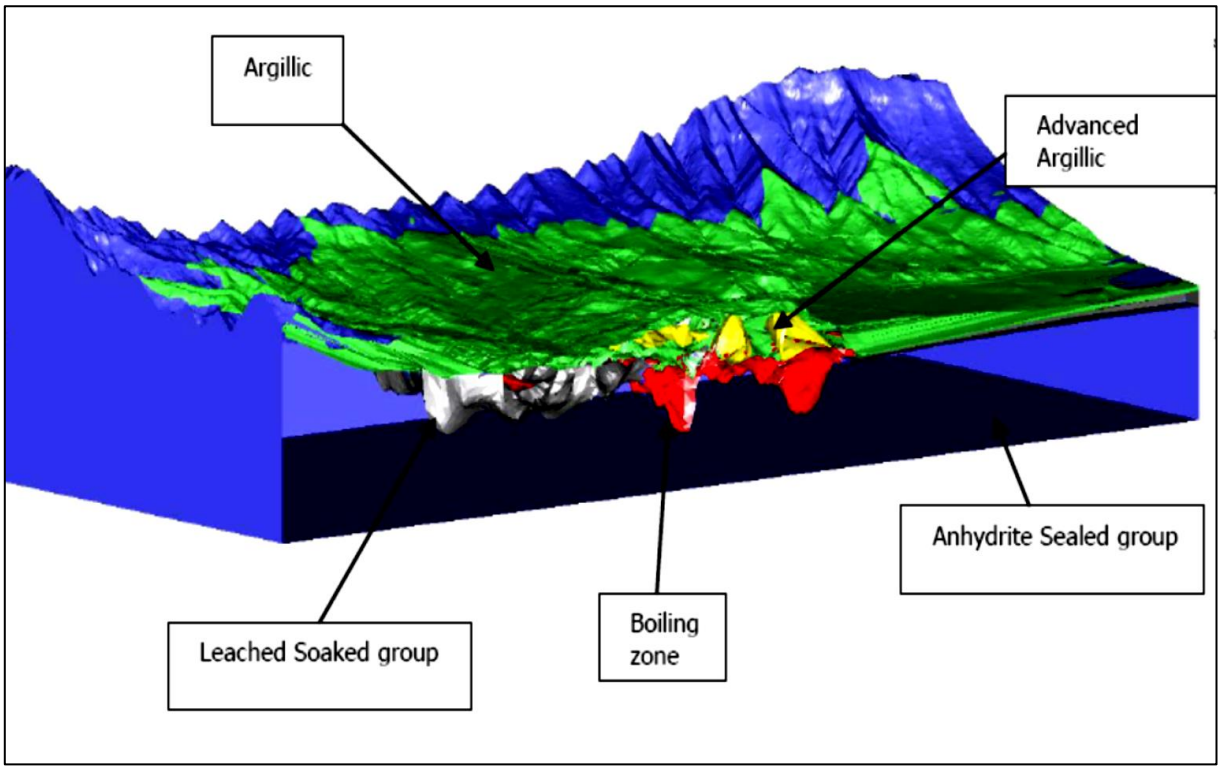

Figure 4.1: 3D representation of Lihir alteration domains (Rankin, 2013)

4.3 Ore Characterisation

The advanced argillic ore (*AA ore*) from the Kapit mineralised area is the sample of interest in this study. This is because the AA ore samples contain a wide range of pyrite types, a high sulfide sulfur grade and future mining at Lihir is expected to extend to the Kapit mineralised area. The various structural domains at Lihir are shown in Figure 4.2. The AA ore is highly refractory in nature yielding less than 30% gold recovery by direct cyanidation. This means that the gold is associated with the fine-grained reactive sulfides and requires pre-treatment such as pressure oxidation to recover the contained gold values (Marsden and House, 2006). The gold associated with the sulfides (*as inclusions*) in the AA ore occurs in the sub-microscopic form in pyrite as shown in Figure 4.3 (*also the relationship between Au content and Arsenic concentration*).

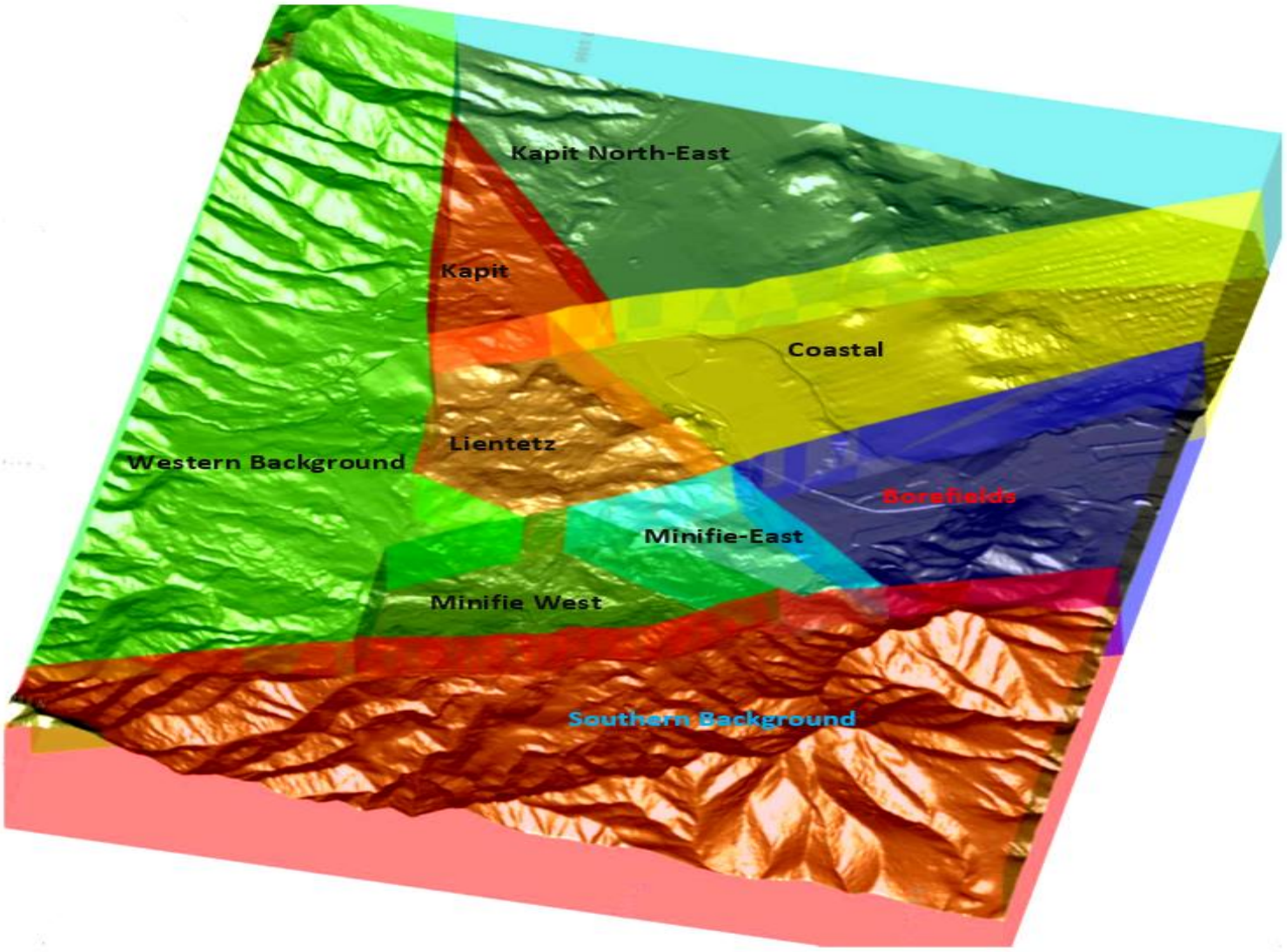

Figure 4.2: Structural domains at Lihir (Colin, 2013)

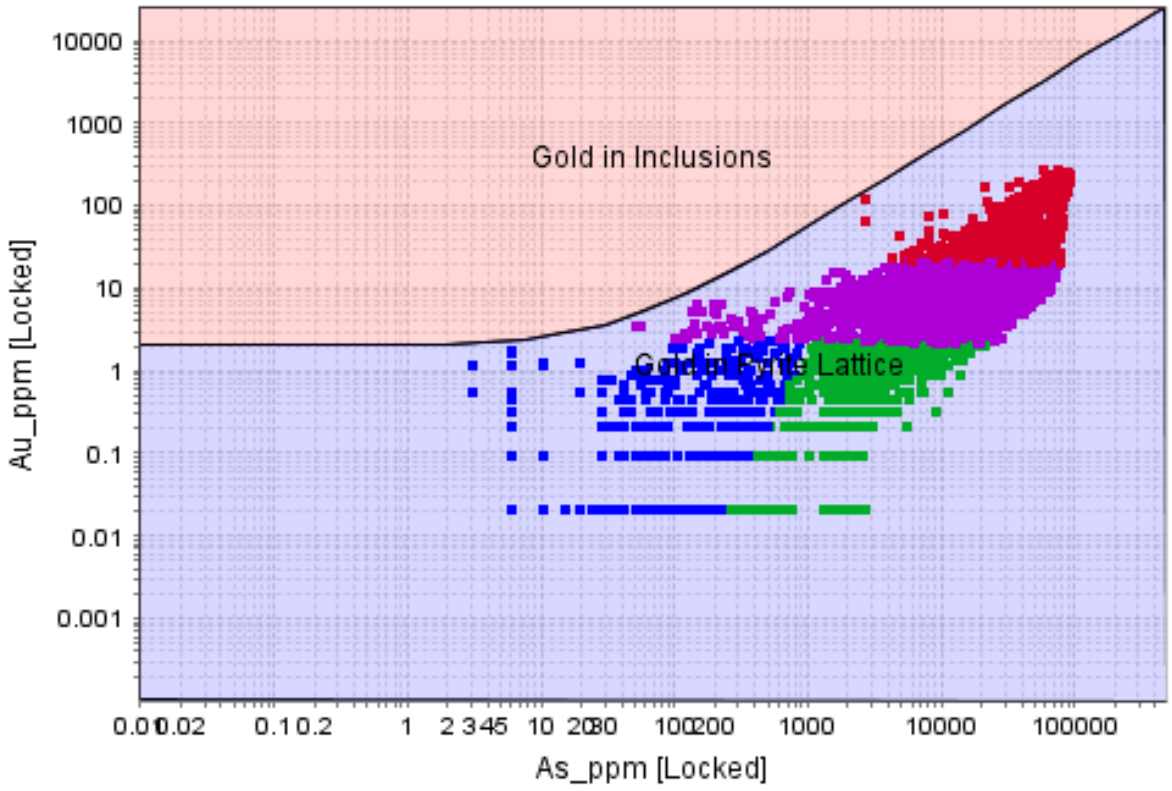

Figure 4.3: Gold solubility in pyrite for Lihir AA ore

(*Courtesy: Newcrest unpublished data; LA-ICPMS measurement undertaken at CODES*)

The advanced argillic ore is high clay, soft and sticky containing significant amounts of alunite (Ketcham et al., 1993). The head assay of the sample confirms the high sulfide sulfur grade of the sample as reported in Table 4.1.

Table 4.1: Elemental composition of the AA ore

Au (*ppm*)	As (*ppm*)	S_{total} (%)	$S_{sulfide}$ (%)	Fe (%)	Cu (*ppm*)
3.6	**500**	**14.4**	**13.9**	**9.9**	**167**

The AA ore samples contain pyrite, pyrophyllite, and some jarosite, as well as illite, smectite, kaolinite and muscovite. The sample can be classified as advanced argillic because it contains significant amounts of alunite as shown in Figure 4.4, which differentiates it from argillic ore which contains little alunite.

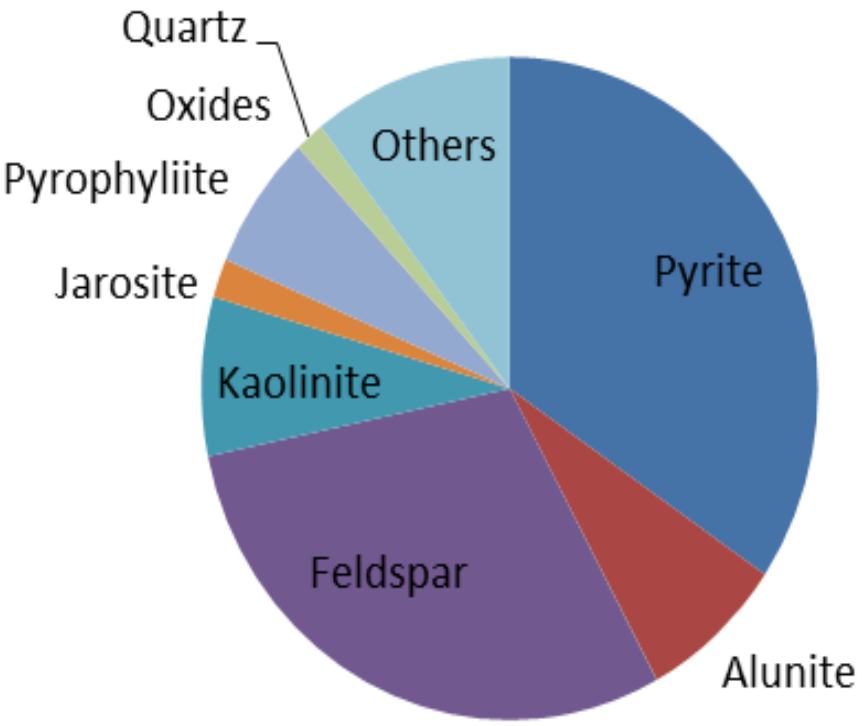

Figure 4.4: Modal mineralogy of the ore

The advanced argillic samples also contain pyrophyllite, and some jarosite, as well as illite, kaolinite and muscovite. However, despite containing pyrophyllite, no attempt was made to float the ore without a collector. This is because standard Lihir flotation practices (*PAX as the collector*) were adopted in this testwork which will be discussed further in the flotation section of this chapter. The advanced argillic alteration is mainly characterised by K feldspar-sulfide mineralisation and alunite (*shown in Appendix 1.3*).

4.4 Range of pyrite types

Pyrite was found to be the sole source of sulfur (*integrated assays and MLA measurements*) and the high sulfur grade of the ore signifies the presence of a wide range of pyrite types which forms Table 4.2. The various types of pyrite in the AA ore also contain variable levels of gold, some pyrite types which are low in gold e.g. blocky pyrite and others that are higher in gold tenor e.g. laminated pyrite. The five main pyrite types in AA ore are:

1. Blocky
2. Euhedral
3. Resorbed
4. Zoned
5. Laminated

Table 4.2: Pyrite types and subtypes in the AA ore

Type	Sub-Type	Description
Image of a low-grade blocky pyrite (*stained*) taken by a reflected light microscope. Pyrite is approx. 500 x 700 µm		Cubic crystal shape with a flat face. Has a coarse texture with no visible porosity and no intense bands of As and Au. Small surface area for oxidation.
Image of a variable grade euhedral pyrite (*stained*) taken by a reflected light microscope. Pyrite is approx. 700 x 900 µm	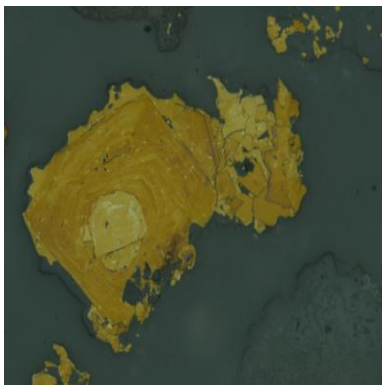	Multiple Au and As oscillatory zones with intense bands towards the outer rims: crystalline pyrites, similar to blocky, but significantly porous in nature.
Image of a high grade resorbed pyrite (*stained*) taken by a reflected light microscope. Pyrite is approx. 500 µm in length	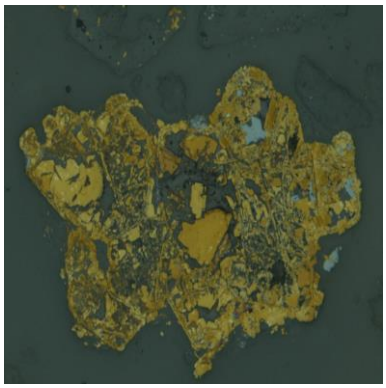	Inclusion rich cores with an amorphous frothy skeleton. High concentration bands of arsenic and gold around the resorbed zones. The outer zones are variable in grade and the distribution of Au and As bands outgrown from the resorbed skeleton. High surface area for oxidation.

Image of a zoned pyrite (*stained*) taken by a reflected light microscope. Pyrite is approx. 600 µm in length	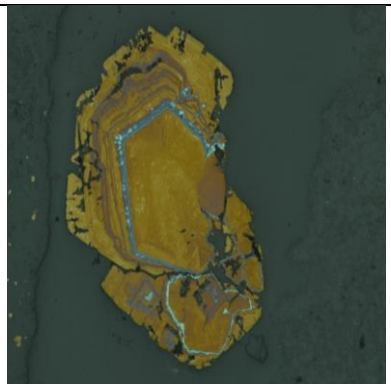	The surface of the faces shows multiple striations. The larger the crystal, heavier the striations. Multiple intense oscillatory bands of As and Au with high surface area for oxidation.
Image of a laminated pyrite (*stained*) taken by a reflected light microscope. Pyrite is approx. 700 µm in length		Contain multiple layers of variable grade Au and As with intense zones observed towards the centre. Have high volume/surface area ratios for oxidation.

4.5 Relation to arsenic

Gold mineralisation studies of refractory ores have revealed that the bulk of the gold is highly associated with As-rich zones in pyrite as exemplified by the double refractory Carlin trend ores at Nevada as shown in Figure 4.5 (Kappes et al., 2009).

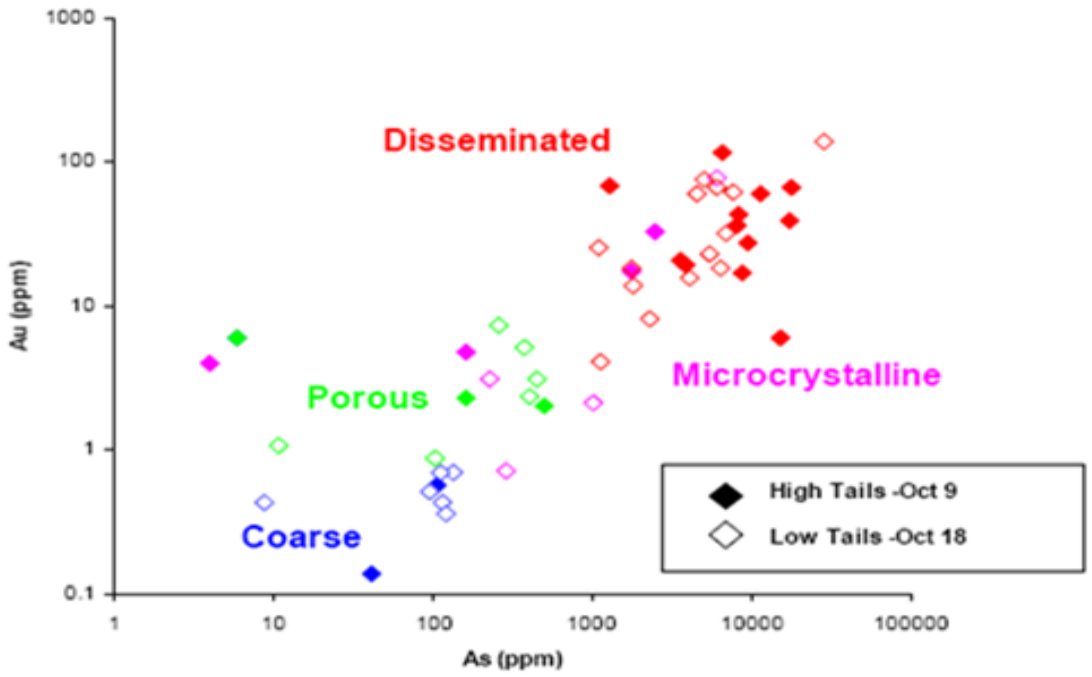

Figure 4.5: Gold and arsenic loading in different types of pyrite for a Carlin Ore (Kappes et al., 2009)

Positive correlations between the occurrence of gold (*Au*) and arsenic (*As*) in pyrite have also been noted in investigations of refractory gold ores by other researchers (Paktunc et al., 2006, Lamb, 2004, Kappes et al., 2009, Fleet et al., 1993, Wightman, 2005). LA-ICPMS of the advanced argillic ore (*AA ore*) sample used in this study shows a similar correlation between arsenic and gold as well. This direct relationship between arsenic and gold was established by the LA-ICPMS analysis of the various pyrite types as shown in detail in Figure 4.6.

LA-ICPMS map of Au and As grade across a low grade blocky pyrite grain

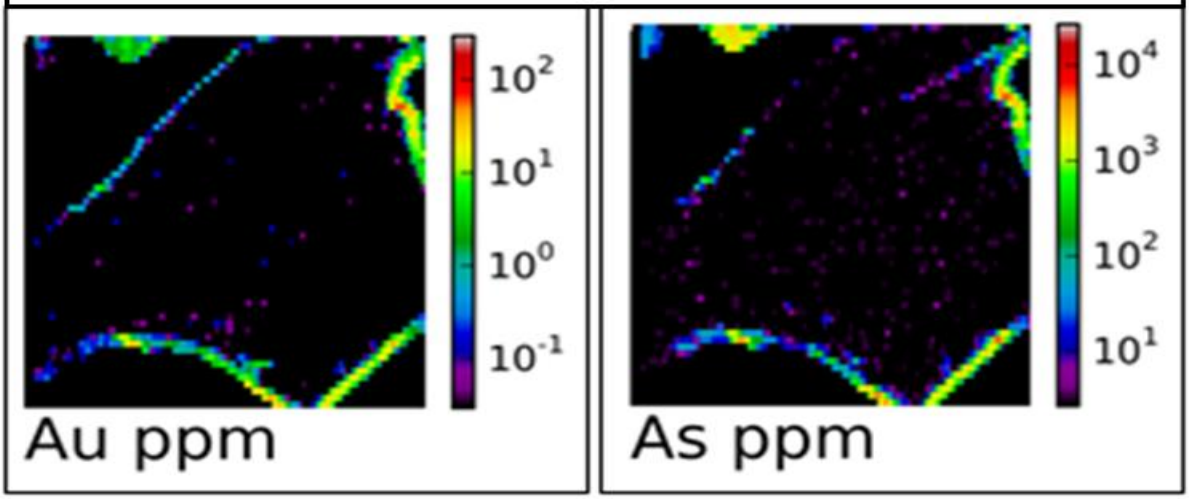

LA-ICPMS map of Au and As grade across a variable grade euhedral pyrite grain

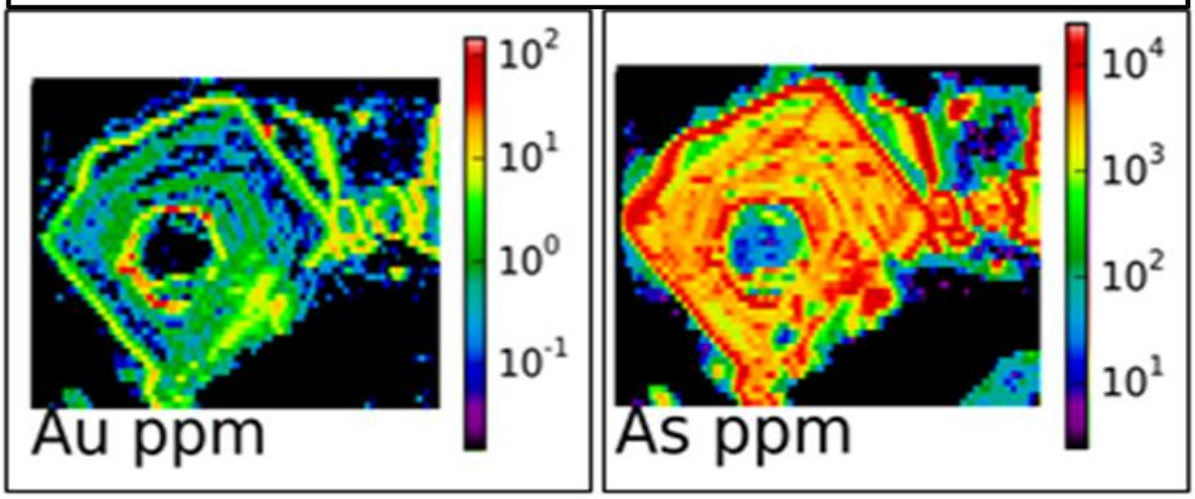

LA-ICPMS map of Au and As grade across a variable grade resorbed pyrite grain

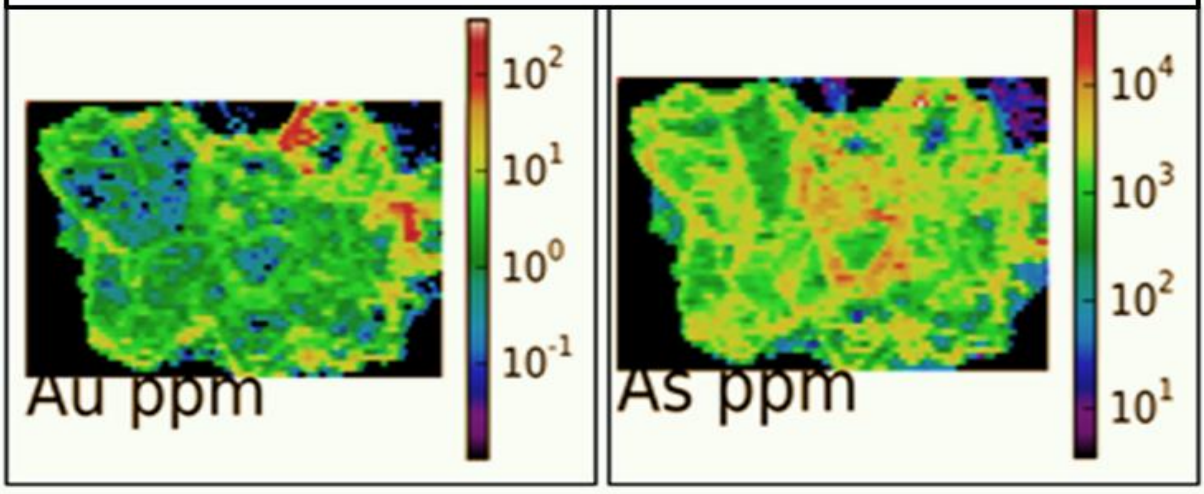

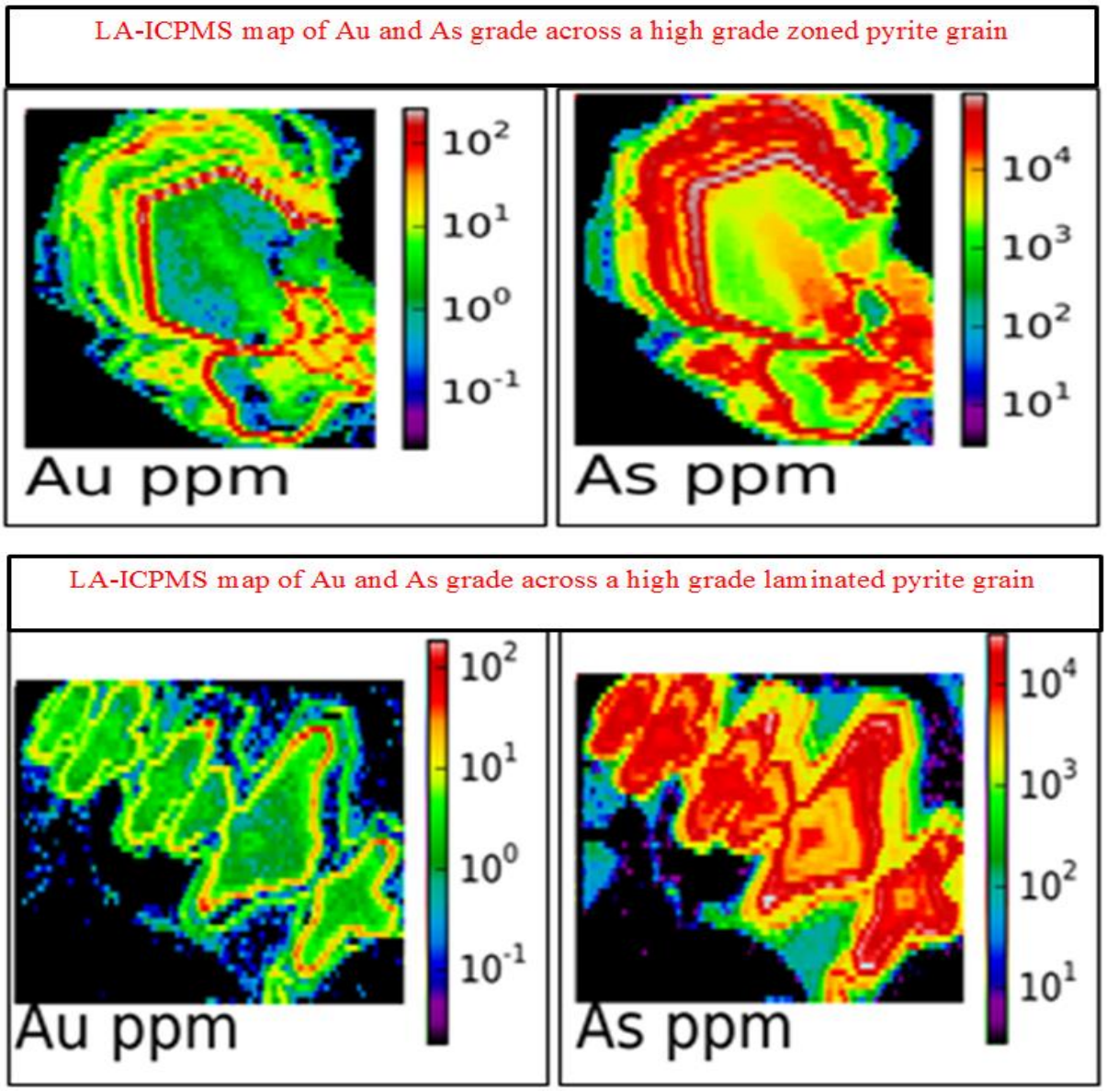

Figure 4.6: Laser ablation mass spectrometry images of the various pyrite types in AA ore, Lihir Mine. The grade of each element is shown by colour scale at the right of LA-ICPMS maps. (*Courtesy: Newcrest unpublished data; LA-ICPMS measurement undertaken at CODES*)

Confidential Lihir technical reports have quantified the distribution of gold in the various pyrite types as shown in Table 4.3. The focus was on a different ore sample using LA-ICPMS analysis. However, in this study, no attempts were made to quantify the gold content in various pyrite types. This is because according to the Newcrest mineralogist, "*LA-ICPMS method does provide information regarding the metal deportments of Au and other interested elements such as As but is not a reliable technique for quantification".*

Table 4.3: Gold content in different types of pyrite (Lamb, 2004, Wightman, 2005)

Pyrite Type	Gold Content of pyrite (*ppm*)
Blocky	5
Porous	12
Disseminated	26
Microcrystalline	52

However, almost without exception, it can be stated that the gold tenor in different types of pyrite is varied supporting the fact that the processing performance of the various types of pyrite is diverse (Lamb, 2004, Wightman, 2005, Mason, 1992, Paktunc et al., 2006, Ketcham et al., 1993). This clearly indicates that not all pyrite types are contributing equally to the economic performance of the Lihir mine. Therefore, development of a method (*based on hydrometallurgical practices*) to selectively remove the low gold pyrite from the high gold pyrite would increase the Au:S ratio to the autoclave feed resulting in higher autoclave throughput (Lamb, 2004; John et al. 2013). Accordingly, this work is novel and prospectively of practical relevance and economic benefit to the processing of future Lihir ore deposits.

4.6 Aggregates of various pyrite types

Despite many suggestions pencilled in qualitatively in many Lihir reports and a few publications such as Mason (1992) and John et al. (2013), it is probably fair to say that no study has been conducted to address this issue. This could be mainly because despite the various types of pyrite containing different gold loading, they do not exist as just discrete pyrite grains. Aggregates of different kinds of pyrite occurring together in the ore (*Figures 4.7 and 4.8*) is a major obscuring factor that could hinder a 100 percent separation of the various pyrite types.

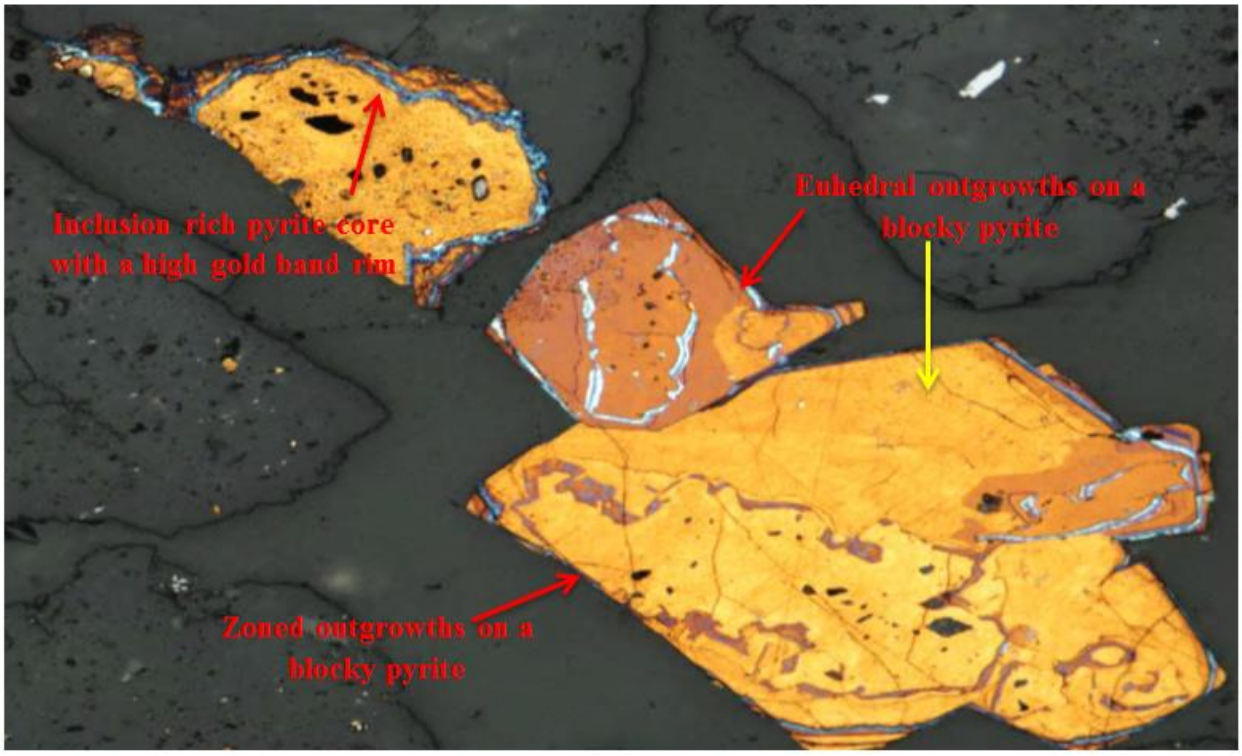

Figure 4.7: Stained images of an inclusion rich core pyrite with a high band gold rim (*Courtesy: Newcrest unpublished data; LA-ICPMS measurement undertaken at CODES*)

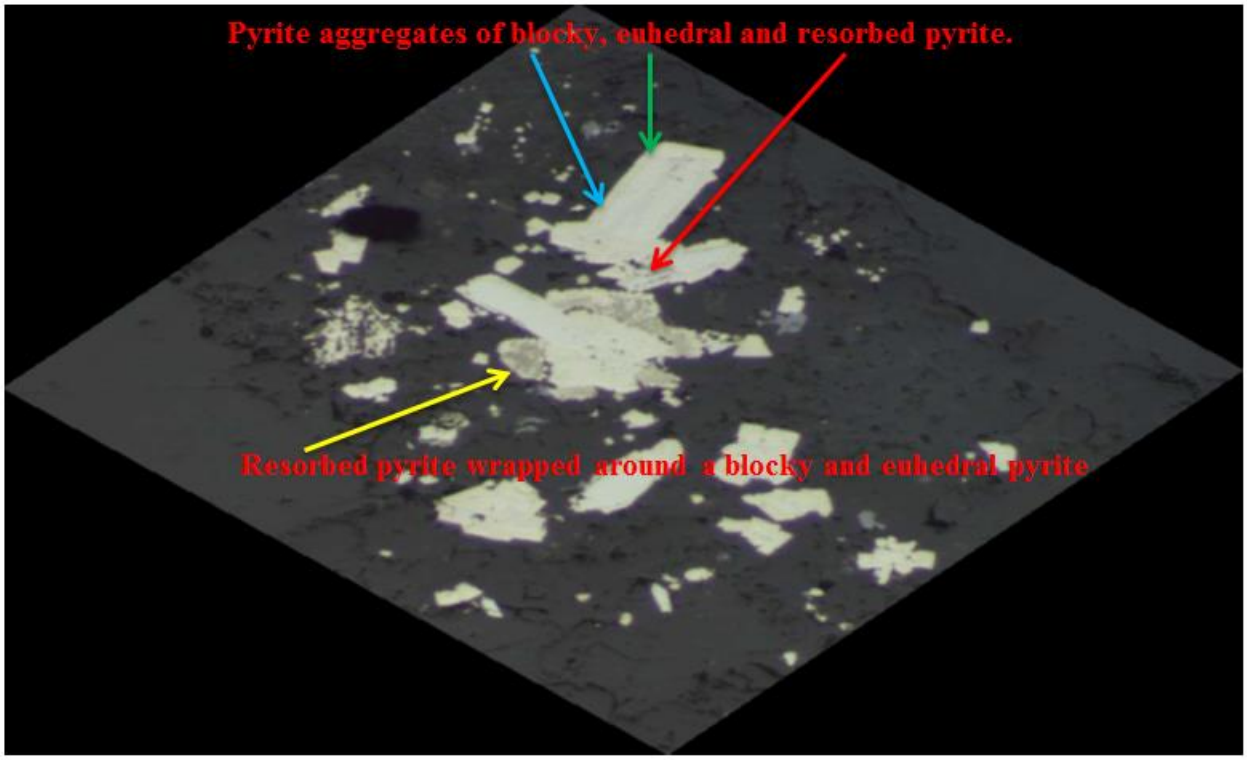

Figure 4.8: Pyrite aggregate of inclusion rich, blocky and microcrystalline pyrite (*Courtesy: Newcrest unpublished data)*

4.7 Chemical and Mineralogical Analysis

4.7.1 Mill Feed

The chemical analysis of the sized mill feed *(-850+425 µm*) is shown in Table 4.4. The fire assay results showed the gold content was 3.65 g/tonne. The elemental assay results showed the existence of arsenic, sulfur and copper in the ore indicating the existence of sulfides such pyrite and copper sulfides.

Table 4.4: Chemical analysis data of the Ore *(-850+425 µm*)

Elements	Values
Au (*ppm*)	3.65
Total Carbon (*%*)	0.1
Inorganic Carbon (*%*)	0.02
Organic Carbon (*%*)	0.12
Total Sulfur (*%*)	14.4
Sulfide Sulfur (*%*)	13.9
Sulfates (*%*)	0.5
Arsenic (*ppm*)	510
Aluminium (*%*)	8.85
Copper (*ppm*)	160

The best estimate of NTS 037 mineralogy was integrated using QXRD, MLA and assay inputs by the Newcrest mineralogist (*Dr Kathryn Stewart*) which forms Table 4.5 and Figure 4.9. The weight of pyrite in the ore was estimated at 19 % classifying it as a major mineral phase in the ore. The results showed that the ore was mainly composed of K-feldspar, alunite, muscovite and illite with minor amounts of kaolinite and jarosite.

Table 4.5: NTS 037 mineralogy estimated by QXRD and MLA

NTS 037 AA Ore Sample	Proportion (*Wt %*)	Abundance
Pyrite	19.09	Major
Other sulfides	0.01	Minor
K Feldspar	39.40	Major
Quartz	2.55	Minor
Plagioclase	0.35	Minor
Biotite	0.20	Minor
Muscovite/Illite	13.73	Minor
Pyrophyllite	3.09	Minor
Kaolinite	3.98	Minor
Jarosite	2.40	Minor
Anhydrite/Gypsum	0.00	None
Alunite	14.00	Major
Barite	0.24	Minor
Minor minerals	0.94	Minor
Total	**100**	

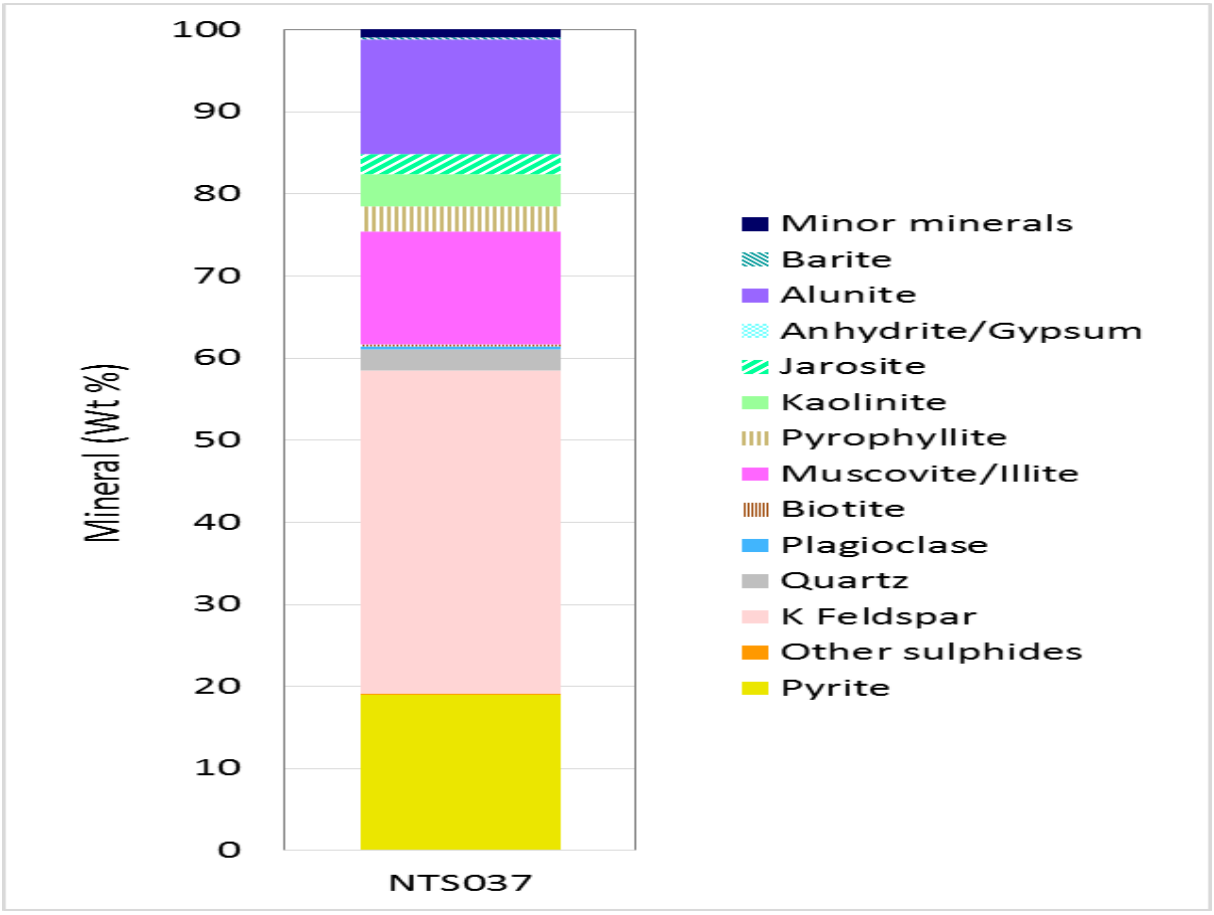

Figure 4.9: Proportion of minerals (*wt %)* in NTS 037 ore sample estimated by QXRD and MLA

4.8 Flotation

The metallurgical response of the NTS 37 AA ore was investigated by conducting preliminary flotation tests. It should be noted that significant amount of flotation study has been performed on this ore by Newcrest Testing Site (*NTS*). Metallurgical responses at various grind sizes and using various chemical reagent schemes were tested at the NTS laboratory. However, in this work metallurgical characterisation of the AA ore was done to reflect the standard Lihir practice as closely as possible. Therefore, operating variables, reagents and dosage were selected based on existing confidential Lihir reports. However, it should be noted slight modifications have been made in certain cases due to the mineralogical differences in the NTS 37 ore sample.

After the grinding calibration was carried out to achieve a P80 of 106 μm, consistent with the current Lihir practice, metallurgical tests were conducted to optimise the sulfide sulfur and gold recovery (*as a function of pH*). Although the current standard flotation practice at Lihir involves floating at natural pH (*pH 7*), using PAX and Nascol 422 as collector and frother respectively, slight pH modifications were done in this work. This is mainly because the natural pH of the AA ore sample was 1.65 suggesting that some pyrite alteration had already occurred and under such acidic conditions, floatability of pyrite decreases mainly due to rapid collector decomposition (Mermillod-Blondin et al., 2005).

The aim of the rougher stage (*in this work*) was to produce a pyrite-rich concentrate for further oxidation and subsequent cleaner flotation tests. Preliminary flotation tests were performed at three different pH conditions (*using lime as a pH modifier and PAX as the collector*) to understand the sulfide flotation behaviour. Flotation data regarding gold grade and gold recovery are shown in Figure 4.10. Although a better gold grade is observed with the natural pH sample, better recoveries were found at pH 5 as shown in Table 4.6.

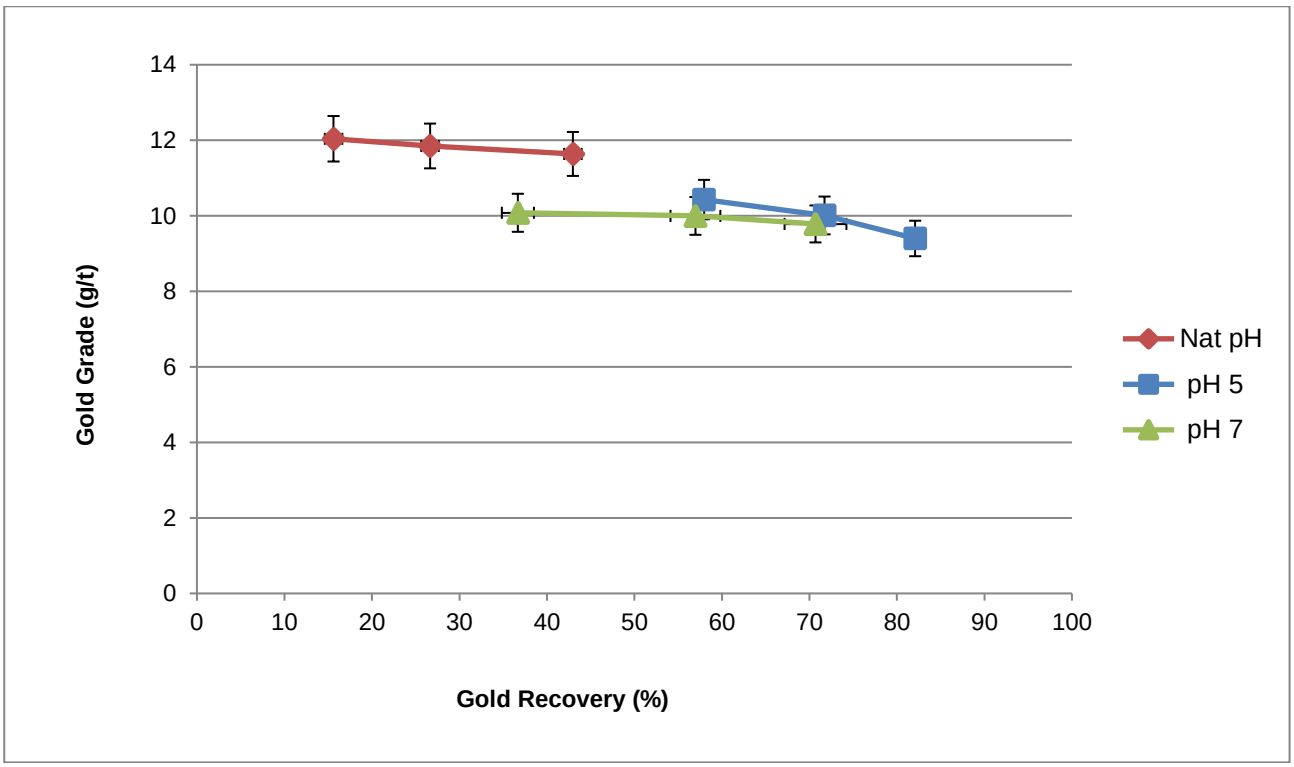

Figure 4.10: Gold grade-recovery curves at different pH conditions

Sulfide flotation at different pH conditions is shown in Figure 4.11. It can also be seen that with floating at natural pH, the sulfides recovery decreased to almost 50% suggesting collector decomposition at highly acidic pH conditions (*Table 4.6*). Although sulfide flotation remained high at pH 5, a significant drop is observed at pH 7.

Table 4.6: Metallurgical responses of AA ore floated at different pH conditions

	Metallurgical Responses			
pH	**Gold Recovery (%)**	**Sulfide Sulfur Recovery (%)**	**Arsenic Recovery (%)**	**Water Recovery (%)**
Natural pH	43.0	51.0	53.5	11.1
pH 5	82.0	84.3	83.0	43.9
pH 7	70.7	75.6	73.3	35.8

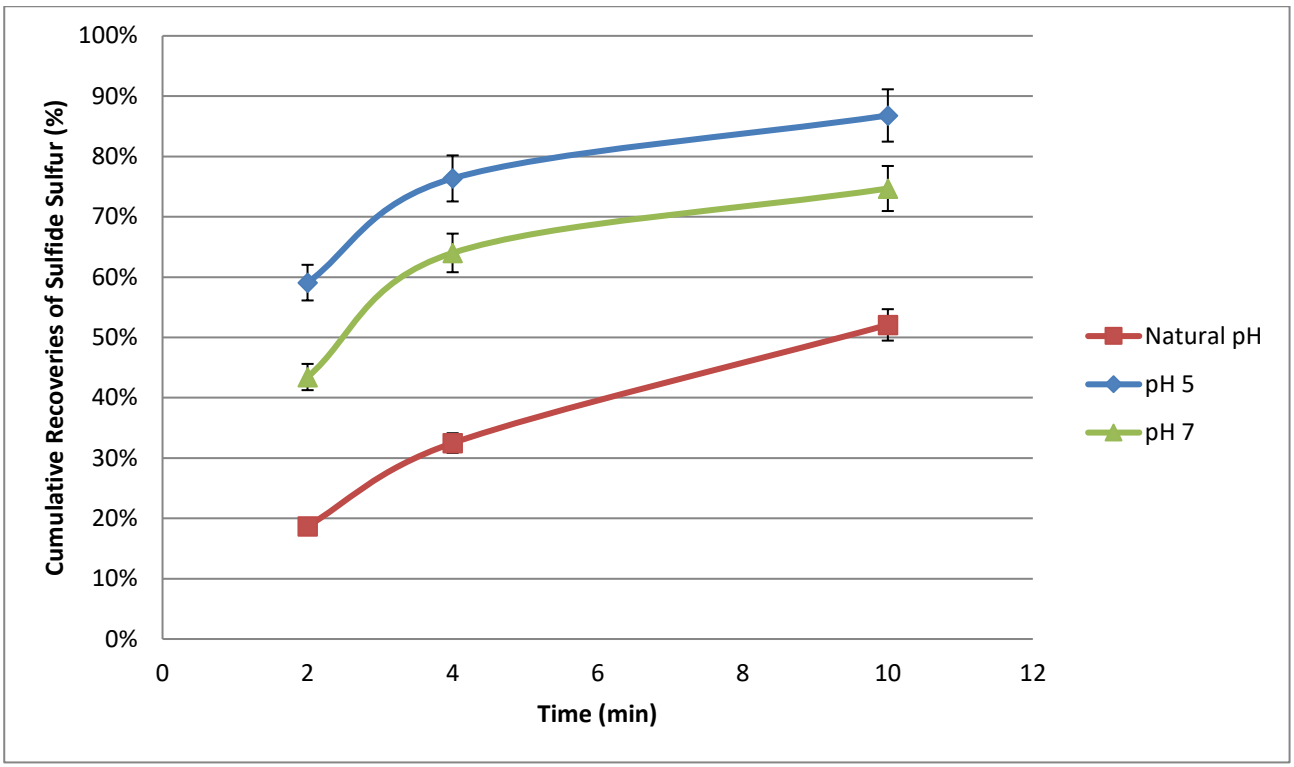

Figure 4.11: Cumulative recovery of sulfides at different pH conditions

This high recovery of sulfides and gold at a near neutral pH of 5 can be described in terms of pyrite-dixanthogen interaction (Wang, 1995). Fornasiero and Ralston (1992) have shown that at a pH value below 6, the positively charged pyrite surfaces preferentially attract the negatively charged xanthate ions to form a metal-xanthate complex due to an ion-exchange reaction. This metal-xanthate complex oxidises to form hydrophobic dixanthogen (Fornasiero et al., 1992) resulting in high gold and sulfide sulfur recoveries as shown in Figures 4.10 and 4.11 respectively.

But as the pH of the slurry increases above 6, the pyrite surface becomes relatively more oxidised than the xanthate complex resulting in comparatively less formation of hydrophobic dixanthogen (Gardner and Woods, 1979, Mermillod-Blondin et al., 2005, Marsden and House, 2006) causing relatively low gold and sulfide sulfur recoveries compared to pH 5. Also since the positive correlation between arsenic and gold content has been established (*discussed in mineralogical section Figures 4.4 and 4.5*), a higher arsenic recovery can also be expected in the flotation stage and this is shown in Figure 4.12.

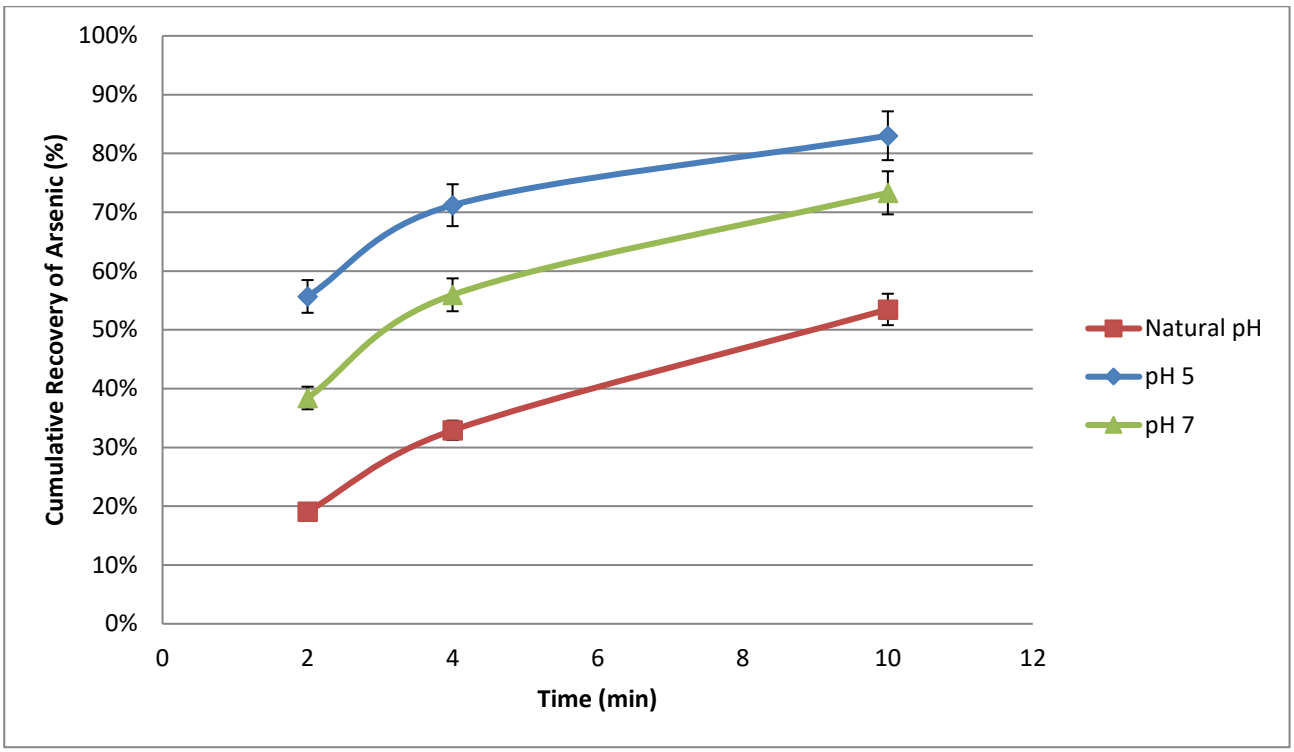

Figure 4.12: Cumulative recovery of arsenic at different pH conditions

In the flotation experiments (*induced floatability due to collector*), the recovery of water in the sulfide stage was high suggesting that the primary mechanism for the recovery of sulfides was by true flotation and not entrainment. However, a significantly higher water recovery was observed at pH 5 (*Table 4.6 and Figure 4.13*), suggesting entrainment did have some contribution towards the recovery of sulfides, arsenic and gold.

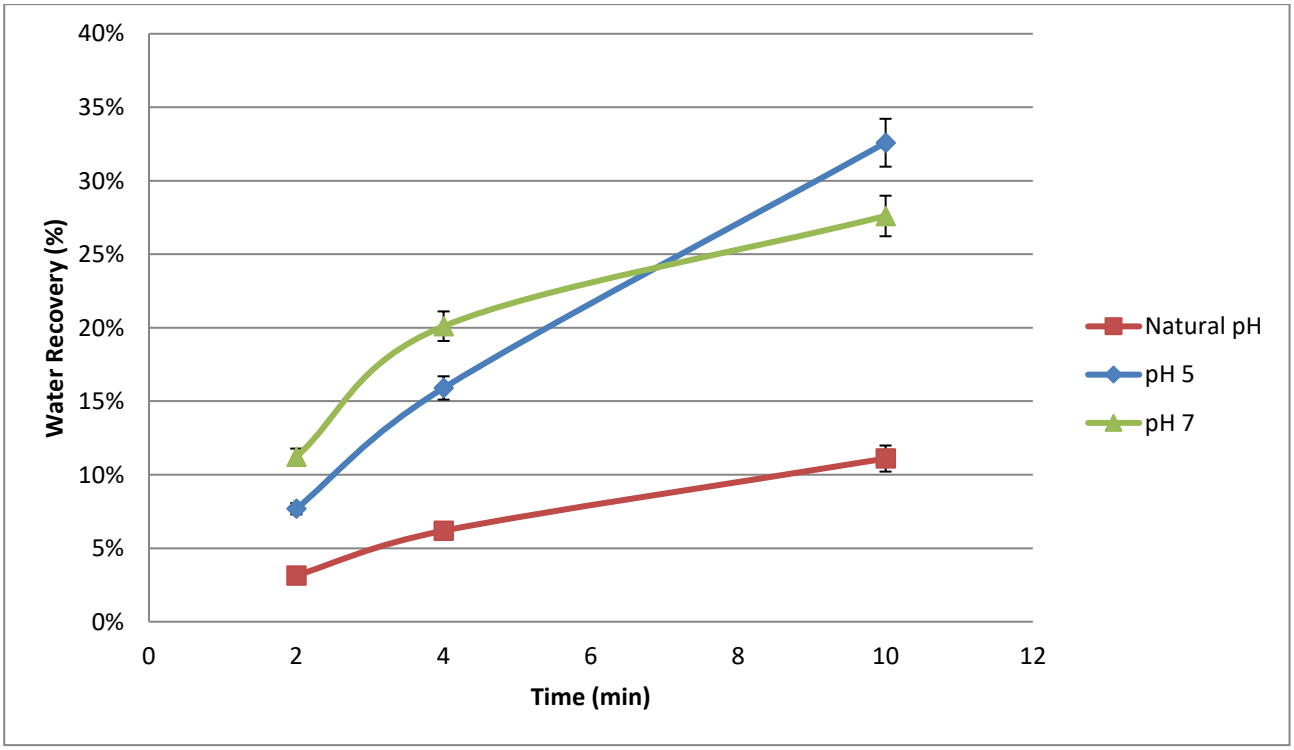

Figure 4.13: Water recovery at different time intervals and pH conditions

4.9 Conclusions

1. The AA ore sample was found to have a wide range of pyrite types with varying gold content and therefore was an excellent ore material for this study.

2. Positive correlations between the occurrence of gold and arsenic in pyrite were also noted in investigations of the AA ore by LA-ICPMS.

3. Aggregates of various pyrite types added to the complexity of the ore.

4. Since the rougher flotation stage was aimed at increasing the recovery of sulfide minerals and minimising non-the sulfide gangue, pH 5 was selected as the optimum pH condition in the roughing stage to generate a pyrite-rich concentrate for subsequent oxidation and cleaner flotation tests.

4.10. Bibliography

FLEET, M. E., CHRYSSOULIS, S. L., MACLEAN, P. J., DAVIDSON, R. & WEISENER, C. G. 1993. Arsenian pyrite from gold deposits; Au and As distribution investigated by SIMS and EMP, and colour staining and surface oxidation by XPS and LIMS. *The Canadian Mineralogist,* 31**,** 1-17.

FORNASIERO, D., EIJT, V. & RALSTON, J. 1992. An electrokinetic study of pyrite oxidation. *Colloids and surfaces,* 62**,** 63-73.

GARDNER, J. & WOODS, R. 1979. An electrochemical investigation of the natural flotability of chalcopyrite. *International journal of mineral processing,* 6**,** 1-16.

GOKTEPE, F. 2002. Effect of pH on pulp potential and sulfide mineral flotation. *Turk. J. Eng. Sci,* 26**,** 309-318.

KAPPES, R., BROSNAHAN, D. & GATHJE, J. Utilising mineral liberation analysis (MLA) to determine pyrite, arsenopyrite and arsenian pyrite floatabilities for Carlin trend ores. SME Annual Meeting and Exhibit and CMA's 111th National Western Mining Conference, 2009. 736-741.

KETCHAM, V., O'REILLY, J. & VARDILL, W. 1993. The Lihir gold project; Process plant design. *Minerals Engineering,* 6**,** 1037-1065.

LAMB, W. 2004. Optimising the value of the Lihir low-grade resource. Rio Tinto Technical Report No: AR2163. Project Code: GAL 144.

MARSDEN, J. & HOUSE, I. 2006. *The chemistry of gold extraction,* SME. Littleton, Colorado, USA ISBN-13: 978-0-87335-240-6 ISBN-10: 0-87335-240-8.

MASON, P. 1992. Examining the economics of some pressure oxidation process options. *Hydrometallurgy,* 29**,** 479-492.

MERMILLOD-BLONDIN, R., KONGOLO, M., DE DONATO, P., BENZAAZOUA, M., BARRÈS, O., BUSSIÈRE, B. & AUBERTIN, M. Pyrite flotation with xanthate under alkaline

conditions-application to environmental desulfurization. Proc. of the Centenary of Flotation Symposium, Brisbane, QLD, 2005.

MÜLLER, D., FRANZ, L., HERZIG, P. M. & HUNT, S. 2001. Potassic Igneous rocks from the vicinity of epithermal gold mineralisation, Lihir Island, Papua New Guinea. *Lithos,* 57**,** 163-186.

PAKTUNC, D., KINGSTON, D., PRATT, A. & MCMULLEN, J. 2006. Distribution of gold in pyrite and products of its transformation resulting from the roasting of refractory gold ore. *The Canadian Mineralogist,* 44**,** 213-227.

RANKIN, W. J. 2013. *New flagship AusIMM Monograph 28: Australasian mining and metallurgical operating practices*. (The Sir Maurice Mawby Memorial Volume), Third Edition.

TABATABAEI, R. H. 2012. The Causes for the Poor Flotation Performance of a Double-Refractory Gold Ore. Ph.D. Thesis. The University of Queensland, Sustainable Minerals Institute, 2012-03-01.

WANG, X.-H. 1995. Interfacial electrochemistry of pyrite oxidation and flotation II. FTIR studies of xanthate adsorption on pyrite surfaces in neutral pH solutions. *Journal of colloid and interface science,* 171**,** 413-428.

WHITE, P., USSHER, G. & HERMOSO, D. Evolution of the Ladolam Geothermal System on Lihir Island, Papua New Guinea. Proceedings World Geothermal Congress 2010, 2010.

WIGHTMAN, E. 2005. Bench scale testing to determine the potential for removal of low gold pyrite from Lihir ores. Rio Tinto Technical Report No: AR2448. Project Code: GAL 161.

CHAPTER 5

The Effect of Acid Media on High Arsenic and Low Arsenic Pyrite

This study describes the development of a novel mineral characterisation technique for distinguishing between low arsenic pyrite and high arsenic pyrite species in a refractory gold ore using BSE images from an SEM-based automated mineralogy system, in this case, an MLA system. The technique is based on a chemical etching process which is used to oxidise the polished surface of the prepared blocks prior to measurement in the MLA system. Although the MLA system can identify and quantify the arsenian pyrite without etching, the coupling of BSE images and image processing software such as ImageJ provides an alternative and rapid means of quantifying arsenian pyrite in a sample on a pixel by pixel basis. This rapid and high-resolution technique allows tracking of pyrite responses to etching by acid which would be more difficult using standard EDS x-ray automated mineralogy. In the refractory gold ore investigated in this work, it was found that pyrite which has high levels of arsenic oxidises more readily than the blocky pyrite which has low levels of arsenic.

Keywords: Chemical Etching, MLA, ImageJ, Arsenic, Pyrite

5. Introduction

Automated mineralogical analysis based on SEM (*scanning electron microscope*) platforms is utilised in the mining industry to understand the mineral characteristics of ores and mineral processing streams to provide quantitative mineralogy i.e. data that can be used for better economic treatment(s), process optimisation and beneficiation. Numerous studies have been conducted on ore samples and processed flotation products to understand mineral abundance, liberation potential and grain size. Nonetheless, there is limited understanding regarding the characterisation and texture of oxidised metallurgical products. It is hard to overlook the significance of this aspect especially considering that the majority of the existing gold ore deposits are refractory or double refractory. This is because one of the challenges of treating refractory ores is that pre-treatment processes are necessary for the adequate liberation of gold from the pyrite matrix to allow maximum recovery (Petruk, 2000, Marsden and House, 2006, Thomas, 1991). Although studies regarding the mechanism of pyrite oxidation are extensive and readily available in the scientific literature, relatively little work has been published which focuses on the effect of oxidation on the different types of pyrite.

This is important because refractory gold ores typically contain a number of species of pyrite with different morphologies, trace element compositions and varying gold content. These various species of pyrite can be distinguished visually under the optical microscope based on characteristics such as the grain shape, crystallinity, texture or, after staining, variations in colour; however, such work must be performed by an experienced mineralogist. Within gold mining companies treating refractory ores there is a need to measure many samples routinely and for these applications, a SEM-based mineralogy system often replaces the optical microscope. SEM-based automated mineralogy systems identify different minerals using their chemistry, as detected from their X-ray spectra. Sub-types of a single mineral can only be identified if there is a compositional difference which is obtainable from the detectors on SEM based mineralogy systems (*for example sphalerite with low and high levels of Fe or pyrite with arsenic levels above the detection limit vs. those with arsenic levels below the detection limit*).

5.2 Correlation between arsenic and gold

Laser Ablation Inductively Coupled Plasma Mass Spectrometry (*LA-ICPMS*) of the advanced argillic ore (*AA ore*) sample used in this study showed a correlation between arsenic and gold. The relationship between Au and As content in low gold and high gold pyrite is shown in Figures 5.1 and 5.2 respectively.

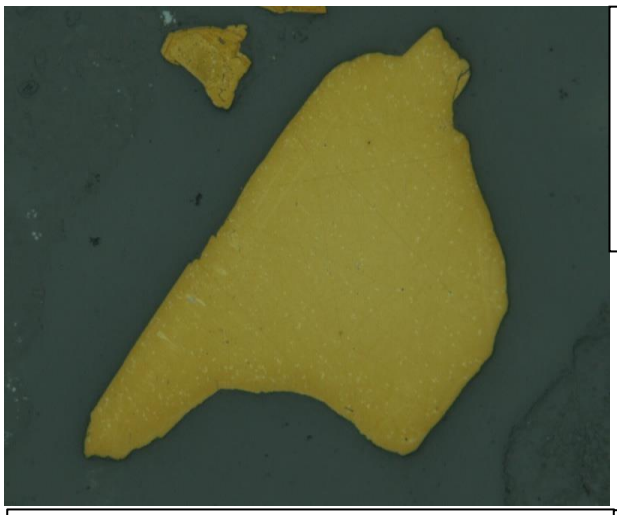

Image of a low grade pyrite (stained) taken by reflected light microscope. Pyrite is approx. 500 x 700 µm.

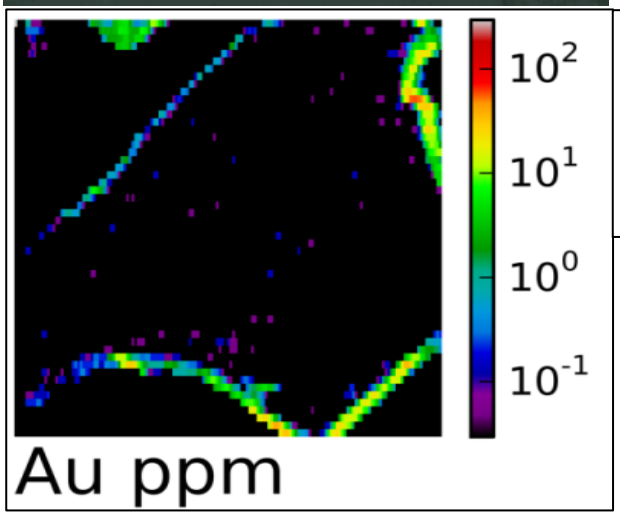

LA-ICPMS map of Au grade across the same pyrite grain.

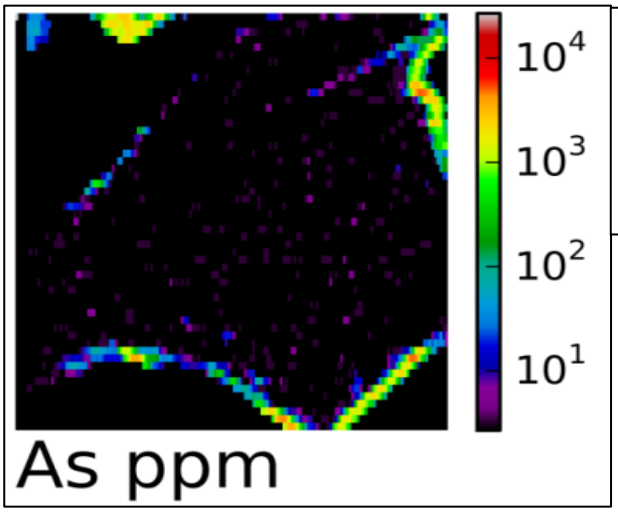

LA-ICPMS map of As grade across the same pyrite grain.

Figure 5.1: Laser ablation mass spectrometry images of a single grain of blocky pyrite from AA ore, Lihir Mine. The blocky pyrite has a cubic crystal shape and is coarse in nature with a discontinuous narrow rim that is higher in As & Au (grade of each element is shown by colour scale at the right of LA-ICPMS maps). (*Courtesy: Newcrest Mining unpublished data; LA-ICPMS measurements undertaken at CODES*)

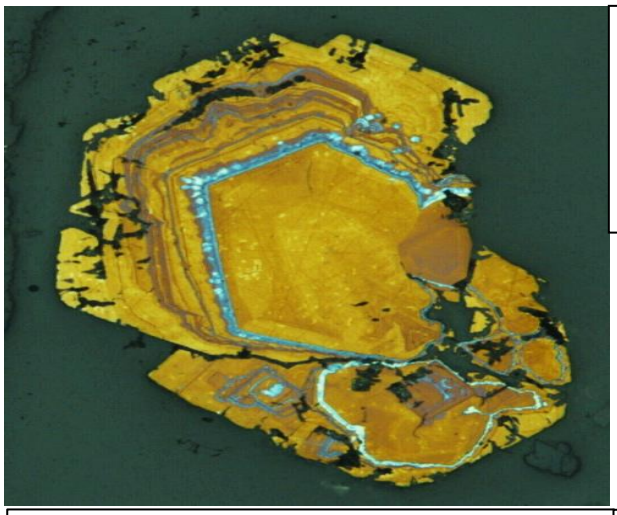

Image of a zoned pyrite (stained) taken by reflected light microscope. Pyrite is approx. 600 μm in length.

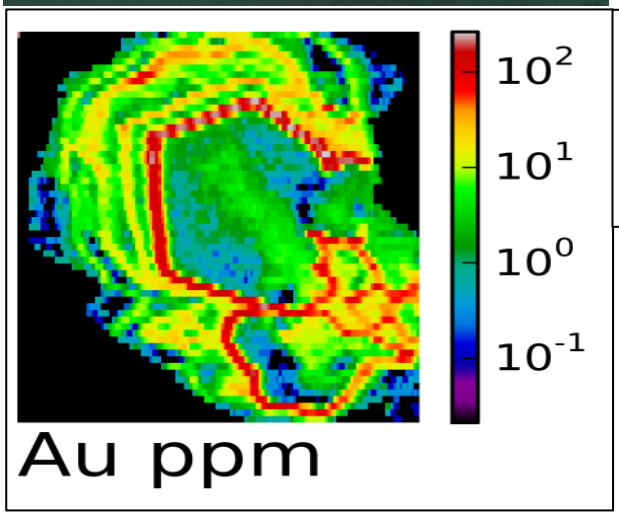

LA-ICPMS map of Au grade across the pyrite grain, showing multiple zones with variable grade.

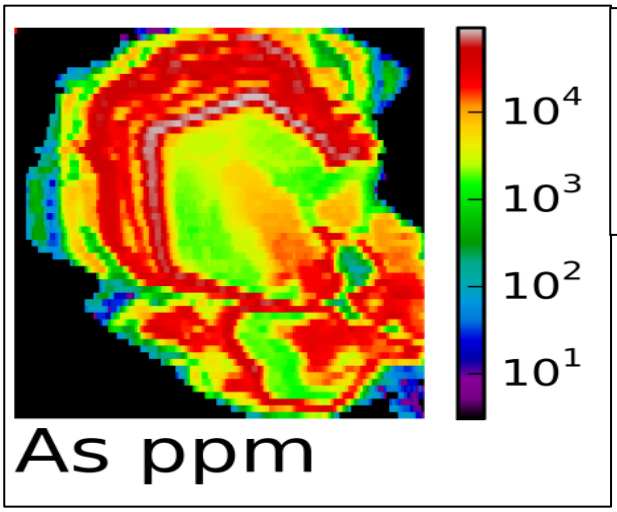

LA-ICPMS map of As grade across the pyrite grain, showing multiple zones with variable grade.

Figure 5.2: Laser ablation mass spectrometry images of a single grain of arsenian zoned pyrite from AA ore, Lihir Mine. The grade of each element is shown by colour scale at right of LA-ICPMS maps. (*Courtesy: Newcrest Mining unpublished data; LA-ICPMS measurements undertaken at CODES*)

The images displayed in Figures 5.1 and 5.2 indicate that Au in pyrite occurs associated with As in specific zones suggesting that the presence of As facilitates the accommodation of Au into the sulfide lattice (Cook and Chryssoulis, 1990, Morishita et al., 2008). Despite this relationship, the actual ratio of Au:As may vary and this correlation is illustrated in Figure 5.2 (*As and Au laser ablation mass spectrometry images*) showing variation in gold grade across a zone of consistently high arsenic content. In simple words, *'where there is Au in pyrite there is As, but there may be As in pyrite with little or even no associated Au'*. Researchers have confirmed this concept previously in other samples from various geological environments (Morishita et al., 2008, Fleet et al., 1993, Reich et al., 2005). In this study, it is the As facet that will be explored. This is because the BSE imagery (*from MLA or any BSE system per se*) can only register the arsenic content in pyrite and not the gold distribution because only As is present above the SEM detection limits. Therefore, the thrust of this chapter was to evaluate the responses of the high As pyrite and low As pyrite to treatment by two different acid media (*nitric acid and sulfuric acid*).

5.3. Experimental Procedure

A pyrite rich concentrate was generated from the AA ore using the standard flotation conditions outlined in Chapter 3. The concentrate was dry screened to +53 μm prior to preparation of the MLA blocks. The carbon coated MLA blocks were then subjected to two sets of acid etching series; one with nitric acid and the other with sulfuric acid. The blocks were sequentially oxidised for 10 minutes for six consecutive days and the BSE images were collected after each etching stage using the MLA system as shown in Figure 5.3. The collected BSE images were then evaluated for textural alterations. The scientific image analysis program ImageJ was used to perform a full set of imaging manipulations of the unoxidised and oxidised samples as outlined previously in Chapter 3 (*Figure 3.12 in section 3.4.5*).

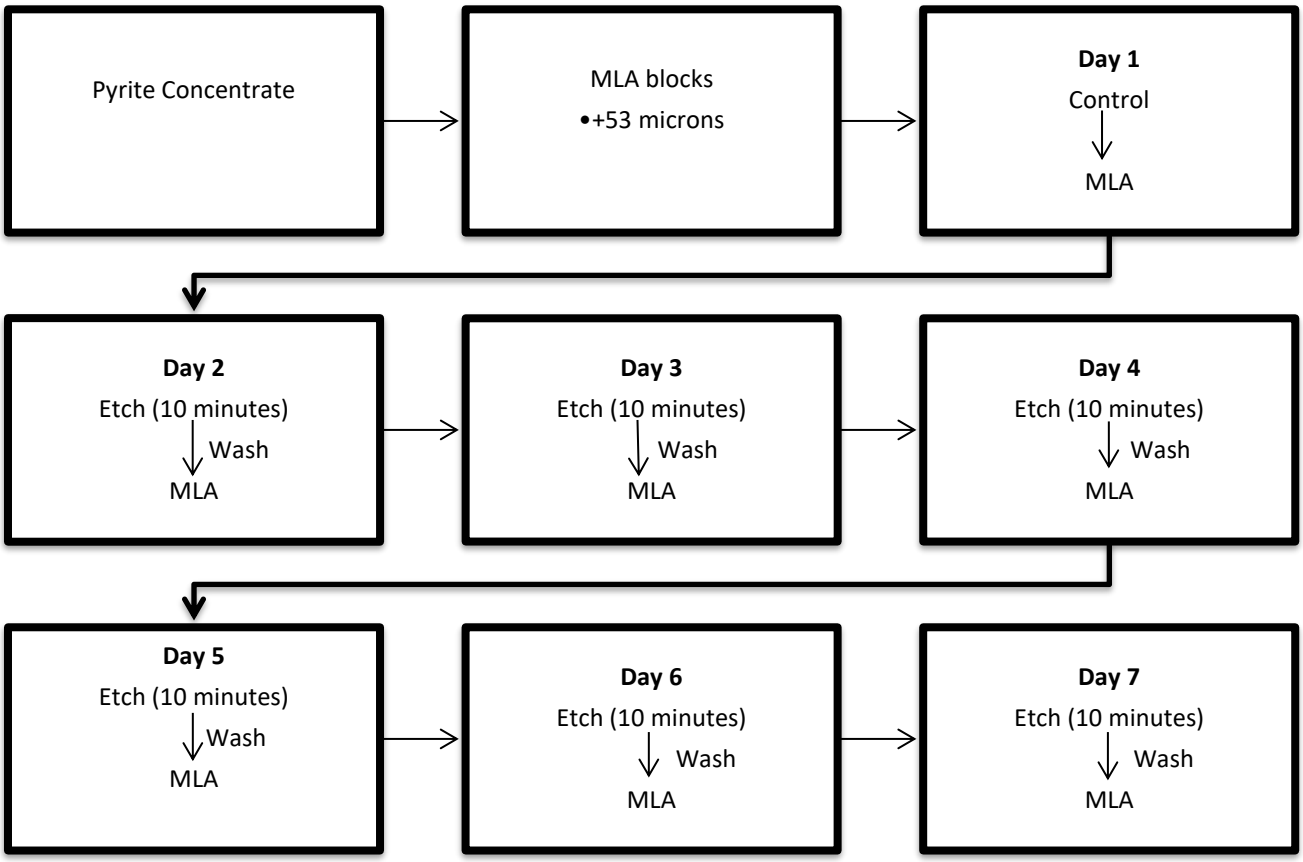

Figure 5.3: Detailed etching experimental procedure of the pyrite MLA blocks. The MLA blocks were rinsed with water post-treatment. MLA runs were completed overnight to generate the BSE images.

5.4 Results and Discussion

5.4.1 Nitric acid etch of high As arsenian pyrite

Despite the extensive arsenian pyrite studies in the literature (Bakken et al., 1989, Cline, 2001, Cook and Chryssoulis, 1990), there is no published information regarding the differences in oxidation response of high As pyrite and As poor pyrite. Therefore, tests were conducted to establish the relative response of arsenian vs. non-arsenian pyrite to oxidation by nitric acid.

Figure 5.4 shows a BSE image (*after ImageJ thresholding*) of an untreated, zoned pyrite grain. The image is a small area captured from a larger, whole block BSE image. The bright red zones within the pyrite indicate very high arsenic concentration which in turn may relate to high gold content (Morishita et al., 2008).

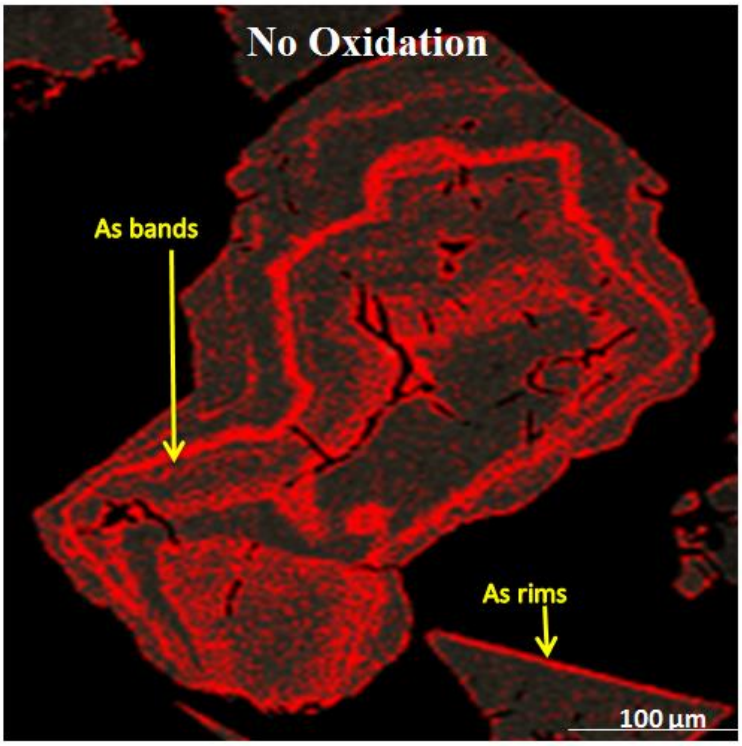

Figure 5.4: Zoomed BSE image (*after ImageJ thresholding*) of the unoxidised high As pyrite grain.

In the unoxidised sample, arsenic zonation textures are inert and the pyrite shows no signs of reactivity. Oxidation using nitric acid was then conducted as per the flow diagram in Figure 5.3. The results of sequential oxidation by nitric acid on arsenian pyrite were tracked both by using a selected pyrite grain to provide an image sequence of oxidation (*Figure 5.5*), and also by using image analysis of BSE images of the entire sample block to quantify the proportion of arsenian pyrite remaining at each stage (*Figure 5.6, Table 5.1*).

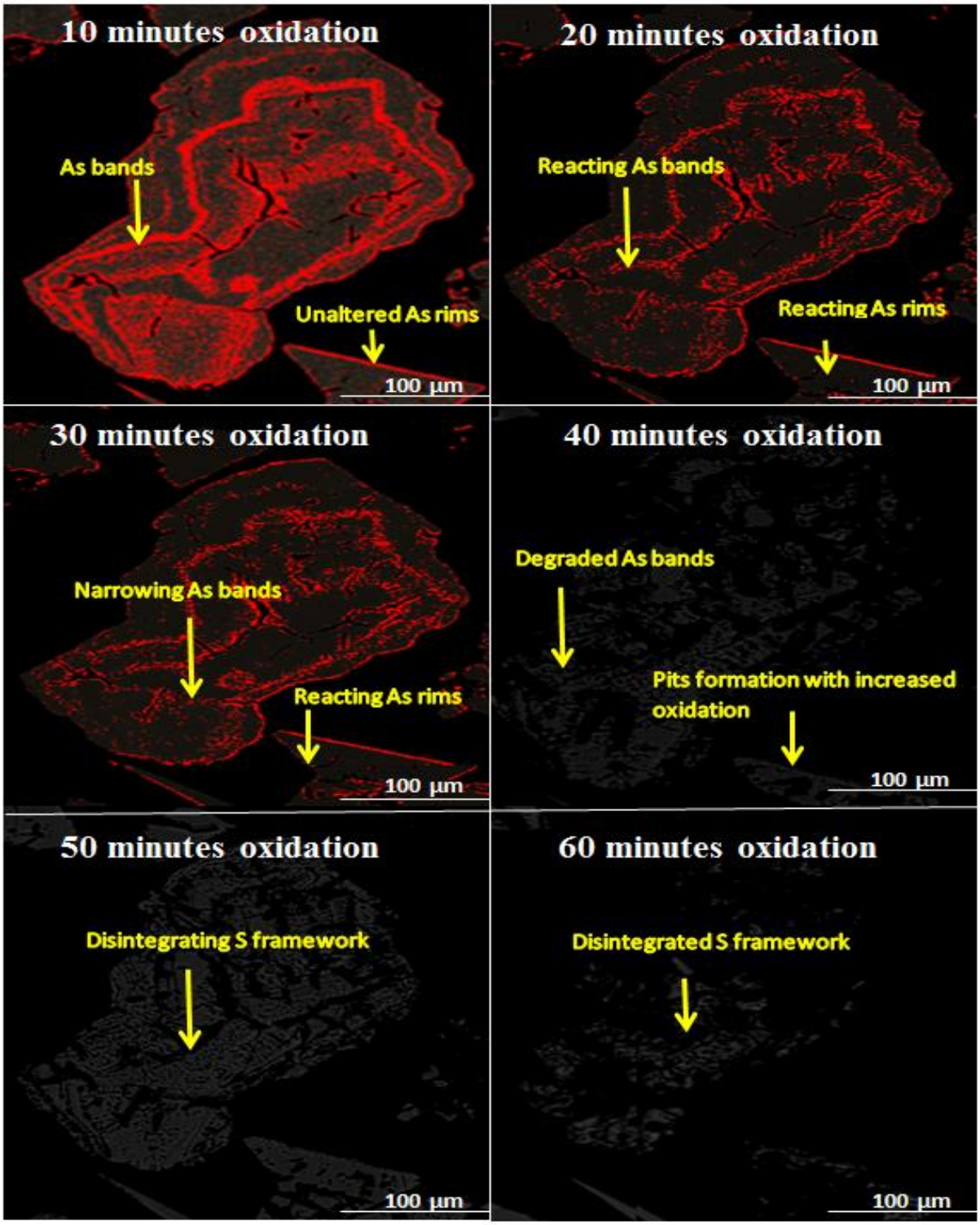

Figure 5.5: BSE image (*after ImageJ thresholding*) of a high As pyrite grain showing changes during sequential treatment with nitric acid

After 10 minutes of exposure to nitric acid, etched samples showed little difference to their unetched precursor, suggesting that low oxidation of arsenian pyrite had taken place at this point. However, after 20 minutes of oxidation, a reduction of arsenian pyrite was evident. Textural changes in the As zoned coliform bands suggest the effect of oxidation after 20 minutes of etching was moderate. Striking changes are evident from the 30 minutes oxidation stage onwards with

many arsenian pyrite zones exhibiting distinct narrowing, and noticeable reduction in the overall amount of arsenian pyrite.

Alteration in textural characteristics becomes very pronounced from 40-minute oxidation onwards. After 40 minutes of etching the arsenic zones have completely reacted leaving behind a sulfide skeleton, as illustrated in Figure 5.5, and no arsenian pyrite was detected at the 50 and 60-minute oxidation stages as shown in Figure 5.6. This suggests that pyrite oxidation by the nitric acid solution is governed by As and sulfur (*S*) reaction with arsenic having a higher rate of oxidation sensitivity than sulfur. It is clear that sequential treatment with nitric acid removes arsenic from the pyrite surface and this effect of repeated oxidation on arsenian pyrite was quantified using the histogram function of ImageJ as previously mentioned in Figure 3.11 in Chapter 3.

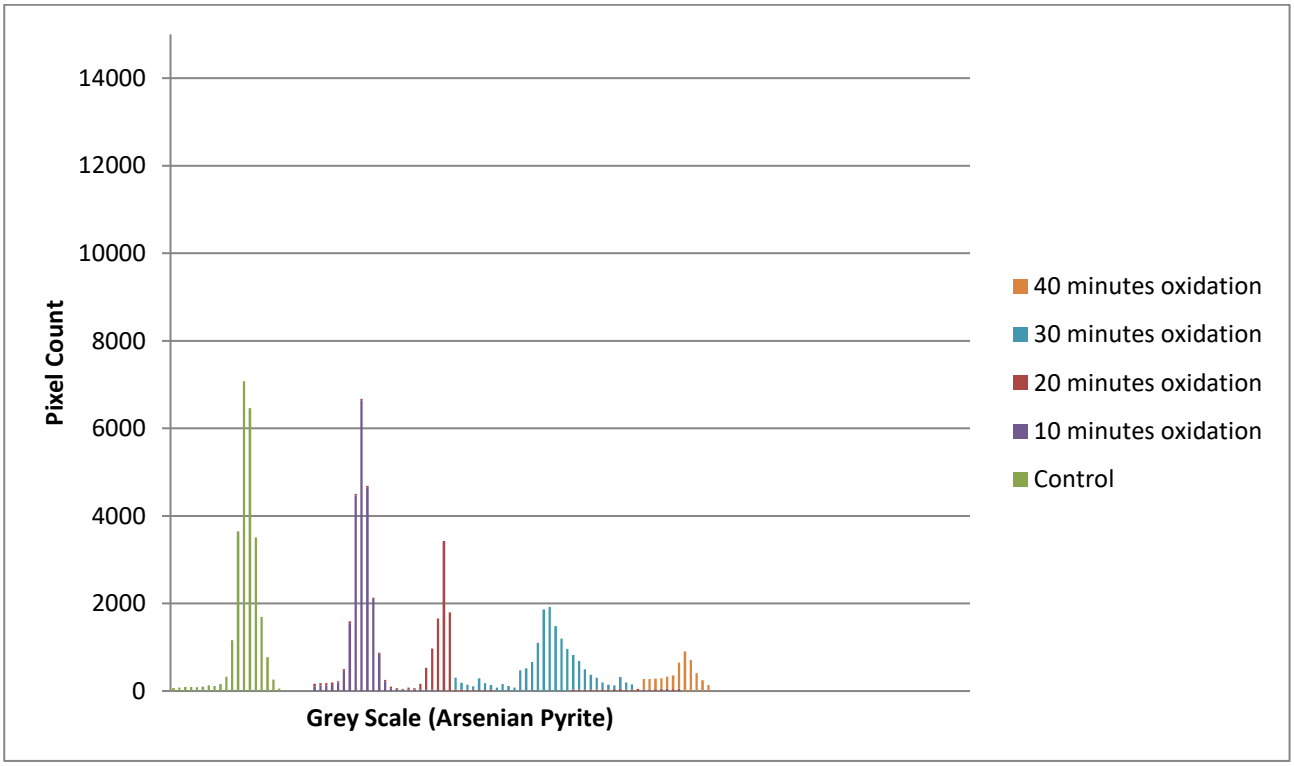

Figure 5.6: The effect of nitric acid sequential treatment on arsenian pyrite

Histogram analysis detected almost 7.4 wt. % arsenian pyrite in the control sample. This quantification based on the arsenic value decreases as the oxidation reaction advances with no arsenian pyrite detected after the 40 minutes oxidation stage as shown in Table 5.1.

Table 5. 1: ImageJ histogram quantification of Au-bearing arsenian pyrite *(wt. %)* after sequential nitric acid oxidation. n.d. = not detected

Oxidation Time (*minutes*)	**Arsenian Pyrite (*wt. %*)**	**Proportion of Arsenian Pyrite oxidised (*as % of original Arsenian Pyrite*)**
Control	7.4	0
10	6.9	7
20	3.1	58
30	0.9	88
40	0.1	99
50	n.d.	100
60	n.d.	100

5.4.2 Nitric acid etch of low As blocky pyrite

Publications related to arsenian pyrite do not focus on characteristics of low arsenic blocky pyrite, probably because of its low value in gold processing. In this study, however, recording the response of blocky pyrite to the same sequential etch program is essential to reveal the relative responses of different pyrite types to oxidation, with implications for understanding the behaviour of low As vs. As-rich pyrite, especially in treating refractory gold ores. The reaction of blocky pyrite to sequential exposures of nitric acid was tracked using image analysis on a selected pyrite (*refer to Figure 5.7*), similar to the process reported for arsenian pyrite in the previous section. The un-etched precursor grain showed no evidence of arsenian pyrite in the BSE image (*although arsenic could have been present at a level below the SEM detection limit*). The lack of BSE detectable arsenian pyrite precluded the use of the ImageJ program for histogram analysis or to illustrate As distribution in the blocky pyrite grain, if arsenic was, in fact, present.

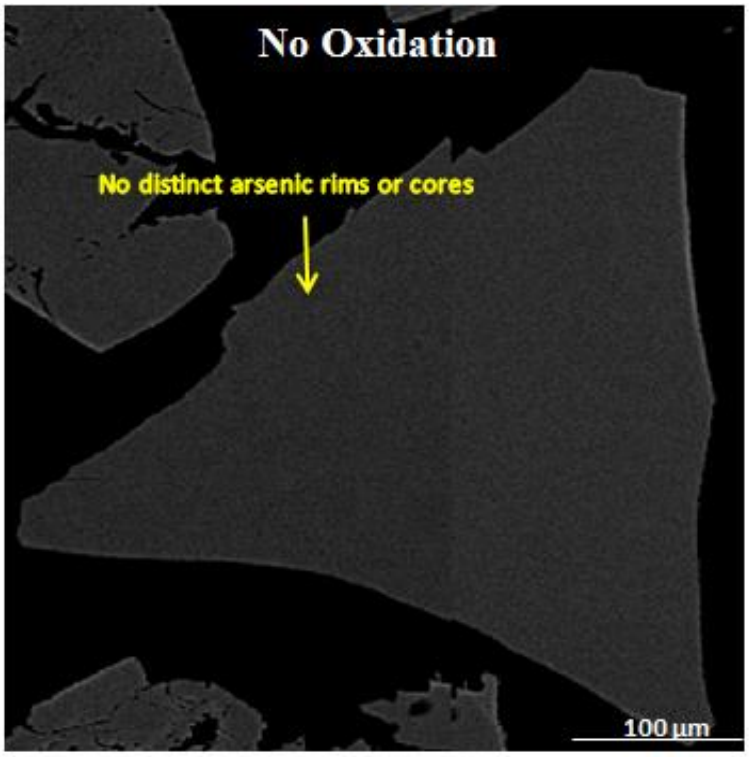

Figure 5.7: BSE image of the untreated, triangular, low As blocky pyrite grain. No arsenian pyrite is seen in the main grain of the image (*lighter greyscale values in the pyrite on the lower edge of the image indicate As*)

The image sequence which tracks the response of the selected blocky pyrite grain through the sequential oxidation steps forms Figure 5.8. The low As pyrite remained relatively unchanged despite being exposed to the same conditions which oxidised all of the arsenian pyrite (*Table 5.1*). The blocky pyrite grain remained largely unaffected. After the 30 minutes cumulative oxidation the appearance of small surface pits is the only response to the exposure to nitric acid; however, the intensity of the pitting does not change after the 40 minutes oxidation stage. The oxidation reaction-path of low As blocky pyrite grain (*Figure 5.8*) was found to be sluggish and not intensive as seen earlier with the high As pyrite.

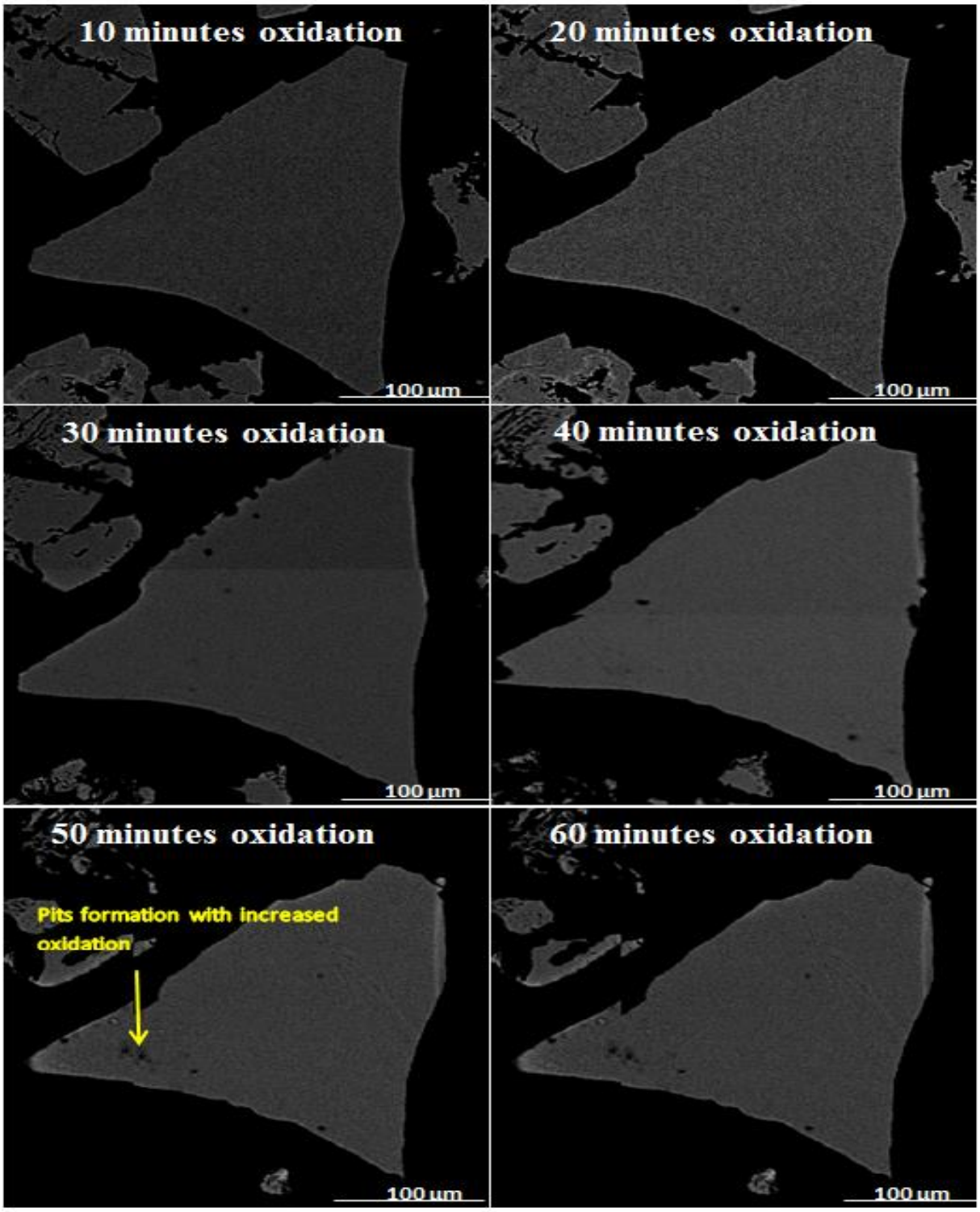

Figure 5.8: BSE image of the low As blocky pyrite grain after sequential treatment with nitric acid. Formation of pits increases as the extent of oxidation increases and is the only response to the nitric acid etching process. In contrast, higher As pyrite grains on the lower and left side of the image become corroded or even oxidised completely by the end of the sequential oxidation process.

This implies that the degree of oxidation of pyrite would be greater when As was present in the interstitial lattice sites, confirming that high arsenic pyrite oxidises at a relatively faster rate compared to low As pyrite when treated with an oxidising acid such as nitric acid. This fundamental understanding has great potential application in Lihir type refractory gold deposits which contain different types of pyrite – including blocky pyrite with low As grade and very low gold tenor. The observed oxidation rate differential of pyrite types opens up new potential processing options, such as modification of pyrite surfaces followed by their separation in a flotation process.

5.4.3 Sulfuric acid etch of low and high As pyrite

To further investigate the reaction of various pyrite types to etching, a program of sequential etching and imaging based on the flow sheet shown in Figure 5.3 was carried out, this time using sulfuric acid as the chemical etchant.

The images which form Figures 5.9 a and b illustrate the reaction of high As and low As pyrite to sequential etching by sulfuric acid. As seen previously in Figure 5.5, the As-rich growth zones in pyrite are preferentially destroyed, such that at the end of 60 minutes cumulative etching arsenian pyrite is no longer present on the face of the block. As time progresses, less and less arsenian pyrite remains, indicating oxidation time is an important parameter (*as is etchant concentration*).

After 10 minutes exposure, no signs of reaction were evident in the arsenian pyrites. Slight changes were noticed after the 20 minutes oxidation stage with some modification of high As pyrite structures as shown in Figure 5.9a. With further etching As-enriched zones progressively disappear i.e. after 30 minutes treatment the amount of arsenian pyrite present is markedly less, and after 40 minutes of cumulative exposure to sulfuric acid, the arsenian pyrite is effectively gone.

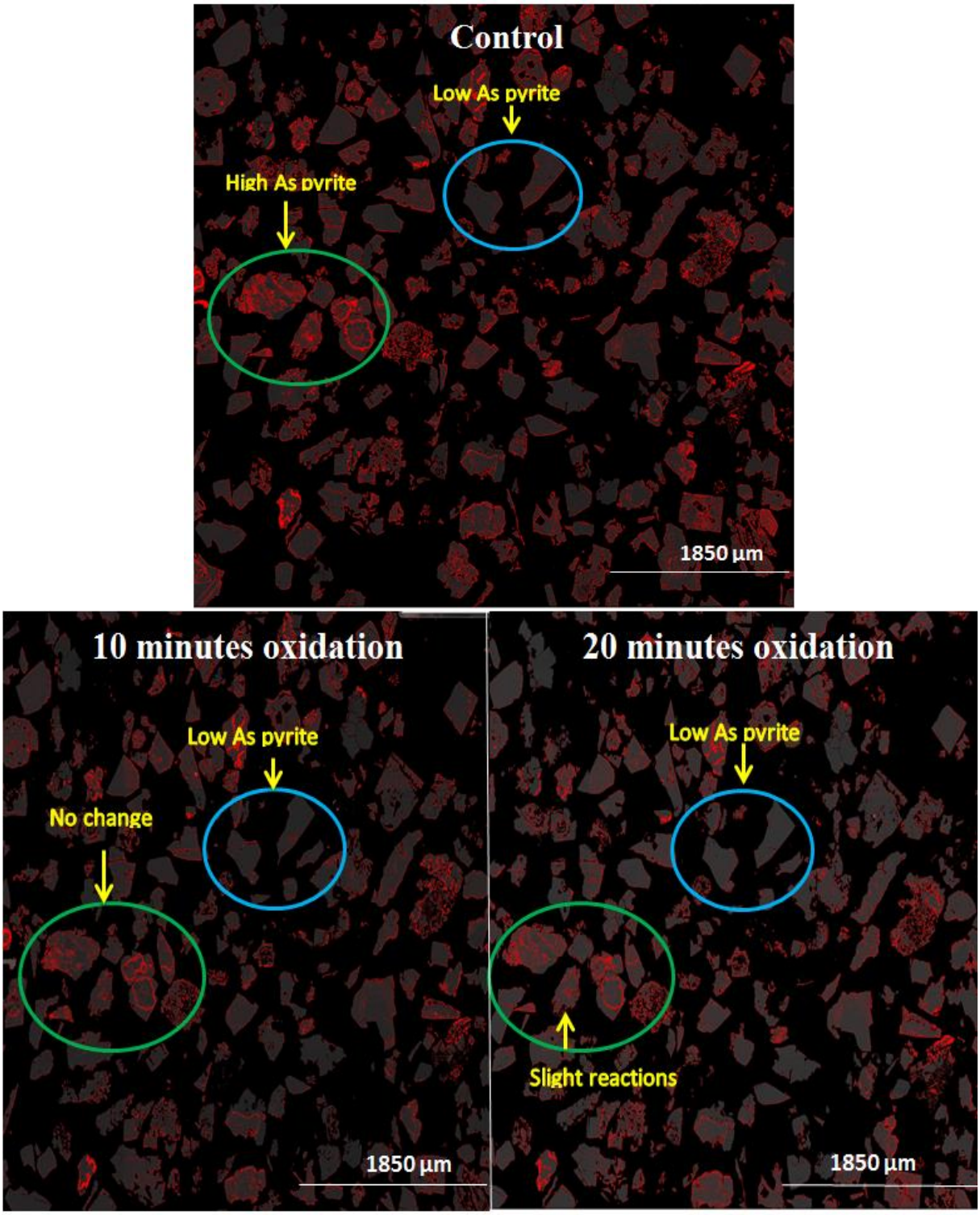

Figure 5.9a: BSE image (*after ImageJ thresholding*) of high As and low As pyrite grains after sequential treatment with sulfuric acid for 10 and 20 minutes (*cumulative time*). Arsenian pyrite is shown in red (*from thresholding*), while low As pyrite is grey. Coloured ellipses simply provide positional references, and do not indicate that all pyrite they contain is either entirely low or high arsenic.

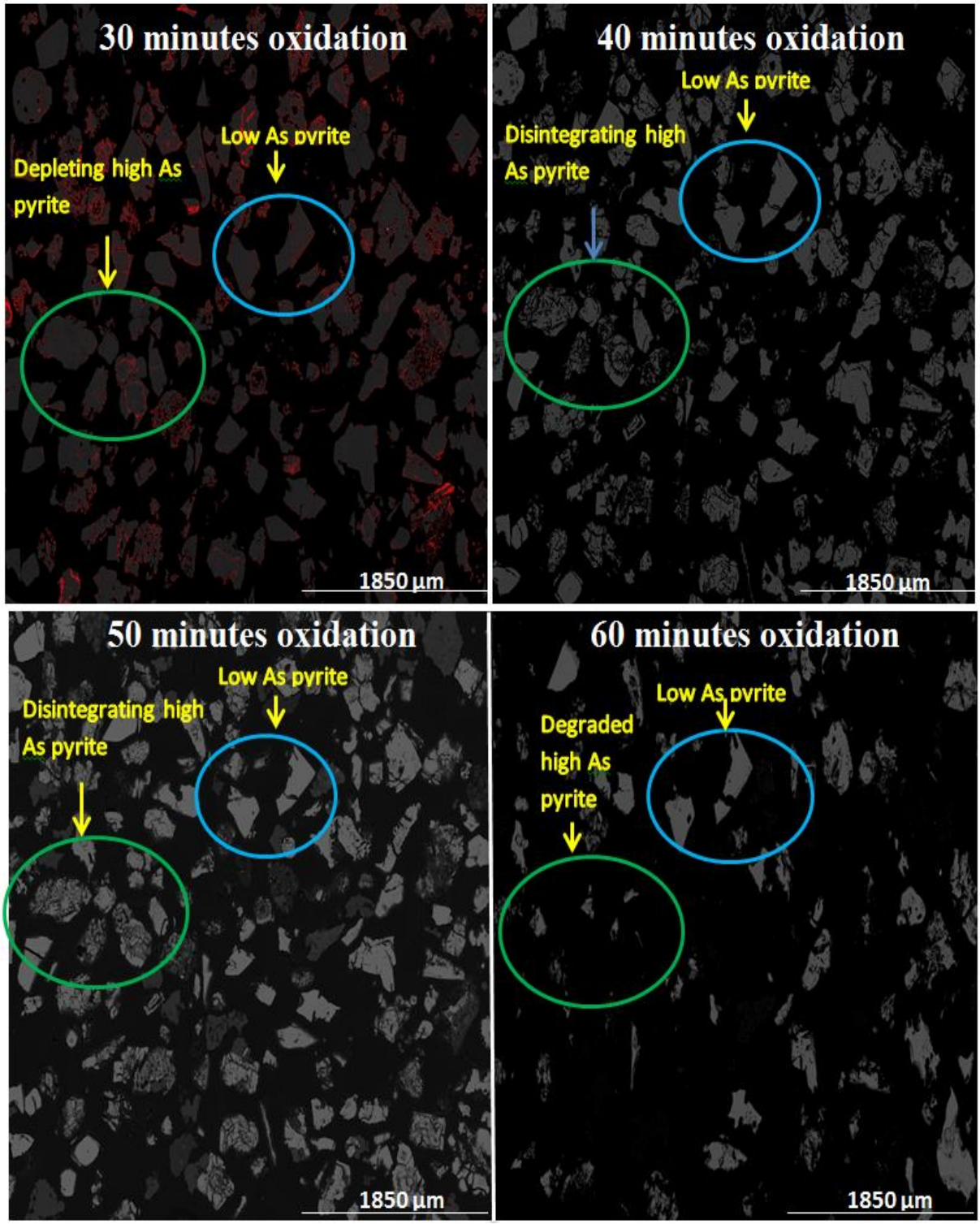

Figure 5.9b: BSE images (*after ImageJ thresholding*) of the high As and low As pyrite grains after sequential treatment with sulfuric acid from 30 to 60 minutes treatment (*cumulative time*). The appearance of pits is observed from the 30 minutes oxidation stage and this substantially increases as the reaction progresses.

The results using sulfuric acid as the etchant are similar to those obtained in the allied nitric acid study, confirming that high As pyrite (*arsenian pyrite*) has a faster reaction rate of reaction by exposure to acid, relative to low As pyrite (*blocky pyrite*). The dissolution of As-rich pyrite by sulfuric acid was quantified using the ImageJ software. Histogram analysis of BSE imaging detected 6.9 wt. % arsenian pyrite in the control sample, with progressively lower levels detected as the cumulative etch time increased (*Table 5.2 and Figure 5.10*).

Table 5.2: ImageJ histogram quantification of Au-bearing arsenian pyrite (*wt. %*) after sequential oxidation in sulfuric acid media. Under this oxidation scheme, the arsenian pyrite concentration is substantially lowered and is not detected (*n.d.*) with the 50 and 60 minutes oxidation stages.

Treatment Time (*minutes*)	**Arsenian Pyrite (*wt. %*)**	**Proportion of Arsenian Pyrite etched (*as % of original Arsenian Pyrite*)**
Control	6.9	0
10	6.2	18
20	2.9	62
30	0.5	93
40	0.1	99
50	n.d.	100
60	n.d.	100

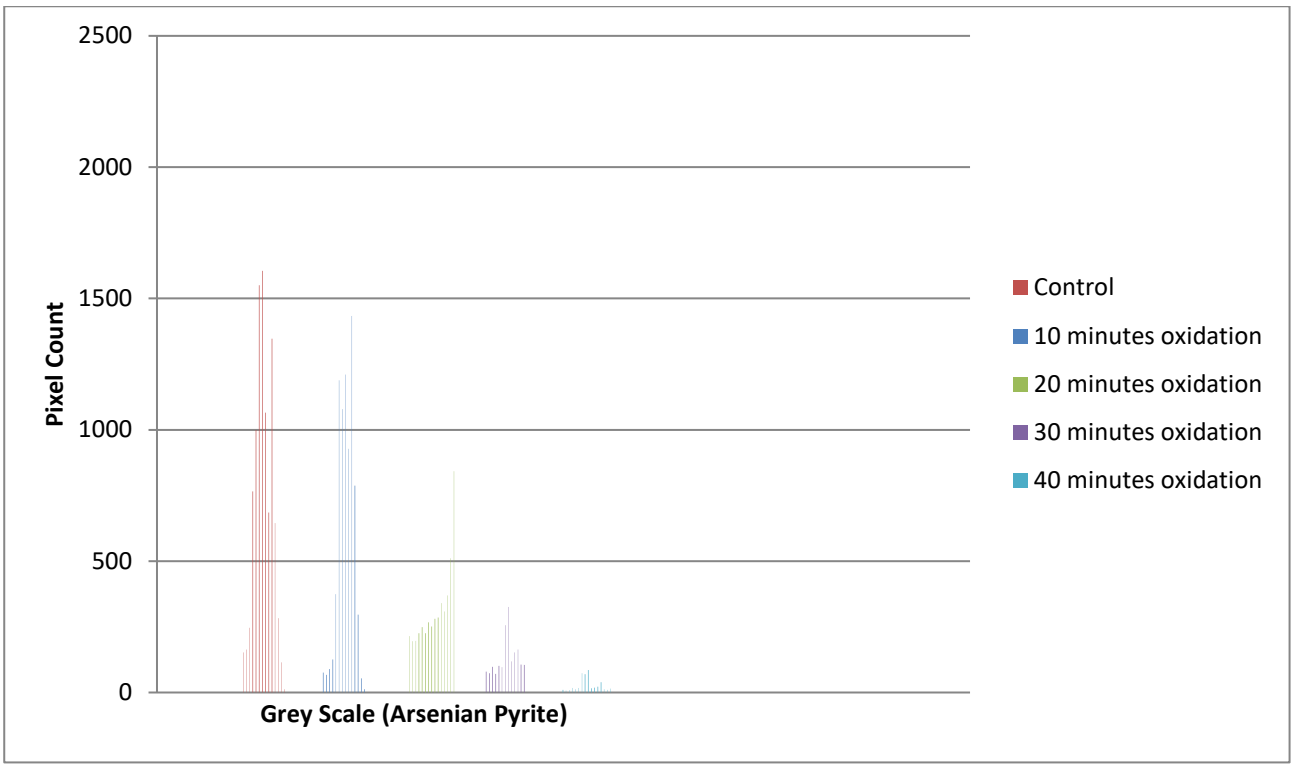

Figure 5.10: The effect of sulfuric acid sequential treatment on arsenian pyrite

5.5 Future Applications

Different oxidation characteristics for low As blocky pyrite and the high As arsenian pyrite have been demonstrated by combining data from MLA with advanced image analysis tools. Being able to understand the reactivity of different types of pyrite may lead to better understanding of their relative processing behaviours, in turn, providing opportunities to optimise recovery of gold from refractory ores. The conditions in oxidation and flotation tests may be able to be manipulated to oxidise and separate one type of pyrite preferentially from the other forms i.e. the surface of the blocky pyrite which is more resistant to oxidation, remains unchanged whereas high-As arsenian pyrite, which is more susceptible to oxidation undergoes surface modification. The differences in surface properties of the oxidised pyrite and the unoxidised pyrite may then be exploited in a subsequent separation process.

Since many pyrite textures seen in Lihir gold ores appear to be part of a morphological and compositional continuum between low As and high As pyrite, it is possible that the oxidation process may be manipulated to optimise the overall metallurgical outcome to produce a product which maximises productivity through downstream processing e.g. an autoclave (Mason, 1992, John et al., 2013).

5.6 Conclusions

1. A rapid and high-resolution mineral characterisation technique to understand the oxidation characteristics of high As pyrite and low As pyrite has been developed.
2. This method involved utilising BSE images from an SEM-based automated mineralogy system and image processing software (*ImageJ*) to track pyrite oxidation on a pixel by pixel basis.
3. Nitric acid and sulfuric acid were used as chemical etchants to understand the relative responses of the high As pyrite and low As pyrite with respect to alterations in texture.
4. It was found that sequential treatment with nitric acid removed arsenic from the pyrite surface and this effect of repeated oxidation on arsenian pyrite was quantified using the histogram function of ImageJ.
5. The low As pyrite remained relatively unchanged despite being exposed to the same conditions which oxidised all of the arsenian pyrite. The degree of pyrite oxidation was found to be greater when As was present in the interstitial lattice site proving that high arsenic pyrite oxidised at a relatively faster rate compared to low As pyrite.
6. The results using sulfuric acid as the etchant were similar to those obtained in the allied nitric acid study.
7. Being able to understand the reactivity of different types of pyrite may lead to better understanding of their relative processing behaviours, in turn, providing opportunities to optimise gold production from Lihir type ores.

5.7 Bibliography

BAKKEN, B. M., HOCHELLA, M. F., MARSHALL, A. & TURNER, A. 1989. High-Resolution Microscopy Of Gold In Unoxidized Ore From The Carlin Mine, Nevada. *Economic Geology,* 84**,** 171-179.

CLINE, J. S. 2001. Timing Of Gold And Arsenic Sulfide Mineral Deposition At The Getchell Carlin-Type Gold Deposit, North-Central Nevada. *Economic Geology,* 96**,** 75-89.

COOK, N. J. & CHRYSSOULIS, S. L. 1990. Concentrations Of Invisible Gold In The Common Sulfides. *The Canadian Mineralogist,* 28**,** 1-16.

FANDRICH, R., GU, Y., BURROWS, D. & MOELLER, K. 2007. Modern SEM-Based Mineral Liberation Analysis. *International Journal Of Mineral Processing,* 84**,** 310-320.

FLEET, M. E., CHRYSSOULIS, S. L., Maclean, P. J., Davidson, R. & Weisener, C. G. 1993. Arsenian Pyrite From Gold Deposits; Au And As Distribution Investigated By SIMS And Emp, And Color Staining And Surface Oxidation By XPS And LIMS. *The Canadian Mineralogist,* 31**,** 1-17.

JOHN, J., JOHNSON, N., STEWART, K., TURNER, D. & BRADSHAW, D. 2013. A Review Of Pretreatment Methods To Separate The Different Types Of Pyrites In Gold Processing. 5th World Gold 2013 Conference, AusIMM: Australasian Institute Of Mining And Metallurgy, 347-355.

KAPPES, R., BROSNAHAN, D. & GATHJE, J. 2009. Utilising Mineral Liberation Analysis (MLA) To Determine Pyrite, Arsenopyrite And Arsenian Pyrite Floatabilities For Carlin Trend Ores. SME Annual Meeting And Exhibit And CMA's 111th National Western Mining Conference, 2009. 736-741.

LAMB, W. 2004. Optimising The Value Of The Lihir Low-Grade Resource. Rio Tinto Technical Report No: AR2163. Project Code: GAL 144.

MARSDEN, J. & HOUSE, I. 2006. *The Chemistry Of Gold Extraction*, SME. Littleton, Colorado, USA ISBN-13: 978-0-87335-240-6 ISBN-10: 0-87335-240-8.

MASON, P. 1992. Examining The Economics Of Some Pressure Oxidation Process Options. *Hydrometallurgy,* 29**,** 479-492.

MORISHITA, Y., SHIMADA, N. & SHIMADA, K. 2008. Invisible Gold And Arsenic In Pyrite From The High-Grade Hishikari Gold Deposit, Japan. *Applied Surface Science,* 255**,** 1451-1454.

PAKTUNC, D., KINGSTON, D., PRATT, A. & MCMULLEN, J. 2006. Distribution Of Gold In Pyrite And In Products Of Its Transformation Resulting From Roasting Of Refractory Gold Ore. *The Canadian Mineralogist,* 44**,** 213-227.

PETRUK, W. 2000. *Applied Mineralogy In The Mining Industry,* Elsevier.

REICH, M., KESLER, S. E., UTSUNOMIYA, S., PALENIK, C. S., CHRYSSOULIS, S. L. & EWING, R. C. 2005. Solubility Of Gold In Arsenian Pyrite. *Geochimica Et Cosmochimica Acta,* 69**,** 2781-2796.

THOMAS, K. G. 1991. Alkaline And Acidic Autoclaving Of Refractory Gold Ores. *JOM,* 43**,** 16-19.

CHAPTER 6

The Influence of Lime and NaOH Conditioning on Sulfide Sulfur in Pyrite Flotation

The influence of two alkaline pH modifiers, namely sodium hydroxide (*NaOH*) and calcium hydroxide ($Ca(OH)_2$) was investigated to evaluate and compare their effectiveness in floating of a high sulfide sulfur grade pyrite ore, averaging 13% S^{2-}, using potassium amyl xanthate (*PAX*) as the collector and Nascol 422 as the frother. The focussing question for this study was to determine if there is a promising premise for substituting lime with NaOH as a pH regulator in the flotation of Lihir ores where there is excess sulfur to be treated for the amount of gold present. If this is possible, then the sulfide sulfur levels of the concentrate samples could be regulated and optimised for a direct autoclave feed. The sulfide sulfur results from the flotation tests show that, for the same experimental conditions (*pH =5, PAX = 50g/t and Nascol =50g/t*), the use of NaOH increased the gold to the sulfur ratio (*Au:S*) of the rougher concentrates and enhanced the gold recovery rates compared to lime.

Keywords: Flotation, pH Modifier, Sodium Hydroxide, Lime, Sulfide Sulfur, XPS

6. Introduction

Sodium hydroxide and lime are the most commonly used industrial and laboratory pH modifiers for pyrite flotation. However, they are both depressants of pyrite with $Ca(OH)_2$ being more effective than NaOH and there have been numerous studies confirming this perception (Li et al. 2012). Lime has always been preferred as a neutralising agent/pH modifier mainly due to its low cost and easy procurement. The local presence of a limestone quarry and a 200 t/d design capacity lime kiln at Lihir lowers the acquisition and operating costs with lime as opposed to using other pH modifiers.

As discussed in Chapter 1, the blend feed sulfide sulfur grade to the autoclave at Lihir is 7.2% S^{2-} (Collins et al., 1993) resulting in autoclave issues due to its fixed sulfide oxidation capacity. The use of lime does not offer any advantage in terms of increasing the Au:S ratio of the flotation concentrates to overcome the limiting capabilities of the autoclave circuit.

Therefore, the driving force was to understand if the use of an alkaline pH modifier such as sodium hydroxide (*NaOH*) which is corrosive in nature oxidises the bulk of the sulfide sulfur during the conditioning stage of flotation as opposed to lime ($Ca(OH)_2$) which is a pH modifier and does not oxidise the sulfide matrices. It has already been reported (Li et al., 2006) that NaOH could be used for sulfide oxidation; however, the impact on the sulfide sulfur grade remains to be explored.

Therefore, the hypothesis being tested is: does substituting lime with NaOH outweigh the advantage of easy procurement of lime and significantly upgrade the Au:S ratio in the flotation concentrate? The key questions that are addressed in this work are: How does the use of NaOH for Au-pyrite roughing (*using PAX as the collector*) affect the sulfur and gold recoveries compared to lime? Is there a significant upgrade of the Au:S value by using NaOH in the conditioning step? If so, does this modification warrant the replacement of lime with NaOH? All the above questions are investigated in the context of producing a gold-rich concentrate of high grade and minimal sulfide sulfur content (Agorhom et al., 2013).

6.2 Results and Discussion

6.2.1 Back-Scattered Electron Imaging

To demonstrate the effect of NaOH (*if any*) oxidation on the pyrite texture, BSE images of the ($Ca(OH)_2$) and NaOH treated samples were collected and processed using ImageJ software to highlight the arsenic zones in pyrite (*highlighted in red*). The BSE images presented in Figures 6.1 and 6.2 show the effect of ($Ca(OH)_2$) and NaOH solution on the texture of pyrite grains. No major pitting of the pyrite grains was observed with any of the lime conditioned samples suggesting there was little or minimal oxidation.

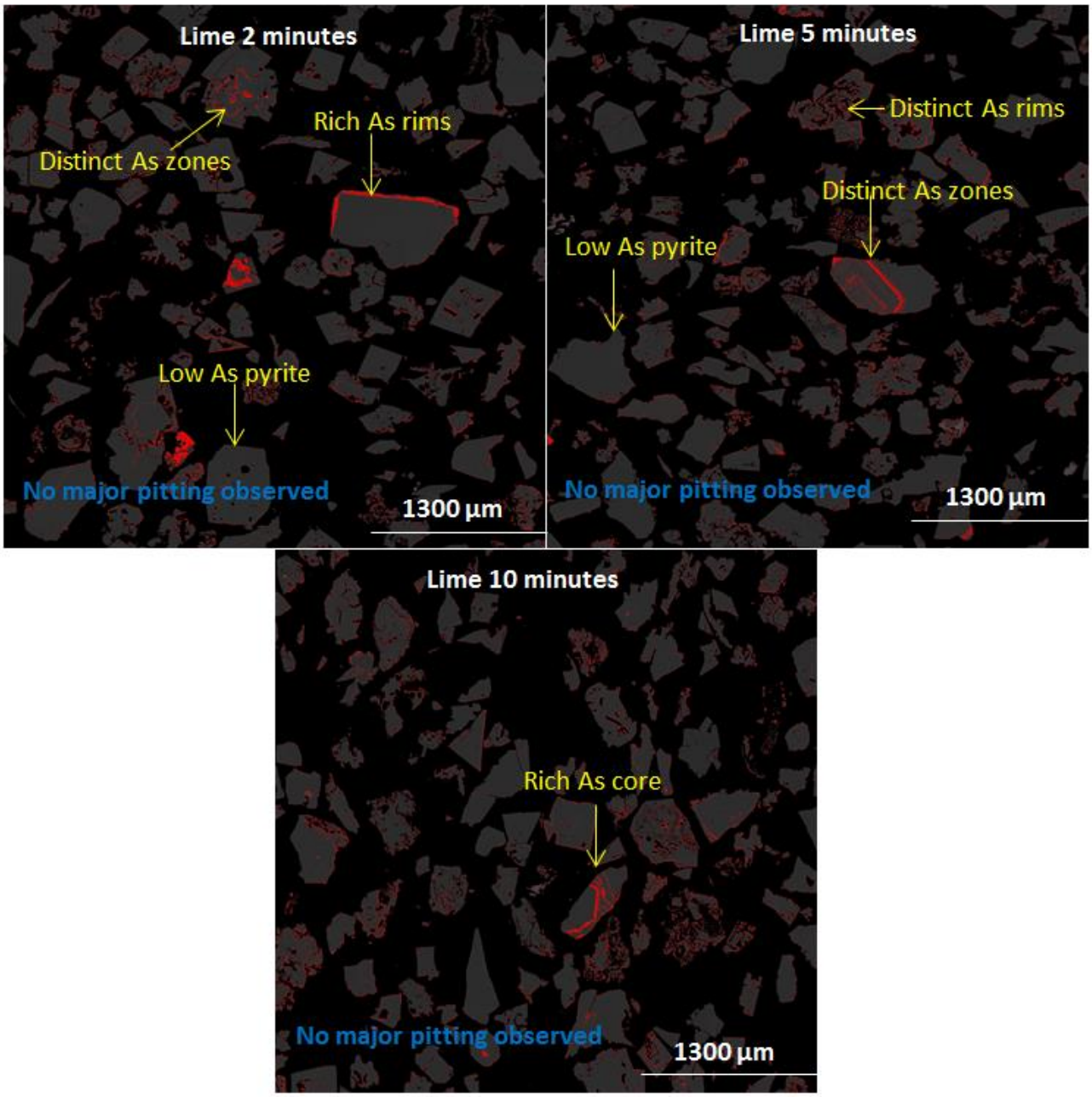

Figure 6.1: BSE images of pyrite treated with lime a) 2 mins b) 5 mins c) 10 mins at pH 4 and ambient temperature. No major pitting was observed with any of the conditioning times.

Although the formation of a fragmented product layer/oxidation layer would be expected in the case of NaOH treated samples (*due to oxidation*), no such formation was detected in the BSE images. This could be because the products from oxidation could have been removed during the preparation of MLA blocks through polishing. Similar to the lime conditioned samples, no pitting effects were observed with NaOH 2 and 5 minute conditioned samples. However, major pitting effects were observed with the NaOH 10 minutes conditioned sample. Suffice to say that conditioning with NaOH did not oxidise the pyrite significantly enough to disintegrate the As-rich zones as shown in Figure 6.2.

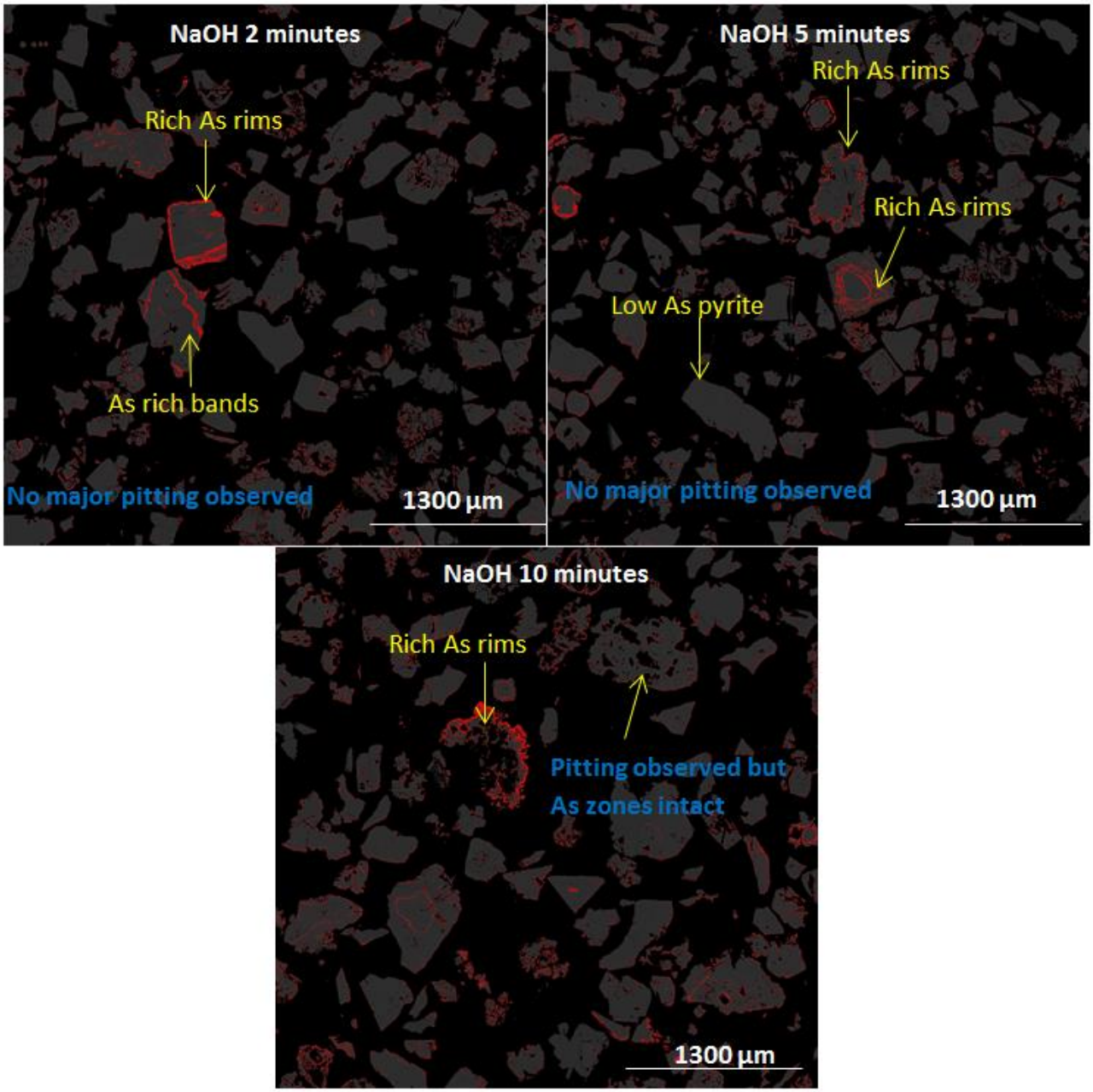

Figure 6.2: BSE images of pyrite treated with NaOH a) 2 mins b) 5 mins c) 10 mins at pH 4 and ambient temperature. Major pitting observed with NaOH 10 minutes conditioned sample.

6.2.2 BET and Sulfide Sulfur oxidation (SOx)

The lime and NaOH conditioned concentrate samples (*2, 5 and 10 mins*) were analysed by more sensitive techniques such as BET surface area analysis and sulfide sulfur oxidation measurement (*SOx*). The results of the BET measurement, as shown in Figure 6.3, suggests that increased exposure to NaOH treatment resulted in higher surface area for NaOH samples which reaches a plateau but lime has no significant effect.

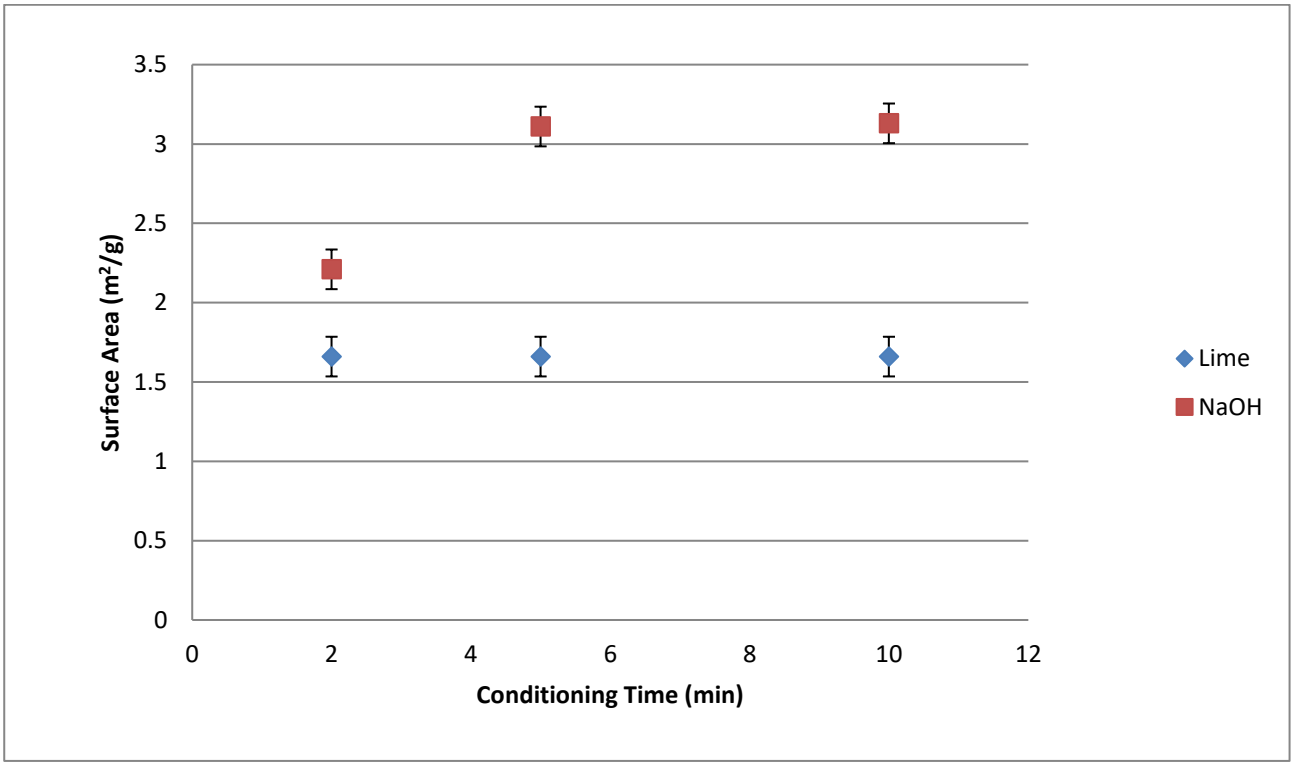

Figure 6.3: Effect of lime and NaOH conditioning on sample surface area

Despite all the samples exhibiting relatively low specific surface area values, a two-fold increase was observed when the samples were conditioned with NaOH indicating that the extent of oxidation directly influences the surface area of the pyrite concentrate. Therefore, the extent of sulfide sulfur oxidation (*lime and NaOH conditioning*) was quantified by SOx measurements. SOx analysis revealed that the sulfide sulfur oxidation values for the lime conditioned samples (*2, 5 and 10 minutes*) remained the same.

However, with increasing NaOH conditioning times, the extent of sulfide sulfur oxidation increased from 5% oxidation for the 2 minutes conditioned concentrate to 6.8% oxidation for the 5 minutes conditioned concentrate and finally to 8.1% oxidation for the 10 minutes conditioned concentrate as illustrated in Figure 6.4. The high level of oxidation of the 10 minutes NaOH conditioned sample (*8.1%*) explains the pitting effects observed with textural analysis. This also aligns quite well with

the findings from BET measurements where no changes in surface area were observed with lime conditioned samples and higher surface area values observed with the NaOH samples.

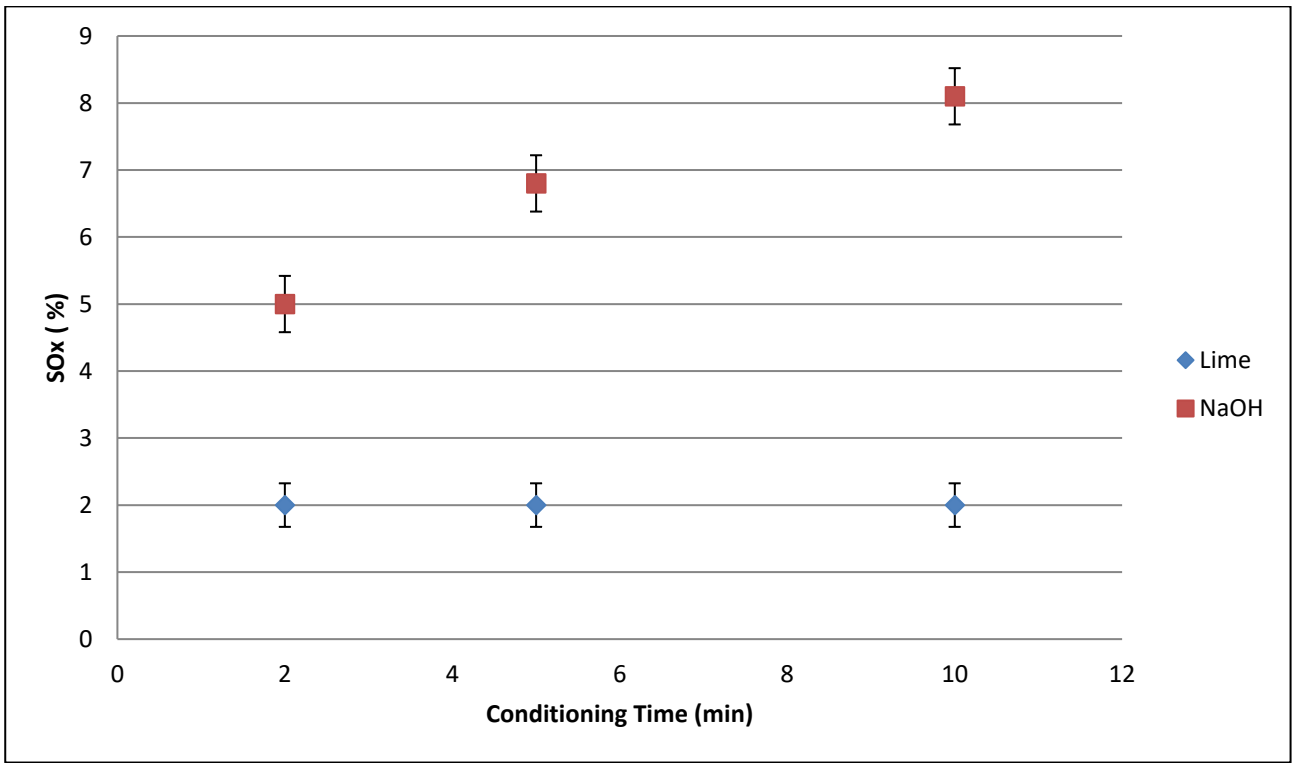

Figure 6.4: SOx (%) of lime and NaOH samples at different time intervals

6.2.3 X-Ray Photoelectron Spectroscopy (XPS)

The oxides and sulfate species formed due to pyrite oxidation can have a considerable impact on the following rougher flotation process. For example, it has been reported in other work that metal deficient sulfides can facilitate flotation by forming hydrophobic species while metal hydroxides can inhibit flotation due to their hydrophilic nature (Buckley and Woods, 1987, Smart, 1991, Buckley and Woods, 1984). This is because oxidation of the mineral surface can facilitate or inhibit interactions with the flotation collectors thereby significantly altering the metallurgical responses (Buckley and Woods, 1987).

Therefore, the effect of lime and NaOH on the pyrite concentrate surface was investigated by the surface analytical technique, XPS. XPS S2p peaks of pyrite have been analysed extensively and use of these can be found in the literature; therefore, just sulfide sulfur and sulfate peaks were used to understand signs of oxidation with either treatment as illustrated in Figure 6.5.

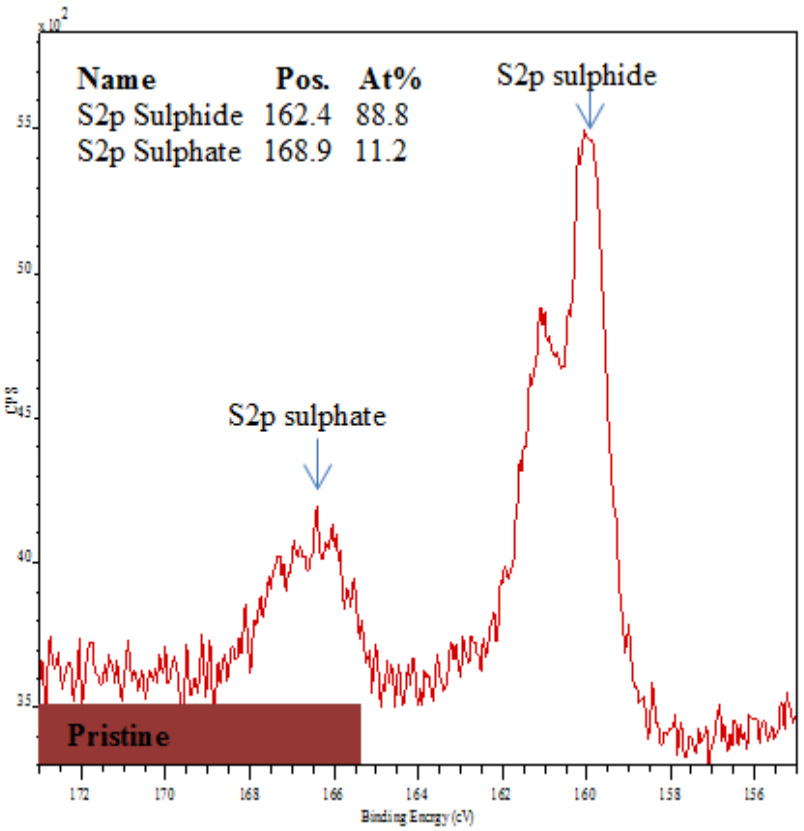

Figure 6.5: S (2p) spectra of an unconditioned pyrite concentrate.

The doublet with the S2p binding energy between 162.4 and 162.7 eV is attributed to S^{2-} from FeS_2 (Buckley and Woods, 1987). The broad peak observed between 166.1 and 169.1 eV is due to the formation of sulfate species (SO_4^{2-}). Comparing the intensities of the S2p spectra of the lime and NaOH concentrate samples, an increase in the surface concentration of sulfates after oxidation in NaOH solution is observed as shown in Figure 6.6.

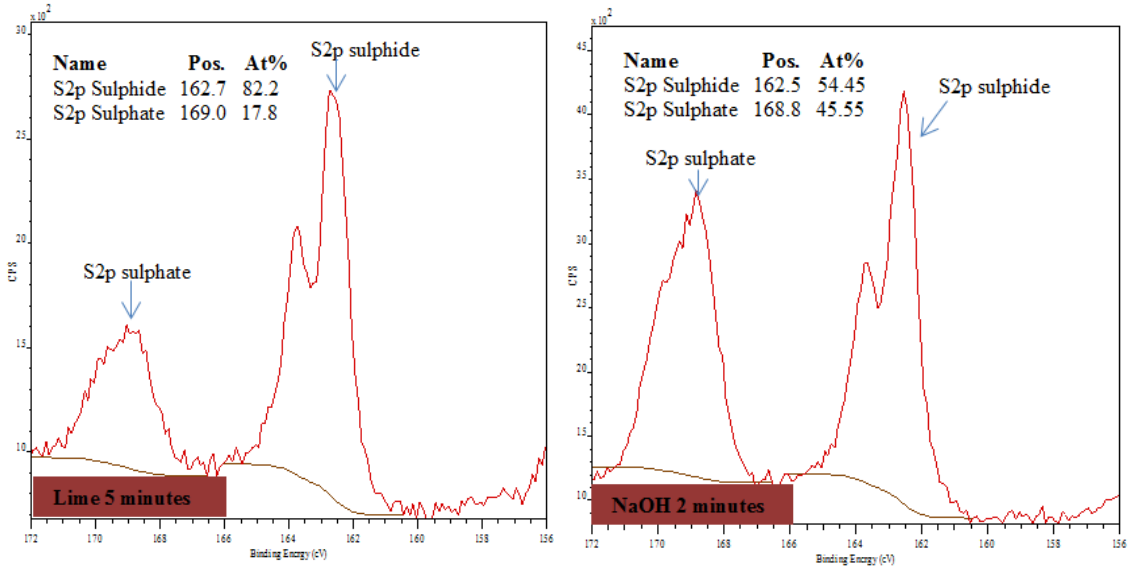

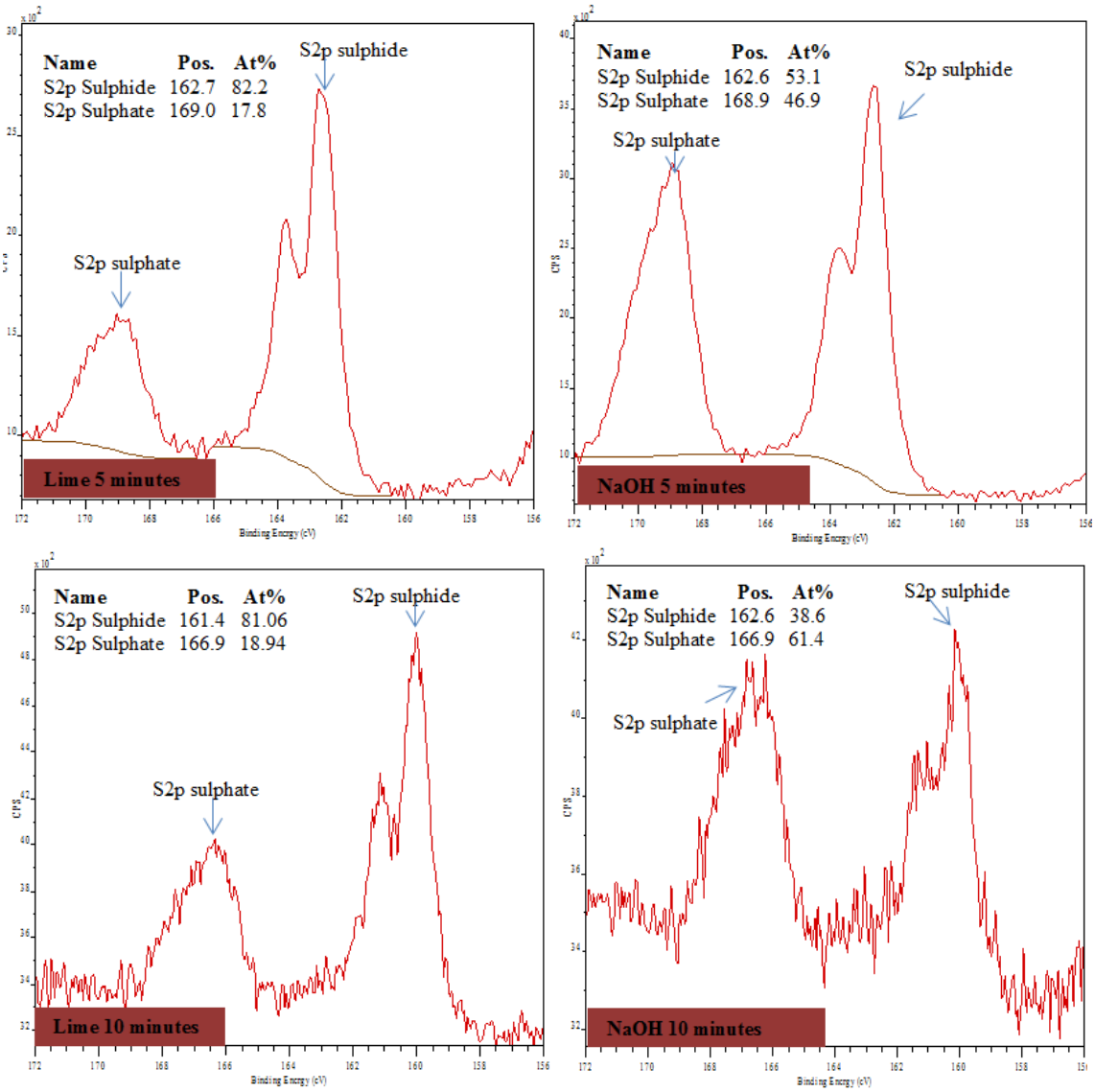

Figure 6.6: S (2p) spectra of lime and NaOH conditioned concentrates. The 2 minutes NaOH conditioned concentrate sample shows a higher percentage of sulfate species signifying the onset of pyrite concentrate oxidation. This trend continues with 5 minutes conditioning stage with increased concentration of sulfate species detected with NaOH concentrate compared to the 5 minutes lime sample. As the conditioning time advances (*10 minutes*), a marked difference is seen with the S2p spectra with the formation of more sulfate precipitates in the case of NaOH conditioned concentrate.

The S2p spectrum for the 2 minutes NaOH conditioned concentrate shows the presence of a stronger sulfate peak (*168.8 eV*) compared to the lime 2 minutes sample. This trend continues with the 5 minutes NaOH conditioned sample showing a more marked oxidised sulfate peak from oxidation. Finally, the measured surface composition (*at %*) of the sulfate species with the 10 minutes NaOH conditioned sample confirms more than 50% oxidation of the sulfide sulfur to sulfate species.

The concentration of sulfate species increases as the residence time of NaOH conditioning increases. In all the NaOH samples, the hydrophilic sulfate to sulfide (*potentially hydrophobic*) ratio increased suggesting that there is significant oxidation of the pyrite surface to cause an impact on the metallurgical response. Quantification of the sulfide sulfur and sulfate species confirmed that the concentration ratio of SO_4^{2-} species (*at %)* increased from 36.4 % (*2 mins lime*) to 75.4 % (*2 mins NaOH*) indicating an increase in oxidation of the pyrite surfaces by NaOH. Correspondingly, while the lime 2 minutes showed a decrease of 7.7 % sulfide sulfur compared to the unconditioned sample, a massive 62.9% decrease was seen with NaOH sample for the same conditioning time. This trend is seen across other NaOH conditioning times as well as shown in Table 6.1.

Table 6.1: S2p quantification of pyrite concentrates conditioned with lime and NaOH

Sample	S^{2-} (*at %*)	SO_4^{2-} (*at %)*	% decrease in sulfide sulfur	% increase in sulfate
Unconditioned	88.8	11.2	0	0
Lime 2 minutes	82.4	17.6	-7.7	36.4
Lime 5 minutes	82.2	17.8	-8.0	37.1
Lime 10 minutes	81.0	18.9	-9.6	40.7
NaOH 2 minutes	54.5	45.6	-62.9	75.4
NaOH 5 minutes	53.1	47.0	-67.2	76.2
NaOH 10 minutes	38.6	61.4	-130.0	81.8

6.2.4 Rougher flotation

The metallurgical responses of the lime and NaOH conditioned pyrite concentrates are shown in Table 6.2. The high flotation response in the acidic pH range 5 is due to the formation of dixanthogen (*and hydrophobic xanthates*) (Fornasiero et al., 1992, Mermillod-Blondin et al., 2005).

Using lime as a pH modifier, gold recoveries of 78.9%, 77.6% and 77.1% are seen for the 2, 5 and 10 minutes conditioning time samples. Although other studies have reported a decrease in gold recoveries due to oxidation of ferrous ions to ferric hydroxides imparting a hydrophilic character to the pyrite surface, that is not the case here. This is because, despite no significant oxidation of the lime conditioned samples (*from XPS and SOx values*), calcium salts (Ca^{2+}) form a dense layer on the pyrite surface and the density of this layer increases with conditioning time. This dense coating not only inhibits further oxidation of pyrite but also reduces the dixanthogen concentration on the pyrite surface (Mermillod-Blondin et al., 2005) resulting in lower gold recoveries as shown in Figure 6.7.

Table 6.2: Rougher flotation data of lime and NaOH samples floated at pH 5. Significant upgrades in Au:S values (blue column). *= untreated/unoxidised concentrate

Oxidation			Metallurgical Response				
Treatment	**Conditioning (*minutes*)**	**Sox (*%*)**	**Gold Recovery (*%*)**	**Gold Grade (*g/t*)**	**Sulfide Sulfur Recovery (*%*)**	**Sulfide Sulfur Grade (*%*)**	**Au:S Ratio**
Lime	2	**0**	78.9	9.6	79.4	39.2	**0.25**
Lime	5	**0**	77.6	9.8	77.7	38.6	**0.25**
Lime	10	**0**	77.1	9.2	70.4	39.6	**0.23**
NaOH	2	**5**	82.7	7.0	83.7	24.9	**0.28**
NaOH	5	**7.9**	81.6	7.4	81.3	23.4	**0.32**
NaOH	10	**8.1**	83.9	7.2	86.7	25.5	**0.28**

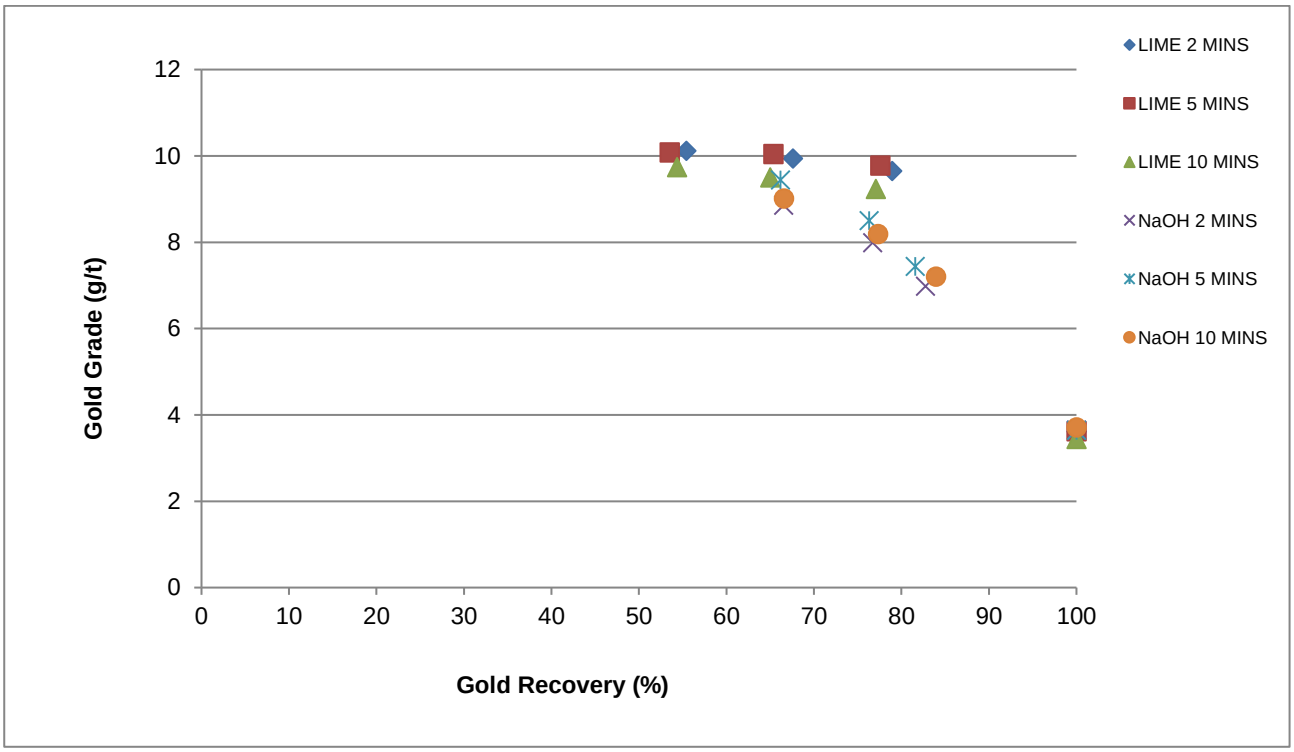

Figure 6.7: Gold grade-recovery curves of lime and NaOH conditioned concentrates

A similar trend is also observed with sulfide sulfur recoveries suggesting that lime inhibits the flotation response of pyrite (*agrees with other studies reported in the literature*) (Mermillod-Blondin et al., 2005, Fornasiero et al., 1992, Li et al., 2006). Previous research (Mermillod-Blondin et al., 2005) has shown that this detrimental effect caused by lime is because the rate of oxide nucleation is lower in the lime system resulting in adhering of much larger particles on the surface to form a dense precipitate layer. Oxide nucleation is a 'cohesive factor' that is directly related to the ionic strength of the solution and inversely to the size of the particles that attach to the mineral surface (Charles, 1952). Hence it is possible that the integrity of the lime coating on the pyrite is maintained despite the high stirring forces involved during the conditioning process. This precipitated dense layer on the pyrite surface could have reduced its floatability and this effect is reflected in the low sulfide sulfur recoveries (*79.4%, 77.7% and 70.4 % for 2 mins, 5 mins and 10 mins samples).*

However, a different trend is observed with NaOH conditioning. The gold recoveries were comparatively higher at 82.7%, 81.6% and 83.9% for 2, 5 and 10 minutes conditioning times. The relatively higher gold recoveries can be attributed to the adsorption density factor of sodium which is 20 times lower than calcium (Gaudin and Charles, 1953). This means that the hydrophilic thin fragmented oxide layer formed on the pyrite surface due to NaOH oxidation (*equation 34*), disintegrates with time and stirring. This allows for more collector attachment on the pyrite surface resulting in relatively high sulfide sulfur recoveries (*83.7%, 81.3% and 86.7% for 2 mins, 5 mins and 10 mins samples*).

$$8FeS_2 + 30NaOH \xrightarrow{\text{yields}} 4Fe_2O_3 + 14Na_2S + Na_2S_2O_3 + 15H_2O \quad \ldots\ldots\ldots\ldots\ldots\ldots\ldots\ldots\ldots\ldots\ldots\ldots\ldots\ldots 34$$

Moreover, it is possible that the NaOH oxidation of the sulfide surfaces is localised i.e. unoxidised regions are available for the collector to attach. It is possible that the localised regions are absent in the lime conditioned samples resulting in relatively low gold and sulfide sulfur recoveries. It can be argued that mild oxidation in the NaOH system leads to the formation of metal-deficient sulfides rendering the mineral surface moderately hydrophobic (Buckley and Woods, 1987). This hydrophobic nature could have resulted in higher gold recoveries as shown in Figure 6.8. However, this not true because in all the systems (*lime and NaOH*) induced floatability due to collector addition and attachment would have overpowered the hydrophobic metal deficient sulfides. Hence, it can be said that the differences in the recoveries between the lime and NaOH system are due to the variations in collector attachment.

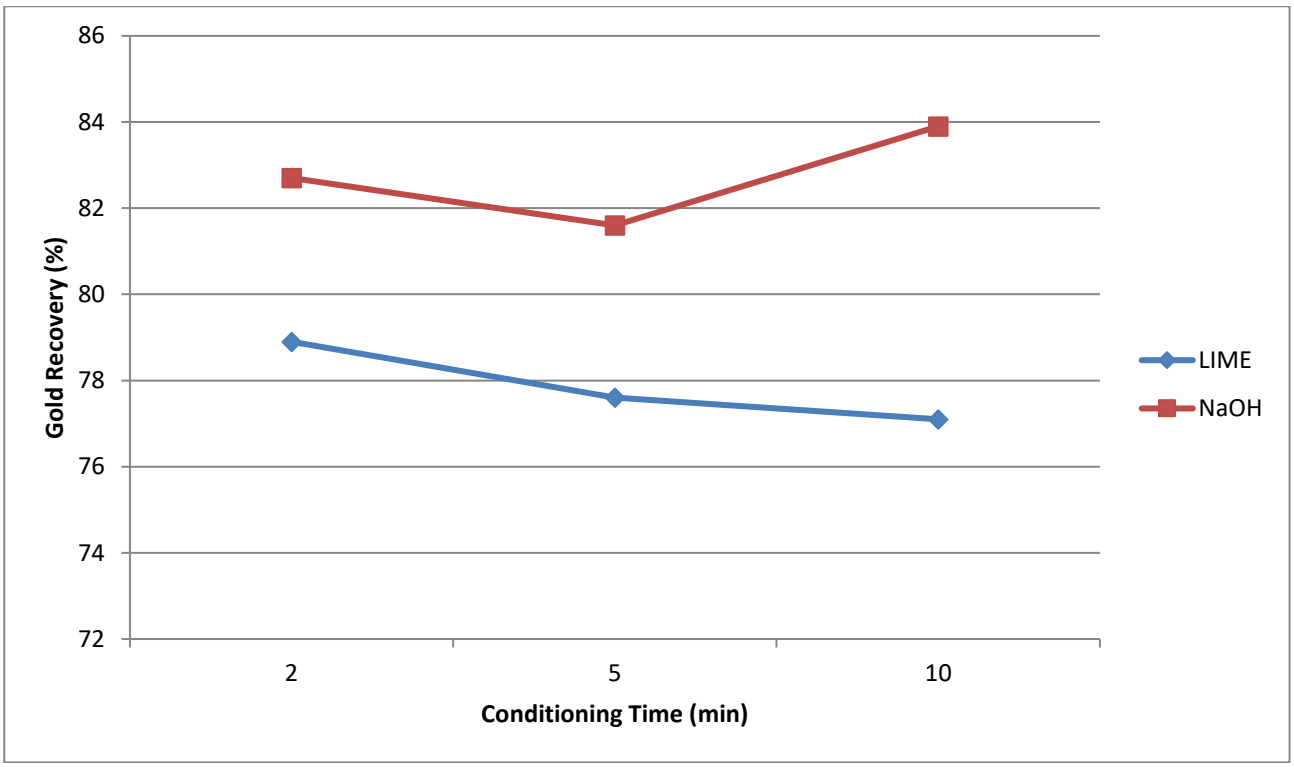

Figure 6.8: Effect of conditioning time on the flotation response of oxidised pyrite

6.2.4.1 Water Recovery

The water recovery patterns in both the lime and NaOH systems are shown in Figure 6.9. It can be seen that the water recoveries are higher by a considerable amount with the NaOH system. Although higher gold recoveries compared to water recoveries recorded in both the systems (*Lime and NaOH*) suggest that the flotation behaviour was 'true and genuine', the significant contribution of entrainment mechanism (*and also higher mass pulls*) to cause higher gold and sulfide sulfur recoveries cannot be ruled out with the NaOH system.

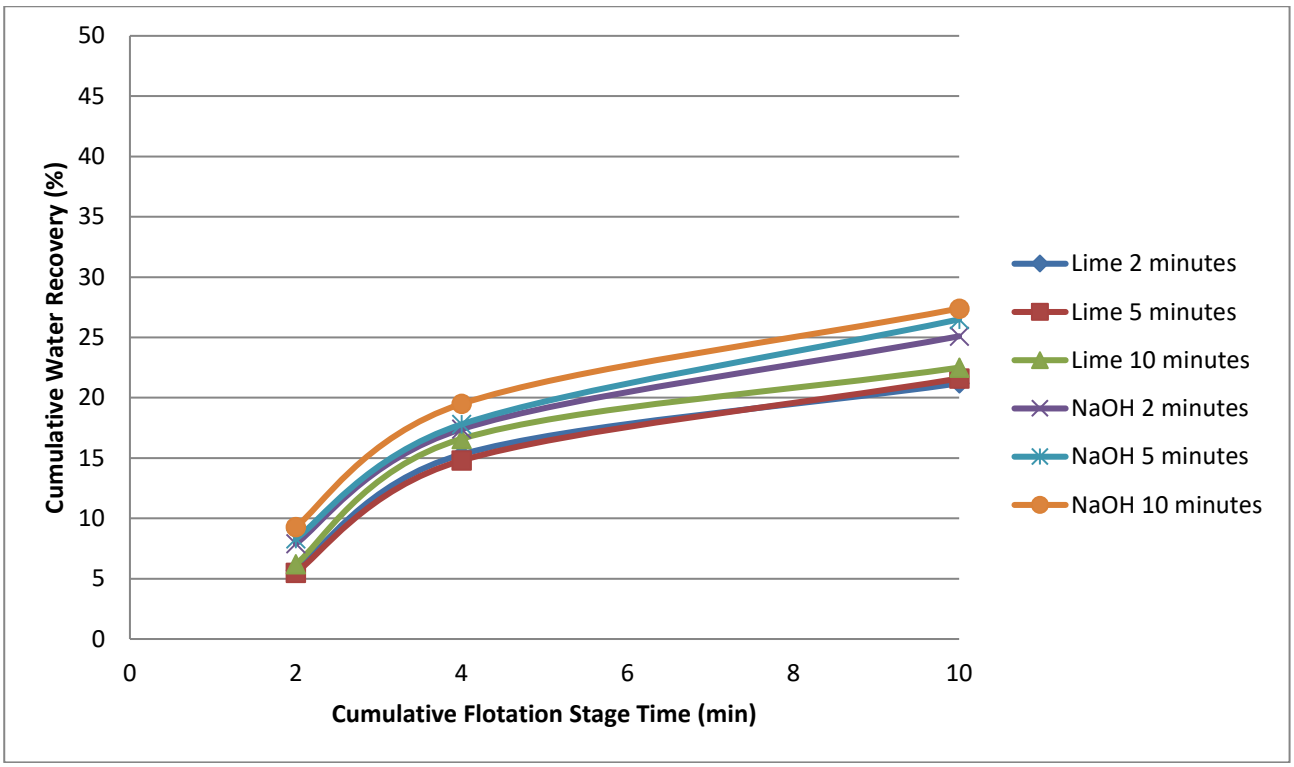

Figure 6.9: Water recovery analysis for the lime and NaOH conditioned flotation concentrates

6.2.5 Gold to Sulfur Ratio (Au:S)

Rougher flotation tests of lime and NaOH conditioned concentrates have displayed different metallurgical responses with an increase in Au:S ratios discerned with the NaOH samples as shown in Figure 6.10. The Au:S ratio for the lime samples stays very low between 0.23 and 0.25 which is quite similar to the typical Lihir flotation performance of 0.25 (Rankin, 2013). However, interestingly for the same flotation conditions, higher Au:S values are observed with the NaOH samples shown in Figure 6.10. Although it can be argued the higher mass pull in the NaOH system could have contributed to the higher Au:S values, this is not true. This is because Au:S values are based on the gold and sulfide sulfur grades and not their recoveries.

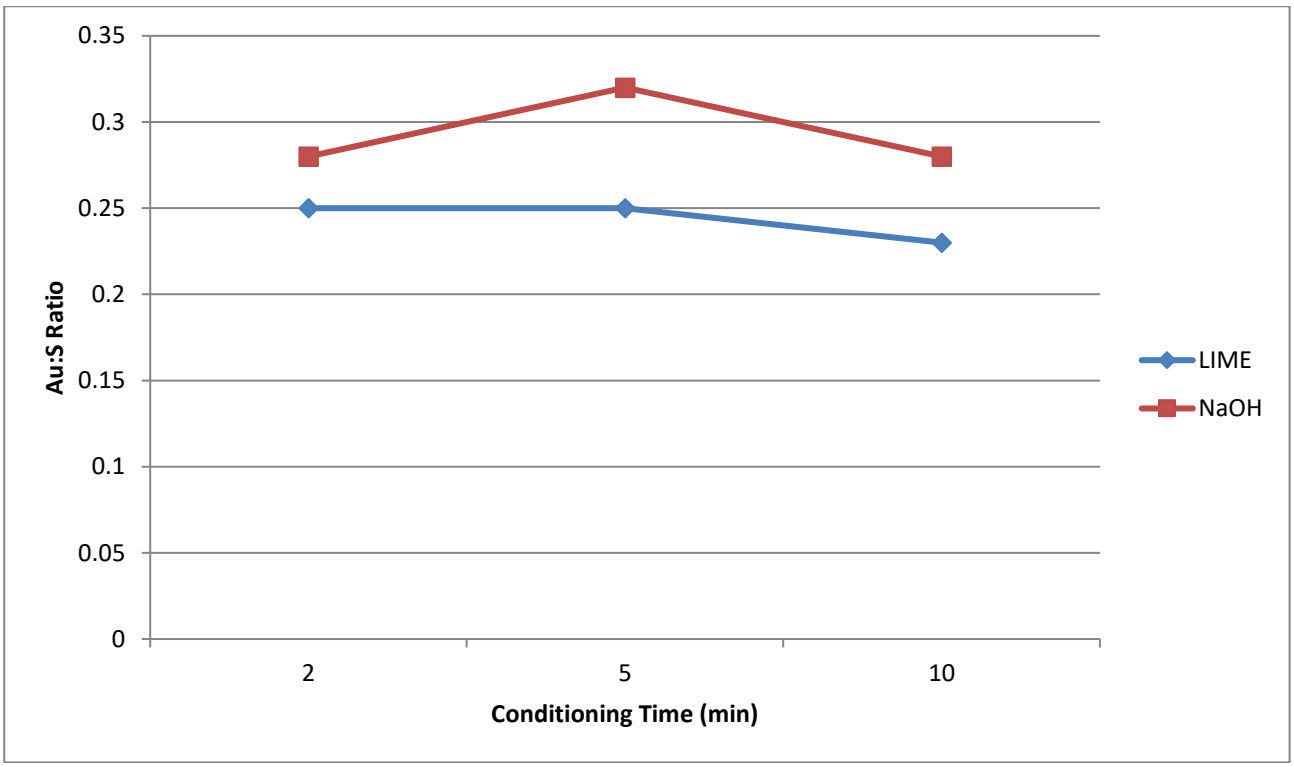

Figure 6.10: Au:S values of lime and NaOH conditioned samples floated at pH 5

Therefore, to explain the upgrade in Au:S values it is necessary to examine the gold and sulfide sulfur grades of the lime and NaOH conditioned samples and this forms Figure 6.11.

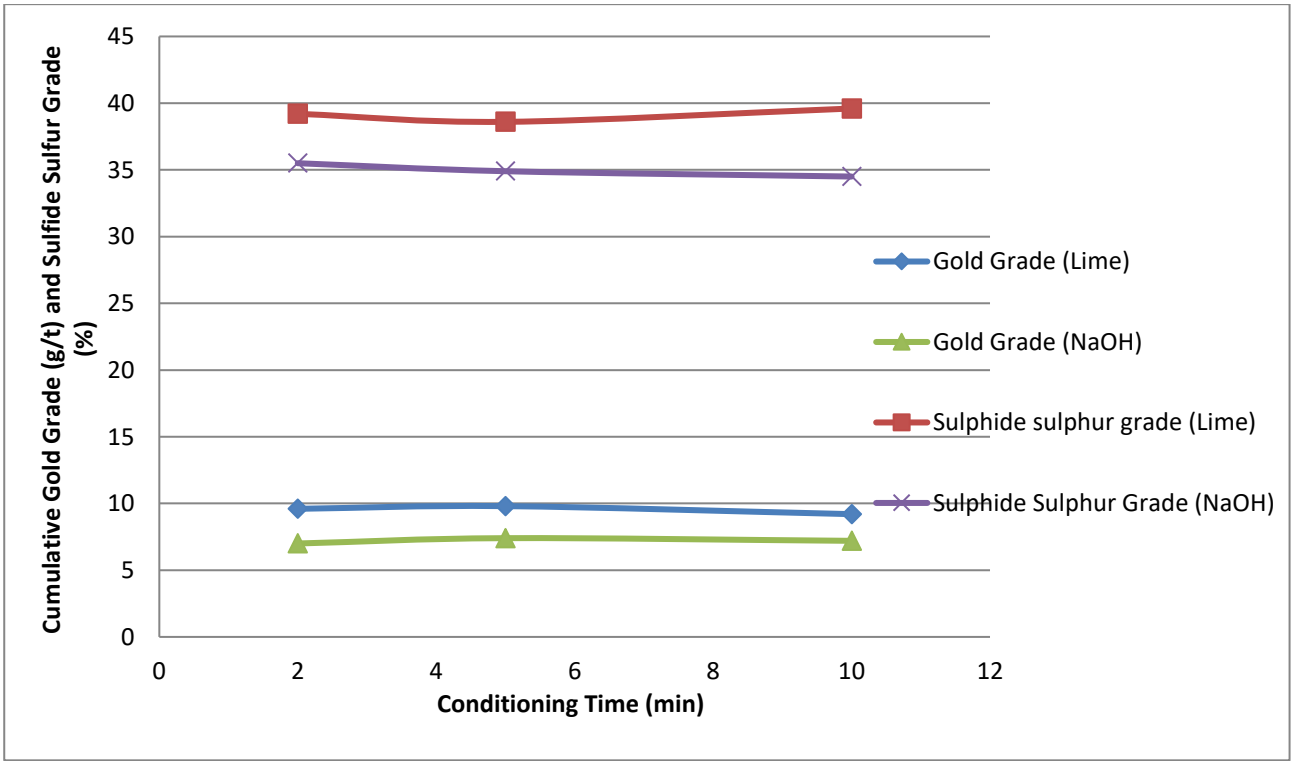

Figure 6.11: Cumulative gold and sulfide sulfur grades of lime and NaOH samples

Despite the fact that a relatively lower gold grade is seen for the NaOH samples, it is evident that it is the sulfide sulfur grade that gets modified to a greater extent in the conditioning process. The change is probably because the AA ore has a wide range of pyrite types some with high gold and some with a low gold tenor.

It is likely that, due to the oxidising environment of the NaOH solution, some of the pyrite types must be oxidising relatively faster compared to the other types. This oxidation reaction must be transforming the highly reactive pyrite types into an 'oxidised pyrite phase' allowing them to be recovered in the following flotation process. This is further confirmed by examining the % changes as a function of sulfide sulfur grade as shown in Table 6.3. It can be seen that the higher the extent of oxidation, the greater is the reduction in sulfide sulfur grade. However, despite a higher mass pull, there is a significant reduction in sulfide sulfur grade as the extent of oxidation increases signifying that the pyritic sulfur is getting oxidised in the NaOH system.

Table 6.3: Percentage reduction in gold, mass and sulfide sulfur recoveries and sulfide sulfur grade (*orange column*) with respect to the extent of oxidation (*blue column*)

Oxidation			**Metallurgical Response**			
Treatment	**Conditioning Time (*minutes*)**	**Sox (*%*)**	**Gold Recovery (*% change*)**	**Mass Recovery (*% change*)**	**Sulfide Sulfur Recover) (*% change*)**	**(Sulfide Sulfur Grade (*% change*)**
Lime	2	**0**	0	0	0	0
Lime	5	**0**	-1.7	0	-2.1	1.6
Lime	10	**0**	-2.3	-2.37	-11.3	-1.0
NaOH	2	**5**	+4.8	+46.8	+5.4	-9.4
NaOH	5	**6.8**	+3.4	+35.6	+2.4	-11.0
NaOH	10	**8.1**	+6.3	+46.8	+9.2	-12.0

6.2.6 Gold to Arsenic Ratio (Au:As)

A trend similar to the Au:S values was observed with the gold to arsenic (*Au:As*) ratios as well which forms Figure 6.12. The improvements in Au:As values with the NaOH system suggests that the high gold arsenian pyrite types are being relatively more oxidised in the NaOH system resulting in higher Au:As ratios compared to the lime environment. This complements the earlier finding (*seen with the ratio of Au:S*) that some of the pyrite types must be oxidising relatively faster compared to the other types. It is likely that the oxidised pyrite types (*with a reduced sulfide sulfur grade*) possess a hydrophobic nature due to mild oxidation resulting in true flotation behaviour.

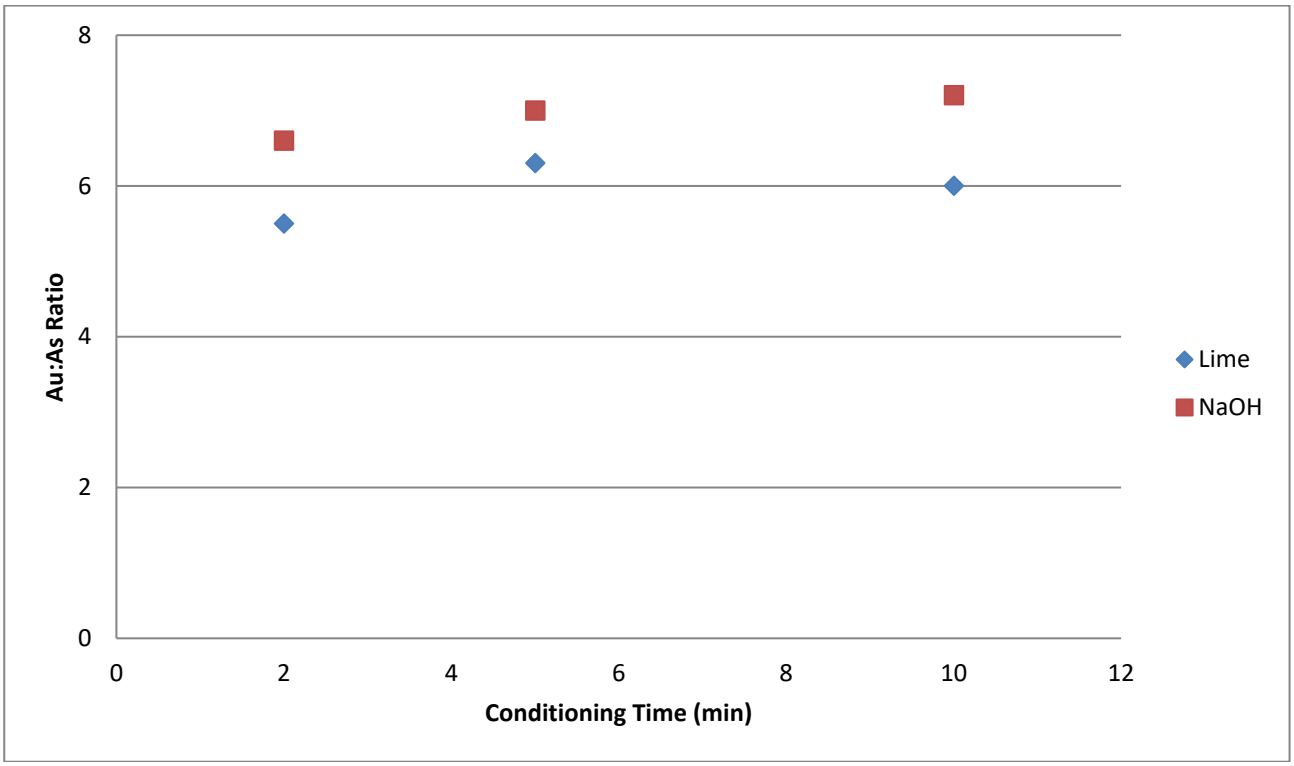

Figure 6.12: Au:As ratio of lime and NaOH conditioned concentrates.

6.3 Conclusions

1. The impact of NaOH conditioning was demonstrated from BET, SOx and XPS results. Higher gold and sulfide sulfur recoveries were recorded with NaOH conditioned concentartes than those treated with lime and this was probably due to metal sulfides that rendered the pyrite surface moderately hydrophobic.

2. Metallurgical responses of the NaOH oxidised concentrates displayed higher Au:S values, compared to the relatively non-oxidised lime concentrate samples, by oxidising the sulfide sulfur of the flotation concentrate. Although 9 to 12% reduction in the sulfide sulfur grade of the flotation concentrate was seen with NaOH conditioning without compromises in gold recoveries, higher water recoveries (*mass pulls*) were also recorded.

3. Textural analysis of NaOH conditioned concentrate samples by BSE and ImageJ thresholding showed that there was no degradation of As-rich zones in the pyrite although some pitting was observed with the 10 minutes NaOH sample. This is probably because mild oxidation only affected the arsenic-rich rims of the pyrite surface and not the As-rich interior zones.

4. However, despite the interesting technical aspects of these findings, the Au:S upgrade does not justify the replacement of lime with NaOH in practice at Lihir. This is because the easy availability and economic factors of lime procurement outweigh the advantages of the small differences in Au:S values between NaOH and lime.

6.4 Bibliography

ADAMS, M. 2005. Advances in gold ore processing, Vol.15. *Elsevier Science*.

AGORHOM, E. A., SKINNER, W. & ZANIN, M. 2013. Influence of gold mineralogy on its flotation recovery in a porphyry copper–gold ore. *Chemical Engineering Science,* 99**,** 127-138.

BRUNAUER, S., EMMETT, P. H. & TELLER, E. 1938. Adsorption of gases in multimolecular layers. *Journal of the American Chemical Society,* 60**,** 309-319.

BUCKLEY, A. & WOODS, R. 1987. The surface oxidation of pyrite. *Applied Surface Science,* 27**,** 437-452.

BUCKLEY, A. N. & WOODS, R. 1984. An X-ray photoelectron spectroscopic study of the oxidation of chalcopyrite. *Australian Journal of Chemistry,* 37**,** 2403-2413.

CHARLES, W. D. 1952. *Adsorption of calcium and sodium on pyrite*. *Transactions AIME – Mining Engineering*, February, pp 195.

COLLINS, M., BEREZOWSKY, R., VARDILL, W., KETCHAM, V. & STOJSIC, A. The Lihir Gold project: pressure oxidation process development. IV International Symposium on Hydrometallurgy, Salt Lake City, UT (August 1993), 1993.

COOK, N. J. & CHRYSSOULIS, S. L. 1990. Concentrations of invisible gold in the common sulfides. *The Canadian Mineralogist,* 28**,** 1-16.

EGGLESTON, C. M., EHRHARDT, J.-J. & STUMM, W. 1996. Surface structural controls on pyrite oxidation kinetics: An XPS-UPS, STM, and modelling study. *American Mineralogist,* 81**,** 1036-1056.

FANDRICH, R., GU, Y., BURROWS, D. & MOELLER, K. 2007. Modern SEM-based mineral liberation analysis. *International journal of mineral processing,* 84**,** 310-320.

FLEET, M. E., CHRYSSOULIS, S. L., MACLEAN, P. J., DAVIDSON, R. & WEISENER, C. G. 1993. Arsenian pyrite from gold deposits; Au and As distribution investigated by SIMS and

EMP, and colour staining and surface oxidation by XPS and LIMS. *The Canadian Mineralogist,* 31**,** 1-17.

FORNASIERO, D., EIJT, V. & RALSTON, J. 1992. An electrokinetic study of pyrite oxidation. *Colloids and surfaces,* 62**,** 63-73.

GAUDIN, A. & CHARLES, W. D. 1953. Adsorption of calcium and sodium on pyrite. *Transactions AIME – Mining Engineering*, February, pp 195-200.

KAPPES, R., BROSNAHAN, D. & GATHJE, J. Utilising mineral liberation analysis (MLA) to determine pyrite, arsenopyrite and arsenian pyrite floatabilities for Carlin trend ores. SME Annual Meeting and Exhibit and CMA's 111th National Western Mining Conference, 2009. 736-741.

KETCHAM, V., O'Reilly, J. & VARDILL, W. 1993. The Lihir gold project; Process plant design. *Minerals Engineering,* 6**,** 1037-1065.

KING, J. & KNIGHT, D. 1992. Autoclave operations at Porgera. *Hydrometallurgy,* 29**,** 493-511.

LAMB, W. 2004. Optimising the value of the Lihir low-grade resource. Rio Tinto Technical Report No: AR2163. Project Code: GAL 144.

LI, J., DABROWSKI, B., MILLER, J., ACAR, S., DIETRICH, M., LEVIER, K. & WAN, R. 2006. The influence of pyrite pre-oxidation on gold recovery by cyanidation. *Minerals Engineering,* 19**,** 883-895.

LONG, H. & DIXON, D. G. 2004. Pressure oxidation of pyrite in sulfuric acid media: a kinetic study. *Hydrometallurgy,* 73**,** 335-349.

MARCHBANK, A. R., THOMAS, K. G., DREISINGER, D. & FLEMING, C. 1996. Gold recovery from refractory carbonaceous ores by pressure oxidation and thiosulfate leaching. U.S. Patent No. 5,536,297. Washington, DC: U.S. Patent and Trademark Office.

MARSDEN, J. & HOUSE, I. 2006. *The chemistry of gold extraction*, SME. Littleton, Colorado, USA ISBN-13: 978-0-87335-240-6 ISBN-10: 0-87335-240-8.

MASON, P. 1992. Examining the economics of some pressure oxidation process options. *Hydrometallurgy,* 29**,** 479-492.

MERMILLOD-BLONDIN, R., KONGOLO, M., DE DONATO, P., BENZAAZOUA, M., BARRÈS, O., BUSSIÈRE, B. & AUBERTIN, M. Pyrite flotation with xanthate under alkaline conditions-application to environmental desulfurization. Proc. of the Centenary of Flotation Symposium, Brisbane, QLD, 2005.

MORISHITA, Y., SHIMADA, N. & SHIMADA, K. 2008. Invisible gold and arsenic in pyrite from the high-grade Hishikari gold deposit, Japan. *Applied Surface Science,* 255**,** 1451-1454.

O'CONNOR, C. & DUNNE, R. 1991. The practice of pyrite flotation in South Africa and Australia. *Minerals Engineering,* 4**,** 1057-1069.

PAKTUNC, D., KINGSTON, D., PRATT, A. & MCMULLEN, J. 2006. Distribution of gold in pyrite and products of its transformation resulting from the roasting of refractory gold ore. *The Canadian Mineralogist,* 44**,** 213-227.

RANKIN, W. J. 2013. *New flagship AusIMM Monograph: Australasian mining and metallurgical operating practices*. (The Sir Maurice Mawby Memorial Volume), Third Edition.

SMART, R. S. C. 1991. Surface layers in base metal sulfide flotation. *Minerals Engineering,* 4**,** 891-909.

THOMAS, K. G. 1991. Alkaline and acidic autoclaving of refractory gold ores. *JOM,* 43**,** 16-19.

THOMAS, K. G., PIETERSE, H. J., BREWER, R. E. & FRASER, K. S. 1991. Process for recovery of gold from refractory ores. U.S. Patent No 5071477 A. Washington, DC: U.S. Patent and Trademark Office.

WIGHTMAN, E. 2005. Bench scale testing to determine the potential for removal of low gold pyrite from Lihir ores. Rio Tinto Technical Report No: AR2448. Project Code: GAL 161.

CHAPTER 7

Nitric Acid Oxidation of Iron Sulfides to Modify the Au:S Ratio of a Flotation Concentrate

In this chapter, the oxidation of iron sulfides by nitric acid and the subsequent effect on Au:S ratio has been investigated. This chapter is an attempt to establish the effectiveness of a preparation step, with its origins from hydrometallurgical practice, to modify the flotation response of gold-rich pyrite and low gold pyrite so that the Au:S ratio of the final flotation concentrate can be upgraded.

Keywords: Refractory ore, Sulfide minerals, Gold to Sulfur ratio, Pyrite, Nitric Acid Oxidation, Flotation, Image processing

7. Introduction

Several processes involving nitric acid leaching of highly complex refractory/double refractory sulfide ores are available in the literature (Gao et al., 2009, La Brooy et al., 1994, Li, 2009, Flatt and Woods, 1995). The effect of nitric acid oxidation on the various pyrite types has also been demonstrated in Chapter 5. Therefore, it was used as a starting basis to oxidise the pyrite-rich flotation concentrate and understand the metallurgical behaviour in a following cleaner flotation process. However, since the approach in this work was to preferentially oxidise the high gold pyrite relative to the low gold pyrite, a "mild to moderate oxidation" process was designed to prevent the complete destruction of the sulfide matrix of the pyrite. This process objective presented a challenge to establish and define the "mild oxidation operating window" where one type of pyrite may be differentially oxidised over the other types. Furthermore, it is well documented that other existing nitric acid oxidation processes such as pressure oxidation/autoclaving, Nitrox process, Activox process and Electrochemical slurry processes are designed to liberate the refractory gold by the complete destruction of the sulfide matrix as shown below in equations 35 and 36.

$$2FeS_2 + 10\ HNO_3 \xrightarrow{\text{yields}} H_2SO_4 + 4Fe_2(SO_4)_3 + 10\ NO + 4\ H_2O \quad \ldots\ldots 35$$

$$2FeAsS + 8\ HNO_3 + H_2SO_4 \xrightarrow{\text{yields}} Fe_2(SO_4)_3 + 2H_3AsO_4 + 8\ NO + 2\ H_2O \quad \ldots\ldots 36$$

Therefore, the challenge was to selectively control the extent of oxidation to target specific mineral types (*in this case the high gold pyrite*).

7.2 Hydrometallurgical Test Work

To address the above questions, hydrometallurgical and regrinding test work methods were developed as shown in Figure 7.1 to manipulate the flotation response to allow separation of the low gold bearing pyrite from the gold-rich pyrite.

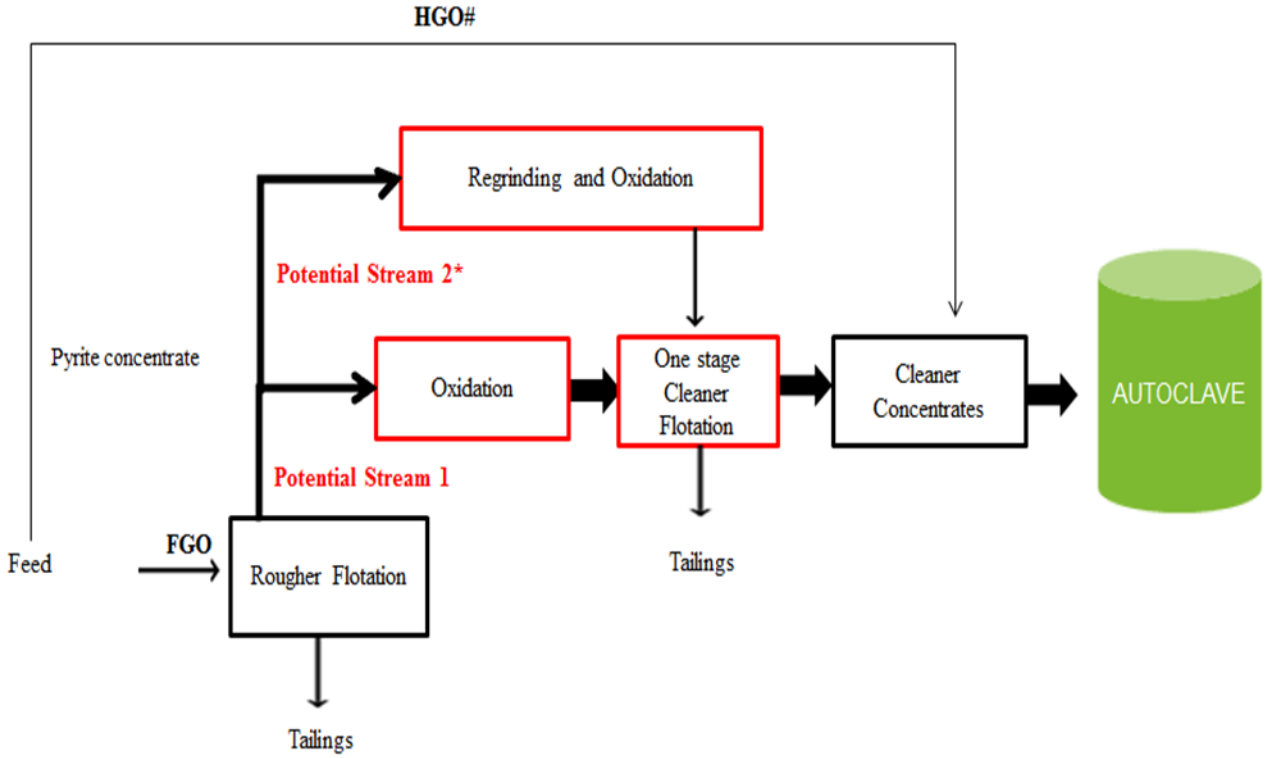

Figure 7.1: Process flow sheet depicting the potential processes

Numerous method development studies were conducted in the laboratory to understand the reaction between a pyrite rougher concentrate and nitric acid solution. This included trialling various conditions such as reacting the sulfide concentrate over a range of acid strengths from 5-50 g/L at ambient temperature and altering oxidation time intervals from 10 to 70 minutes. Visually, 5 g/L was too low a concentration to induce any change in the concentrate and the SO_x analysis and flotation data confirmed this (*not shown here*). Among the other concentrations, 10 g/L nitric acid was found optimum because it did not char the surface of the rougher concentrate but was still effective for oxidising the pyrite concentrate as confirmed by SOx and XPS measurements. Ambient temperature ranges were employed (*10 to 23.5 ^0C*) during the experimental work and therefore, the discussion of mineral leaching below will be based on this temperature region.

7.3. Results and Discussion

7.3.1 Back-Scattered Electron Imaging

To demonstrate the effect of 10 g/L nitric acid oxidation on the pyrite texture, backscattered electron images (*BSE*) of the pyrite concentrate (*pre and post-oxidation*) were collected. The BSE images were then processed using ImageJ software, as mentioned in Chapters 3 and 5 to highlight the arsenic zones in pyrite (*in red*). The differences among the test products were marked suggesting the oxidation was sufficient to induce surface alterations in the various pyrite types. The

10 minutes etched pyrite concentrate sample showed As-rich bands similar to the untreated (*control*) pyrite concentrate suggesting that the effect of oxidation was minimal (*Figure 7.2 and Figure 7.3*). Slight changes were observed with the 20 minutes oxidation stage with alterations in the textural features of the As-rich pyrite types which are shown in Figure 7.4. Noticeable changes were apparent from the 30 minutes oxidation stage with considerable depletion of arsenic zones as shown in Figure 7.5.

Similar to the nitric acid oxidation effects discussed in Chapter 5, visible differences in the textural characteristics become more pronounced from the 40 minutes oxidation stage (*Figure 7.6*) with the appearance of more surface irregularities and pits due to the etching effects of nitric acid. Furthermore, as seen in Chapter 5, the degradation of the As-rich bands is strongly dependent on the reaction time and this trend is further confirmed with the 50 and 60 minutes etched samples (*Figure 7.7 and Figure 7.8*). As –rich pyrite types have been fully oxidised at the end of 70 minutes oxidation stage and minor oxidation effects for the low As blocky pyrite started to appear as seen in Figure 7.9. These observations confirm the aim of this work which was to differentially oxidise the various types of pyrite.

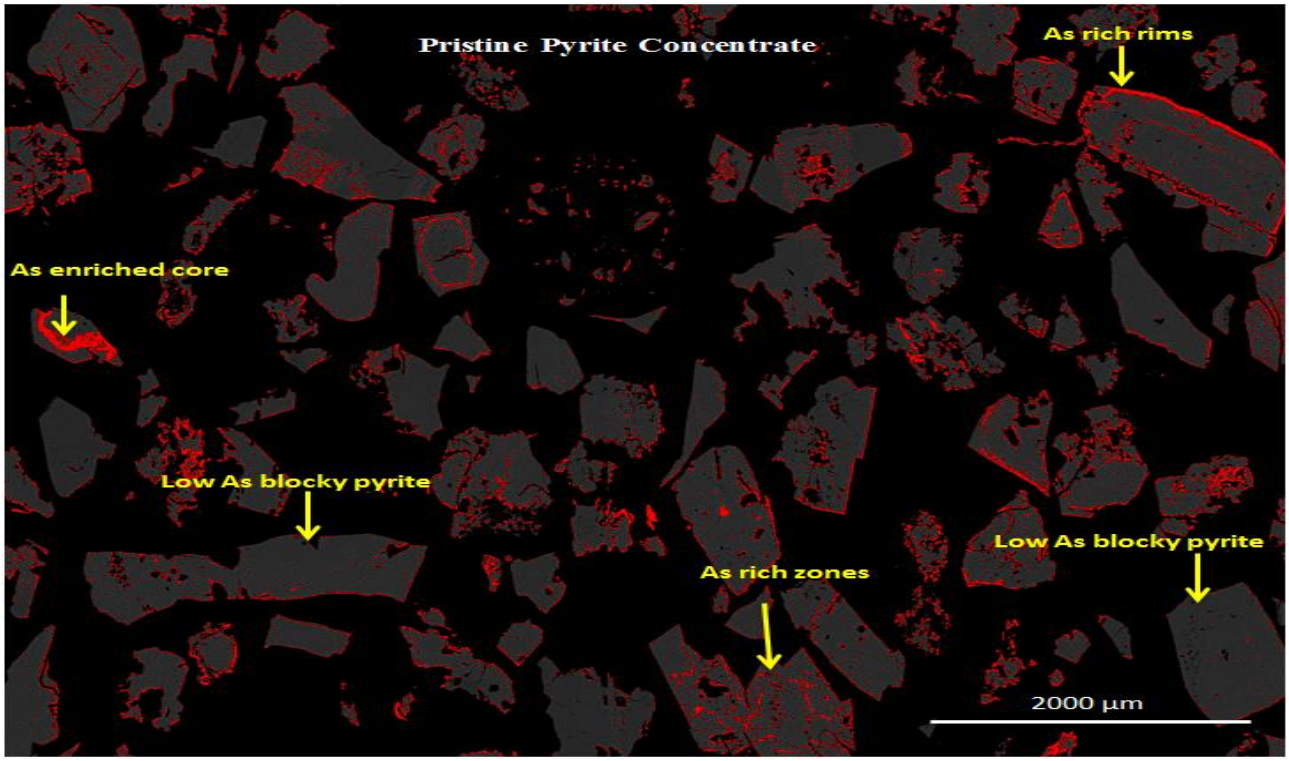

Figure 7.2: BSE image (*after ImageJ thresholding*) of the pristine (*unoxidised*) concentrate

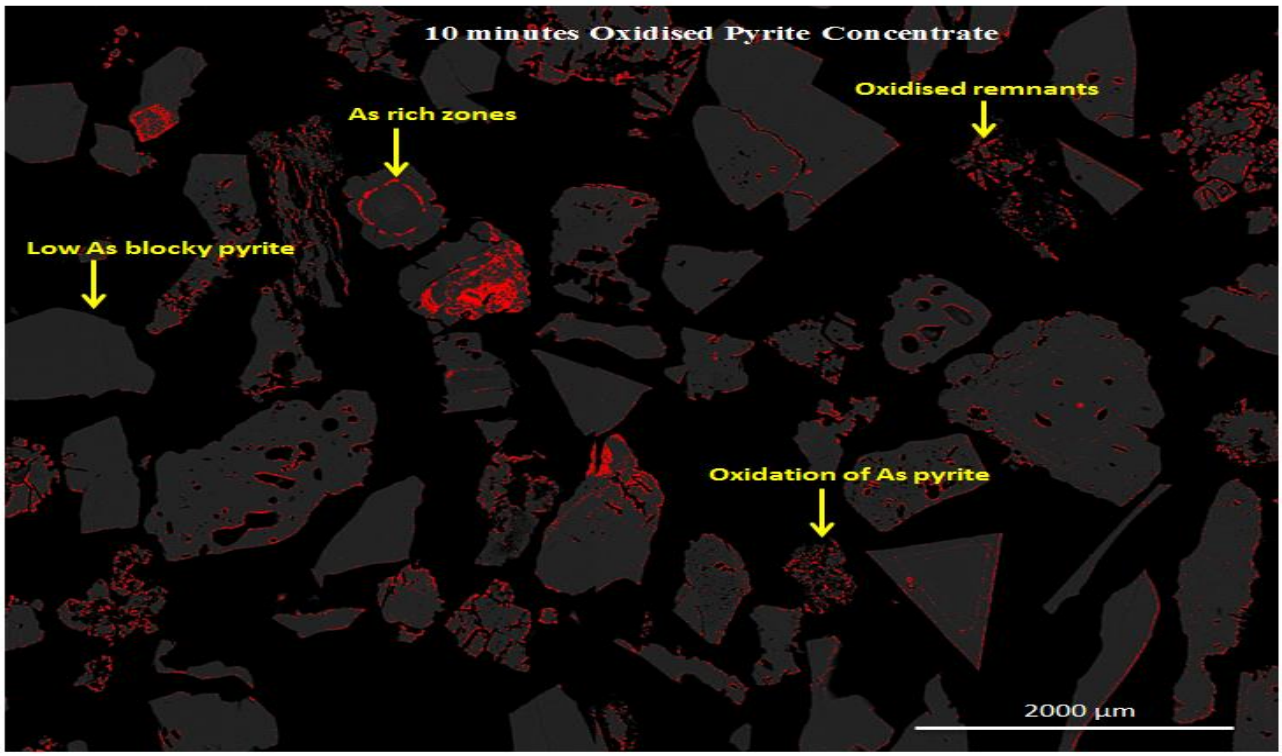

Figure 7.3: BSE image (*after ImageJ thresholding*) of the 10 minutes oxidised concentrate. Slight oxidation of high As pyrite, however, etching effects on the rim are not prominent.

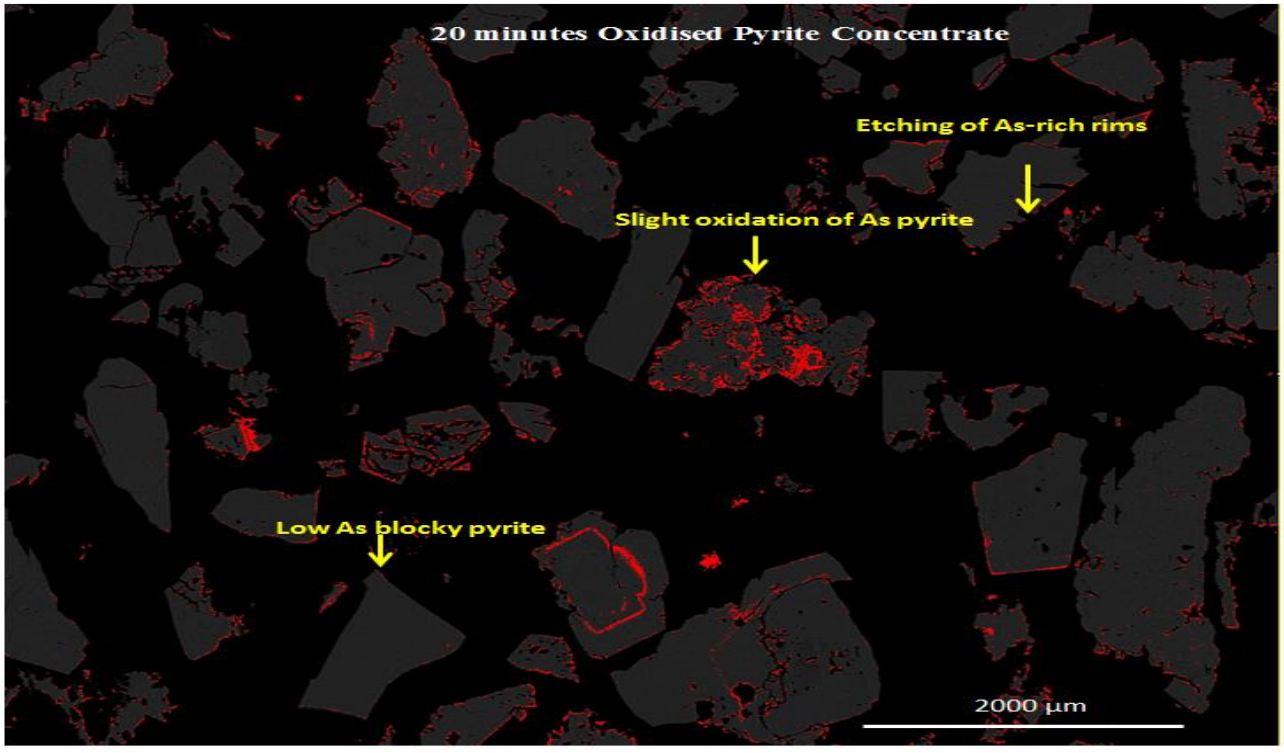

Figure 7.4: BSE image (*after ImageJ thresholding*) of the 20 minutes oxidised concentrate. Oxidation of high As pyrite and etching of As-rich rims. Low As blocky pyrite remains inert to the effects of oxidation.

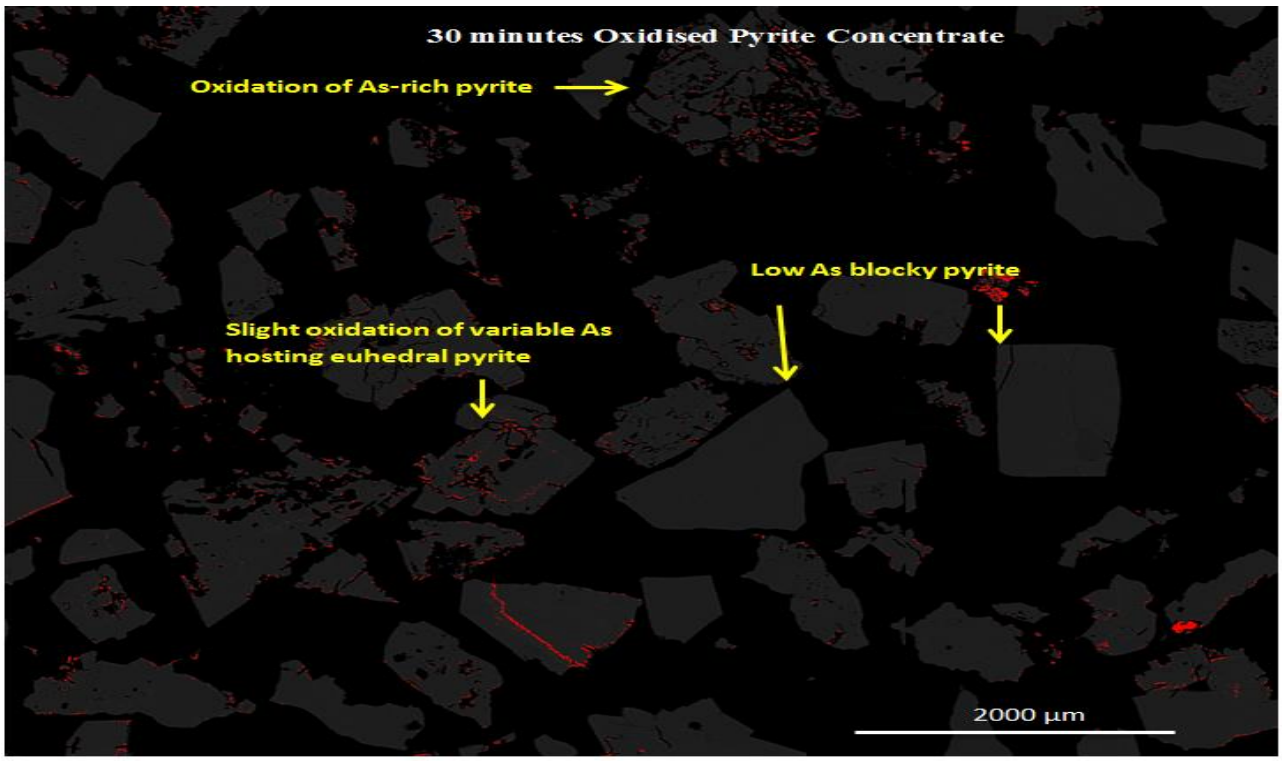

Figure 7.5: BSE image (*after ImageJ thresholding*) of the 30 minutes oxidised concentrate. Oxidation of high As pyrite and slight oxidation of variable As containing euhedral pyrite. Low As blocky pyrite remains inert to the effects of oxidation.

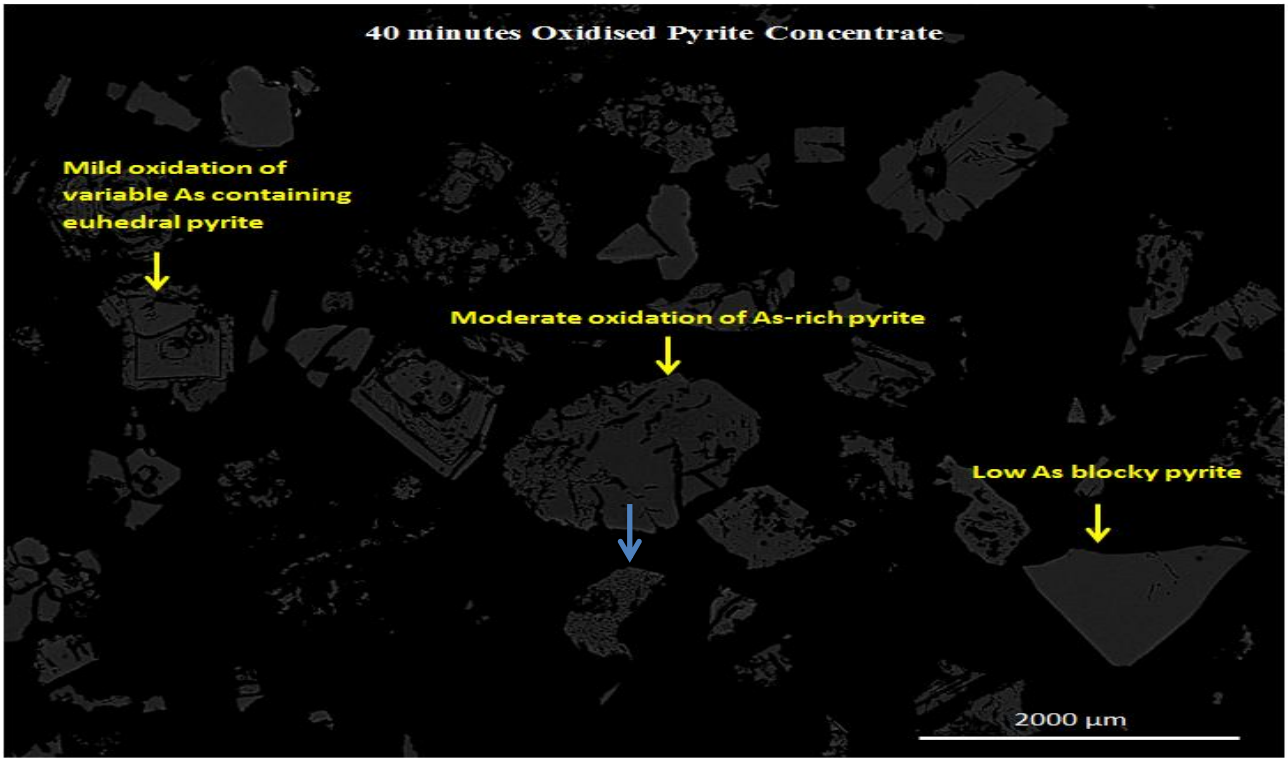

Figure 7.6: BSE image (*after ImageJ thresholding*) of the 40 minutes oxidised concentrate. Moderate oxidation of high As pyrite and variable As containing euhedral pyrite. Low As blocky pyrite remains inert to the corrosive action of nitric acid.

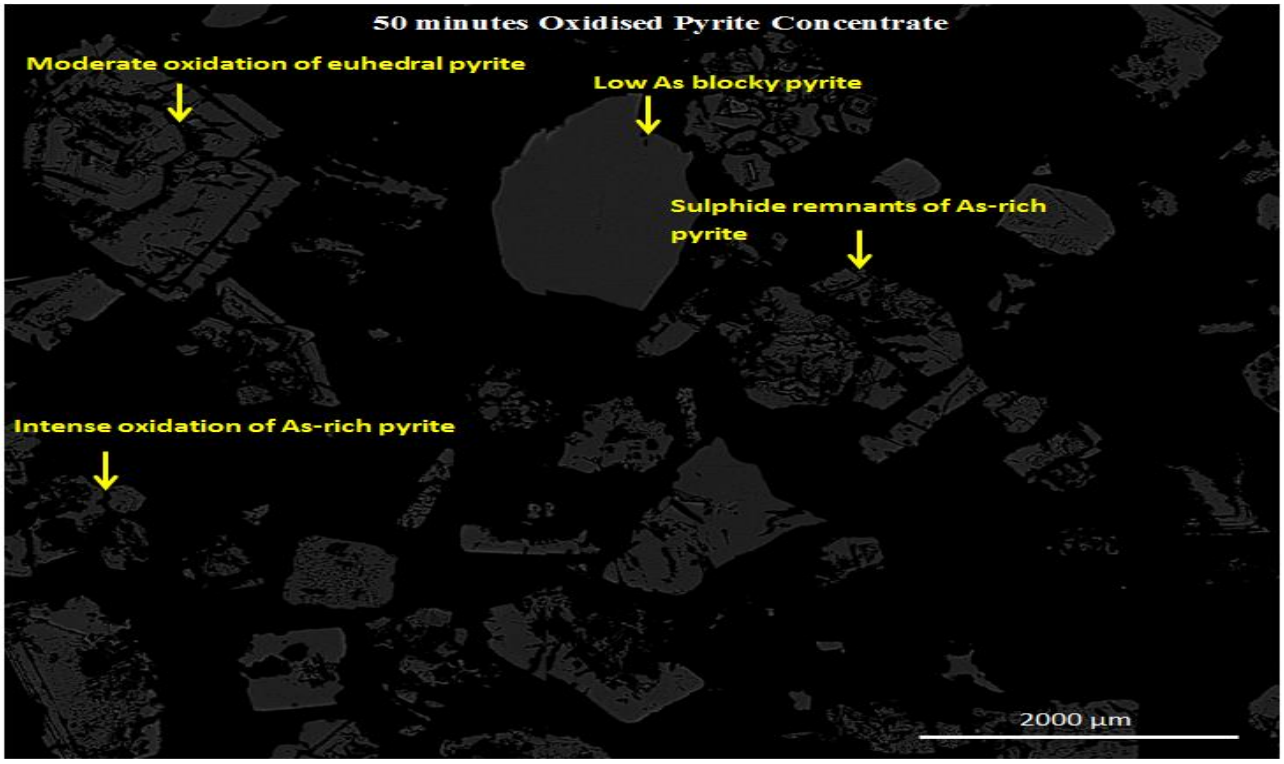

Figure 7.7: BSE image (*after ImageJ thresholding*) of the 50 minutes oxidised concentrate. Intense oxidation of high As pyrite. Some high As-rich pyrite types are completely oxidised leaving behind sulfide skeletons. Moderate oxidation of the variable As containing euhedral pyrite. Low As blocky pyrite remains unaltered.

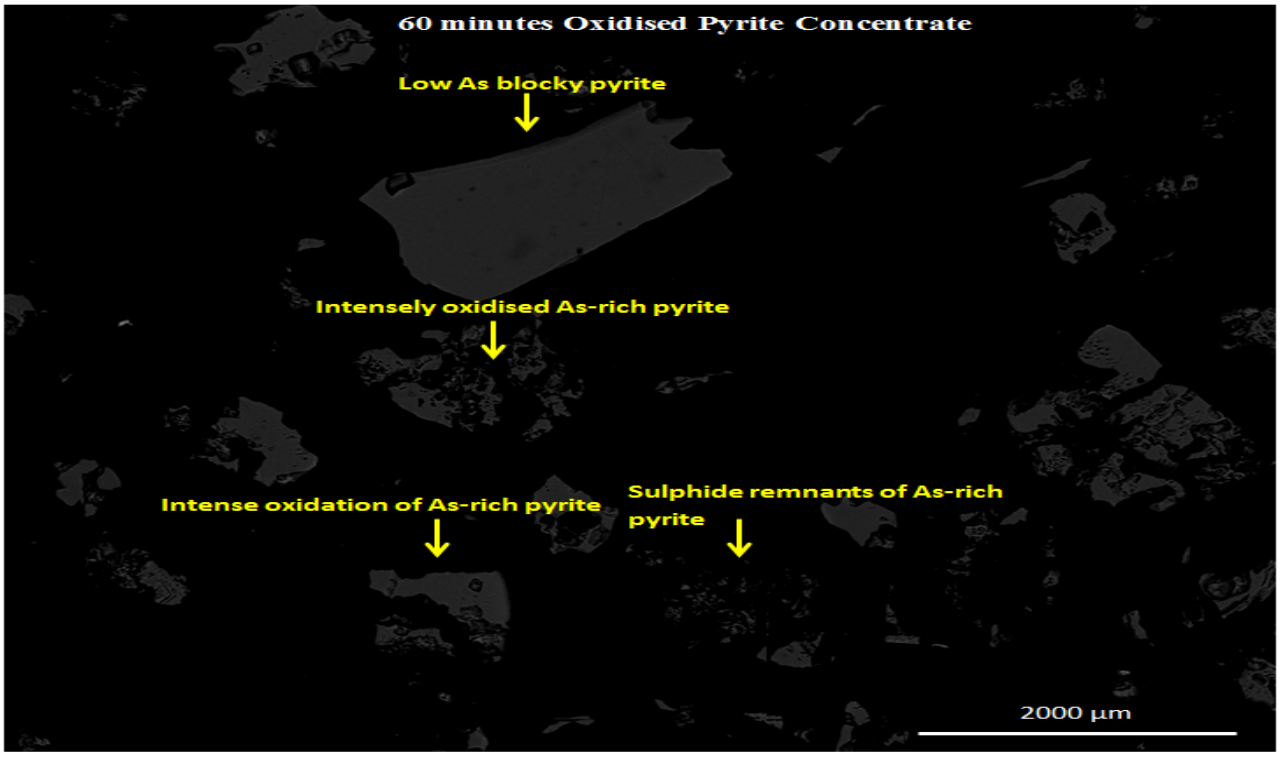

Figure 7.8: BSE image (*after ImageJ thresholding*) of the 60 minutes oxidised concentrate. Intense oxidation of high As and variable As containing pyrite types. The As-rich pyrite types are corroded but the low As blocky pyrite remains inert to the effects of oxidation.

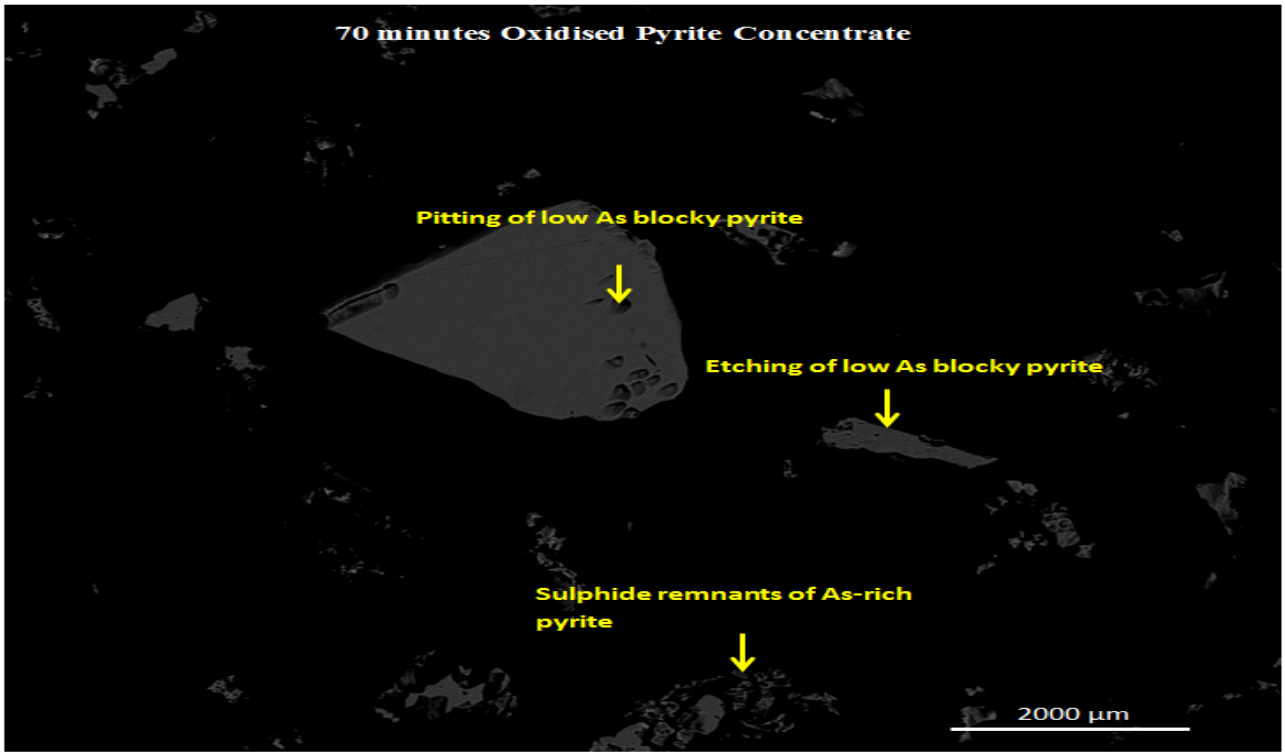

Figure 7.9: BSE image (*after ImageJ thresholding*) of the 70 minutes oxidised concentrate. Oxidised sulfide frameworks from As-rich and variable As containing pyrite types. Low As blocky pyrite starts to oxidise with the appearance of pits and etching of edges becoming prominent due to the effects of oxidation.

7.3.2 Sulfide Sulfur Oxidation (SOx)

The intention of the work was to establish a 'mild to moderate oxidation regime' for preferential oxidation and therefore, the extent of oxidation of the pyrite concentrate was quantified through SOx measurements. SOx analysis revealed that with increasing oxidation times, the extent of sulfide sulfur oxidation also increased from no oxidation for the control sample to 27% oxidation for the 70 minutes oxidised sample as shown Figure 7.10. This not only confirms the increase in SOx with oxidation time but also pinpoints the fact that the extent of oxidation values must be determined to establish the "window of interest" for the desired Au:S range. It is also important to understand that as the extent of oxidation increases, the nature of the oxidised pyrite phase might also change resulting in varying metallurgical responses.

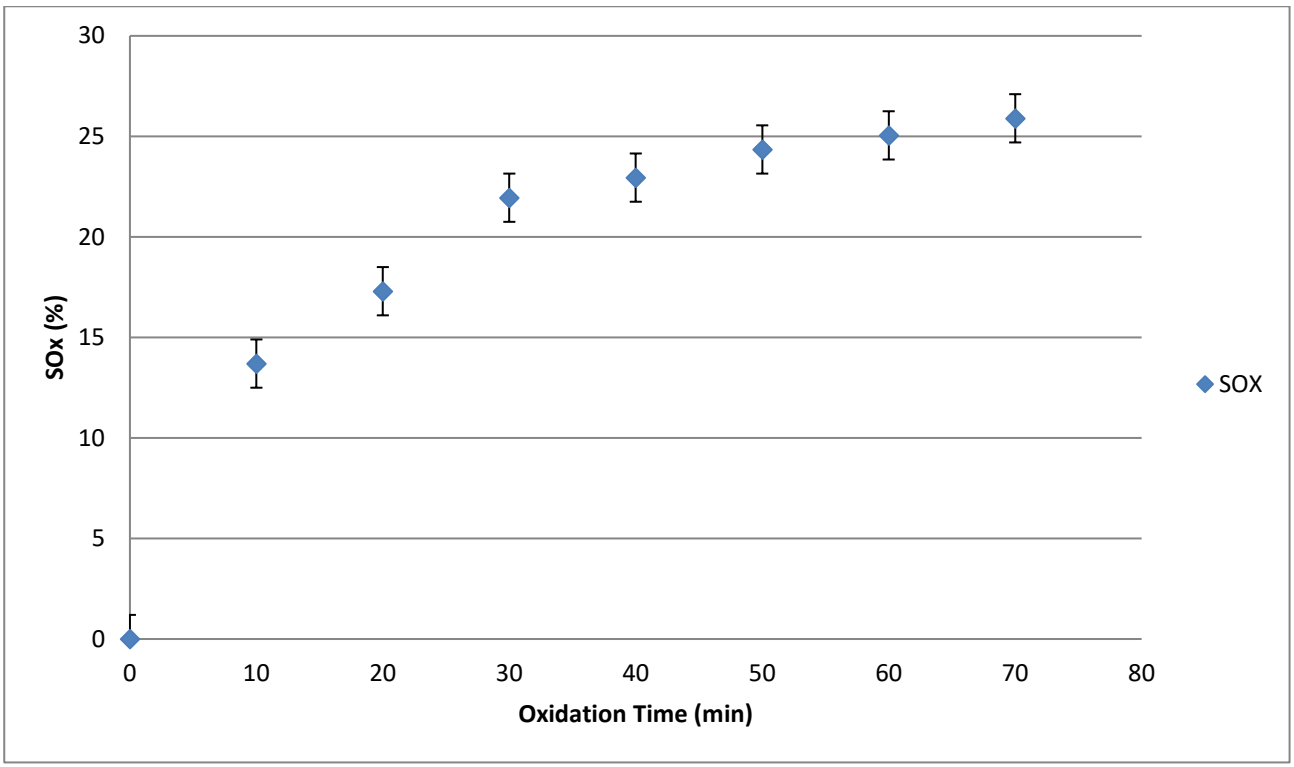

Figure 7.10: Quantification of the extent of 10 g/L nitric acid oxidation of pyrite concentrates at different time intervals by sulfide sulfur measurement which was converted to the SOx values.

7.3.3 Total surface area analysis (BET)

Surface area is a crucial parameter in understanding the impact of oxidation of the pyrite concentrate. Although all the samples exhibited relatively low specific surface area values, an increase was observed when the sample was oxidised and this trend continued as the extent of oxidation increased as shown in Table 7.1.

Table 7. 1: BET measurements (*pink column*) of the control and oxidised samples. Pristine*= untreated/unetched sample

Sample	Oxidation Time (*mins*)	BET Surface Area (m^2/g)
Pyrite Concentrate	0 (Pristine*)	1.6
	10	3.8
	20	4.6
	30	5.1
	40	5.6
	50	6.0
	60	6.7
	70	7.9

BET analysis alone cannot be used as a characterisation technique; however, it does emphasise the effect of chemical modification of the pyrite concentrate by nitric acid. This surface texture modification by nitric acid on the pyrite surface, rims, fractures and pits has already been shown in the BSE images *(Figures 7.2 to 7.9*). As the leaching process advances, so does the surface area change, as presented in Figure 7.11, indicating pyrite reaction. This dependence of extent of oxidation on surface area is positively correlated as shown in Figure 7.12.

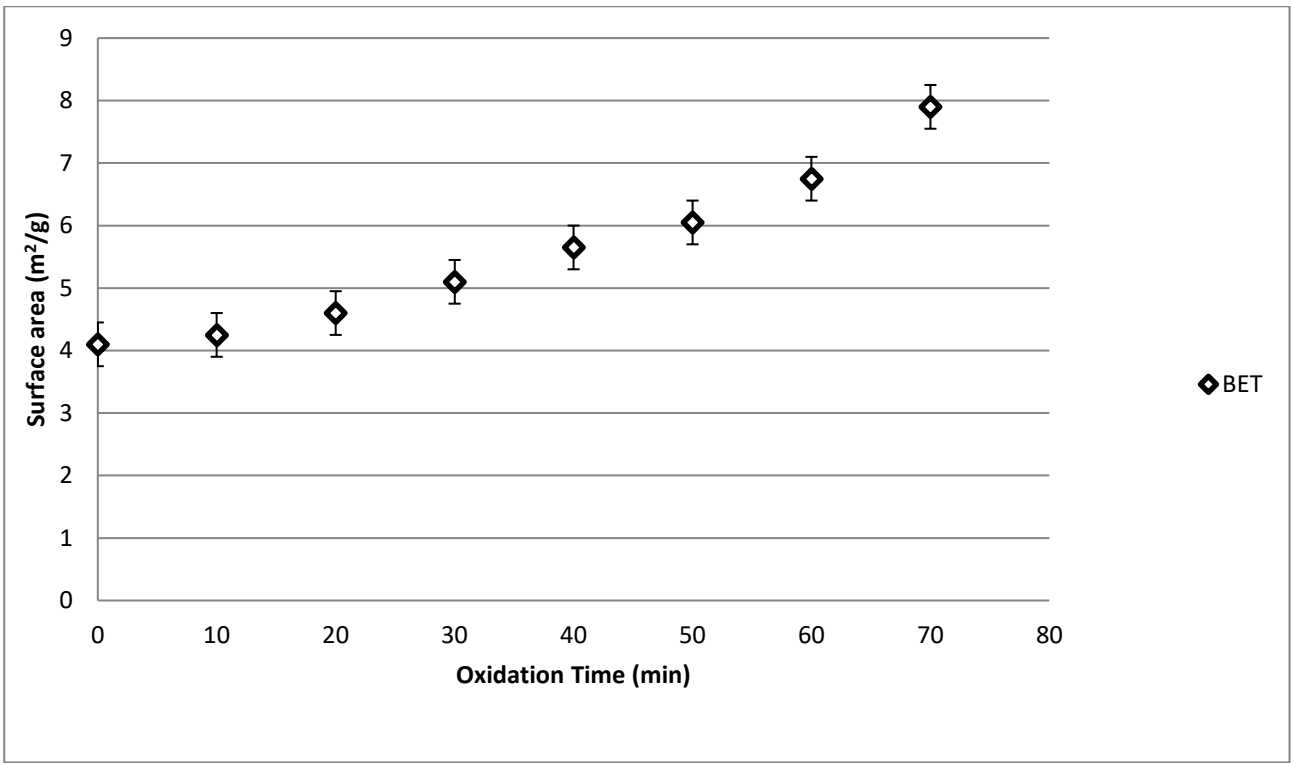

Figure 7.11: Quantification of the total surface area of pyrite concentrates after nitric acid oxidation at different time intervals by BET measurement analysis.

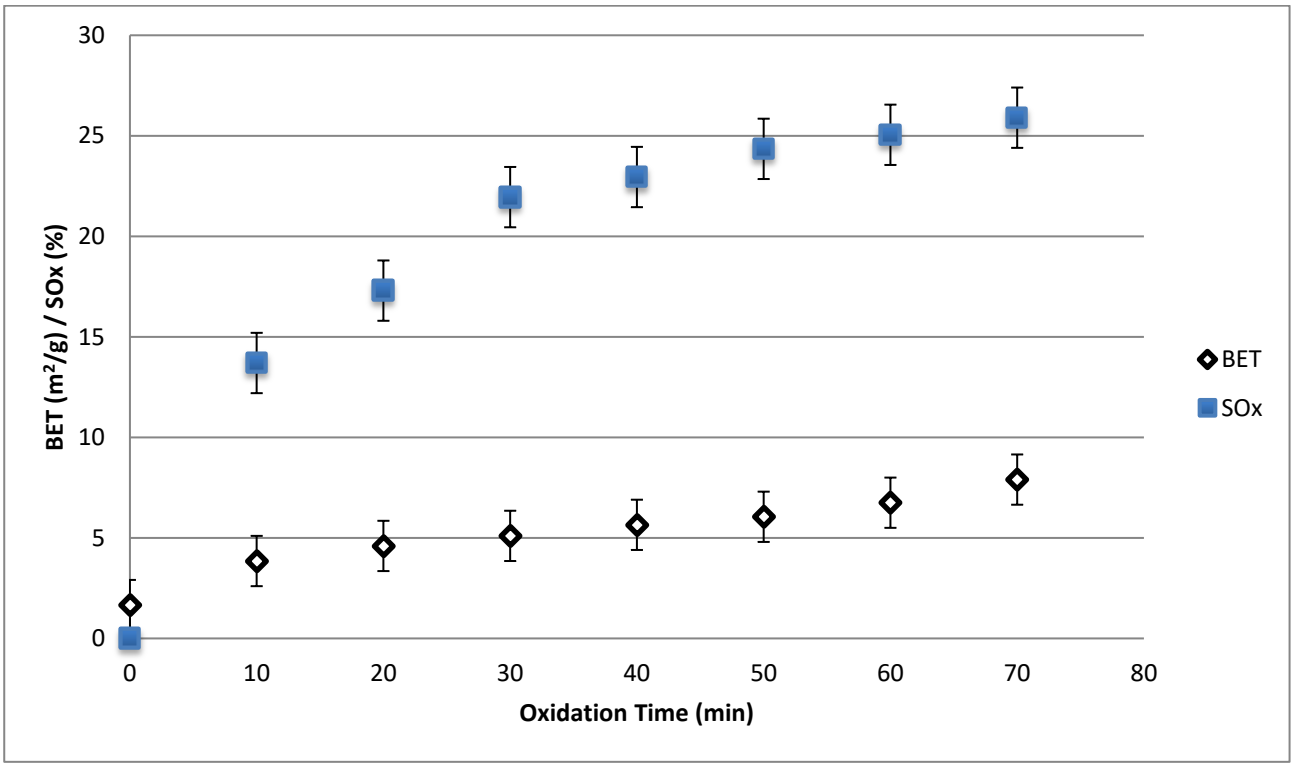

Figure 7.12: Correlation between sulfide sulfur oxidation extent and total surface area values of the pyrite concentrates oxidised at various time intervals.

7.3.4 X-Ray Photoelectron Spectroscopy (XPS)

Oxidation species formed as a part of oxidation can influence the response behaviour of the pyrite in a subsequent flotation process. This is because in self-induced flotation process (*without any collector additions*), oxidation products can contribute to a hydrophobic or hydrophilic character of the mineral surface thereby facilitating or inhibiting interactions with the flotation collectors (Buckley and Woods, 1987). For example, as seen in Chapter 6, metal-deficient sulfides can result in a hydrophobic pyrite surface while pyrite metal hydroxides can inhibit flotation due to their hydrophilic nature (Buckley and Woods, 1987, Smart, 1991, Buckley and Woods, 1984).

The effect of oxidation on the pyrite surface was investigated by the surface analytical technique, XPS. The objective was not to collect detailed XPS spectra of pyrite oxidation but rather to gain surface analytical results to complement oxidation results from SOx and BET analysis. XPS S2p peaks of pyrite have been analysed extensively and the methodology can be found in the literature; therefore, a minimum number of the main peaks were used to understand the effect of oxidation with time. The Fe (2p) and S (2p) core level peaks of the pyrite surface before oxidation are shown in Figure 7.14. The S 2p3/2 binding energy at 162.7 eV is due to S^{2-} from FeS_2 (Buckley and Woods, 1987). The doublet at 162.8 eV is a result of polysulfides (Buckley and Woods, 1987, Smart, 1991, Buckley and Woods, 1984) and the broad peak at 167.9 eV is due to the sulfate species (SO_4^{2-}). The binding energy of the Fe (2p) level of the pyrite sample was measured at 707.2 eV which is common for pyrite (Eggleston et al., 1996).

An increase in the surface concentration of iron hydroxides and sulfates after oxidation in nitric acid solution is observed as shown in Figure 7.13. For example, the S(2p) spectrum for the 10 minutes oxidised sample indicates the presence of a stronger sulfate peak in the latter spectrum near 168.5 eV. However, for the 20 minutes oxidised sample a drastic shift in the sulfide sulfur and sulfate peak is observed. Comparing the Fe (2p) spectra of both the 10 and 20 minutes oxidation stages, it can be seen that a broader Fe peak is observed with the 20 minutes sample. This suggests that it is due to the higher extent of oxidation that more iron hydroxide layers are precipitated on the pyrite surface.

Fe Spectra **S Spectra**

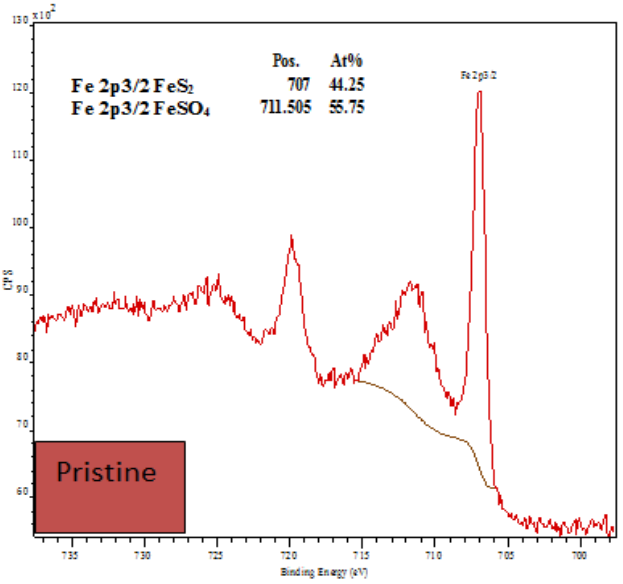

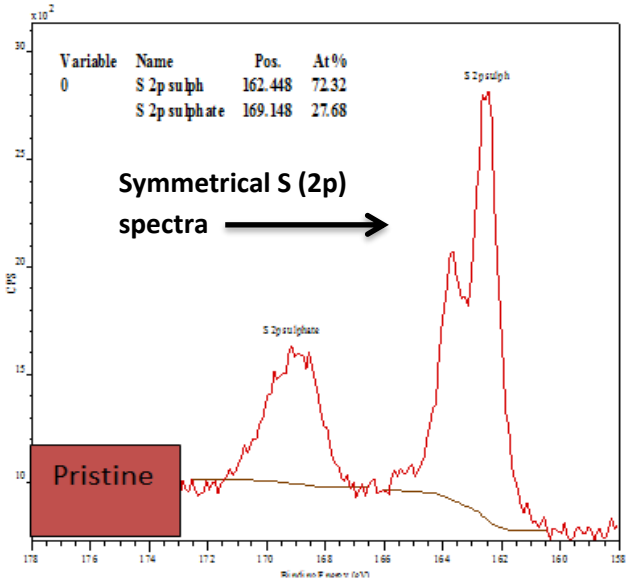

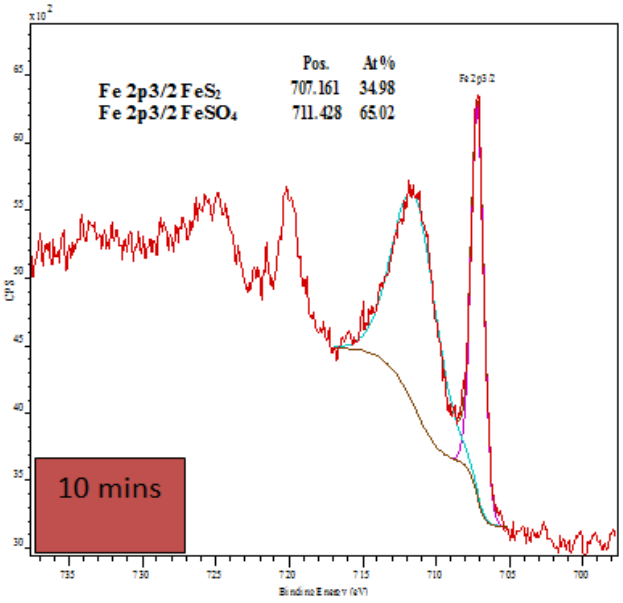

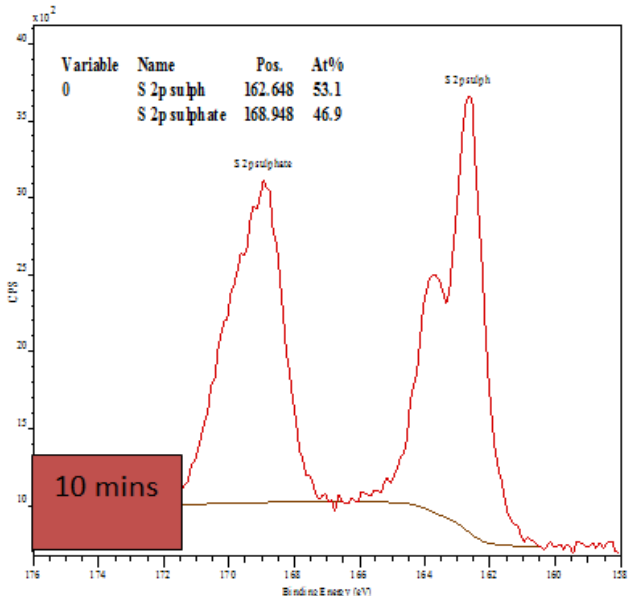

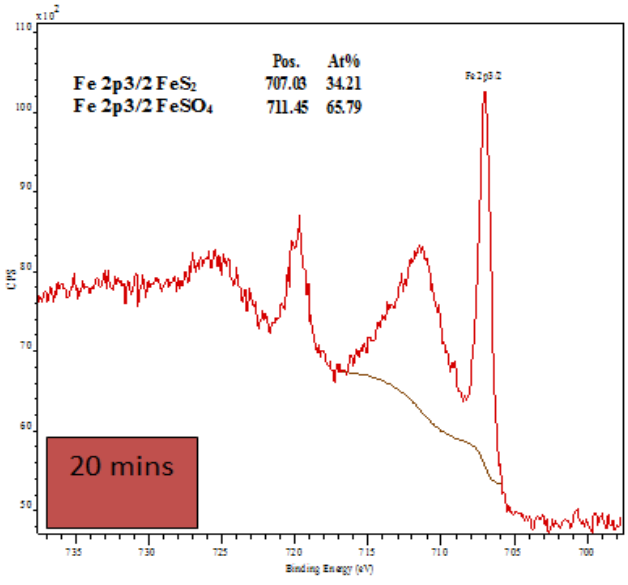

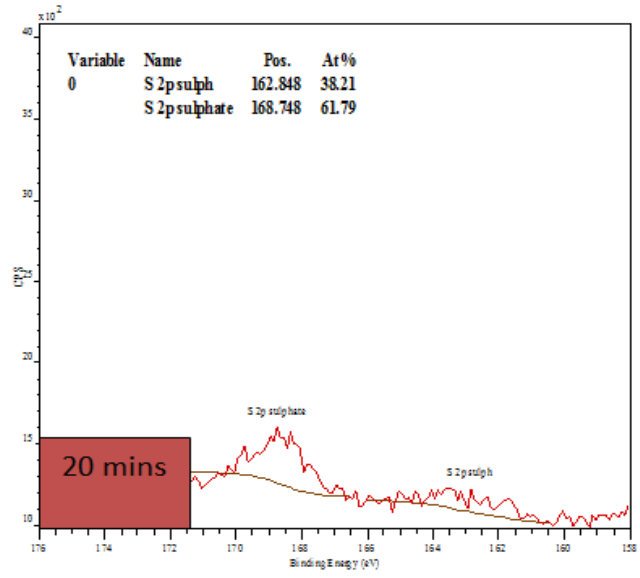

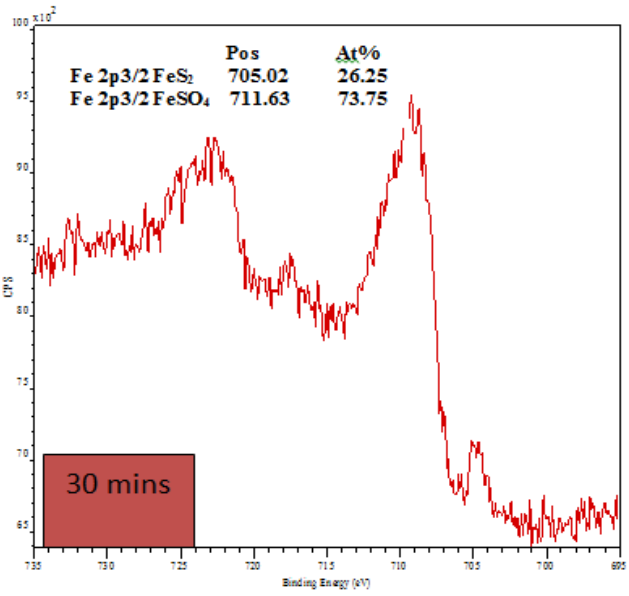
Pos At%
Fe 2p3/2 FeS2 705.02 26.25
Fe 2p3/2 FeSO4 711.63 73.75
30 mins

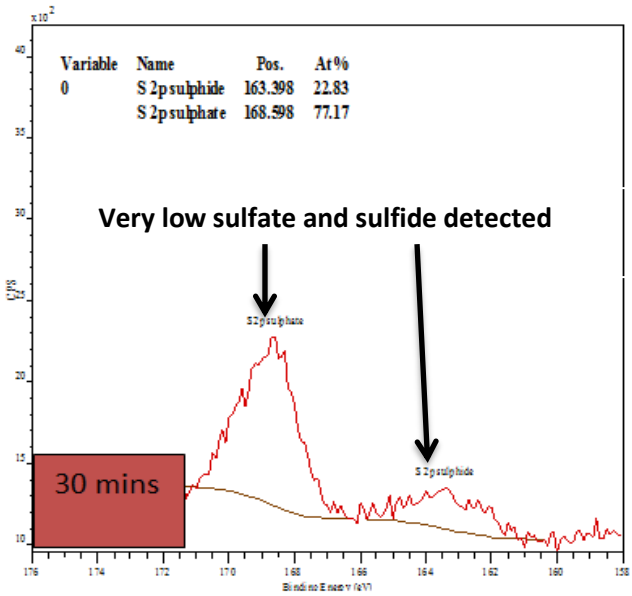
Variable Name Pos. At%
0 S 2p sulphide 163.398 22.83
S 2p sulphate 168.598 77.17
Very low sulfate and sulfide detected
30 mins

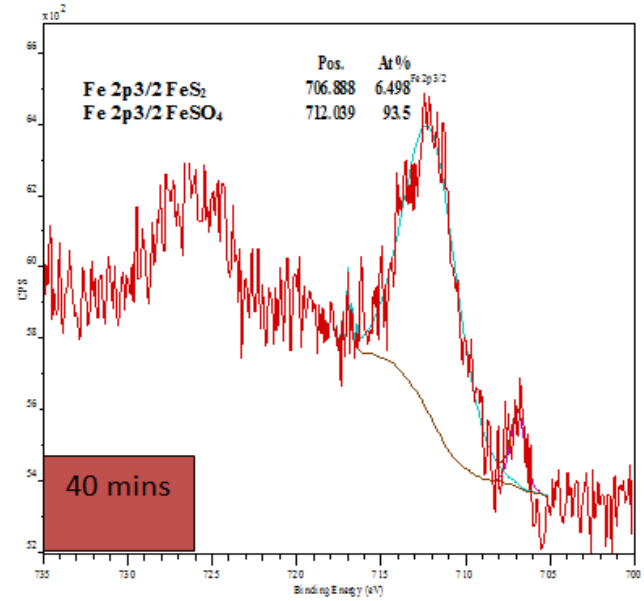
Pos. At%
Fe 2p3/2 FeS2 706.888 6.498
Fe 2p3/2 FeSO4 712.039 93.5
40 mins

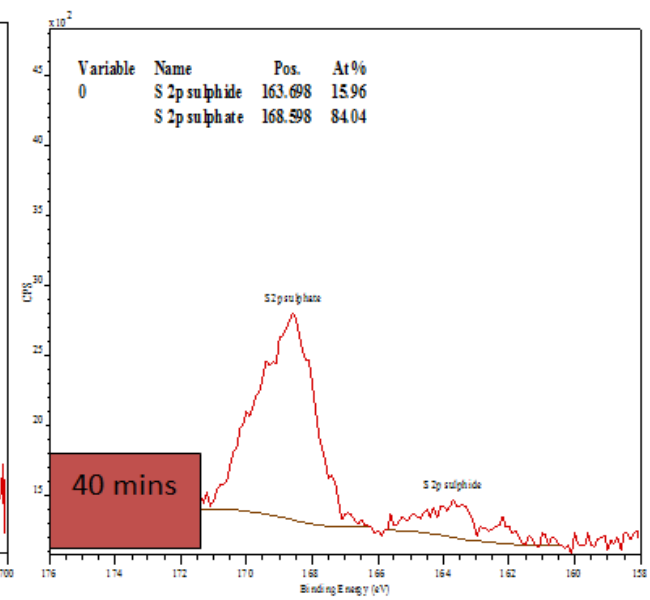
Variable Name Pos. At%
0 S 2p sulphide 163.698 15.96
S 2p sulphate 168.598 84.04
40 mins

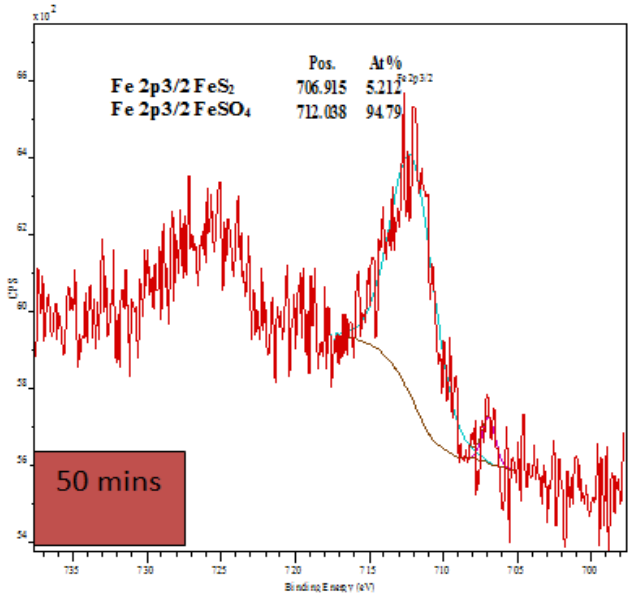
Pos. At%
Fe 2p3/2 FeS2 706.915 5.212
Fe 2p3/2 FeSO4 712.038 94.79
50 mins

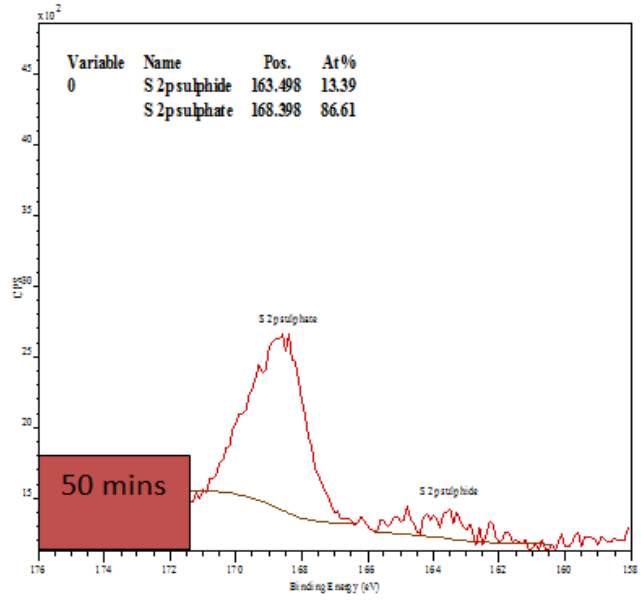
Variable Name Pos. At%
0 S 2p sulphide 163.498 13.39
S 2p sulphate 168.398 86.61
50 mins

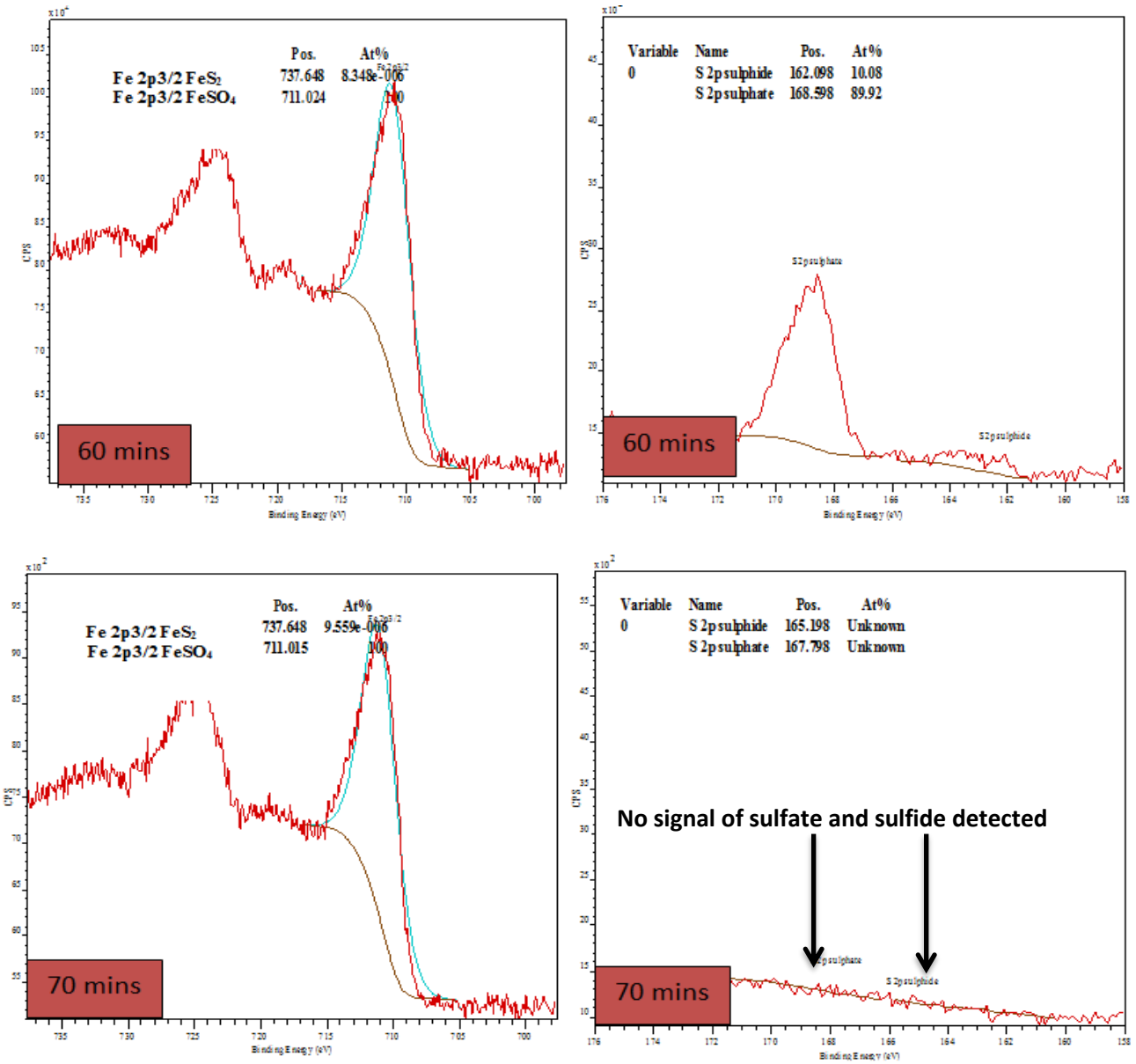

Figure 7.13: Fe (2p) and S (2p) spectra of the pristine and oxidised concentrates. The 10 minutes oxidised sample shows a higher percentage of sulfate species signifying the onset of pyrite oxidation and this trend continues with the 20 minutes oxidation stage. As the oxidation reaction advances (*70 minutes oxidation*), the XPS system is unable to quantify the sulfide sulfur species due to increased presence of iron and sulfate precipitates.

With increasing extent of oxidation, the higher concentrations of the iron species passivate the pyrite surface and this formation of Fe precipitates is obvious in the 20 minutes oxidised sample. It was observed that the Fe(2p) spectrum exhibited energy peaks at 711 eV signifying the presence of hydrated iron oxides and iron sulfates (Pietrzak et al., 2007). The surface composition of the pyrite surfaces after the 30 minutes oxidation stage was very different compared to the pristine, 10 minutes and 20 minutes oxidation samples with comparatively more noise in the data. The reason for this is, compared to the control sample, the surface sulfide sulfur layer reconstructed to form

separate unstable sulfur phases (*metal deficient sulfides and elemental sulfur*) with increasing extent of oxidation.

In all the oxidised samples, the ratio of sulfate to sulfur on the surface increased with increase in the extent of oxidation suggesting that oxidation had significantly altered the pyrite surface to have an impact on the metallurgical response. Although the presence of metal-deficient sulfides provides surface hydrophobicity for higher mineral recovery (*in the absence of collector*), the formation of hydroxides, oxides, sulfates and precipitates on the pyrite surface can hamper the flotation response and this had to be tested.

7.3.5 Cleaner (Reverse) Flotation

Pyrite flotation relies on manipulating the differences in hydrophilic and hydrophobic nature of the sulfide and non-sulfide minerals (Newell et al., 2006). Nevertheless, when it comes to flotation separation within the same mineral family, understanding the flotation behaviour of the highly oxidised pyrite relative to the unoxidised/mildly oxidised pyrite particles can be a difficult challenge *per se.* This is because the usual practice in evaluating the flotation performance is relying on the grade-recovery curves. In this case, it is possible to obtain a grade recovery for the total pyrite; it is not a standard procedure to obtain separate grade-recovery curves for the two types of pyrite due to a lack of readily available measurements and assays. Simply assessing the flotation curves will not enable an appreciation of the potential of an oxidative hydrometallurgical process and its effect on the sulfide concentrate. Therefore, the best course and the most straight forward indication would be evaluating the metallurgical response in terms of Au:S values of the pristine and the nitric acid leached pyrite concentrate.

The nitric acid test work involved oxidising the rougher flotation pyrite concentrates at different time intervals from 10 to 70 minutes, as described earlier, and the gold and sulfide sulfur flotation were then examined in a one-step cleaner flotation step where multiple concentrates were collected. PAX collector and Nascol 422 frother were used as reagents in the cleaner flotation stage as shown in Table 7.2.

Table 7.2: Reverse flotation test conditions. Lime (*upfront addition*) was used to raise the pH of the oxidised concentrates to 5

Test Conditions	Cleaner Float
Float Cell Size	2.5L
Agitation	250 rpm
Air	5 L/min
Reagents	20g/t PAX Nascol 422
Pulp Density	10% solid by weight
Conditioning (*minutes*)	2 minutes
Float pH	**5 (*Lime*)**
Flotation time (*minutes*)	incremental time of 2, 2, 4 and 4 minutes for a total time of 12 minutes
Concentrates	4
Scraping Frequency	10 seconds

Good recoveries have been achieved due to the strong interaction of collector with pyrite surfaces (Zhang et al., 1997, Chen et al., 2013, Leppinen et al., 1988). The key assumption was that the low gold pyrite which is more resistant to oxidation would float and the oxidised high gold pyrite would be left behind with the tails. The key results for the reverse one-step cleaner flotation tests are shown in Table 7.3.

Table 7.3: Reverse cleaner flotation data of control and oxidised samples floated at pH 5

Oxidation			**Metallurgical Response**				
Reagent	**Sample**	**SOx (%)**	**Gold Recovery (%)**	**Gold Grade (*g/t*)**	**Sulfide Sulfur Recovery (%)**	**Sulfide Sulfur Grade (%)**	**Au:S Ratio**
None	Control*	**0**	92.8	10.6	91.1	41.2	**0.26**
HNO_3	30	**12**	90.0	10.5	92.9	39.2	**0.27**
HNO_3	40	**21**	86.7	10.8	87.6	39.3	**0.27**
HNO_3	60	**25**	83.1	9.9	91.3	37.0	**0.27**

For the control (*pristine*) test, a high gold and sulfide sulfur recovery of 92.8% and 91.1% respectively was achieved. The SOx values seen from Table 7.3 quantifies that there has been sufficient oxidation to show metallurgical variations between the control and oxidised samples. This is because, with increasing residence times in nitric acid solution, the pyrite concentrate undergoes mild to moderate oxidation for surface modification (*as shown previously with the BSE images, BET analysis and XPS measurements*). The only indication of this surface alteration from the assays is the decreasing gold recoveries possibly due to the formation of hydrophilic iron oxide/hydroxides reducing the floatability (Senior and Trahar, 1991, Smart, 1991). Despite an increased extent of oxidation, there was no significant upgrade of the Au:S values as shown in Figure 7.14.

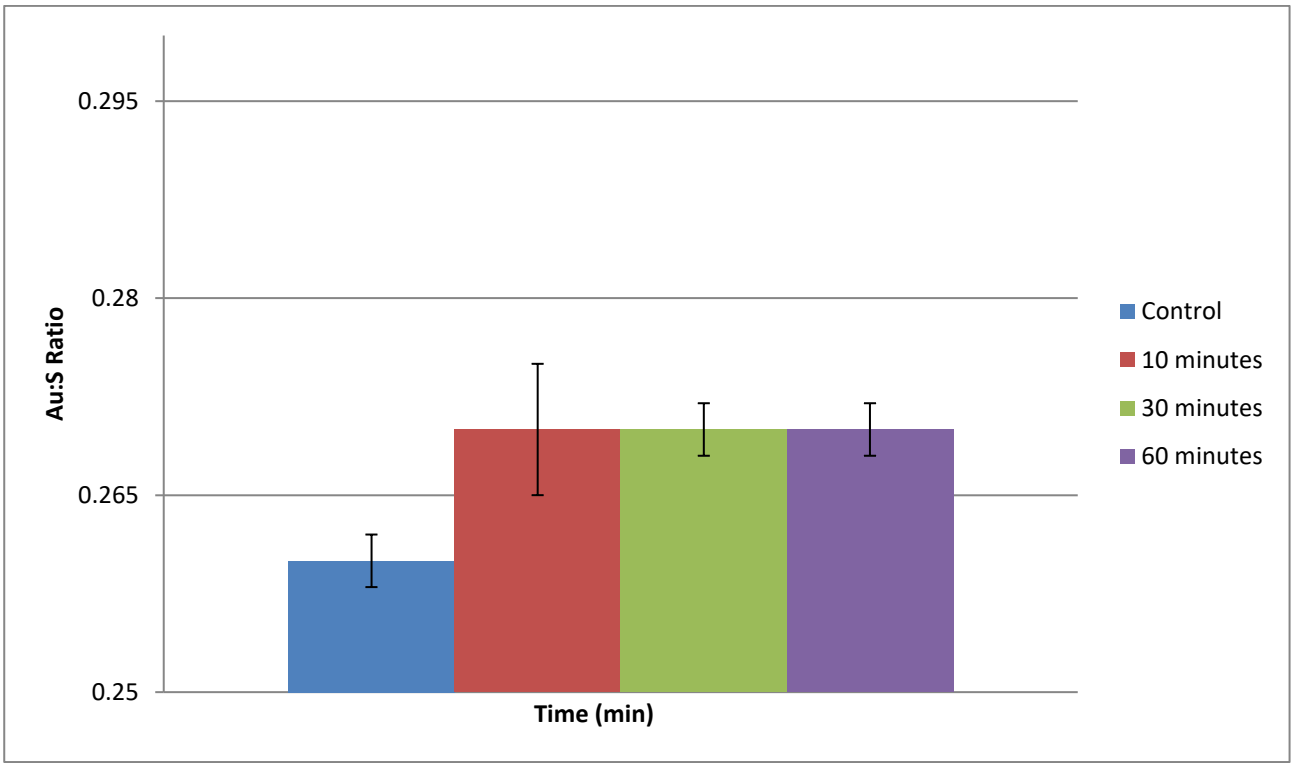

Figure 7.14: Au:S values of the control and oxidised samples. Despite higher levels of oxidation, no significant upgrade of Au:S values is seen due to the non-selective behaviour of sulfides

7.3.6 Direct Cleaner Flotation

Sulfide minerals can be easily oxidised (Buckley and Woods, 1984, Zachwieja et al., 1989) and this has been confirmed by SOx, BET and XPS analysis of the oxidised sulfide concentrate in this study. BSE images (*Figures 7.2 to 7.9*) revealed that, with an increase in the extent of oxidation by nitric acid, the corrosion effects were significant with marked alterations in the pyrite texture. This led to the decision to change the float pH from 5 to 11. The logic behind this was that some

oxidative modification would alter the pyrite phase resulting in the formation of an oxidised species as shown in equation 37 (Li, 2009).

$$2FeS_2 + 10HNO_3 \xrightarrow{\text{yields}} H_2SO_4 + Fe_2(SO_4)_3 + 10NO + 4H_2O \ldots\ldots\ldots\ldots\ldots\ldots\ldots\ldots\ldots\ldots\ldots\ldots\ldots\ldots 37$$

Alkaline pH conditions are usually employed in copper flotation plants to produce a high-quality copper concentrate by rejecting pyrite at the cleaner stage by depressing it at pH 11 (Chen et al., 2014, Wills, 2011). This is because pyrite has low floatability under alkaline conditions (Chen et al., 2014) and therefore, the postulation was the unoxidised pyrite would not float due to the depressing environment and the oxidised pyrite phase would float due to its different surface properties. This is an experiment based method to infer the effect of oxidation on mineral phases and their subsequent flotation behaviour as compared to more expensive surface analytical methods. A series one stage cleaner flotation tests were performed using the conditions shown in Table 7.4.

Table 7.4: Reverse flotation test conditions

Test Conditions	Cleaner Float
Float Cell Size	2.5L
Agitation	250 rpm
Air	5 L/min
Reagent	20g/t PAX Nascol 422
Density	10% solid by weight
Conditioning (*minutes*)	2 minutes
Float pH	11(***Lime***)
Flotation time (*minutes*)	incremental time of 2, 2, 4 and 4 minutes for a total time of 12 minutes
Concentrates	4
Scraping Frequency	10 seconds

The metallurgical responses of the pristine and nitric acid treated pyrite concentrates floated at pH 11 are shown in Table 7.5. Despite the fact that lime depresses pyrite in alkaline conditions, the control sample yielded high gold and sulfide sulfur recoveries of 87.5% and 87.1% respectively. One theory to explain this high pyrite recovery with the control sample can be attributed to the copper ions (Finkelstein, 1997, Leppinen, 1990, Chen et al., 2014, Chandra and Gerson, 2009). Although this was not expected, on further review of several Lihir and technical services reports, it was found that Lihir ores contain 150 to 300 ppm of copper which would be sufficient to activate pyrite (*if able to enter the aqueous phase*). Furthermore, the mineralogy of AA ore has shown around 167 ppm of copper which is ample enough to cause metal ion activation.

Table 7.5: Direct cleaner flotation data of oxidised samples floated at pH 11

Oxidation			Metallurgical Response				
Reagent	**Sample**	**SOx (%)**	**Gold Recovery (%)**	**Gold Grade (*g/t*)**	**Sulfide Sulfur Recovery (%)**	**Sulfide Sulfur Grade (%)**	**Au:S Ratio**
None	Control*	**0**	87.5	10.0	87.1	37.0	**0.27**
HNO_3	10	**13.7**	78.8	8.7	84.2	33.8	**0.26**
HNO_3	20	**17.3**	75.4	8.8	69.0	26.9	**0.33**
HNO_3	30	**21.9**	68.5	9.9	70.4	28.7	**0.34**
HNO_3	40	**22.9**	57.4	10.9	55.6	26.1	**0.42**
HNO_3	50	**24.3**	56.6	11.6	31.5	19.4	**0.60**
HNO_3 **Best Result**	60	**25.0**	56.3	11.5	24.0	17.3	**0.66**
HNO_3	70	**26**	54.6	10.0	23.1	28.0	**0.36**

The chemistry of surface activation by copper ions (Cu^{2+}) is a three stage process (Leppinen et al., 1988, Shen et al., 2001) involving:

1. Adsorption of Cu^{2+} on pyrite surfaces
2. Reduction to Cu^{+}.
3. Cu^{+}–xanthate interaction enhancing pyrite floatability

It is possible that the pyrite concentrate in the roughing stage had its surfaces already activated by Cu^{2+}. This Cu^{2+} was then reduced to Cu^{+} and the addition of collector (*PAX*) facilitated the Cu^{+}–xanthate interaction thereby enhancing pyrite floatability. This reduction in the valency states of copper was confirmed by XPS as shown in Figure 7.15. However, identifying and distinguishing the Cu^{+} $2p_{3/2}$ component at 932.5 eV from Cu^{2+} $2p_{3/2}$ at about 934.0 eV was difficult as the peaks overlapped.

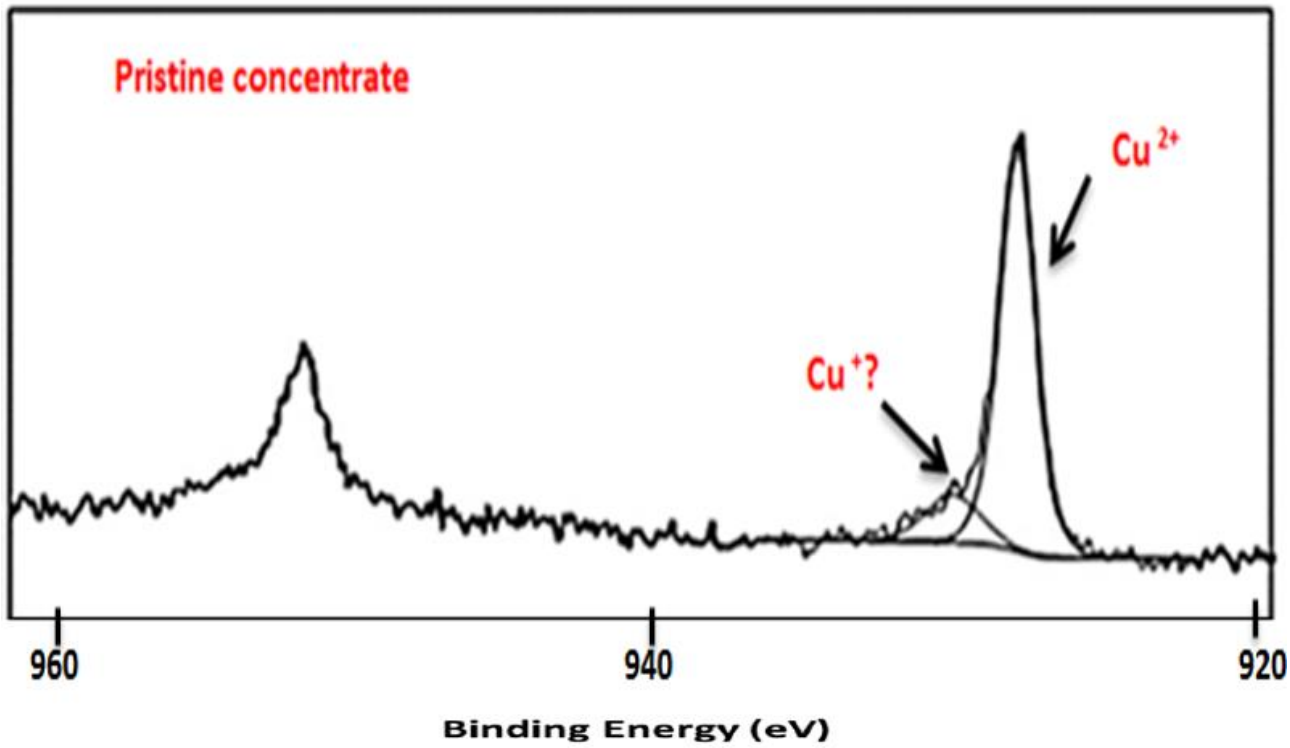

Figure 7.15: Cu 2p XPS spectra of the pristine pyrite concentrate

Therefore, to investigate further the distribution behaviour of copper species on pyrite in both the cleaner concentrate and tailing, ToF-SIMS was applied to measure the intensity of copper ions with the hope this information would aid the understanding of the mechanism involved in copper ion activation of pyrite. The ToF-SIMS spectrum is shown in Figure 7.16. The higher concentrations of copper ions, on the cleaner concentrate compared to the cleaner tail, confirmed the copper activation mechanism of the pyrite in an alkaline pH range, thereby agreeing with other studies in the literature (Finkelstein, 1997, Chen et al., 2014, Dichmann and Finch, 2001).

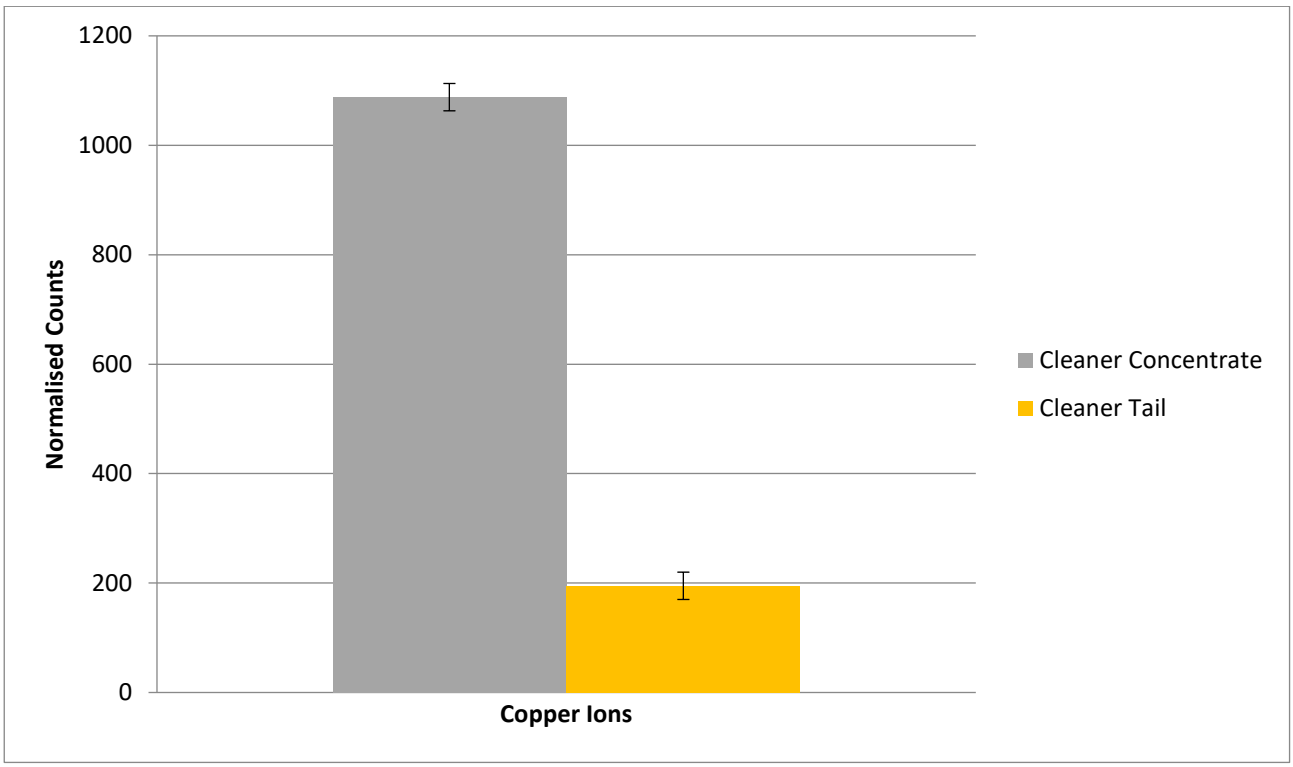

Figure 7.16: ToF-SIMS plot of copper ion concentration on the cleaner concentrate and tail

However, at the same alkaline pH of 11, the situation changes drastically for oxidised samples. As the extent of oxidation increases, significant decreases in gold recoveries were observed i.e. 78.8 % and 54.6% gold recoveries for the 10 minutes and 70 minutes oxidised concentrates respectively. Although the trend is disturbing in the traditional gold grade recovery sense, a closer look at the percentage differences in gold, mass and sulfide sulfur recoveries reveal some positive results as presented in Table 7.6. As the extent of oxidation increases, relatively sharp reductions in the sulfide sulfur and mass recoveries are observed for corresponding gold recoveries i.e. with the 50 to 70 minutes oxidised concentrates, 35 to 38 % reduction in gold recoveries are seen for corresponding 52 to 61 % and 64 to 74% reduction in sulfide sulfur and mass recoveries respectively. This decrease in gold recoveries is further explained in section 7.4.11 (*under collector attachment and copper ion activation of oxidised pyrite phase).*

Table 7.6: Percentage reduction in gold, mass and sulfide sulfur recoveries (*Gold column*) as a function of oxidation (*Blue column*). *= untreated/unoxidised concentrate

Oxidation			Metallurgical Response			
Treatment	**Oxidation (*minutes*)**	**SOx (%)**	**Gold Recovery (*Reduction %*)**	**Mass Recovery (*Reduction %*)**	**Sulfide Sulfur Recovery (*Reduction %*)**	**Au:S Ratio**
None	Control*	**0**	-	-	-	0.27
HNO_3	10	**13.7**	**9.9**	**5.4**	**3.3**	0.26
HNO_3	20	**17.3**	**13.8**	**11.8**	**20.8**	0.33
HNO_3	30	**21.9**	**21.7**	**36.7**	**19.2**	0.34
HNO_3	40	**22.9**	**34.4**	**26.5**	**36.2**	0.42
HNO_3	50	**24.3**	**35.3**	**52.2**	**63.8**	0.60
HNO_3	60	**25.0**	**35.7**	**61.0**	**72.4**	0.66
HNO_3	70	**26.0**	**37.6**	**61.0**	**73.5**	0.36

The low sulfide sulfur and mass recoveries but relatively high gold recoveries suggest that only the gold-rich pyrite species is reporting to the concentrate. However, the significant decline in gold recoveries reveals that a perfect separation is not likely to be achieved. This is mainly because there are many pyrite textures in the AA ore that represent part of a morphological and compositional continuum between the high gold and low gold pyrite types. The other possible reason is that the high-grade pyrite could be intergrown with other pyrite types (*some of which may have low gold tenor*) and therefore absolute separation of just the high-grade pyrite types may not be possible.

The present work has raised many questions. Foremost of these is the low flotation recoveries as a consequence of sulfur oxides, precipitates and oxyhydroxides formed on the oxidised pyrite surface. Nevertheless, this fundamental work is based on 'separation elucidation' within the same pyrite family i.e. low gold pyrite from high gold pyrite or *vice versa* rather than optimising gold recovery to concentrate. Therefore, over emphasis on flotation recoveries alone will result in ambiguity

regarding the potential of an oxidative hydrometallurgical treatment to separate within the same mineral family. The approach embraced in this work is evaluating the metallurgical response in terms of Au:S ratios of both the untreated/pristine concentrate and nitric acid leached pyrite concentrate. This is because the sole objective remains to produce a lower sulfur and relatively high gold concentrate as an autoclave feed (*as an alternative to the current practice*). It is unrealistic to expect high recoveries considering the nature of the mineral assembly while enhancing the Au:S ratio; this would otherwise defy the logic behind this work.

7.3.7 Gold to Sulfur Ratios (Au:S)

Cleaner flotation tests of pristine and oxidised samples have displayed different metallurgical responses with an increase in Au:S ratios achieved for oxidised samples as previously shown in Tables 7.5 and 7.6. The Au:S ratio for the control sample stays very low at 0.27 and is close to the typical Lihir flotation performance of 0.25 (Rankin, 2013). However, interestingly for the same cleaner flotation conditions, changes in Au:S values are observed with the oxidised samples. The 10 minutes oxidised samples exhibited an Au:S value lower than the control sample although this could be due to the unfortunate errors inherent in gold assays (Flatt and Woods, 1995). Improvements in Au:S ratios were observed from the 20 minutes oxidation stage; however, there was no steady progression suggesting no direct relationship between the extent of oxidation and the Au:S values as illustrated in Figure 7.17. The odd result with the 70 minutes oxidised sample is probably due to oxidising more than 25% of the sulfide sulfur i.e., destroying more than 1/4 of the pyrite in the sample as opposed to changing the surface of the pyrite by mild oxidation.

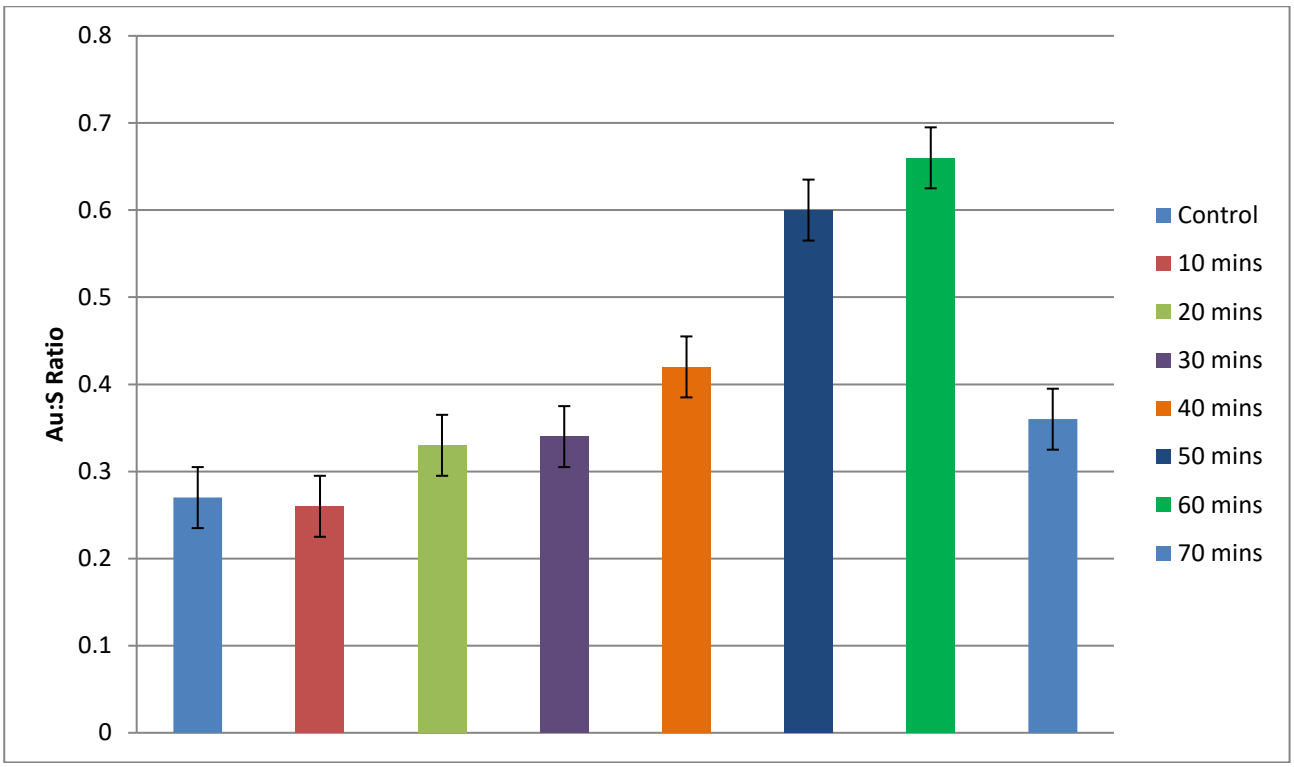

Figure 7.17: Au:S values of control and oxidised samples floated at pH 11

The 50 minutes and 60 minutes oxidised concentrates displayed the best results with 122% and 145 % increase in Au:S values respectively. However, interestingly the Au:S ratio decreases with the 70 minutes oxidation case. This is probably due to the excessive formation of sulfates and hydroxides by-products that interfere with the flotation response of high gold pyrite. This signifies that the extent of oxidation dictates the pyrite separation behaviour in a following cleaner flotation process and therefore, a moderate oxidation of approximately 25% SOx is the optimum oxidation level for optimum separation. Since the aim of this work is to oxidise the bulk of the sulfide sulfur to overcome the fixed sulfide oxidation capacity constraint of the Lihir autoclave, the sulfide sulfur grade-recovery curves of the highest Au:S value concentrate (*in this case the 60 minutes oxidised sample*) was compared with the pristine cleaner concentrate and is shown in Figure 7.18.

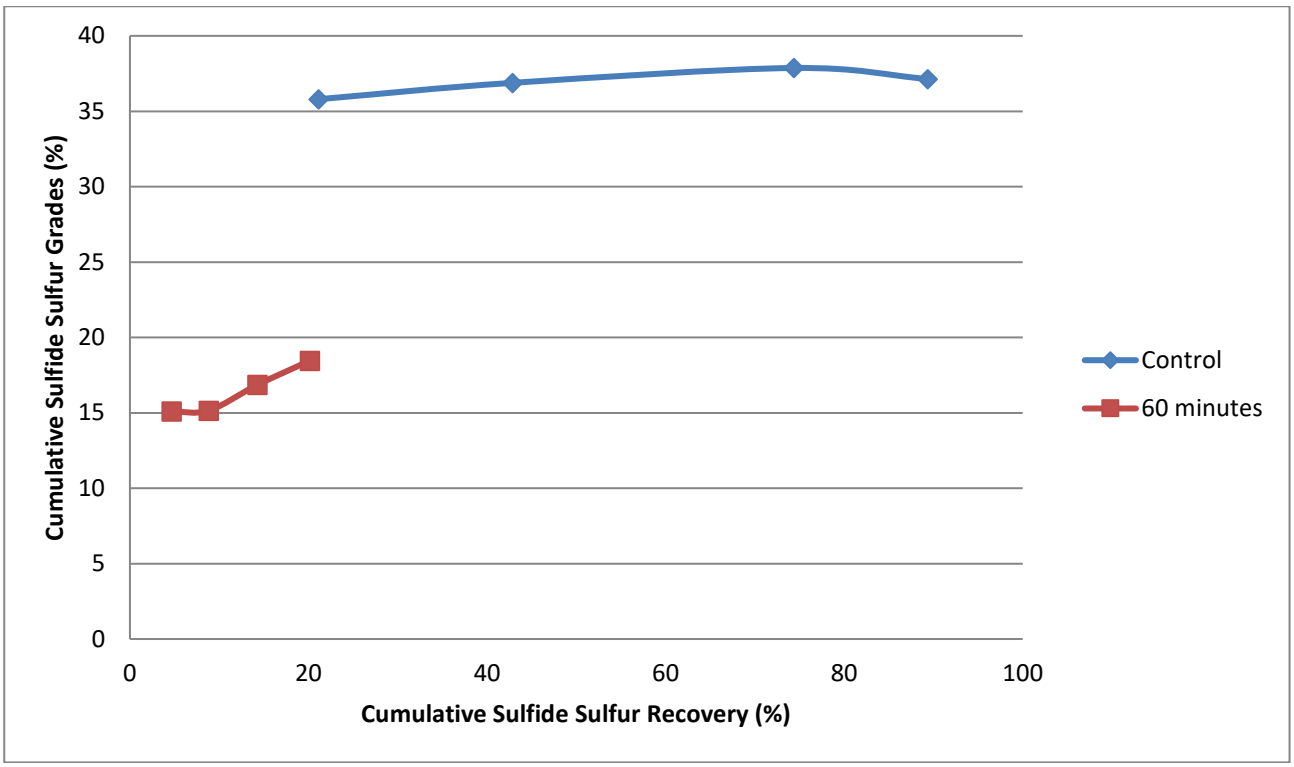

Figure 7.18: Sulfide sulfur grade-recovery curve for the pristine and 60 minutes oxidised concentrates

As seen, the sulfide sulfur grade of the 60 minutes oxidised concentrate decreases significantly and rigorous analysis of these experimental data revealed an interesting trend that is presented in Table 7.7.

Table 7.7: Gold and sulfide sulfur grade of the control and oxidised concentrates

Oxidation Time (*minutes*)	Gold Grade (*g/t*)	Sulfide Sulfur Grade (%)
0	10.0	37.0
10	8.7	33.7
20	8.7	26.8
30	9.8	28.6
40	10.9	26.1
50	11.6	19.3
60	11.5	17.2
70	10.0	28.0

The gold grade for all the samples (*unoxidised and oxidised*) remains more or less the same. The minor changes in gold grades among the various sets of samples could be attributed to the errors in gold assaying (Flatt and Woods, 1995). Although the literature is of little help in providing information regarding the impact of nitric acid oxidation on gold grades, from the experimental data, it is evident that it is the sulfide sulfur grade that gets modified to a great extent in the oxidation process. Therefore, it can be confidently stated that it is not possible to improve the gold grade of the final pyrite concentrate by nitric acid oxidation. However, there is convincing evidence that the sulfide sulfur grade of a pyrite concentrate can be significantly reduced without affecting the gold grade as shown in Figure 7.19.

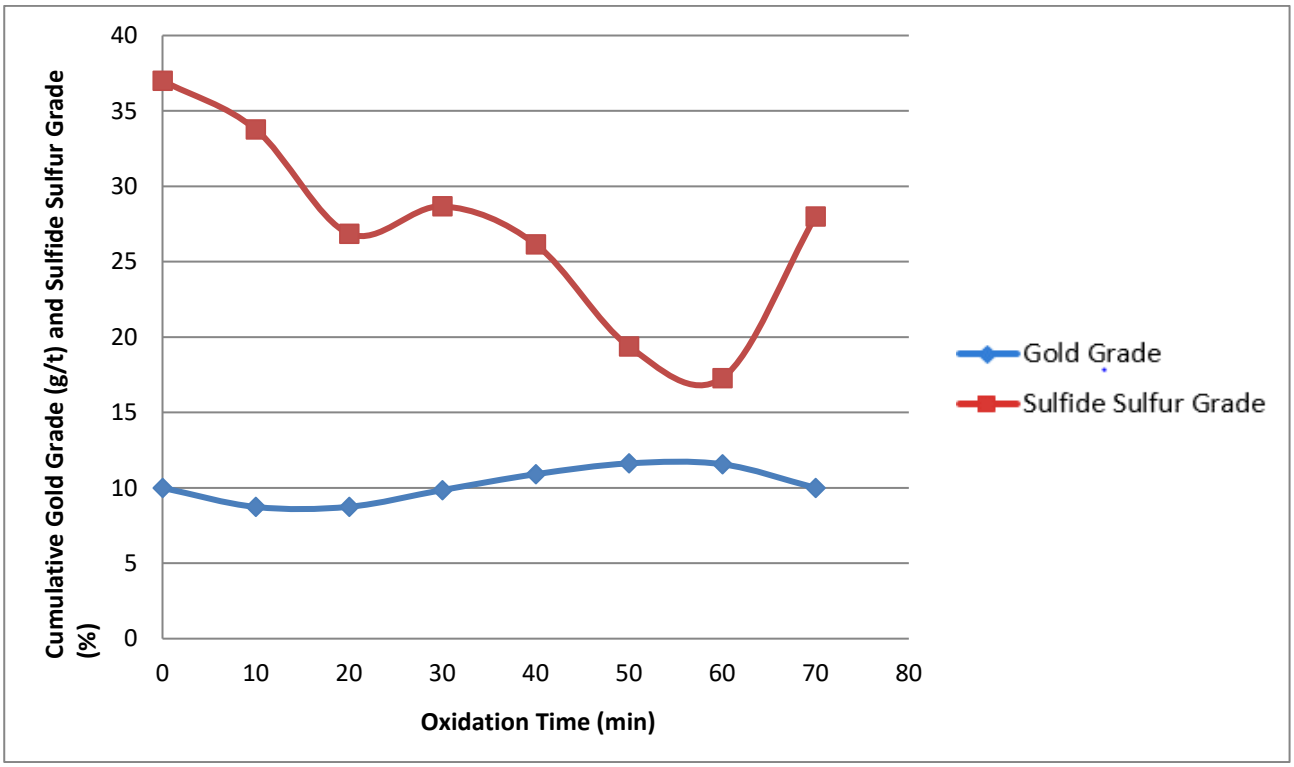

Figure 7.19: Cumulative gold and sulfide sulfur grades vs. oxidation time

This change in sulfide sulfur grades explains the varying Au:S values between unoxidised and oxidised samples. This trend was further confirmed looking at actual Au:S ratios of the individual concentrates as shown in Figure 7.20. As shown, the control sample shows low Au:S for all individual concentrates. With oxidation, there is an increase in Au:S ratios with all the individual concentrates. A standout difference is observed with 50 minutes and 60 minutes oxidised samples again confirming that a moderate oxidation of approximately 25% SOx is the optimum oxidation level for significant upgrades in individual (*actual*) Au:S values of flotation concentrates as well as cumulative ratios.

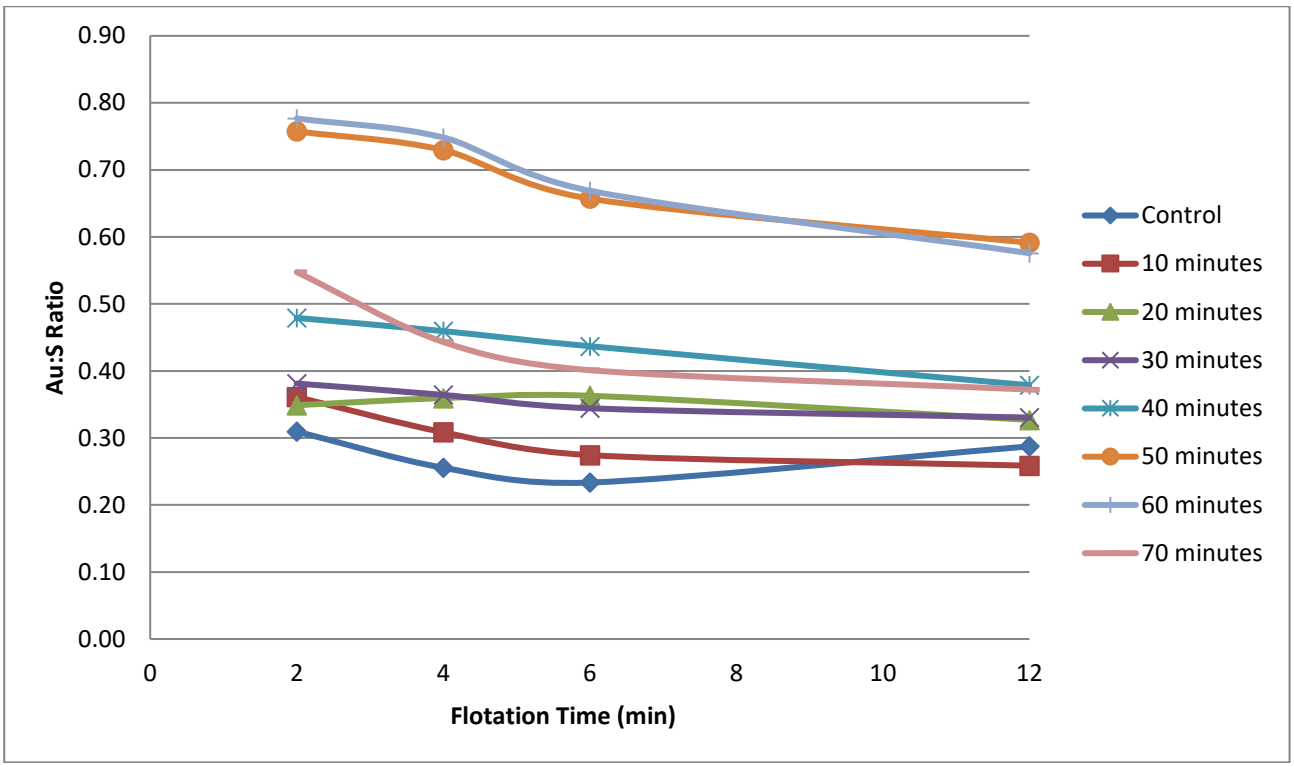

Figure 7.20: Actual Au:S ratios of the control and oxidised samples

The presence of sulfide sulfur in the oxidised cleaner concentrates revealed that sulfides were not completely depressed. Moreover, the high Au:S values of the oxidised concentrates compared to the respective tails established conclusive evidence that the high gold low sulphur pyrite was floating and the low gold pyrite types were not and this is presented in Table 7.8. However, Au:S ratio and extent of oxidation do not share a linear relationship and this is seen with the 10 minutes oxidation case. The high Au:S value of the tail, in the case of 10 minutes oxidation with 13% SOx, is either due to the incomplete surface modification of the high gold pyrite types or formation of oxidation intermediates such as nitrates inhibiting pyrite flotation in an alkaline environment. Therefore, oxidising a pyrite concentrate does not necessarily elevate the Au:S ratio and in order to achieve preferential oxidation of the high gold pyrite types, it is necessary to adopt an oxidation regime within a strict operating window.

Table 7.8: Au:S ratios of pristine and oxidised cleaner concentrates and tails

Oxidation			Metallurgical Response	
Treatment	**Oxidation (*minutes*)**	**SOx (*%*)**	**Au:S Ratio Concentrate**	**Au:S Ratio Tail**
None	Control*	**0**	0.27	0.25
HNO_3	10	**13.7**	0.27	0.38
HNO_3	20	**17.3**	0.33	0.22
HNO_3	30	**21.9**	0.34	0.28
HNO_3	40	**22.9**	0.42	0.17
HNO_3	50	**24.3**	0.60	0.15
HNO_3	60	**25.0**	0.66	0.10
HNO_3	70	**26.0**	0.36	0.10

7.3.8 Eh-pH window

The standard practice in mineral oxidation studies is to establish an Eh-pH operating window that allows significant optimisation of the process. However, this approach is not valid in this work mainly because this is not an extensive oxidation experiment and hence, there is no significant difference among the Eh-pH values. The Eh-pH values of the various conditioning stages are shown in Table 7.9. At 10 g/L of nitric acid, the pH value increases (*and Eh values decrease*) indicating that nitric acid was consumed in the process resulting in oxidising conditions. After 50 minutes oxidation, the pH stabilised at 1.26 (*greater than the stock solution by 0.38*) then decreased to 1.21 indicating that nitric acid was not completely consumed in the process and hence, a wash liquor stage is necessary to neutralise the excess acid prior to further flotation tests. Excess nitric acid from the pre-treatment stage could be regenerated from an economical and processing point of view, however, this topic is beyond the scope of this study.

A moderate Eh is required for collector adsorption and to facilitate pyrite flotation (Owusu et al., 2014). High Eh values between 580 and 543 mV (*shown in Table 7.9*) would have inhibited the adsorption of xanthate collectors on to sulfide surfaces contributing to low sulfide sulfur recoveries leading to higher Au:S values in the case of oxidised samples.

Table 7.9: Eh-pH values of the nitric acid oxidation process

Oxidation Time (*minutes*)	**E_h (*SHE*)**	**pH**
10	580	0.88
20	573	1.05
30	567	1.11
40	562	1.13
50	555	1.26
60	555	1.26
70	543	1.21

High Au:S values of the oxidised concentrates compared to the oxidised tails (*shown in Table 7.8*) clearly signifies that the floating pyrite had an 'active phase characteristic' compared to the passive (*depressed*) pyrite. The differences in the Au:S values observed with different stages of oxidation reveal that the oxidation level for separating one type of pyrite from another is quite sensitive and dependent on the pH/Eh conditions. Pyrite oxidation was found to increase with operating pH, and therefore the pH used to control the preferential oxidation should be between ~ 1.15 and ~ 1.28 for optimum Au:S upgrades (*0.6V with 50 and 60 minutes oxidation*). Similar to the pH condition, the Eh of the nitric acid leach solution did not vary significantly between the different sets of oxidation (*due to short residence times and the presence of ferrous ions according to reaction 38*) (Li, 2009) providing an optimum range of 0.5 to 0.6 V with respect to SHE.

$$FeS_2 + 8\,H_2O \xrightarrow{\text{yields}} Fe^{2+} + 2\,SO_4^{2-} + 16H^+ + 14e^- \quad \ldots\ldots 38$$

The difference in Au:S values with varying oxidation times and extent of oxidation reveals that oxidising a pyrite concentrate does not necessarily elevate the Au:S value and this upgrade is pinned by a sensitive oxidation window. Operating Eh, pH and SOx are, therefore, the key variables in the preferential oxidation and separation of high gold pyrite. Thus for pH and Eh values of 1.26 and 0.55 V (*vs.SHE*) respectively, the highest Au:S values were obtained with a SOx value of 25% for both 50 minutes and 60 minutes oxidised samples as shown in Figure 7.21.

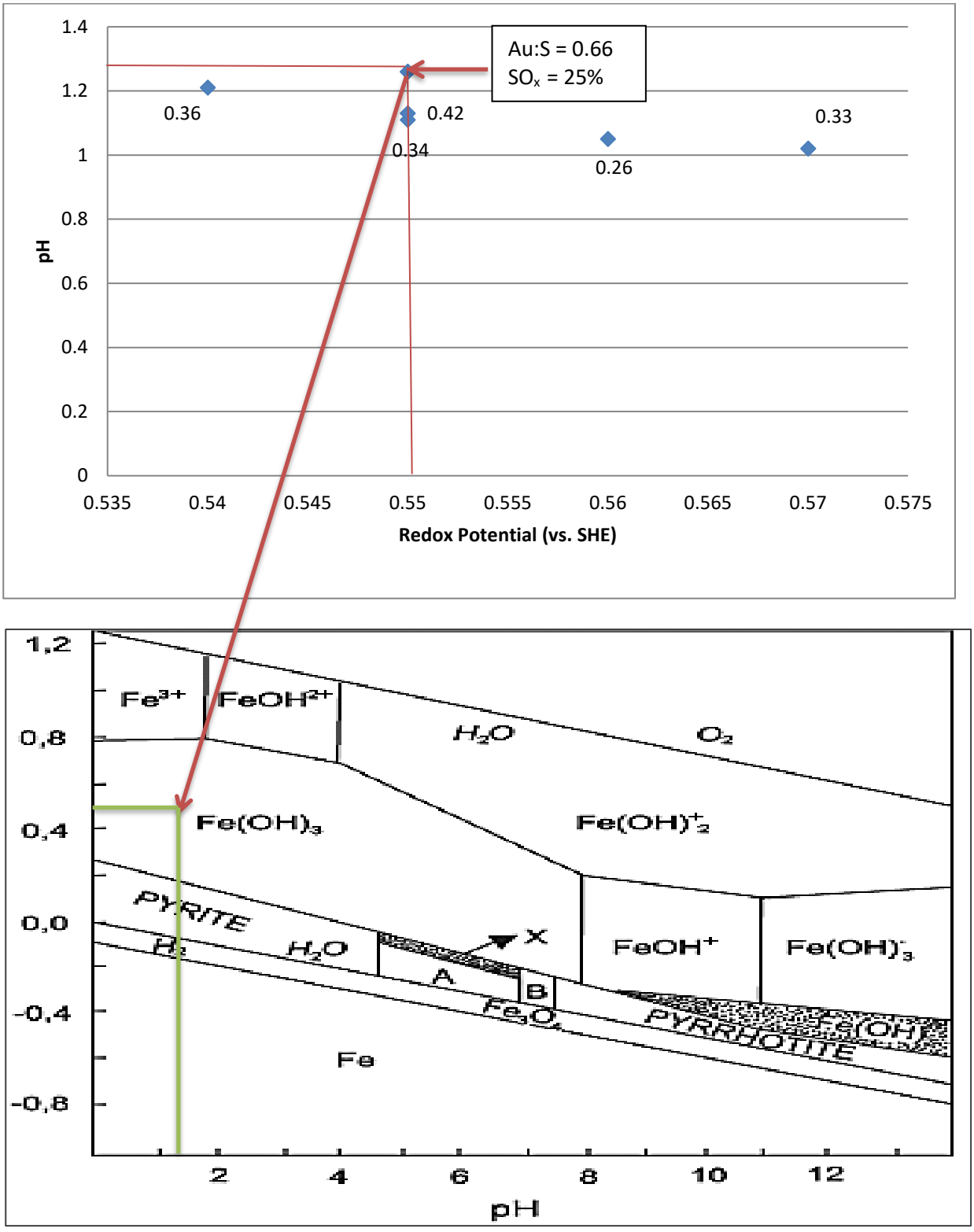

Figure 7.21: Operating window for optimum Au:S ratio upgrade by nitric acid oxidation. pH and ORP values of 1.26 and 0.55 V vs. SHE are critical for 25 % sulfide sulfur oxidation for optimum Au:S ratio upgrade

7.3.9 Nature of the oxidised pyrite phase

Metallurgical and mineralogical data have provided clues regarding the effect of oxidation; however, it does not clarify the cause of the upgrade in Au:S values. To demonstrate this, it is necessary to understand the nature of both the active (*oxidised*) and passive (*unoxidised*) pyrite phases. Therefore, the purpose of this section is to discuss the oxidised pyrite behaviour in the following cleaner flotation process.

The suggested mechanism of reaction is a direct pyrite oxidation process with dissolved oxygen and ferric ions (Fe^{3+}) as the main oxidising agents. The role of oxygen is to regenerate fresh ferric ions by oxidation of ferrous ions. The concentration of ferric can be much greater than that of oxygen so the contributions of the oxidants can vary. According to the literature, the main reactions taking place are (Chinchón-Payá et al., 2012):

$$FeS_2 + \frac{7}{2}O_2 + H_2O \xrightarrow{\text{yields}} Fe^{2+} + 2SO_4^{2-} + 2H^+ \quad \ldots\ldots 39$$

$$Fe^{2+} + \frac{1}{4}O_2 + H^+ \xrightarrow{\text{yields}} Fe^{3+} + \frac{1}{2}H_2O \quad \ldots\ldots 40$$

$$FeS_2 + 14Fe^{3+} + 8H_2O \xrightarrow{\text{yields}} 15Fe^{2+} + 2SO_4^{2-} + 16H^+ \quad \ldots\ldots 41$$

These equations are very straightforward from a chemical reaction perspective. Extensive literature exists on pyrite oxidation with a number of studies overlapping with each other and they have all confirmed and illustrated the nature of pyrite oxidation. However, this is because the majority of the oxidation studies found in the literature consider only oxidation of pure mineral systems and do not account for the interference of other elements/minerals and galvanic effects. Conflicting results arise when studies are conducted on real ores with complex mineralogy. This is because "no two ores are the same" and the presence of different elements in the ore system can inhibit or promote the oxidation process resulting in the formation of various oxidised species.

There is always a potential risk for undertaking mineral-industry research on a 'real world' samples as some of the more fundamental aspects could be overlooked. Drawing conclusions and developing a fundamental understanding of the oxidation and flotation processes are often limited without recourse to some further investigations using model systems. Significant efforts were made during the initial stages of this work to undertake tests on pure mineral samples (*arsenian pyrite and pyrite*) to understand the behaviour of a single mineral sample and underpin the behaviours observed with the Lihir sample. Although it was easy to source pure pyrite minerals, the difficulty

in obtaining arsenian pyrite samples restricted the opportunity to understand the more applied work which was completed during the course of this research.

An investigation (*by the candidate*) revealed that no published information considers the interference of various elements during the oxidation of pyrite. Although this could be a crucial part of oxidation studies dealing with real ore and concentrate samples, this aspect will not be covered in this thesis considering the broad nature of this investigation. Also, the lack of a specific surface analysis diagnostic technique to identify the various pyrite types leads to the conclusion that identification and 'labelling' of the oxidised pyrite phase is a separate investigation in its own right. Therefore, as discussed, the reliable approaches embraced here would be to focus on the Au:S ratio and the gold to arsenic ratio (*Au:As*) to investigate the characteristics of the oxidised pyrite phase and resistant pyrite.

7.3.10 Gold to Arsenic Ratios (Au:As)

It has already been shown in Chapter 5 that the high arsenic pyrite had a faster oxidation rate compared to the low arsenic pyrite. As the extent of oxidation increases, trivalent arsenic is oxidised to pentavalent arsenic as shown in Figure 7.22, resulting in the formation of *ferric arsenate* in the low pH conditions of the nitric acid system (*Table 7.10*).

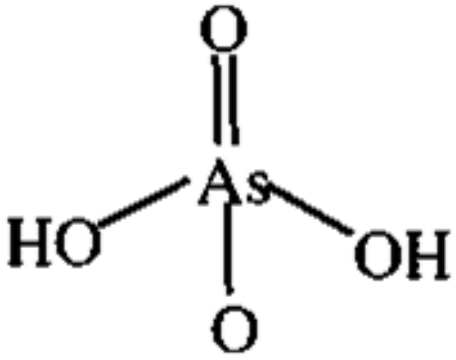

Figure 7. 22: Structural Configuration of Arsenate (Nazari et al., 2016)

Table 7.10: Oxidation Products in the Nitric Acid System

System	pH	Oxidation products
FeS_2 / HNO_3	0.88 to 1.26	$Fe^{2+} \xrightarrow{yields} Fe^{3+}$ $As(III) \xrightarrow{yields} As\ (V)$

Arsenates could have then adsorbed onto haematite and floated under alkaline conditions in the cleaner stage contributing to higher Au:As ratios compared to the corresponding tail values as shown in Table 7.11. The best approach to defining the characteristic of the active oxidising pyrite is to compare the gold to arsenic ratios (*Au:As*) of the control and oxidised concentrates as shown in Figure 7.23. There is a significant upgrade in Au:As ratios of the oxidised samples especially with 50 minutes and 60 minutes oxidation stage samples. This follows the same trend as Au:S ratios shown before suggesting that the oxidised high gold arsenian pyrite (*ferric arsenate*) was floating while the low arsenic pyrite remained depressed in the cleaner stage. This relates well to the BSE images (*Figures 7.3 to 7.9*) where ImageJ thresholding was not possible beyond the 40 minutes' oxidation stage due to very low arsenic concentrations. A very similar trend is observed with the Au:As ratios as well with a significant upgrade seen from the 40 minutes oxidation stage.

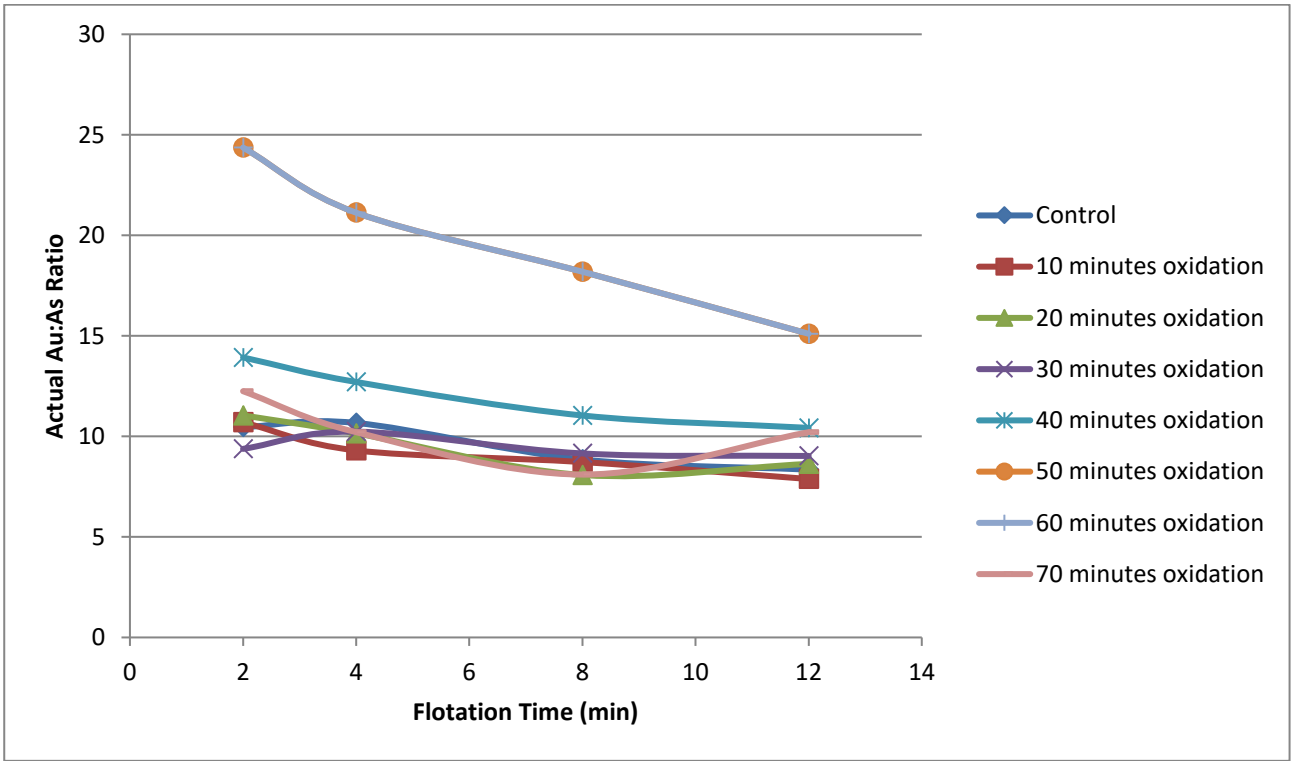

Figure 7. 23: Actual Au:As ratios of control (*pristine or non-oxidised*) and oxidised pyrite concentrates. 50 minutes and 60 minutes oxidation data points are overlapped.

The variable gold hosting pyrite types are oxidised as well explaining the relatively low Au:As values of the tails from the 50 minutes oxidation stage samples as seen in Table 7.11. This can be further confirmed by closer examination of the 60 and 70 minutes oxidation case where the Au:As ratio of the tail is very low signifying extreme oxidation of the arsenic hosting pyrite types. The high Au:As tail value of the 10 minutes oxidation case, as seen previously with the Au:S ratio, is either due to the incomplete surface modification of the high gold pyrite types or formation of oxidation intermediates inhibiting pyrite flotation in an alkaline environment.

Table 7.11: Au:As values of the control and oxidised cleaner concentrates and tails

Oxidation Time (*minutes*)	**Cumulative Au:As Ratio Concentrate**	**Cumulative Au:As Ratio Tail**
Control	10.6	5.7
10	9.2	11.1
20	9.3	7.8
30	10.4	9.2
40	11.5	7.6
50	11.4	4.6
60	13.7	2.9
70	10.0	3.0

The typical mass and metal balances for nitric acid oxidation tests (*10 minutes oxidation stage*) are included for clarity in Figure 7.24. Appendix section 4.2 gives detailed metallurgical accounting for other oxidation stages.

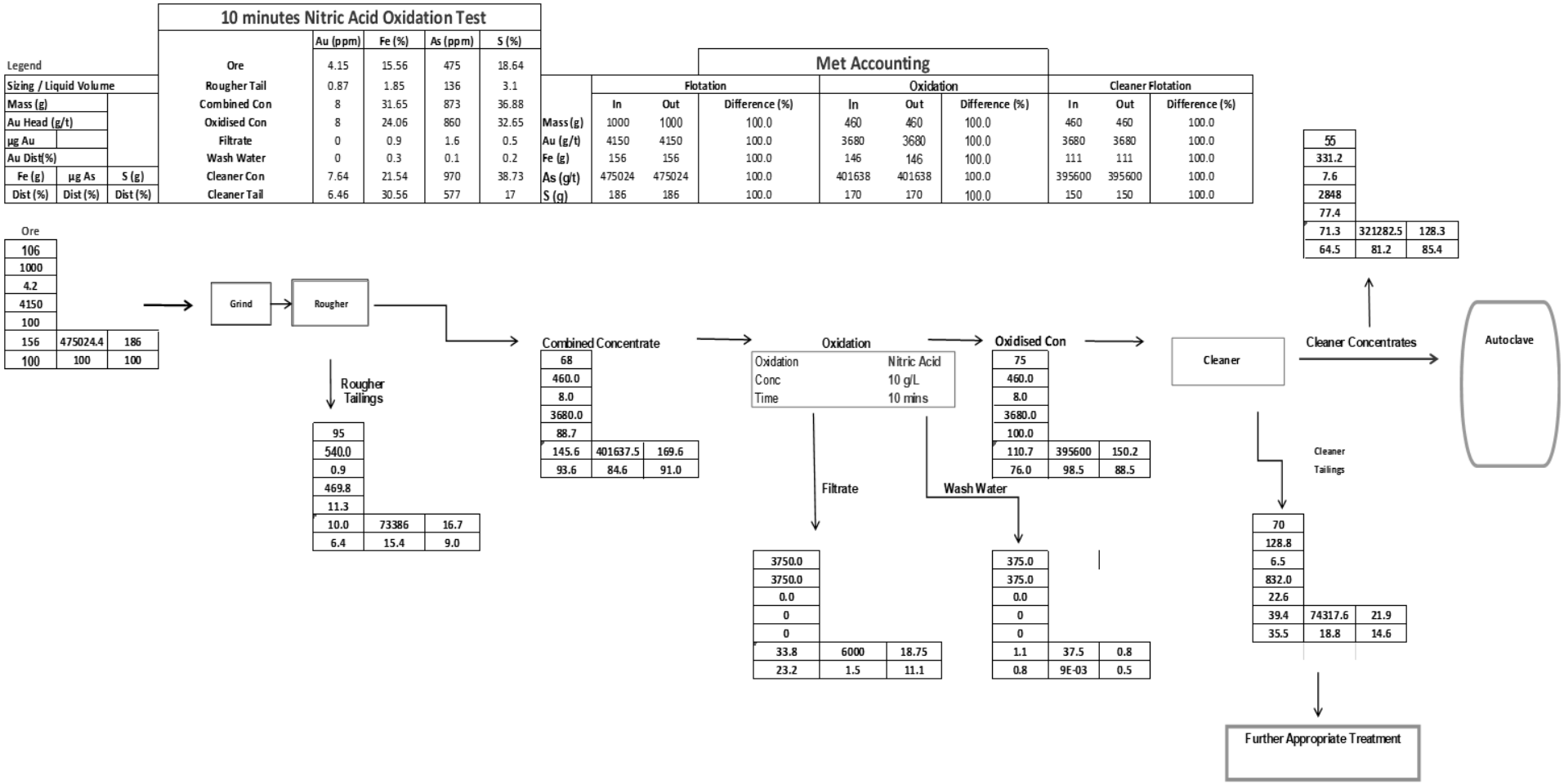

Figure 7. 24: Metallurgical Accounting of the Nitric Acid Oxidation Process

The distribution values are for three steps: Step 1: Rougher Tail + Combined Concentrate

Step 2: Filtrate + Wash Water + Oxidised Concentrate

Step 3: Cleaner concentrate + Cleaner Tail

7.3.11 Collector and copper ion attachment on the oxidised pyrite phase

To obtain a conclusive understanding of the oxidised species, ToF-SIMS analysis was undertaken to understand the collector attachment on pristine and oxidised pyrite surfaces as shown in Figure 7.25.

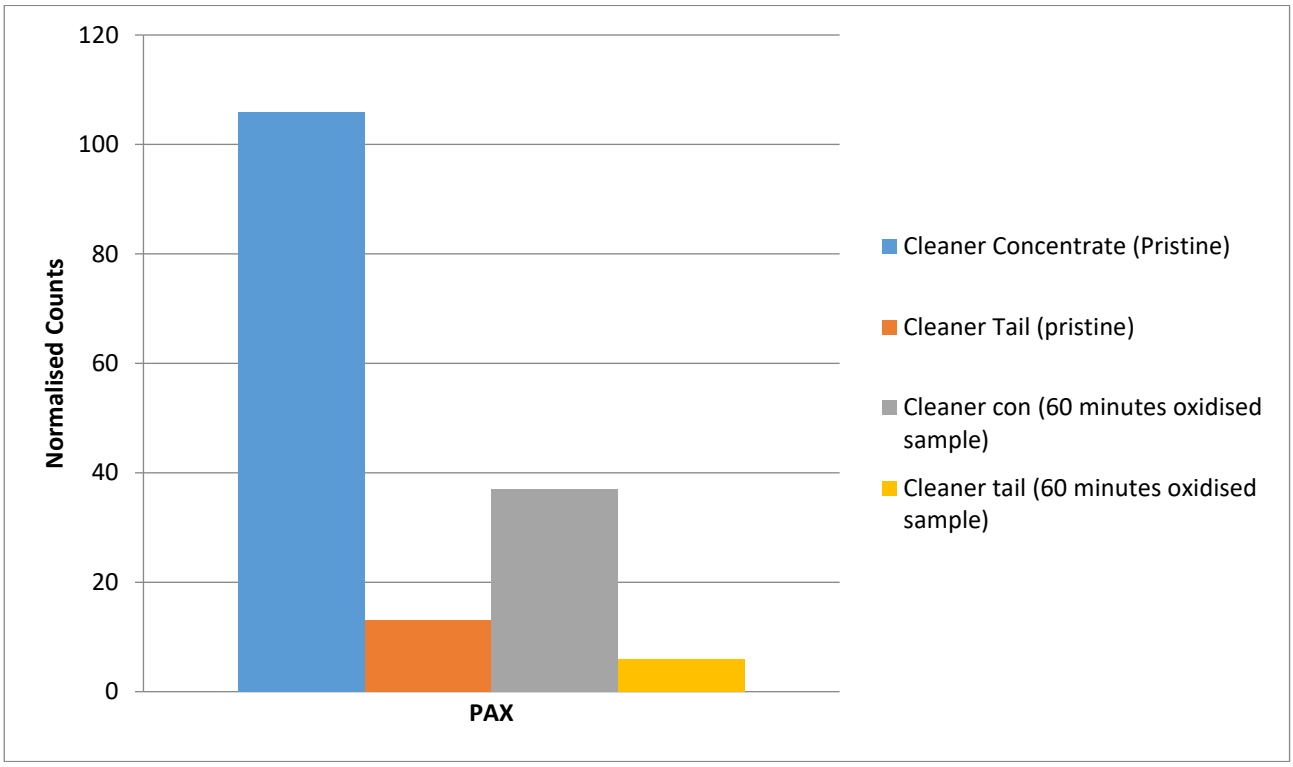

Figure 7.25: ToF-SIMS graphs of collector attachment on pristine and oxidised (*60 minutes oxidation stage*) pyrite concentrate and tailing

From the ToF-SIMS graphs, it is clear that there is relatively low collector attachment on the oxidised pyrite concentrate compared to the pristine concentrate attributing to low gold recoveries. This is because iron oxidation products on the oxidised concentrate inhibited xanthate adsorption on pyrite surface (Jiang et al., 1998). However, the reasonably high collector attachment on the oxidised pyrite concentrate compared to the oxidised tail confirms the relatively moderate hydrophobic nature of the oxidised pyrite phase. Although it can be argued that the addition of more collector may further improve the floatability of the oxidised pyrite phase, it is less probable that the Au:S values will improve due to the non-selective flotation character of all pyrite types in the presence of a xanthate (*PAX*) collector.

A similar trend is observed with the copper ion concentration graphs as well, as shown in Figure 7.26. It has been reported earlier that an oxidising environment inhibits the copper activation of sulfides (Chen et al., 2013, Peng and Grano, 2010) and this could be the reason why low copper ion concentration is observed with the 60 minutes oxidised cleaner concentrate compared to the pristine concentrate.

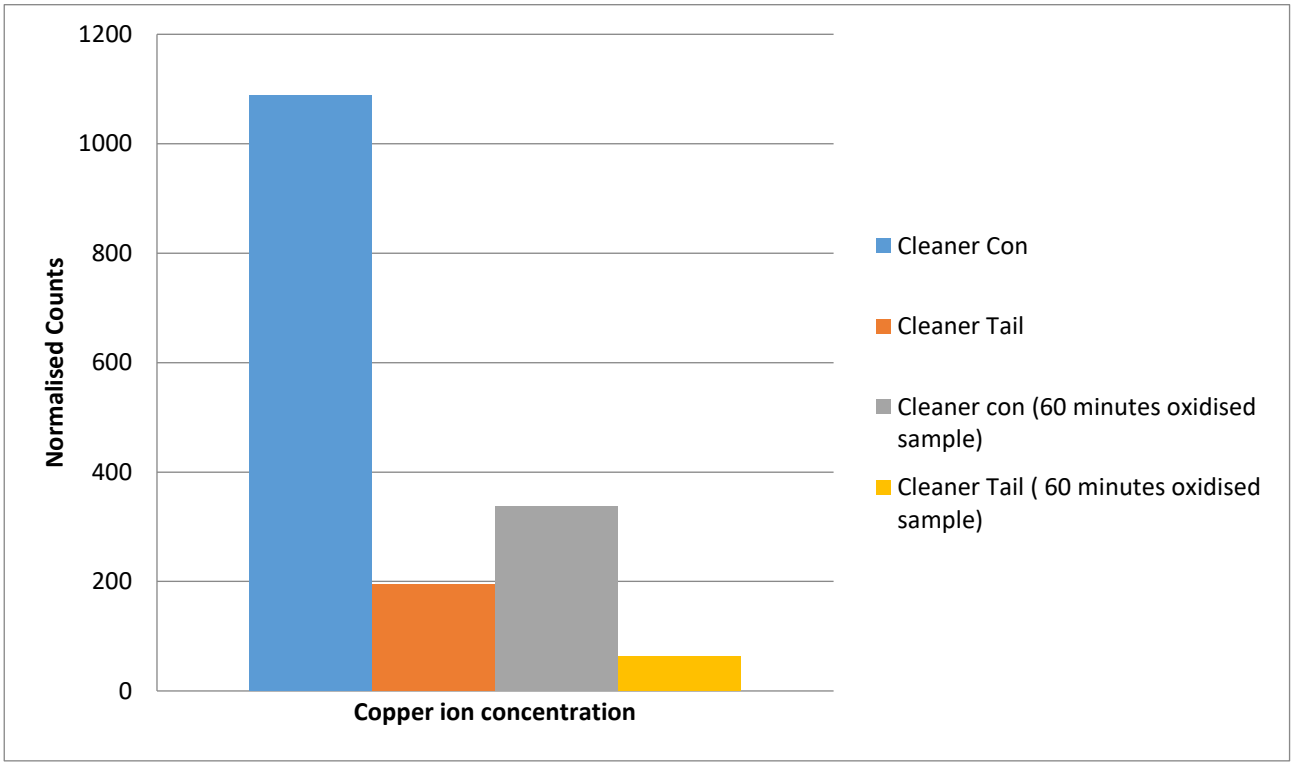

Figure 7.26: ToF-SIMS graphs of copper ion attachment on pristine and oxidised (*60 minutes oxidation stage*) pyrite concentrate and tailing

This suggests that with 60 minutes oxidation, the oxidised pyrite phase must be in hydrophobic state (*due to sulfides and polysulfides on the surface and also contribution from the collector*) explaining the very high Au:S values. However, with 70 minutes' oxidation, the oxidised pyrite may not be able to retain its hydrophobic nature due to extensive formation of iron oxide/hydroxides. This confirms that the oxidation level for separating one type of pyrite from another is quite sensitive and therefore for optimum Au:S values the SOx cut-off range is between 24 to 25%. For this reason, the path with promise might be to select an oxidation time that upgrades the Au:S ratio to serve as an optimal autoclave feed at reasonable gold recoveries that fit within the process economics.

7.3.12 Flotation of high gold pyrite phase (Bottle roll tests)

Bottle roll tests were conducted on an unoxidised pyrite concentrate and the 60 minutes oxidised concentrate and tailing as per the conditions illustrated in Table 7.12.

Table 7.12: Bottle Roll test conditions

Variables	Values
Leach residence time	24h
Temperature	25^{o}C
Slurry density	40%
Initial cyanide concentration	1000 mg/L
Target free cyanide concentration	500 mg/L
Target pH	10.5

Note: Kinetic samples were not required in the bottle roll tests.

The overall bottle roll leaching data indicate that the gold recovery from the 60 minutes oxidised cleaner concentrate is higher than the unoxidised concentrate suggesting that 60 minutes oxidation improved the amenability of gold to cyanidation as seen in Table 7.13. This is because, with 60 minutes oxidation, the arsenian pyrite (*that is high in gold tenor*) undergoes significant textural alteration as seen previously with the BSE images. This surface modification (*with different surface properties compared to unoxidised pyrite*) must have enabled the oxidised pyrite (*modified arsenian pyrite*) to float at an alkaline pH resulting in higher cyanide soluble gold. The low gold pyrite (*which is more resistant to oxidation and hence less or no surface alterations*) is seen depressed into the tailings at an alkaline pH resulting in a lower cyanide soluble gold value.

Table 7.13: Bottle roll test results for three samples

Sample	Cyanide soluble gold (*% Au*)
Unoxidised Con (*pristine/control*)	21.7
60 minutes Oxidised Cleaner Con	36.3
60 minutes Oxidised Cleaner Tail	14.8

7.4 Regrinding

Regrinding to a very fine particle size is a common practice (Chen et al., 2013) of processing low-grade ores to improve the liberation of valuable minerals and thereby their subsequent separation in flotation and leaching (Owusu et al., 2014, Chen et al., 2014). Regrinding reduces the intermediate and coarse particles to fine and ultra-fine fractions and therefore, it was expected that the significant reduction in particle size would have a substantial effect on the Au:S values compared to just primary grinding. This is because the floatability of mineral particles is attributed to both their mechanical (*size*) and chemical (*hydrophobicity*) properties (Vizcarra et al., 2011). Also, new surfaces that are formed during regrinding provides more active sites for pyrite surface oxidation and this, in turn, would result in more surface area of pyrite ultimately affecting its flotation performance (Ye et al., 2010, Owusu et al., 2014).

Literature that relates to the effect of regrinding on Au:S values appears to be scarce and therefore this study investigates the effect of 'the intrinsic relationship of mechanical and chemical properties' in separating the various pyrite types. The focussing question in this section is "Are there differences in the mechanical properties of low gold pyrite relative to the gold-rich pyrite and would the exploitation of these variances allow the separation of various types of pyrite and upgrade the Au:S ratio of a flotation concentrate after oxidation"? This hypothesis is framed on the assumption that if one particular type of pyrite (*low or high gold*) possesses a different grain size (*texture*) and harder sulfide framework compared to the other form; it will be less liberated after regrinding, in the following flotation process. This effect will be reflected in the metallurgical responses, after oxidation and cleaner flotation, mainly through gold and sulfur recoveries.

7.4.1 Impact of regrinding on sulfide sulfur oxidation

Although the intention was to establish a 'mild to moderate oxidation regime' for preferential oxidation and separation, the synergistic effect of particle size reduction on oxidation was expected to increase the SOx values compared to no regrinding. If this substantial improvement in the extent of oxidation can be justified, will depend on the flotation performance of the valuable mineral, in this case, the high gold pyrite. Due to the shortage of AA ore sample, the pyrite concentrate was processed at slightly different oxidation intervals of 15, 30, 45 and 60 minutes. Similar to the previous study and as expected, the extent of sulfide sulfur oxidation increased from no oxidation for the control sample to 47% oxidation for the 60 minutes oxidised sample as shown in Figure 7.27.

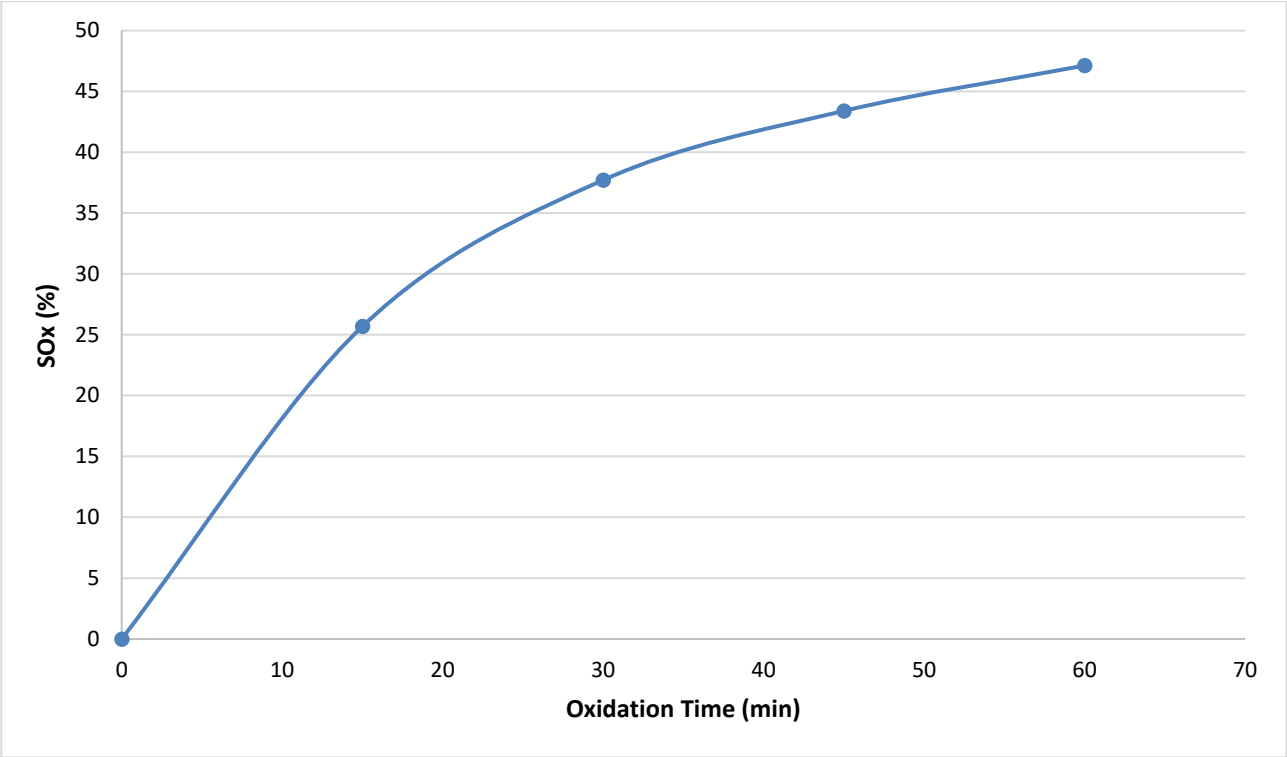

Figure 7.27: Quantification of the extent of nitric acid oxidation of reground pyrite concentrates at different time intervals by sulfide sulfur measurements

7.4.2 Impact of regrinding on pyrite surface area

The surface area of the pyrite concentrate increased from 1.6 m^2/g to 2.8 m^2/g after regrinding, indicating the creation of new surfaces as a result of the regrinding process as shown in Table 7.14.

Table 7.14: Surface area measurement of the pyrite concentrate feed and regrinding product

Parameters	Regrind Feed	Regrind Product
80% Passing Size (μm)	70	38
Surface Area(m^2/g)	1.6	2.8
% Fresh Surfaces		75

As the leaching process advances, the surface area also increases as shown in Table 7.15 suggesting depletion of the pyrite granular zones. The relationship between sulfide sulfur oxidation and surface area is positively correlated (*previously illustrated*) as shown in Figure 7.28.

Table 7.15: BET derived surface area measurements of the pristine and oxidised reground samples. Pristine*= untreated/unetched sample

Sample	Oxidation Time (*minutes*)	BET Surface Area (m^2/g)	Sulfide Sulfur Oxidation (*SOx %*)
Reground Pyrite Concentrate	0 (*Pristine**)	1.6	0
	15	4.4	25.7
	30	5.4	37.7
	45	7.5	43.4
	60	7.7	47.1

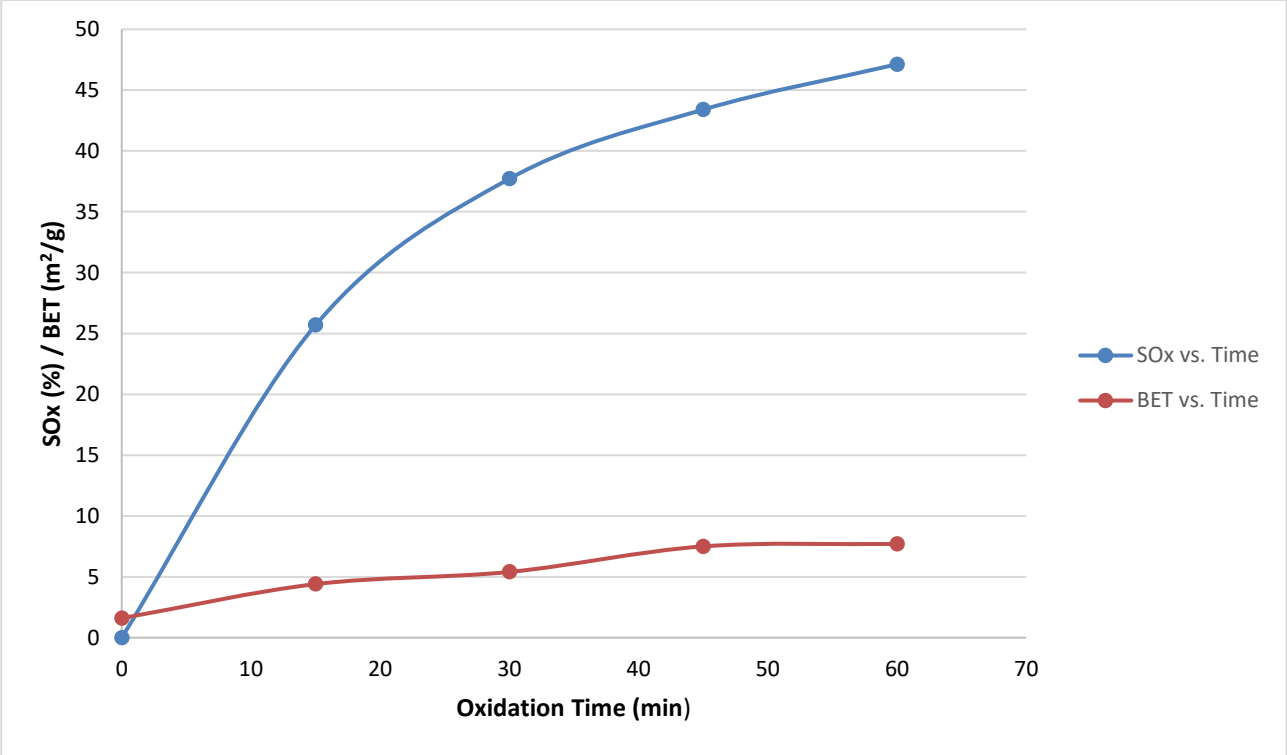

Figure 7.28: Correlation between sulfide sulfur oxidation and total surface area values of the pyrite concentrates oxidised at different time intervals.

7.4.3 XPS analysis

The XPS measured atomic concentrations of iron, sulfur and oxygen on the pyrite surfaces are given in Table 7.16.

Table 7.16: Normalised surface concentrations of O, Fe, S^{2-} and SO_4^{2-} on the surfaces of reground pyrite concentrate before and after oxidation. *Unknown=cannot be detected

Samples	Atomic concentration of elements (at. %)			
	O	**Fe**	**S^{2-}**	**SO_4^{2-}**
Control Sample	25.2	44.2	68.0	31.9
15 mins	57.2	8.5	28.7	71.3
30 mins	92.3	1.2	7.6	92.4
45 mins	Unknown*	10.115e-006	Unknown*	Unknown*
60 mins	Unknown*	Unknown*	Unknown*	Unknown*

The concentration of oxygen increases as the residence time of nitric acid oxidation increases suggesting the formation of more oxidised species. However, the species is undetectable beyond the 30 minutes oxidation stage and this could be attributed to the sensitivity of the XPS technique to measure first 20 superficial layers. A similar trend is observed with the sulfide sulfur species in the pristine sample corresponding to the lower surface oxidation. However, as the extent of oxidation increases sulfide sulfur oxidation occurs resulting in lower concentrations of the hydrophobic sulfide sulfur and relative increase in hydrophilic sulfate species as shown in equation 42.

$$2FeS_2 + 8\,HNO_3 + H_2O \xrightarrow{\text{yields}} Fe_2(SO_4)_3 + 2H_2SO_4 + 2S + 2\,H_2O \quad \ldots\ldots 42$$

In this study, the sulfur oxidation species on mineral surfaces were investigated by S 2p XPS spectra as shown in Figure 7.29. Due to the proximity of the two peaks observed at 160.9 eV and 161.5 eV they could not be decoupled and hence were attributed to S^{2-} from the pyrite (Chen et al., 2013, Smart, 1991). No iron peaks are shown in this case because no discrepancies are observed with sulfur signals and the decreasing sulfide sulfur trend is obvious compared to the previous study shown in this chapter (*without regrinding*). The complementary approach of comparing the "normalised surface concentrations" (*atomic %*) of the sulfide and sulfate species of each oxidation stage has still been followed as shown in Table 7.16.

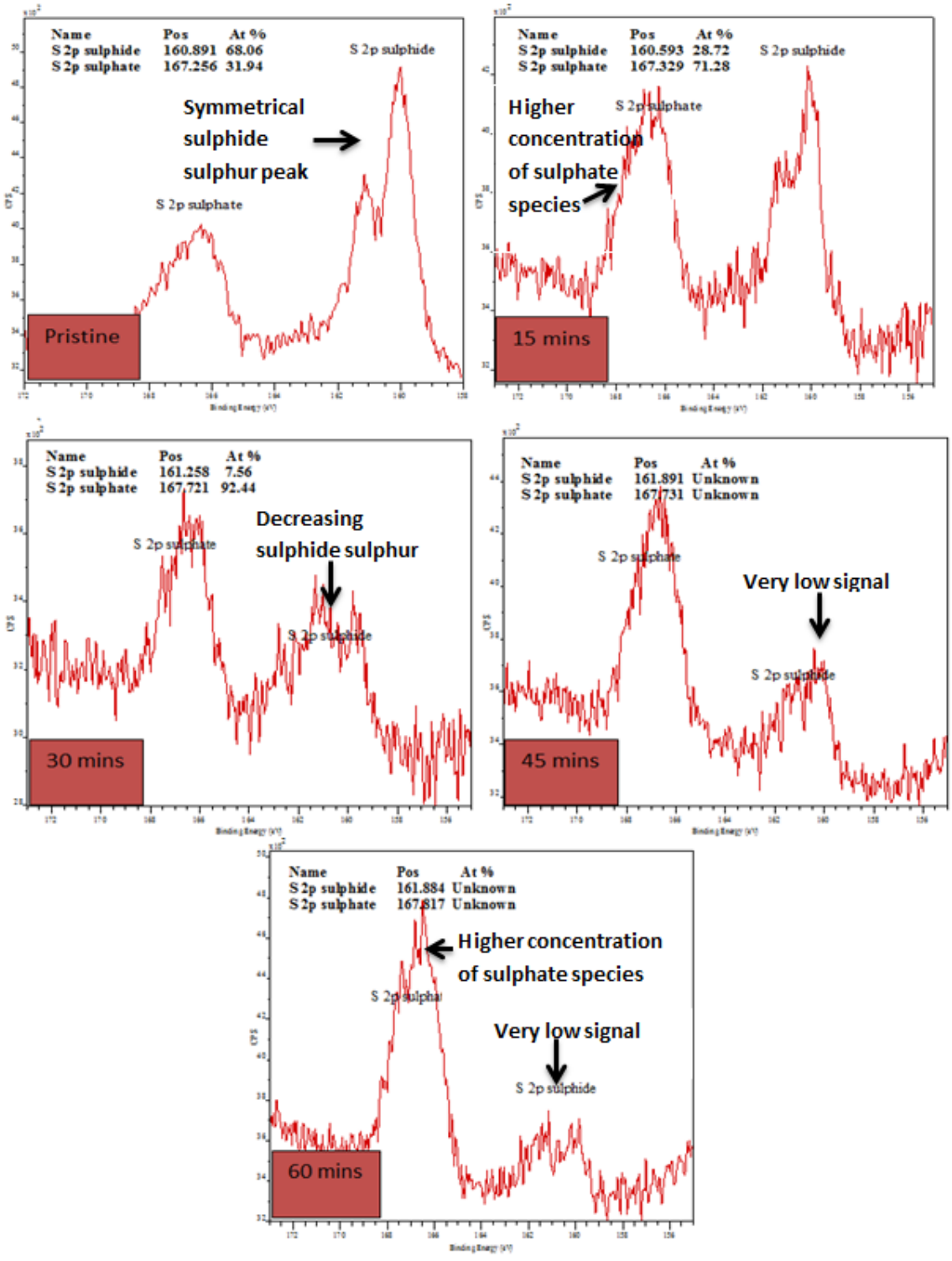

Figure 7.29: S (2p) spectra of reground oxidised samples. The 15 minutes oxidised sample shows a higher percentage of sulfate species signifying the effect of pyrite oxidation. This trend continues with 30 minutes oxidation stage. As the oxidation reaction advances, the XPS system is unable to quantify the sulfide sulfur species due to increased presence of iron and sulfate precipitates.

7.4.4 Direct cleaner flotation

Similar to the previous study (*without regrinding*), the effect of oxidation on pyrite was tested by conducting one-step cleaner flotation tests at pH 11. The metallurgical responses in terms of gold grade, sulfide sulfur grade and Au:S values are shown in Table 7.17.

Table 7.17: One stage cleaner flotation data of Au:S values (*Gold*) of reground pristine and oxidised samples as a function of SOx values (*Blue*)

Oxidation			**Metallurgical Response**				
Treatment	**Oxidation Time (*minutes*)**	**SOx (*%*)**	**Gold Recovery (*%*)**	**Gold Grade (*g/t*)**	**Sulfide Sulfur Recovery (*%*)**	**Sulfide Sulfur Grade (*%*)**	**Au:S Ratio**
None	0	0	90.0	6.7	94.0	23.8	**0.28**
HNO_3	15	25.7	78.1	7.4	80.2	25.1	**0.29**
HNO_3	30	37.7	81.4	7.3	86.9	28.3	**0.26**
HNO_3	45	43.4	59.5	7.3	43.5	25.3	**0.29**
HNO_3	60	47.1	60.6	10.4	53.3	36.3	**0.29**

This leads to the conclusion that particle size from regrinding plays a pivotal role in pyrite and gold flotation. As seen with the control sample, the regrinding process may liberate the gold from pyrite as seen from better gold recovery with reground samples as opposed to no regrinding (*90% vs. 87.5% gold recovery from Table 7.5*). However, there is also an increase in sulfide sulfur recovery (*94% vs. 87.1% from Table 7.5*). This is because depression of sulfides can be challenging because the probabilities of newly exposed pyrite surfaces being activated by copper ions are greater in contrast to no regrinding (Chen et al., 2013).

However, with oxidation, the scenario with gold and sulfur recovery is different compared to the pristine sample. The Au:S value of the control sample is very close to the previous study at 0.28, however, no significant upgrade is observed with oxidation. Although regrinding the pyrite concentrate enhances the oxidation process due to the increase in mineral surface area, these accelerated oxidation rates do not improve the Au:S value significantly. This is because accelerated oxidation rates can completely destroy the pyrite surface resulting in no preferential oxidation of the

gold-rich pyrite types relative to the low gold pyrite types and thereby no major differences in their hydrophobic states. Since the effect of regrinding did not have much of a positive effect on the Au:S ratio compared to tests with just chemical oxidation and no mechanical reduction, no further tests (*ToF-SIMS, bottle roll tests*) were done on the oxidised samples. Sample shortage, time constraints and budget restrictions were other important factors which limited further investigations of the reground samples. The typical mass and metal balances for regrinding and nitric acid oxidation tests (*15 minutes oxidation stage*) are included for clarity in Figure 7.30. Appendix section 4.5 gives a detailed metallurgical accounting for other oxidation stages.

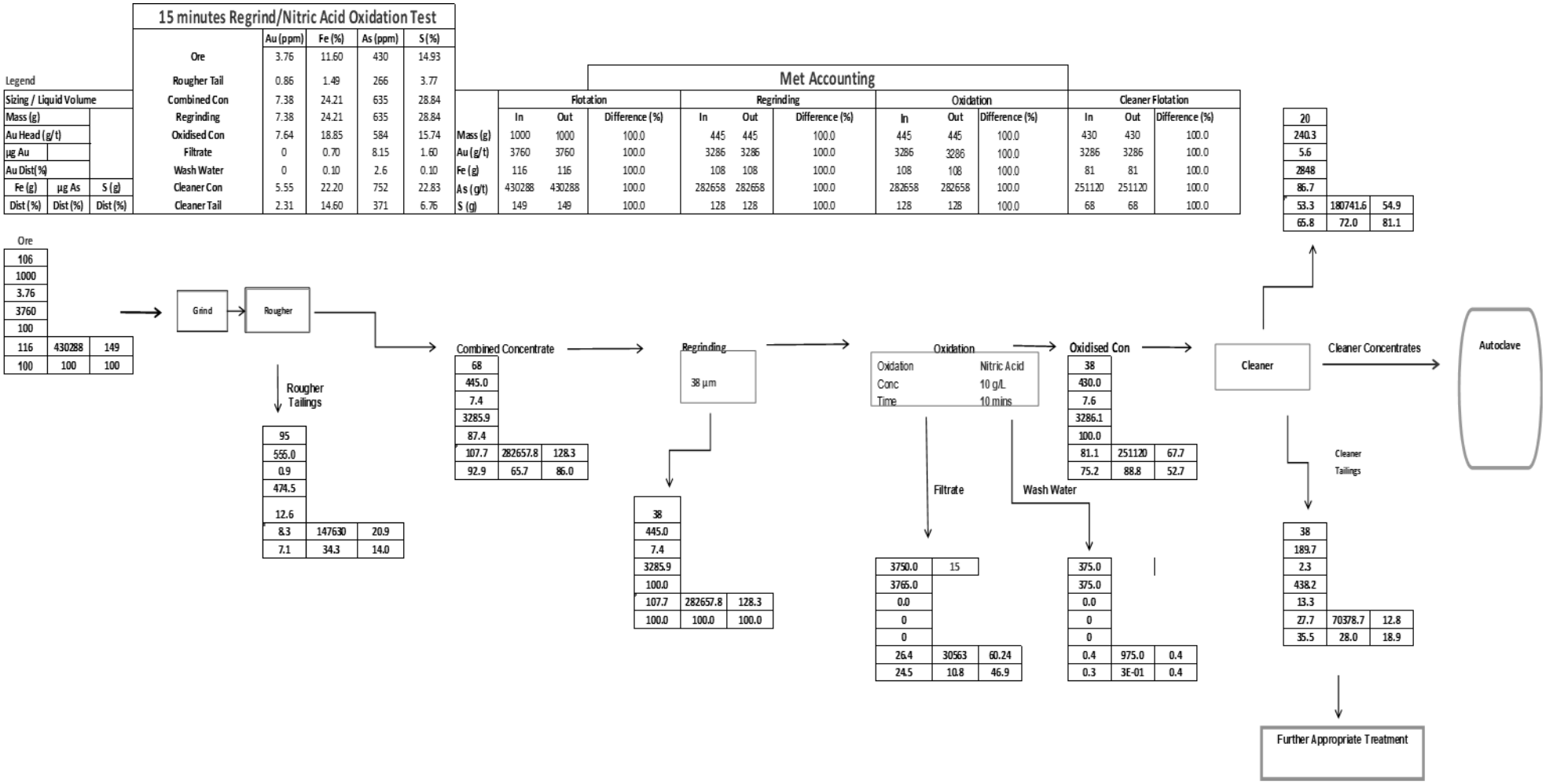

Figure 7. 30: Metallurgical Accounting of the Nitric Acid Oxidation of Reground Pyrite Concentrate

The distribution values are for three steps: Step 1: Rougher Tail + Combined Concentrate

Step 2: Filtrate + Wash Water + Oxidised Concentrate

Step 3: Cleaner concentrate + Cleaner Tail

7.5 Conclusions

The following conclusions can be drawn:

- ✓ The sole objective was to produce a low sulfide sulfur and relatively high gold concentrate as an autoclave feed by oxidising the bulk of the sulfide sulfur to overcome the fixed sulfide oxidation capacity constraint of the Lihir autoclave.

- ✓ This has been successfully achieved by means of a preparation step, with its origins from hydrometallurgical practice, by modifying the flotation response of gold-rich pyrite and low gold pyrite resulting in an upgrade of the Au:S value of the final flotation concentrate.

- ✓ Nitric acid oxidising conditions have been productively established to oxidise one type of pyrite relative to the other type and separate them in a following one stage cleaner flotation process using standard Lihir reagents (*PAX as the collector*).

- ✓ The high Au:S values of the oxidised concentrates compared to the corresponding tails established definite evidence that the high gold pyrite was floating and the low gold pyrite was depressed at pH 11.

- ✓ The difference in the Au:S values observed with different stages of oxidation revealed that the oxidation level for separating one type of pyrite from another is sensitive to oxidation level.

- ✓ Operating Eh, pH and the extent of oxidation (*SOx*) are therefore the key variables in the preferential oxidation and separation of high gold pyrite from low-grade pyrite. Thus for a pH and ORP range of 1.26 and 0.55 V (*vs. SHE*) respectively, a 144% increase in Au:S value (*0.66*) was obtained with a SOx value of 25% for the 60 minutes oxidised concentrate.

- ✓ Accelerated oxidation rates due to mechanical reduction (*particle size reduction*) did not differentiate the high gold and low gold pyrite resulting in no significant upgrade of Au:S ratios compared to normal concentrates that were oxidised without regrinding. This is because the enhanced oxidation conditions completely destroyed the pyrite surface resulting in no preferential oxidation of low gold and high gold pyrite types and separation in a following cleaner flotation process.

7.6 Bibliography

ADAMS, M. 2005. Advances in gold ore processing. *Elsevier Science*. ISBN: 0-444-51730-8.

BUCKLEY, A. & WOODS, R. 1987. The surface oxidation of pyrite. *Applied Surface Science,* 27**,** 437-452.

BUCKLEY, A. N. & WOODS, R. 1984. An X-ray photoelectron spectroscopic study of the oxidation of chalcopyrite. *Australian Journal of Chemistry,* 37**,** 2403-2413.

CHANDRA, A. & GERSON, A. 2009. A review of the fundamental studies of the copper activation mechanisms for the selective flotation of the sulfide minerals, sphalerite and pyrite. *Advances in Colloid and Interface Science,* 145**,** 97-110.

CHEN, X., PENG, Y. & BRADSHAW, D. 2013. Effect of regrinding conditions on pyrite flotation in the presence of copper ions. *International journal of mineral processing,* 125**,** 129-136.

CHEN, X., PENG, Y. & BRADSHAW, D. 2014. The separation of chalcopyrite and chalcocite from pyrite in cleaner flotation after regrinding. *Minerals Engineering,* 58**,** 64-72.

CHINCHÓN-PAYÁ, S., AGUADO, A. & CHINCHÓN, S. 2012. A comparative investigation of the degradation of pyrite and pyrrhotite under simulated laboratory conditions. *Engineering Geology,* 127**,** 75-80.

COLLINS, M., BEREZOWSKY, R., VARDILL, W., KETCHAM, V. & STOJSIC, A. The Lihir Gold project: pressure oxidation process development. IV International Symposium on Hydrometallurgy, Salt Lake City, UT (August 1993), 1993.

DICHMANN, T. K. & FINCH, J. 2001. The role of copper ions in sphalerite-pyrite flotation selectivity. *Minerals Engineering,* 14**,** 217-225.

EGGLESTON, C. M., EHRHARDT, J.-J. & STUMM, W. 1996. Surface structural controls on pyrite oxidation kinetics: An XPS-UPS, STM, and modelling study. *American Mineralogist,* 81**,** 1036-1056.

FINKELSTEIN, N. 1997. The activation of sulfide minerals for flotation: a review. *International journal of mineral processing,* 52**,** 81-120.

FLATT, J. & WOODS, R. 1995. A Voltammetric investigation of the oxidation of pyrite in nitric acid solutions: relation to the treatment of refractory gold ores. *Journal of applied electrochemistry,* 25**,** 852-856.

FLEMING, C. 1992. Hydrometallurgy of precious metals recovery. *Hydrometallurgy,* 30**,** 127-162.

GAO, G., LI, D., ZHOU, Y., SUN, X. & SUN, W. 2009. Kinetics of high-sulfur and high-arsenic Refractory gold concentrate oxidation by dilute nitric acid under mild conditions. *Minerals Engineering,* 22**,** 111-115.

JIANG, C., WANG, X., PAREKH, B. & LEONARD, J. 1998. The surface and solution chemistry of pyrite flotation with xanthate in the presence of iron ions. *Colloids and Surfaces A: Physicochemical and Engineering Aspects,* 136**,** 51-62.

JOHN, J., JOHNSON, N., STEWART, K., TURNER, D. & BRADSHAW, D. A review of pretreatment methods to separate the different types of pyrites in gold processing. 5th World Gold 2013 Conference, 2013. AusIMM: Australasian Institute of Mining and Metallurgy, 347-355.

KETCHAM, V., O'REILLY, J. & VARDILL, W. 1993. The Lihir gold project; Process plant design. *Minerals Engineering,* 6**,** 1037-1065.

KING, J. & KNIGHT, D. 1992. Autoclave operations at Porgera. *Hydrometallurgy,* 29**,** 493-511.

LA BROOY, S., LINGE, H. & WALKER, G. 1994. Review of gold extraction from ores. *Minerals Engineering,* 7**,** 1213-1241.

LEPPINEN, J. 1990. FTIR and flotation investigation of the adsorption of ethyl xanthate on activated and non-activated sulfide minerals. *International Journal of Mineral Processing,* 30**,** 245-263.

LEPPINEN, J., BASILIO, C. & YOON, R. 1988. FTIR study of thiocarbamate adsorption on sulfide minerals. *Colloids and surfaces,* 32**,** 113-125.

LI, D. 2009. Developments in the pretreatment of refractory gold minerals by nitric acid. *World Gold Conference 2009, The Southern African Institute of Mining and Metallurgy, 2009.*

LONG, H. & DIXON, D. G. 2004. Pressure oxidation of pyrite in sulfuric acid media: a kinetic study. *Hydrometallurgy,* 73**,** 335-349.

MARCHBANK, A. R., THOMAS, K. G., DREISINGER, D. & FLEMING, C. 1996. Gold recovery from refractory carbonaceous ores by pressure oxidation and thiosulfate leaching. U.S. Patent No. 5,536,297. Washington, DC: U.S. Patent and Trademark Office.

MARSDEN, J. & HOUSE, I. 2006. *The chemistry of gold extraction*, SME. Littleton, Colorado, USA ISBN-13: 978-0-87335-240-6 ISBN-10: 0-87335-240-8.

MASON, P. 1992. Examining the economics of some pressure oxidation process options. *Hydrometallurgy,* 29**,** 479-492.

MONTE, M., LINS, F. & OLIVEIRA, J. 1997. Selective flotation of gold from pyrite under oxidising conditions. *International Journal of Mineral Processing,* 51**,** 255-267.

MONTE, M., LINS, F. & OLIVEIRA, J. Adsorption of thiol compounds on gold and pyrite and its influence in their selective flotation. Proceedings of the XXI International Mineral Processing Congress, Rome, vol. B, 2000. 23-28.

NAZARI, A. M., RADZINSKI, R., & GHAHREMAN, A. 2016. Review of arsenic metallurgy: Treatment of arsenical minerals and the immobilization of arsenic. *Hydrometallurgy*.

NEWELL, A., BRADSHAW, D. & HARRIS, P. 2006. The effect of heavy oxidation upon flotation and potential remedies for Merensky type sulfides. *Minerals Engineering,* 19**,** 675-686.

OWUSU, C., E ABREU, S. B., SKINNER, W., ADDAI-MENSAH, J. & ZANIN, M. 2014. The influence of pyrite content on the flotation of chalcopyrite/pyrite mixtures. *Minerals Engineering,* 55**,** 87-95.

PENG, Y. & GRANO, S. 2010. Effect of iron contamination from grinding media on the flotation of sulfide minerals of different particle size. *International Journal of Mineral Processing,* 97**,** 1-6.

PIETRZAK, R., GRZYBEK, T. & WACHOWSKA, H. 2007. XPS study of pyrite-free coals subjected to different oxidising agents. *Fuel,* 86**,** 2616-2624.

RANKIN, W. J. 2013. *New flagship AusIMM Monograph: Australasian mining and metallurgical operating practices*. (The Sir Maurice Mawby Memorial Volume), Third Edition.

SENIOR, G. & TRAHAR, W. 1991. The influence of metal hydroxides and collector on the flotation of chalcopyrite. *International journal of mineral processing,* 33**,** 321-341.

SHEN, W. Z., FORNASIERO, D. & RALSTON, J. 2001. Flotation of sphalerite and pyrite in the presence of sodium sulfide. *International Journal of Mineral Processing,* 63**,** 17-28.

SMART, R. S. C. 1991. Surface layers in base metal sulfide flotation. *Minerals Engineering,* 4**,** 891-909.

SOKIĆ, M. D., MARKOVIĆ, B. & ŽIVKOVIĆ, D. 2009. Kinetics of chalcopyrite leaching by sodium nitrate in sulfuric acid. *Hydrometallurgy,* 95**,** 273-279.

THOMAS, K. G. 1991. Alkaline and acidic autoclaving of refractory gold ores. *JOM,* 43**,** 16-19.

THOMAS, K. G., PIETERSE, H. J., BREWER, R. E. & FRASER, K. S. 1991. Process for recovery of gold from refractory ores. U.S. Patent No 5071477 A. Washington, DC: U.S. Patent and Trademark Office.

VIZCARRA, T., HARMER, S., WIGHTMAN, E., JOHNSON, N. & MANLAPIG, E. 2011. The influence of particle shape properties and associated surface chemistry on the flotation kinetics of chalcopyrite. *Minerals Engineering,* 24**,** 807-816.

WILLS, B. A. 2011. *Wills' Mineral Processing Technology: an introduction to the practical aspects of ore treatment and mineral recovery*, Butterworth-Heinemann.

YE, X., GREDELJ, S., SKINNER, W. & GRANO, S. R. 2010. Regrinding sulfide minerals—Breakage mechanisms in milling and their influence on surface properties and flotation behaviour. *Powder Technology,* 203**,** 133-147.

ZACHWIEJA, J. B., MCCARRON, J. J., WALKER, G. W. & BUCKLEY, A. N. 1989. Correlation between the surface composition and collectorless flotation of chalcopyrite. *Journal of colloid and interface science,* 132**,** 462-468.

ZHANG, Q., XU, Z., BOZKURT, V. & FINCH, J. 1997. Pyrite flotation in the presence of metal ions and sphalerite. *International Journal of Mineral Processing*, 52**,** 187-201.

CHAPTER 8

Sulfuric Acid Treatment of Iron Sulfides to Modify the Au:S Ratio of a Flotation Concentrate

As mentioned in Chapter 2, the PARTOX Process is a selective partial oxidation process that was developed to extract valuable metals from pyrite (*and other sulfide minerals*) as per the following equation:

Pyrite: $FeS_2 + H_2SO_4 + 0.5O_2 \xrightarrow{\text{yields}} FeSO_4 + 2S + H_2O$ ……43

The PARTOX Process (2005) selectively oxidises arsenian pyrite to give reasonable gold recoveries by cyanidation without having to oxidise all the pyrite. This selective treatment is a better representation of what is being discussed in this Chapter. Therefore, this chapter is an attempt to establish the effectiveness of a sulfuric acid treatment step, with its origins from hydrometallurgical practice, to modify the flotation response of gold-rich pyrite and low gold pyrite so that the Au:S ratio of the final flotation concentrate can be upgraded.

Keywords: Refractory ore, Sulfide minerals, Gold to Sulfur ratio, Pyrite, Sulfuric Acid, Flotation, Image processing

8. Introduction

In this test work, sulfuric acid was the preferred choice as the conditioning agent for surface modification. This is because traditionally pyrite has been one of the raw materials for sulfuric acid production. About half of the sulfuric acid produced worldwide is from sulfur and one-third from pyrite (Chepushtanova and Luganov, 2007). Therefore, considering that the Lihir mineral deposit is rich in sulfur containing a wide range of pyrite types, it would be preferable from an economic, logistical and operating point of view to select an acidic agent that can be generated onsite. Sulfuric acid is not an oxidising acid *per se* (*except at very high concentrations*) and it is the oxygen and ferric ions that are the usual oxidants for sulfides in acid sulfate media as shown in equations 44 to 46.

$$FeS_2 + \frac{7}{2}O_2 + H_2O \xrightarrow{\text{yields}} Fe^{2+} + 2SO_4^{2-} + 2H^+ \quad \ldots\ldots 44$$

$$Fe^{2+} + \frac{1}{4}O_2 + H^+ \xrightarrow{\text{yields}} Fe^{3+} + \frac{1}{2}H_2O \quad \ldots\ldots 45$$

$$FeS_2 + 14Fe^{3+} + 8H_2O \xrightarrow{\text{yields}} 15Fe^{2+} + 2SO_4^{2-} + 16H^+ \quad \ldots\ldots 46$$

8.2. Results and Discussion

8.2.1 Back-Scattered Electron Imaging

To demonstrate the effect of sulfuric acid on the pyrite texture, BSE images of the control and conditioned samples were collected. For this purpose, Mineral Liberation Analysis (*MLA*) blocks were made from a control and etched (*conditioned/treated/oxidised*) pyrite concentrate and a JKMRC-FEI Mineral Liberation Analyser was used to generate the BSE images as shown in Figures 8.1 to 8.5. The BSE images were then processed using ImageJ software to highlight the arsenic zones in pyrite (*highlighted in red*).

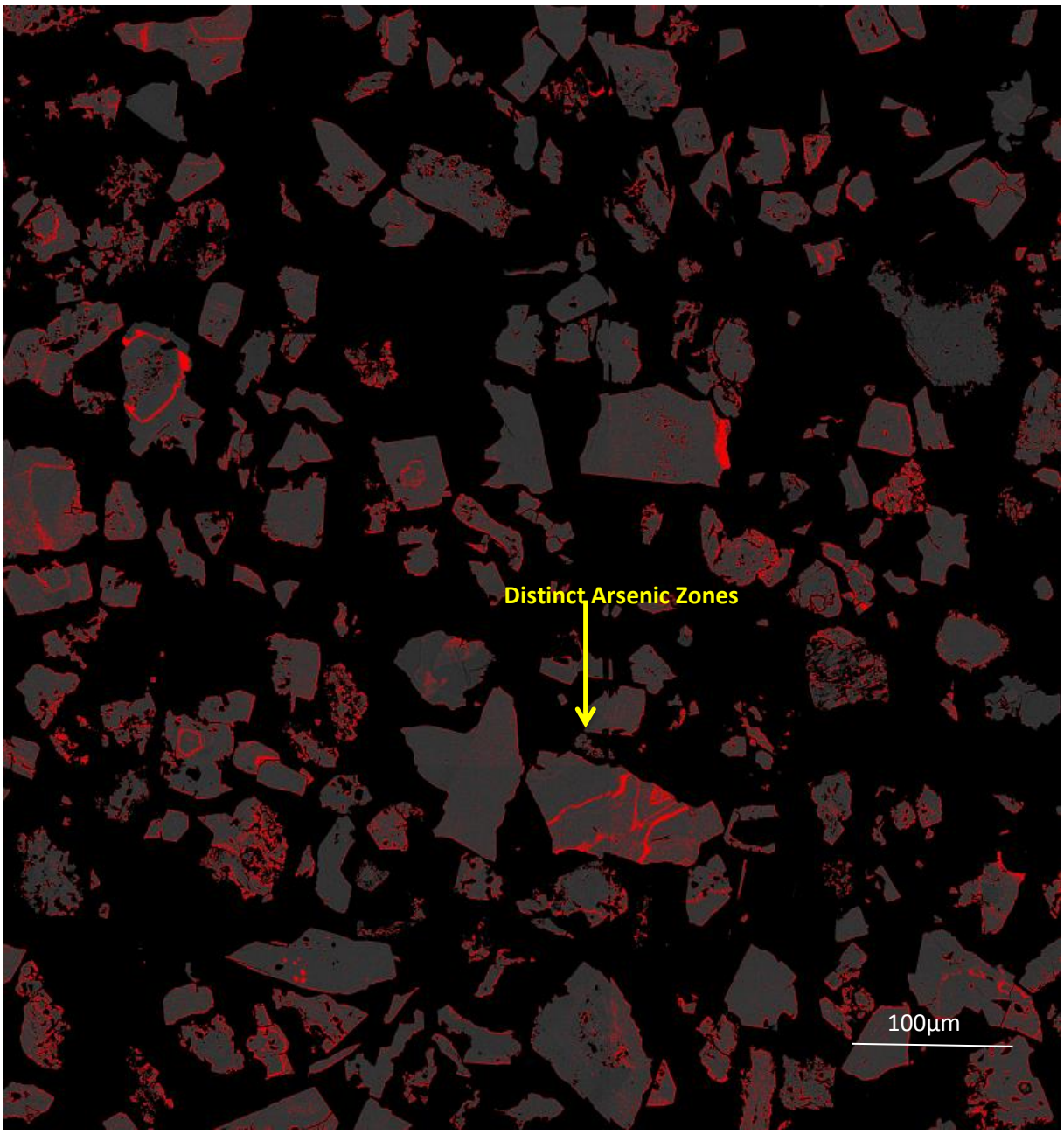

Figure 8. 1: BSE image (*after ImageJ thresholding*) of the pristine (*unetched*) concentrate

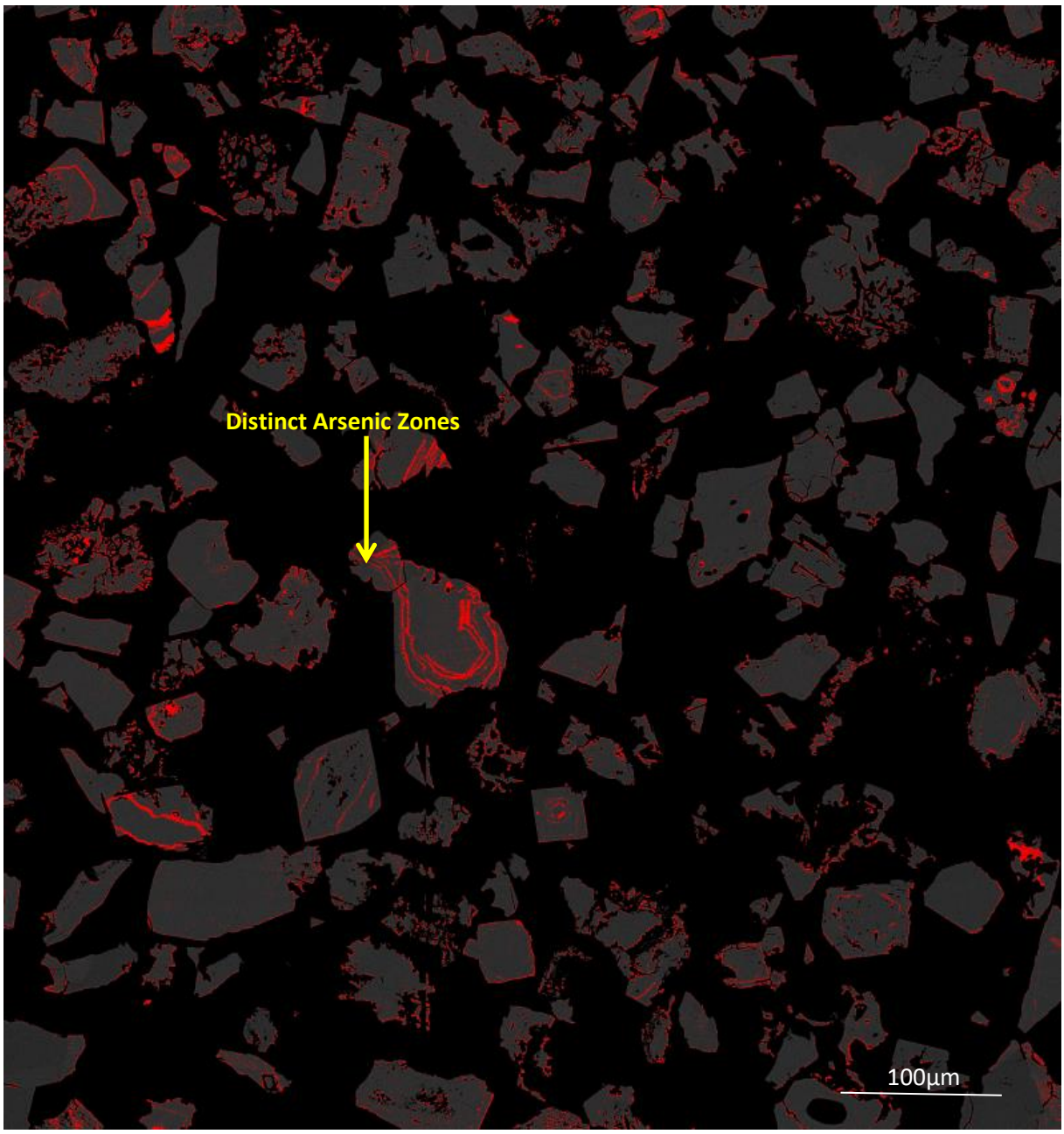

Figure 8. 2: BSE image (*after ImageJ thresholding*) of the 10 minutes conditioned concentrate

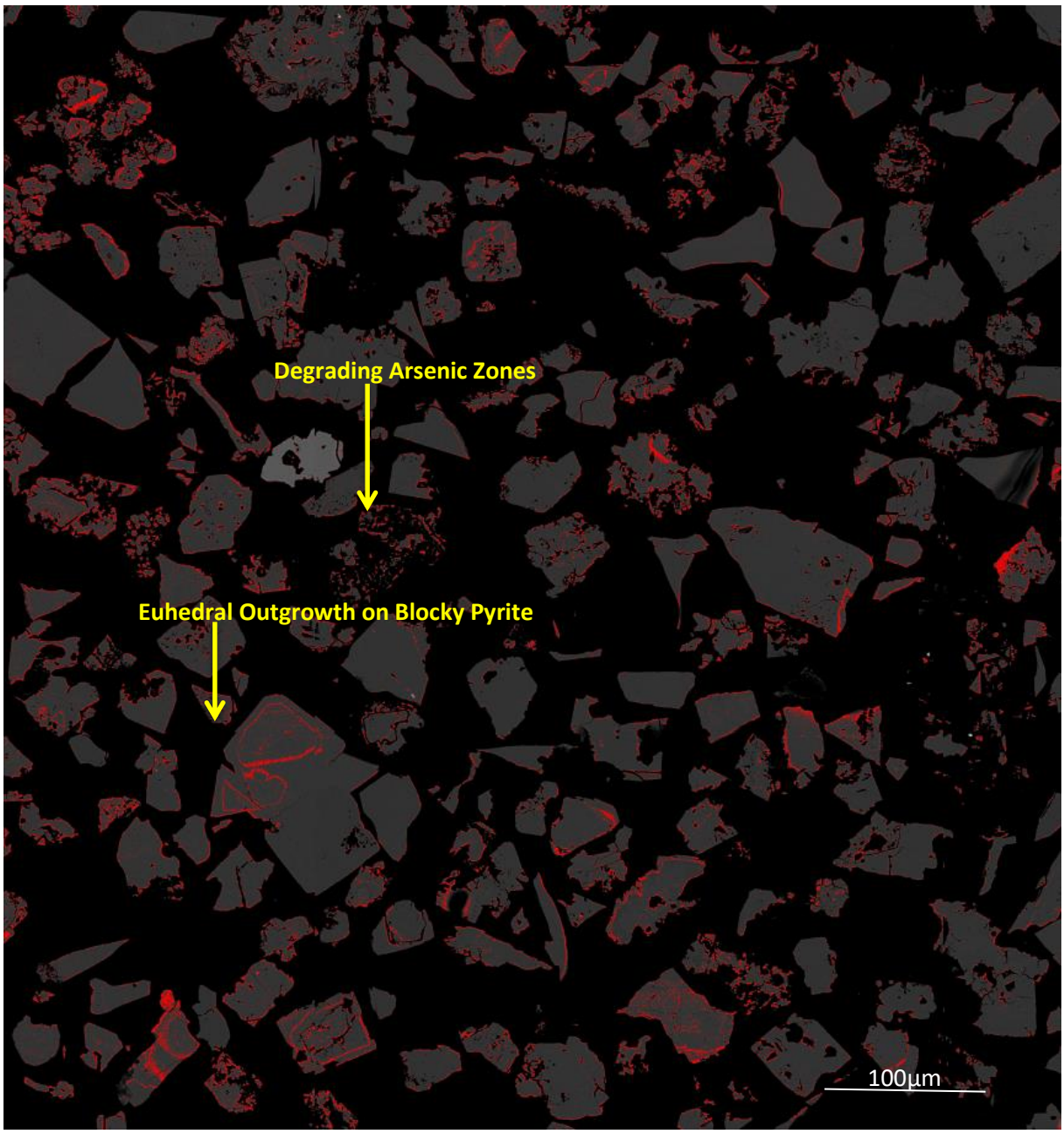

Figure 8. 3: BSE image (*after ImageJ thresholding*) of the 20 minutes conditioned concentrate

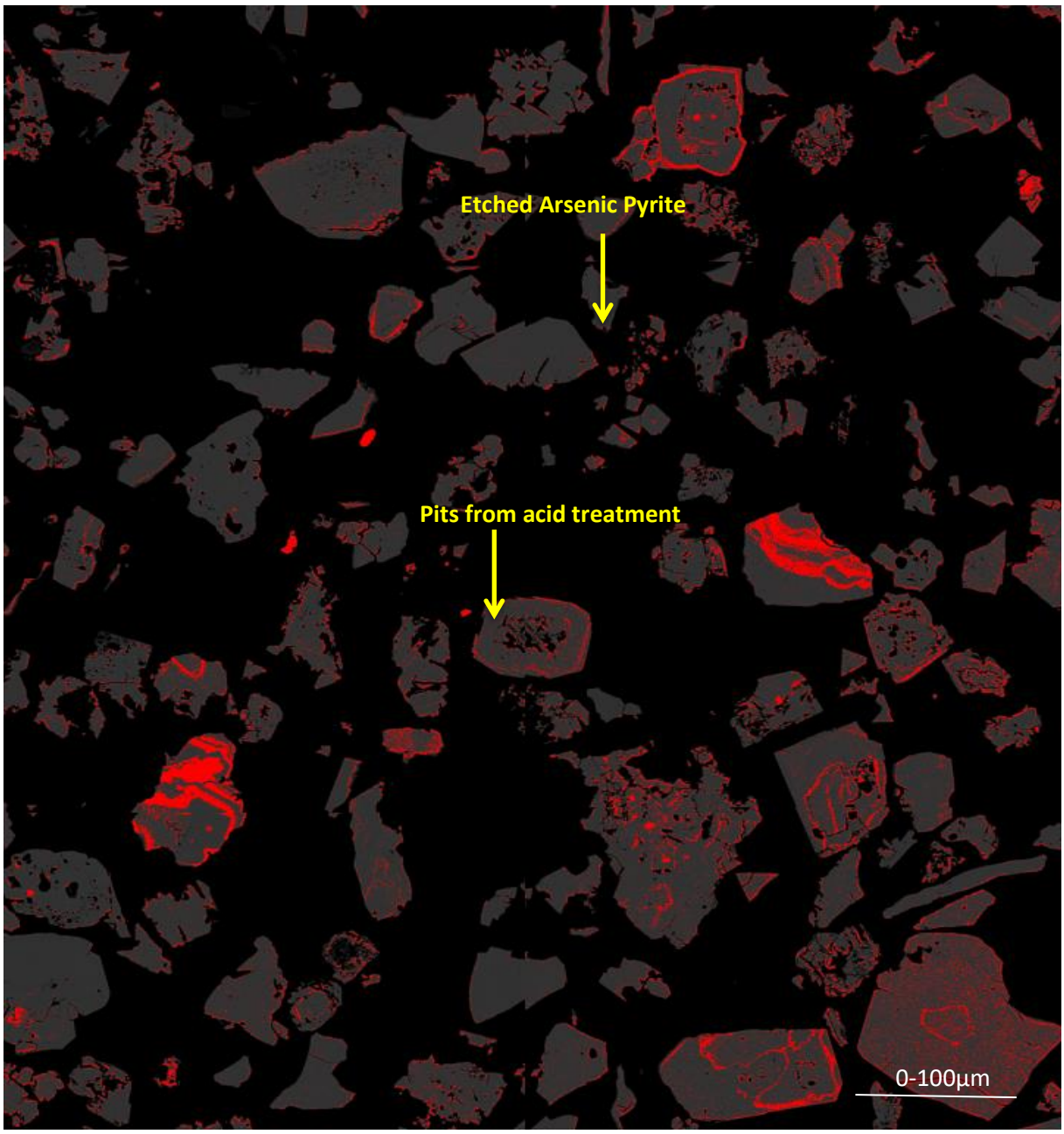

Figure 8. 4: BSE image (*after ImageJ thresholding*) of the 30 minutes conditioned concentrate

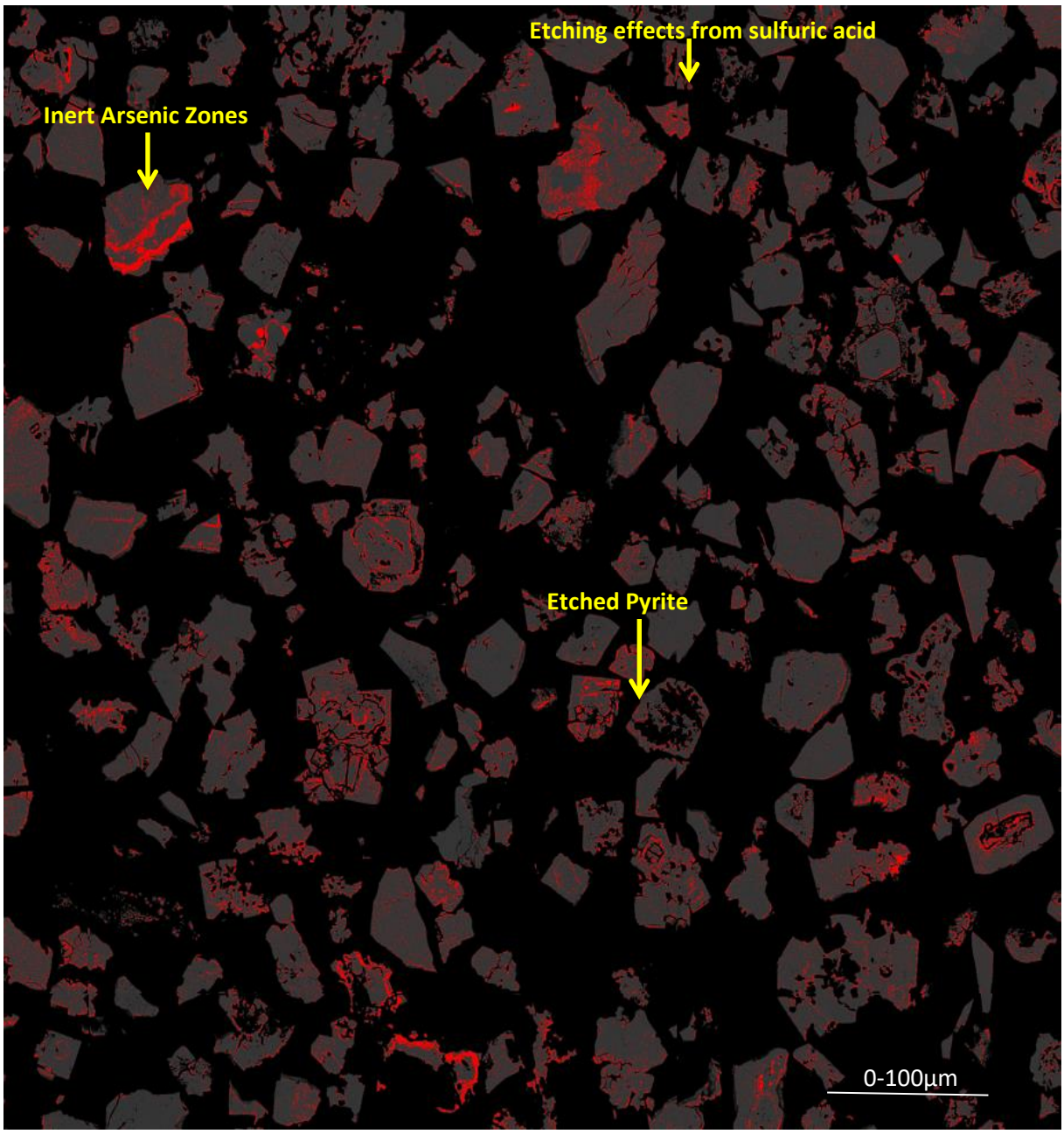

Figure 8. 5: BSE image (*after ImageJ thresholding*) of the 40 minutes conditioned concentrate

From the BSE images, the differences among the different samples are subtle suggesting that sulfuric acid treatment did not char the pyrite surface completely. Visible differences become more pronounced in the 40 minutes conditioning stage (*Figure 8.5*) with the appearance of more surface irregularities and pits due to the etching effects of sulfuric acid. This aligns entirely with the aim of the work to differentially modify the surface of the various types of pyrite and not completely annihilate the whole pyrite matrix. There is no published information on the application of the MLA system and image processing software (*ImageJ)* to understand the effect of acid treatment on arsenic-rich minerals and therefore this investigation holds significant potential for future studies to understand the effect of acid treatment on mineral texture.

8.2.2 Sulfide Sulfur Oxidation (SOx)

As mentioned earlier in Chapter 7, the intention is to identify an oxidation regime to preferentially oxidise the surface of gold-rich and low gold pyrite types. Therefore, the extent and effect of sulfuric acid treatment on the pyrite concentrate were confirmed by SOx, BET and XPS measurements prior to conducting any cleaner flotation tests. SOx analysis revealed that with increasing etching times, the extent of sulfide sulfur oxidation also increased from no oxidation for the control sample to 13.3% oxidation for the 40 minutes sample as shown Figure 8.6.

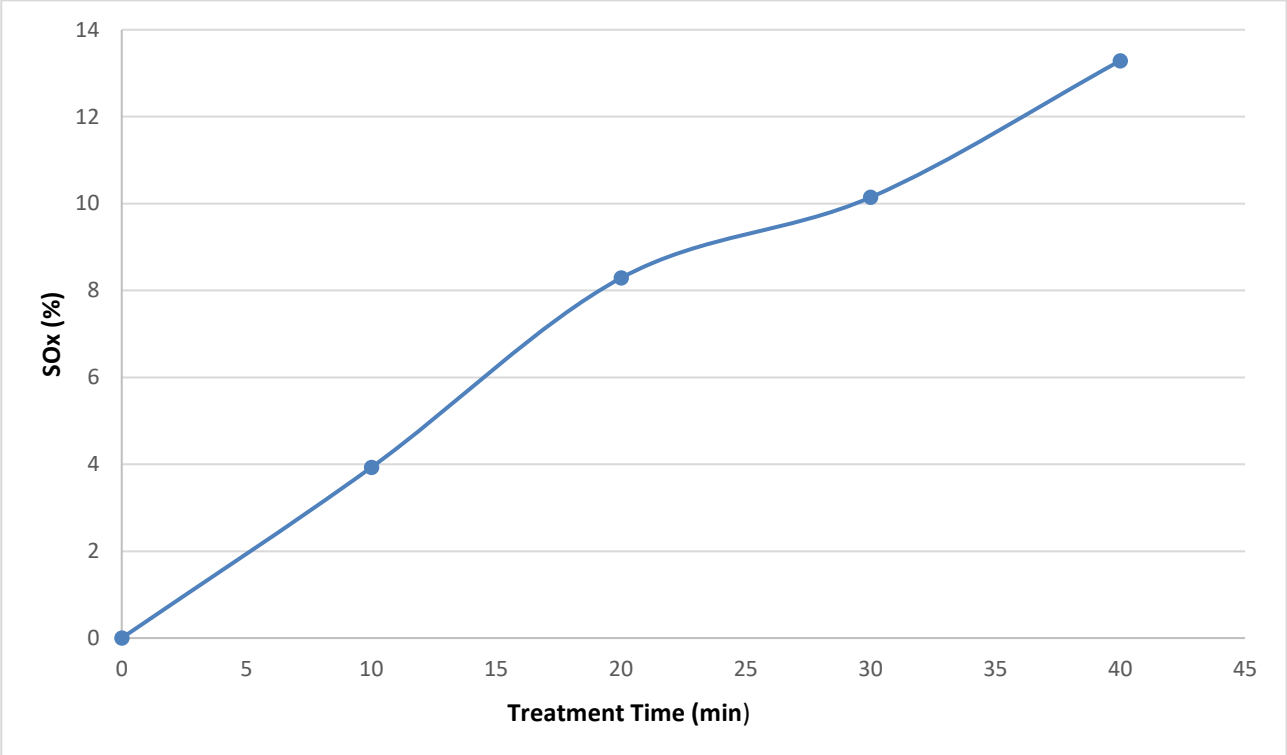

Figure 8. 6: Extent of sulfide oxidation at different time intervals

8.2.3 Surface Area Determination

Quantitative determination of surface area by BET measurements showed an increase from 1.6 m^2/g to 9.1 m^2/g for the control and etched samples respectively. A systemic dependence was observed between the extent of surface oxidation and the oxidation time (*also seen in Chapter 7*) as shown in Table 8.1 and Figure 8.7.

Table 8.1: BET measurements of the pristine* and conditioned samples. *= untreated/unetched/control sample

Sample	Conditioning Time (*minutes*)	BET Surface Area (m^2/g)
Pyrite Concentrate	Pristine*	1.6
	10	5.4
	20	7.5
	30	7.8
	40	9.1

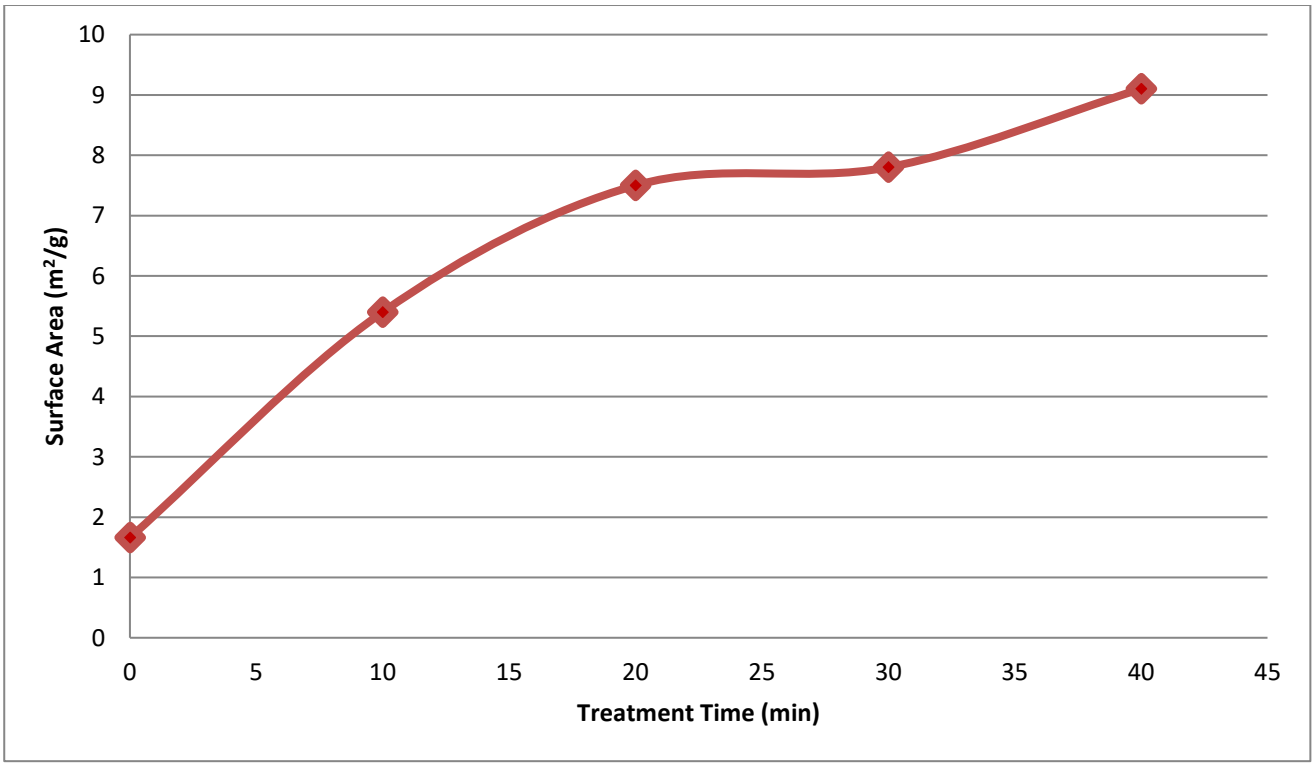

Figure 8. 7: Increase in surface area with increasing conditioning time

A coherent relationship was also indicated between the extent of etching and surface area as shown in Figure 8.8. This reflects the fact that the extent of sulfuric acid conditioning directly influences the surface area of the pyrite concentrate.

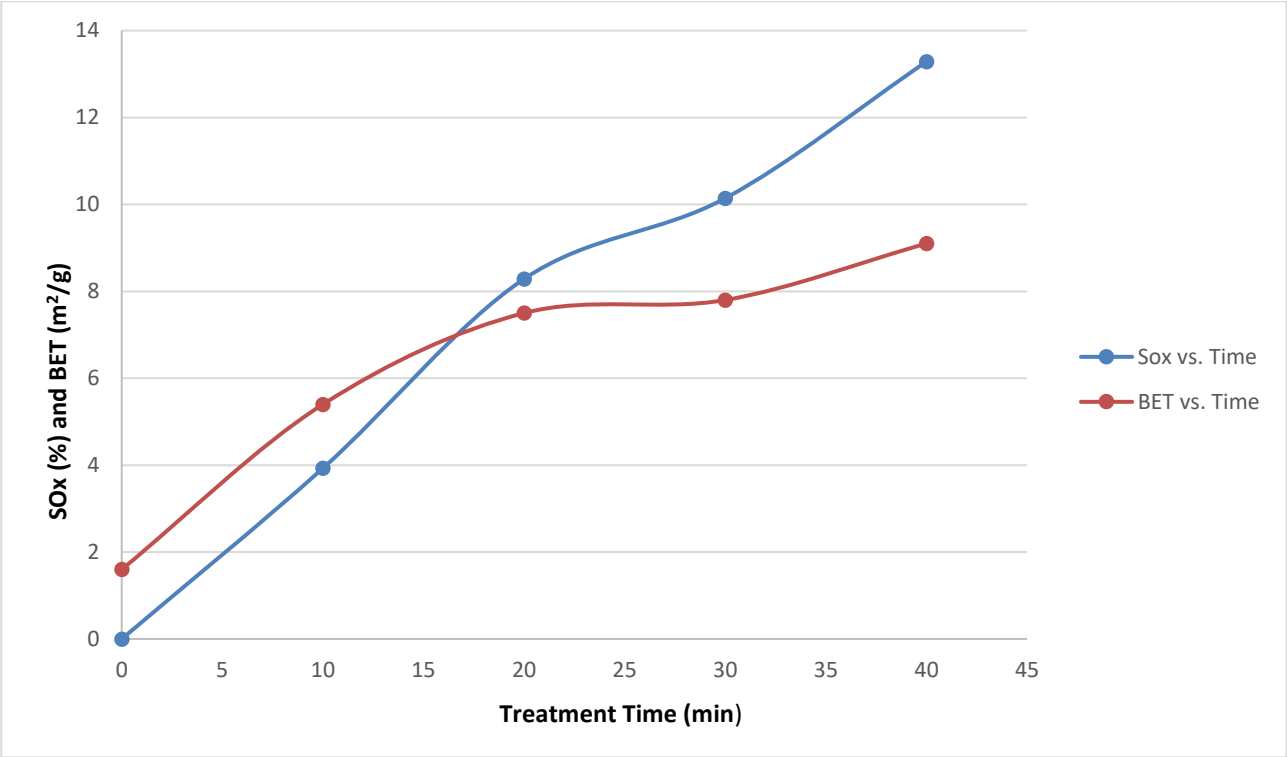

Figure 8. 8: Relationship between surface area and sulfide sulfur oxidation

8.2.4 X-Ray Photoelectron Spectroscopy

The effect of sulfuric acid treatment on the pyrite surface was investigated by the surface analytical technique, XPS. XPS S 2p peaks of pyrite have been analysed extensively and can be found in the literature; therefore, a minimum number of peaks were used to understand the trend. The Fe (2p) and S (2p) core level peaks from the pyrite surface before acid conditioning are shown in Figure 8.9. The doublet with the S 2p3/2 binding energy at 162.4 eV is attributed to S^{2-} from FeS_2 and is in good agreement with previously reported values (Buckley and Woods, 1987). The doublet at 162.8 eV is attributed to the formation of polysulfide (Buckley and Woods, 1984; Smart et al., 1999). The broad peak observed at 167.9 eV is attributed to the sulfate species (SO_4^{2-}). The binding energy of the Fe (2p) level of the pyrite sample was measured at 707.2 eV which is common for pyrite (Eggleston et al., 1996).

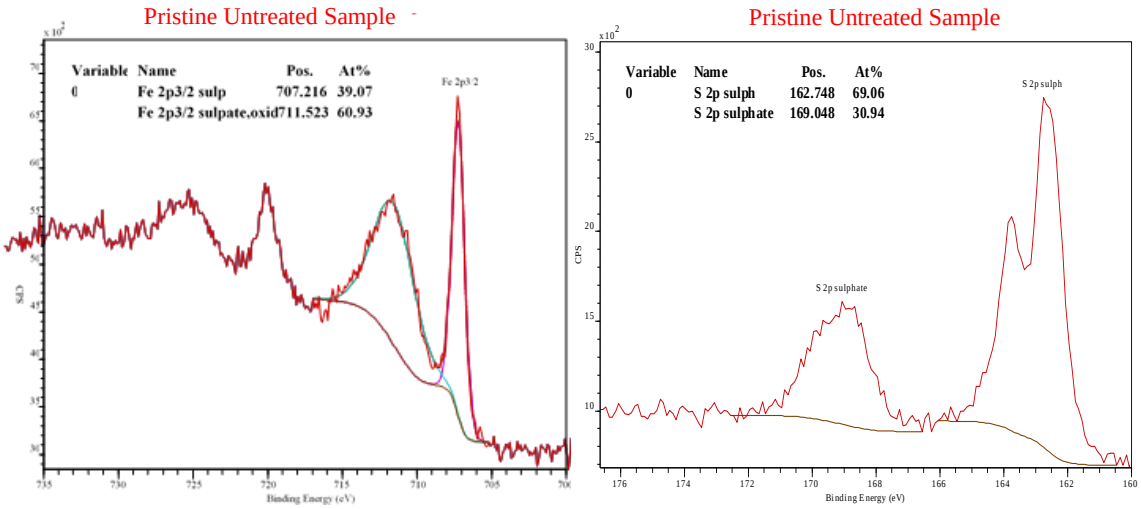

Figure 8. 9: Fe (2p) and S (2p) spectra of the pristine pyrite surface before conditioning

Comparing the pristine and conditioned samples, an increase in the surface concentration of iron hydroxides and sulfates after treatment in sulfuric acid solution is observed as shown in Figure 8.10. The Fe (2p) and S(2p) spectrum of the other etched samples (*Figures 8.11, 8.12 and 8.13*) also shows the presence of stronger Fe and sulfate peaks (*near 711 eV and 168.5 eV*).

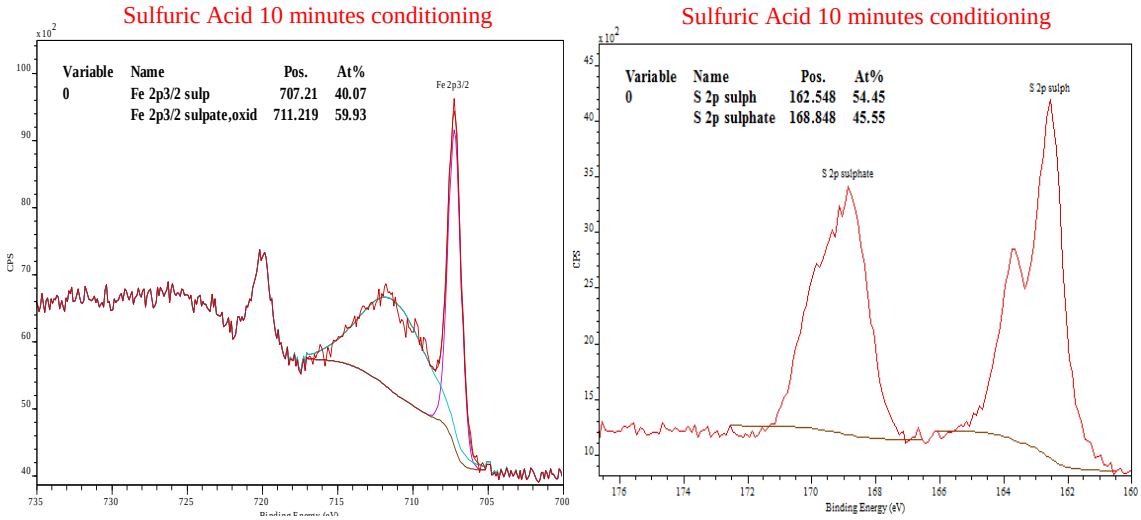

Figure 8. 10: Fe (2p) and S (2p) spectra of the pyrite surface after 10 minutes acid conditioning

The S(2p) spectrum for the 20 minutes acid treated sample (*Figure 8.11*) shows the presence of a weaker sulfide sulfur and sulfate peak in the range near 168.5 eV. However, comparing the Fe (2p) spectra for both conditioning times, it can be seen that a broader Fe peak is observed with the 20 minutes sample.

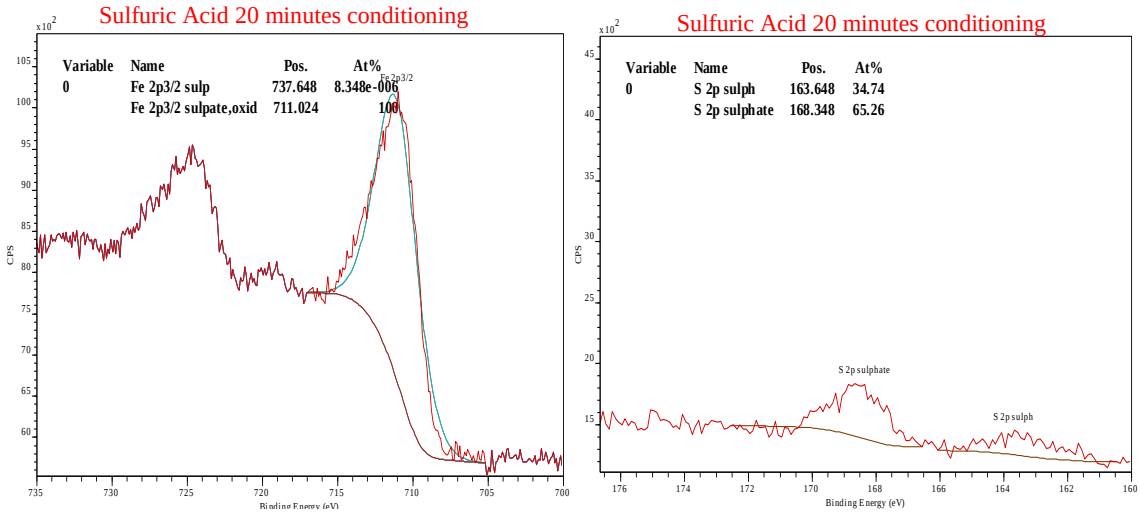

Figure 8. 11: Fe (2p) and S (2p) spectra of the pyrite surface after 20 minutes conditioning

This suggests that due to the higher extent of oxidation (*as an effect of sulfuric acid conditioning*), more iron hydroxide layers are formed on the pyrite surface as seen with nitric acid oxidation in the previous chapter. This is because higher concentrations of iron species (*due to pyrite oxidation*) forms a blanket of hydrophilic oxidation products on the mineral surface. This is evident from the XPS spectra of the 20 minutes oxidised sample (*Figure 8.11*) where a new spectral intensity at 711 eV is observed, indicating hydrated oxidised iron products (Pietrzak et al., 2007). The surface composition of pyrite surfaces after 30 minutes and 40 minutes conditioning was distinguishable compared to the pristine, 10 minutes and 20 minutes conditioned samples as shown in Figures 8.12 and 8.13.

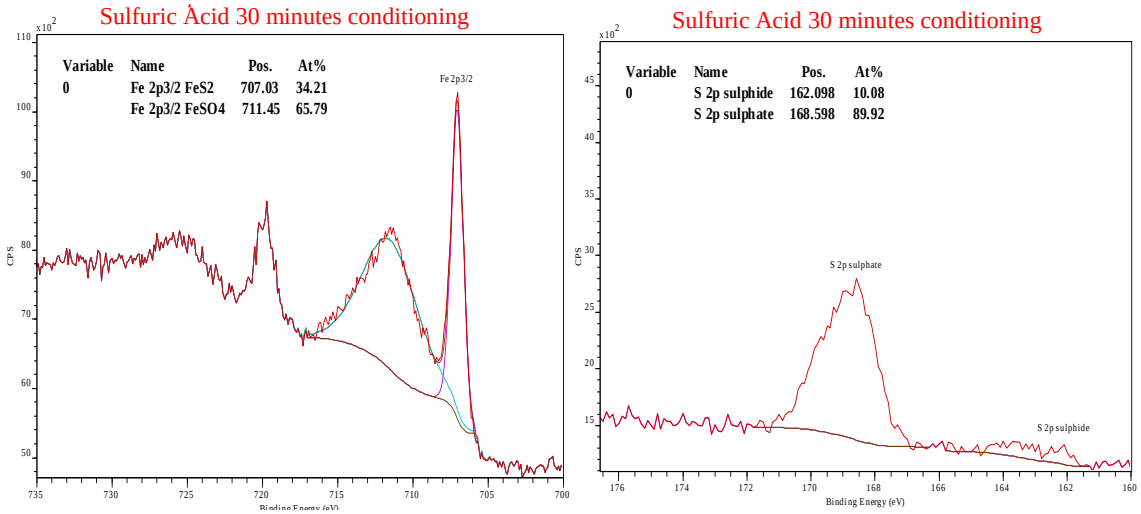

Figure 8. 12: Fe (2p) and S (2p) spectra of the pristine pyrite surface after 30 minutes conditioning

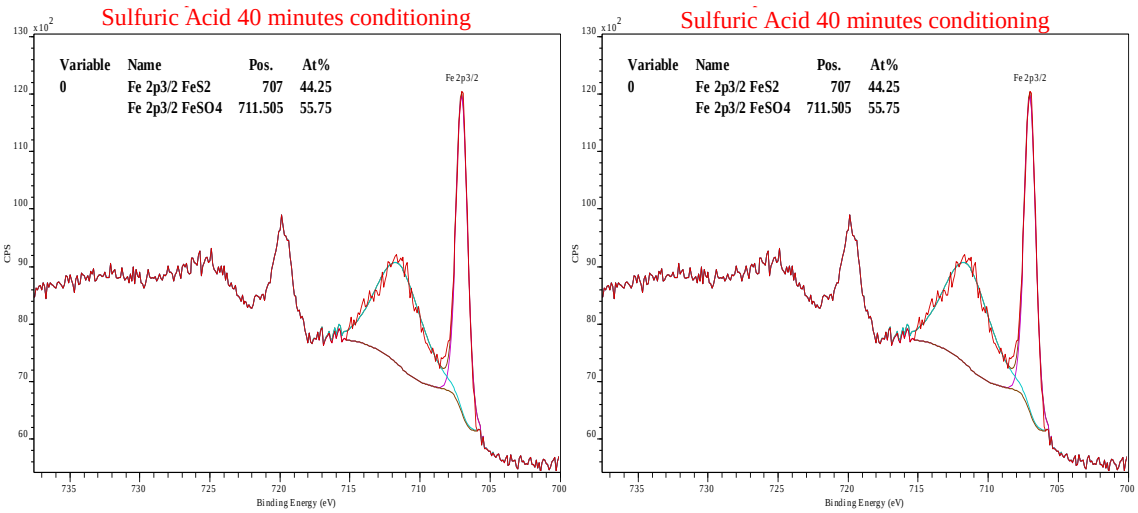

Figure 8. 13: Fe (2p) and S (2p) spectra of the pristine pyrite surface after 40 minutes conditioning

A noticeable difference was observed in the sulfide sulfur peak with the 30 minutes and 40 minutes samples compared to the control sample confirming the effect of sulfuric acid conditioning on sulfide sulfur. There was a significant change in the S (2p) spectrum with 30 minutes and 40 minutes acid etched samples indicating that the surface sulfur layer reconstructs to form separate unstable sulfur phases (*metal deficient sulfides and elemental sulfur*) with increasing extent of conditioning.

In all the acid treated samples, the ratio of sulfate to sulfur increased with increase in time suggesting that sulfuric acid conditioning had significantly altered the pyrite surface to have an impact on the metallurgical response. Although the presence of metal-deficient and polysulfide oxidation products provide sufficient surface hydrophobicity for high pyrite recovery, the presence of iron hydroxides and precipitates can hamper the flotation response and this had to be tested.

8.2.5 Gold and Sulfur Recovery

The impact of surface chemical alterations of pyrite on the flotation behaviour was investigated by one stage cleaner flotation step (*cleaner conditions mentioned in Chapter 3 and 7*). The metallurgical responses of the pristine and sulfuric acid treated concentrates are shown in Table 8.2. Although pyrite exhibits low floatability in an alkaline environment (Chen et al., 2014), the control sample yielded a relatively high gold and sulfur recoveries of 80.5% and 84.0 % respectively signifying that pyrite flotation was not depressed (*as seen previously in Chapter 7*).

Table 8.2: Direct cleaner flotation data of sulfuric acid conditioned concentrates at pH 11

	Oxidation			Metallurgical Response	
Test	**Pre-treatment**	**Conditioning Time (*minutes*)**	**SOx (%)**	**Gold Recovery (%)**	**Sulfide Sulfur Recovery (%)**
1	None	0	0	80.5	84.0
2	H_2SO_4	10	3.9	54.9	35.0
3	H_2SO_4	20	8.3	43.3	27.0
4	H_2SO_4	30	10.1	28.5	14.8
5	H_2SO_4	40	13.3	22.5	8.7

The high gold and sulfur recovery with the control sample was found to be an aftermath of copper ion activation as explained in Chapter 7 (Chen et al., 2014, Leppinen et al., 1988, Finkelstein, 1997, Leppinen et al., 1988, Shen et al., 2001).This suggested mechanism of copper ion activation of pyrite was confirmed by ToF-SIMS analysis a shown in Figure 8.14.

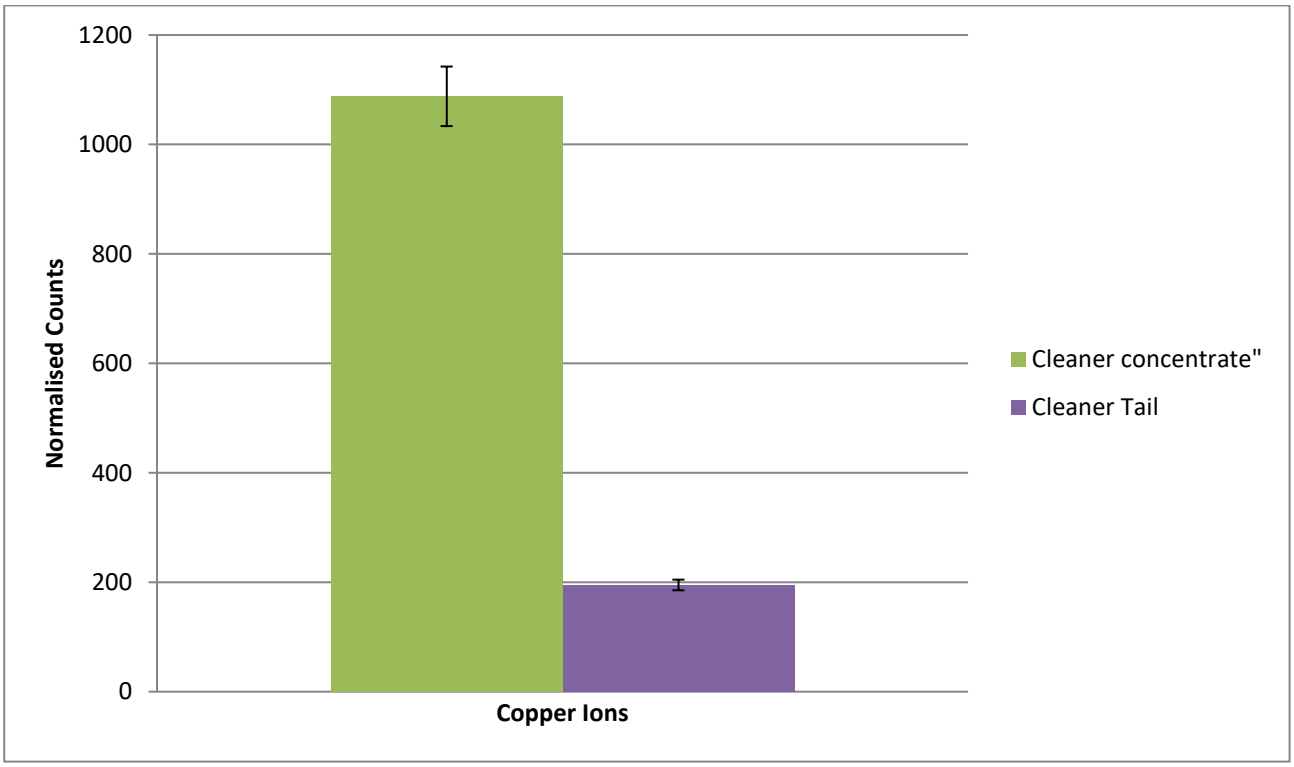

Figure 8. 14: ToF-SIMS plot of copper ions on the cleaner concentrate and tail (*non-oxidised/ pristine /control samples*)

It has been shown in chapter 7 (*and other studies in literature*) that in an alkaline pH condition, Cu+–xanthate interaction is high (Dichmann and Finch, 2001, Leppinen et al., 1988, Zhang et al., 1997, Mermillod-Blondin et al., 2005). This Cu+–xanthate interaction could be another reason for high sulfur recoveries with the control sample and was confirmed by ToF-SIMS analysis as shown in Figure 8.15.

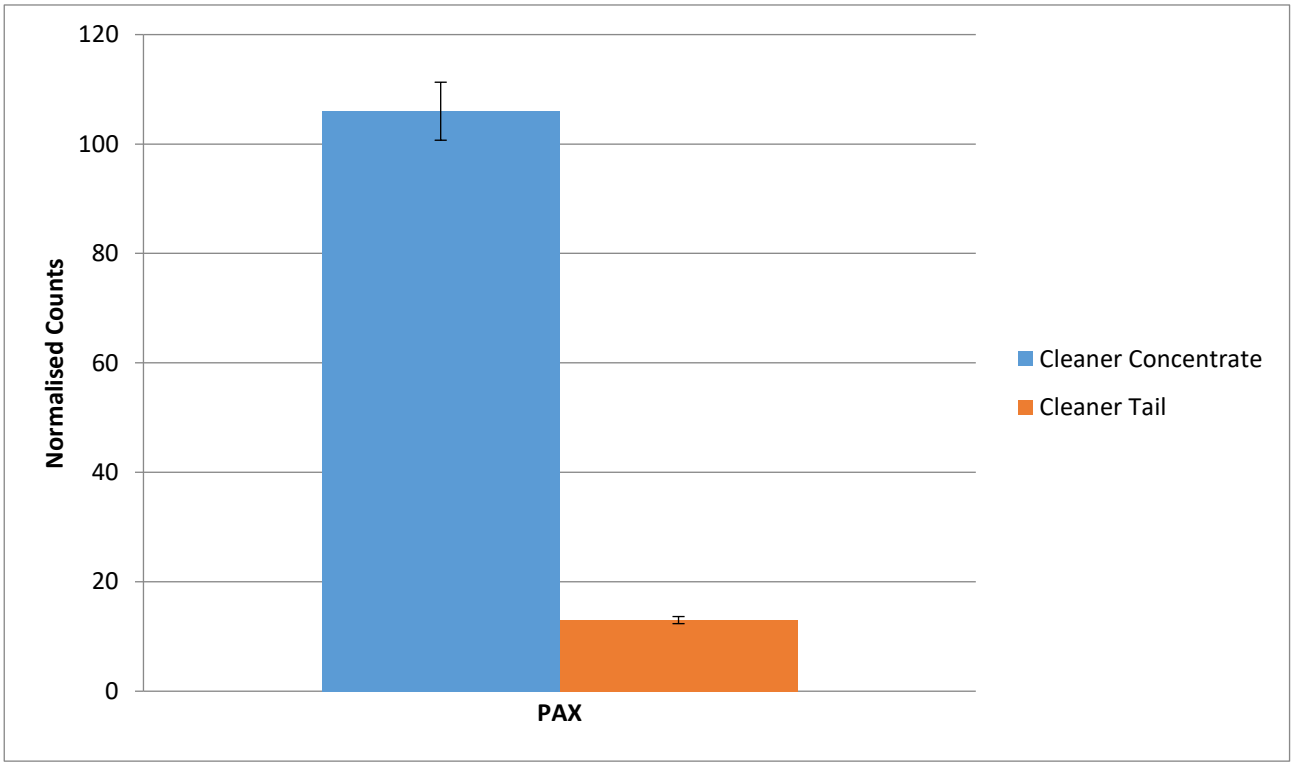

Figure 8. 15: ToF-SIMS plot of collector on the cleaner concentrate and tail (*non-oxidised/ pristine /control samples*)

Nonetheless, the flotation recoveries change drastically with oxidised samples as shown in Figure 8.16. The flotation recovery of gold drops from 80% to 55% after 10 minutes of sulfuric acid conditioning. In general, the flotation recoveries of gold decreased (*with increasing conditioning time*) with a very low gold recovery of 22.5% for the 40 minutes sample. This is because as the extent of acid treatment increases, the concentration of hydrophilic products on the mineral surface also increases (*as confirmed by XPS spectra*).

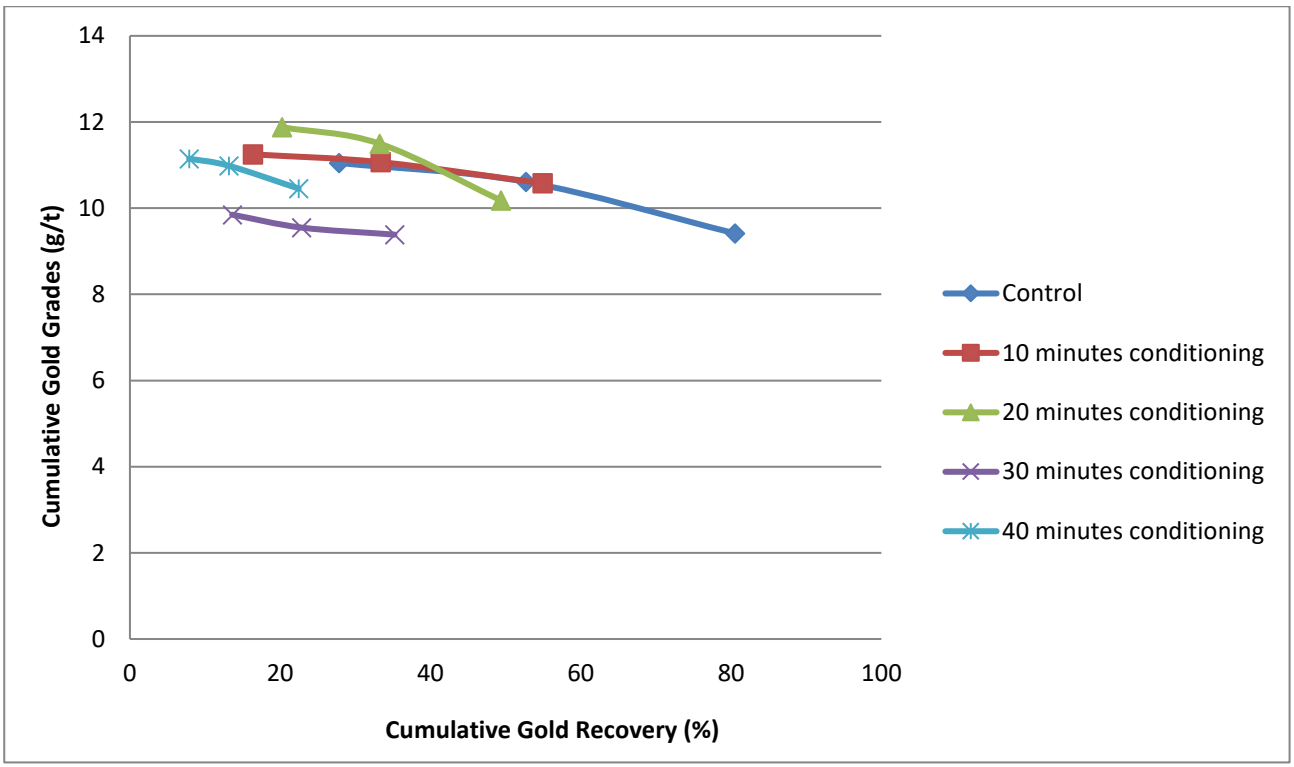

Figure 8. 16: Flotation behaviour of gold from control and acid conditioned concentrates

These hydrophilic oxidation layers formed on the pyrite surface impeded the electrochemical reactions between the collector and the mineral surface resulting in relatively low flotation recoveries. This is due to the precipitation of iron caused by the hydrolysis and subsequent oxidation of ferrous hydroxides to ferric hydroxides as shown in equations 47 and 48 (Ekmekçi and Demirel, 1997).

$$Fe^{2+} + 2H_2O \xrightarrow{\text{yields}} Fe(OH)_2 + 2H^+ \quad \ldots\ldots\ldots\

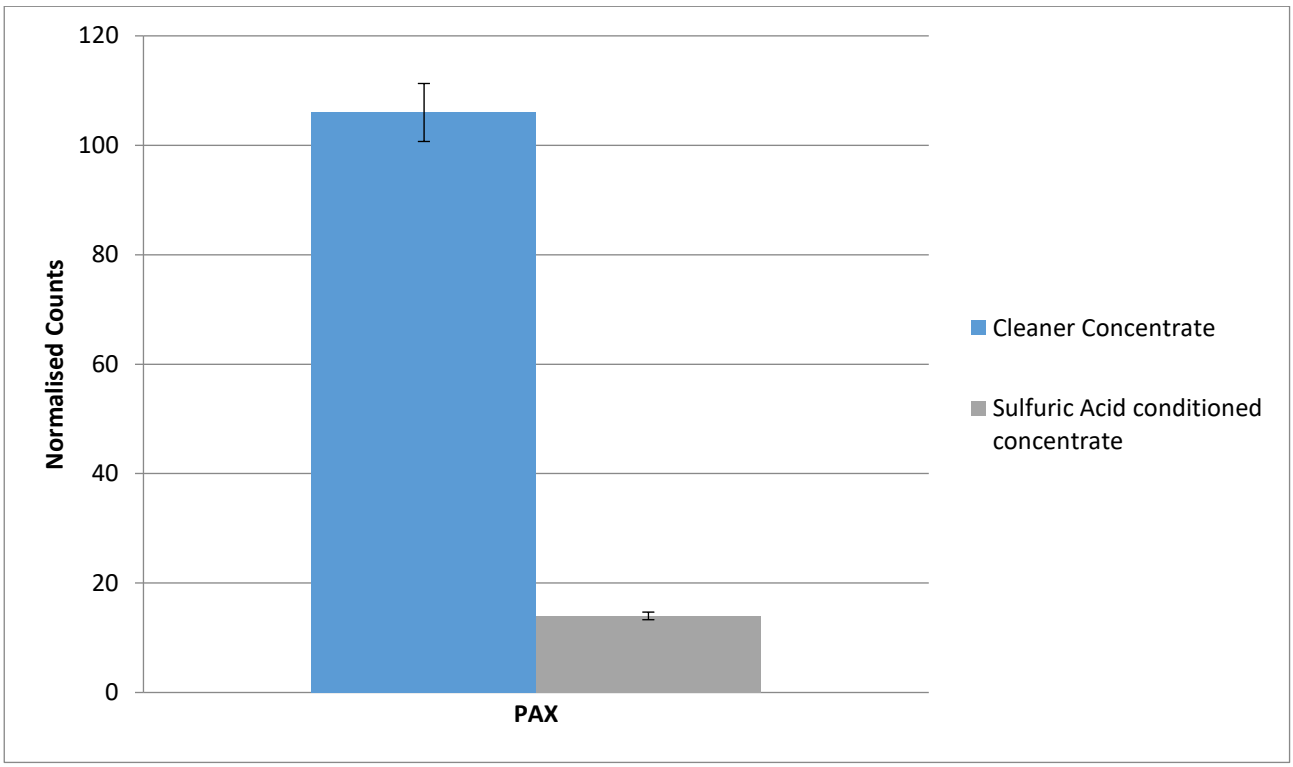

Figure 8. 17: ToF-SIMS plots of collector attachment on control and sulfuric acid oxidised surfaces.

It can be seen from Figure 8.17 that the collector adsorption is very low on the conditioned concentrate as compared to the control (*untreated*) concentrate. This suggests that pyrite flotation was strongly depressed as a result of hydrophilic iron hydroxy/hydroxides and sulphoxy species resulting in lower collector attachment (Rimstidt and Vaughan, 2003).

8.2.6 Eh-pH window

The normal practice in mineral oxidation studies is to establish an Eh-pH operating window that allows significant upgrade of the process. However, this approach is not valid in this work mainly because this is not an extensive oxidation experiment and hence, there are minimal differences among the Eh-pH values. The Eh-pH values of the various conditioning stages are shown in Table 8.3. At 10 g/L of sulfuric acid, the pH value increases (*and Eh values decrease*) indicating that sulfuric acid was consumed in the process. After 30 minutes conditioning, the pH stabilised at 1.11 which is only greater than the stock solution by 0.23. The excess sulfuric acid from the pre-treatment stage could be regenerated from an economical perspective, however, this topic is beyond the scope of this study. The excess acid present in the system was neutralised with wash liquor and lime (*during the conditioning stage of cleaner flotation*) as per the following equation:

$$CaCO_3 + H_2SO_4 + H_2O \xrightarrow{\text{yields}} CaSO_4.2H_2O + CO_2(g) \quad \ldots\ldots\ldots\

Table 8.3: Eh-pH values of the sulfuric acid treatment process

Conditioning Time (*minutes*)	Eh (*SHE*) mV	pH
10	513	0.88
20	505	0.96
30	502	1.11
40	496	1.12

A moderate Eh is favourable for collector adsorption and mineral flotation (Owusu et al., 2014), high Eh values between 495 and 515 mV (*confirming an oxidising environment similar to nitric acid oxidation*) would have inhibited adequate pyrite-xanthate interaction (*and subsequent dixanthogen formation*) contributing to low sulfide sulfur recoveries as shown in Figure 8.18.

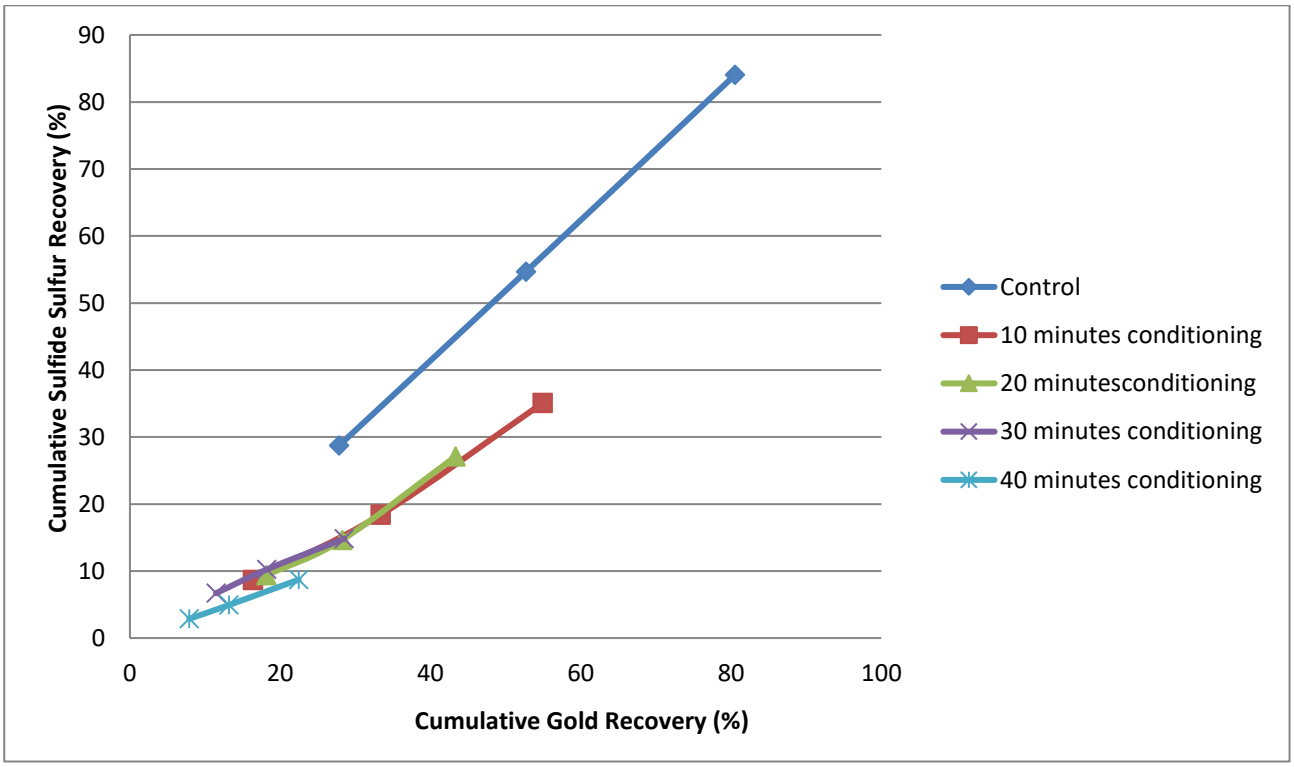

Figure 8. 18: Gold and sulfide recoveries of control and acid conditioned concentrates

This explains that the decreasing sulfide sulfur recoveries as a function of conditioning time (*from 84.0% in case of the control sample to 8.7 % with 40 minutes etched sample*) are due to the higher formation rate of oxidised species as the extent of conditioning increases. Hence conditioning time and extent of oxidation are critical parameters that need to be considered. This is because 'mild oxidation' can promote sulfide flotation by forming hydrophobic sulfides and (Zachwieja et al.,

1989) while 'moderate to extensive oxidation' impedes flotation performance by forming hydrophilic precipitates (Smart, 1991, Senior and Trahar, 1991).

However, with AA ore, collector attachment is not the only factor that governs pyrite floatability. Copper ions also played a pivotal role as seen from the flotation of the control sample (*also in Chapter 7*). Therefore, due consideration must be given to copper ion activation of the oxidised pyrite concentrates as well. It has been reported in other work that an oxidising environment inhibits the copper activation of sulfides (Chen et al., 2013, Peng and Grano, 2010, Peng et al., 2003). Similar observations were encountered in this study as well as shown in the ToF-SIMS plots in Figure 8.19.

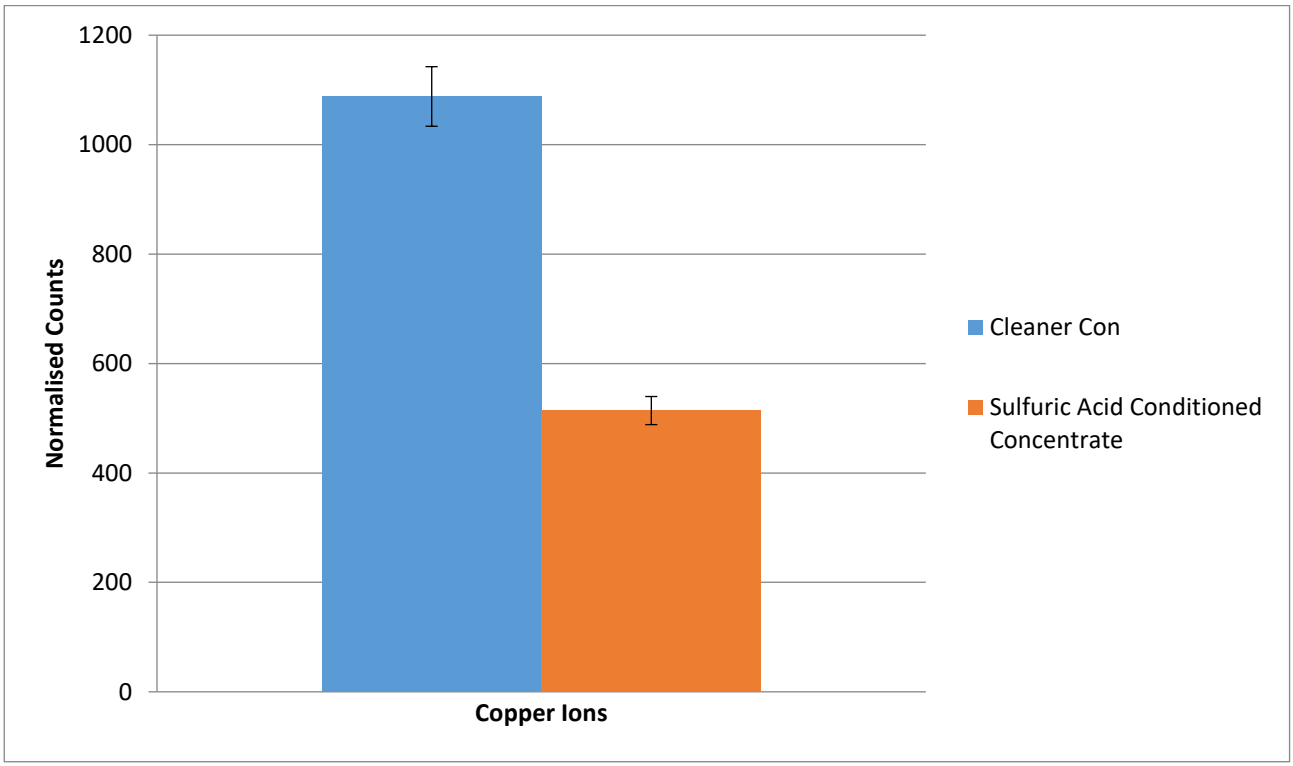

Figure 8. 19: ToF-SIMS plots of copper ions on control and sulfuric acid modified pyrite surfaces.

This behaviour is because hydrophilic iron and sulfur precipitates from pyrite modification, caused by sulfuric acid media, inhibited the adsorption of Cu^{2+} on oxidised pyrite surfaces decreasing the subsequent Cu^{+}–xanthate interaction. This was indicated by the reduced intensity of copper ion concentration on the etched surfaces as shown in Figure 8.19 and this contributed to the low sulfur recoveries of conditioned samples.

8.2.7 Mass Recovery

Although this project is not governed by process economics, the samples were not treated beyond 40 minutes due to the unacceptably low mass recoveries (*probably due to extensive passivation compared to nitric acid treatment*) for sample assays as shown Table 8.4 and Figure 8.20.

Table 8.4: Mass recoveries of control and acid conditioned samples after cleaner flotation

	Oxidation			**Metallurgical Response**	
Test	**Pre-treatment**	**Conditioning Time (*minutes*)**	**SOx (%)**	**Mass Recovery (%)**	**Au:S Ratio**
1	None	0	0	**52.9**	0.24
2	H_2SO_4	10	3.9	**34.3**	0.39
3	H_2SO_4	20	8.3	**35.4**	0.44
4	H_2SO_4	30	10.1	**29.1**	0.54
5	H_2SO_4	40	13.3	**15.1**	0.63

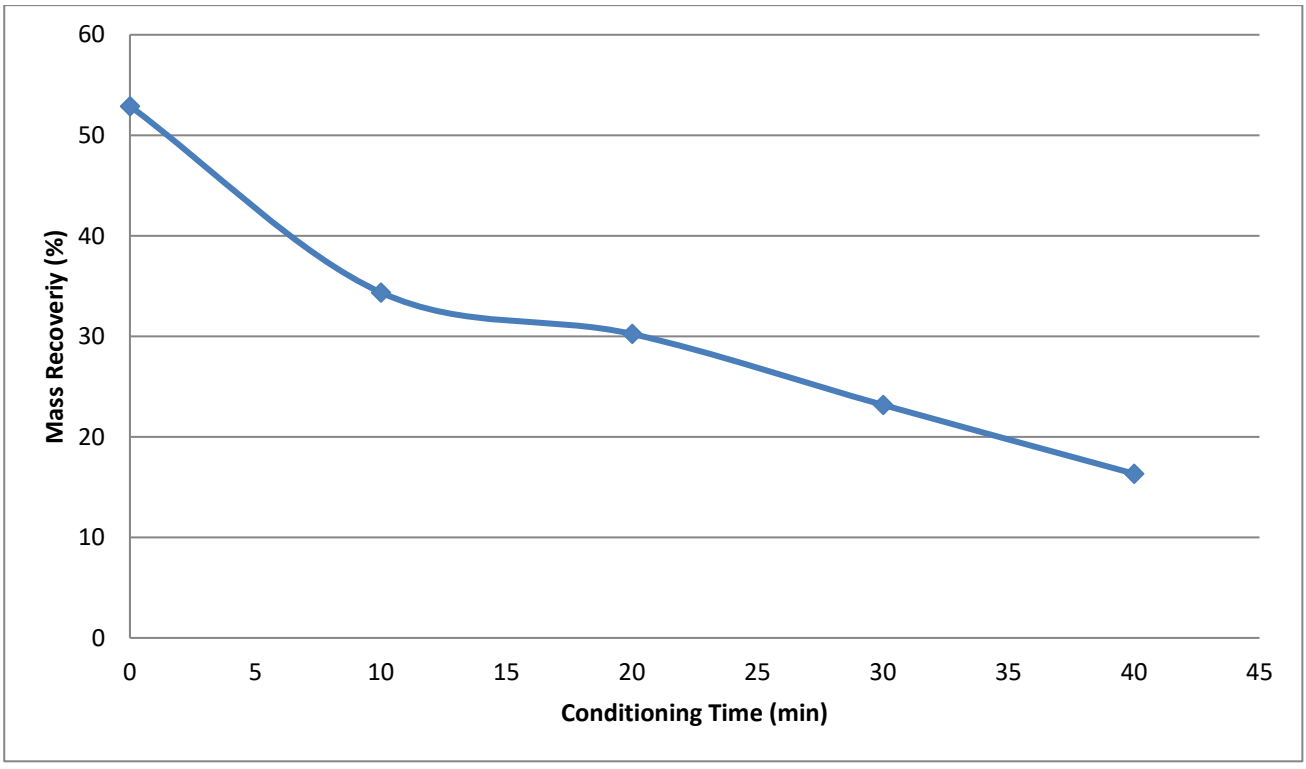

Figure 8.20: The effect of sulfuric acid conditioning on mass recovery of cleaner concentrates

The extremely low mass recoveries could be due to higher concentrations of sulphoxy intermediates resulting in a passivating film inhibiting collector attachment as shown in Figure 8.21 and Equations 50 to 56 (Zhang and Dreisinger, 2002; Ahern, 2006; Kleinjan, 2005; Melashvili et al., 2015).

Figure 8.21: Sulfur Intermediates formed during pyrite oxidation (Melashvili et al., 2015)

$$4FeS_2 + 7O_2 + 2H^+ \xrightarrow{\text{yields}} 4Fe^{3+} + 4S_2O_3^{2-} + 2H_2O \quad \text{.....50}$$

$$4S^O + 4OH \xrightarrow{\text{yields}} 2HS^- + S_2O_3^{2-} + H_2O \quad \text{.....51}$$

$$2HS^- + 2O_2 \xrightarrow{\text{yields}} S_2O_3^{2-} + H_2O \quad \text{.....52}$$

$$2S_2O_3^{2-} + H_2O + 0.5O_2 \xrightarrow{\text{yields}} S_4O_6^{2-} + 2OH^- \quad \text{.....53}$$

$$4S_4O_6^{2-} + 6OH^- \xrightarrow{\text{yields}} 5S_2O_3^{2-} + S_3O_6^{2-} + 3H_2O \quad \text{.....54}$$

$$2S_3O_6^{2-} + 6OH^- \xrightarrow{\text{yields}} S_2O_3^{2-} + 4SO_3^{2-} + 3H_2O \quad \text{.....55}$$

Sulfates are further formed by the oxidation of sulfite by O_2:

$$4SO_3^{2-} + 0.5O_2 \xrightarrow{\text{yields}} SO_4^{2-} \quad \text{.....56}$$

8.2.8 Gold to Sulfur Ratios

The approach in this work is not optimising conditions for high recoveries. This fundamental work is based on 'separation elucidation' within the same pyrite family i.e. low gold pyrite from high gold pyrite or *vice versa*. Therefore, emphasis on flotation recoveries will result in ambiguity regarding the potential of an oxidative hydrometallurgical treatment to separate within the same mineral family.

The approach embraced in this work is evaluating the metallurgical response in terms of Au:S ratio of both the sulfuric acid treated sulfide concentrate and the untreated/pristine concentrate. This is

because the sole objective remains to produce a low sulfur and relatively high gold concentrate as an autoclave feed. It is usual to expect high recoveries considering the nature of the mineral industry but not at the expense of Au:S ratio which would otherwise defy the logic behind this work. Cleaner flotation tests of control and etched samples have displayed different metallurgical responses with an increase in Au:S ratio seen with conditioned samples as shown in Table 8.5.

Table 8.5: Change in the Au:S ratio in the flotation concentrate after sulfuric acid treatment

Test	**Pre-treatment**	**Conditioning Time (*minutes*)**	**SOx (*%*)**	**Au:S Ratio**	**Au:S Ratio (*% Increase*)**
1	None	0	0	**0.24**	**-**
2	H_2SO_4	10	3.9	**0.39**	**62.5**
3	H_2SO_4	20	8.3	**0.44**	**83.3**
4	H_2SO_4	30	10.1	**0.54**	**125.0**
5	H_2SO_4	40	13.3	**0.63**	**162.5**

The Au:S value of the control sample is low at 0.24 and is close to the typical Lihir flotation performance of 0.25 (Rankin, 2013). However, interestingly for the same cleaner float conditions, steady positive progression in Au:S values are observed. For example, there is a 162.5 % upgrade in Au:S value with 40 minutes acid conditioned sample compared to the control sample as shown in Table 8.5 and Figures 8.22 and 8.23.

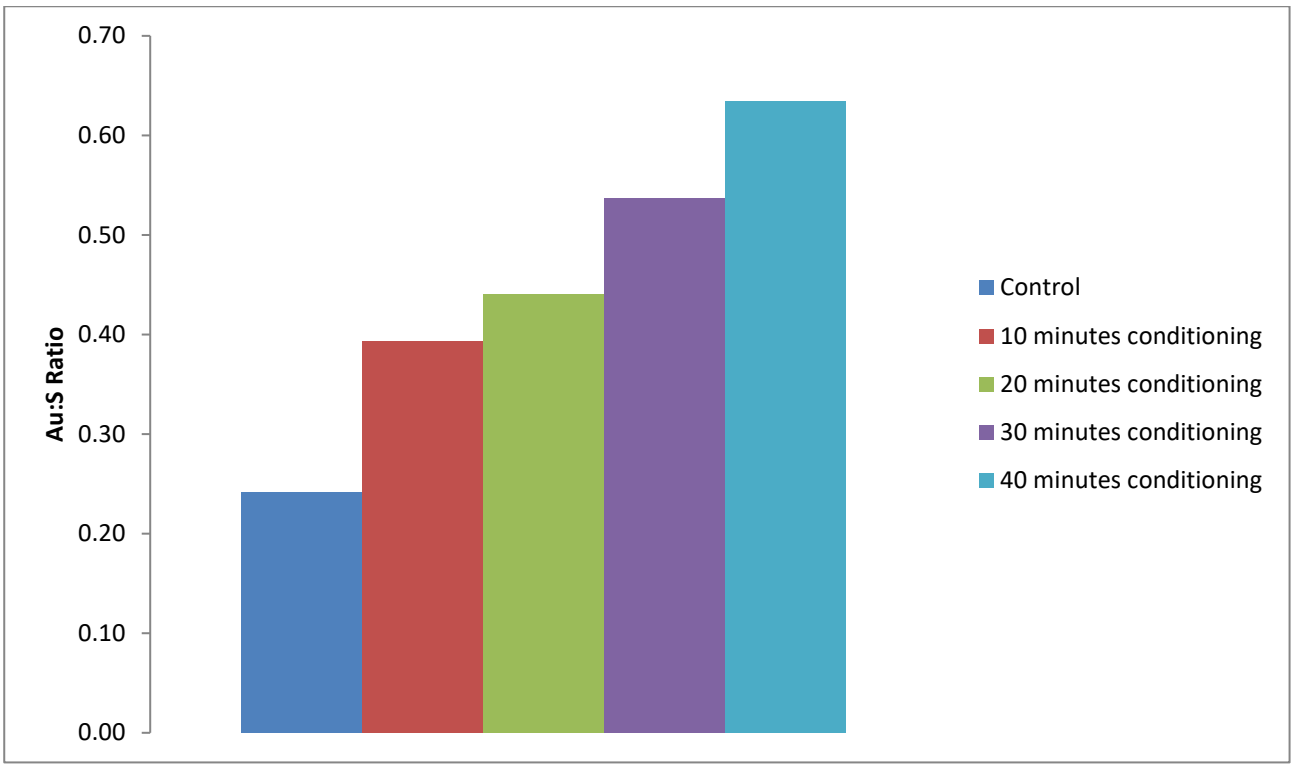

Figure 8.22: Au:S of control and acid conditioned samples floated at pH 11

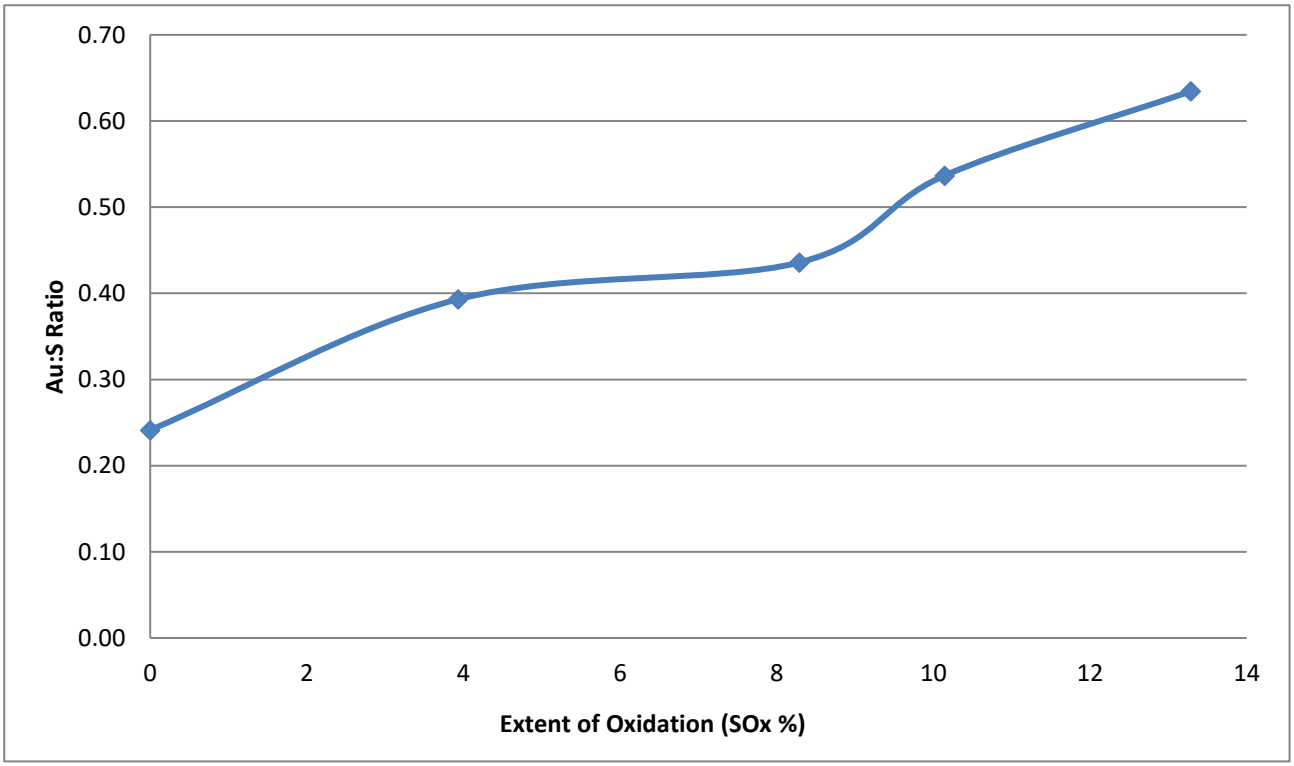

Figure 8.23: The effect of sulfide sulfur oxidation on Au:S values

The 40 minutes conditioned sample with 13.3% oxidation yielded the highest Au:S ratio of 0.63. This signifies that the conditioning time and extent of oxidation dictated pyrite flotation and the changes were reflected in the flotation responses. This was confirmed by the sulfide sulfur grade-recovery curves of the samples as shown Figure 8.24.

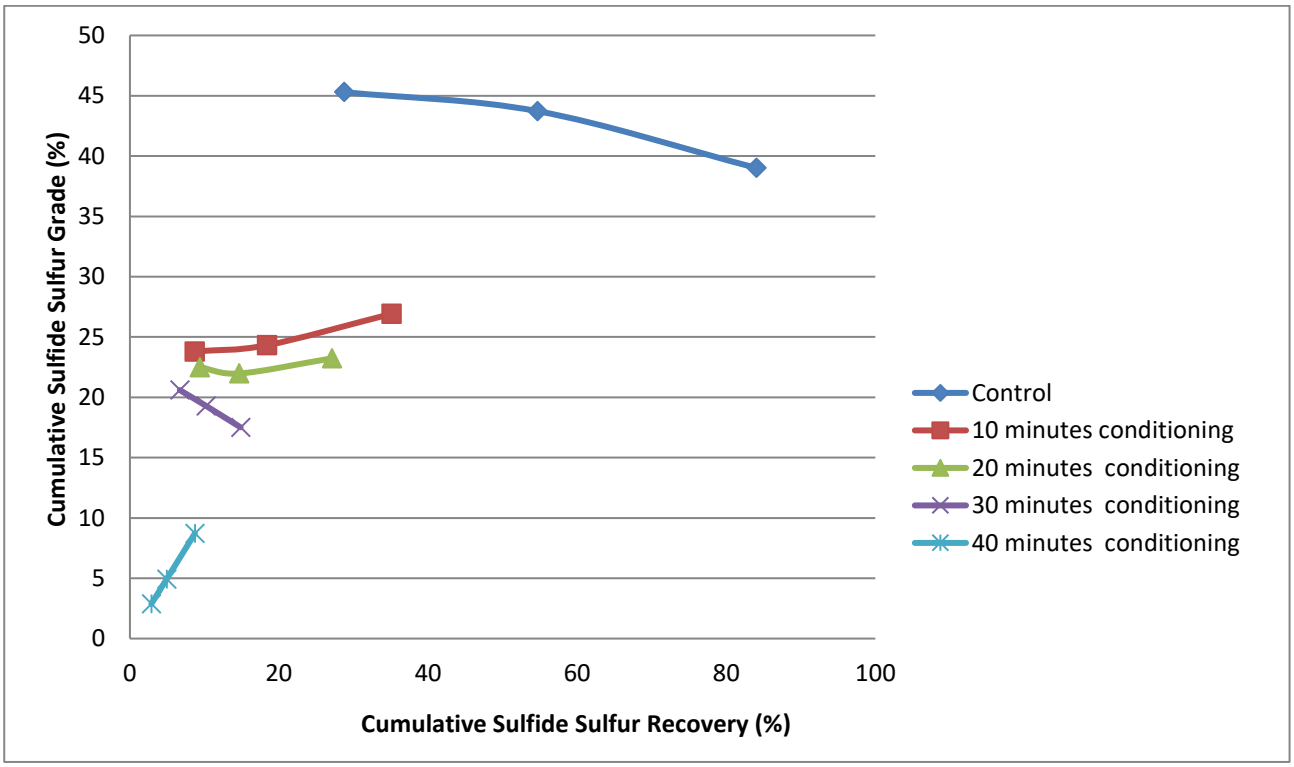

Figure 8.24: Sulfide sulfur grade-recovery curve for the control and acid conditioned samples

This establishes that the sulfide sulfur grade of the sample decreases significantly with oxidation. The consistency of this pattern is indicated by the cumulative gold and sulfide sulfur grades of the control and treated samples with respect to conditioning time as shown in Table 8.6.

Table 8.6: Gold and sulfide sulfur grade of the control and acid conditioned samples

Conditioning Time (*minutes*)	Gold Grade (*g/t*)	Sulfide Sulfur grade (%)
0	9.4	39.0
10	10.5	26.9
20	10.1	23.2
30	9.4	17.5
40	10.4	16.4

Rigorous analysis of these experimental data revealed an interesting trend. The gold grade for all the samples (*control and conditioned*) remains more or less the same. Although the literature is of little help in providing information regarding the impact of oxidation on gold grades, from the experimental data, it is obvious that it is the sulfide sulfur grade that gets modified to a great extent in the oxidation process. Therefore, it can be proposed that it is not possible to improve the gold grade of the final pyrite concentrate by sulfuric acid conditioning. However, there is convincing evidence that the sulfide sulfur grade of a pyrite concentrate can be significantly reduced without affecting the gold grade as shown in Figure 8.25.

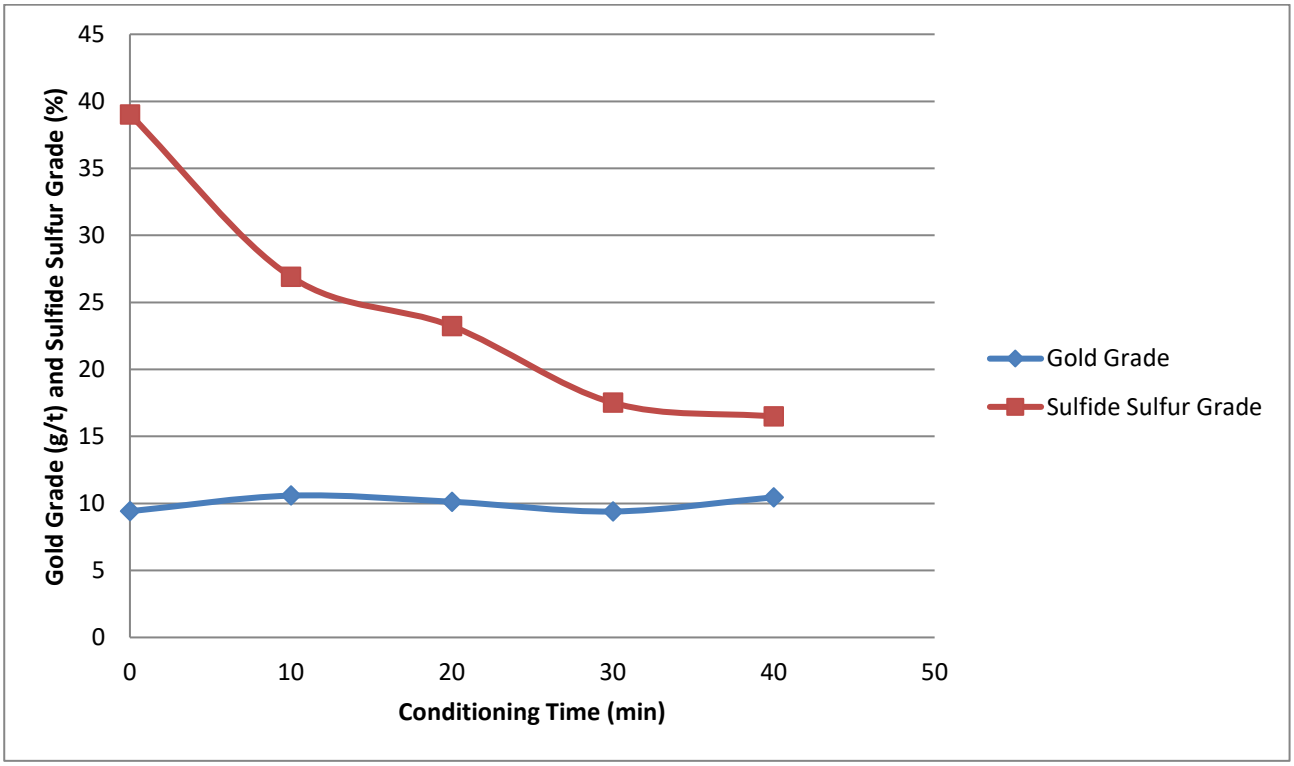

Figure 8.25: Cumulative gold and sulfide sulfur grades of the control and acid conditioned samples

This change in sulfide sulfur grades explains varying Au:S values between control and conditioned samples. The presence of sulfur in the sulfuric acid treated cleaner concentrates revealed that sulfides were not completely depressed. Additionally, the high Au:S values of the conditioned concentrates compared to the respective tails (*shown in Table 8.7*) established definite evidence that one type of pyrite was floating and the other was not.

Table 8.7: Au:S ratios of pristine and oxidised cleaner concentrates and tails

	Oxidation			Metallurgical Response	
Test	**Pre-treatment**	**Conditioning Time (*minutes*)**	**SOx (*%*)**	**Au:S Ratio Concentrate**	**Au:S Ratio Tail**
1	None	0	0	**0.24**	**0.25**
2	H_2SO_4	10	3.9	**0.39**	**0.18**
3	H_2SO_4	20	8.3	**0.44**	**0.22**
4	H_2SO_4	30	10.1	**0.54**	**0.25**
5	H_2SO_4	40	13.3	**0.63**	**0.23**

This trend was further confirmed looking at actual Au:S ratios of the individual concentrates as shown in Figure 8.26. As shown, the control sample shows low Au:S value for all individual concentrates. With the 30 minutes and 40 minutes samples, there is an upsurge in Au:S ratio with all the individual concentrates. However, with the 10 and 20 minutes conditioned samples, a different Au:S kinetics is observed. This probably due to the interference of intermediate and unstable oxidised species formed causing a different flotation response compared to other time intervals. High Au:S values of the sulfuric acid treated concentrates compared to the oxidised tails clearly signifies that the floating pyrite had an 'active phase characteristic' compared to the passive (*depressed*) pyrite. The low Au:S value of the tail, in the case the 40 minutes oxidation with 13% SOx, signifies that it is not the incomplete surface modification of the high gold pyrite types but rather the formation of oxidation intermediates such as nitrates with nitric acid oxidation that depressed the high gold pyrite types in an alkaline environment.

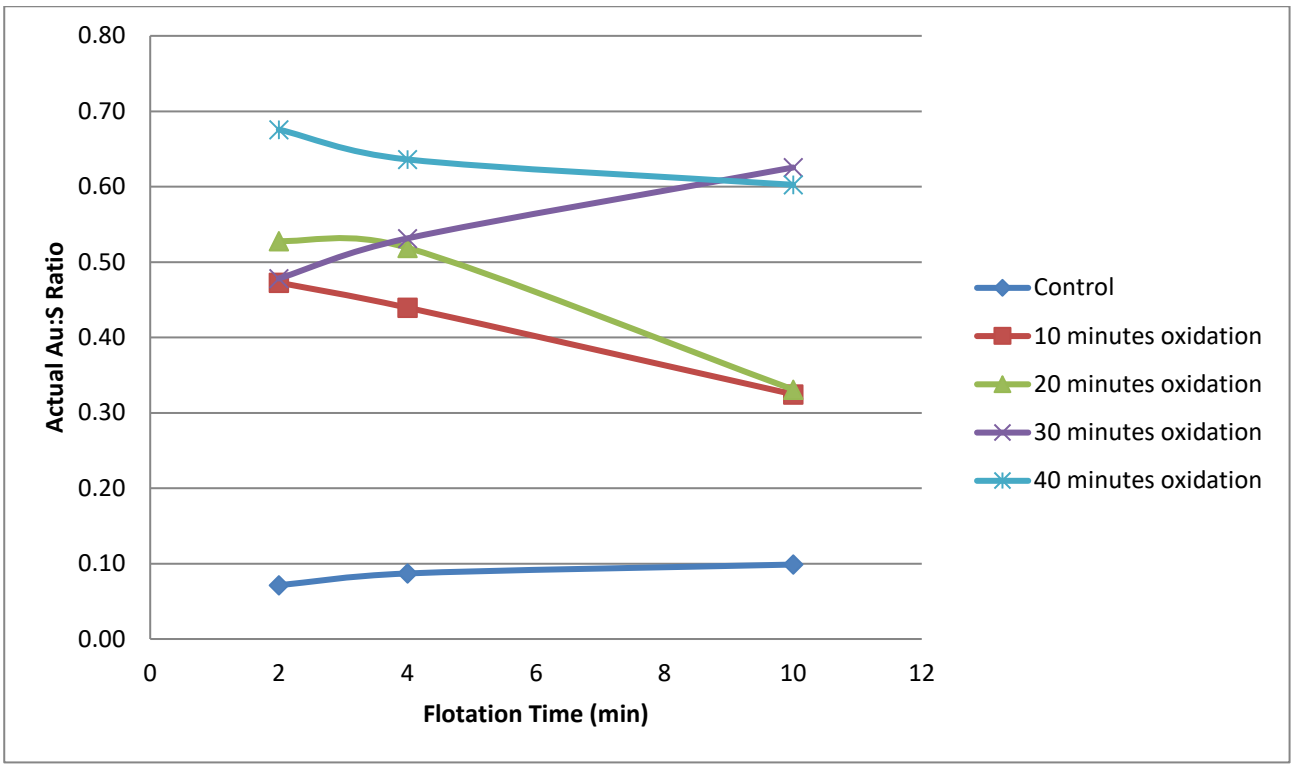

Figure 8.26: Actual Au:S ratios of individual cleaner concentrates of control and acid conditioned samples

8.2.9 True Flotation

Metallurgical and mineralogical data have provided clues regarding the effect of sulfuric acid conditioning, however; it does not clarify the upgrade in Au:S values. To demonstrate this, there is a need to understand the modified pyrite behaviour in the following cleaner flotation process. As shown in Table 8.8, the oxidation of pyrite is governed by Fe^{3+}ions resulting in the formation of basic ferric sulfate, hydronium jarosite and haematite as shown in equations 57 to 60 (Dreisinger, 2006).

Table 8.8: Oxidising conditions in the Sulfuric Acid System

System	pH	Oxidation products
FeS_2 / H_2SO_4	0.88 to 1.11	$Fe^{2+} \xrightarrow{yields} Fe^{3+}$ $As(III) \xrightarrow{yields} As\ (V)$

$$FeS_2 + 0.5O_2 + H_2SO_4 \xrightarrow{\text{yields}} FeSO_4 + 2S + H_20 \quad \text{.....57}$$

$$Fe_2(SO_4)_3 + 2H_3\ AsO_4 + H_2SO_4 \xrightarrow{\text{yields}} 2FeAsO_4 + 2S + 3H_2SO_4 \quad \text{.....58}$$

$$FeSO_4 + 0.25O_2 + 0.5H_2SO_4 \xrightarrow{\text{yields}} 0.5Fe_2(SO_4)_3 + 0.5H_20 \quad \text{.....59}$$

$$Fe_2(SO_4)_3 + 3H_20 \xrightarrow{\text{yields}} Fe_2O_3 + 3H_2SO_4 \quad \text{.....60}$$

It has already been shown in Chapter 5 that the high arsenic pyrite had a faster oxidation rate compared to the low arsenic pyrite. Therefore, the best approach to defining the characteristic of the active oxidising pyrite is to compare the Gold to Arsenic ratios (*Au:As*) of the control and conditioned concentrates as shown in Figure 8.27.

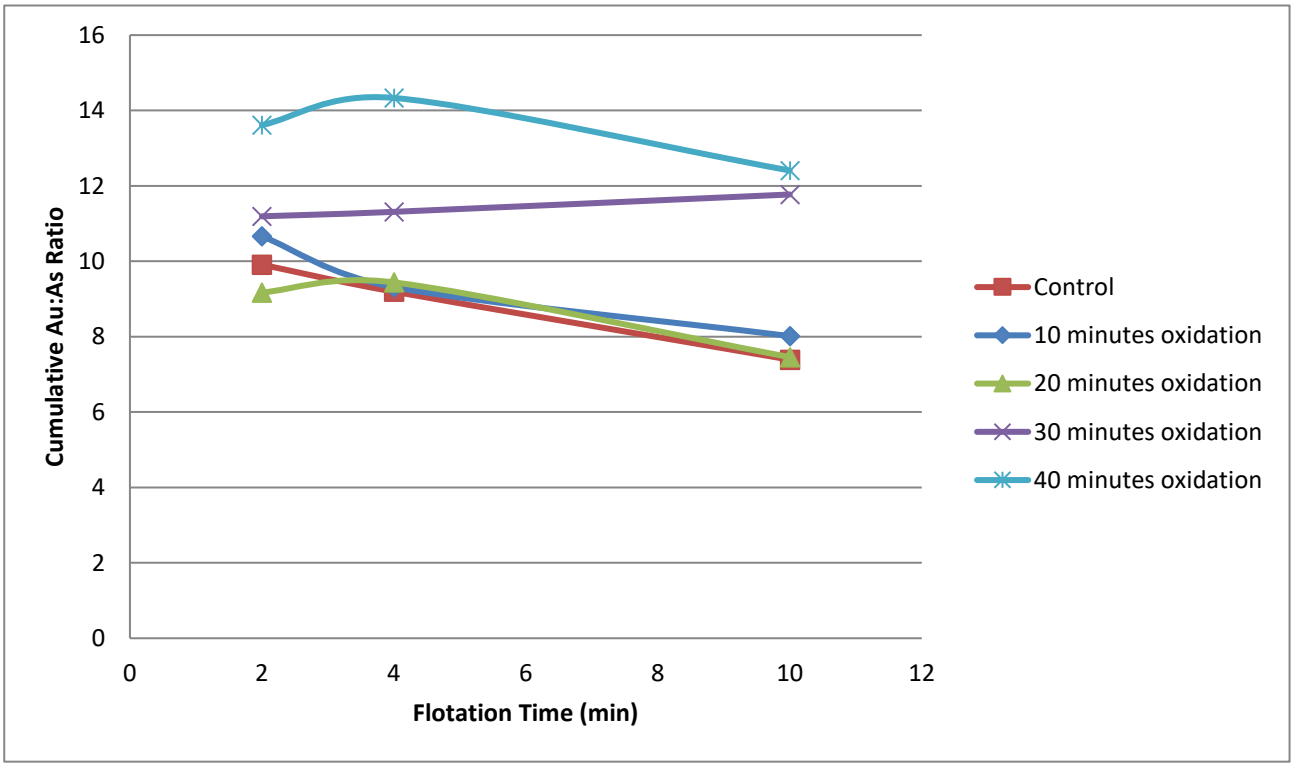

Figure 8.27: Cumulative Au:As ratios of control and acid conditioned pyrite concentrates

There is a significant upgrade in Au:As ratio of the acid conditioned samples especially with 30 minutes and 40 minutes samples. This follows the same trend as Au:S ratios shown before suggesting that the oxidised arsenian pyrite was floating while the low arsenic pyrite remained depressed in the cleaner stage post sulfuric acid treatment. This was further confirmed by the Au: As values of the tailings as shown in Table 8.9. The increasing Au:As values of the concentrates

indicate that the oxidation rate of the arsenian pyrite was faster and it was reporting in an oxidised form to the concentrate (*arsenate as discussed in Chapter 7*). As the extent of oxidation increases, the Au:As values of the oxidised tailings also increases. This suggests that while the low arsenic pyrite types remained depressed in an alkaline pH, formation of arsenates increases with the extent of oxidation and is no longer depressed.

Table 8.9: Au:As values of the control and acid conditioned cleaner concentrate and tail

Conditioning Time (*minutes*)	**Au:As Ratio Concentrate**	**Au:As Ratio Tail**
Control	8.6	5.4
10	9.0	5.2
20	8.5	7.8
30	11.4	8.8
40	13.2	9.7

8.2.10 Collector and copper ion attachment on the oxidised pyrite phase

ToF-SIMS analysis was performed to understand the collector and copper ion attachment on control and modified surfaces as shown in Figures 8.28 and 8.29. From the ToF-SIMS plots, it is clear that there are low collector and copper ion attachments on the conditioned pyrite concentrate compared to the tailing. However, it must be noted that ToF-SIMS is a semi-quantitative method and especially in this type of separation within the same mineral family, ToF-SIMS data can only be used as an indication and not for pure quantification purposes. Nevertheless, from the ToF-SIMS plot, it is clear that the oxidised pyrite phase (*active pyrite*) has a hydrophobic nature. This is because, despite very low collector and copper ion attachment on the conditioned pyrite concentrate, high Au:S values are observed with the concentrates. Moreover, since the gold tenor in different types of pyrite is different, (*Chapter 4, Table 4.3*) the chances are as the conditioning time increases, only the extremely gold-rich pyrite types are likely to remain hydrophobic and float resulting in high Au:S values despite low gold and sulfur recoveries. i.e. 80.5 % gold recovery vs. 84.0 % sulfide sulfur recovery for a control sample and 22.5% gold recovery vs. 8.7 % sulfide sulfur recovery for the 40 minutes sample as shown in Table 8.10.

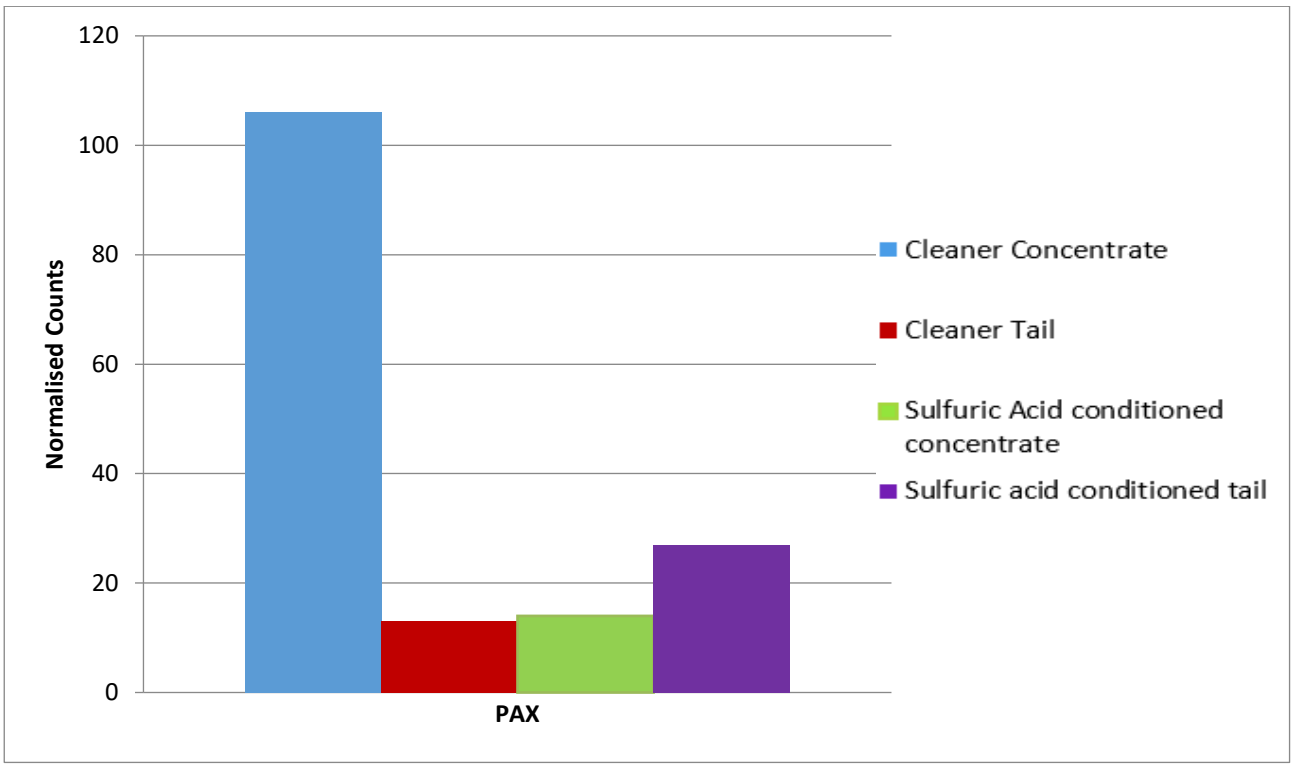

Figure 8.28: ToF-SIMS plots of collector attachment on acid conditioned pyrite concentrate and tail

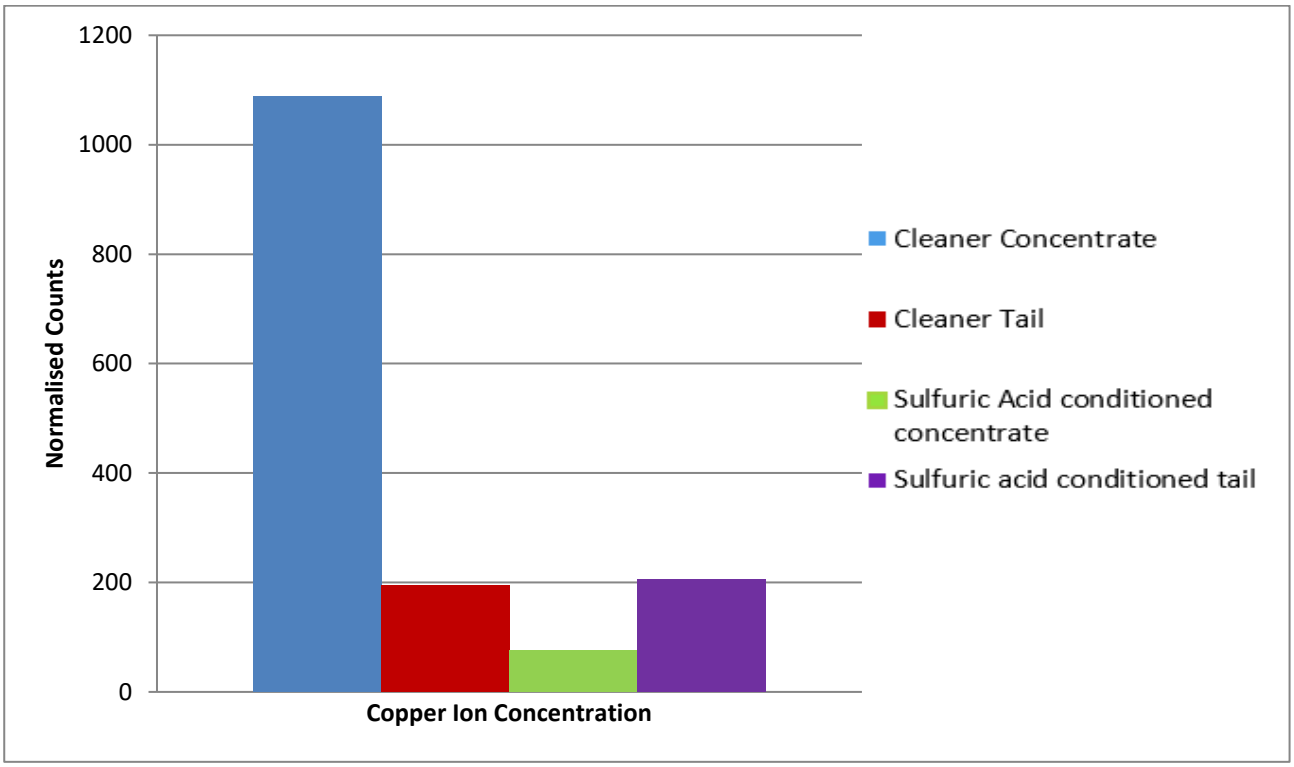

Figure 8.29: ToF-SIMS plots of copper ion attachment on acid conditioned pyrite concentrate and tail

Table 8.10: Gold and Sulfur recoveries of control and acid conditioned samples

	Oxidation			Metallurgical Response		
Test	**Pre-treatment**	**Conditioning Time (*minutes*)**	**SOx (%)**	**Gold Recovery (%)**	**Sulfide Sulfur Recovery (%)**	**Au:S Ratio**
1	None	0	0	**80.5**	**84.0**	0.24
2	H_2SO_4	10	3.9	**54.9**	**35.0**	0.39
3	H_2SO_4	20	8.3	**49.3**	**27.0**	0.44
4	H_2SO_4	30	10.1	**35.2**	**14.8**	0.54
5	H_2SO_4	40	13.3	**22.5**	**8.7**	0.63

The relatively high gold recoveries compared to sulfide sulfur recoveries applies with all conditioned samples but not with the control sample as shown in Table 8.9. This clearly signifies the hydrophobic nature of the active pyrite reduces with increasing extent of oxidation. This is because as the conditioning time proceeds, the active hydrophobic phase is transformed to a passive hydrophilic phase by forming intermediate oxidation products with hydrophilic oxides and sulfates being the final product. Therefore, one path with promise might be to select a conditioning time that upgrades the Au:S ratio to serve as an optimal autoclave feed at reasonable gold recoveries that fit within the process economics. The typical mass and metal balances for the sulfuric acid treatment tests (*10 minutes stage*) are included for clarity in Figure 8.30. Appendix section 5.2 gives detailed metallurgical accounting for other treatment stages.

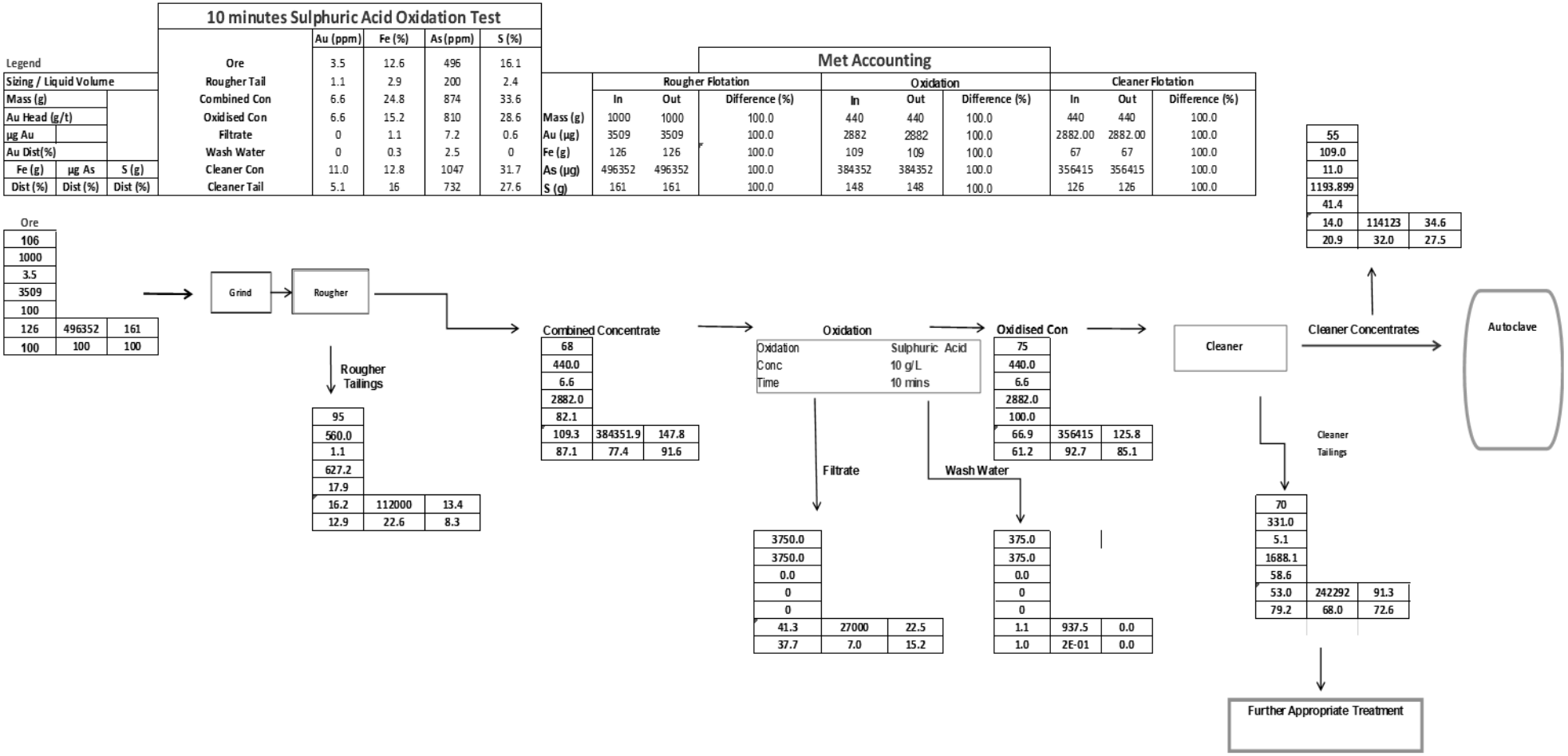

Figure 8.30: Metallurgical Accounting of the Sulfuric Acid Treatment Process

The distribution values are for three steps: Step 1: Rougher Tail + Combined Concentrate

Step 2: Filtrate + Wash Water + Oxidised Concentrate

Step 3: Cleaner concentrate + Cleaner Tai

8.2.11 Water vs. Solids Recovery

While true flotation is a chemically selective process based on hydrophobicity (Yianatos et al., 2009), entrainment is the recovery of hydrophilic gangue in the concentrate reducing the quality of the final products (Stewart, 2010). This study of entrainment is quite significant in this work as there are two major phases which are the active pyrite and passive pyrite with significantly different chemical and physical properties. The entire curves for the control sample are better described as more convex than linear as shown in Figure 8.31.

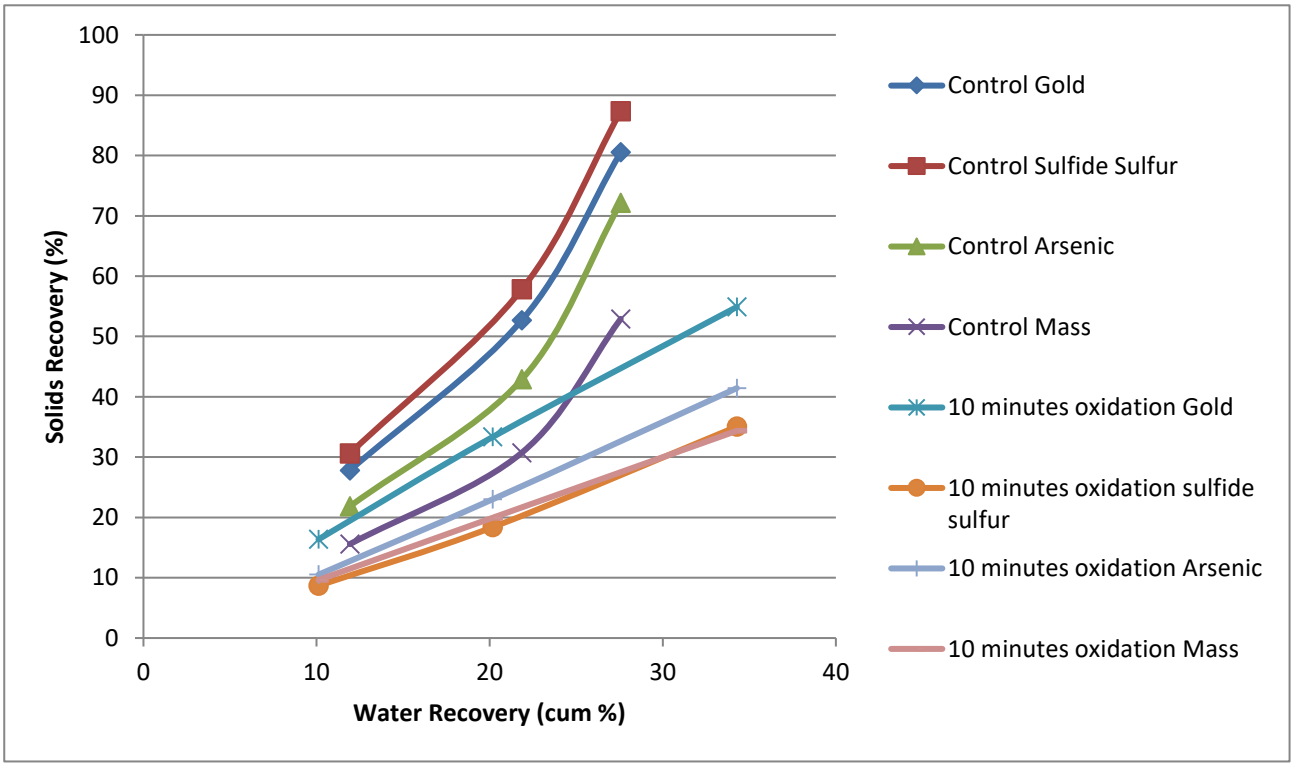

Figure 8.31: Water and solids recovery of control and 10 minutes acid conditioned samples

However, with 10 minutes and 20 minutes treatment (*Figures 8.31 and 8.32*), the correlation between the solids recovery and water recovery appears to be close to linear. It can be seen that the gold recovery with the control and conditioned samples is greater than the corresponding water recovery. The difference between the gold recovery and the water recovery decreases with increase in conditioning times i.e. 81% gold recovery for 28% water recovery with the control sample, 55% gold recovery for 34% water recovery with 10 minutes conditioning and 49 % gold recovery for 13% water recovery with 20 minutes conditioning. When treated with H_2SO_4, the lines do not start asymptotic suggesting that the conditions are close to zero order which could mean the response could be entrainment dominated. For instance, the last concentrate point of the conditioned sample

in Figure 8.32 looks like a pure entrainment concentrate whereas the first two points suggest some true flotation occurring for all species plotted, gold being faster floating than As or S^{2-}.

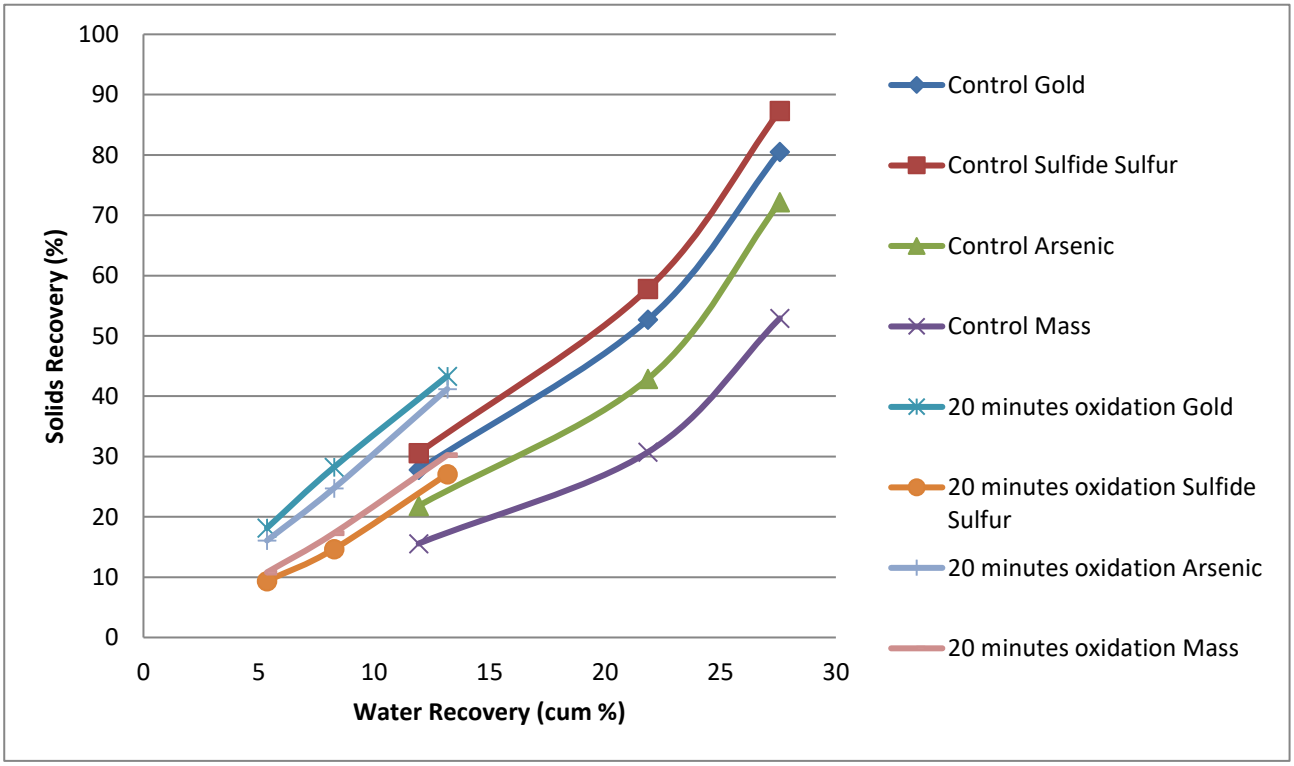

Figure 8.32: Water and solids recovery of control and 20 minutes acid conditioned samples

However, with 20 minutes treatment in Figure 8.32, all the three concentrate points suggest true flotation occurring for every species plotted with gold being faster floating than As and S^{2-}. The reason for this difference in flotation behaviour between the 10 minutes and 20 minutes conditioning could be attributed to the nature of the oxidised species formed as the oxidation reaction proceeds. The finer distribution of gold supports the fact that it would be more readily entrained than the S^{2-}. This is also supported by the fact that the As distribution is so much finer than the S^{2-}.

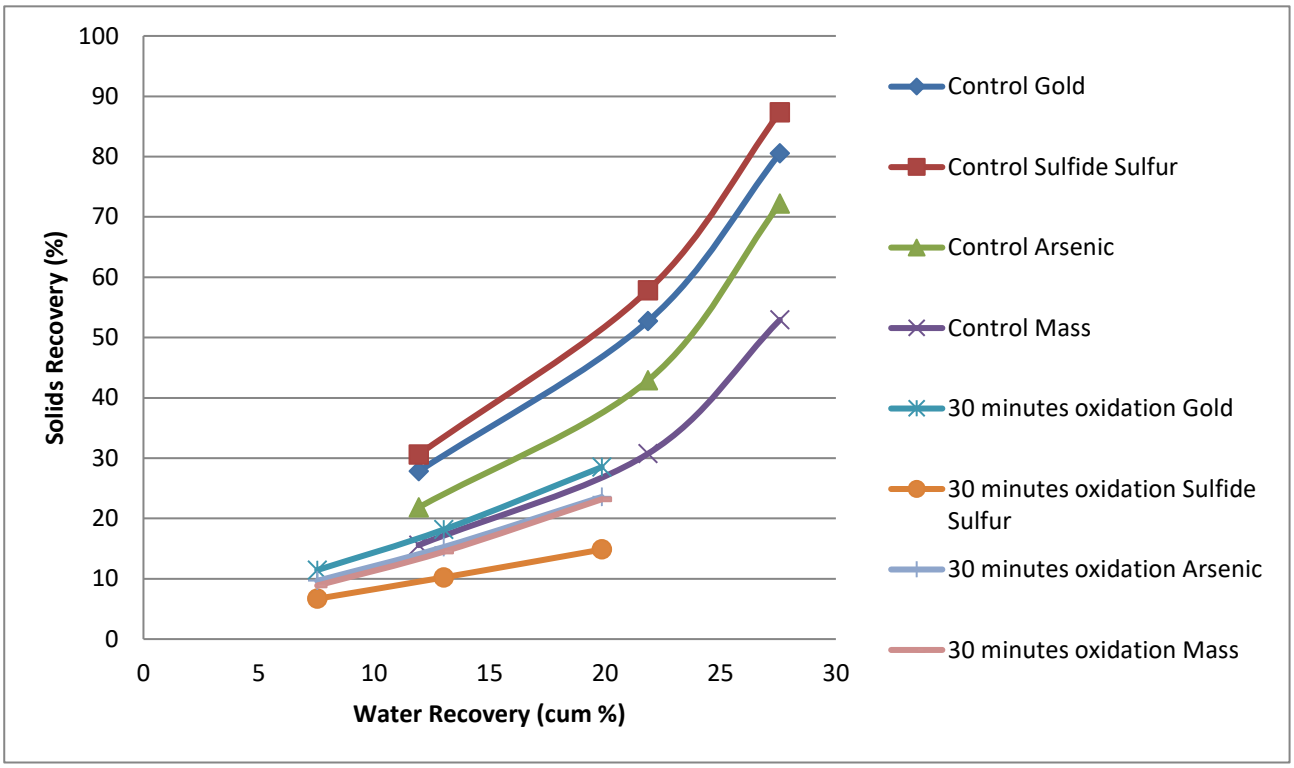

Figure 8.33: Water and solids recovery of control and 30 minutes acid conditioned samples

Similar trends are also observed with 30 minutes and 40 minutes treatment as shown Figures 8.33 and 8.34 respectively. All the three concentrate points with 30 minutes conditioning suggest true flotation occurring for every species plotted again with gold being faster floating than As and S^{2-}. Similar is the case with 40 minutes conditioning as well.

These results suggest that the sulfides are not totally depressed, however, the recovery is not completely governed by entrainment. Sulfides are in a form that is floating and is being recovered similar to hydrophobic particles by true flotation probably due to the chemical state of the oxidised species.

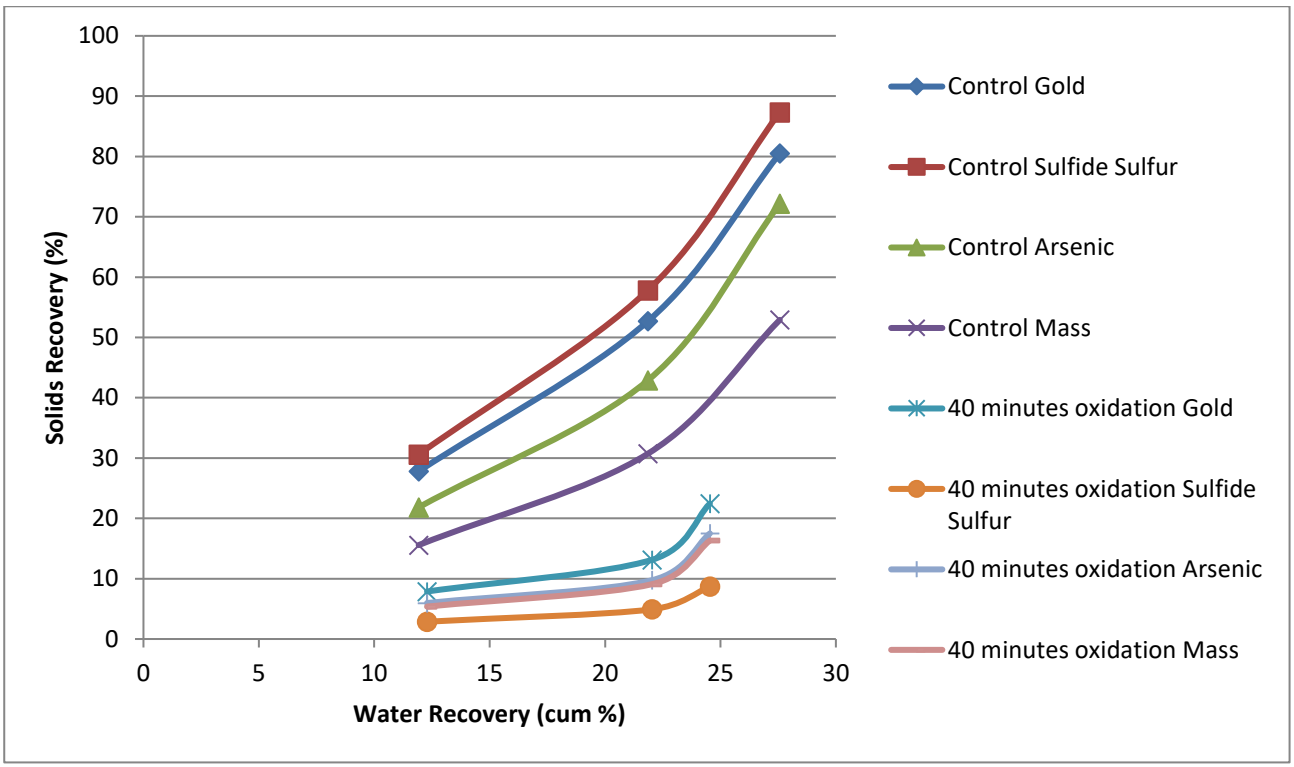

Figure 8.34: Water and solids recovery of control and 40 minutes acid conditioned samples

8.3. Conclusions

1. The principal mechanism suggested for the floatability of the pyrite at an alkaline pH is copper ion activation.

2. Two phases are formed after pyrite modification by sulfuric acid media: an active pyrite phase and a passive pyrite phase. The active pyrite phase has a hydrophobic nature while the passive pyrite remains depressed in the flotation process.

3. True flotation and entrainment are the two most important mechanisms suggested for the floatability of the active pyrite phase.

4. Low flotation recoveries were observed with conditioned samples. However, the logic behind this work was to minimise the sulfide sulfur grade of the final pyrite concentrate and upgrade the Au:S value of the autoclave feed. This has been successfully achieved using standard hydrometallurgical conditions.

5. The established acidic conditions have upgraded the Au:S values by 62.5, 83.3, 125.0 and 162.5 % for corresponding conditioning times of 10, 20, 30 and 40 minutes. A similar

upgrade was also observed with Au:As values establishing the fact that the oxidation rates of pyrite vary based on their gold and arsenic tenor.

6. There are multiple variables that affect oxidation; however, being a moderate oxidation study only the duration and extent of oxidation were considered. This is because the Eh-pH of the sulfuric acid system did not prove amenable to manipulation due to the short duration of conditioning. While the effect of gold recovery may be a function of oxidation time, the effects of the Au:S ratio shown in this work should be valid and valuable to the gold industry.

8.4. Bibliography

ADAMS, M. 2005. Advances in gold ore processing, Vol.15. *Elsevier Science*. ISBN: 0-444-51730-8.

AHERN, N., 2005. Thiosulfate Degradation During Gold Leaching in Ammoniacal Thiosulfate Solutions: A Focus on Trithionate. Ph.D. Thesis. The University of British Columbia.

BRUNAUER, S., EMMETT, P. H. & TELLER, E. 1938. Adsorption of gases in multimolecular layers. *Journal of the American Chemical Society,* 60**,** 309-319.

BUCKLEY, A. & WOODS, R. 1987. The surface oxidation of pyrite. *Applied Surface Science,* 27**,** 437-452.

CHANDRA, A. & GERSON, A. 2009. A review of the fundamental studies of the copper activation mechanisms for the selective flotation of the sulfide minerals, sphalerite and pyrite. *Advances in Colloid and Interface Science,* 145**,** 97-110.

CHEN, X., PENG, Y. & BRADSHAW, D. 2013. Effect of regrinding conditions on pyrite flotation in the presence of copper ions. *International journal of mineral processing,* 125**,** 129-136.

CHEN, X., PENG, Y. & BRADSHAW, D. 2014. The separation of chalcopyrite and chalcocite from pyrite in cleaner flotation after regrinding. *Minerals Engineering,* 58**,** 64-72.

CHEPUSHTANOVA, T. & LUGANOV, V. 2007. Processing of the Pyrite Concentrates to Generate Sulfurous Anhydride for Sulfuric Acid Production. *Journal of Minerals & Materials Characterization & Engineering,* 6**,** 103-108.

CHINCHÓN-PAYÁ, S., AGUADO, A. & CHINCHÓN, S. 2012. A comparative investigation of the degradation of pyrite and pyrrhotite under simulated laboratory conditions. *Engineering Geology,* 127**,** 75-80.

COLLINS, M., BEREZOWSKY, R., VARDILL, W., KETCHAM, V. & STOJSIC, A. The Lihir Gold project: pressure oxidation process development. IV International Symposium on Hydrometallurgy, Salt Lake City, UT (August 1993), 1993.

DICHMANN, T. K. & FINCH, J. 2001. The role of copper ions in sphalerite-pyrite flotation selectivity. *Minerals Engineering,* 14**,** 217-225.

DREISINGER, D. 2006. Copper leaching from primary sulfides: Options for biological and chemical extraction of copper. *Hydrometallurgy*, *83*(1), 10-20.

EGGLESTON, C. M., EHRHARDT, J.-J. & STUMM, W. 1996. Surface structural controls on pyrite oxidation kinetics: An XPS-UPS, STM, and modelling study. *American Mineralogist,* 81**,** 1036-1056.

EKMEKÇI, Z. & DEMIREL, H. 1997. Effects of galvanic interaction on collectorless flotation behaviour of chalcopyrite and pyrite. *International journal of mineral processing,* 52**,** 31-48.

FINKELSTEIN, N. 1997. The activation of sulfide minerals for flotation: a review. *International journal of mineral processing,* 52**,** 81-120.

FLEMING, C. 1992. Hydrometallurgy of precious metals recovery. *Hydrometallurgy,* 30**,** 127-162.

JOHN, J., JOHNSON, N., STEWART, K., TURNER, D. & BRADSHAW, D. A review of pretreatment methods to separate the different types of pyrites in gold processing. 5th World Gold 2013 Conference, 2013. AusIMM: Australasian Institute of Mining and Metallurgy, 347-355.

KETCHAM, V., O'REILLY, J. & VARDILL, W. 1993. The Lihir gold project; Process plant design. *Minerals Engineering,* 6**,** 1037-1065.

KLEINJAN, WILFRED E., DE KEIZER, ARIE, JANSSEN, ALBERT J.H., 2005. Kinetics of the chemical oxidation of polysulfide anions in aqueous solution. Water Res. 39, 4093–4100.

KING, J. & KNIGHT, D. 1992. Autoclave operations at Porgera. *Hydrometallurgy,* 29**,** 493-511.

LAMB, W. 2004. Optimising the value of the Lihir low-grade resource. Rio Tinto Technical Report No: AR2163. Project Code: GAL 144.

LEPPINEN, J., BASILIO, C. & YOON, R. 1988. FTIR study of thionocarbamate adsorption on sulfide minerals. *Colloids and surfaces,* 32**,** 113-125.

LONG, H. & DIXON, D. G. 2004. Pressure oxidation of pyrite in sulfuric acid media: a kinetic study. *Hydrometallurgy,* 73**,** 335-349.

MARCHBANK, A. R., THOMAS, K. G., DREISINGER, D. & FLEMING, C. 1996. Gold recovery from refractory carbonaceous ores by pressure oxidation and thiosulfate leaching. U.S. Patent No. 5,536,297. Washington, DC: U.S. Patent and Trademark Office.

MARSDEN, J. & HOUSE, I. 2006. *The chemistry of gold extraction*, SME. Littleton, Colorado, USA ISBN-13: 978-0-87335-240-6 ISBN-10: 0-87335-240-8

MASON, P. 1992. Examining the economics of some pressure oxidation process options. *Hydrometallurgy,* 29**,** 479-492.

MELASHVILI, M., FLEMING, C., DYMOV, I., MATTHEWS, D., & DREISINGER, D. 2015. Equation for thiosulfate yield during pyrite oxidation. *Minerals Engineering*, *74*, 105-111.

MERMILLOD-BLONDIN, R., KONGOLO, M., DE DONATO, P., BENZAAZOUA, M., BARRÈS, O., BUSSIÈRE, B. & AUBERTIN, M. Pyrite flotation with xanthate under alkaline conditions-application to environmental desulfurization. Proc. of the Centenary of Flotation Symposium, Brisbane, QLD, 2005.

OWUSU, C., E ABREU, S. B., SKINNER, W., ADDAI-MENSAH, J. & ZANIN, M. 2014. The influence of pyrite content on the flotation of chalcopyrite/pyrite mixtures. *Minerals Engineering,* 55**,** 87-95.

PENG, Y. & GRANO, S. 2010. Effect of iron contamination from grinding media on the flotation of sulfide minerals of different particle size. *International journal of mineral processing,* 97**,** 1-6.

PENG, Y., GRANO, S., FORNASIERO, D. & RALSTON, J. 2003. Control of grinding conditions in the flotation of chalcopyrite and its separation from pyrite. *International journal of mineral processing,* 69**,** 87-100.

PIETRZAK, R., GRZYBEK, T. & WACHOWSKA, H. 2007. XPS study of pyrite-free coals subjected to different oxidising agents. *Fuel,* 86**,** 2616-2624.

RANKIN, W. J. 2013. *New flagship AusIMM Monograph: Australasian mining and metallurgical operating practices*. (The Sir Maurice Mawby Memorial Volume), Third Edition.

RIMSTIDT, J. D. & VAUGHAN, D. J. 2003. Pyrite oxidation: a state-of-the-art assessment of the reaction mechanism. *Geochimica et Cosmochimica Acta,* 67**,** 873-880.

SENIOR, G. & TRAHAR, W. 1991. The influence of metal hydroxides and collector on the flotation of chalcopyrite. *International journal of mineral processing,* 33**,** 321-341.

SHEN, W. Z., FORNASIERO, D. & RALSTON, J. 2001. Flotation of sphalerite and pyrite in the presence of sodium sulfide. *International journal of mineral processing,* 63**,** 17-28.

SMART, R. S. C. 1991. Surface layers in base metal sulfide flotation. *Minerals Engineering,* 4**,** 891-909.

SOKIĆ, M. D., MARKOVIĆ, B. & ŽIVKOVIĆ, D. 2009. Kinetics of chalcopyrite leaching by sodium nitrate in sulfuric acid. *Hydrometallurgy,* 95**,** 273-279.

STEWART, P. 2010. Floatation plant optimisation: a metallurgical guide to identifying and solving problems in flotation plants. *Mineral Processing and Extractive Metallurgy,* 119**,** 247-247.

THOMAS, K. G. 1991. Alkaline and acidic autoclaving of refractory gold ores. *JOM,* 43**,** 16-19.

THOMAS, K. G., PIETERSE, H. J., BREWER, R. E. & FRASER, K. S. 1991. Process for recovery of gold from refractory ores. U.S. Patent No 5071477 A. Washington, DC: U.S. Patent and Trademark Office.

YIANATOS, J., CONTRERAS, F., DÍAZ, F. & VILLANUEVA, A. 2009. Direct measurement of entrainment in large flotation cells. *Powder Technology,* 189**,** 42-47.

ZACHWIEJA, J. B., MCCARRON, J. J., WALKER, G. W. & BUCKLEY, A. N. 1989. Correlation between the surface composition and collectorless flotation of chalcopyrite. *Journal of colloid and*

interface science, 132**,** 462-468.

ZHANG, Q., XU, Z., BOZKURT, V. & FINCH, J. 1997. Pyrite flotation in the presence of metal ions and sphalerite. *International journal of mineral processing,* 52**,** 187-201.

ZHANG, H., DREISINGER, D.B., 2002. The kinetics for the decomposition of tetrathionate in alkaline solutions. Hydrometallurgy 66, 59–65.

CHAPTER 9

Process Implications of the Potential Process System

The practical relevance of this thesis work to maximise the autoclave throughput at Lihir has been discussed in Chapter 1. Therefore, this chapter discusses the various aspects that are likely to be encountered in the industrial implementation of the oxidation and one stage cleaner flotation process developed as a part of this work.

9.1 Elemental Sulfur

A major concern regarding the oxidation of pyrite is the production of elemental sulfur (Hiskey et al., 1982). This is because layers of elemental sulfur can interfere with the oxidation of sulfides resulting in unreacted sulfides (*in this case pyrite*). A minimum temperature of 195 ^{o}C is required to eliminate elemental sulfur (Flatt and Woods, 1995) and considering the oxidation process in this thesis is performed at ambient temperature (*20 to 23 ^{o}C*), it is possible that accumulation of elemental sulfur could inhibit the oxidation of the various pyrite types and cause deposition issues in the autoclave. Nevertheless, considering the short residence times associated with the oxidation process, it is less likely that extent of elemental sulfur formation is high enough to complicate the autoclave system.

9.2 Operating window

The differences in Au:S values with varying oxidation times and the extent of oxidation (*seen in Chapters 7 and 8*) reveal that oxidising a pyrite concentrate to upgrade the Au:S value is pinned by a sensitive oxidation window. Operating Eh, pH and the resulting extent of oxidation (*SOx*) are therefore the key variables in the preferential oxidation and subsequent separation of high gold pyrite. Thus, in the case of nitric acid oxidation, a pH and Eh range of 1.20 to 1.26 and 0.58 to 0.53 V (*vs.SHE*) respectively yielded the highest Au:S values. These values change with sulfuric acid oxidation with a pH and Eh range of 1.12 to 0.88 and 0.45 to 0.50 V (*vs.SHE*) respectively yielding the highest Au:S values (*above 0.55*). Since electrochemical experimentation is a crucial part of

hydrometallurgical investigations, it might be beneficial to seek the advice of experienced electrochemists to evaluate the mechanism involved in the oxidation system developed in this work.

There is also a rigid correlation between SOx and the Au:S values. A SOx value of 25% oxidation of pyrite concentrates by nitric acid resulted in an Au:S value of 0.66 for a gold recovery of ~55%. However, it is a different story with sulfuric acid oxidation. High Au:S values of 0.63 were observed for a SOx value of 13% oxidation but at the expense of gold recoveries (*~23%*). Therefore, to significantly upgrade the Au:S values without much compromise in gold recoveries, operating within the sensitive pH, Eh and SOx range is critical. Although all these parameters were closely monitored and reinforced during the laboratory scale oxidation tests, the necessary industrial scale practice can be challenging where multiple factors can come into play and interfere with the oxidation process. An example could be that an extended residence time in an oxidation reactor can completely destroy the sulfides resulting in no preferential separation.

9.3 Advanced Argillic ore samples

The tests in this thesis have only been conducted on the AA ore samples. Therefore, the application of the oxidation process developed/used in this work needs to be tested with other ore samples. Working with other ore types from Lihir might lead to metallurgical trends contrary to (*better results or not so encouraging*) those seen in this work.

9.4 Washing of oxidised concentrates

Washing of oxidised concentrates was performed prior to the cleaner flotation step to minimise/nullify further oxidation and remove traces of sulfates and hydroxides which may otherwise have interfered with the metallurgical responses. The washing process was monitored by regular pH testing of the washings and continued till neutral readings were obtained (*pH 7*). However, in a plant design, continuous monitoring and attention would be required to ensure adequate washing of the oxidised concentrates which could otherwise raise the reagent costs and yield unsatisfactory metallurgical results.

9.5 Temperature dependence

Temperature is a critical factor in hydrometallurgical oxidation techniques that significantly affect the pyrite oxidation kinetics. In this test work, no temperature controls were enforced and oxidation tests were performed at ambient temperature *(accepted the resulting temperature ~23 ^{o}C)*. Although Lihir has a hot and humid climate with average temperatures ranging between 19 and 35 ^{o}C, similar to Brisbane, care will be required to ensure optimum conditions are being used.

9.6 Total System Considerations

It is noteworthy to mention that the current process circuit at Lihir does not include a cleaner flotation stage nor regrinding stage. A simplified flow diagram is shown in Figure 9.1.

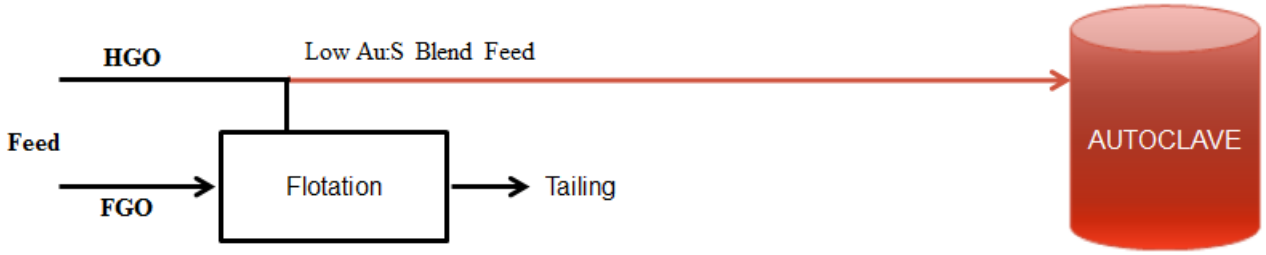

Figure 9. 1: Generalised process circuit at Lihir

The potential implications that could arise from incorporating a cleaner flotation step and regrinding as shown in Figure 9.2 are well beyond the scope of this thesis.

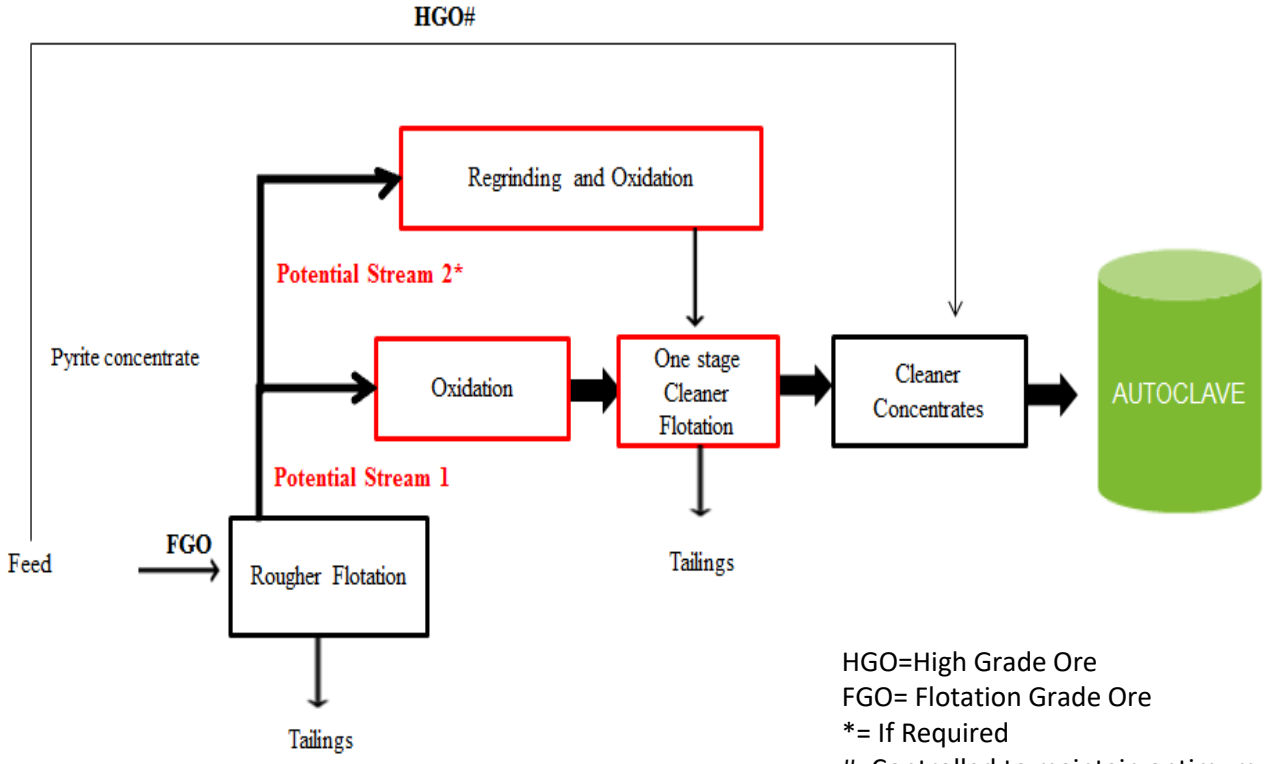

Figure 9. 2: Potential process circuit proposed to upgrade the Au:S Ratio at Lihir

9.7 Metal recoveries vs. Au:S

Although upgrades in Au:S values (*especially with nitric acid oxidation*) were very encouraging, compromises in gold recoveries were observed. Therefore, while process economics are outside the scope of the project, upgrades in Au:S values vs. gold recoveries should be costed. This is critical because, as seen in Chapter 7, high Au:S values were obtained for a gold recovery of almost 55%. This suggests that the remaining 45% of the gold in the tailings (*low Au:S*) would have to be processed further probably by a much more vigorous oxidation process (*compared to the process in this thesis*) such as leaching in the Albion process to release the gold. This also helps to prevent further thermal throttling issues in the autoclave caused by processing low Au:S feed blends (*HGO and FGO*).

9.8 Nitric Acid vs. Sulfuric Acid Treatment

The sole objective of this work was to produce a low sulfide sulfur and relatively high gold concentrate as an autoclave feed by oxidising the bulk of the sulfide sulfur to overcome the fixed sulfide oxidation capacity constraint of the Lihir autoclave. This was successfully achieved by nitric acid oxidation of pyrite, with its origins from hydrometallurgical practice, resulting in significant

upgrades of Au:S values of the final flotation concentrate. However, sulfuric acid treatment yielded comparatively lower Au:S values for substantially lower gold recoveries and this is shown in Table 9.1.

Table 9. 1: Metallurgical responses of nitric acid and sulfuric acid oxidised samples floated at pH 11. Best results (*in terms of Au:S Ratio*) within both systems are highlighted.

Oxidation			**Metallurgical Response**		
Reagent	**Sample**	**SOx (%)**	**Gold Recovery (%)**	**Sulfide Sulfur Recovery (%)**	**Au:S Ratio**
None	Control*	0	87.5	87.1	0.27
HNO_3	10	13.7	78.8	84.2	0.26
HNO_3	20	17.3	75.4	69.0	0.33
HNO_3	30	21.9	68.5	70.4	0.34
HNO_3	40	22.9	57.4	55.6	0.42
HNO_3	50	24.3	56.6	31.5	0.60
HNO_3 Best Result	**60**	**25.0**	**56.3**	**24.0**	**0.66**
HNO_3	70	26.0	54.6	23.1	0.36
H_2SO_4	10	3.9	54.9	35.0	0.39
H_2SO_4	20	8.3	43.3	27.0	0.44
H_2SO_4	30	10.1	28.5	14.8	0.54
H_2SO_4 Best Result	**40**	**13.3**	**22.4**	**8.7**	**0.63**

9.9 References

FLATT, J. & WOODS, R. 1995. A Voltammetric Investigation Of The Oxidation Of Pyrite In Nitric Acid Solutions: Relation To Treatment Of Refractory Gold Ores. *Journal Of Applied Electrochemistry,* 25**,** 852-856.

HISKEY, J., SCHLITT, W. & JACKSON, J. Aqueous Oxidation Of Pyrite In Situ, 1982. Marcel Dekker Inc 270 Madison Ave, New York, NY 10016, 59-59.

CHAPTER 10

Conclusions and Recommendations

10.1 Conclusions

1. The refractory AA ore from the Kapit mineralised area of the Lihir deposit was the sample of interest in this study. This is because the AA ore sample contained a wide range of pyrite types and a high sulfide sulfur grade. Comprehensive gold and arsenic deportment studies using LA-ICPMS confirmed the variable gold tenor in the various pyrite types.

2. The effect of acid media (*HNO_3 and H_2SO_4*) on high arsenic and low arsenic pyrite**,** using BSE images from an SEM-based automated mineralogy system, confirmed the different rates of oxidation of the various pyrite types. The degree of pyrite oxidation was found to be greater when As was present in the interstitial lattice site proving that high arsenic pyrite (*possibly high gold pyrite*) oxidised at a relatively faster rate compared to low As pyrite (*possibly low gold pyrite*).

3. The Influence of Lime and NaOH Conditioning on Sulfide Sulfur in Pyrite Flotation was investigated. Although it was found that the pyrite concentrate after NaOH treatment had less sulfide sulfur compared to lime treatment, there was more mass to be treated.

4. The high Au:S values of the nitric acid oxidised concentrates compared to the untreated concentrates established definite evidence that hydrometallurgical oxidising conditions could be utilised to separate the low gold pyrite from the gold rich pyrite. The low sulfide sulfur and mass recoveries but relatively high gold recoveries with the oxidised concentrates suggested that only the high gold pyrite species was reporting to the concentrate post oxidation. A significant decline in gold recoveries revealed that a perfect separation of the high gold pyrite from the low gold pyrite types was not likely to be achieved due to the presence of many pyrite textures in the AA ore that represent part of a morphological and compositional continuum between the high gold and low gold pyrite types.

5. Differences in the Au:S values observed with different stages of nitric acid oxidation revealed that the outcome was sensitive to the oxidation level (*for separating one type of pyrite from another*). The 50 minutes and 60 minutes oxidised concentrates displayed the best results with 122% and 145% increase in Au:S values respectively (*Au:S values of 0.60 and 0.66*). Interestingly, the Au:S ratio decreased with 70 minutes oxidation suggesting that the extent of oxidation dictated the pyrite separation behaviour in the following cleaner flotation process. Hence, from a SOx point of view, a moderate oxidation of approximately 25% SOx was found to be the optimum oxidation level for separation of the various pyrite types in an AA ore.

6. Fine grinding of the concentrate samples increased the rate of oxidation of the pyrite concentrate and this was confirmed by BET, SOx and XPS analysis. A significant upgrade of Au:S ratios was observed with samples after regrinding and oxidation as compared to non-regrind samples. However, accelerated oxidation rates due to mechanical reduction did not differentiate the high gold and low gold pyrite resulting in no significant upgrade of Au:S ratios compared to normal concentrates that were oxidised without regrinding.

7. Sulfuric acid conditioning of the pyrite concentrate resulted in SOx values of up to 13% oxidation for the 40 minutes oxidised concentrate yielding a high Au:S value of 0.63 and extremely low gold recovery of 22.5%.

8. Comparing the metallurgical responses of the nitric acid and sulfuric acid conditioned samples, nitric acid treatment displayed better results. Although sulfuric acid might be a better processing agent from the perspective of reagent costs, substantial differences in the Au:S values and gold recoveries suggest that nitric acid is a better oxidising agent to suit the purpose of this study.

10.2 Recommendations

1) This thesis investigation has been conducted only on the advanced argillic ore sample. However, considering the current problems encountered at Lihir due to high sulfide sulfur grades, it would be valuable to investigate the effect of oxidation in mitigating the autoclave bottleneck issues posed with other ores.

2) MLA software: Fine tuning of the MLA software suite is an excellent postgraduate project to differentiate the high gold and low gold pyrite.

3) Electrochemical investigations: If the electrochemical responses of the various pyrite types can be developed, these responses can be utilised as a diagnostic tool to confirm the nature of cleaner concentrates and tailings post oxidation. Such work would include constructing electrodes with high and low gold pyrite types.

4) From a processing perspective, replacement of lime with NaOH cannot be justified and recommended for Lihir. This is mainly because the easy availability and economic factors of lime procurement outweighed the advantages of the difference in Au:S ratios between NaOH and lime. However, the technical finding from this chapter might be of relevant interest to other mine sites.

5) Flotation Reagents: The use of different flotation reagents should be tested in the one step cleaner flotation stage to selectively depress the low gold pyrite and activate the high gold pyrite. This is because the standard collector used at Lihir and in this work (*PAX*) is a non-selective sulfide collector.

6) Oxidised species: Understanding the nature of the oxidised pyrite species is a topic of interest from a scientific point of view. Although preliminary elemental mapping by MLA was undertaken in this work, it could not be pursued further due to time limitations. Understanding the oxidised species would aid the establishment of the floatable characteristics of the oxidised pyrite vs. unoxidised pyrite and explain the complex mechanisms that are involved.

7) Regrinding: The proposition from Lihir confidential reports and Newcrest personnel that the blockier, low gold pyrite is “more resistant” to regrinding compared to the gold rich pyrite is worthwhile pursing further.

8) Cleaner step conditions: Cleaner step conditions post regrinding could be investigated and optimised further to reflect better Au:S values compared to those obtained in this thesis. This includes trying other flotation agents and opting for longer conditioning times.

9) Sulfuric acid may appear to be a better candidate for preferential separation of the gold-rich and low gold pyrite types from the perspective of reagent costs, however, metallurgical test work suggests that further optimisation such as controlling oxygen levels during the etching process is required. This is because sulfuric acid is not an oxidising acid *per se* (*except at very high concentrations*) and it is the oxygen and ferric ions that are the usual oxidants for sulfides in acid sulfate media.

10) The aim of the thesis was to modify the surface properties of the different gold-bearing pyrite minerals so as to promote differential flotation in order to separate the high-gold pyrite from the low-gold pyrite types. However, the extent of oxidation required to promote a high Au:S ratio in the final concentrate was significant (*15-25 % sulfide oxidation*) and this poses the question of the process economics of this approach. Considering that the upgraded product is intended as a feedstock to the autoclave, the degree of oxidation required will involve some capital and reagent/processing costs and this may have an impact on the overall operating costs of the gold recovery circuit. Whether any additional cost(s) of the new circuit modification and operation is offset by improved gold recovery or lower downstream costs should be further investigated and costed.

11) The treatment of the barren flotation water containing nitrates (*as a consequence of sulfide oxidation*) and regeneration of the excess acid (*nitric and sulfuric acid*) from the pre-treatment stage is a potential Master's thesis.

APPENDIX

Appendix 1: Mineralogical Data

1.1 Elemental composition of the AA ore

Au (ppm)	As (ppm)	S_{total} (%)	$S_{sulfide}$ (%)	Fe (%)	Cu (ppm)
3.6	**500**	**14.4**	**13.9**	**9.9**	**167**

1.2 Elemental Assay of the Mill Feed

Bulk	Au (ppm)	As (ppm)	S_{total} (%)	$S_{sulfide}$ (%)	Fe (%)	Cu (ppm)	C %	C inorganic	C organic
-850+425	**3.65**	**510**	**14.4**	**13.9**	**9.9**	**171**	**0.1**	**0.03**	**0.11**

1.3 Simplified MLA Mineralogy

Mineral	NTS37
Pyrite	34.48
Other sulfides	0.03
Fe (Ti) oxides	0.01
Rutile	0.20
Quartz	1.39
K-Feldspar	30.88
Plagioclase Gp	0.03
Hornblende	0.00
Biotite	0.23
Muscovite Group	3.15
Chlorite/smectite	0.00
Kaolinite	7.73
Illite/Smectite	5.89
Montmorillonite	4.80
Calcite	0.00
Mn-bearing carbonates	0.00
Anhydrite	0.02
Alunite	9.73
Barite (Sr & high Sr)	0.49
Apatite & Trolleite	0.12
Jarosite	0.44
Leucoxene	0.37
Other minerals	0.01
Total	**100.00**

1.4 Laser Ablation Images

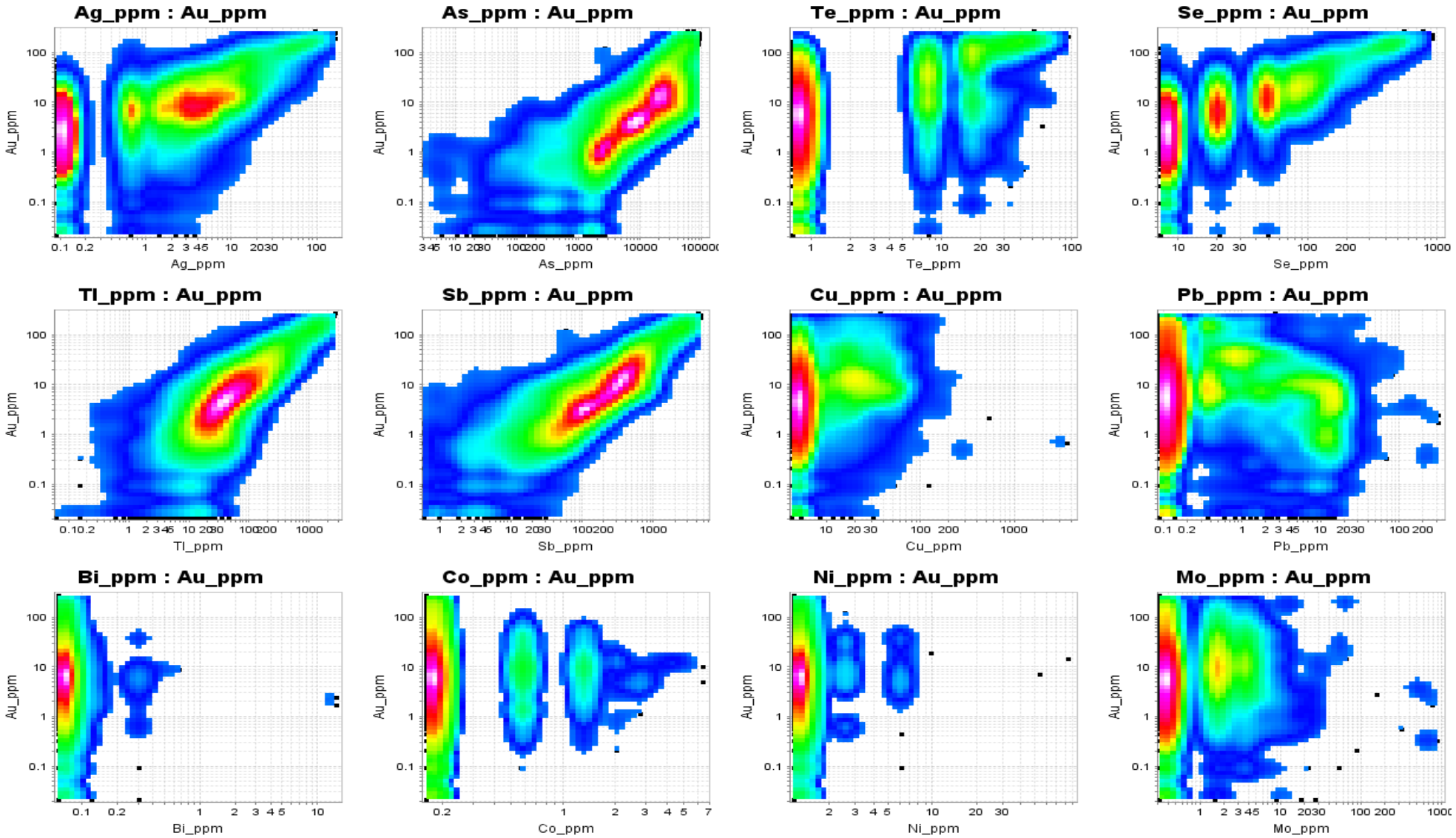

1.5 Laser Ablation Plots

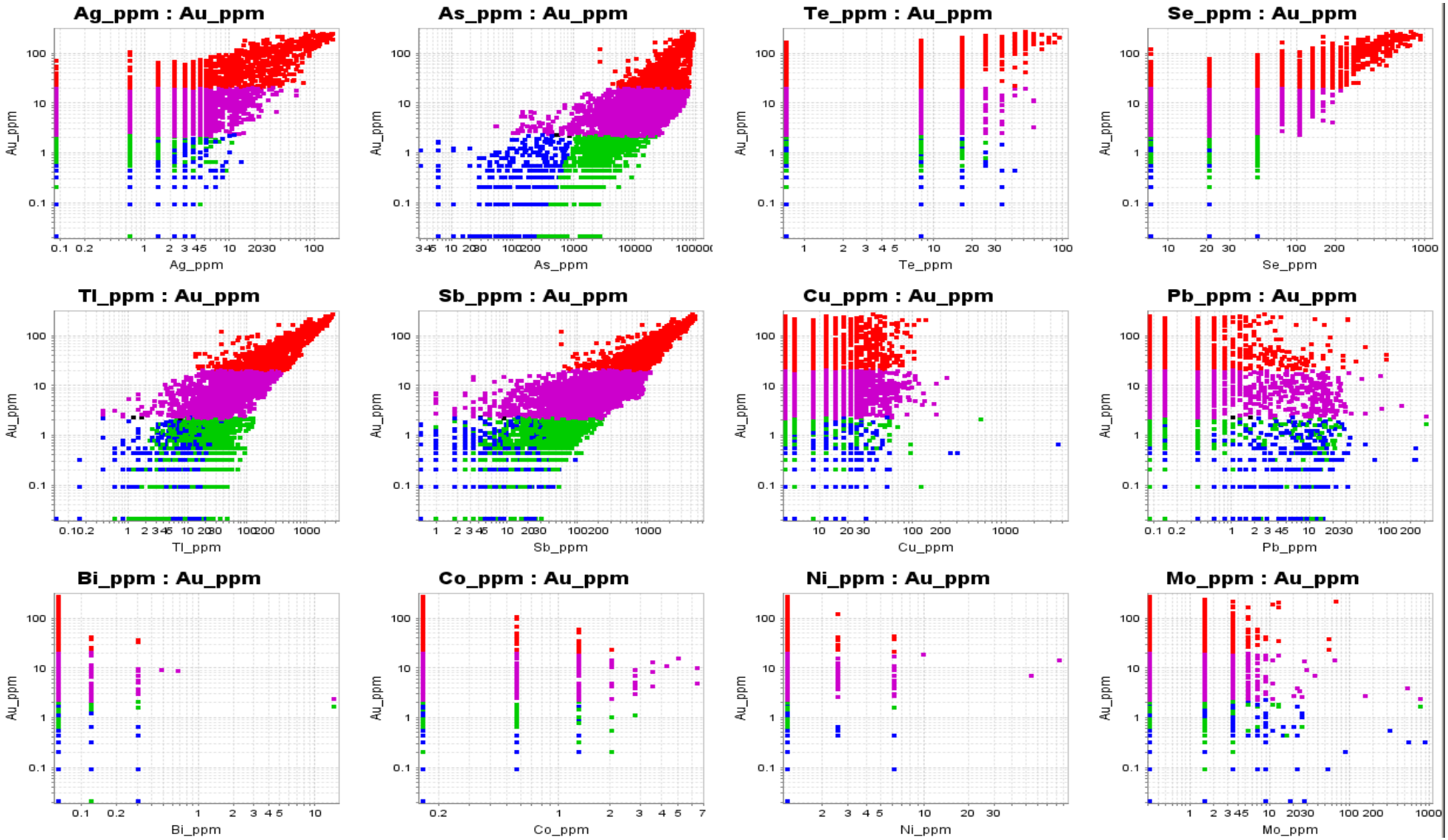

1.6 Gold Solubility in Pyrite

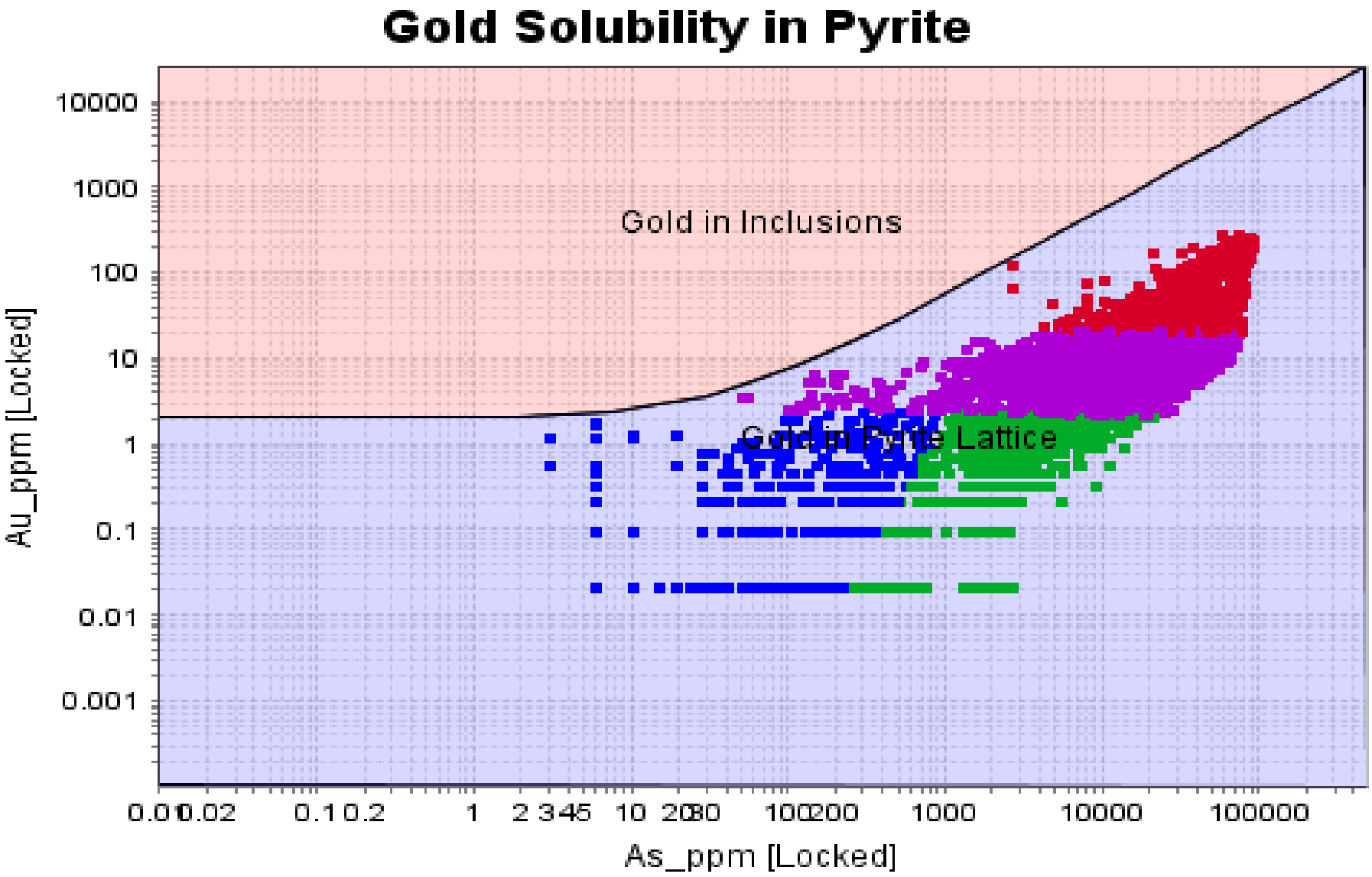

Appendix 2: Rougher Flotation Optimisation Data

Natural pH	Gold Grade (g/t)			Gold Recovery (%)			Sulfide Sulfur Grade (%)			Sulfide Sulfur Recovery (%)			Arsenic Grade (ppm)			Arsenic Recovery (%)		
	Test 1	Test 2	Test 3	Test 1	Test 2	Test 3	Test 1	Test 2	Test 3	Test 1	Test 2	Test 3	Test 1	Test 2	Test 3	Test 1	Test 2	Test 3
Rougher 1	12.08	13.43	10.59	15.6	17.1	14.0	48.64	59.20	42.46	18.3	21.4	16.3	1764	2180	1665	18.2	21.6	17.3
Rougher 2	11.63	12.93	10.20	11.0	10.8	11.2	48.83	59.43	42.63	13.9	13.3	14.2	1745	2157	1647	14.0	13.4	14.1
Rougher 3	11.35	12.61	9.95	16.3	16.1	16.7	45.73	55.65	39.92	19.7	18.9	20.2	1708	2110	1611	20.8	19.9	21.0
Rougher Tail	2.42	2.69	2.12	57.0	56.1	58.2	6.83	8.31	5.96	48.2	46.3	49.3	236	291	223	47.0	45.1	47.5
				100.0	**100.0**	**100.0**				**100.0**	**100.0**	**100.0**				**100.0**	**100.0**	**100.0**

Tests 3	Natural pH			Gold				Arsenic				Sulfide Sulfur			
				Average		Cumulative		Average		Cumulative		Average		Cumulative	
Product	Mass Recovery (%)	Recovery (%)	Water Recovery (%)	Grade (g/t)	Recovery (%)	Grade (g/t)	Recovery (%)	Grade (g/t)	Recovery (%)	Grade (g/t)	Recovery (%)	Grade (%)	Recovery (%)	Grade (%)	Recovery (%)
Con 1	4.7	4.7	3.1	12.0	15.6	12.0	15.6	1870.0	19.1	1870.0	19.1	54.7	18.2	54.7	18.2
Con 2	3.5	8.2	6.2	11.6	11.0	11.8	26.6	1850.0	13.8	1861.5	32.9	54.7	13.4	54.7	31.6
Con 3	5.3	13.5	11.1	11.3	16.3	11.6	43.0	1810.0	20.6	1841.4	53.5	52.2	19.4	53.7	51.0
Feed	86.5	**100.0**	**100.0**	2.4	57	2.4	**100.0**	250.0	46.5	537.9	**100.0**	7.03	49	7.03	**100.0**

pH 5	Gold Grade (g/t)			Gold Recovery (%)			Sulfide Sulfur Grade (%)			Sulfide Sulfur Recovery (%)			Arsenic Grade (ppm)			Arsenic Recovery (%)		
	Test 1	Test 2	Test 3	Test 1	Test 2	Test 3	Test 1	Test 2	Test 3	Test 1	Test 2	Test 3	Test 1	Test 2	Test 3	Test 1	Test 2	Test 3
Rougher 1	9.90	11.30	10.09	56.7	59.9	57.1	42.37	49.47	42.28	59.1	62.8	59.0	1618	2000	1527	54.2	59.4	52.8
Rougher 2	8.13	9.27	8.28	14.2	13.1	14.0	42.75	49.91	42.65	17.3	15.7	17.3	1557	1924	1469	16.0	14.2	16.5
Rougher 3	6.28	7.16	6.39	10.7	9.9	10.6	26.54	30.98	26.48	10.4	9.5	10.5	1217	1504	1148	12.2	10.8	12.6
Rougher Tail	1.08	1.24	1.10	18.5	17.1	18.3	3.35	3.91	3.34	13.2	12.0	13.2	175	216	165	17.5	15.5	18.1
				100.0	**100.0**	**100.0**				**100.0**	**100.0**	**100.0**				**100.0**	**100.0**	**100.0**

Tests 3	pH 5			Gold				Arsenic				Sulfide Sulfur			
				Average		Cumulative		Average		Cumulative		Average		Cumulative	
Product	Mass Recovery (%)	Recovery (%)	Water Recovery (%)	Grade (g/t)	Recovery (%)	Grade (g/t)	Recovery (%)	Grade (g/t)	Recovery (%)	Grade (g/t)	Recovery (%)	Grade (%)	Recovery (%)	Grade (%)	Recovery (%)
Con 1	22.7	22.7	10.3	10.4	57.9	10.4	57.9	1715.0	55.7	1715.0	55.7	55.4	62.0	55.4	62.0
Con 2	6.6	29.3	21.4	8.6	13.8	10.0	71.7	1650.0	15.5	1700.4	71.2	41.0	13.3	52.2	75.3
Con 3	6.4	35.7	43.9	6.6	10.4	9.4	82.0	1290.0	11.8	1626.8	83.0	28.3	8.9	47.9	84.3
Feed	22.7	64.3	**100.0**	1.14	17.9	1.14	**100.0**	185.0	17	1715.0	**100.0**	3.53	15.7	3.53	**100.0**

pH 7	Gold Grade (g/t)			Gold Recovery (%)			Sulfide Sulfur Grade (%)			Sulfide Sulfur Recovery (%)			Arsenic Grade (ppm)			Arsenic Recovery (%)		
	Test 1	Test 2	Test 3	Test 1	Test 2	Test 3	Test 1	Test 2	Test 3	Test 1	Test 2	Test 3	Test 1	Test 2	Test 3	Test 1	Test 2	Test 3
Rougher 1	9.57	10.92	9.75	35.5	38.6	35.9	34.48	41.96	30.09	42.7	47.6	39.4	908	1046	861	37.6	41.0	36.4
Rougher 2	9.35	10.67	9.53	20.7	19.7	20.5	28.84	35.10	25.18	20.8	19.1	22.0	733	844	695	17.8	16.8	18.1
Rougher 3	8.53	9.74	8.70	14.0	13.3	13.9	20.21	24.60	17.64	10.8	9.9	11.4	978	1126	927	17.6	16.6	17.9
Rougher Tail	2.64	3.01	2.69	29.9	28.4	29.7	6.93	8.44	6.05	25.6	23.5	27.1	218	251	206	27.0	25.6	27.6
				100.0	**100.0**	**100.0**				**100.0**	**100.0**	**100.0**				**100.0**	**100.0**	**100.0**

Tests 3	pH 7			Gold				Arsenic				Sulfide Sulfur			
				Average		Cumulative		Average		Cumulative		Average		Cumulative	
Product	Mass Recovery (%)	Recovery (%)	Water Recovery (%)	Grade (g/t)	Recovery (%)	Grade (g/t)	Recovery (%)	Grade (g/t)	Recovery (%)	Grade (g/t)	Recovery (%)	Grade (%)	Recovery (%)	Grade (%)	Recovery (%)
Con 1	18.2	18.2	15.6	10.1	30.8	10.1	30.8	938.0	32.7	938.0	32.7	45.6	37.7	45.6	37.7
Con 2	17.9	36.1	26.3	9.9	29.8	10.0	60.6	757.0	26.1	848.0	58.7	38.5	31.4	42.0	69.1
Con 3	9.1	45.2	35.8	9.0	13.7	9.8	70.7	1010.0	17.6	880.6	73 .3	23.1	9.5	38.2	75.6
Feed	18.2	18.2	**100.0**	2.78	29.3	2.78	**100.0**	225	26.7	225	**100.0**	7.14	24.4	7.14	**100.0**

Appendix 3: Lime and Sodium Hydroxide Flotation Data

LIME 2 mins	Gold Grade (g/t)			Gold Recovery (%)			Sulfide Sulfur Grade (%)			Sulfide Sulfur Recovery (%)			Arsenic Grade (ppm)			Arsenic Recovery (%)		
	Test 1	Test 2	Test 3	Test 1	Test 2	Test 3	Test 1	Test 2	Test 3	Test 1	Test 2	Test 3	Test 1	Test 2	Test 3	Test 1	Test 2	Test 3
Rougher 1	9.61	11.63	9.12	54.1	58.8	52.8	39.56	48.15	34.53	55.8	60.6	52.4	1459	1525	1576	53.6	54.7	55.5
Rougher 2	8.72	10.56	8.28	12.5	11.3	12.9	34.47	41.95	30.08	11.8	10.5	12.7	1286	1344	1389	11.9	11.7	11.4
Rougher 3	7.79	9.44	7.40	11.7	10.5	12.0	33.36	40.60	29.12	11.9	10.6	12.8	1190	1244	1285	11.5	11.2	11.0
Rougher Tail	1.03	1.24	0.97	21.7	19.5	22.3	4.10	4.99	3.58	20.6	18.4	22.2	168	176	181	22.9	22.4	22.0
				100.0	**100.0**	**100.0**				**100.0**	**100.0**	**100.0**				**100.0**	**100.0**	**100.0**

Tests 3	Lime	2 mins	Gold				Arsenic				Sulfide Sulfur				Au:S
			Average		Cumulative		Average		Cumulative		Average		Cumulative		
Product	Mass Recovery (%)	Recovery (%)	Grade (g/t)	Recovery (%)	Grade (g/t)	Recovery (%)	Grade (g/t)	Recovery (%)	Grade (g/t)	Recovery (%)	Grade (%)	Recovery (%)	Grade (%)	Recovery (%)	
Con 1	19.8	19.8	10.1	55.4	10.1	55.4	1520.0	54.7	1890.0	58.2	40.8	55.8	40.8	55.8	**0.25**
Con 2	4.8	24.6	9.2	12.2	9.9	67.6	1340.0	11.7	1832.6	74.6	35.5	11.8	39.7	67.6	**0.25**
Con 3	5.0	29.5	8.2	11.3	9.6	78.9	1240.0	11.2	1741.3	89.3	34.4	11.9	39.2	79.4	**0.25**
Feed	70.5	**100.00**	1.1	21.1	3.6	**100.0**	175.0	22.4	3238.4	**100.0**	4.2	20.6	14.4	**100.0**	**0.25**

LIME 5 mins	Gold Grade (g/t)			Gold Recovery (%)			Sulfide Sulfur Grade (%)			Sulfide Sulfur Recovery (%)			Arsenic Grade (ppm)			Arsenic Recovery (%)		
	Test 1	Test 2	Test 3	Test 1	Test 2	Test 3	Test 1	Test 2	Test 3	Test 1	Test 2	Test 3	Test 1	Test 2	Test 3	Test 1	Test 2	Test 3
Rougher 1	10.96	9.07	10.21	55.6	50.9	53.8	41.54	39.68	42.92	60.0	58.9	60.8	1785	1499	1563	56.7	52.4	53.4
Rougher 2	10.75	8.90	10.02	11.3	12.5	11.8	35.12	33.55	36.28	11.4	11.7	11.2	1812	1522	1588	11.8	12.9	12.6
Rougher 3	9.29	7.70	8.66	11.7	12.9	12.2	29.10	27.80	30.06	11.3	11.6	11.1	1337	1123	1171	10.4	11.4	11.2
Rougher Tail	1.24	1.03	1.16	21.4	23.7	22.3	3.24	3.10	3.35	17.3	17.8	17.0	199	167	174	21.2	23.3	22.8
				100.0	**100.0**	**100.0**				**100.0**	**100.0**	**100.0**				**100.0**	**100.0**	**100.0**

Tests 3	Lime	5 mins	Gold				Arsenic				Sulfide Sulfur				Au:S
			Average		Cumulative		Average		Cumulative		Average		Cumulative		
Product	Mass Recovery (%)	Recovery (%)	Grade (g/t)	Recovery (%)	Grade (g/t)	Recovery (%)	Grade (g/t)	Recovery (%)	Grade (g/t)	Recovery (%)	Grade %)	Recovery (%)	Grade (%)	Recovery (%)	
Con 1	19.2	19.8	10.1	53.5	10.1	53.5	1615.0	54.2	1615.0	54.2	41.4	59.9	41.4	59.9	**0.24**
Con 2	4.3	24.6	9.9	11.8	10.0	65.3	1640.0	12.4	1619.6	66.6	35.0	11.4	40.2	71.3	**0.25**
Con 3	5.2	29.5	8.6	12.2	9.8	77.6	1210.0	11.0	1545.7	77.6	29.0	11.3	38.6	77.7	**0.25**
Feed	71.2	**100.0**	1.1	22.4	3.6	**100.0**	180.0	22.4	572.7	**100.0**	3.2	17.3	13.3	**100.0**	**0.27**

LIME 10 mins	Gold Grade (g/t)			Gold Recovery (%)			Sulfide Sulfur Grade (%)			Sulfide Sulfur Recovery (%)			Arsenic Grade (ppm)			Arsenic Recovery (%)		
	Test 1	Test 2	Test 3	Test 1	Test 2	Test 3	Test 1	Test 2	Test 3	Test 1	Test 2	Test 3	Test 1	Test 2	Test 3	Test 1	Test 2	Test 3
Rougher 1	9.78	10.86	8.57	54.4	57.0	51.1	39.71	48.33	34.66	56.4	61.2	53.1	1486	1836	1402	52.6	57.8	51.2
Rougher 2	8.48	9.42	7.43	10.6	10.0	11.4	36.15	43.99	31.55	11.9	10.6	12.9	1498	1852	1414	12.7	11.3	13.1
Rougher 3	8.06	8.96	7.06	12.1	11.4	12.9	33.69	41.00	29.41	13.3	11.9	14.3	1171	1447	1105	11.9	10.6	12.2
Rougher Tail	1.11	1.24	0.98	22.9	21.6	24.5	3.38	4.11	2.95	18.3	16.3	19.7	164	203	155	22.8	20.3	23.5%
				100.0	**100.0**	**100.0**				**100.0**	**100.0**	**100.0**				**100.0**	**100.0**	**100.0**

Tests 3	Lime	10 mins	Gold				Arsenic				Sulfide Sulfur				Au:S
			Average		Cumulative		Average		Cumulative		Average		Cumulative		
Product	Mass Recovery (%)	Recovery (%)	Grade (g/t)	Recovery (%)	Grade (g/t)	Recovery (%)	Grade (g/t)	Recovery (%)	Grade (g/t)	Recovery (%)	Grade (%)	Recovery (%)	Grade (%)	Recovery (%)	
Con 1	19.2	19.2	9.7	54.3	9.7	54.3	1575.0	54.1	1575.0	54.1	40.9	57.2	40.9	57.2	**0.24**
Con 2	4.3	23.6	9.5	10.6	9.5	65.0	1588.0	12.3	1577.4	66.4	37.2	11.7	40.2	68.9	**0.24**
Con 3	5.2	28.8	9.2	12.1	9.2	77.1	1241.0	11.5	1516.7	77.9	34.7	13.1	39.6	70.4	**0.23**
Feed	71.2	**100.0**	3.4	22.9	3.4	**100.0**	174.0	22.1	560.1	**100.0**	3.5	18.0	13.8	**100.0**	**0.25**

NaOH 2 mins	Gold Grade (g/t)			Gold Recovery (%)			Sulfide Sulfur Grade (%)			Sulfide Sulfur Recovery (%)			Arsenic Grade (ppm)			Arsenic Recovery (%)		
	Test 1	Test 2	Test 3	Test 1	Test 2	Test 3	Test 1	Test 2	Test 3	Test 1	Test 2	Test 3	Test 1	Test 2	Test 3	Test 1	Test 2	Test 3
Rougher 1	9.88	8.89	7.79	68.9	66.6	63.6	36.74	30.42	34.25	73.6	69.8	72.0	1519	1276	1331	69.5	65.7	66.7
Rougher 2	5.43	4.89	4.28	9.4	10.1	11.1	14.67	12.15	13.68	7.5	8.6	8.0	718	603	629	8.3	9.3	9.0
Rougher 3	2.99	2.69	2.36	5.6	6.0	6.6	6.38	5.28	5.95	3.5	4.0	3.8	414	348	363	5.2	5.8	5.6
Rougher Tail	1.24	1.11	0.98	16.0	17.2	18.8	4.01	3.32	3.74	15.3	17.5	16.3	199	167	174	17.1	19.2	18.7
				100.0	**100.0**	**100.0**				**100.0**	**100.0**	**100.0**				**100.0**	**100.0**	**100.0**

Tests 3	NaOH	2 mins	Gold				Arsenic				Sulfide Sulfur				Au:S
			Average		Cumulative		Average		Cumulative		Average		Cumulative		
Product	Mass Recovery (%)	Recovery (%)	Grade (g/t)	Recovery (%)	Grade (g/t)	Recovery (%)	Grade (g/t)	Recovery (%)	Grade (g/t)	Recovery (%)	Grade (%)	Recovery (%)	Grade (%)	Recovery (%)	
Con 1	27.4	27.4	8.9	66.5	8.9	66.5	1375.0	67.4	1375.0	67.4	33.8	72.0	33.8	72.0	**0.26**
Con 2	7.6	35.0	4.9	10.2	8.0	76.7	650.0	8.9	1217.3	76.2	13.5	8.0	29.4	80.0	**0.27**
Con 3	8.2	43.3	2.7	6.0	7.0	82.7	375.0	5.5	1057.1	81.7	5.9	3.8	24.9	83.7	**0.28**
Feed	56.7	**100.0**	1.1	17.3	3.6	**100.0**	180.0	18.3	559.4	**100.0**	3.7	16.3	12.9	**100.0**	**0.28**

NaOH 5 mins	Gold Grade (g/t)			Gold Recovery (%)			Sulfide Sulfur Grade (%)			Sulfide Sulfur Recovery (%)			Arsenic Grade (ppm)			Arsenic Recovery (%)		
	Test 1	Test 2	Test 3	Test 1	Test 2	Test 3	Test 1	Test 2	Test 3	Test 1	Test 2	Test 3	Test 1	Test 2	Test 3	Test 1	Test 2	Test 3
Rougher 1	10.30	9.47	8.56	68.1	66.2	63.9	32.26	30.89	31.06	70.2	69.3	69.7	1407	1360	1299	66.2	65.4	64.4
Rougher 2	5.62	5.17	4.67	9.6	10.1	10.8	13.87	13.28	13.35	8.3	8.5	8.4	753	727	695	9.6	9.8	10.1
Rougher 3	2.89	2.66	2.40	5.0	5.3	5.6	5.22	5.00	5.02	3.1	3.2	3.2	379	366	350	4.9	5.0	5.1
Rougher Tail	1.22	1.12	1.02	17.4	18.4	19.6	3.69	3.53	3.55	18.4	18.9	18.7	182	176	168	19.3	19.8	20.4
				100.0	**100.0**	**100.0**				**100.0**	**100.0**	**100.0**				**100.0**	**100.0**	**100.0**

Tests 3	NaOH	5 mins	Gold				Arsenic				Sulfide Sulfur				Au:S
			Average		Cumulative		Average		Cumulative		Average		Cumulative		
Product	Mass Recovery (%)	Recovery (%)	Grade (g/t)	Recovery (%)	Grade (g/t)	Recovery (%)	Grade (g/t)	Recovery (%)	Grade (g/t)	Recovery (%)	Grade (%)	Recovery (%)	Grade (%)	Recovery (%)	
Con 1	25.6	25.6	9.4	66.2	9.4	66.2	1355.0	65.4	1355.0	65.4	31.4	69.7	31.4	69.7	**0.30**
Con 2	7.2	32.7	5.2	10.1	8.5	76.3	725.0	9.8	1216.7	75.2	13.5	8.4	27.5	78.1	**0.30**
Con 3	7.2	40.0	2.7	5.3	7.4	81.6	365.0	5.0	1062.4	80.2	5.1	3.2	23.4	81.3	**0.31**
Feed	60.0	**100.0**	1.1	18.4	3.6	**100.0**	175.0	19.8	529.8	**100.0**	3.6	18.7	11.5	**100.0**	**0.31**

NaOH 10 mins	Gold Grade (g/t)			Gold Recovery (%)			Sulfide Sulfur Grade (%)			Sulfide Sulfur Recovery (%)			Arsenic Grade (ppm)			Arsenic Recovery (%)		
	Test 1	Test 2	Test 3	Test 1	Test 2	Test 3	Test 1	Test 2	Test 3	Test 1	Test 2	Test 3	Test 1	Test 2	Test 3	Test 1	Test 2	Test 3
Rougher 1	9.04	10.05	7.93	66.6	68.9	63.6	33.65	40.95	29.37	74.1	77.7	71.4	1216	1503	1147	64.4	69.0	63.0
Rougher 2	5.27	5.86	4.62	10.8	10.0	11.7	12.71	15.47	11.09	8.0	6.9	8.8	608	751	573	9.5	8.2	9.8
Rougher 3	3.00	3.33	2.63	6.6	6.2	7.2	6.31	7.68	5.51	4.3	3.7	4.7	331	409	312	5.6	4.8	5.8
Rougher Tail	1.05	1.17	0.92	16.0	14.9	17.4	2.90	3.53	2.53	13.6	11.7	15.0	177	219	167	20.6	17.9	21.4
				100.0	**100.0**	**100.0**				**100.0**	**100.0**	**100.0**				**100.0**	**100.0**	**100.0**

Tests 3	NaOH	10 mins	Gold				Arsenic				Sulfide Sulfur				Au:S
			Average		Cumulative		Average		Cumulative		Average		Cumulative		
Product	Mass Recovery (%)	Recovery (%)	Grade (g/t)	Recovery (%)	Grade (g/t)	Recovery (%)	Grade (g/t)	Recovery (%)	Grade (g/t)	Recovery (%)	Grade (%)	Recovery (%)	Grade (%)	Recovery (%)	
Con 1	27.4	27.4	9.0	66.5	9.0	66.5	1289.0	65.7	1289.0	65.7	34.7	74.6	34.7	74.6	**0.26**
Con 2	7.6	35.0	5.3	10.8	8.2	77.3	644.0	9.1	1148.7	74.8	13.1	7.8	30.0	82.5	**0.27**
Con 3	8.2	43.3	3.0	6.6	7.2	83.9	351.0	5.4	996.9	80.2	6.5	4.2	25.5	86.7	**0.28**
Feed	56.7	**100.0**	1.1	16.1	3.7	**100.0**	188.0	19.8	537.9	**100.0**	3.0	13.3	12.7	**100.0**	**0.29**

Appendix 4: Nitric Acid Oxidation

Appendix 4.1: Nitric Acid Sulfide Sulfur Oxidation Data

Test	Acid Media	Treatment Time (mins)	S^{2-} Head (g)	S^{2-}sample (g)	S^{2-}Residue (g)	S^{2-} Residue / S^{2-} Head	Final SOx Mass (%)
1	10 g/L Nitric Acid	10	144	120.1	23.9	0.1659	**16.6**
2		10	144	128.3	15.7	0.109	**10.9**
3		20	144	116.9	27.1	0.188	**18.8**
4		20	144	121.2	22.8	0.158	**15.8**
5		30	144	111.6	32.4	0.225	**22.5**
6		30	144	113.2	30.8	0.2138	**21.4**
7		40	144	112.0	32.0	0.222	**22.2**
8		40	144	109.8	34.1	0.237	**23.7**
9		50	144	112.1	31.9	0.221	**22.1**
10		50	144	105.7	38.3	0.265	**26.6**
11		60	144	108.4	35.6	0.247	**24.7**

SOx Data Continued							
12	**10 g/L Nitric Acid**	60	144	104.9	39.1	0.271	**27.1**
13		70	144	106.8	37.2	0.258	**25.8**
14		70	144	106.4	37.6	0.261	**26.1**

Appendix 4.2: Nitric Acid MET Accounting

Test	Time	Au	Fe	As	S	Distribution
Nitric Acid	20 minutes	µg	g	µg	g	%
Ore		3900	143	515000	144	
Rougher Tail		459.4	11.4	104857	16.2	
Combined Con		3440.6	131.6	410143	127.8	
Oxidised Con		3440.6	74.7	409050	107.1	
Filtrate		0	47.5	1000	18.8	**100.0**
Wash Water		0	9.4	93.0	1.9	
Cleaner Con		2542.4	44.3	294638	68.7	
Cleaner Tail		898.2	30.4	114412	38.4	
	30 minutes	µg	g	µg	g	%
Ore		3405	158	490000	144	
Rougher Tail		767.5	11.4	117288.5	16.2	
Combined Con		2637.5	146.6	372711.5	127.8	
Oxidised Con		2637.5	74.5	366616	87.3	
Filtrate		0	48	6000	29.5	**100.0**
Wash Water		0	24.1	95.5	11	
Cleaner Con		1664.6	29.6	173362	24.9	
Cleaner Tail		972.9	44.9	193254	62.4	
	40 minutes	µg	g	µg	g	%
Ore		3870	136	475000	144	
Rougher Tail		432.4	12.4	126477	16.2	
Combined Con		3437.6	123.6	348523	127.8	
Oxidised Con		3437.6	66.5	347270	98	
Filtrate		0	55.7	1100	29.5	**100.0**
Wash Water		0	1.4	153	0.3	
Cleaner Con		2317.2	31.6	209446	37.3	
Cleaner Tail		1120.4	34.9	137824	60.7	
	50 minutes	µg	g	µg	g	%
Ore		3710	135	459000	141	
Rougher Tail		701	9.8	135240	16.2	
Combined Con		3009	125.2	323760	147.0	

Oxidised Con		3009	68.3	323010	94.6	**100.0**
Filtrate		0	37.6	700	29.9	
Wash Water		0	19.3	50	0.3	
Cleaner Con		1450.35	19.8	131087	39.9	
Cleaner Tail		1558.6	49.0	191923	54.7	
	60 minutes	**µg**	**g**	**µg**	**g**	**%**
Ore		3250	124	535000	165	
Rougher Tail		1417	11.9	107088	16.2	
Combined Con		1833	112.1	427912	148.8	
Oxidised Con		1833	70.0	426610	123.1	
Filtrate		0	41.7	1198	23	**100.0**
Wash Water		0	0.3	104	2.7	
Cleaner Con		886.65	15.8	107394	33.9	
Cleaner Tail		946.35	54.2	319216	89.2	

The distribution values are for three steps: Step 1: Rougher Tail + Combined Concentrate

Step 2: Filtrate + Wash Water + Oxidised Concentrate

Step 3: Cleaner concentrate + Cleaner Tail

Appendix 4.3: Nitric Acid Flotation Data

Control (Nitric Acid Series)	Gold Grade (g/t)			Gold Recovery (%)			Sulfide Sulfur Grade (%)			Sulfide Sulfur Recovery (%)			Arsenic Grade (ppm)			Arsenic Recovery (%)		
	Test 1	Test 2	Test 3	Test 1	Test 2	Test 3	Test 1	Test 2	Test 3	Test 1	Test 2	Test 3	Test 1	Test 2	Test 3	Test 1	Test 2	Test 3
Cleaner 1	10.91	10.34	7.99	13.4	12.8	10.2	37.95	40.07	29.34	20.2	21.1	16.3	1209	1145	885	20.8	19.9	16.1
Cleaner 2	9.95	9.42	7.29	11.9	12.0	12.4	40.28	42.54	31.15	17.2	17.0	18.0	1038	983	760	13.6	13.7	14.4
Cleaner 3	9.51	9.01	6.97	19.0	19.1	19.7	41.66	43.99	32.21	32.9	32.6	34.5	1181	1118	865	28.6	28.9	30.2
Cleaner 4	9.68	9.17	7.09	13.1	13.2	13.6	35.94	37.95	27.79	18.0	17.8	18.8	1326	1256	971	20.3	20.5	21.5
Cleaner Tail	4.09	3.90	3.02	42.6	42.9	44.2	15.32	16.18	11.84	11.7	11.6	12.3	719	681	526	16.8	17.0	17.8
Au:S	**0.27**	**0.24**	**0.25**	**100.0**	**100.00**	**100.0**				**100.0**	**100.0**	**100.0**	**5.6**	**5.7**	**5.7**	**100.0**	**100.0**	**100.0**

3 Tests	Nitric Acid	Control		Gold				Arsenic				Sulfide Sulfur			
				Average		Cumulative		Average		Cumulative		Average		Cumulative	
Product	Mass Recovery (%)	Recovery (%)	Water Recovery (%)	Grade (g/t)	Recovery (%)	Grade (g/t)	Recovery (%)	Grade (g/t)	Recovery (%)	Grade (g/t)	Recovery (%)	Grade (%)	Recovery (%)	Grade (%)	Recovery (%)
Con 1	16.8	16.8	14.6	9.74	20.0	9.74	20.0	860.0	16.2	860.0	16.2	23.3	15.5	23.3	15.5
Con 2	14.3	31.1	28.7	9.5	20.4	9.5	40.5	934.0	18.0	897.4	34.1	18.7	12.7	21.0	28.1
Con 3	26.5	57.6	41.1	8.2	23.2	9.0	63.7	1010.0	25.7	942.5	59.8	22.7	20.3	21.6	48.4
Con 4	16.8	74.4	53.3	8.2	11.7	10.0	87.5	944.0	12.1	942.7	71.9	37.7	17.0	37.0	87.1
Feed		100.0	100.0		**Au:S**	**0.27**	**100.0**				**100.0**				**100.0**

Nitric Acid 10 mins	Gold Grade (g/t)			Gold Recovery (%)			Sulfide Sulfur Grade (%)			Sulfide Sulfur Recovery (%)			Arsenic Grade (ppm)			Arsenic Recovery (%)		
	Test 1	Test 2	Test 3	Test 1	Test 2	Test 3	Test 1	Test 2	Test 3	Test 1	Test 2	Test 3	Test 1	Test 2	Test 3	Test 1	Test 2	Test 3
Cleaner 1	9.91	9.68	9.35	21.1	20.7	20.1	26.40	25.79	24.91	15.9	15.6	15.2	927	887	892	18.9	18.2	18.5
Cleaner 2	9.61	9.38	9.06	20.3	20.5	20.6	33.39	32.61	31.50	20.0	20.1	20.2	1033	989	994	20.9	21.1	21.0
Cleaner 3	9.05	8.84	8.54	26.9	27.1	27.3	39.35	38.43	37.12	33.2	33.3	33.5	1038	993	999	29.5	29.7	29.6
Cleaner 4	7.64	7.46	7.21	10.6	10.6	10.7	38.73	37.83	36.54	15.2	15.2	15.3	970	929	934	12.8	12.9	12.9
Cleaner Tail	6.46	6.31	6.10	21.1	21.2	21.3	17.00	16.61	16.04	15.7	15.8	15.8%	577	553	556	18.0	18.1	18.1
				100.0	**100.00**	**100.0**				**100.0**	**100.0**	**100.0**	**11.1**	**11.4**	**10.9**	**100.0**	**100.0**	**100.0**

3 Tests	Nitric Acid	10 mins		Gold				Arsenic				Sulfide Sulfur			
				Average		Cumulative		Average		Cumulative		Average		Cumulative	
Product	Mass Recovery (%)	Recovery (%)	Water Recovery (%)	Grade (g/t)	Recovery (%)	Grade (g/t)	Recovery (%)	Grade (g/t)	Recovery (%)	Grade (g/t)	Recovery (%)	Grade (%)	Recovery (%)	Grade (%)	Recovery (%)
Con 1	17.6	17.6	5.1	12.6	25.0	12.6	25.0	902.0	18.5	902.0	18.5	25.7	15.6	25.7	15.6
Con 2	17.9	35.5	9.7	11.4	23.0	12.0	48.0	1005.0	21.0	954.0	39.5	32.5	20.1	29.1	35.7
Con 3	25.2	60.7	15.9	9.8	27.9	11.1	76.0	1010.0	29.6	977.3	69.1	38.3	33.3	32.9	69.0
Con 4	11.7	72.4	21.0	8.2	10.8	8.7	78.8	944.0	12.9	945.0	81.9	37.7	15.2	33.8	84.2
Feed		**100**	**100.0**				**100.0**				**100.0**				**100.0**
Au:S						**0.26**				**9.2**					

Nitric Acid 20 mins	Gold Grade (g/t)			Gold Recovery (%)			Sulfide Sulfur Grade (%)			Sulfide Sulfur Recovery (%)			Arsenic Grade (ppm)			Arsenic Recovery (%)		
	Test 1	Test 2	Test 3	Test 1	Test 2	Test 3	Test 1	Test 2	Test 3	Test 1	Test 2	Test 3	Test 1	Test 2	Test 3	Test 1	Test 2	Test 3
Cleaner 1	9.76	9.53	9.21	20.0	19.7	19.1	27.84	27.19	26.27	16.5	16.1	15.7	884	846	851	16.6	16.0	16.2
Cleaner 2	9.74	9.51	9.19	20.4	20.5	20.7	30.46	29.75	28.74	17.9	18.0	18.1	960	919	924	17.9	18.0	18.0
Cleaner 3	8.38	8.19	7.91	23.2	23.3	23.5	25.33	24.73	23.89	19.7	19.7	19.8	1038	993	999	25.5	25.7	25.7
Cleaner 4	8.37	8.18	7.90	11.7	11.7	11.8	38.73	37.83	36.54	15.1	15.2	15.3	970	929	934	12.0	12.1	12.1
Cleaner Tail	6.16	6.02	5.82	24.6	24.7	24.9	27.53	26.89	25.98	30.8	30.9	31.1	789	755	760	28.0	28.2	28.1
	0.22	**0.22**	**0.22**	**100.0**	**100.00**	**100.0**				**100.0**	**100.0**	**100.0**	**7.8**	**7.9**	**7.6**	**100.0**	**100.0**	**100.0**

3 Tests	Nitric Acid	20 mins		Gold				Arsenic				Sulfide Sulfur			
				Average		Cumulative		Average		Cumulative		Average		Cumulative	
Product	Mass Recovery (%)	Recovery (%)	Water Recovery (%)	Grade (g/t)	Recovery (%)	Grade (g/t)	Recovery (%)	Grade (g/t)	Recovery (%)	Grade (g/t)	Recovery (%)	Grade (%)	Recovery (%)	Grade (%)	Recovery (%)
Con 1	16.7	16.7	7.3	9.5	20.0	9.5	20.0	860.0	16.2	860.0	16.2	23.3	15.5	23.3	15.5
Con 2	17.0	33.7	14.1	9.5	20.4	9.5	40.5	934.0	18.0	897.4	34.1	18.7	12.7	21.0	28.1
Con 3	22.5	56.2	21.4	8.2	23.2	9.0	63.7	1010.0	25.7	942.5	59.8	22.7	20.3	21.6	48.4
Con 4	11.3	67.5	27.6	8.2	11.7	8.8	75.4	944.0	12.1	942.7	71.9	37.7	17.0	26.9	69.0
Feed		**100.0**	**100.0**			**0.33**	**100.0**			**9.3**	**100.0**				**100.0**

Nitric Acid 30 mins	Gold Grade (g/t)			Gold Recovery (%)			Sulfide Sulfur Grade (%)			Sulfide Sulfur Recovery (%)			Arsenic Grade (ppm)			Arsenic Recovery (%)		
	Test 1	Test 2	Test 3	Test 1	Test 2	Test 3	Test 1	Test 2	Test 3	Test 1	Test 2	Test 3	Test 1	Test 2	Test 3	Test 1	Test 2	Test 3
Cleaner 1	11.05	10.16	9.18	23.3	21.8	20.2	33.60	30.90	27.92	23.4	22.0	20.3	1110	1062	1068	22.4	21.6	21.7
Cleaner 2	11.84	10.89	9.83	20.2	20.6	21.1	34.36	31.61	28.55	19.4	19.8	20.2	1089	1043	1048	18.9	19.0	19.0
Cleaner 3	9.77	8.99	8.12	14.2	14.4	14.8	30.11	27.69	25.02	14.4	14.7	15.0	1006	963	968	14.8	14.9	14.9
Cleaner 4	8.20	7.55	6.82	11.4	11.6	11.8	29.89	27.49	24.83	13.7	13.9	14.3	856	819	824	12.0	12.1	12.1
Cleaner Tail	3.48	3.12	3.73	30.9	31.5	32.2	12.71	11.69	10.56	29.0	29.6	30.2	457	438	440	32.0	32.3	32.3
Au:S	**0.27**	**0.27**	**0.30**	**100.0**	**100.00**	**100.0**				**100.0**	**100.0**	**100.0**	**9.8**	**9.4**	**8.4**	**100.0**	**100.0**	**100.0**

3 Tests	Nitric Acid	30 mins		Gold				Arsenic				Sulfide Sulfur			
				Average		Cumulative		Average		Cumulative		Average		Cumulative	
Product	Mass Recovery (%)	Recovery (%)	Water Recovery (%)	Grade (g/t)	Recovery (%)	Grade (g/t)	Recovery (%)	Grade (g/t)	Recovery (%)	Grade (g/t)	Recovery (%)	Grade (%)	Recovery (%)	Grade (%)	Recovery (%)
Con 1	14.5	14.5	7.0	10.2	20.7	10.2	20.7	881.0	15.6	881.0	15.6	23.6	12.9	23.6	12.9
Con 2	12.8	27.2	13.9	10.2	18.2	10.2	39.0	920.0	14.4	899.3	30.1	28.1	13.6	25.7	26.6
Con 3	10.8	38.1	20.8	8.6	13.0	9.7	52.0	962.0	12.8	917.2	42.9	29.8	12.3	26.9	38.8
Con 4	10.3	48.4	27.1	8.2	11.8	9.9	68.5	944.0	12.0	950.0	54.9	37.7	14.8	28.7	70.4
Feed		**100.0**	**100.0**				**100.0**				**100.0**				**100.0**
Au:S						**0.34**									

Nitric Acid 40 mins	Gold Grade (g/t)			Gold Recovery (%)			Sulfide Sulfur Grade (%)			Sulfide Sulfur Recovery (%)			Arsenic Grade (ppm)			Arsenic Recovery (%)		
	Test 1	Test 2	Test 3	Test 1	Test 2	Test 3	Test 1	Test 2	Test 3	Test 1	Test 2	Test 3	Test 1	Test 2	Test 3	Test 1	Test 2	Test 3
Cleaner 1	13.04	11.99	10.83	18.9	17.6	16.2	27.82	25.59	23.11	9.6	8.9	8.1	882	844	849	12.5	12.1	12.2
Cleaner 2	12.60	11.59	10.47	15.6	15.8	16.1	36.22	33.31	30.09	10.6	10.7	10.8	934	894	899	12.0	12.1	12.1
Cleaner 3	12.16	11.19	10.11	12.6	12.8	13.0	44.51	40.94	36.98	10.9	11.0	11.1	1038	993	999	11.2	11.3	11.2
Cleaner 4	10.71	9.85	8.90	11.0	11.2	11.4	40.36	37.12	33.53	9.9	10.0	10.0	968	927	932	10.4	10.5	10.4
Cleaner Tail	6.64	6.11	5.52	41.9	42.5	43.3	39.38	36.22	32.72	59.0	59.4	59.9	818	783	787	53.8	54.1	54.0
Au:S	**0.17**	**0.17**	**0.17**	**100.0**	**100.00**	**100.0**				**100.0**	**100.0**	**100.0**	**8.1**	**7.8**	**7.0**	**100.0**	**100.0**	**100.0**

3 Tests	Nitric Acid	40 mins		Gold				Arsenic				Sulfide Sulfur			
				Average		Cumulative		Average		Cumulative		Average		Cumulative	
Product	Mass Recovery (%)	Recovery (%)	Water Recovery (%)	Grade (g/t)	Recovery (%)	Grade (g/t)	Recovery (%)	Grade (g/t)	Recovery (%)	Grade (g/t)	Recovery (%)	Grade (%)	Recovery (%)	Grade (%)	Recovery (%)
Con 1	11.7	11.7	8.3	12.0	16.3	12.0	16.3	858.0	11.4	858.0	11.4	25.9	8.5	25.9	8.5
Con 2	10.9	22.6	16.3	11.6	14.7	11.8	31.0	909.0	11.3	882.6	22.7	33.5	10.2	29.6	18.7
Con 3	19.1	41.7	23.7	11.2	11.9	11.5	42.9	1010.0	22.0	941.0	44.7	41.0	21.9	24.8	40.5
Con 4	14.5	56.2	30.7	9.8	10.4	10.9	57.4	942.0	15.5	941.0	60.3	37.3	15.1	26.1	55.6
Feed		**100.0**	**100.0**			**0.42**	**100.0**				**100.0**				**100.0**

Nitric Acid 50 mins	Gold Grade (g/t)			Gold Recovery (%)			Sulfide Sulfur Grade (%)			Sulfide Sulfur Recovery (%)			Arsenic Grade (ppm)			Arsenic Recovery (%)		
	Test 1	Test 2	Test 3	Test 1	Test 2	Test 3	Test 1	Test 2	Test 3	Test 1	Test 2	Test 3	Test 1	Test 2	Test 3	Test 1	Test 2	Test 3
Cleaner 1	14.01	13.55	12.94	17.4	16.9	16.3	21.97	20.99	22.73	6.4	6.1	6.6	638	617	589	6.0	5.8	5.5
Cleaner 2	12.77	12.34	11.79	16.2	16.2	16.4	20.17	19.27	20.87	6.2	6.2	6.2	825	798	762	7.8	7.9	7.9
Cleaner 3	11.06	10.69	10.21	13.8	13.9	14.0	28.60	27.32	29.58	8.7	8.7	8.7	872	843	805	8.2	8.2	8.2
Cleaner 4	8.58	8.30	7.93	9.6	9.6	9.7	37.73	36.04	39.03	10.2	10.3	10.2	936	905	865	7.8	7.9	7.9
Cleaner Tail	5.15	4.98	4.75	43.1	43.3	43.7	33.61	32.11	34.78	68.5	68.7	68.3	1116	1079	1030	70.2	70.3	70.5
Au:S	**0.15**	**0.15**	**0.15**	**100.0**	**100.00**	**100.0**				**100.0**	**100.0**	**100.0**	**4.6**	**4.6**	**4.6**	**100.0**	**100.0**	**100.0**

3 Tests	Nitric Acid	50 mins		Gold				Arsenic				Sulfide Sulfur			
				Average		Cumulative		Average		Cumulative		Average		Cumulative	
Product	Mass Recovery (%)	Recovery (%)	Water Recovery (%)	Grade (g/t)	Recovery (%)	Grade (g/t)	Recovery (%)	Grade (g/t)	Recovery (%)	Grade (g/t)	Recovery (%)	Grade (%)	Recovery (%)	Grade (%)	Recovery (%)
Con 1	9.1	9.1	5.9	13.5	15.5	13.5	15.5	1015.0	10.5	1015.0	10.5	28.90	7.6	28.9	7.6
Con 2	9.6	18.7	11.1	12.3	15.0	12.9	30.5	1075.0	11.8	1045.8	22.4	33.30	9.3	31.2	23.9
Con 3	9.5	28.1	20.2	10.7	12.8	12.1	43.2	1040.0	11.3	1043.9	33.7	43.50	12.0	35.3	40.1
Con 4	8.4	36.6	28.3	8.3	8.9	11.6	56.6	902.0	8.7	1011.1	42.4	37.60	9.2	19.4	31.5
Feed		**100.0**	**100.0**				**100.0**				**100.0**				**100.0**
Au:S						**0.60**				**11.4**					

Nitric Acid 60 mins	Gold Grade (g/t)			Gold Recovery (%)			Sulfide Sulfur Grade (%)			Sulfide Sulfur Recovery (%)			Arsenic Grade (ppm)			Arsenic Recovery (%)		
	Test 1	Test 2	Test 3	Test 1	Test 2	Test 3	Test 1	Test 2	Test 3	Test 1	Test 2	Test 3	Test 1	Test 2	Test 3	Test 1	Test 2	Test 3
Cleaner 1	13.24	12.79	12.22	18.0	17.5	16.9	18.56	17.73	19.20	4.5	4.3	4.7	579	560	535	4.3	4.1	3.9
Cleaner 2	12.30	11.89	11.36	16.1	16.2	16.4	21.77	20.80	22.53	5.3	5.3	5.3	714	690	659	5.1	5.1	5.1
Cleaner 3	9.98	9.64	9.21	13.0	13.1	13.2	30.80	29.42	31.87	7.5	7.5	7.5	806	779	744	5.7	5.7	5.7
Cleaner 4	8.19	7.92	7.56	9.4	9.5	9.6	31.30	29.90	32.39	6.7	6.7	6.7	992	959	916	6.2	6.2	6.2
Cleaner Tail	3.62	3.50	3.35	43.4	43.7	44.0	34.11	32.59	35.29	76.0	76.2	75.9	1220	1179	1126	78.9	79.0	79.1
Au:S	**0.10**	**0.10**	**0.10**	**100.0**	**100.00**	**100.0**				**100.0**	**100.0**	**100.0**	**2.9**	**2.9**	**2.9**	**100.0**	**100.0**	**100.0**

3 Tests	Nitric Acid	60 mins		Gold				Arsenic				Sulfide Sulfur			
				Average		Cumulative		Average		Cumulative		Average		Cumulative	
Product	Mass Recovery (%)	Recovery (%)	Water Recovery (%)	Grade (g/t)	Recovery (%)	Grade (g/t)	Recovery (%)	Grade (g/t)	Recovery (%)	Grade (g/t)	Recovery (%)	Grade (%)	Recovery (%)	Grade (%)	Recovery (%)
Con 1	7.7	7.7	5.5	11.4	13.6	11.4	13.6	558.0	4.1	558.0	4.1	14.1	3.6	14.1	3.6
Con 2	7.7	15.4	11.4	12.3	14.6	11.8	28.2	688.0	5.1	623.0	9.2	16.5	4.2	15.3	7.8
Con 3	7.6	23.0	17.3	12.2	14.5	11.9	42.7	776.0	5.7	673.8	14.8	22.7	5.8	17.7	13.5
Con 4	6.7	29.8	22.8	10.1	10.5	11.5	56.3	956.0	6.2	837.7	21.0	32.1	7.2	17.3	24.0
Feed		**100.0**	**100.0**				**100.0**				**100.0**				**100.0**
Au:S						**0.66**									

Nitric Acid 70 mins	Gold Grade (g/t)			Gold Recovery (%)			Sulfide Sulfur Grade (%)			Sulfide Sulfur Recovery (%)			Arsenic Grade (ppm)			Arsenic Recovery (%)		
	Test 1	Test 2	Test 3	Test 1	Test 2	Test 3	Test 1	Test 2	Test 3	Test 1	Test 2	Test 3	Test 1	Test 2	Test 3	Test 1	Test 2	Test 3
Cleaner 1	13.49	12.31	10.49	18.5	16.9	14.8	23.18	22.14	23.98	5.7	5.5	5.9	1026	991	947	7.0	6.8	6.5
Cleaner 2	10.87	9.92	8.45	13.4	13.6	14.0	20.87	19.94	21.59	5.1	5.2	5.1	991	958	915	6.5	6.5	6.6
Cleaner 3	9.71	8.86	7.55	11.9	12.1	12.4	27.59	26.36	28.55	6.8	6.8	6.7	1116	1079	1030	7.3	7.3	7.3
Cleaner 4	10.88	9.93	8.46	11.7	12.0	12.3	25.59	24.44	26.47	5.5	5.5	5.5	992	959	916	5.7	5.7	5.8
Cleaner Tail	3.96	3.61	3.08	44.5	45.4	46.5	34.11	32.59	35.29	76.8	77.0	76.7	1220	1179	1126	73.4	73.6	73.8
				100.0	**100.00**	**100.0**				**100.0**	**100.0**	**100.0**	**3.2**	**3.0**	**2.7**	**100.0**	**100.0**	**100.0**
		0.10												**3.0**				

3 Tests	Nitric Acid	70 mins		Gold				Arsenic				Sulfide Sulfur			
				Average		Cumulative		Average		Cumulative		Average		Cumulative	
Product	Mass Recovery (%)	Recovery (%)	Water Recovery (%)	Grade (g/t)	Recovery (%)	Grade (g/t)	Recovery (%)	Grade (g/t)	Recovery (%)	Grade (g/t)	Recovery (%)	Grade (%)	Recovery (%)	Grade (%)	Recovery (%)
Con 1	7.7	7.7	5.5	12.1	14.9	12.1	14.9	988.0	6.8	988.0	6.8	20.9	5.2	20.9	5.2
Con 2	7.7	15.4	11.4	9.8	12.0	10.9	27.0	955.0	6.5	971.5	13.3	20.8	5.1	20.9	10.3
Con 3	7.6	23.0	17.3	8.7	10.7	10.2	37.7	1075.0	7.3	1005.9	20.6	23.6	5.8	21.8	16.1
Con 4	6.7	29.8	22.8	9.8	10.6	10.0	54.6	956.0	5.7	994.6	26.4	32.1	7.0	28.0	23.1
Feed		**100.0**	**100.0**				**100.0**				**100.0**				**100.0**
Au:S						**0.36**									

Appendix 4.4: Regrinding Oxidation Data

Test	Acid Media	Condition	Treatment Time (mins)	S^{2-} Head (g)	S^{2-}sample (g)	S^{2-}Residue (g)	S^{2-} Residue / S^{2-}Head	Final SOx Mass (%)
1	10 g/L Nitric Acid	Regrinding	15	153	113.7	39.3	0.257	**25.7**
2			30	153	95.3	57.7	0.377	**37.7**
3			45	153	86.6	66.4	0.434	**43.4**
4			60	153	80.9	72.1	0.471	**47.1**

Appendix 4.5: Regrinding MET Accounting

Test	Time	Au	Fe	As	S	Distribution
Regrinding+ Nitric Acid	30 minutes	µg	g	µg	g	%
Ore		4252	116	491160	141	
Rougher Tail		474.5	8.3	147630	20.9	
Combined Con		3777.5	107.7	343530	120.1	
Regrind		3777.5	107.7	343530	120.1	
Oxidised Con		3777.5	81.1	311993	110.5	**100.0**
Filtrate		0	26.4	26885	9.1	
Wash Water		0	0.2	4652	0.5	
Cleaner Con		2848	53.3	204471	49.7	
Cleaner Tail		929.5	27.8	107522	60.8	
	45 minutes	µg	g	µg	g	%
Ore		4350	113	526000	141	
Rougher Tail		377.4	8.3	147630	20.9	
Combined Con		3972.6	104.7	378370	120.1	
Regrind		3972.6	104.7	378370	120.1	
Oxidised Con		3972.6	78.2	347440	103.5	**100.0**
Filtrate		0	26.4	28450	15.8	
Wash Water		0	0.1	2480	0.8	
Cleaner Con		1959.4	44.8	170286	50.3	
Cleaner Tail		2013.2	33.4	177154	53.2	
	60 minutes	µg	g	µg	g	%
Ore		4000	113	506000	163	
Rougher Tail		377.4	8.6	125630	20.9	
Combined Con		3622.6	104.4	380370	142.1	
Regrind		3622.6	104.4	380370	142.1	
Oxidised Con		3622.6	77.6	337650	119	**100.0**
Filtrate		0	25.8	35720	22.9	
Wash Water		0	1.0	7000	0.2	
Cleaner Con		1942.6	37.9	136150	56.2	
Cleaner Tail		1680	39.7	201500	62.8	

Appendix 4.6: Regrinding Flotation Data

Regrind Control (Nitric Acid Series)	Gold Grade (g/t)			Gold Recovery (%)			Sulfide Sulfur Grade (%)			Sulfide Sulfur Recovery (%)			Arsenic Grade (ppm)			Arsenic Recovery (%)		
	Test 1	Test 2	Test 3	Test 1	Test 2	Test 3	Test 1	Test 2	Test 3	Test 1	Test 2	Test 3	Test 1	Test 2	Test 3	Test 1	Test 2	Test 3
Cleaner 1	9.27	8.45	7.21	29.0	27.1	24.1	31.00	29.62	32.08	29.3	28.4	30.1	1016	982	938	23.0	22.5	21.7
Cleaner 2	8.82	8.04	6.86	22.9	23.5	24.5	28.19	26.93	29.17	24.6	24.9	24.3	1038	1003	958	21.0	21.1	21.3
Cleaner 3	7.06	6.44	5.49	25.0	25.7	26.8	24.28	23.19	25.12	29.0	29.4	28.7	979	946	904	27.1	27.3	27.5
Cleaner 4	4.80	4.37	3.73	13.4	13.8	14.4	12.34	11.79	12.77	11.6	11.8	11.5	712	688	658	15.6	15.7	15.8
Cleaner Tail	1.59	1.45	1.24	9.7	9.9	10.3	2.67	2.55	2.76	5.4	5.5	5.4	283	274	262	13.4	13.5	13.6
				100.0	**100.00**	**100.0**				**100.0**	**100.0**	**100.0**				**100.0**	**100.0**	**100.0**

3 Tests	Regrind Nitric Acid	Control		Gold				Arsenic				Sulfide Sulfur			
				Average		Cumulative		Average		Cumulative		Average		Cumulative	
Product	Mass Recovery (%)	Recovery (%)	Water Recovery (%)	Grade (g/t)	Recovery (%)	Grade (g/t)	Recovery (%)	Grade (g/t)	Recovery (%)	Grade (g/t)	Recovery (%)	Grade (%)	Recovery (%)	Grade (%)	Recovery (%)
Con 1	15.8	15.8	19.1	8.3	26.8	8.3	26.8	979.0	22.4	979.0	22.4	31.50	28.9	31.50	28.90
Con 2	14.6	30.3	35.3	7.9	23.6	8.1	50.4	1000.0	21.2	989.1	43.5	28.70	24.3	30.15	53.24
Con 3	19.9	50.2	55.7	6.3	25.8	7.4	76.2	943.0	27.3	970.8	70.8	24.90	28.9	28.07	82.14
Con 4	15.8	66.0	79.6	4.3	13.9	6.7	90.0	686.0	15.7	902.8	86.5	12.95	11.9	23.81	94.02
Feed		**100.0**	**100.0**				**100.0**				**100.0**				**100.00**
Au:S						**0.28**									

Regrind 15 min (Nitric Acid Series)	Gold Grade (g/t)			Gold Recovery (%)			Sulfide Sulfur Grade (%)			Sulfide Sulfur Recovery (%)			Arsenic Grade (ppm)			Arsenic Recovery (%)		
	Test 1	Test 2	Test 3	Test 1	Test 2	Test 3	Test 1	Test 2	Test 3	Test 1	Test 2	Test 3	Test 1	Test 2	Test 3	Test 1	Test 2	Test 3
Cleaner 1	7.47	9.05	7.09	18.6	21.7	17.8	18.73	23.14	17.67	14.1	16.8	13.4	838	1020	731	16.9	19.9	15.1
Cleaner 2	7.81	9.46	7.41	20.5	19.7	20.7	25.00	30.90	23.59	19.9	19.3	20.1	948	1153	827	19.7	19.0	20.1
Cleaner 3	7.31	8.85	6.94	21.9	21.1	22.1	27.74	34.28	26.17	25.3	24.5	25.5	896	1091	782	21.3	20.5	21.8
Cleaner 4	5.55	6.72	5.27	16.8	16.2	17.0	22.83	28.22	21.54	21.0	20.3	21.1	752	915	656	18.0	17.4	18.4
Cleaner Tail	2.31	2.79	2.19	22.2	21.3	22.4	6.76	8.36	6.38	19.7	19.1	19.9	371	385	276	24.1	23.2	24.6
				100.0	**100.00**	**100.0**				**100.0**	**100.0**	**100.0**				**100.0**	**100.0**	**100.0**

3 Tests	Regrind Nitric Acid	15 mins		Gold				Arsenic				Sulfide Sulfur			
				Average		Cumulative		Average		Cumulative		Average		Cumulative	
Product	Mass Recovery (%)	Recovery (%)	Water Recovery (%)	Grade (g/t)	Recovery (%)	Grade (g/t)	Recovery (%)	Grade (g/t)	Recovery (%)	Grade (g/t)	Recovery (%)	Grade (%)	Recovery (%)	Grade (%)	Recovery (%)
Con 1	12.6	12.6	14.5	7.9	19.4	7.9	19.4	863.0	17.3	863.0	17.3	20.3	14.9	20.30	14.86
Con 2	12.6	25.1	27.7	8.2	20.3	8.1	39.7	976.0	19.6	919.5	36.9	26.9	19.7	23.60	34.55
Con 3	14.4	39.5	43.2	7.7	21.7	7.9	61.4	923.0	21.2	920.8	58.1	29.8	24.9	25.85	59.49
Con 4	14.5	54.0	66.1	5.9	16.6	7.4	78.1	774.0	17.9	881.4	76.0	24.5	20.7	25.10	80.22
Feed		**100.0**	**100.0**				**100.0**				**100.0**				**100.00**
Au:S						**0.29**									

Regrind 30 min (Nitric Acid Series)	Gold Grade (g/t)			Gold Recovery (%)			Sulfide Sulfur Grade (%)			Sulfide Sulfur Recovery (%)			Arsenic Grade (ppm)			Arsenic Recovery (%)		
	Test 1	Test 2	Test 3	Test 1	Test 2	Test 3	Test 1	Test 2	Test 3	Test 1	Test 2	Test 3	Test 1	Test 2	Test 3	Test 1	Test 2	Test 3
Cleaner 1	9.17	7.70	8.03	23.3	20.3	21.0	25.22	20.88	23.51	17.9	15.3	16.8	857	1043	748	19.4	22.6	17.3
Cleaner 2	8.85	7.43	7.75	20.4	21.2	21.0	38.48	31.86	35.87	25.1	25.9	25.4	911	1108	795	21.2	20.3	21.7
Cleaner 3	8.34	7.01	7.31	21.9	22.8	22.6	37.72	31.23	35.16	28.1	29.0	28.4	890	1083	777	23.7	22.7	24.3
Cleaner 4	6.10	5.12	5.34	16.2	16.8	16.7	22.17	18.36	20.67	16.6	17.2	16.8	662	806	578	17.8	17.0	18.2
Cleaner Tail	2.22	1.87	1.95	18.2	18.9	18.7	5.34	4.42	4.97	12.4	12.8	12.5	217	265	190	18.0	17.3	18.5
				100.0	**100.00**	**100.0**				**100.0**	**100.0**	**100.0**				**100.0**	**100.0**	**100.0**

3 Tests	Regrind Nitric Acid	30 mins		Gold				Arsenic				Sulfide Sulfur			
				Average		Cumulative		Average		Cumulative		Average		Cumulative	
Product	Mass Recovery (%)	Recovery (%)	Water Recovery (%)	Grade (g/t)	Recovery (%)	Grade (g/t)	Recovery (%)	Grade (g/t)	Recovery (%)	Grade (g/t)	Recovery (%)	Grade (%)	Recovery (%)	Grade (%)	Recovery (%)
Con 1	12.7	12.7	14.4	8.3	21.6	8.3	21.6	883.0	19.8	883.0	19.8	23.60	16.7	23.60	16.66
Con 2	12.7	25.5	27.7	8.0	20.8	8.2	42.4	938.0	21.1	910.5	40.9	35.70	25.2	29.65	41.86
Con 3	14.6	40.0	43.1	7.6	22.4	7.9	64.9	917.0	23.5	912.9	64.4	35.00	28.2	31.60	70.10
Con 4	14.7	54.7	66.0	5.5	16.5	7.3	81.4	682.0	17.7	850.9	82.1	20.70	16.8	28.34	86.93
Feed		**100.0**	**100.0**				**100.0**				**100.0**				**100.00**
Au:S						**0.26**									

Regrind 45 min (Nitric Acid Series)	Gold Grade (g/t)			Gold Recovery (%)			Sulfide Sulfur Grade (%)			Sulfide Sulfur Recovery (%)			Arsenic Grade (ppm)			Arsenic Recovery (%)		
	Test 1	Test 2	Test 3	Test 1	Test 2	Test 3	Test 1	Test 2	Test 3	Test 1	Test 2	Test 3	Test 1	Test 2	Test 3	Test 1	Test 2	Test 3
Cleaner 1	10.18	9.16	8.03	15.1	13.8	12.3	31.41	26.01	29.28	15.8	13.4	14.7	869	1074	820	14.2	16.9	14.9
Cleaner 2	11.93	10.74	9.41	15.5	15.7	16.0	24.78	20.52	23.10	11.2	11.5	11.3	820	1013	774	13.8	13.4	13.7
Cleaner 3	11.60	10.44	9.15	14.9	15.1	15.4	32.17	26.64	29.99	14.4	14.8	14.5	826	1021	780	13.8	13.4	13.7
Cleaner 4	9.76	8.78	7.70	13.0	13.2	13.4	22.07	18.27	20.57	10.2	10.5	10.3	795	983	750	13.7	13.3	13.6
Cleaner Tail	8.88	7.99	7.00	41.5	42.1	42.9	29.89	24.75	27.86	48.5	49.9	49.1	733	906	692	44.5	43.0	44.1
				100.0	**100.00**	**100.0**				**100.0**	**100.0**	**100.0**				**100.0**	**100.0**	**100.0**

3 Tests	Regrind Nitric Acid	45 mins		Gold				Arsenic				Sulfide Sulfur			
				Average		Cumulative		Average		Cumulative		Average		Cumulative	
Product	Mass Recovery (%)	Recovery (%)	Water Recovery (%)	Grade (g/t)	Recovery (%)	Grade (g/t)	Recovery (%)	Grade (g/t)	Recovery (%)	Grade (g/t)	Recovery (%)	Grade (%)	Recovery (%)	Grade (%)	Recovery (%)
Con 1	13.4	13.4	16.7	9.1	13.8	9.1	13.8	921.0	14.9	921.0	14.9	28.5	12.6	28.5	12.6
Con 2	13.1	26.5	31.4	10.7	15.7	9.9	29.5	869.0	13.7	869.0	28.6	22.3	9.6	25.4	22.3
Con 3	13.0	39.5	57.8	10.4	15.2	10.1	44.7	876.0	13.7	876.0	42.3	29.2	12.5	26.7	34.8
Con 4	13.4	52.9	81.0	8.8	13.2	7.3	59.5	843.0	13.6	843.0	55.9	19.8	8.8	25.3	43.5
Feed		**100.0**	**100.0**				**100.0**				**100.0**				**100.0**
Au :S						**0.29**									

Regrind 60 min (Nitric Acid Series)	Gold Grade (g/t)			Gold Recovery (%)			Sulfide Sulfur Grade (%)			Sulfide Sulfur Recovery (%)			Arsenic Grade (ppm)			Arsenic Recovery (%)		
	Test 1	Test 2	Test 3	Test 1	Test 2	Test 3	Test 1	Test 2	Test 3	Test 1	Test 2	Test 3	Test 1	Test 2	Test 3	Test 1	Test 2	Test 3
Cleaner 1	11.87	14.37	11.26	16.7	19.5	16.0	30.10	36.63	26.27	11.2	9.9	14.7	900	942	973	14.6	15.2	15.6
Cleaner 2	11.25	13.62	10.68	16.3	15.7	16.4	32.62	39.70	28.47	12.2	12.4	11.3	839	878	907	13.9	13.8	13.7
Cleaner 3	9.78	11.84	9.28	14.0	13.5	14.1	37.28	45.37	32.54	13.8	14.0	14.5	811	849	877	13.3	13.2	13.1
Cleaner 4	8.92	10.80	8.47	13.2	12.8	13.4	40.97	49.86	35.76	15.7	15.9	10.3	738	773	798	12.5	12.4	12.4
Cleaner Tail	7.63	9.24	7.24	39.8	38.4	40.1	34.95	42.54	30.51	47.1	47.8	49.1	766	802	828	45.7	45.3	45.1
				100.0	**100.00**	**100.0**				**100.0**	**100.0**	**100.0**				**100.0**	**100.0**	**100.0**

3 Tests	Regrind Nitric Acid	60 mins		Gold				Arsenic				Sulfide Sulfur			
				Average		Cumulative		Average		Cumulative		Average		Cumulative	
Product	Mass Recovery (%)	Recovery (%)	Water Recovery (%)	Grade (g/t)	Recovery (%)	Grade (g/t)	Recovery (%)	Grade (g/t)	Recovery (%)	Grade (g/t)	Recovery (%)	Grade (%)	Recovery (%)	Grade (%)	Recovery (%)
Con 1	13.4	13.4	16.7	12.5	17.4	12.5	17.4	939.0	15.2	939.0	15.2	31.4	11.6	31.4	11.6
Con 2	13.1	26.5	31.4	11.9	16.1	12.2	33.5	875.0	13.8	907.4	29.0	34.1	12.3	32.7	23.8
Con 3	13.0	39.5	57.8	10.3	13.9	11.6	47.4	846.0	13.2	887.2	42.2	38.7	13.8	34.7	37.6
Con 4	13.4	52.9	81.0	9.4	13.1	10.4	60.5	770.0	12.4	857.5	54.6	42.4	15.6	36.3	53.3
Feed		**100.0**	**100.0**				**100.0**				**100.0**				**100.0**
Au:S						**0.29**									

Appendix 5: Sulfuric Acid

Appendix 5.1: Sulfuric Acid Sulfide Sulfur Oxidation Values

Test	Acid Media	Treatment Time (mins)	S^{2-} Head (g)	S^{2-}sample (g)	S^{2-}Residue (g)	S^{2-} Residue / S^{2-}Head	Final SOx Mass (%)
1	10 g/L Sulfuric Acid	10	140	134.5	5.5	0.039	**3.9**
2		20	140	128.4	11.6	0.083	**8.3**
3		30	140	125.8	14.2	0.101	**10.1**
4		40	140	121.4	18.6	0.133	**13.3**

Appendix 5.2: Sulfuric Acid MET Accounting

Test	Time	Au	Fe	As	S	Distribution
Sulfuric Acid	20 minutes	µg	g	µg	g	%
Ore		3891	131	582750	152	
Rougher Tail		632.6	21.5	124985	16.5	
Combined Con		3258.4	109.1	457765	135.5	
Oxidised Con		3258.4	66.8	429803	110.5	
Filtrate		0	41.3	27025	25.0	**100.0**
Wash Water		0	1.0	937	0	
Cleaner Con		1418.84	19.9	192602	35.9	
Cleaner Tail		1839.6	46.9	237201	74.6	
	30 minutes	µg	g	µg	g	%
Ore		4251	132	566100	152	
Rougher Tail		528	15.8	141900	16.5	
Combined Con		3723	116.2	424200	135.5	
Oxidised Con		3723	59.1	396060	108.9	
Filtrate		0	56.3	27100	22.5	**100.0**
Wash Water		0	0.8	1040	4.1	
Cleaner Con		1206.58	13.2	104188	15	
Cleaner Tail		2516.42	43.1	291872	93.9	
	40 minutes	µg	g	µg	g	%
Ore		4280	151	520000	174	
Rougher Tail		313.5	12.8	101650	8.0	
Combined Con		3966.5	138.2	418350	166	
Oxidised Con		3966.5	61.8	383625	135.7	
Filtrate		0	75	34125	30	**100.0**
Wash Water		0	1.4	600	0.3	
Cleaner Con		1118.86	11.1	76230.2	16.2	
Cleaner Tail		2847.6	50.7	307395	119.5	

The distribution values are for three steps: Step 1: Rougher Tail + Combined Concentrate

Step 2: Filtrate + Wash Water + Oxidised Concentrate

Step 3: Cleaner concentrate + Cleaner Tail

Appendix 5.3: Sulfuric Acid Flotation Data

Control (Sulfuric Acid Series)	Gold Grade (g/t)			Gold Recovery (%)			Sulfide Sulfur Grade (%)			Sulfide Sulfur Recovery (%)			Arsenic Grade (ppm)			Arsenic Recovery (%)		
	Test 1	Test 2	Test 3	Test 1	Test 2	Test 3	Test 1	Test 2	Test 3	Test 1	Test 2	Test 3	Test 1	Test 2	Test 3	Test 1	Test 2	Test 3
Cleaner 1	10.49	12.70	9.95	26.8	30.7	25.8	43.01	52.34	37.54	30.0	34.3	30.6	1069	1119	1156	21.1	21.9	21.8
Cleaner 2	9.65	11.68	9.15	25.2	23.9	25.6	39.32	47.85	34.32	27.5	25.8	27.2	1059	1109	1145	21.3	21.0	21.1
Cleaner 3	7.37	8.92	6.99	28.2	26.7	28.6	29.13	35.45	25.42	29.8	28.0	29.5	1006	1054	1088	29.6	29.3	29.3
Cleaner Tail	4.0	3.94	4.31	19.8	18.7	20.0	15.88	17.16	15.14	12.8	12.0	12.7	450	472	487	28.1	27.8	27.8
Au:S	**0.25**	**0.23**	**0.28**	**100.0**	**100.0**	**100.0**				**100.0**	**100.0**	**100.0**	**5.4**	**6.2**	**4.7**	**100.0**	**100.0**	**100.0**
		0.25												**5.4**				

3 Tests	Sulfuric Acid	Control		Gold				Arsenic				Sulfide Sulfur			
				Average		Cumulative		Average		Cumulative		Average		Cumulative	
Product	Mass Recovery (%)	Recovery (%)	Water Recovery (%)	Grade (g/t)	Recovery (%)	Grade (g/t)	Recovery (%)	Grade (g/t)	Recovery (%)	Grade (g/t)	Recovery (%)	Grade (%)	Recovery (%)	Grade (%)	Recovery (%)
Con 1	7.7	7.7	3.9	11.04	22.6	11.04	27.8	558.0	21.83	1114	21.1	14.1	28.7	14.1	28.7
Con 2	7.7	15.4	7.9	12.3	24.5	11.8	52.7	688.0	21.06	760.6	42.8	16.5	26.0	15.3	54.6
Con 3	7.6	52.9	13.3	12.2	33.4	9.4	80.5	776.0	29.28	1049.3	72.17	22.7	29.3	39.0	84.0
Feed		**100.0**	**100.0**				**100.0**				**100.0**				**100.0**
Au:S						**0.24**			**Au:As**	**8.6**					

Sulfuric Acid 10 mins	Gold Grade (g/t)			Gold Recovery (%)			Sulfide Sulfur Grade (%)			Sulfide Sulfur Recovery (%)			Arsenic Grade (ppm)			Arsenic Recovery (%)		
	Test 1	Test 2	Test 3	Test 1	Test 2	Test 3	Test 1	Test 2	Test 3	Test 1	Test 2	Test 3	Test 1	Test 2	Test 3	Test 1	Test 2	Test 3
Cleaner 1	12.43	10.44	10.89	17.8	15.4	15.9	24.13	19.98	22.49	9.1	7.6	8.5	1024	1247	894	10.5	12.5	9.3
Cleaner 2	12.04	10.11	10.55	16.7	17.2	17.1	25.22	20.88	23.51	9.4	9.5	9.4	1136	1382	992	12.5	12.2	12.7
Cleaner 3	11.0	9.19	9.58	21.2	21.8	21.7	31.74	26.28	29.58	16.4	16.7	16.5	1047	1459	1199	18.4	18.0	18.7
Cleaner Tail	5.1	4.22	4.40	44.3	45.6	45.3	27.61	22.86	25.73	65.1	66.2	65.5	732	1019	837	58.6	57.3	59.4
Au:S	**0.18**	**0.18**	**0.17**	**100.0**	**100.0**	**100.0**				**100.0**	**100.0**	**100.0**	**6.8**	**4.1**	**5.2**	**100.0**	**100.0**	**100.0**
		0.18												**5.2**				

3 Tests	Sulfuric Acid	10 mins		Gold				Arsenic				Sulfide Sulfur			
				Average		Cumulative		Average		Cumulative		Average		Cumulative	
Product	Mass Recovery (%)	Recovery (%)	Water Recovery (%)	Grade (g/t)	Recovery (%)	Grade (g/t)	Recovery (%)	Grade (g/t)	Recovery (%)	Grade (g/t)	Recovery (%)	Grade (%)	Recovery (%)	Grade (%)	Recovery (%)
Con 1	6.9	6.9	4.5	11.3	20.4	11.3	20.4	1055.0	10.51	1055.0	10.51	22.2	8.69	22.2	8.69
Con 2	5.9	12.8	9.1	10.9	17.1	11.1	37.5	1170.0	12.49	1108.4	23.01	23.2	9.70	22.7	18.38
Con 3	12.5	34.3	15.3	4.4	14.4	10.5	54.9	1235.0	18.43	1171.0	41.44	29.2	16.67	26.9	35.06
Feed		**100.0**	**100.0**				**100.0**				**100.0**				**100.0**
Au:S						**0.39**			**Au:As**	**9.0**					

Sulfuric Acid 20 mins	Gold Grade (g/t)			Gold Recovery (%)			Sulfide Sulfur Grade (%)			Sulfide Sulfur Recovery (%)			Arsenic Grade (ppm)			Arsenic Recovery (%)		
	Test 1	Test 2	Test 3	Test 1	Test 2	Test 3	Test 1	Test 2	Test 3	Test 1	Test 2	Test 3	Test 1	Test 2	Test 3	Test 1	Test 2	Test 3
Cleaner 1	12.83	10.62	11.96	18.1	15.4	17.0	20.97	25.52	18.31	7.8	7.6	6.9	1431	1202	1254	17.5	16.1	16.7
Cleaner 2	11.90	9.86	11.09	10.1	10.4	10.2	19.22	23.40	16.78	5.2	9.5	5.3	1282	1076	1123	8.5	8.7	8.6
Cleaner 3	8.96	7.42	8.35	15.1	15.6	15.3	22.72	27.65	19.83	12.4	16.7	12.5	1221	1025	1070	16.2	16.5	16.3
Cleaner Tail	6.24	5.17	5.82	56.7	58.6	57.5	25.44	30.96	22.20	74.6	66.2	75.3	810	680	710	57.8	58.8	58.4
Au:S	**0.24**	**16.7**	**0.26**	**100.0**	**100.0**	**100.0**				**100.0**	**100.0**	**100.0**	**7.7**	**7.6**	**8.1**	**100.0**	**100.0**	**100.0**
		0.22												**7.8**				

3 Tests	Sulfuric Acid	20 mins		Gold				Arsenic				Sulfide Sulfur			
				Average		Cumulative		Average		Cumulative		Average		Cumulative	
Product	Mass Recovery (%)	Recovery (%)	Water Recovery (%)	Grade (g/t)	Recovery (%)	Grade (g/t)	Recovery (%)	Grade (g/t)	Recovery (%)	Grade (g/t)	Recovery (%)	Grade (%)	Recovery (%)	Grade (%)	Recovery (%)
Con 1	14.6	14.6	5.1	11.9	18.15	11.9	18.15	1295.0	16.08	1295.0	16.08	18.3	9.37	18.3	9.37
Con 2	6.9	21.6	8.0	11.0	10.7	11.6	28.22	1160.0	8.67	1244.8	24.75	21.1	5.29	19.2	14.66
Con 3	14.4	35.4	12.8	8.24	15.10	10.1	43.32	1105.0	16.45	1184.6	41.20	25.6	12.43	23.2	27.09
Feed		**100.0**	**100.0**				**100.0**				**100.0**				**100.0**
Au:S						**0.44**			**Au:As**	**8.5**					

Sulfuric Acid 30 mins	Gold Grade (g/t)			Gold Recovery (%)			Sulfide Sulfur Grade (%)			Sulfide Sulfur Recovery (%)			Arsenic Grade (ppm)			Arsenic Recovery (%)		
	Test 1	Test 2	Test 3	Test 1	Test 2	Test 3	Test 1	Test 2	Test 3	Test 1	Test 2	Test 3	Test 1	Test 2	Test 3	Test 1	Test 2	Test 3
Cleaner 1	10.71	8.87	9.98	11.4	9.7	10.8	18.74	22.80	16.36	5.4	6.5	4.7	972	817	852	9.7	8.2	8.6
Cleaner 2	9.93	8.23	9.26	6.7	6.9	6.8	d5	18.43	13.22	3.4	3.3	3.4	893	750	782	5.6	5.7	5.7
Cleaner 3	9.89	8.19	9.22	10.3	10.6	10.4	12.28	14.95	10.72	4.2	4.2	4.2	854	717	748	8.3	8.4	8.4
Cleaner Tail	7.73	6.40	7.20	71.5	72.9	72.1	28.74	34.97	25.08	87.1	86.0	87.7	890	747	779	76.4	77.6	77.4
Au:S	**0.27**	**0.18**	**0.29**	**100.0**	**100.0**	**100.0**				**100.0**	**100.0**	**100.0**	**8.6**	**8.5**	**9.2**	**100.0**	**100.0**	**100.0**
		0.25												**8.8**				

3 Tests	Sulfuric Acid	30 mins		Gold				Arsenic				Sulfide Sulfur			
				Average		Cumulative		Average		Cumulative		Average		Cumulative	
Product	Mass Recovery (%)	Recovery (%)	Water Recovery (%)	Grade (g/t)	Recovery (%)	Grade (g/t)	Recovery (%)	Grade (g/t)	Recovery (%)	Grade (g/t)	Recovery (%)	Grade (%)	Recovery (%)	Grade (%)	Recovery (%)
Con 1	10.0	10.0	9.1	9.9	11.44	9.9	11.44	880.0	8.66	880.0	9.66	19.3	6.69	19.3	6.69
Con 2	7.4	17.4	15.6	9.1	6.72	9.5	18.16	808.0	5.61	849.4	15.26	15.6	3.53	17.7	10.22
Con 3	9.6	29.1	23.9	9.1	10.34	9.4	28.5	773.0	8.30	822.3	23.56	12.7	4.62	17.5	14.85
Feed		**100.0**	**100.0**				**100.0**				**100.0**				**100.0**
Au:S						**0.54**			**Au:As**	**11.4**					

Sulfuric Acid 40 mins	Gold Grade (g/t)			Gold Recovery (%)			Sulfide Sulfur Grade (%)			Sulfide Sulfur Recovery (%)			Arsenic Grade (ppm)			Arsenic Recovery (%)		
	Test 1	Test 2	Test 3	Test 1	Test 2	Test 3	Test 1	Test 2	Test 3	Test 1	Test 2	Test 3	Test 1	Test 2	Test 3	Test 1	Test 2	Test 3
Cleaner 1	12.43	11.19	9.81	7.9	7.1	6.3	16.09	13.32	14.99	3.1	2.4	2.7	773	955	729	6.0	7.3	5.7
Cleaner 2	11.99	10.79	9.46	5.3	5.3	5.4	16.52	13.68	15.40	2.0	2.1	2.0	708	874	668	3.8	3.7	3.8
Cleaner 3	10.92	9.83	8.61	9.3	9.4	9.5	15.82	13.10	14.74	3.8	3.8	3.8	744	920	702	7.7	7.6	7.8
Cleaner Tail	7.86	7.08	6.20	77.5	78.2	78.9	32.83	27.18	30.60	91.1	91.7	91.5	686	848	647	82.5	81.4	82.8
Au:S	**0.24**	**0.26**	**0.20**	**100.0**	**100.0**	**100.0**				**100.0**	**100.0**	**100.0**	**11.4**	**8.3**	**9.5**	**100.0**	**100.0**	**100.0**
		0.23												**9.7**				

3 Tests	Sulfuric Acid	40 mins		Gold				Arsenic				Sulfide Sulfur			
				Average		Cumulative		Average		Cumulative		Average		Cumulative	
Product	Mass Recovery (%)	Recovery (%)	Water Recovery (%)	Grade (g/t)	Recovery (%)	Grade (g/t)	Recovery (%)	Grade (g/t)	Recovery (%)	Grade (g/t)	Recovery (%)	Grade (%)	Recovery (%)	Grade (%)	Recovery (%)
Con 1	6.5	6.5	3.8	11.2	7.88	11.2	7.88	819.0	7.2	819.0	7.2	14.8	3.1	14.8	3.1
Con 2	6.9	13.3	6.7	10.8	5.26	10.9	13.14	750.0	6.9	783.5	14.1	15.2	2.2	15.0	4.92
Con 3	8.4	15.1	11.2	9.8	9.31	10.4	22.46	789.0	9.0	785.7	23.1	14.6	4.12	16.4	8.72
Feed		**100.0**	**100.0**				**100.0**				**100.0**				**100.0**
Au:S						**0.63**			**Au:As**	**13.2**					

Appendix 6: ToF-SIMS Data

	Cleaner Con			Cleaner Tail			Cleaner Con (Nitric oxidised)			Cleaner Tail (Nitric oxidised)		
	Average	**Std Dev**	**95% C.I.**	**Average**	**Std Dev**	**95% C.I.**	**Average**	**Std Dev**	**95% C.I.**	**Average**	**Std Dev**	**95% C.I.**
CH3	0.009781	0.001741	0.000682	0.010567	0.001133	0.000444	0.007552	0.001102	0.000432	0.007709	0.001324	0.000519
Na	0.160872	0.04634	0.018165	0.137885	0.047905	0.018779	0.2439	0.025304	0.009919	0.19268	0.027329	0.010713
Mg	0.023851	0.006118	0.002398	0.025686	0.004694	0.00184	0.024504	0.002181	0.000855	0.026059	0.003585	0.001405
Al	0.139208	0.028297	0.011092	0.133718	0.026768	0.010493	0.143844	0.012887	0.005052	0.164148	0.022196	0.008701
Si	0.12802	0.032155	0.012605	0.10831	0.026479	0.01038	0.183107	0.019822	0.00777	0.187981	0.038073	0.014925
K	0.105848	0.020021	0.007848	0.133373	0.023192	0.009091	0.105022	0.012004	0.004705	0.16299	0.037609	0.014743
Ca	0.250135	0.085895	0.033671	0.258128	0.058823	0.023059	0.205467	0.023422	0.009181	0.18662	0.047594	0.018657
Fe	0.170354	0.02613	0.010243	0.178076	0.023875	0.009359	0.079844	0.015066	0.005906	0.068175	0.026976	0.010575
Cu	0.011787	0.008067	0.003162	0.014089	0.009838	0.003857	0.006598	0.008876	0.003479	0.003469	0.002976	0.001167
Au	0.000144	6.44E-05	2.52E-05	0.000168	6.77E-05	2.66E-05	0.000163	0.000101	3.95E-05	0.000168	9.5E-05	3.72E-05

	Cleaner Con (Sulfuric oxidised)			Cleaner Tail (Sulfuric oxidised)		
	Average	**Std Dev**	**95% C.I.**	**Average**	**Std Dev**	**95% C.I.**
CH3	0.006738	0.000751	0.000295	0.006225	0.00105	0.000412
Na	0.192702	0.028521	0.01118	0.188183	0.041324	0.016199
Mg	0.024052	0.002664	0.001044	0.021469	0.012202	0.004783
Al	0.136193	0.01677	0.006574	0.113719	0.020746	0.008133
Si	0.148183	0.020038	0.007855	0.12391	0.022426	0.008791
K	0.180092	0.022016	0.00863	0.161409	0.044445	0.017423
Ca	0.251109	0.034344	0.013463	0.314159	0.072842	0.028554
Fe	0.05768	0.015578	0.006107	0.066447	0.01934	0.007581
Cu	0.003101	0.002069	0.000811	0.004362	0.002501	0.000981
Au	0.000151	7.19E-05	2.82E-05	0.000116	7.54E-05	2.96E-05

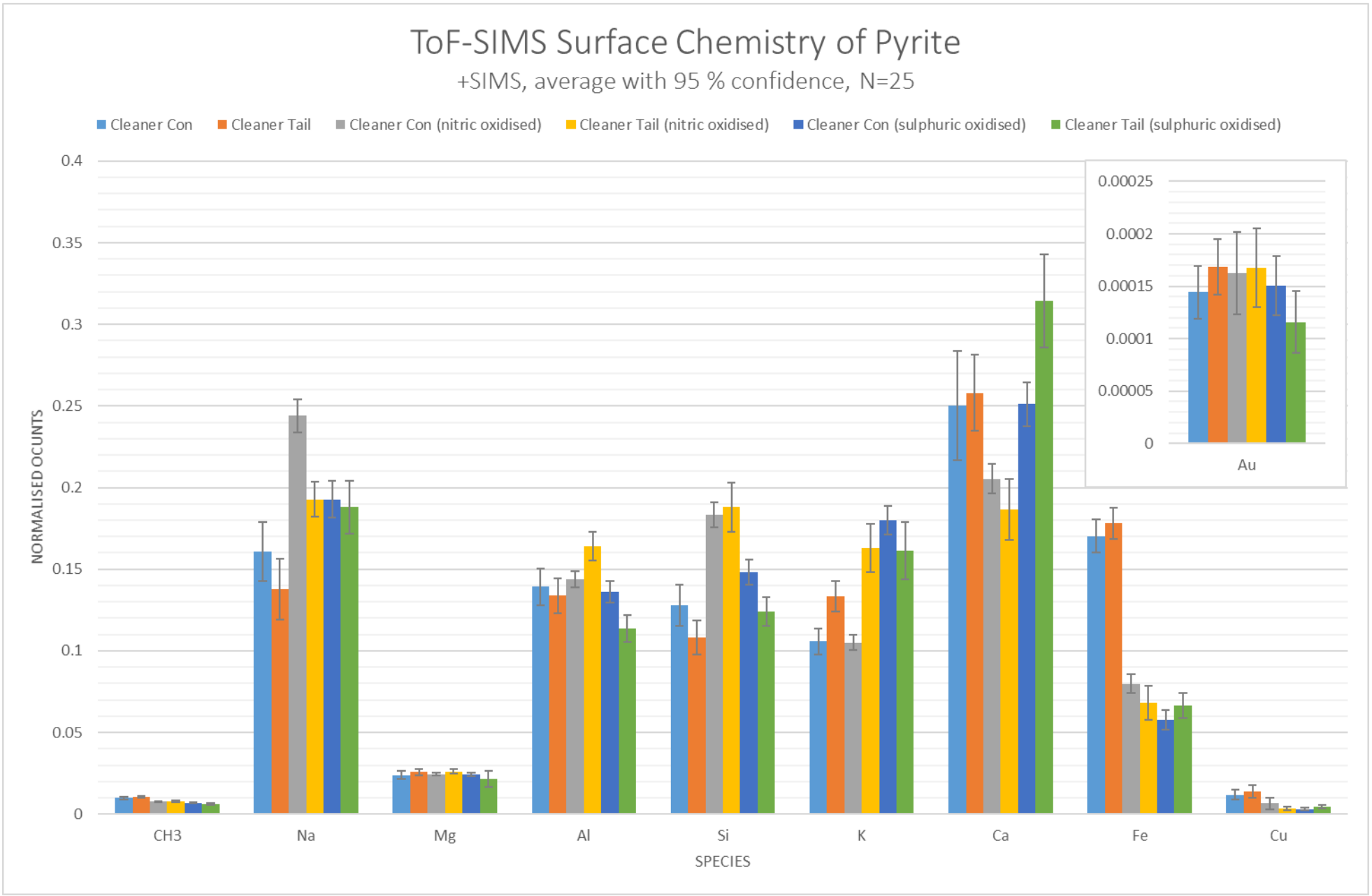
ToF-SIMS Surface Chemistry of Pyrite
+SIMS, average with 95 % confidence, N=25
Cleaner Con
Cleaner Tail
Cleaner Con (nitric oxidised)
Cleaner Tail (nitric oxidised)
Cleaner Con (sulphuric oxidised)
Cleaner Tail (sulphuric oxidised)
NORMALISED OCUNTS
0.4
0.35
0.3
0.25
0.2
0.15
0.1
0.05
0
CH3
Na
Mg
Al
Si
K
Ca
Fe
Cu
SPECIES
0.00025
0.0002
0.00015
0.0001
0.00005
0
Au

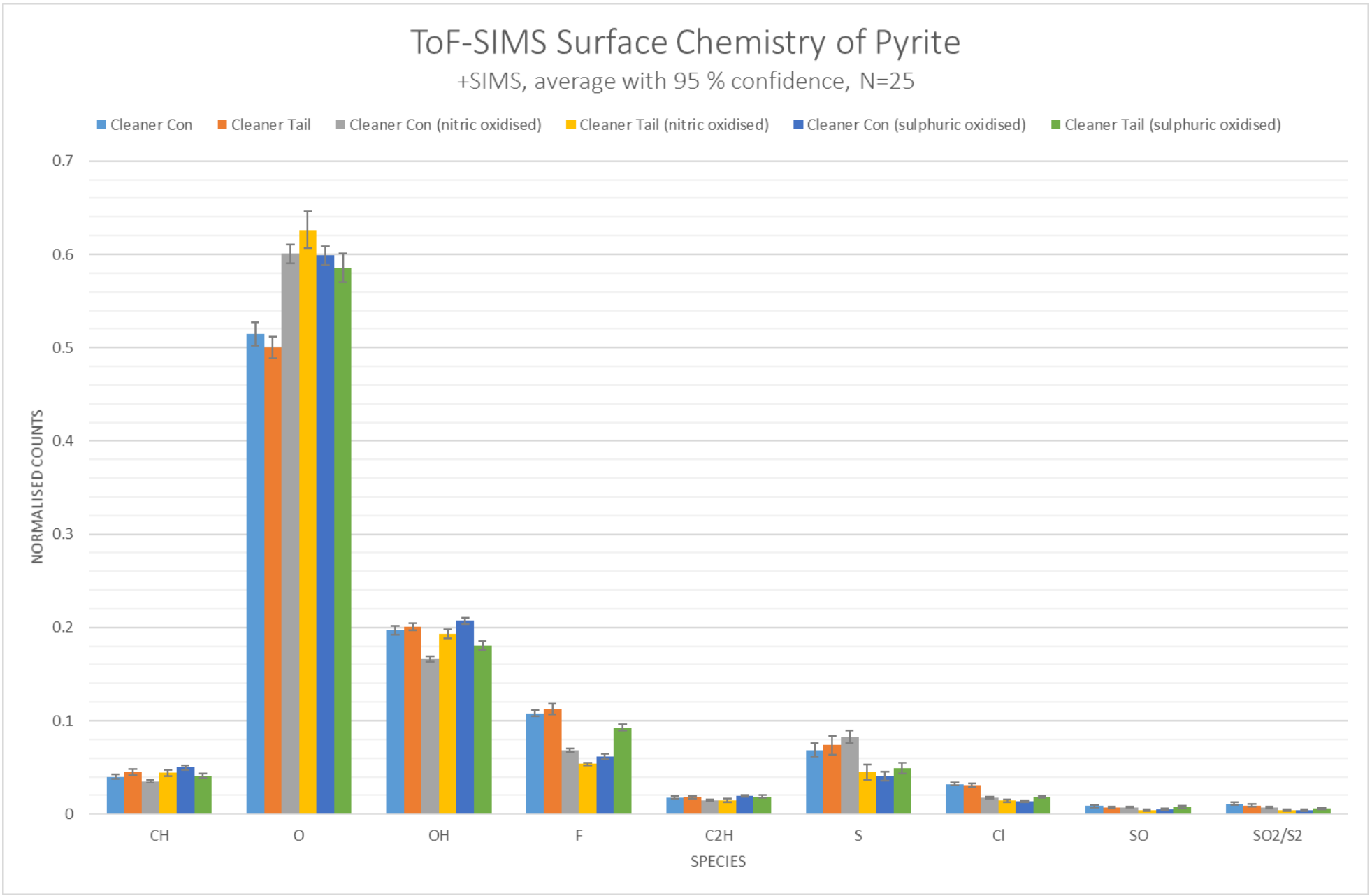
ToF-SIMS Surface Chemistry of Pyrite
+SIMS, average with 95 % confidence, N=25
Cleaner Con
Cleaner Tail
Cleaner Con (nitric oxidised)
Cleaner Tail (nitric oxidised)
Cleaner Con (sulphuric oxidised)
Cleaner Tail (sulphuric oxidised)
NORMALISED COUNTS
0.7
0.6
0.5
0.4
0.3
0.2
0.1
0
CH
O
OH
F
C2H
S
Cl
SO
SO2/S2
SPECIES

310

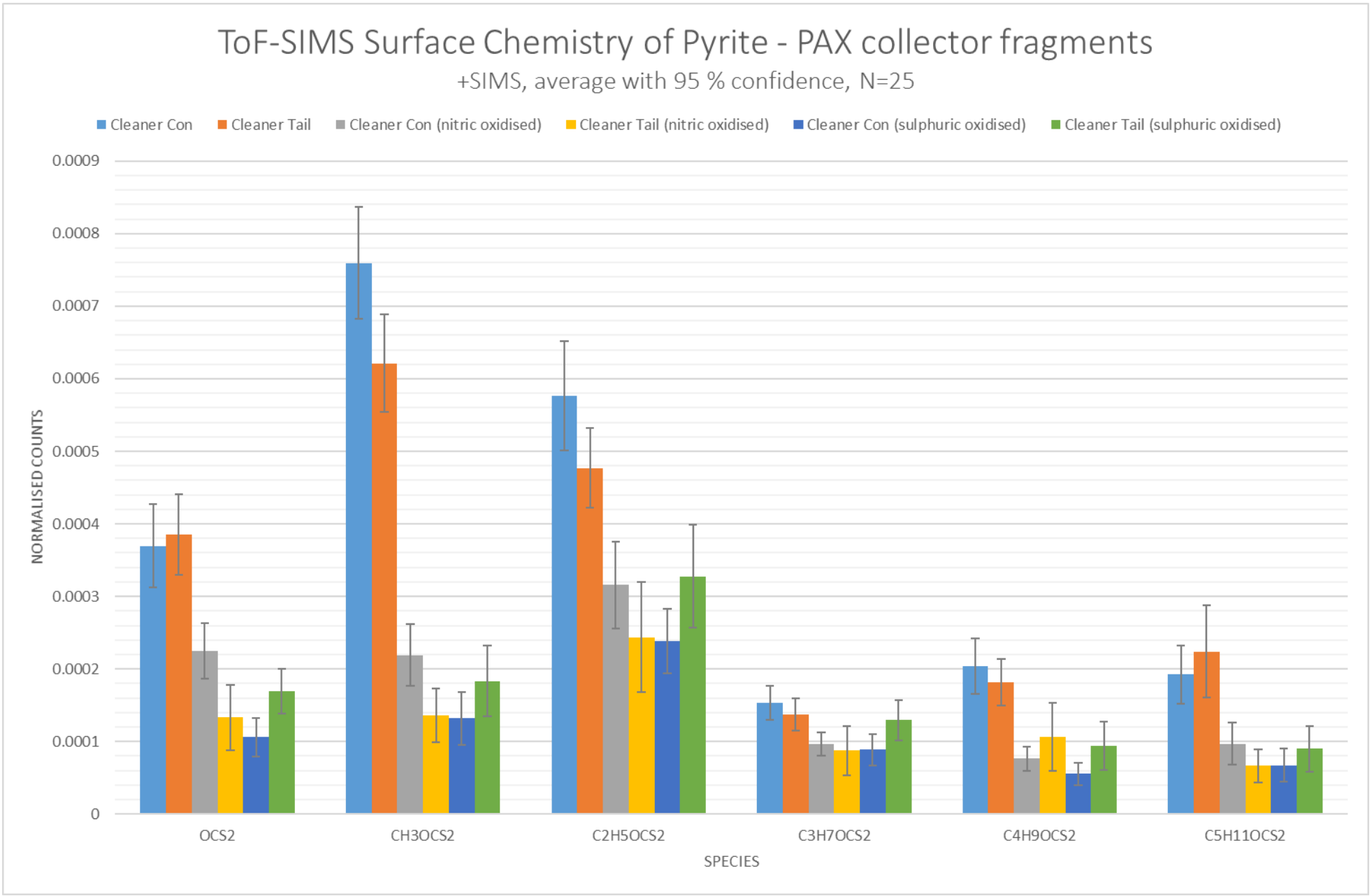
ToF-SIMS Surface Chemistry of Pyrite - PAX collector fragments
+SIMS, average with 95 % confidence, N=25
Cleaner Con
Cleaner Tail
Cleaner Con (nitric oxidised)
Cleaner Tail (nitric oxidised)
Cleaner Con (sulphuric oxidised)
Cleaner Tail (sulphuric oxidised)
NORMALISED COUNTS
0.0009
0.0008
0.0007
0.0006
0.0005
0.0004
0.0003
0.0002
0.0001
0
OCS2
CH3OCS2
C2H5OCS2
C3H7OCS2
C4H9OCS2
C5H11OCS2
SPECIES